НАЦИОНАЛЬНАЯ АКАДЕМИЯ НАУК УКРАИНЫ
ИНСТИТУТ ГЕОФИЗИКИ

ГЕОФИЗИЧЕСКИЙ ЖУРНАЛ

Geophysical journal

Основан в июле 1979 г. | Выходит 6 раз в год | Том 32

Международный журнал | An International Journal | № 4 • 2010



An International Conference on

GEODYNAMICAL PHENOMENA: From Observations and Experiments to Theory and Modelling

September 20-24, 2010
Kiev, Ukraine



SUPPORTING ORGANIZATIONS:

Institute of Geophysics, National Academy of Sciences of Ukraine, Kiev, Ukraine
University of Minnesota, Twin Cities, USA
University of California, San Diego, USA
Institute of Physics of the Earth, Russian Academy of Sciences, Moscow, Russia
National Technical University (Kiev Polytechnic Institute), Kiev, Ukraine

University of Minnesota
Driven to Discover

UC San Diego
Local Impact, National Influence, Global Reach

SUPPORTING ORGANIZATIONS:

- Institute of Geophysics, National Academy of Sciences of Ukraine, Kiev, Ukraine
- University of Minnesota, Twin Cities, USA
- University of California, San Diego, USA
- Institute of Physics of the Earth, Russian Academy of Sciences, Moscow, Russia
- National Technical University (Kiev Polytechnic Institute), Kiev, Ukraine

ORGANIZATION COMMITTEE

Chairmans:

- Starostenko Vitaly, Institute of Geophysics, National Academy of Sciences of Ukraine (NASU), Kiev, Ukraine
- Yuen David A., University of Minnesota, Twin Cities, USA
- Gliko Alexander, Institute of Physics of the Earth, Russian Academy of Sciences (RAS), Moscow, Russia
- Zgurovsky Michael, National Technical University (Kiev Polytechnic Institute), Kiev, Ukraine

Executive Members:

- Baranov Alexey, Institute of Physics of the Earth, RAS, Moscow, Russia
- Bogdanova Svetlana, Lund University, Lund, Sweden
- Danylenko Vyacheslav, Institute of Geophysics, NASU, Kiev, Ukraine
- Fialko Yuri, University of California, San Diego, USA
- Gerya Taras, ETH Zurich, Switzerland
- Gintov Oleg, Institute of Geophysics, NASU, Kiev, Ukraine
- Grad Marek, Institute of Geophysics, University of Warsaw, Warsaw, Poland
- Guterch Alexander, Institute of Geophysics, Polish Academy of Science, Warsaw, Poland
- Kendzera Alexander, Institute of Geophysics, NASU, Kiev, Ukraine
- Khazan Yakov, Institute of Geophysics, NASU, Kiev, Ukraine
- Kobolev Vladimir, Institute of Geophysics, NASU, Kiev, Ukraine
- Kutas Roman, Institute of Geophysics, NASU, Kiev, Ukraine
- Lapusta Nadia, Caltech, Pasadena, USA
- Makarenko Alexander, Kiev Polytechnic Institute, Kiev, Ukraine
- Mikhailov Valentin, Institute of Physics of the Earth, RAS, Moscow, Russia
- Pankratova Natalia, Kiev Polytechnic Institute, Kiev, Ukraine
- Pasichny Alexis, Kiev Polytechnic Institute, Kiev, Ukraine
- Podladchikov Yuri, PGP, Oslo University, Norway
- Rokityansky Igor, Institute of Geophysics, NASU, Kiev, Ukraine
- Stephenson Randell., University of Aberdeen, UK
- Thybo Hans, University of Copenhagen, Copenhagen, Denmark
- Trubitsyn Valery, Institute of Physics of the Earth, Moscow, Russia
- Tsvetkova Tatiana, Institute of Geophysics, NASU, Kiev, Ukraine
- Yefremov Kostiantyn, Kiev Polytechnic Institute, Kiev, Ukraine

Scientific secretary of the Conference:

- Legostaeva Olga, Institute of Geophysics, NASU, Kiev, Ukraine

The nature and prediction of regional zoning for dynamic phenomena in mines of the Donets Coal Basin

© ***A. Antsiferov*[1], *M. Dovbnich*[2], *V. Kanin*[1], *I. Viktosenko*[2], *2010***

[1]UkrNIMI, National Academy of Sceinces of Ukraine, Donetsk, Ukraine
ukrnimi@ukrnimi.donetsk.ua
[2]National Mining University, Dnepropetrovsk, Ukraine
dovbnichm@mail.ru

The Donets Coal Basin is the basic fuel and energy region of Ukraine. Promotion of safety measures (accident prevention) in mining is the main industrial and functional problem of coal-mining companies that requires the very careful attention and scientific learning. In coal mines of the Donets Coal Basin as, it must be said, in other coal regions, where coal is being mined underground, at all times there is a real hazard of dynamic phenomena in mine entries. First of all a hazard is due to gas-dynamic phenomena — sudden outbursts [Antsiferov et al., 2009]. Generally, sudden outbursts occur after a number of preliminary stages defined by many factors. Together with man-induced impact on rock mass being mined, geological factor is also involved. One of the main characteristics which define the role of geological factor in occurrence of dynamic phenomena in mine entries is tectonic stresses. At its core the natural component of the mechanism of dynamic phenomena in mine entries, in many respects, is similar to earthquake-generating mechanism. The type of dynamic phenomenon is determined by properties of rock mass itself. Neo-tectonic activity within the limits of one or another territory plays the determining role in maintenance of significant level of present tectonic stresses. Accordingly one of the urgent problems in research into geological causes for occurrence of geodynamic phenomena in mine entries is prediction of geodynamically active zones. Strictly speaking, idea to investigate zoning of dynamic phenomena within the limits of the Donets Coal Basin attracting information on neo-tectonic activity is not new (G. A. Konkov, V. S. Vereda, V. A. Privalov et al.). The authors of this work also hold the opinion on confinedness of dynamic phenomena in mine entries to dynamically active zones of tectonosphere.

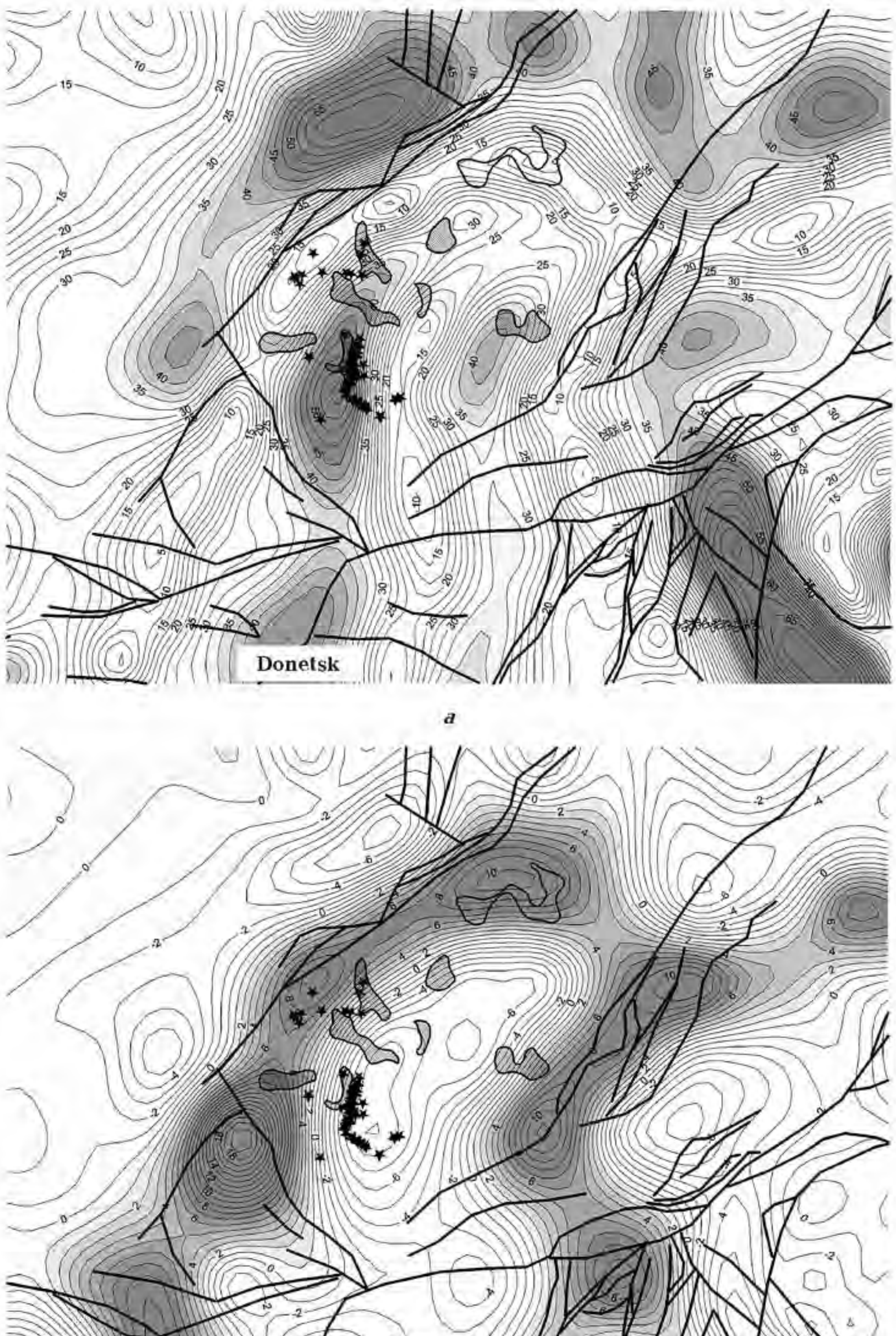
The objective of this work is to consider the main methodical provisions for identification and some outcomes of prediction of regional zoning of dynamic phenomena in mines of the Donets Coal Basin.

The basis for the suggested approach is the equilibrium-state model of the rotated Earth proposed by K. F. Tyapkin and called *geoisostasy* which is the subject of considerable literature [Tyapkin, 1980]. At present based on the analysis of geoid anomalies [Dovbnich, 2008] algorithms are elaborated for computation of tectonosphere stress fields caused by disturbance of equilibrium state. In previously published works [Dovbnich, Demianets, 2009] it was shown that geodynamically active zones of tectonosphere manifest themselves in stress anomalies due to disturbance of equilibrium state. First and foremost, such zones, on the assumption that stresses acting in them are sufficient, manifest them as seismically active. Elements which are tectonic base for seismic generating structures are embodied in stresses under consideration.

The working hypothesis in predicting regional zones for development of dynamic phenomena in mine entries can be the following statement: regional zones for development of dynamic phenomena are defined by degree of deformation processes that develop in sedimentation mass, which in their turn are embodied in stress field local component caused by disturbance of equilibrium state.

In conditions of the Donets Coal Basin assessment of subsurface stressed state caused by disturbance of equilibrium state was made on the basis of land gravity measurement data of the scale 1: 200,000 and relief digital model.

Based on the computed stresses we generated prediction layout of regional zones for development of dynamic phenomena for greater territory of the Donets Coal basin. A detailed comparison of computed stress fields with gas-dynamic phenomena occurred during mining of seams m_3, l_4, l_1 and k_8 (A. F. Zasyadko Mine) was made (Figure). At the first stage comparison of gas-dynamic phenomena occurred during mining of seams m_3, l_4, l_1 and k_8 with local stresses computed by land gravity measurement data was made. The most of phenomena are confined to the



Comparison layout of gas-dynamic phenomena (A. F. Zasyadko Mine) and local geoisostatic stresses (kPa): *a* — shear stresses, *b* — compression-tensile stresses (*1* — gas-dynamic phenomena, *2* — predicted zones of methane accumulation, *3* — tectonic faults).

anomaly of intense shear stresses. Most zones of methane accumulation predicted by a set of independent techniques are also connected with this anomaly. At the second stage for more detailed analysis of deformation processes in sedimentation mass within the limits of mine field analysis of attitude of coal seam m_3 was made. As an outcome we received a layout of local folding that complicates close monoclinal bedding of this seam and represents difference of the seam surface and its approximating surface which is polynomial of third order. Comparing a layout of local folds with dynamic phenomena and predicted zones of methane accumulation we can insist that majority of them is confined to gradient zone of local folds. The nature of this zone is closely connected with the processes that are embodied in anomalies of intensity of local shear stresses. Regularities determined within the limits of A. F. Zasyadko Mine field confirm assumptions on connection of certain components of stress field caused by disturbance of equilibrium state with deformation processes developed in sedimentation mass and zones of development of dynamic processes embodied in it.

The authors are convinced that in investigation of dynamic phenomena in geologic environment, independently of their scale — earthquakes, rock bursts, gas-dynamic phenomena and others — the most important element is study of all whole factors, starting from planetary and ending by local ones, which result in disturbance of equilibrium state of the planet and cause occurrence of mechanical stresses in the outer shells of the Earth.

References

Antsiferov A. V., Golubev A. A., Kanin V. A., Tirkel M. G., Zadara G. Z., Uziyuk V. I., Antsiferov V. A., Suyarko V. G. Gas content and methane resources of coal basins in Ukraine. Vol. 1. — Donetsk: Veber, 2009. — 456 p. (in Russian).

Dovbnich M. M. Disturbance of geoisostasy and tectonoshere stressed state // Geophys. J. — 2008. — **30**, № 4. — P. 123—132 (in Russian).

Dovbnich M. M., Demianets S. N. Tectonoshere stress fields caused by distorsion of geoisostasy and geodynamics of the Azov-Black Sea region // Geophys. J. — 2009. — **31**, № 2. — P. 107—116 (in Russian).

Tyapkin K. F. New rotation hypothesis of structure formation and geoisostasy // Geophys. J. — 1980. — **2**, № 5. — P. 40—46 (in Russian).

Computer-aided investigation of fault zone deformation response to low-amplitude dynamic mechanical actions

© ***S. Astafurov, E. Shilko, A. Grigoriev, A. Panchenko, S. Psakhie, 2010***

Institute of Strength Physics and Materials Sciences, SB RAS, Tomsk, Russia
astaf@ispms.tsc.ru

An important direction in mechanics is investigation of features of mechanical response of geological media. An important feature of geomedium is that its fragments are in complex stressed state. Relation of internal stresses to strength characteristics of interfacial regions (faults and cracks) appreciably defines deformation and relaxation capacity of the mechanism concerned with relative block displacement. As the shear stress at an active block boundary reaches limiting (threshold) value, its local deformation mode can change qualitatively from slow deformation (creeping) to dynamic deformation (referred to as unsTable sliding). Note that according to modern notion, acts of dynamic block sliding are seismogenerating events those magnitude can reach 6—7. Thus, an urgent task in geomechanics is to develop methods of estimating the local stress state at active interfaces of fragments of rock massifs or the earth's crust. Theoretical studies as well as experiments on prestressed rock samples and fragments of plane discontinuities in rock massifs revealed an important effect consisting in deformation response of geomedium to dynamic perturbations of stress state in form of irreversible relative displacement of blocks. This allowed different authors to formulate the idea

about the possibility of estimation of shear stress level in the fragments of active fault zones by measuring deformation response on testing dynamic actions. Nevertheless to transform this idea into practical approach it is necessary to have information about the character of connection between shear stress level in interfacial zone and deformation response to dynamic perturbation of local stress state. This information could be obtained in particular on the base of computer-aided simulation of fragments of block interfaces being under complex stress condition. In the present paper this study was done with use of the movable cellular automaton method (MCA). This method is a variant of particle method and over last decade successfully employed for studying the peculiarities of deformation and fracture of indurated, unconsolidated and loose media.

For solving the problem posed, a two-dimensional structural model of the interface between elements of a block medium was developed in the framework of movable cellular automaton method. The model includes the interface itself and contiguous block fragments. The model blocks were assumed to be monolithic, brittle and of high strength. The mechanical response of interfacial region featured irreversible strain accumulation and simulated the mechanical properties of a cataclasites. For mathematical description of elastoplastic response of the interface and of the blocks in the framework of the MCA method, the model described in was used. The lower surface of the specimen was rigidly fixed while external load was applied to the upper surface. The initial stress state of the system was specified by applying an external force with normal and tangential components to the upper surface of the model specimen with subsequent relaxation of the system. In the calculations, we used different values of normal force, whose specific value varied in the range from 20 to 40 % of the yield stress of interface material. Deformation response of model interface to dynamic pulse testing loading by *P*- and *S*-waves was studied.

Simulation results showed that the dynamically initiated displacement of the upper block along the interface varies over order of magnitude with the shear stress level, and this variation has a clearly defined nonlinear character. If the shear stress level approaches some critical value, qualitative variations occur in deformation response of the interface to dynamic loading. Revealed effect is important for formulation of the approach to diagnostics of stress state of block interfaces in block-structured geomedium. Note that character of interface deformation response defines to a great extent not only by shear stress level, but by applied normal load and by type of incident wave as well. Under large normal load the region of great increase of initiated shear displacement extends far in the stage of so-called quasiplastic interface response. Effective slope of this region therewith decreases nearly proportional to increase of normal stresses. Hence character of change of block boundary deformation response to testing pulse actions by compressive *P*-waves with shear stress level is appreciably defined by normal stress value. At the same time, pulse testing actions with use of elastic *S*-waves looks more promising. Results of investigation shows, that dependencies of shear displacements on shear stresse at different normal stresses are close to each other. The region of great increase of shear displacement is strongly pronounced in all cases, and its completion is associated with the point of transition from quasielastic to quasiplastic response stage. Hence characteristics of interface shear deformation response to dynamic exposure to *S*-waves insignificantly depend on value of normal stress.

Simulation results allowed authors to propose the way to development of an approach to diagnostics of shear stress level at sections of active faults of structural blocks in rock massif. The approach could be based on long-time monitoring of dynamics of natural and man-caused displacements in studied part of active block boundary. It is shown that both theoretical and experimental study of deformation response of real fragments of fault zones to testing pulse dynamic exposure could be carried out with use of local sources of pulse perturbations of stress state, which generate mainly *S*-waves. In that case obtained data about interface deformation response could be interpreted the most unambiguously and will reliably characterize the shear stress level, i.e. the proximity of shear stress at the interface to the current value of stress corresponding to beginning of the stage of “macroscopic” irreversible deformation.

The investigation has been carried out at financial support of the RFBR Grant № 09-05-00968-a, RAS Presidium Project № 11.2, Grant of the President of Russian Federation (MK-130.2010.5) and Russian Science Support Foundation.

On the influence of deformation mechanisms of different scales on regularities of response of shear fault zones under nonequiaxal compression loading

© **S. Astafurov, E. Shilko, V. Sergeev, A. Panchenko, S. Psakhie, 2010**

Institute of Strength Physics and Materials Sciences, SB RAS, Tomsk, Russia
astaf@ispms.tsc.ru

Introduction. It is well known that stress state of geological media is nonuniform and complex and one of its main features are constrained conditions. Degree of constraint, determined through a value of applied stresses, greatly influences on deformation mechanisms and fracture regime of the medium. Significant parts of massifs, are in complex conditions, which could be characterized by the scheme "shear+compression". So, deformation of shearing fault zones takes place under nonequiaxial compression conditions. In this current study is the influence of relationship of normal and lateral pressures on the character of deformation and fracture of the geological medium under shear loading. An important feature of the structure of geological media is a multiscale hierarchical organization of the block structure. The structural blocks separated by a "surface relaxations", characterized by lower effective strength in comparison with the material blocks itself. This helps to alleviate the slipping along interblock interfaces and thus leads to occurrence of large number of additional degrees of freedom (mobility) fragments of the medium. Therefore it is important to analyze the role of the block structure of the medium, in particular, the processes of formation of discontinuities and cracks growth at the interfaces of structural elements. This paper is devoted to the theoretical investigation of the effect of this factor on the deformation parameters, shear strength and other characteristics of the response of block-structured medium under constrained shear loading conditions. The study was carried out on the base of computer-aided simulation by movable cellular automaton method.

In this paper, regularities of response of block-structured media under shear deformation were studied on the example of system with blocks of the same size, separated by interfaces. Analogue interblock interfaces constituted zones with reduced strength and deformation characteristics. It promotes the localization and accumulation of irreversible strains on them. Note that in the case of a real geological medium these features are determined by highest content in the interface zones (in comparison with the blocks) of damages, porosity, etc. This model of block-structured medium was realized in the framework of two-dimensional version of the movable cellular automaton method. For the mathematical description of the elastic-plastic response of the blocks and the interfaces applied the model described in, in approximation, a similar to plain-stress state approximation. For automata that simulate the blocks linear response function was used. Response functions of automata that simulate the interfaces were characterized by a long section, corresponding to the accumulation of irreversible deformation. Initial stress state of the sample set by nonequiaxial compression by forces. Constrained specimen was subjected to a shear deformation with a small constant velocity. Degree of nonequiaxiality of compression of the specimen was characterized by the dimensionless parameter, which is defined as the ratio of the relative values of compresses in the horizontal direction force to a specific value of the vertical compressive force. This parameter characterizes the relative magnitude of compression of the system in the direction of shear.

The results of the theoretical investigation of the general regularities of behavior of block-structured, including geology, media in conditions of shear deformation have shown that an important factor in determining the relative contribution of different deformation mechanisms in the integrated mechanical response of the block system is the degree of nonequiaxiality of compression of the specimen. Thus, the increase in compressive stress in the direction of application of shear loading leads to reducing of contribution of deformation mechanisms of low scale levels, leading to the accumulation of irreversible deformation in the interblock interface areas. The reason for this is increasing of the degree of degradation of medium in the initial stress-strain state,

which leads to rapid formation of discontinuities in the most weak interfaces in the process of shear deformation. At high degrees of constraint formation of these "mesoscopic" flaws and their association into interblock cracks become the dominant deformation mechanism in the block-structured medium. Changing of the dominant mechanism of deformation is manifested as a change of the trend and in some cases of the sign of the integral characteristics of the deformation response of the medium, such as shear strength, the ultimate value of shear strain and changing of the width of shearing zone. In general, results suggest the possibility of introducing of some dimensionless parameter characterizing regime of the mechanical response of the medium during shear deformation. This parameter should be a function which links the applied stresses and rheological characteristics of the medium (in particular, the elastic limit of the material of interblock interfaces).

This work was supported by grant of the President of Russian Federation (MK-130.2010.5), RFBR grant № 09-05-00968-a and project of program of the Presidium of RAS 16.8.

Recent stress deformation in disjunctive zones on the base of remote sensing data

Scientific Centre for Aerospace Research of the Earth, IGS,
National Academy of Sciences of Ukraine, Kiev, Ukraine
azimov@casre.kiev.ua

It is identified that by their formation mechanisms the known and forecasted fracture dislocations at a recent stage of their geotectonic development manifest themselves mainly as the zones of stretching. The disjunctive structures of this type are always well decoded on different-scale remote sensing data (RSD) of any region of study. Their geoindicators are characteristic of zones of increased fluid-geological permeability.

Let's consider a territory of the Chernobyl Exclusion Zone and an adjacent region of the Korosten pluton. For its landscape-geological conditions the geoindication constituents of fractures are represented usually by the negative relief forms, super-humid sites with developed species of hygrophilous vegetation, elongated lines of anomalous phototone change to darker hues, etc. At once for mentioned region as an example (specifically for the Tovstyi Lis site within its borders) we classified the basic landscape geoindicators of the discriminating geodynamic fields at the recent tectogenesis stage. The fields are related to the Earth's crust disjunctive structures. Peculiarities of the fields' reflection in the RSD are characterised too [Azimov, 2008; 2009].

During investigation first of all it was taking as a base the framework of a tectonic structure of the studied area (Fig. 1, 2) chosen in the course of the regional research stage [Azimov, 2001; 2002; 2003]. It was worked out in detail within the Tovstyi Lis site and its adjacent areas [Azimov, 2004; 2006; Geological …, 2006]. For example, determination of the rectilinear known and forecasted structural elements of disjunction character (or structural lines, lineaments) on the remote images of high space resolution and topographic materials was performed with using a set of criteria (geoindicators): boundaries of sites with a different degree of the relief dissection and dynamics of erosion processes; rectified boundary segments of hypsometric benches, gradient steps of the relief, river valleys, banks of small lakes and swamps, erosion network, troughs, grooves, gullies, water divides, bent water courses and valleys, linearly elongated chains of suffusion depressions, mikrodepressions, erosion-denudation bodies, sandy ranges, as well as boundaries of the Quaternary deposit complexes and their lithofacies, sections with specific facies of hygrophilous vegetation, elongated lines of anomalous variations of image phototone, etc.

A location scheme for the lineament structures obtained by decoding show high lineaments density, for this reason direct identification of the fracture dislocations is difficult. For finding regularities of the lineaments distribution, their typification was done according to their manifestation indicators at remote images or the site, their relation with geological objects and inter-correlation between each other, elongation, width, etc. Usually zones of decoded lineaments appear to be wider than zones of fractures revealed by geological-geophysical methods. The latter ones are located in the middle of linea-

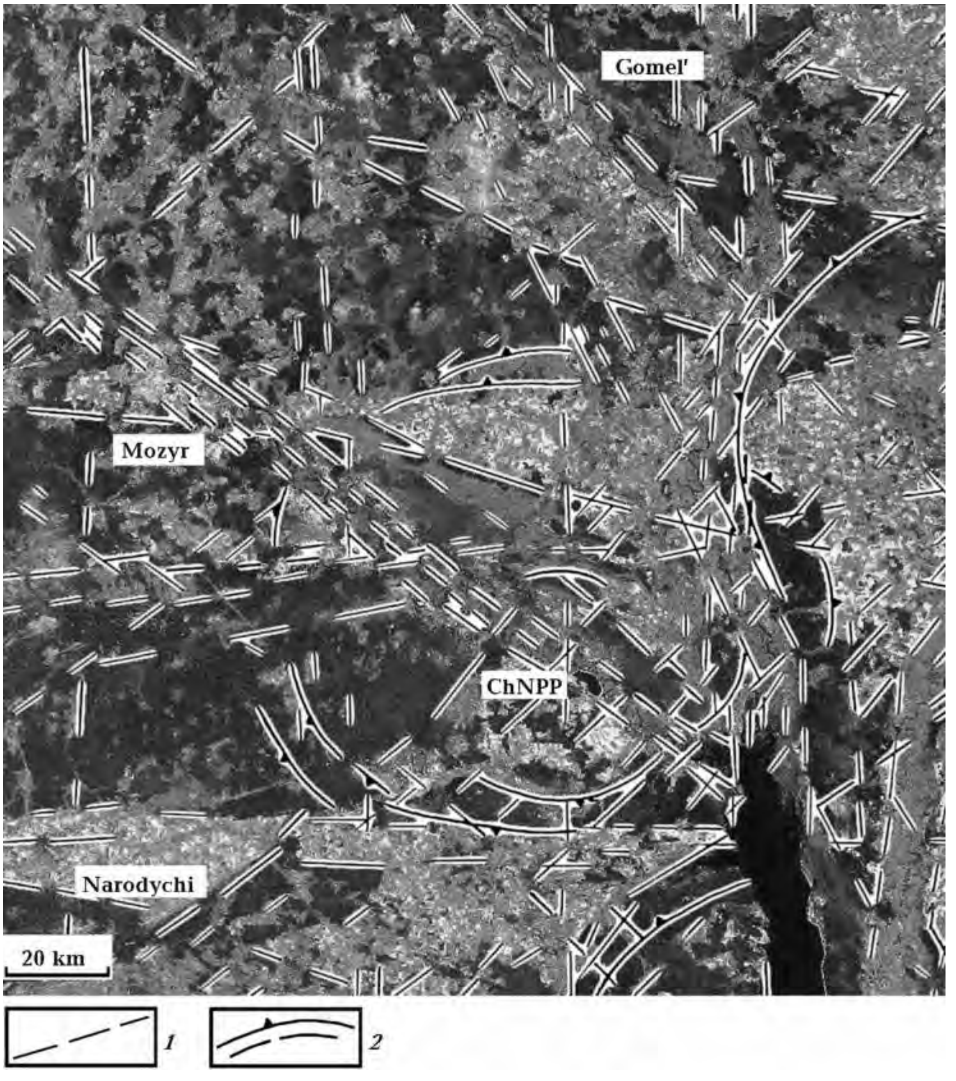


Fig. 1. General synthesized multiband space image LANDSAT MSS (07.09.1977) on the ChNPP Exclusion Zone territory and adjacent regions with elements of the regional structural decoding: *1* — lineaments and their zones depicting the fault-block frame of the crystalline basement and sedimentary cover, *2* — contours of ring-type and arc-type landscape elements conditioned of the presence of deep lithosphere structures.

ment zones. This gave possibility to refine the areas of anomalous geodynamic influence of fractures activated at the recent stage of the Earth's crust evolution.

In the course of direct study of the general structure of an elementary lineament field within studied the Tovstyi Lis site it was found that differently oriented separate elementary structural lines are grouped in lineaments and their zones, saturating and depicting their internal construction. They are grouped into regularly built systems of definite directions, mainly diagonal with prevailing azimuths from 40 to 50° (north-eastern), and 310° (north-western), and orthogonal ones directed with azimuth 0±5° (submeridional), and 270°±5° (sublatitudinal). These systems control each other by stretch and size. Practically each of them finds its orthogonal system, forming with it a dynamic pair, and one system from this pair prevails in its development. Within boundaries of the definite site the structural lines of definite direction dominate (Fig. 3). Linear elements correspond well by their directions to the main fracture systems of Ukraine revealed by different methods [Chebanenko, 1977]. The latter ones during the platform stage had been developing in correlation, forming the entire dynamic system of co-subordinated stably coupled fractures of diagonal and orthogonal orientations.

The above data enable to conclude that the majority of lineaments and their zones decoded from

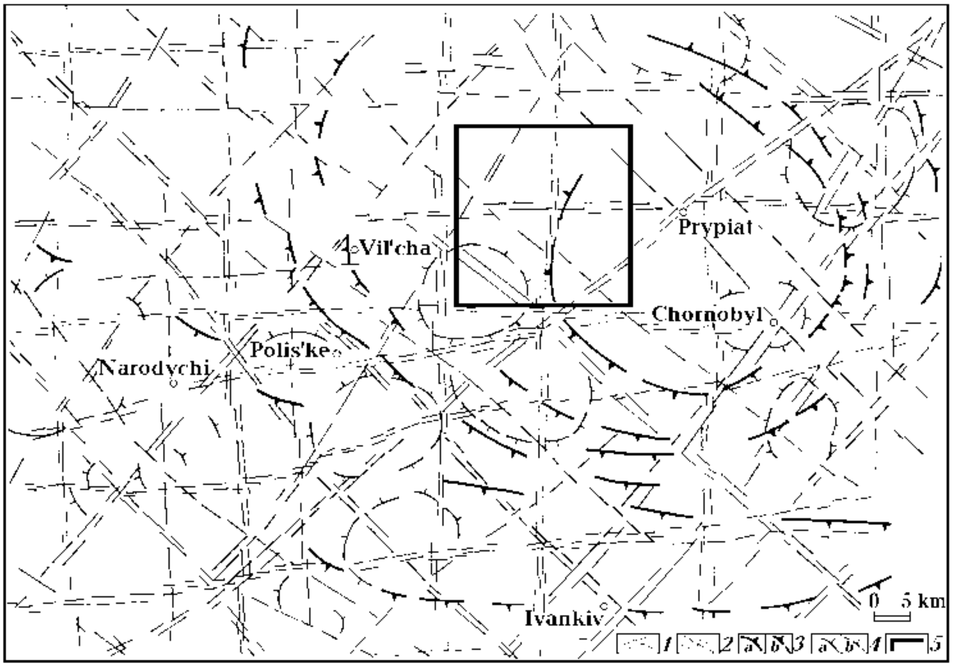


Fig. 2. Scheme of lineaments and ring-type structures of the Chornobyl NPP Exclusion Zone and adjacent region of the Korostensky crystalline massif (on the basis of the results of remote sensing data decoding): *1*, *2* — lineaments and their zones depicting the fault-block frame of the crystalline basement and sedimentary cover (*1* — confidently recognized, *2* — indefinitely recognized); *3* — contours of ring-type and arc-type landscape elements decoded on space images of high generalization level, depicting probably structures related with the under-crust magmatism (*a* — confidently recognized, *b* — indefinitely recognized); *4* — curvilinear landscape elements decoded on middle- and large-scale space images, depicting blocks of the crystalline basement activated at the recent tectogenesis stage (*a* — confidently recognized, *b* — indefinitely recognized); *5* — contour of the Tovstyi Lis site of detailed investigation.

the RSD come along the axes of discharge of stress-deformed rock state, that indicate a presence of the local disjunctive fractures or components of break structures of various lower-rank morphogenetic types developed in the Earth's crust within studied area. They represent the boundaries of main block fields within which the localization of anomalous geodynamic stresses takes place.

In the course of interpreting the neo- and recent geodynamical situation the known facts were taken into account [Chebanenko, 1977; Pavlinov, 1977; Geodynamic …, 1989] stating that during the tensile deformations the fractures are formed followed by faults, separations, rifts, combined shift-faults, and during the compressing stress deformations — by uplifts, joints, thrusts and coverings with combined forms of shift-uplifts and shift-thrusts.

Linear contraction zones within the Tovstyi Lis site are of significantly scarcer occurrence, or their distinguishing by aerospace decoding materials is difficult (see Fig. 3). This is obvious. Structures of this type are indicated mainly by additional relief forms, such as: rectified sections of water divides, erosion-denudation bodies, sandy ranges, etc., which are often distinguished in the aerosurvey data by the anomalous (lighter) image phototone. Sometimes fractures change their characteristic along their stretching direction from strain to contraction zones, that is evident from the interaction of stresses and location of axes of regional and local stresses in each particular tectonic block formed by the disjunction system.

According to morphological assessments, the majority of fracture deformations studied in more detail are represented in plane by typical shift faults (proper shifts and transformed fractures) related with horizontal movements of rock masses. This follows from the analysis of an internal structure of zones represented by bands of shingling longitudinal separate chips, and their spatial relation. The latter is most prominently seen in the regions of intersection nodes of these dislocations.

At the Tovstyi Lis site right shears prevail (except for zones 4—4, 5—5, 7—7, the south-eastern part of zone 6—6 and the submeridional zone without number located to south-east from Tovstyi Lis village). Some elongated shear dislocations in their stretch direction change their movement sign to the

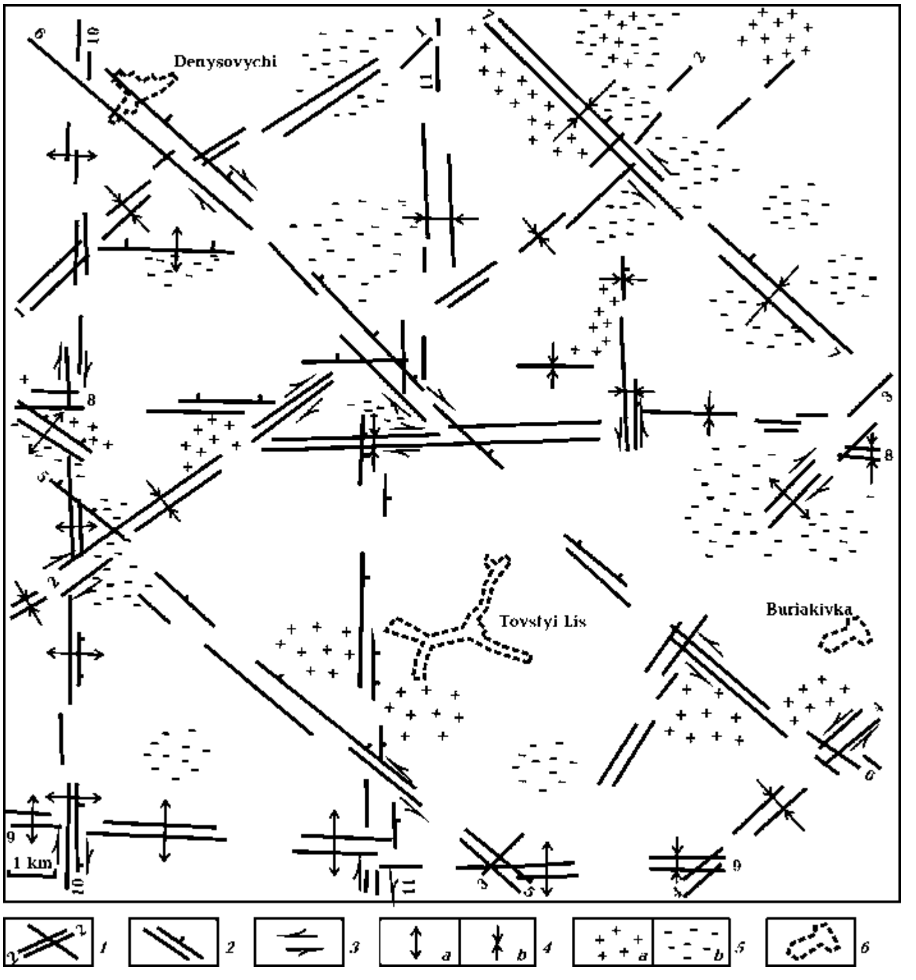


Fig. 3. Scheme of the fault-block structure of the Tovstyi Lis site with elements of the recent geodynamics (via results of remote sensing data decoding): *1* — lineaments and their zones depicting the fault-block framework of the crystalline basement and sedimentary cover; *2* — forecasted direction of descending of the disjunctive structures area; *3* — sections of revealed and forecasted fractures with the clearly distinguished shift component; *4* — forecasted linear zones of stretching (*a*) and contraction (*b*); *5* — local areas of stress (*a*) and strain (*b*) deformation development; *6* — settlement borders.

opposite (from left to right and vice versa). This is caused also by changing the active direction of shear stresses.

Hence, based on the tectonic-physical interpretation of available aerospace image decoding materials and geological-geophysical survey data, within the studied area the regularities of a systematic hierarchy of the fault-blocked structures are revealed. More detailed analysis of the distribution of different-directed deformations at the studied site enable to separate the local areas of predominant development of the strain and compression stresses which concentrate around the nodes of intersection of paragenetically related diagonal and orthogonal fractures (see Fig. 3).

Characteristic landscape elements of the local blocks areas subjected to compression forces are the positive relief forms (mainly water divides), increasing of the part of sandy litho-facies, etc. Characteristic for the areas of dominating development of the strain deformations are the negative relief forms manifesting in swamped areas, small lakes, reservoirs, homogeneously distributed microdepressions, suffusion forms, etc., determined by runoff-less character of surface waters. On the aerospace images they can be identified by presence of characteristic soil-geobotanic features manifesting themselves mainly by anomalous (darker) image phototone, as compared to neighboring areas.

Thus, considered aspects of RSD using are evidence of the high geologic unformativity of aerospace survey materials. Methodological techniques of RSD using can be employed efficiently for solving a whole number of the interiorusing problems.

References

Azimov O. T. Complex geological aerospace investigation of the Chornobyl estrangement zone and the adjacent Korosten' pluton region in the search for deep deposition of radioactive waste // Space Science and Technology. — 2002. — **8**, № 2/3. — P. 134—142 (in Ukrainian).

Azimov O. T. Investigation of the tectonic features of the Korostensky crystalline massif region and the ChNPP Exclusion Zone on the base of aero- and space images decoding with the purpose of promising sites selection for the RAW deep disposal // Sci. collection, Nat. Acad. of Mines of Ukraine. — **1**, № 12. — Dnepropetrovsk, 2001. — P. 284—289 (in Ukrainian).

Azimov O. T. Landscape geoindicators of the fractures' descriptions as the foundation of their investigation via remote sensing methods. 2. Geodynamic features of the disjunctive structures // Geoinformatics. — 2009. — № 2. — P. 71—79 (in Ukrainian).

Azimov O. T. Practical results of using the automated systems for remote sensing data processing during specification the block structure of the ChNPP Exclusion Zone territory (with connection of the problem of the radioactive waste disposal within its borders in deep boreholes) // Sci. collection, Ukrainian State Inst. for Geological Prosp. — Kiev, 2003. — № 1. — P. 78—86 (in Ukrainian).

Azimov O. T. Research of disjunctive dislocations in the Earth's crust with remote sensing methods (by the examples of some Ukraine's regions): Thesis in speciality 04.00.01 — General and Regional Geology // Inst. of Geological Sci., NAS of Ukraine. — Kiev, 2008. — 485 p. (in Ukrainian).

Azimov O. T. Results of the structural and geodynamic decoding of remote sensing data in connection with the problem of grounds most promising for the radioactive waste isolation // Intern. Conf. "Twenty Years after Chernobyl Accident. Future Outlook", (Kiev, Ukraine, April 24—26, 2006). — Kiev: Innovation Publ. Centre "HOLTEH", 2006. — P. 221—225.

Azimov O. T. The block structure scheme of the Tovstyi Lis site (the Korosten pluton) with elements of the modern dynamics by the results of decoding of remote sensing data // Rep. of the Nat. Acad. Sci. of Ukraine. — 2004. — № 10. — P. 114—119 (in Ukrainian).

Chebanenko I. I. Theoretical aspects of the Earth's crust tectonic divisibility (Ukraine as an example). — Kiev: Nauk. dumka, 1977. — 84 p. (in Russian).

Geodynamic reconstructions: (Methodical supply for regional geological investigation) / Ed. V. A. Unksov. — Leningrad: Nedra, 1989. — 278 p. (in Russian).

Geological disposal of radioactive weste in Ukraine (Problems and solutoins) / Ed. V. M. Shestopalov — Kiev: Radioecol. Center, Nat. Acad. Sci. of Ukraine, 2006. — 398 p. (in Russian).

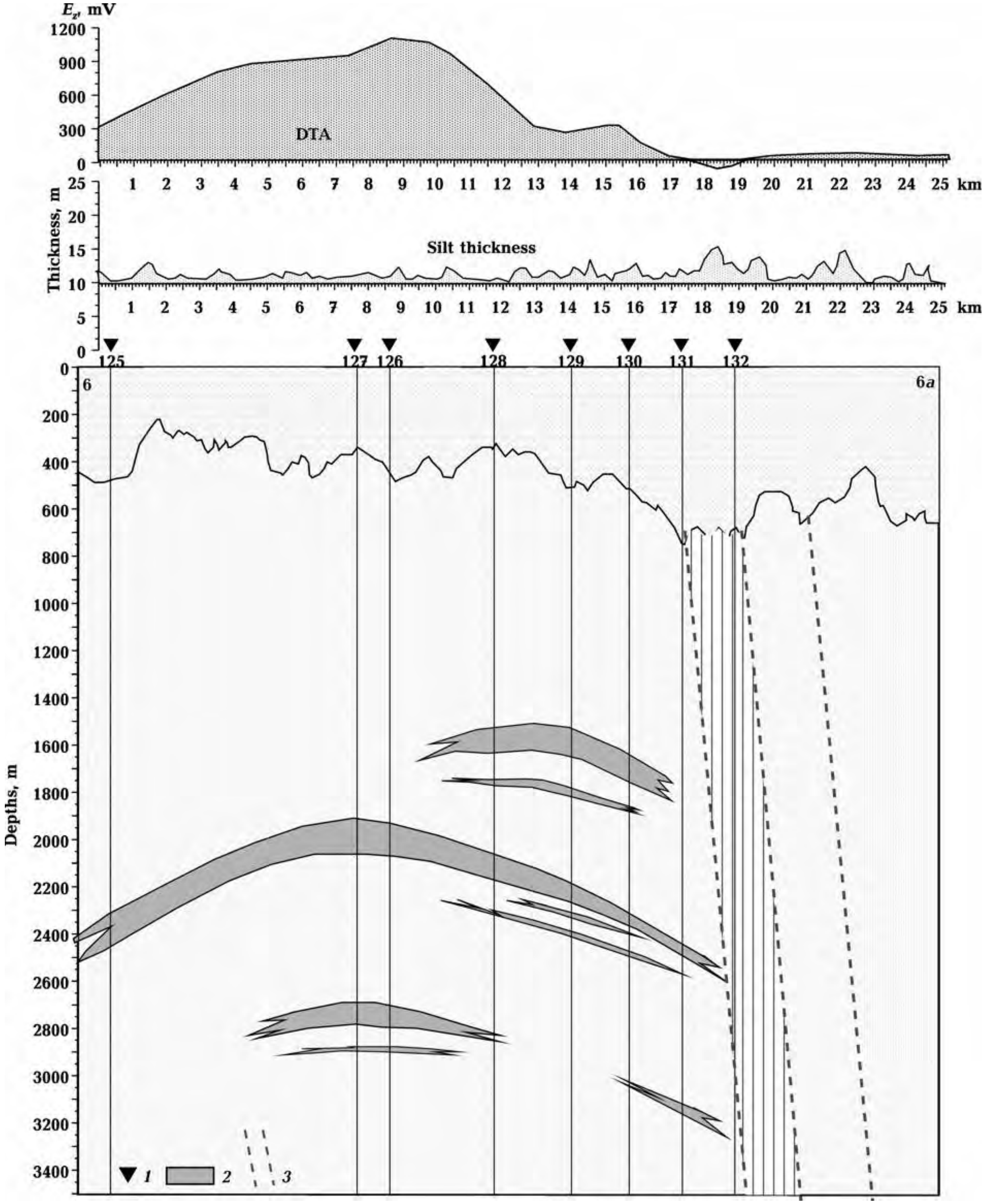
Pavlinov V. N. Deep landslides and disjunctive structures paragenicly connected with them. Article I // Proc. of Inst. of Higher Education. Geology and Prospecting. — 1977. — № 8. — P. 3—14 (in Russian).

Drake Passage: crustal structure, tectonic evolution and new prognosis for local HC accumulations along the Antarctic Peninsula margin

© ***V. Bakhmutov*[1], *V. Solovyov*[1], *I. Korchagin*[1], *S. Levashov*[2], *N. Yakymchuk*[2], *D. Bozhezha*[2], 2010**

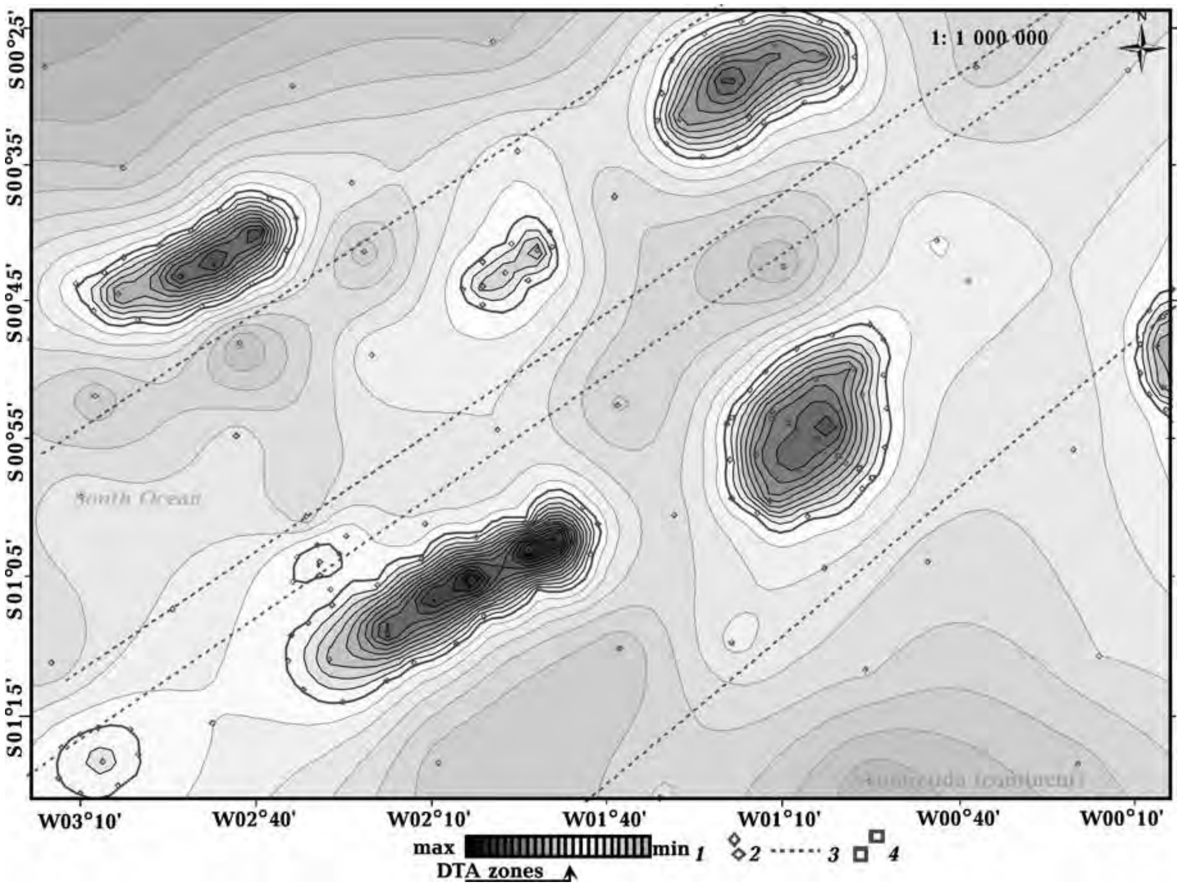
[1]Institute of Geophysics, National Academy of Sciences of Ukraine, Kiev, Ukraine
bakhm@igph.kiev.ua
[2]Institute of the Applied Problems of Ecology, Geophysics and Geochemistry, National Academy of Sciences of Ukraine, Kiev, Ukraine
yakymchuk@karbon.com.ua
bozhezha@gmail.com

New geological and geophysical data that have been obtained during last years for bottom structures of West Antarctica are of particular importance for evolution and geodynamics processes of this region understanding. The 2004 (9^{th}) and 2006 (11^{th}) Ukrainian Antarctic expeditions acquired new geo-



a

The VERS sounding data and geoelectric anomalous zone of the “hydrocarbon deposit” type in the Antarctic Peninsula region (*a*): *1* — the sounding points; *2* — anomalous polarized layers of “hydrocarbon deposit” type; *3* — tectonic fracture zone. Map of anomalous zones of «oil deposit” type in the Antarctic region (relative coordinates, near Ukrainian Antarctic Station «Academician Vernadsky»), allocated by the satellite data special processing and interpretation results (*b*): *1* — the scale of the anomalous response intensity; *2* — points of the anomalous response values determination; *3* — predicted tectonic fractures; *4* — points of «deposit» type anomalies by geoelectric methods FSPEF and VERS.



b

electrical data ('short-impulse electromagnetic field formation' — FSPEF, and 'vertical electric-resonance sounding' — VERS) along profiles across Drake Passage with the aim of studying the crustal structure down to depths of >30 km. Obtained crustal inhomogeneities could be connected with some evolution stages of tectonic and magmatic processes at this region — the fluid regime, tectonic disturbances and crush zones in basement and local places of submarine volcanic activity too [Levashov et al., 2006; Drake …, 2007]. Analysis has been provided new data of the sedimentary horizons deep structure and Moho crust-mantle discontinuity of Drake Passage. Beneath the Drake Passage, Moho is interpreted at shallow depths of 8—12 km and more. Both Moho and the deeper layer show strong variations in depth and thickness in the vicinity of the Shackleton Fracture Zone (SFZ). It's forming was connected with episodes of Drake Passage opening, which led to the final separation of the South America and Antarctic continents. The trough system near this zone was formed when stress field regime was extensional and local rifting and spreading processes had been developed. SFZ is characterized by thickened oceanic crust, deformed by deep local faults, which cut across layers 2 and 3 of the oceanic crust.

The gravity models show in detail the deep structure of the fracture zone and suggest that crustal thickness remains approximately constant along SFZ, whereas central valley of rifted West Scotia Ridge shows crustal thinning. Obtained results assure the no Table role of continental fragments (extending from the northwestern Antarctic Peninsula towards the Pacific margin of the south-western top of South America) in crustal structural transformations and rifting processes at the central part of Drake Passage. As oil and gas exploration activities are focused along continental margins, where fragmenting and presumably petroleum deposit formation has taken place, the FSPEF and VERS geoelectric methods were used also in Antarctic expeditions for the hydrocarbon (HC) resources prospecting along the Antarctic Peninsula margin. During the expedition one «deposit» type anomaly was mapped by FSPEF survey in area not far from the Ukrainian Antarctic Station «Academician Vernadsky» [Drake …, 2007]. Some anomalous polarized layers of «oil deposit» type were mapped by VERS sounding in depth interval up to 3500 m. (Figure, *a*).

The special method of satellite data processing and interpretation for this anomaly region was applied. Four relatively large anomalous zones of «oil deposit» type were identified and mapped within the surveyed segment of the Antarctic Peninsula margin. The mapped (during 2006 expedition) geoelectric anomaly of «oil deposit» type completely falls into one of the anomalous zones that were selected by satellite data (Figure, *b*).

The multi-channel seismic data acquired on the South Shetland margin [Jin et al., 2003] show that Bottom Simulating Reflectors (BSRs) are widespread in the area, implying large volumes of gas hydrates. Satellite data over the site of BSR zones extension, identified by seismic studies, have been processed and interpreted. The various processing parameters were analyzed during investigation that allowed revealing and mapping the anomalous zone of «gas hydrates deposit» type within this region. In general, the revealed and mapped anomalous zone of «gas hydrates deposit» type satisfactorily correlate with BSRs zones, defined by seismic data. The anomalous zones of «gas deposit» and «oil deposit» type were not detected there by the satellite data processing and interpretation results.

Conclusions. New data about geodynamics and Drake Passage earth's crust structure have demonstrated high efficiency of the VERS method using. New prognosis for local HC accumulations along the Antarctic Peninsula margin confirms the high oil and gas potential perspectives of the Antarctic Peninsula region.

References

Jin Y. K., Lee M. W., Kim Y., Nam S. H., Kim K. J. Gas hydrate volume estimations on the South Shetland continental margin, Antarctic Peninsula // Antarctic Sci. — 2003. — **15**, № 2. — P. 271—282. — DOI: 10.1017/S0954102003001275.

Levashov S. P., Bakhmutov V. G., Korchagin I. N., Pischaniy Yu. M., Yakymchuk N. A. Geoelectric investigations during the seasonal work of 11th Ukrainian Antarctic expedition // Geoinformatika. — 2006. — № 2. — P. 24—33 (in Russian).

Levashov S. P., Yakymchuk N. A., Korchagin I. N., Bakhmutov V. G., Solovyov V. D., Bozhezha D. N. Drake Passage and Bransfield Strait — new geophysical data and modelling of the crustal structure, in Antarctica // A Keystone in a Changing World — Online Proc. of the 10th ISAES X. — USGS Open-File Report. — 2007. — P. 1047.

Numerical modeling of cloud and precipitation evolution and its connection with entropy

© ***T. Belyi*[1], *A. Pirnach*[2], 2010**

[1]Institute of Geophysics, National Academy of Sciences of Ukraine, Kiev, Ukraine
tbelyi@mail.ru
[2]Ukrainian Hydrometeorological Institute, Kiev, Ukraine
hanna@uhmi.org.ua

A recent work devoted to sources of entropy connected with mesoscale frontal cloudiness. Three-dimensional nowacasting and forecasting numerical models developed in UHRI [Pirnach, 1998; 2008; Belyi et al., 2009] for modeling of the winter and summer frontal cloud systems were adapted for theoretical interpretation of the investigated phenomena.

The integration of full thermodynamic equations, which included equations for air motion, water vapor content, temperature transfer, the continuity and thermodynamic state equations are used in these models. Cloud microphysics is considered explicitly by solving the kinetic equations for the droplet and crystal size distribution. The size distribution function of the cloud and precipitation particles is formed due to cloud condensation nucleation, ice nucleation, growth (evaporation) by deposition, and freezing, riming, collection by raindrops of cloud drops. Droplet and ice nucleation is accounted by parameterization in the model. Cartesian coordinates (x, y, z) and terrain-following sigma coordinates ξ, η, ζ have been used. In second case the system of equation will be described as follows:

$$\frac{dS_i}{dt} = F_i + \Delta S_i \,, \qquad (1)$$

$$\frac{\partial \rho u}{\partial \xi}+\frac{\partial \rho v}{\partial \eta}+\frac{\partial \rho w}{\partial \zeta}=0\,,$$

$$\rho=\frac{p}{RT}\,,$$

$$S_i=\left(u,v,w,T,q,\,f_k\right),$$

$$i=1,2,...,8\,;\;k=1,2,3\,,$$

u, v, w are components of wind velocity across ζ, η, ζ axis, which are directed on east, north and perpendicular to the ground surface respectively. F_i are describes separate physical processes: F_1—F_3 presented right parts of wind velocity projections, which included Carioles parameter, free-fall acceleration, pressure gradients and etc.; F_4—F_5 describe heat and moisture fluxes; F_6—F_8 represent processes of droplets and crystal nucleation, cloud and precipitation particles falling velocities, their transfer, condensation and coagulation processes etc; ΔS_i is turbulent transfer; p and ρ are pressure and density; T is temperature; q is specific humidity; f_k are cloud particle size distribution functions.

A splitting method had been used for sintegration of the system (1). The solution scheme was described as follows:

$$\frac{\partial S_i}{\partial t}=\sum_{n=1}^{6}F_{in}\,,\;\;n=1,2,...,6\,;\;i=1,2,...,8\,.$$

System (5) to split up on 6 equations as follows:

$$\frac{\partial S_{in}}{\partial t}=F_{in}\,,\;\;n=1,2,...,6\,.$$

F_{i1} presented the advection, convection and turbulent transfer; F_{i2} included the pressure gradients; F_{i3} included Carioles acceleration; F_{i4} described a vertical motion solution schemes; F_{i5} presented condensation processes; F_{i6} included coagulation solution schemes.

Entropy S calculated by relationship [Khrgian, 1969]:

$$S=C_p\ln\theta+\mathrm{const}\,,$$

θ is potential temperature, C_p is specific heat capacity at the constant pressure.

Production of entropy calculated by relationship as follows:

$$\frac{dS}{dt}=\frac{d\theta}{dt}\frac{C_p}{\theta}\,.$$

Numerical simulation of atmospheric phenomena connected with atmospheric fronts and their cloud systems that caused the damages events have been fulfilled for several synoptic situations observed in steppe part and mountain regions of Ukraine. Diagnostic and forecast models have been constructed for mesoscale cloud formations followed by high floods in Carpathian region. Numerical experiments are carried out with aim to determine the role of various dynamics and microphisics parameters in formation of strong and catastrophic precipitation. Series of numerical experiments have been carried out with aim to research the key parameters caused features of development of dangerous events and their activity. Special numerical experiments have been carried out with a main goal to research the temporal and spatial distribution of entropy and its production. Numerical study interaction between entropy and cloud and precipitation had been carried out.

It is found, the unlimited growth of water and ice supersaturation is possible if mechanisms of cloud precipitation formation are insufficiently effective for precipitating of whole moisture. In turn, it can cause intensive activation of cloud condensation nuclei and unlimited growth of large drops as well. Therefore the unlimited growth of precipitation intensities may occur.

Some key parameters, meteorological conditions and predictors caused the occurrence of dangerous phenomena were defined. The main features of strong precipitation have been noted as follows: interaction of flows of different physical nature coming from opposite directions; presence of ice supersaturation layers; strong vortical motions in single air mass advanced to mountain ridge; chimney clouds with ice tops and cirrus clouds above; high tropopause achieved 10 km and more, strong ascending and compensative descending motions; the necessary combination of precipitation-forming mechanisms.

Coupling modeling of evolution entropy and precipitation found their perfect agreement. Regions of the low entropy coincided with regions of heavy precipitation. Regions with high entropy located in cloudless space. Regions of the low entropy can to be good predictors of heavy precipitation with a high confidence probability.

References

Belyi T. A., Dudar C. M., Pirnach G. M. Numerical investigation effect on evolution of mesoscale cloud clusters of different mechanisms of cloud and precipitation formation caused heavy precipitation in Car-

patian in 2008 during July 21—29 // Geophys. J. — 2009. — **31**, № 6. — P. 107—123 (in Russian).

Khrgian A. Kh. Atmospheric physics. — Leningrad: Hydrometeoisdat, 1969. — 647 p. (in Russian).

Pirnach A. M. Numerical modeling of clouds and precipitation in atmospheric frontal systems. — Kiev: Nika-Center, 2008. — 294 p.

Pirnach A. M. The construction and application of numerical models to the study of cloud dynamics and the structure of winter frontal rainbands // J. Atmospher. Res. — 1998. — **45**—**47**. — P. 356—376.

The effect of variable viscosity in the Earth's mantle on the stress field of the mantle and an overlying continent, moving self-consistently due to mantle flow

© ***A. Bobrov, A. Baranov, 2010***

Laboratory of Theoretical Geodynamics, Institute of Physics of the Earth, RAS, Moscow, Russia
bobrov@ifz.ru
baranov@ifz.ru

In numerical two-dimensional experiments we investigate the spatial field of stresses in the mantle and continent and its evolution. A continent moves self-consistently with changing mantle flows. Velocity of a continent in the process of movement varies in accordance with time-dependent forces which act from underlying viscous mantle as well as with mantle forces acting on the end faces of continent. This model is described in [Bobrov, Trubitsyn, 2008]. Continent viscosity is equal to 1e5 with respect to average viscosity of the mantle. For convection modeling we used Citcom code with high Rayleigh numbers, strong viscosity variations and active markers for simulating continent [Moresi, Gurnis, 1996]. We consider three model laws for viscosity: isoviscous mantle case; *P*,*T*-dependent viscosity case and viscosity=*f*(*P*, *T*, stress_ invariant). For these three models we analyze how a form of viscosity.

law can change stress fields in the mantle and continent. We research what model law gives the results more close to actual data. The horizontal stress field in moving continent greatly depends on variations of horizontal velocity in the underlying mantle, and also on continent position between the ascending and descending mantle streams. Sub-continental upwelling mantle flows have the extensive effect; sub-continental downwelling ones- the compressive effect. Mantle plumes near continent's borders demonstrate compressive effect on continent, downwelling flows produce its extension. If the horizontal stresses are presented in dimensionless form then our cases show rather big but not principal differences. Thus, the mantle model with constant viscosity can be regarded as qualitatively representative. However, after transition to dimensional parameters it appears, that in isoviscous mantle model stresses values bigger in several times, than in the cases of variable viscosity. In this case isoviscous mantle model leads to strongly overestimated stresses and is not representative in this aspect. Mantle model with variable viscosity has typical horizontal stress values in the major portion of mantle — (2÷6) MPa; in continent at different stages of its movement — (2÷15) MPa.

It should be noted that all examined models should give approximately equal Nusselt number (i. e., should have the same efficiency of bearing-out of heat, as surface heat flow is the observational value). For this reason, the values of the adopted Rayleigh number Ra, in all computations, were different.

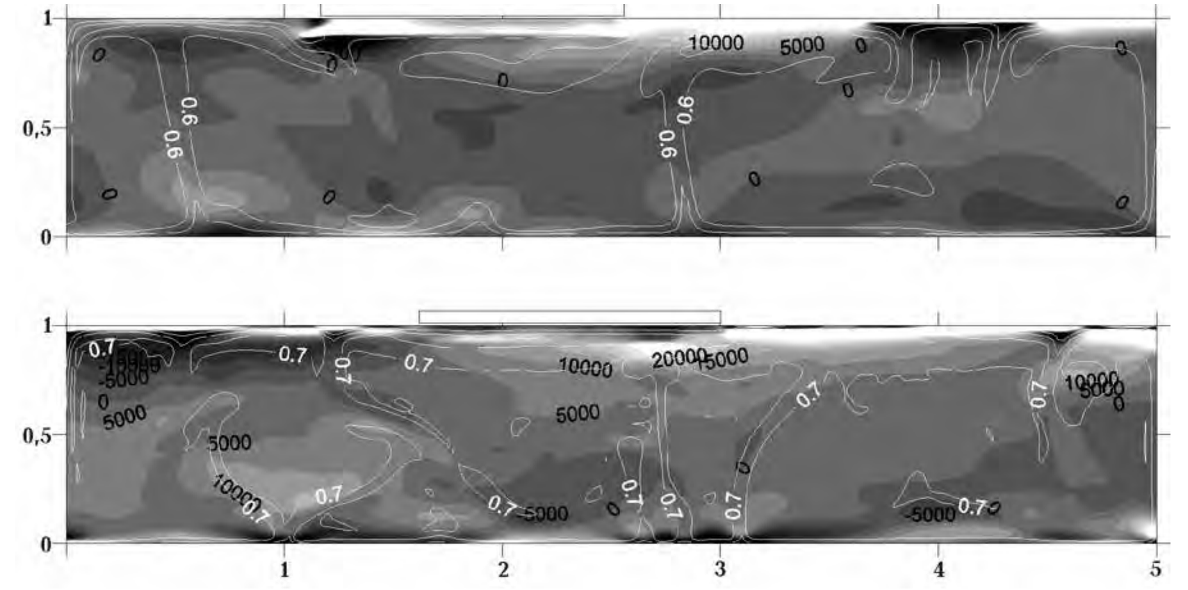
Figure presents a comparison of temperature and stress fields for the isoviscous mantle case and for the variable viscosity case. All values are given in dimensionless form. This comparison allows identification of a number of interesting effects.

Results. The models in this work are simplified in several aspects. However our purpose was to reveal only the main features and patterns of the process of mantle flow in the presence of floating continental material. From the numerical results, the following conclusions can be derived.

1. The distribution of horizontal stress in a moving continent over a viscous mantle greatly depends

on the spatial variations of mantle velocities in the subcontinental mantle and also on continent position between the ascending and descending mantle streams at the given moment. Subcontinental upgoing currents have an extensive effect on the continent, while subcontinental downgoing ones a compressive effect. On the contrary, suboceanic upgoing mantle plumes near continent's borders result in compressive actions on the continent, while downwellings result in its extension.

2. If the horizontal stresses are expressed in non-dimensional units for the three cases considered here (constant and variable viscosity), they show considerable, but not fundamental differences (Figure). It should be noted that the stress values in the case of variable viscosity are higher.



Dimensionless horizontal stress fields $\sigma_{xx}(x, z)$ for isoviscous model (upper panel) and *P,T*-dependent viscosity model (lower panel). Light grey depicts positive values, dark grey — negative values. The stresses $\sigma_{xx}(x, z)$ are determined by the relation $\sigma_{xx}(x,z)= p(x, z)-2\partial v_x(x, z)/\partial x$, i. e., compressive stresses are considered to be positive. White isolines show the non-dimensional temperature field. The position of the continent is shown with a rectangle on the upper surface.

3. Transition to dimensional stresses (that is, to the stresses measured in MPa or bars) shows that for the isoviscous model the stress values are significantly higher than in the case of variable viscosity. This arises from the imposed condition of equality of the surface heat flow in both models. If we would not equalize the models by heat flow, but simply calculate them using the same Rayleigh number — that is, with the same intensity of convection — then we wouldn't have such significant difference. However, the difference in Rayleigh number values (namely, for account of increasing of viscosity in isoviscous model) leads to a difference of dimensional stresses. As a result, the isoviscous mantle model leads to overestimated dimensional stresses. This model, however, is necessary for comparison, as it allows to evaluate the effect of the variable viscosity on the final results.

4. For the considered model of variable mantle viscosity the following typical horizontal stress values are found: for the largest part of the mantle values between 2 to 5 MPa (that is 20—50 bars); in continent at different stages of its movement and in different areas 2—10 MPa, depending on the impact of the mantle these stresses may be compressive or tensile.

References

Moresi L. N., Gurnis M. Constraints on the lateral strength of slabs from three-dimensional dynamic flow models // Earth Planet. Sci. Lett. — 1996. — **138**. — P. 15—28.

Bobrov A. M., Trubitsyn A. P. Numerical model of the supercontinental cycle stages: integral transfer of the oceanic crust material and mantle viscous shear stresses // Stud. Geophys. Geod. — 2008. — **52**. — P. 87—100.

First instrumental recognition of the Earth eigenmodes in radio frequency electromagnetic radiation

© Yu. Bogdanov[1], A. Kvasnyuk[2], V. Kobolev[1], N. Loyko[3], O. Rusakov[1], V. Pavlovych[2], V. Shuman[1], 2010

[1]Institute of Geophysics, National Academy of Sciences of Ukraine, Kiev, Ukraine
[2]Institute for Nuclear Research, National Academy of Sciences of Ukraine, Kiev, Ukraine
[3] "Yug-neftegeologia" Ltd, Kiev, Ukraine

At present time eigenmodes of the Earth and earthquakes-related long period oscillations are reliably registered by seismic and gravitational methods. A special term has been put forward for the definition of such oscillations, namely seismic — gravitational oscillations of the Earth [Linkov et al., 1989]. There have been determined the structure of oscillations spectrum with periods above one hour and delineated the regions of the most intensive Earth oscillations.

A new relevant geodynamic conception has been developed in the past several years. It states that "the mechanism of forced cyclic relative build-up and wandering of the Earth's core and mantle over the geological periods of time is a single and main mechanism controlling the plate tectonic and plume tectonic activity of the Earth" [Barkin, 2002; Barkin, Vilke, 2004]. The periods of free oscillations of the dynamic system (the elastic mantle — Earth's core) have been revealed to be as 3.47, 4.06 and 4.89 hours. An analysis of different experimental observations has demonstrated that the variations with periods from 1.497 to 24 hours are characteristic of all planetary processes.

New methods and technologies are employed to examine long period waves, with these methods being particularly based on the use of natural electromagnetic emission of the Earth. The present study is aimed at detecting some regularities of the Earth oscillations processes in the spectrum of the Earth's electromagnetic radiation (EMR). Experimental observations have been performed to reveal EMP oscillations frequencies already registered by seismic — gravitational methods and to finding new harmonics of oscillations. They have been carried out on the Ukrainian Antarctic Station (ö= 64º15?S, ë= 65º15′W) and at 3 sites in Ukraine (φ=50ºN, λ=35º51′E; φ=44º51′N, λ=34º58′E; φ=44º35′N, λ=33º39′E) during 2004—2009.

A three component EMR detector has been used to measure 1—100 Hz frequencies (at a level of 3dB) in a dynamic range of 1—20 nT. A quantity of pulses has been registered in time (*N*) unit exceeding the specified threshold. It is proportional to root-mean-square value of carrier frequency.

A method for revealing latent periodicity and Wavelet — analysis have been applied to mathematical processing, interpretation and visualization of results. An analysis of graphs from four stations demonstrates that the strong negative correlation is observed in some vicinity of characteristic frequencies of 0.15, 0.20, 0.21, 0.28, 0.2 MHz in periods from 10 to 90 min. The full spectrum of EMR oscillations from Antarctica and in Ukraine contains sufficient frequencies. Their analysis exhibits that the properties of a signal in the interval of 0— 250 min, including its frequency characteristic and duration, correspond to seismic-gravitational multiplets and to natural oscillations of the inner Earth's core with a period of about 200 min.

The periods have been also registered to be needed for explanation, for example, the Shuler period of 84.4 min. The oscillations with the Shuler period are expressed more intensively in Antarctica than in the middle latitudes of Ukraine. In Figure the time series data cover 1440 min, i. e. one day. The graphs of Wavelet decomposition are situated for Antarctica and Ukrainian on the right and left of the Figure respectively. The following periods of oscillations are observed: the eigenmodes of the core with the basic oscillations of ~14 hour (the 2^{th} row of the graphs), the oscillations with a period of ~5 hour (the 3^{th} row of the graphs), the variations in the synodic month duration, the oscillations of the inner core with a period of~3 hour 18 min (the 4^{th} row of the graphs), the Shuler period ~84 min (the 5^{th} row of the graphs). According to Petrova the oscillations with periods of 78 min (the 6^{th} row of the graphs), 67 min (the 7^{th} row of the graphs), and 54 min (the 8^{th} row of the graphs) are main harmonics reliably registered in Ukraine. On the contrary, the amplitudes of these oscillations are negligible in Antarctica.

The above results indicate the existence of both inner and cosmic sources of oscillation processes in the Earth. The indicator of these global processes is background electromagnetic radiation. The paradigm of originating electromagnetic oscillations in the Earth implies that any eigenmodes of planet oscillations leads to change in the Earth deformation mode resulting in the generation of EMR. All frequencies of the mechanical eigenmodes in the Earth must be revealed in spectrum of electromagnetic radiation. Based on observations of Earth electromagnetic variations in Antarctica and Ukraine, it has been established that not only generally acknowledged seismic-gravitational oscillations but all planetary processes must additionally oscillate with periods of an hour range, for example, the Shuler period ($T \approx 84$ min), and with different daily periods from 14 days to 28 days which are not shown in the Figure).

In conclusion, for the first time our instrumental observations have recognized the frequencies of the Earth mechanical eigenmodes in the spectrum of its background electromagnetic radiation.

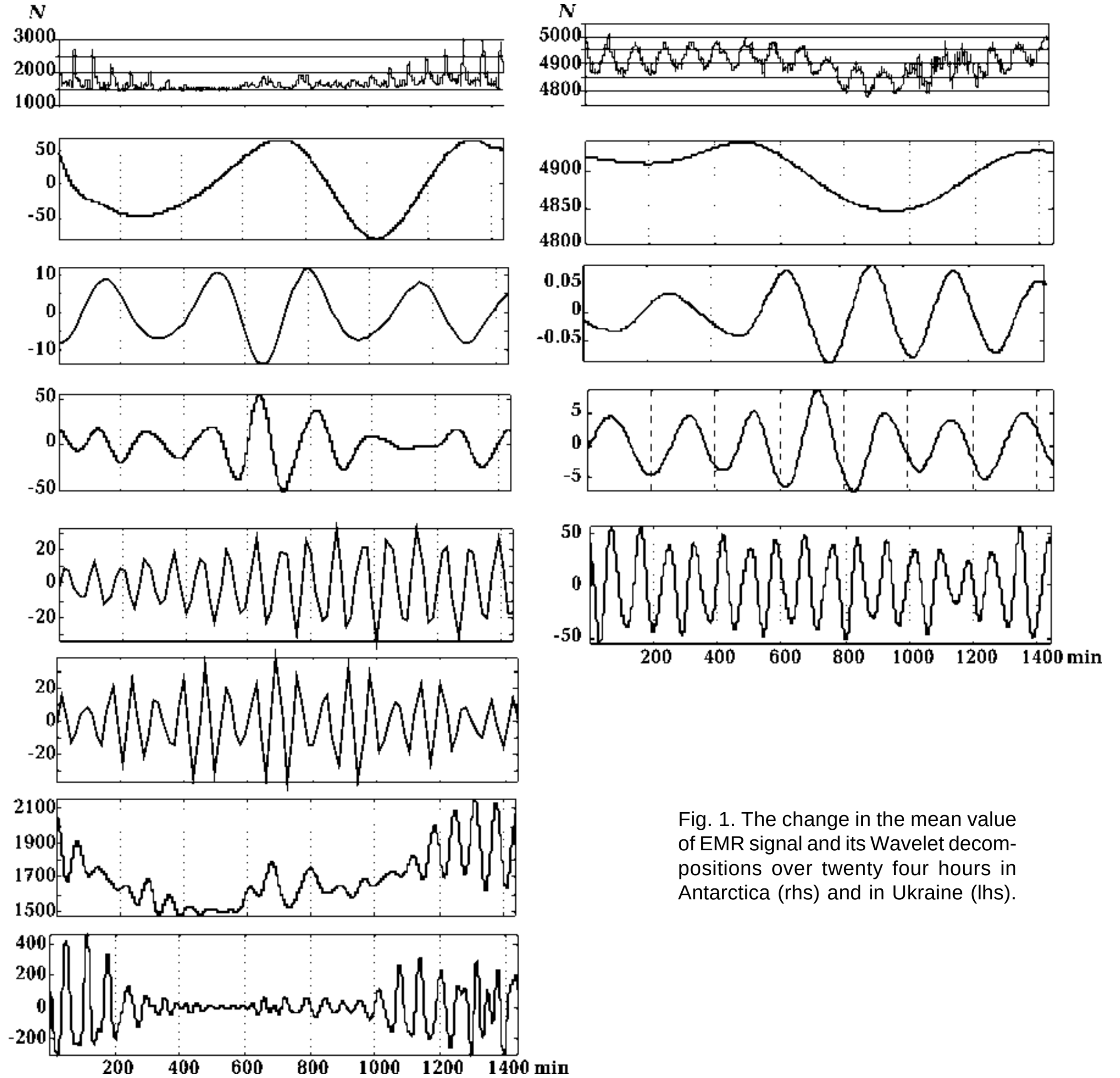


Fig. 1. The change in the mean value of EMR signal and its Wavelet decompositions over twenty four hours in Antarctica (rhs) and in Ukraine (lhs).

References

Linkov E. M., Petrova K. M., Zuroshvili D. D. Sesmic-gravitational oscillations of the Earth and related with them perturbations of the atmosphere // Dok. AN SSSR. — 1989. — **306**, № 2. — P. 314—317 (in Russian).

Barkin Yu. V. The explanation of the endogenous activity of the planets and satellites: the mechanism of its cyclicity // Izv.of RAEN. Earth science section. — 2002. — № 9. — P. 45—97 (in Russian).

Barkin Yu., Vilke V. G. Celestial Mechanics of Planet Shells // Astronom. Astrophys. Transactions. — 2004. — **23**, № 6. — P. 533—553.

The exotic Volgo-Uralia: circular-and-linear structures of the crystalline crust defined by Paleoproterozoic mantle upwelling

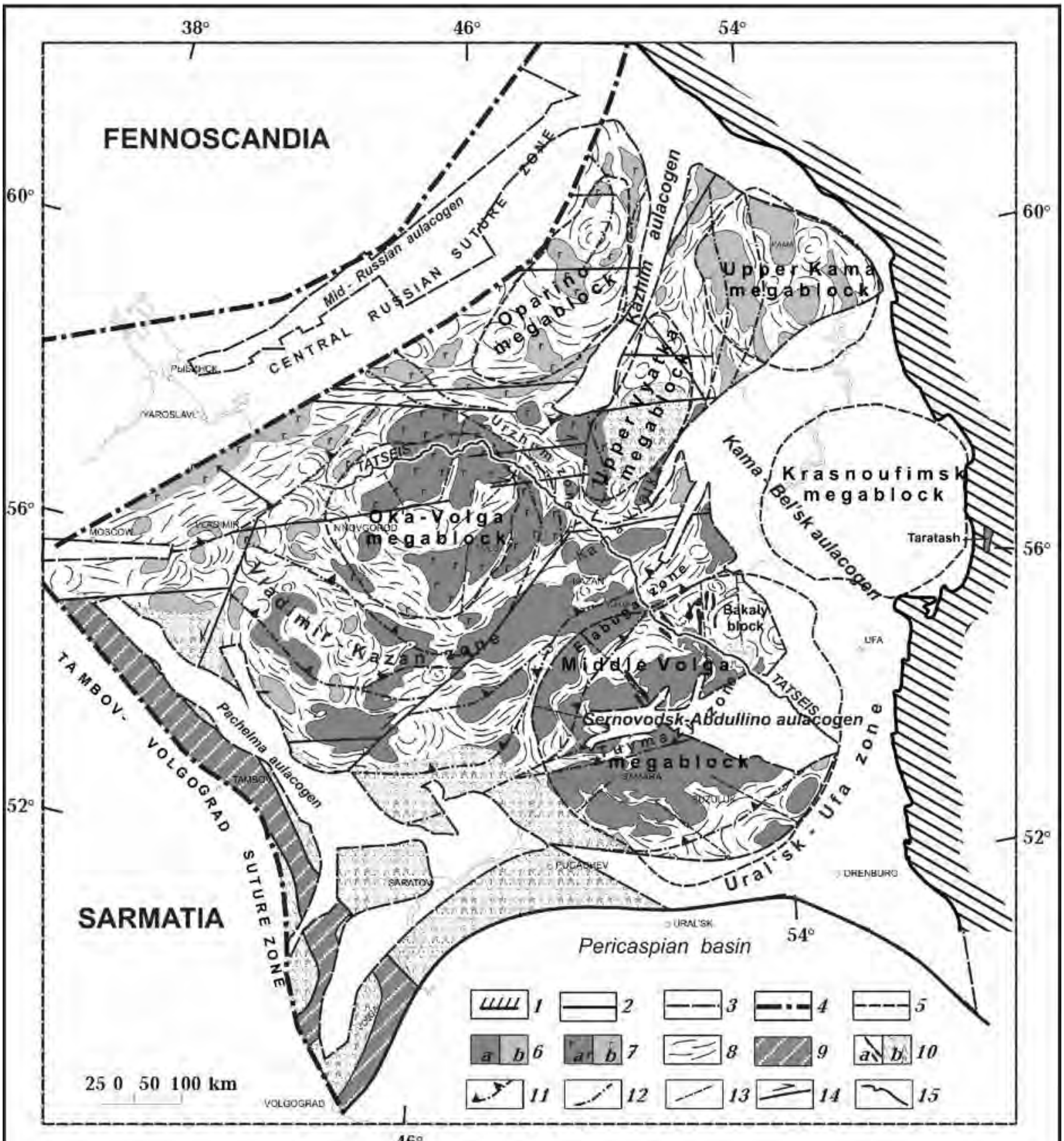
© **S. Bogdanova[1], A. Postnikov[2], V. Trofimov[3], 2010**

[1]Department of Earth' and Ecosystems, Lund University, Sweden
Svetlana.Bogdanova@geol.lu.se
[2]Department of Lithology, Gubkin State University of Oil and Gas, Moscow, Russia
apostnikov@mtu-net.ru
[3]Insitute of Geology and Development of Fossil Fuels (IGIRGI), Moscow, Russia
vatgeo@yandex.ru

The crystalline crust of Volgo-Uralia, one of the major crustal segments of the East European Craton, is buried beneath a Phanerozoic, mostly Devonian to Triassic, sedimentary cover and underlying 2 to 10 km thick Meso- to Neoproterozoic sedimentary deposits intercalated with rare volcanics. The only exposed parts of the crystalline basement are isolated small blocks involved in the adjacent Paleozoic Uralides belt (Figure). Knowledge of the basement is therefore founded on geophysical data and drill cores alone. These are particularly numerous due to the high oil and gas potential of the region. Twenty drillings reach down into the crystalline crust for distances between 100 and 1000 m, some others even penetrating three kilometres and more. This provides valuable information on rock relationships and abundances [Bogdanova, 1986; The Crystalline …, 1996; Postnikov, 2002].

Essentially, Volgo-Uralia is a high-grade terrain composed of granulite- and amphibolite-facies supracrustal and plutonic rocks both Archean and Paleoproterozoic in age. It features several megablocks with more or less circular, "mosaic" patterns of magnetic and gravity anomalies, separated by belts of linear anomalies (see Figure). Previously, the megablocks were assumed to represent stable massifs of Archean crust, while the intervening zones of linear anomalies were interpreted as Paleoproterozoic ("Svecokarelian") fold belts [Goodwin, 1991; International …, 1979]. This view was challenged by the idea that the circular anomaly patterns of the megablocks had been caused by the doming of strongly stacked Archean crust during the Paleoproterozoic [Bogdanova, 1986]. That could explain why intense Paleoproterozoic structural and metamorphic reworking of the Archean crust follows the circular geophysical patterns of the megablocks and the distribution of Paleoproterozoic metasedimentary cover within these megablocks. In this model, the zones of linear anomalies, i.e. the former "Svecokarelian fold belts", are interdomal areas less affected by Paleoproterozoic reworking. Recently, such a picture has been corroborated by the "TATSEIS" seismic reflection profiling, which transected both megablocks and linear zones in central Volgo-Uralia [Trofimov, 2006]. This profiling revealed an up-doming mantle and the lower crust beneath the Oka-Volga megablock and the presence of an associated, up to 10 km thick highly metamorphosed volcano-sedimentary sequence atop its Neoarchean crust. As different from the Oka-Volga megablock, the Middle Volga megablock has Paleoproterozoic deposits within mostly troughs along the radial faults of the domal structure, and within small cover remains elsewhere. The deposition of the Paleoproterozoic cover must have taken place before 2,4—2,1 Ga, which is the age of the cutting granitoid intrusions and the metamorphism. Subsequently, both metamorphism of the cover rocks and granitoid magmatism continued episodically until 1,90—1,85 Ga. K-Ar ages of amphibole and biotite show several tectonothermal events by 1,65 Ga, when the Neoarchean fault zones were reactivated.

The Paleoproterozoic tectonics in Volgo-Uralia may suggest mantle-plume geodynamics, most probably related to the rifting of the Archean crust between 2,5 and 2,0 Ga, i. e. during a period of rifting well known from the Fennoscandian, Laurentian and other Precambrian cratons. However, the large sizes of the Volgo-Uralian "dome-and-basin" structures, reaching ca. 300 km across, and their good preservation are extraordinary features requiring additional study.



The main tectonic units of the crystalline basement structure of Volgo-Uralia (modified after S. V. Bogdanova, 1986 with additions by A. V. Postnikov): *1* — the Timan-Uralian boundary of the East European Craton; *2* — boundary of the Pericaspian basin; *3* — boundaries of the Meso-Neoproterozoic (Riphean) aulacogens; *4* — boundaries of the crustal segments; *5* — outlines of the circular cores of the megablocks; *6* — blocks of dominant granulites as defined by (*a* — drill core materials and geophysics, *b* — geophysical data); *7* — amphibolites, mafic granulites and various intrusions of the assumed Paleoproterozoic cover over the Oka-Volga megablock (*a* — by drill core materials and geophysics, *b* — by geophysical data); *8* — amphibolite facies rocks, granitoids and migmatites, undivided Archean and Paleoproterozoic; *9* — Tersa marginal magmatic belt; *10* — Palaeoproterozoic supracrustals (*a* — in troughs along the radial faults within the Middle Volga megablock; *b* — the Paleoproterozoic metasedimentary schists, migmatites and granitoids); *11* — thrust faults; *12* — faults unspecified; *13* — faults of the radial system within the circular cores of the megablocks; *14* — strike slips; *15* — TATSEIS transect.

It is remarkable that the Paleoproterozoic circular structural patterns are mirrored by the structure of the Proterozoic-Paleozoic sedimentary cover [Postnikov, 2002]. Particularly important are radial fault system of the basement structures controlling the position of Paleozoic cover swells and the distribution of the oil ore deposits [Trofimov et al., 2004]. Notably, large recent circular/ring structures recorded by satellite images coincide with some of the basement-cover structural features [The Crystalline ..., 1996].

References

Bogdanova S. V. The Earth's Crust of the Russian Platform in the Early Precambrian as exemplified by the Volgo-Uralian segment. — Moscow: Nauka, 1986. — 224 p (in Russian).

Goodwin A. Precambrian Geology. — New York: Academ. Press, 1991. — 666 p.

International Tectonic Map of Europe and Adjacent Areas / Eds. A. V. Peive, A. A. Bogdanov, V. E. Khain. — Scale 1:2 500 000. — IGC/CGMW, 1979. — 20 sheets.

Postnikov A. V. The basement of the eastern part of the East European platform and its influence upon the structure of oil-and-gas-bearing sedimentary cover. — Moscow: Geological Faculty, Gubkin State University of Oil and Gas, 2002. — 55 p. (in Russian).

The Crystalline Basement in Tatarstan and Problems of its Oil and Gas Deposits / Eds. R. K. Muslimov, T. A. Lapinskaya. — Kazan: Denta, 1996. — 488 p. (in Russian).

Trofimov V. A. Deep CMP Seismic Surveying along the Tatseis-2003 Geotraverse across the Volga-Ural Petroliferous Province Geotectonics // Geotektonika. — 2006. — **40**. — P. 249—262 (in Russian and English).

Trofimov V. A., Romanov Yu. A., Khromov V. T. Large radial-ring structures — potential objects for hydrocarbon prospecting in the Volga — Ural province / / Geology, Geophysics and Development of Oil and Gas Deposits. — 2004. — **4**. — P. 36—41 (in Russian).

The scenarios of repeatability of catastrophic climatic phenomena in Europe and Ukraine under the influence of climate changes (with use of historical records and manuscripts for the last millennium)

© ***S. Boychenko, 2010***

Institute of Geophysics, National Academy of Sciences of Ukraine, Kiev, Ukraine
uaclimate@gmail.com

The climatic catastrophic phenomena, such as droughts, floods, extremely cold or warm winter, occurring at a large scale and great intensity are rather rare events. These phenomena, typically, occur only a few times per century. Because of this, statistically estimating the basic characteristics of the dynamics of repeatability of these events is very difficult. The instrumental observations are not helpful because of the short time-series. It is therefore necessary to use other proxy data as well. In our opinion, different historical records and manuscripts are most suiTable for this purpose. These records were very carefully compiled and described in the monasteries located in territory Europe [Borisenkov, Pasetsky, 1988].

The analysis is carried out on the basis of historical records and manuscripts for the last millennium (900—1800) [Borisenkov, Pasetsky, 1988]. The following phenomena were considered: droughts, rainy summers, floods, cold winters, late springs, colds at the beginning of a summer, catastrophic thunderstorms and catastrophic storms. It was used the names of these events, which are described in historical records and manuscripts.

The statistical analysis of these data shows that the long-term dynamics of repeatability of the climatic catastrophic phenomena in the territory Europe, Ukraine and Russian Plain was not similar to an ordinary stationary Poisson's flux of events [Boychenko, 2002]. It is supposed by our hypothesis

that the temperature fluctuations in Europe could be as main factor Influencing dynamics of repeatability of the phenomena [Voloshchuk, Boychenko, 2001; Boychenko, 2003; 2008]. Namely, the repeatability of the considered events is a non-monotonic function of temperature fluctuations: repeatability of catastrophic climatic phenomena in the territory of Europe was higher, when the temperature of Europe was increased (the Little Climatic Optimum) or, on the contrary, decreased (the Little Ice Age) [Boychenko, 2003; 2008; Voloshchuk, Boychenko, 2001]. Necessary characteristics of anomalies of temperature on Northern hemisphere for last millennium were restored Mann, Crouly etc and time-series for territory of the East Europe of Imbrie etc (quoted by [Boychenko, 2008]).

It is used the theory of similarity. The following basic criteria of the similarity theory of dynamics of frequency of the catastrophic climatic phenomena are worked out: collective rating of group of catastrophic climatic events X; index of level of climatic anomalies Q; dimensionless optimum level q of a thermal regime for considered geographical region.

Definitions of these criteria of similarity are formulated and proved and algorithms for calculation of their values are given on the basis of empirical materials or the given different modeling calculations:

$$X(t)=\sum_{k=1}^{N}\frac{n_k(t)-a_k}{s_k}\ ,\quad Q(t)=\frac{1}{s_T^2}\left(\Delta T(t)+s_T\,q\right)^2 ,$$

$$\delta t = 50-100 \text{ years}\ ,\ \Pi=\{900-1800 \text{ years}\}, \qquad (1)$$

where δt — elementary time unit; X — a collective rating of events; $n_k(t)$, a_k and s_k^2 — repeatability for time t, average repeatability during period Π and a dispersion of repeatability during the same period of time k-the events; $\Delta T(t)$ — anomalies of annual temperature for the East Europe or Northern hemisphere, for a time t; q — an optimum regional level of temperature which can accept different values for different regions.

Developed semi-empirical model of probability of dynamics of repeatability of the catastrophic climatic phenomena for different physic-geographical regions shows that:

$$\begin{gathered} X(t)\approx\chi(t)=\beta Q(t)\pm s_\chi\ , \\ \nu_k(t)=[a_k+s_k\,\chi(t)]\Delta t\ , \\ P_m(k,t;\Delta t)=\frac{\nu_k^m}{m!}e^{-\nu_k}\ , \\ \beta=0{,}8\pm0{,}2\ ,\ \ s_\chi=0{,}6\ , \end{gathered} \qquad (2)$$

where m — amount of occurrences k^{th} events during for time t, P_m — probability occurrences of k^{th} events for time t, $s\chi$ — a root-mean-square error of a collective rating of events, Δt — interval time in elementary units δt.

It was for the first time established existence excitation effect of the catastrophic climatic phenomena in different regions of Europe to an index of climatic anomaly Q (Fig. 1).

On a basis of the criteria's equation the scenarios of increase of frequency of occurrence of different catastrophic climatic phenomena in territory of Ukraine, East European plain and the Western Europe in 21[th] century are constructed. Validity of the semi-empirical models are checked up by the decision of a return problem: comparison of results of

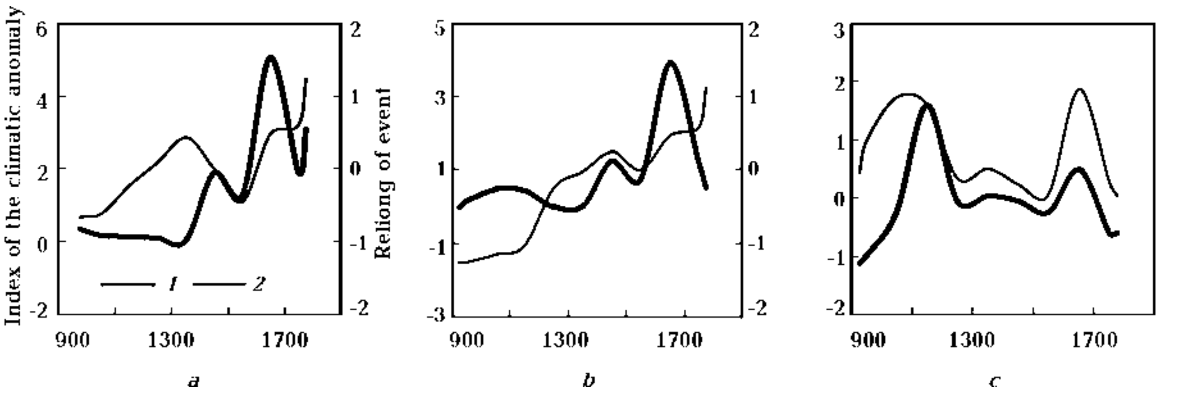


Fig. 1. A century course of an index of the climatic anomay (*1*) and a rating of catastrophic climatic events (*2*) in territories: *a* — Western Europe, *b* — Russian plain, *c* — Ukraine (the rating for Russian plain is displaced for 100 years forward).

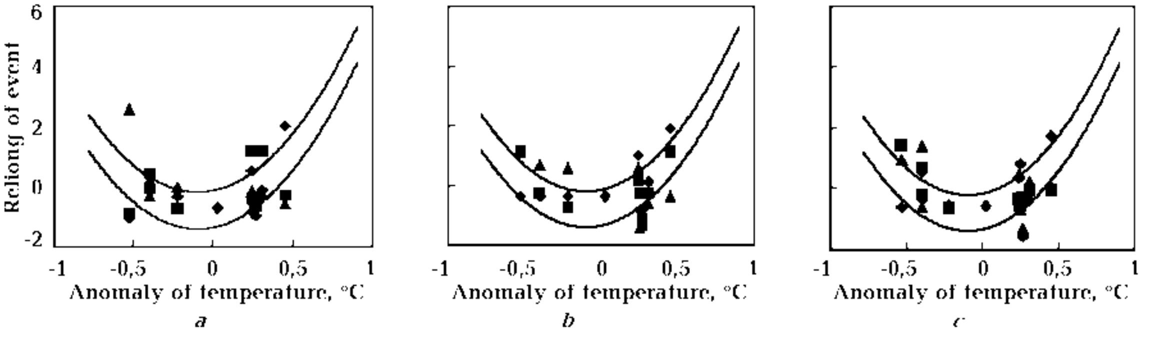


Fig. 2. Scenarios of dynamics of frequency of catastrophic climatic events in territory: *a* — Western Europe, *b* — Russian plain, *c* — Ukraine (droughts, flooding, unknown storms), calculations on ratio formule (1); on an axis $0X$ anomalies of temperature for Northern hemisphere.

modeling calculations with the fact for last millennium (11—13 century). By the developed scenarios it is possible to draw a conclusion, that the expected average amount of the considered catastrophic climatic events in 21th century in territories of Ukraine, the Western Europe and Russian plain in 1.5—2 times will exceed their fixed quantity in 12th century — for epoch of known global warming in the last millennium (Fig. 2).

It is found that the repeatability of the considered events is a non-monotonic function of temperature fluctuations, namely: repeatability of catastrophic climatic phenomena in the territory of Ukraine was higher, when the global temperature was deviating in either direction from some optimum level (at global warming or cooling from some optimum level of global temperature) [Boychenko, 2002; 2003]. It is established, that this effect takes place also for all Europe. Semi-empirical models for rating of intensity of climatic catastrophic phenomena in Ukraine as function of index of climatic anomality are constructed. A scenario of possible dynamics of repeatability of climatic catastrophic phenomena in the territory of Ukraine at the further global warming is considered [Voloshchuk, Boychenko, 2001; Boychenko, 2008].

References

Borisenkov Ye. P., Pasetsky V. M. The thousand-year annals of extraordinary natural phenomena. — Moscow: Mysl, 1988. — 524 p. (in Russian).

Boychenko S. Frequency of catastrophic phenomena in Ukraine under the influence of global warming // Water Resources Systems — Hydrological Risk, Management and Development (Proceedings of symposium HS02b held during IUGG2003 at Sapporo, 2003). — IAHS Publ, 2003. — № 281. — P. 18—25.

Boychenko S. Semi-empirical models and scenarios of global and regional changes of climate. — Kiev: Nauk. dumka, 2008. — 310 p. (in Russian).

Boychenko S. Semi-empirical statistical models of connection of repeatability of the catastrophic phenomena in Europe with global temperature anomalies in last millennium (on the basis of historical records and annals). Proceedings of Third International Conference on Water Resources and Environment Research (CWRER). — Germany, 2002. — **1**. — P. 224—229.

Voloshchuk V., Boychenko S. The effect of intense increase in repeatability of catastrophic processes and phenomena in the territory of Ukraine under the conditions of global warming or cooling // Ann. of the National Academy of Sciences of Ukraine. — 2001. — № 5. — P. 105—112 (in Russian).

Distribution of elastic parameters in the Earth's core

© **V. Burmin, 2010**

Institute of Physics of the Earth, RAS, Moscow, Russia
burmin@ifz.ru

The travel-time curves of refracted and reflected short-longitudinal seismic waves propagating in the Earth's core were constructed by record-sections of seismic vibrations from deep earthquakes recorded by the global network. These travel-time obtained velocity section core, in good agreement with observed data. The velocity curve for the Earth's core is well explain the nature of the so-called «precursors» — vibrations that go in the first arrival in the Earth's surface at epicentral distances of 134—142°. Features velocity section of the outer core is the presence of his bottom of the layer thickness of about 500 km from the high positive velocity gradient and immediately beneath a low-velocity layer thickness of about 200 km (zone F). In the inner core velocity first increases rather strongly to a depth of approximately 5500 km, and then to the center of the Earth varies almost linearly, with a slightly higher gradient than is usual in the standard model.

Density, elastic parameters and viscosity of the Earth's core were obtained on the basis of velocity curve for the longitudinal seismic waves. The density distribution for the new model differs from the distribution obtained in the standard model PREM only in the inner core. Distributions of modulus and shear modulus, depending on the physical processes occurring inside the Earth, may have a different character. In particular, the bulk modulus can have a negative jump at the boundary of the outer and inner core of the Earth, and the shear modulus may be different from zero at the bottom of the outer core. It is concluded that the shear modulus in the bottom of the outer core to fluctuations in the order of 1 Hz should be different from zero, and reach values of $\sim 2\times 10^{12}$ Pa. This conclusion is based on the fact that the gradient of the velocity of longitudinal waves in the lower outer core increases and the assumption that the bulk modulus in the core is a monotonic function. Estimates of the coefficient of shear viscosity for the outer and inner core have been made. These estimates imply that in the outer core directly adjacent to the upper boundary of the outer core viscosity is low, which corresponds to the liquid state of matter in the Earth's core. As we move to the lower boundary of the outer core viscosity increases, and the substance goes into the vitreous state. Low viscosity, apparently, takes place at the bottom of the outer core in zone F.

The methodology of operative prognosis of hydrocarbons by gravity-magnetic and space data

© **B. Busygin, S. Nikulin, E. Zatsepin, I. Garkusha, 2010**

National Mining University, Dniepropetrovsk, Ukraine
BusyginB@nmu.org.ua

Introduction. Because of constant growth of consumption of hydrocarbonic raw stock and exhaustion of world's reserves of oil and gas the problem of searches of new hydrocarbonic objects becomes more and more important. Nowadays for its decision the seismic survey in various modifications (for example, 3D, etc.) is used. However, possessing high geological efficiency, it demands large economic expenses, especially at field surveying on the big areas. For this reason the approaches based on using of a complex of cheap gravity-magnetic methods and space images of the various physical nature (multispectral, radar, thermal, etc.) received a wide dissemination.

Using the special geoinformation systems and technologies of the integrated analysis of spatial data [Pivnyak et al., 2007; Busygin, Nikulin, 2009], it is possible to implement the preliminary allocation of the sites on which it is expedient to apply detailed seismic survey. Use of such technique will allow to reduce considerably costs without essential loss of the information and to optimize a location of reconnaissance wells.

Investigated area. The proposed technique has been tested on a site in the size 137×130 km by the area more than 17000 km^2, located within the Dnieper—Donetsk cavity (DDC) (Fig. 1). Now the major strategic direction of searches of oil and gas in the territory of DDC are depths over 5 km. By the most reasonable estimations in the range of depths of 5—8 km it is concentrated over 5 billion tons of conditional fuel. At the beginning of 2009 there was discovered a great number of deposits in this region, amongst them — one of the largest in Europe Shebelinskoye gas-condensate deposit with resource of 650 bil. m^3 (exhausted).



Fig. 1. Area location.

The initial data are presented by gravitational (Δg) and magnetic (*Za*) surveys on a grid 500×500 m, and the radar image received by SRTM (Shuttle Radar Topography Mission) with the resolution of 90 m. In researches were used 29 known hydrocarbons deposits, presented by gas, gas-condensate, and oil-and-gas objects.

Research technique. The apparatus of lineament analysis, based on detection and research of lineaments — the linear sites detected on space images and on physical fields, underlie the proposed technique.

For more accurate allocation of lineaments the radar image and geophysical fields were exposed to the operations of images processing – contrasting, histogram alignment, sharpness increase (Fig. 2). The images received as a result of processing, have allowed to allocate more amount of linear elements, including, visually not distinguishable in initial materials. Then using the Canny «optimal detector» [Canny, 1986] on space image and raster

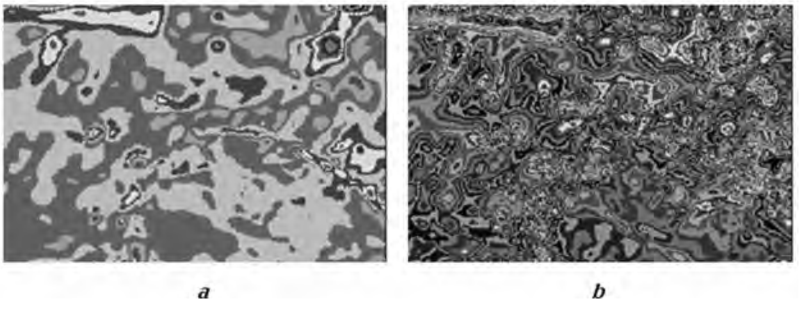


Fig. 2. Fragment of the raster map of magnetic field before (*a*) and after (*b*) operations of images processing (colors of a legend are generated in a random way).

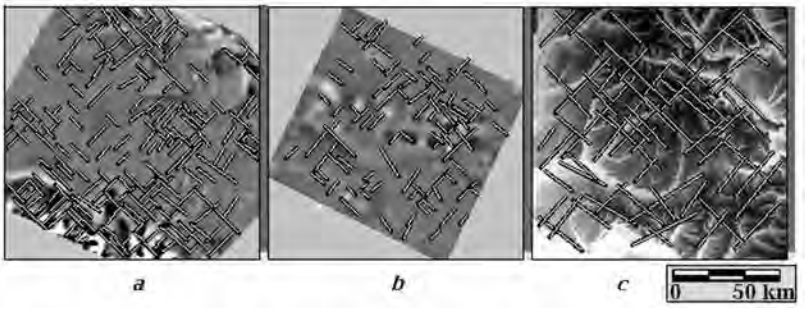


Fig. 3. Orthogonal systems of lineaments with azimuth 45—135º, detected on magnetic (*a*), gravitational (*b*) fields and in a radar image (*c*).

maps of fields the borders of brightness were defined and corresponding maps were built.

The lineaments were allocated using the Hough transformation [Sewisy, 2002] to brightness borders maps. The circle diagram estimation showed that two orthogonal systems of lineaments with azimuth 0—90° and 45—135° are presented on the image. In a Fig. 3 the scheme of lineaments location with azimuths 45 and 135° is presented, and in a Fig. 4 — the density (amount on area unit) of these lineaments, calculated in a sliding window 5000×5000 m, is presented.

The absolute majority of known objects are in conjunction with zones of high density (9 from 28) and with sites of their intersection (8 from 28) or in immediate proximity from them, while no essential relationship between the system of lineaments with azimuths 0—90° is observed (Fig. 5).

Conclusions. Thus, the sites of high lineaments density can be considered as perspective on detection of oil and gas objects and to be recommended for analysis by seismic prospecting of various modifications.

The relationship between location of oil and gas objects and zones of the high lineaments density indicate to the possibility of use the relatively cheap geophysical (gravitational and magnetic), and also space methods for preliminary allocation of promising sites.

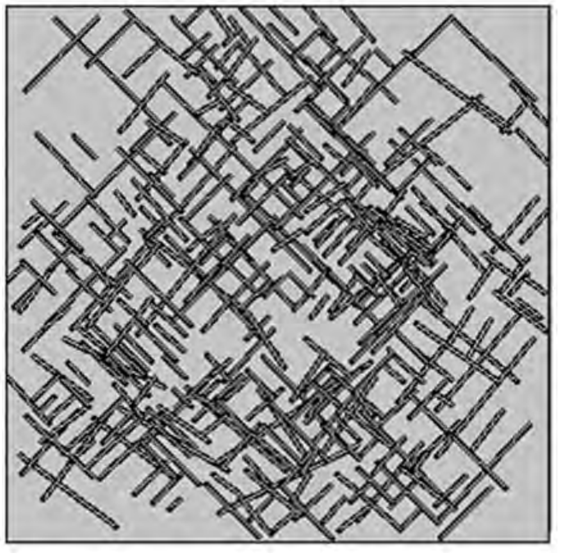


Fig. 4. Lineaments distribution with azimuth 45 and 135º.

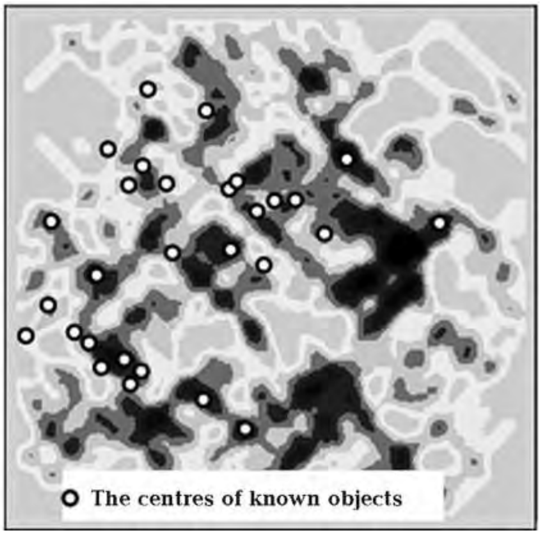


Fig. 5. Lineaments density map (more dark colour corresponds to more density).

References

Busygin B., Nikulin S. The methodology of oil and gas deposits prognosis by space and geophysical data // 71rd EAGE conference. — Amsterdam, 2009. — 4 p.

Canny J. F. A computational approach to edge detection // IEEE Trans Pattern Analysis and Machine Intelligence. — 1986. — № 8. — P. 679—698.

Pivnyak G. G., Busygin B. S., Nikulin S. L. GIS-technology of integrated heterogeneous and different-level geodata analysis // Rep. National Acad. Sci. of Ukraine. — 2007. — № 7. — P. 121—128.

Sewisy A. A. Graphical techniques for detecting lines with the Hough transform // JCM. — 2002. — **79**. — P. 49—64.

Lithosphere structure of Vietnam and adjacent territories based on seismic *P*-waves tomography and gravity

© ***Cao Dinh Trieu*[1]*, V. Starostenko*[2]*, T. Tsvetkova*[2]*, O. Legostaeva*[2]*, L. Zaets*[2]*, Pham Nam Hung*[1]*, Bui Anh Nam*[1]*, Le Van Dung*[1]*, 2010***

[1]Institute of Geophysics, VAST, Hanoi, Vietnam
vag-seg@ftp.vn
[2]Institute of Geophysics, National Academy of Sciences of Ukraine, Kiev, Ukraine

In the framework of this research work, the structural model of lithosphere of Vietnam territory and its adjacent areas is presented, based on the results of seismic *P*-waves tomography in combination with of Bouguer Gravity Anomaly. The combined processing and analysis of these two types of data will greatly contribute to a clarification of structural characteristics of lithosphere of Vietnam territory and its adjacent areas.

3D *P*-velocity model of the mantle under South-East Asia was received as the solution of the seismic tomography problem by Taylor approximation method, which was supposed by V. S. Geyko [Geyko, 2004]. The solution don't depends from the referent model selection and can be imagine in Cartesian and spherical coordinate system. The used tomography method permits recovering the mantle model being optimal in the given metric in respect with the whole totality of *P*-wave first arrival traveltime data within the frame of selected basic model of interpretation. It includes the apriory assumptions, theory and algorithms of numerical inversion, parameterization of velocity function, the smoothing method and other regularizing factors. The results are imagine in horizontal, longitude and latitude sections of the model.

Density model of lithosphere and mantle of Vietnam territory and its adjacent areas. The establishment of lithosphere density model of Vietnam territory and its adjacent areas is made, based on the following principles:

1. Density of sedimentary rocks is determined based on the study of density distribution of mineral and rock in a territory of Vietnam.

2. For the crystalline cover and upper mantle, the Pudiurov's correlated formula on density value and velocity of longitudinal *P*-waves propagation $V_P = 6\rho - 11$ is used, where V_P (km/s), and ρ (g/cm^3).

3. Synthesis of final result for construction of density model is the solution of 3D Gravity inverse problem.

Combined analysis of gravity data and seismic *P*-waves velocity for study the lithosphere structure of Vietnam territory and its' adjacent areas. The structural features of lithosphere of Viet Nam territory was set up, based on data of seismic waves tomography and gravity data in combination with other available material of exploration seismic and electrical and telluric surveys etc [Cao Dình Trieu, 2005].

Underneath lithosphere boundary is established, based on the followings:

- Anomaly cross-sections of seismic *P*-wave tomography. This boundary reflects a lager change of velocity propagation in the underneath part of lithosphere (seismic lithosphere is characterized by high velocities).
- To solve 3D Inverse Gravity Model with an average density values of the top mantle layer is 3,4 g/cm^3, of the asthenosphere is 3,20 g/cm^3, and the earth crust is 2,90 g/cm^3 [Cao Dình Trieu, 2002].

3D P-velocity model of the mantle under South-East Asia was received as the solution of the seismic tomography problem by Taylor approximation method, which was supposed by V. S. Geyko [Geyko, 2004]. The solution don't depends from the referent model selection and can be imagine in Cartesian and spherical coordinate system. The used tomography method permits recovering the mantle model being optimal in the given metric in respect to the whole totality of *P*-wave first arrival travel time data within the frame of selected basic model of interpretation. It includes the a priory assumptions, theory and algorithms of numerical inversion, parameterization of velocity function, the smoothing method and other regularizing factors. The results are imagine in horizontal, longitude and latitude sections of the model.

The thickness of the Earth crust of Vietnam territory and its adjacent is varying in limits of values lesser 12 up to 38 km. Oceanic cover has value of

thickness less than 14 km; continental cover has thickness varying from 24 km up to more than 38 km; and cover of transitional zones has thickness value from 14 to 24 km.

The Vietnam territory and its adjacent areas seismic lithosphere does not pick out for all territory. On the whole, thickness of the lithosphere of Vietnam territory and its adjacent areas is varying from 50 km to larger 110 km. The seismic lithosphere picks up under central part of North Calimantan block up to 50 km, under South China block up to 75 km, under Indochina block up to 50 km. The maximum lithosphere depth is under blocks Central East Sea and East East Sea — 110÷120 km.

References

Geyko V. S. A general theory of the seismic travel-time tomography // Geophys. J. — 2004. — **26**, № 2. — P. 3—32.

Cao Dinh Trieu. Geophysical fields and lithosphere structure of Vietnam territory // Publishing house Science and Technology. — Hanoi, 2005. — P. 330 (in Vietnamese).

Autowave solutions of a nonlocal model for geophysical media taking into account the hysteretic character of their deformation

© ***V. Danylenko, S. Skurativskyy, 2010***

Division of Geodynamics of Explosion, Institute of Geophysics,
National Academy of Sciences of Ukraine, Kiev, Ukraine
skurserg@rambler.ru

Geophysical media as open thermodynamic systems actively display synergetic properties, ability to creation of localized dissipative structures, and an order. Experimental investigations show that dynamics of physical processes in nonequilibrium media is determined substantially by hierarchy and discreteness of a media structure, the set of internal relaxing processes, the nonlocality of interaction between structure elements, the directed exchange of energy between the degrees of freedom. In the papers [Danylenko, Skurativsky, 2007; Danylenko et al., 2008] it is proposed to take into account these features of internal media structure in the dynamical equation of state. This leads to the nonlocal nonlinear mathematical model for structured media:

$$\frac{d\rho}{dt} + \rho\frac{\partial u}{\partial u} = 0\,, \quad \rho\frac{du}{dt} + \frac{\partial p}{\partial u} = \gamma\rho^m\,,$$

$$\tau(\dot{p} - \chi\dot{\rho}) = æ\rho^n - p + \Phi_1 + \sigma\left\{p_{xx} + \rho^{-1}p_x\rho_x - \eta\left(\rho_{xx} - \rho^{-1}\rho_x^2\right)\right\} -$$

$$- h\left(\ddot{p} + \eta\left\{2\rho^{-1}\dot{\rho}^2 - \ddot{\rho}\right\}\right) + \frac{h^2}{\tau}\dddot{p} + \frac{h\chi}{\tau}\left\{\frac{6}{\rho}\dot{\rho}\ddot{\rho} - \frac{6}{\rho^2}\dot{\rho}^3 - \dddot{\rho}\right\}, \qquad (1)$$

where ρ is the density of a medium, u is the velocity, p is the pressure, $\gamma\rho^m$ is the external mass force, τ is the relaxing time, σ and h are parameters of spatial and temporal nonlocalities, the parameters æ and χ are proportional to the squares of equilibrium and frozen speeds of the sound. The function $\Phi_1 = \varepsilon\Phi_1(\rho, p, \dot{\rho}, \dot{p})$ describes hysteretic reaction of a medium under the deformation, ε is the scale parameter.

Previous investigations of the wave solutions of model (1) in the form [Danylenko, Skurativsky, 2009]

$$\rho = R(\omega), \quad p = P(\omega), \quad u = 2\xi t + U(\omega), \quad \omega = x - \xi t^2 \qquad (2)$$

shown that accounting the spatial and temporal nonlocal effects in the dynamical equation of state ex-

pands substantially the class of solutions in comparison with the local model (τ, σ, h are infinitesimal). In particular, the set (2) contains periodic, quasiperiodic, multiperiodic, and chaotic regimes, which are connected with each other by means of bifurcational scenarios. The solitary waves with the oscillating asymptotics were discovered as well.

Thus, basing upon the results of investigations of models that do not take into account the hysteretic character of media deformations, we shall study the influence of the hysteretic function Φ_1 in the dynamical equation of state on the structure of solutions (2). The function Φ_1 describes the histeretic loop in the plane (ρ; p) under the harmonic loading. The form of this loop is defined by the following relation

$$\Phi_1 = \begin{cases} \exp\left(C_2\{\rho-\rho_0\}\right)-1, & \rho \ge \rho_0,\ d\rho/dt \ge 0, \\ \left[\exp\left(C_2\{\rho_{\max}-\rho_0\}\right)-1\right]\dfrac{\exp\left(C_1\{\rho-\rho_0\}\right)-1}{\exp\left(C_1\{\rho_{\max}-\rho_0\}\right)-1}, & \rho \ge \rho_0,\ d\rho/dt < 0, \\ -\left[\exp\left(-C_2\{\rho-\rho_0\}\right)-1\right], & \rho < \rho_0,\ d\rho/dt \le 0, \\ -\left[\exp\left(C_2\{\rho_{\max}-\rho_0\}\right)-1\right]\dfrac{\exp\left(-C_1\{\rho-\rho_0\}\right)-1}{\exp\left(C_1\{\rho_{\max}-\rho_0\}\right)-1}, & \rho < \rho_0,\ d\rho/dt > 0, \end{cases} \tag{3}$$

where $C_2 < C_1$. In the case, when $C_2 < C_1$, the area bounded by the loop is zero. We should note that the set of enclosed loops appears in the plane (ρ; p) instead of one loop, if we use the loading, distinct from harmonic one. The elements of function (3) can be used for description of the simplest cases of enclosed loops (Fig. 1).

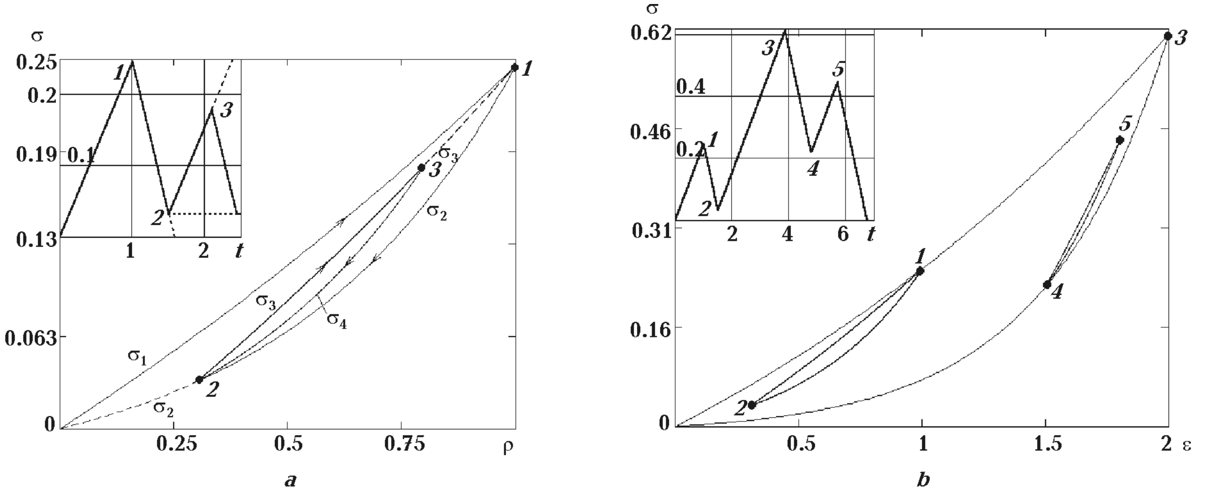


Fig. 1. The construction of two (*a*) and three (*b*) encloset histeretic loops in the plane (ρ; p).

Substituting solution (2) into system (1), we obtain the quadrature $UR=S=\mathrm{const}$ and the dynamical system:

$$R' = W\,,\quad P' = \gamma R^m - 2\xi R = \frac{S^2}{R^2}W\,,\quad W' = Z\,,\quad Z' = \frac{F + R^7\varepsilon\Phi_1}{bS^3\left(\chi - S^2\right)R^2}\,. \tag{4}$$

Here $(\circ)' = d(\circ)/d\omega$, $F = F(R,P,W,Z)$ is the nonlinear function. The analitical expression for the function F is omitted due to its length. Note that analitical expression (3) for the histeretic loop can also be written in terms of invariant variables (2).

Nonlinear dynamical system (4) is investigated by means of the qualitative and numerical methods. Equating the right parts of system (4) to zero, we get the coordinates of the fixed point

$$R_0 = (2\xi/\gamma)^{1/m-1}, \; P_0 = æR_0^n, \; W_0 = 0, \tag{5}$$

which do not depend on the parameters of the histeretic function Φ_1. Analyzing the stability of fixed point (5) under the neglecting the histeretic function Φ_1 we state that at χ = 16; S = 3.2; τ = 1; æ = 0.9; ζ = –0.5; h = 6.74; σ = 0; γ = –0.6; n = 4; m = 8; b = –3.8 the fixed point changes the type from unstable node-focus to stable one. In the vicinity of fixed point (5) the unstable limit cycle appears at increasing the parameter h. Bifurcational analysis of dynamical system (4) in the case when $\Phi_1 \neq 0$ and zero area of histeretic loop shown that for $C_2 = C_1 > 0$ fixed point (5) is a stable node-focus surrounded by both unstable and stable cycles. Consider the case, when $C_1 \neq C_2$ and function (3) describes the loop with nonzero area. Then as a consequence of histeretic loop including the structure of the phase space of system (4) becomes more complicated at increasing the parameter C_1. In particular, at $C_2 = 7.5$; $C_1 = 27$ there are several localized and separated regimes in the phase space of dynamical system (4), namely, fixed point (5), both stable and unstable cycles surrounding it (Fig. 2, *a*), and the chaotic attractor in addition (Fig. 2, *b*). Note that the chaotic attractor does not exist neither at $C_1 = C_2 = 7.5$ nor at $C_1 < C_2 = 27$. So that the chaotic attractor is created due to accounting the histeretic loop.

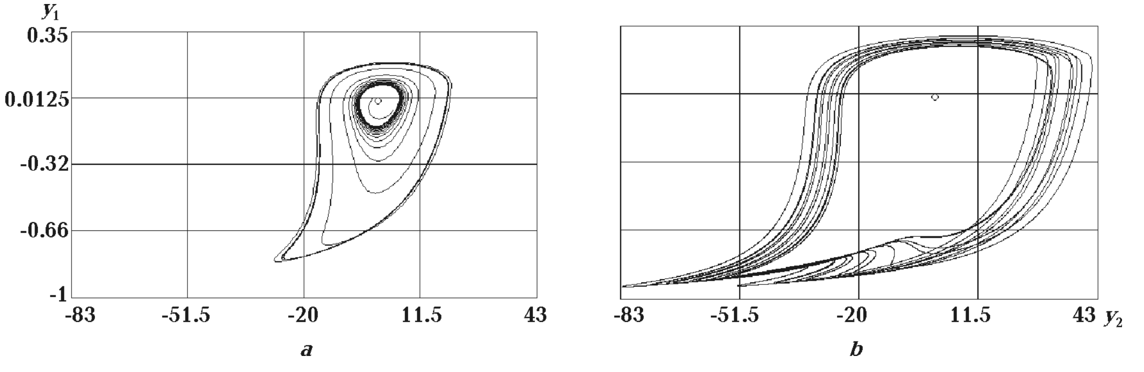


Fig. 2. The structure of the phase space of system (4) at C_1=27 (*a*) and C_2=7.5 (*b*).

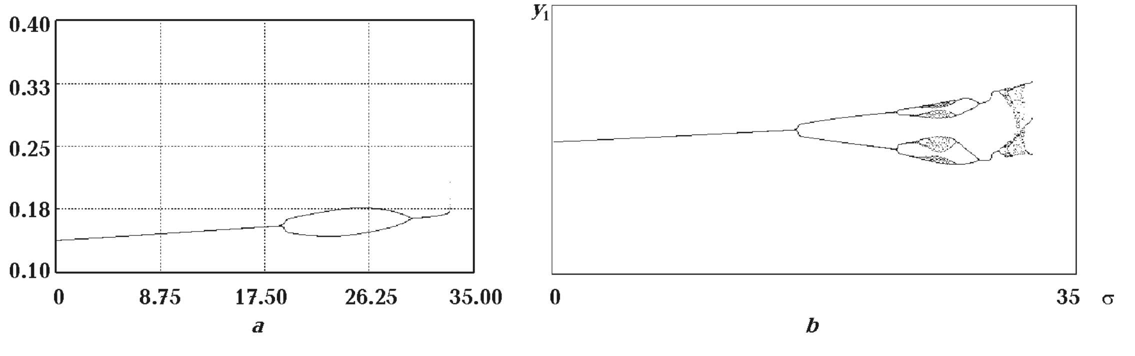


Fig. 3. Poincare diagrames of the limit cycle development at increasing σ: *a* — C_1=C_2=9.5; *b* — C_2=9.5, C_1=19.

Another manifestation of the histeretic function Φ_1 adding is regularization of chaotic oscillations. According to the numerical experiments, at S = 3.8, $C_1 = C_2 = 7.5$, ε = 0,1 the complicated periodic trajectory exists in the vicinity of the fixed point. Analyzing the development of the periodic trajectory by Poincare diagram we show that the period doubling cascade with chaotic attractor creation is actualized at $C_1 \in [7.5;\ 8]$. But if we fix $C_2 = 7.5$ and vary $C_1 \in [7.5;\ 8]$, then the periodic regime exists only instead of the chaotic attractor.

The existence of new wave regimes for model (1) is connected with the effects of spatial nonlocality, which are described by terms with the parameter σ. Analyzing the Poincare diagram of the limit cycle

development at increasing σ and $C_1 = C_2$ (zero loop area) we see that the size of *T*-period cycle is growing and there is an interval of σ corresponding to the existence of 2*T*-period cycle (Fig. 3, *a*). The structure of solutions (2) is much more complicated in the case of nonzero histeretic loop area at C_2 = 9,5, C_1 = 19. Studying the Poincare diagram in picture 3b we can distinguish several period doubling cascade, intervals of the different type chaotic attractor existence, moment of the histeretic transition from one attractor to other.

Thus, the accounting a histeretic loop in the dynamical equation of state causes new wave regimes creation. The histeretic loop is the way of elastic energy utilization and in the same time it is the nonlinear element of media, which can cause unstability generation in media and produce localized dissipative structures.

References

Danylenko V. A., Danevich T. B., Skurativskyy S. I. Nonlinear mathematical models of media with temporal and spatial nonlocalities. — Kiev: Institute of Geophysics NAS of Ukraine, 2008. — 86 p. (in Russian).

Danylenko V. A., Skurativskyy S. I. Autowave solutions of a nonlocal model of geophysical media with regard for the hysteretic character of their deformation // Rep. of the NAS of Ukraine. — 2009. — **1**. — P. 98—102 (in Ukrainian).

Danylenko V. A., Skurativskyy S. I. Invariant chaotic and quasi-periodic solutions of nonlinear nonlocal models of relaxing media // Rep. on Math. Phys. — 2007. — **59**. — P. 45—51.

What does Grace satellite mission tell us about seismic cycle?

© ***M. Diament[1], V. Mikhailov[2,1], I. Panet[3,1], F. Pollitz[4], 2010***

[1]Institut de Physique du Globe de Paris, Université Paris-Diderot, Paris, France
diament@ipgp.fr
[2]Institute of Physics of the Earth, RAS, Moscow, Russia
mikh@ifz.ru
[3]Institut Geographique National, Laboratoire LAREG, Marne-la-Vallée, France
panet@ign.fr
[4]U.S. Geological Survey, California, USA

Launched in March 2002, the GRACE mission measures the temporal variation of the gravity field at a spatial resolution of about 400 km, and at a temporal resolution from ten days to one month.

These information complements ground based geodetic and geophysical ones. The temporal variations of the Earth gravity field are dominated by the effect of the water circulation between the atmosphere, the oceans, the land hydrological systems and the polar ice caps. Such mass redistributions cause geoid variations of a few millimetres at various temporal and spatial scales. Locally, large seismic events also generate geoid variations of similar amplitude, which may also be detectable by GRACE [Gross, Chao, 2001; Mikhailov et al., 2004; Sun, Okubo, 2004; de Viron et al., 2008].

One of the largest earthquakes in recent decades, the M_w 9.2 Sumatra-Andaman, earthquake, occurred on December 26th 2004 at a particularly complex subduction boundary, along which the Indian and Australian plates subduct below a set of microplates comprising the forearc sliver plate, the Burma and the Sunda ones. The Sumatra-Andaman earthquake ruptured at least 1300 km of this subduction boundary. It was followed by numerous aftershocks and by a second very large earthquake, the M_w 8.7 Nias earthquake, on March 28th, 2005. During the following years, slip at depth has continued, as showed by the sequence of recorded aftershocks and regional GPS data.

The December 2004 Sumatra-Andaman event is associated with a large gravity co-seismic anomaly in the Andaman Sea and very fast post seismic relaxation that is well monitored by Grace [Panet et al., 2007; 2010]. This gravity variation is due to vertical displacement of density interfaces (mostly the

upper crust boundary and the Moho), and to rock density changes resulting from variations of the stress field (dilatation/compression). At large scales, the density variation effect dominates that of the vertical displacement. Part of the gravity low has been attributed to non-uniform coseismic subsidence of the Andaman Sea overriding plate [Panet et al., 2007].

Comparison of Grace data with the sparse GPS available information allowed us to construct a relaxation model and to discuss the amount of afterslip. In our post-seismic model the observed GPS displacements and gravity variations are well explained by of visco-elastic relaxation plus small amount of afterslip at the downdip extension of the co-seismically ruptured fault planes. Our model comprises 60 km thick elastic layer above a visco-elastic asthenosphere with Burgers body rheology. The mantle below depth 220 km has Maxwell rheology. Assuming a low transient viscosity in the 60—220 km depth range, the GRACE data are best explained by constant steady-state viscosity throughout the ductile portion of the upper mantle (e.g. 60—660 km). This suggests that the localization of relatively low viscosity in the asthenosphere is chiefly in the transient viscosity rather than the steady-state viscosity. The data indicate that mantle viscosity is as low as $8{,}10^{18}$ Pa s in the 220—660 km depth range, maybe indicating a transient behaviour of the upper mantle in response to the exceptionally high amount of stress released by the earthquakes. The remaining misfit to the GRACE data, larger at the smaller spatial scales, was explained by a cumulative afterslip of about 75 cm at depth continuation of the co-seismic rupture, over 30— months period spanned by the GRACE models. It produces small crustal displacements at the level of GPS errors.

Our results confirm that satellite gravity is an essential complement to the ground geodetic and geophysical networks, for understanding the seismic cycle and the Earth inner structure.

References

Gross R., Chao B. The gravitational signature of earthquakes, in Gravity, Geoid and Geodynamics 2000, IAG Symposia, 123. — New York: Springer-Verlag, 2001. — P. 205—210.

Mikhailov V., Tikhostky S., Diament M., Panet I., Ballu V. Can tectonic processes be recovered from new satellite gravity data? // Earth Planet. Sci. Lett. — 2004. — **228**, № 3/4. — P. 281—297.

Panet I., Mikhailov V., Diament M., Pollitz F., King G., de Viron O., Holschneider M., Biancale R., Lemoine J. M. Co-seismic and post-seismic signatures of the Sumatra December 2004 and March 2005 earthquakes in GRACE satellite gravity // Geophys. J. Int. — 2007. — **171**, № 1. — P. 177—190. — DOI:10.1111/j.1365-246X.2007.03525.x.

Panet I., Pollitz F., Mikhailov V., Diament M., Banerjee P., Grijalva K. Upper mantle rheology from GRACE and GPS post-seismic deformation after the 2004 Sumatra-Andaman earthquake // Geochem. Geophys. Geosyst. — 2010. — DOI:10.1029/2009GC002957.

Sun W., Okubo S. Coseismic deformations detect-Table by satellite gravity missions: a case study of Alaska (1964, 2002) and Hokkaido (2003) earthquakes in the spectral domain // J. Geophys. Res. — 2004. — **109**. — P. B04405.

de Viron O., Panet I., Mikhailov V., Van Camp M., Diament M. Retrieving earthquake signature in GRACE gravity solutions // Geophys. J. Int.— 2008. — **174**, № 1. — P. 14—20.

Numerical study of dynamic phenomena in the coal seam with taking into the account the influence of gas filtration and diffusion

© ***A. Dimaki[1], E. Shilko[1], A. Dmitriev[1], S. Zavsek[2], S. Psakhie[1], 2010***

[1]Institute of Strength Physics and Materials Sciences, SO RAS, Tomsk, Russia
dav@ispms.tsc.ru
[2]Velenje Coal Mine, Velenje, Slovenia
simon.zavsek@rlv.si

Coal beds are media with hierarchically organized structure, in which the processes of gas transfer in solid framework produce the significant influence on the mechanical response. Numerical si-

mulation of such media requires special methods to describe as the motion of a solid frame as the transfer of gas in the pores and channels, taking into account the interconnection between these processes. In the paper the symbiotic cellular automata (SCA) method is proposed, which is the combination of conventional [Wolfram, 1986] and movable cellular automaton [Psakhie et al., 2001] methods (CCA and MCA, consequently). In the framework of SCA method the investigated medium is considered as a superposition of two interrelated media. One of them is described by a set of MCA and another — by a mesh of CCA [Zavsek et al., 2005]. The step of calculation consists of two main substeps. First of them is the step of the MCA model, called “mechanical step”. At this substep motion equations of movable automata are solved. In other words, the process of mass transfer of solid due to mechanical loading is simulated at the first substep. Next for the mechanical — “net” substep is performed on a mesh of CCA. At this substep the process of mass transfer of gas in the pores and channels is considered, as well as the values of the forces acting on the movable cellular automata from gas phase are calculated. The configuration of pores and channels through which gas propagates, is projected to the mesh of classical cellular automata from the MCA layer. This symbiotic approach combines solutions of mechanical and gas dynamic problems and allows description of multiphase heterogeneous media.

During simulation of coal we used the following main assumptions.

1. Isothermal approximation (T=const) is used for considered system “porous solid — gas/liquid”.

2. Description of fluid transfer in filtration volume is done on the basis of linear model of stabilized flow of liquid and gas (Darcy law) [Alekseev et al., 2007].

3. Description of diffusion mechanism of gas transfer (transfer of gas molecules in solid-phase framework) is done using Fick law.

4. Calculation of fluid pressure is done using Van der Waals equation. Possibility of phase transition “gas↔liquid” is taken into account. When considering phase transformation, it is assumed that in two-phase state the pressure is constant. In corresponding interval of fluid specific volumes the Van der Waals dependence of pressure (p) on specific volume (V_{spec}) is replaced by the segment of isobar horizontal line (p=const).

5. Simulation of processes of adsorption and desorption on the outer surface of porous solid is carried out using the equation, which is written on the basis of Darcy law.

6. The influence of pressure of contained gases/liquids on solid-phase framework is calculated within linear approximation of porosity dependence on material mean stress [Borisenko, 1985]. Within the framework of present approach the gas-liquid fluid is considered as homogeneous multicomponent two-phase mixture. Phase composition for each component (fluid) is calculated independently of other components. Influence of absorbed gas molecules (molecules located in crystal lattice) on increase of elastic energy of solid-phase framework is not taken into account.

Verification of proposed approach was carried out by means of comparison of the results of modeling of the samples of fine detritus in the CO_2 atmosphere with the results of experimental studies performed by researchers of Velenje coal mine (Faculty of natural sciences and engineering, University of Ljubljana, Slovenia) [Pezdic et al., 1999]. These results demonstrate a qualitative agreement between model and experimental data. The effect of the CO_2 on the mechanical response and the failure of the samples of fine detritus was studied. Mechanical properties of fine detritus and xylite inclusions were used as given in [Zavsek et al., 2005]. The response and failure of fine detritus under uniaxial compression in the CO_2 atmosphere and in vacuum have been simulated. Results of simulation have shown that the presence of external gas pressure resulted in an increase of strength and ultimate strain of specimens without a noticeable change in Young's modulus. Also, the fracture pattern of specimens has undergone some changes.

It is clear that the proposed approach does not cover the entire spectrum of processes in a multiphase heterogeneous medium. Nevertheless, proper selection of model parameters allows obtaining good agreement with the results of natural experiments. This demonstrates the correct formulation of the problem and qualitatively correct description of the basic processes occurring in the system.

References

Alekseev A. D., Vasilenko T. A., Gumennik K. V. et al. Diffusion-filtration model of methane escape from a coal seam // Tech. Phys. – 2007. – **52**, № 4. – P. 456–465.

Borisenko A. A. Effect of gas pressure on stresses in coal strata // J. Mining Sci. — 1985. — **21**, № 1. — P. 88—92.

Pezdic J., Markič M., Letič M., Popovič A., Zavsek S. Laboratory simulation of adsorption-desorption processes on different lignite lithotypes from the Velenje lignite mine // RMZ — Mater. and Geoenv. — 1999. — **46**, № 3. — P. 555—568.

Psakhie S. G., Horie Y., Ostermeyer G.-P., Korostelev S. Yu., Smolin A. Yu., Shilko E. V., Dmitriev A. I., Blatnik S., Spegel M., Zavsek S. Movable cellular automata method for simulating materials with mesostructure // Theor. Appl. Fracture Mech. — 2001. — № 37. — P. 311—334.

Wolfram S. Theory and applications of cellular automata. — New Jersey: World Scientific, 1986. — 560 p.

Zavsek S., Pezdich J., Shilko E. V., Dmitriev A. L., Dimaki A. V. Application of hybrid cellular automaton approach for computer-aided examination and forecast of strength properties of heterogeneous coalbeds // Proc. 11th Int. Conf. on Fracture, Turin, Italy, 2005. — P. 4502/1–4502/6.

Geodynamic and geotectonic position of the geoisostatic stress fields of seismic active segments of Ukraine

© ***M. Dovbnich, S. Demianets, 2010***

National Mining University, Dniepropetrovsk, Ukraine
dovbnichm@mail.ru

The majority of Ukrainian territory is situated in the Eastern European platform. Meanwhile the most seismic active is the young tectonic structures of its south and south-west framing. First of all it's a zone of articulation of the Eastern and the Southern Carpathians — Vrancea zone and Crimean seismically active segment. In the historical past the earthquakes repeatedly leaded to the catastrophic consequences.

The main geodynamic factor, defined the regions seismicity, is a moving and interaction of separate tectonosphere fragments — tectonic blocks. Studying the nature of tectonic forces, caused different scale geodynamic processes behavior, is an actual question in solving the fundamental and applied problems. The analysis of geological environment stress-deformed state is the key section in chain of the nature and the prognosis of seismic events investigation.

The aim of the work — using the satellite and ground gravity data to make an analysis of the geological environment stress-deformed state, occurred as a result of the disturbances of the tectonosphere equilibrium state and it further usage in the investigation of the nature and the prognosis of seismic events.

Authors investigate the disturbances of the Earth equilibrium state and connected with them tectonosphere stress fields — effects, caused by the deviation of factual Earth Figure — geoid from theoretical equilibrium Figure — ellipsoid. These investigations based on the phenomena called geoisostasy. The model of the equilibrium state of the rotating Earth, offered by K. F. Tyapkin, geoisostasy is well described in geological and geophysical literature [Tyapkin, 1984]. The minimization energy principle, in accordance with which every natural dynamic system is aspired to minimize its interior energy, is the physically mathematics basis of this conception. The equilibrium Figure of our planet is the rotating ellipsoid. In accordance with this principle, the planet will reach the hydrostatic equilibrium in the moment, when the deviation between geoid and ellipsoid in whole Earth will be equivalent to zero. Therefore, evolving Earth aspire to minimize the height of geoid anomalies. Otherwise, the Earth tried to reach the hydrostatic equilibrium, in which its equilibrium form will take the ellipsoid form. Meanwhile, the geoid deviations from ellipsoid, caused by the heterogeneities of tectonic nature inside the planet can be used as an equilibrium criterion. As far as there is the geoid deviations from ellipsoid, so in accordance with the mentioned above principle there must be forces aspired to smooth those deviations, to make it equivalent with the equilibrium Figure. Therefore the mechanic stresses will occur in the tectonosphere of the planet. The law of the stress distribution will be defined as a function of the geoid deviation from the ellipsoid appropriated to it. The value that was taken as a deviation measure from the equilibrium state is suitable because it can be calculated using the results of the Earth gravity field studying based on satellite and ground data. The tectonosphere stresses connect with these disturbances can be estimated using the data of the equilibrium state disturbances in time and in space [Dovbnich, 2008].

Taking into account that tectonosphere has difficult fault-block building it becomes clear that the

density boundaries appeared when the displacements of the tectonic blocks happen. In other words the relative tectonosphere block displacements leaded to appearance of lateral density heterogeneities, reflected in the geoid anomalies relatively the reference ellipsoid of the Earth, and in tectonosphere the stresses will appear as a result of forces aspired to smooth those disturbances of the equilibrium state of the rotating Earth [Demianets, Dovbnich, 2010]. The stress fields' analysis allows to answer the row of questions concern of the nature and the prognosis of the dangerous geodynamic processes.

Nowadays studying the orbits of the artificial Earth satellites broaden our knowledge about the geoid anomalies significantly. In this work we use the geoid anomalies, got in the framework of GRACE project (Gravity Recovery And Climate Experiment). But in spite of the increasing accuracy of satellite measurements of geoid anomalies there usage is possible only in regional investigations in the near future. Authors developed technology of the geoid anomalies restoration using the ground gravity data based on the approximating approach using the gravity force in the Faye's reduction (free-air anomalies).

The calculation of the stress fields using the satellite gravimetry is done in the Ukrainian territory. The comparison of the earthquakes with the geoisostatic nature stress fields is done in the Vrancea zone and in Crimea. It can be seen on the schemes the majority earthquakes are corresponded with the maximums of the tangent stresses. As it was mentioned above, the disturbances of the equilibrium state happen in case if the tectonosphere blocks displacements is vertical. Meanwhile the tangent stresses localized blocks boundaries, for which the relative vertical displacements take place. Therefore, it is possible to assert that the whole seismicity of the regions defines by the relative tectonosphere block displacements with the significant vertical component. It was proved by that in case with the North Anatolian Fault, represented itself as a practically clean shear and which is one of the main seismic generating structures of Turkey, there is no interrelation between the earthquake epicenters and the tangent geoisostatic stresses. It can be seen only correlation between the earthquake epicenters with the chain of compression zone along the fault.

More detailed buildings are done using the results of gravimetry survey in 1:200000 scales. First of all the transformation of gravitational field into the Bouguer reduction based on the frequency selection is done. This transform suggested by author [Dovbnich, 2005], allows to localize anomalygenerating objects in plan and in section. Building the cutsets of results of gravity fields transformation along the profiles, crossing the Vrancea zone and the Crimean segment in the NW-SE direction, there comparison with the earthquake centers allows to assert: In both case seismic events corresponded with the block boundaries, for which the density boundaries corresponded, there nature was described above. Just these boundaries are reflected on these sections. In the same time there are principle differences:

1) the free-air, Bouguer anomalies and the relief are identical for the Crimean segment, in the same time in the Vrancea zone the Bouguer anomaly are rather different than free-air anomaly and relief similar each others;

2) the penetration depth of the vertical density boundaries in tectonosphere are rather different and it is in good agreement with observed seismicity. These facts are the convincing evidence of differs in the forming and in the development of seismogenic Vrancea zone and Crimea: in the first case the seismicity is defined by the raised up blocks of Carpathian orogen relatively the Moesian Platlform, and in the second case — by blocks lowering of the Black Sea relatively to the Crimean orogen.

The calculation and the analysis of the geoisostatic stresses using the ground gravimetry was done for the detailed study of the stress state and of internal structure of seismically active segments: the Carpathian and the Crimea.

The results showed that in the geoisostatic stress fields the different scale block boundaries of the Earth crust are reflected. The block boundaries, on which the vertical displacements happen, reflected as linear elongate anomalies of the maximum of the tangent stresses, subhorizontal block displacement — as a axes of linear elongate anomalies of the maximum of the tangent stresses. The elements that are the tectonic basis of the seismic generating structures are reflected in the stresses.

Just with these stresses, practically with the block boundaries connect the majority of the seismic events. Taking into account the high values of geoisostatic stresses we can assert that the neotectonic activity of the dedicated zones is high. Probably, the high seismicity is connected with it, and also possibly landslide processes, anomaly values of modern displacement of the Earth crust and others. In whole the seismicity of the studying region defined as fracture zones crossings; the earthquake epicenter distribution features are defined by boundaries of interactions of the separate fragments — less order tectonic blocks.

References

Demianets S., Dovbnich M. Satellite and Ground Gravimetry — The Innovative Approaches in Studying the Earthquake Nature and Prognosis // Extended abstracts, 72th EAGE Conference, Exhibition. — Barcelona (Spain), 2010. — CD.

Dovbnich M. M. Disturbance of geoisostasy and tectonoshere stressed state // Geophys. J. — 2008. — **30**, № 4. — P. 123—132 (in Russian).

Dovbnich M. Geological model of greenstone belts of the Ukrainian shield on the gravimetry data // Extended abstracts, 67th EAGE Conference, Exhibition. — Madrid (Spain), 2005. — CD.

Tyapkin K. F. A new isostatic model of the Earth // Trans. Hung. Geophys. Inst. — 1984. — № 30. — P. 3— 10.

The seasonal location of the core of the Earth — is an important geodynamic factor of the planet

© ***O. Drevitska, 2010***

National Medical Academy of Postgraduate Education,
Ministry of Health of Ukraine, Kiev, Ukraine
drevitska@ukr.net

The scientific literature is not elaborate enough to consider the importance of the seasonal location of the core of the Earth as a factor of geodynamic processes [Greiner-Mai et al., 2003; Antonov, Kondratjev, 2004; Malyshkov Yu., Malyshkov S., 2009]. In our work we present a logical rational of the concept.

The first position. Newton's second law of the force of gravity states that there is a direct proportional relation to the mass of bodies and inversely proportional to the distance between them. Weight is calculated as the product of the specific body weight and its volume. The core of the Earth has a larger proportion (this fact is proved by numerous gravimetric studies) [http://uk.wikipedia.org/wiki/Geophysic].

It is known that the Earth's core consists of 90% iron while the mantle contains of only 10 % iron and a proportion of the other elements — oxygen, silicon and magnesium [Allegre et al., 1995].

Therefore, the force of gravity per unit volume of Earth's core is higher and the nucleus constantly presses the inside the mantle. Pressure is directed towards the Sun and as the Earth rotates the constantly changing area of highest pressure is inside the kernel.

So, the Earth's core is heavier, and in accordance with Newton's second law, more attracted to the sun. This is partly accounted for in the scientific literature.

The second position. The axis of the Earth is tilted 23 degrees to the ecliptic plane. Earth is facing the Sun at an angle, in the summer inside the nucleus at an angle of more pressure on the northern hemisphere, and in the winter — on the Southern.

Findings from the provisions of 1 and 2.

The core of the Earth not only rotates inside the planet, but also seasonally shifts to the Northern Hemisphere and then to the Southern, as shown in the picture (Figure).

In the presented picture (when the Earth is right) shows how the Earth's core is offset at an angle of 23 degrees in the direction of the Northern Hemisphere, when we have the summer season.

Inside — the pressure on the mantle. The picture also shows (when the Earth is on the left) as the core is offset at an angle to the Southern Hemisphere, when we have the winter season.

Such internal displacement of the Earth's core (as conventionally shown "on the cut") reaches its highest value in the following periods: December—January and June—July.

The pressure inside the kernel, its friction and seasonal shifts significantly affects:

- earthquakes and volcanoes,
- the movement of continents and the formation of mountain ranges,
- the formation of plumes, subduction, nutation, and other geodynamic processes.

During the summer, forming elevations in the Northern Hemisphere, are active volcanoes, earthquakes that occur in the projections of the nucleus and the more pressure field "breaks" of tectonic

plates. Seasonal shift in the Earth's core could explain the gaps of tectonic plates and their movement.

During our winter season, shaped elevations in the Southern Hemisphere are active volcanoes, earthquakes occur in the relatively "weak" field. In the northern hemisphere, meanwhile, it may also occur from an earthquake, but the land, that "sinks", hence an understanding for the reasons for subduction.

Seasonal location of the core of the Earth is important geodynamic effects, as evidenced by the presence of zones of high tectonic activnosi on both sides of the equator. This increases the tectonic activity in the Southern Hemisphere in December—January, and in the Northern — in June and July.

The core of the Earth — it is almost a "perpetual motion" inside the planet until there is a structure of the Earth's axis and the trajectory of the Earth around the Sun.

This concept should be considered when creating a computer model of the Earth, a view of the seasonal movement of the nucleus, in order to better predict those processes that will occur inside and on the surface of our planet.

References

Allegre C. J., Poirier J. P., Humler E., Hofmann A. W. The Chemical-Composition of the Earth // Earth Planet. Sci. Lett. — 1995. — **134**(3-4). — P. 515—526.

Antonov V. A., Kondratjev B. P. On the problem of the value of the interior Earth's core displacement // Earth Physics. — 2004. — № 4. — P. 63—66 (in Russian).

Greiner-Mai H., Jochmann H., Barthelmes F., Ballani L. Possible infleunces of core processes on the Earth's rotation and the gravity field // J. Geodynam. — 2003. — **36**, № 3. — P. 343—358.

http://www.izdatgeo.ru

http://uk.wikipedia.org/wiki/Geophysic

Malyshkov Yu. P., Malyshkov S. Yu. Periodic variations of geophysical fields and seismic activity, their possible connection with the Earth's core motions // Geology and Geophysics. — 2009. — **50**, № 2. — P. 152—172 (in Russian).

Geoenergogenerated dynamic cataclysms as the launch mechanism of the origin and evolution of the terrestrial life

© ***A. Drozdovskaya, 2010***

Department of Marine Geology and Sedimentary Ore Genesis,
National Academy of Sciences of Ukraine, Kiev, Ukraine
dakaktotak@mail.ru

The author proposes a new conception for the mechanism of the origin and evolution of the terrestrial life in the energetic Earth-Space interactions [Drozdovskaya, 2009]. This conception (named geoenergetic) has been developed in the process of the analysis of the Earth's biological and dynamical history from the viewpoint of the author-made studies of the geochemical evolution history [Drozdovskaya, 1990] that was carried out using geological, physical-chemical, geoecological and eniological methods.

The problem of the mechanism and time of the terrestrial life origin was solved in connection to the physical-chemical and geostructural specifics of the Early Proterozoic Krivoy Rog-type Jaspilite Formation (JFKT) termed in English as the Banded Iron Formation (BIF). BIF is considered as the unique geological phenomenon due to a number of specific features peculiar only to it. The main ones amongst them are *the single-act and geologically short time of the BIF's global origination in the range by isotopic data 24—2,2 billion years with accumulation in it about 90 % of iron ore reserves of the Earth's crust in simplified elemental form, predominantly iron-silicon-oxygen.*

The computer physical-chemical experiments demonstrated [Drozdovskaya, 1990] that BIF is a chemogenic-sedimentary product of geochemical

evolution which origination is themodynamically limited by redox-barrier parameters of chemical interactions between three external shells of the Earth — water (*hydrosphere*), gas (atmosphere) and solid (*lithosphere*) composing the planet **exosphere**. It means that the temporal development of geochemical evolution was predicted by the steady-directed transformation of the terrestrial exosphere from the primary reduced state into recent oxidized one with single-act overcoming of the redox-barrier at the geological time interval of 2,4—2,2 Ga. Accounting this statement, the author's opinion is that BIF is a geological reference point of geochemical evolution that confirm that *during the BIF genesis time* coming into the exosphere free oxygen completed the oxidization of reduced polyvalent elements occurring there. But, in the moment when *BIF finished its development,* free oxygen for the first time became able to remain in the exosphere in a thermodynamically steady state pointing in this way the moment of oxygen era dawn on the planet Earth.

Proceeding from this conclusion, an appearance of one else distinguishing feature of BIF became understand: *a mass burial of blue-green algae appeared in directly covering sediments for the very first time in the history of the Earth crust. That biological phenomenon showed that, as the BIF generation stopped, the first in the Earth's history global and mass origin of unicellular organisms took place, which* ***was initiated*** *by the first occurrence in the* exosphere *of the thermodynamically stable free oxygen.* It means that 2,2 Ga the structuration of the pre-cellular organic matter finished also.

In these links, an attempt was made to determine the time period where that structuration passed — therefore, to recognize the moment of the First Global Life Appearance. Solving those problems, the original explanation of one more BIF's feature was in hand: *all its global ingredients were located in morphologically uniform, fracture-like faults of the coeval global tectonic structure.*

Accounting the planet rotation, we may to presuppose that *before the start of the BIF origination,* an surplus amount of geogenic energy (torsion, most of all) was accumulated in the Earth which, trying to leave this close space, provoked a blast-like geodynamical cataclysm with lithosphere splitting by a number of fracture-like faults, and (geologically, in the one moment) penetrated trough to the day surface. It was a very hard energetic strike onto the exospherical matter world.

At this notion about geodynamical evolution, we can see by "the morning eyes" that before the BIF origination that the results of today biological experiments have shown: some DNA fragments were found after energetic impacts into a mixture of biophilic combinations (including hydrocarbonic). In this connection, we can to assume a massive pulse outburst of geogenic energy in the Early Proterozoic exosphere was able to initiate forming of the primary living matter forms from existing chemical combinations (their important parts were in that time the combinations of reduced biophilic elements including carbon, nitrogen, and sulfur). Therefore, the time of global appearance of initial live matters forms (i. e. the life appearance time) can be reasonably dated with lower BIF's age as 2,4 billion years.

From these positions, the author analyzed and re-comprehended the history of step species composition transformations in the biosphere and complication of its organisms' matter organization that is fixed in the Earth's crust at the lower boundaries of geological epochs (Vendian, Cambrian, Ordovician, Silurian, Devonian, Carboniferous, Permian, Triassic, Jurassic, Cretaceous, Paleogene, Neogene) which are termed as transformation frontiers of biological evolution. It is proved that at each the frontier some organic species with more simple organization exited and new, more complicated appeared. It means that the biosphere developed through the time by the step complication of its organisms' matter organization in the chain: *Unicellulars→Multicellulars→Corals→Crustacea→Fishes→Arthropoda→Quadrupedantae→Amphibians→Reptiles→Mammalia→Hominidae*.

In the comparisons of the biological evolution and geodynamic phenomena histories a mutual relation in time became understood between the biospherical transformations at the frontiers mentioned and formation of global tectonic structures of fluidogenic type in those geological times. An idea appeared that those structures also formed in the origin moments of blast-like dynamic cataclysms which at each transformation frontier maintained the pulse outbursts of geogenic energy to the surface. Its impacts lead to jumps in the species composition and matter organization level of the organisms' in the biosphere. Proceeding from those notions, we should to refer those structures as geoenergogenic ones and to consider them as a kind of fluidogenic structures.

So, we postulate a universal geoenergogenerated mechanism both for the origination and evolution of the terrestrial life. Its action is maintained due three casual-concession geoenergogenerated phenomena (mutually subordinated, which periodically appeared through the geological time due the rotational existence of the Earth and its energetic interaction with the Space:

1) generation and accumulation of geogenic energy surplus amounts in the Earth, which

provoke attempts of its liberation from the closed space outward;
2) origination as a concession of it the blast-like dynamic cataclysms with global origination of numerous fracture-like faults in the lithosphere;
3) pulse breaks of geogenic energy surpluses onto the surface through those faults and its powerful impacts into the matter world of the exosphere. It is stated that through action of this mechanism, 2,4 billion years ago the global transformation of the exosphere's organic combinations into primary forms of terrestrial live matter took place in the first time at the Earth; and jump-like changes of species composition and organization complication of biosphere organisms' matter were carried out at the transformation frontiers of biological evolution.

References

Drozdovskaya A. A. Chemical Evolution of the Ocean and Atmosphere in the Geological History of the Earth. — Kiev: Nauk. dumka, 1990. — 208 p. (in Russian).

Drozdovskaya A. A. The Life: the Origin and evolution under Earth-Space energy interaction. — Kiev: Simvol-T, 2009. — 334 p. (in Russian).

On the ambiguity of 4D gravity monitoring of geological media

© Yu. Dubovenko, O. Chorna, 2010

Institute of Geophysics, National Academy of Sciences of Ukraine, Kiev, Ukraine
dubovenko@igph.kiev.ua

The main concept of 4D gravity monitoring being realized on the short profiles is in common supplied by the analitical relations with the rapidly decreasing kernels. The monitoring perceptible depends on the non-tidal quasiperiodic variation of gravity field and also is influenced by the low-level geophysical factors marked out by the Dvulit's techniques.

1. On the background of monitoring. Now on the amount, methods and opportunity to execute large-scale geophysical workings affect both the increasing accuracy and productivity of gravity surveying (this method at acceptable accuracy remains affordable prospecting and exploration solution due to improved equipment and GPS support) and a markedly sharp decline in volume measurements.

The first trend cause to review the methods of processing of the data acquired, in particular, a more accurate account of a Bouguer corrections [Bychkov, 2007]. The latter one, due to need of detection a deeper sources of anomalies[1] , entails the revision of the measurement method to account for subtle features of gravity anomalies without complicating the mathematical apparatus, measurement techniques and increasing the logistical costs. These features one can "hooks" wit the help of additional variable — the time.

In this regard, the world's "trends" of geophysical observations gradually tend to the continuous 4D monitoring (Geophysics. — 2008. — **73**, № 6) of studied area, studying the evolution of the gravity field during exploitation time of the area or over duration of interval of his abrupt dynamic activation.

Nevertheless in the English-speaking sources the term "gravity variations" means temporal difference between the real anomalies in limited spaces, which sources are the objects with the rapidly changing of deep dynamics, while in the USSR's literature this concept are reserved for a weak *quasi-periodic fluctuations* in the super-long profiles crossing the area of contrasting modern vertical movements of Earth's crust.

[1] The possibilities of regularization methods in solving the problems of building complex cross sections at the present level of model representations on the geological environment are close to the technological limit.

But the idea of monitoring the some of its applications illustrate the work [Bolotnova, 2007]. Nevertheless, in these sources there are no mention on the background of monitoring — the gravity variations in the sense laid in the [Sobakar, 1972] and on their dependence on a series of *low-level* natural and man-made factors.

The use of *repeated* observations in a certain region in gravimetry branch is comparatively well known (its elements are used in the creation of regional density models of the Caucasus, in [Aleksidze, 1985], also [Yurkina, 1978]), although *continuous* in time to call them rather difficult, whereas in seismometry this for a long time there is a common practice. However, the organization of any high-precision measurements with the gravity as a separate parameter, its variational component should always be investigated to take into account.

2. On the variations of gravity. For the first time in the USSR's literature a various components of variation part of the gravity field are examined and a non-tidal *quasi-periodic variations* (QPV) of gravity (with amplitude within 3 to 5 times the measurement error) are picked out in [Sobakar, 1972]. For aim of their measurement was created a new triple basis. The methodological one means a use of the *heterogeneous Earth* model as in a physical-chemical as in a energy-efficient treatment. The methodological one relies on the fact that QPV have *maximum* at the intersection of tectonic structures of *different ages* and in the areas of *contrasted* modern vertical movements. The metrological one relies upon the observations on the network with *optimal density* and configuration by the multiple devices with a high coefficient of *reliability* and comparison of QPV gradients and the observed gravity anomalies.

The QPV itself obviously are closely related to endogenous processes of formation and development of density inhomogeneities of the Earth's crust and mantle, although not confined by them. The Earth's moment of inertia is changing during the redistribution of matter inside it, and as a consequence — the rotation regime and the corresponding gravity. Equilibrium Figure of the Earth is disturbed in the process of the redistribution, changing the gravity intensity. During isostatic restoration of the equilibrium patterns gravity changes once again. The range of processes mentioned generates the QPV gravity of the Earth. The reversible part of the process thus creates a periodic part of variation, and the irreversible part — a *non-periodic* part of the variations, which forms a stationary gravity anomalies.

There are correlation of large-scale mantle density inhomogeneities and tidal parameters of Earth, characterizing its tidal deformation. Earth tidal parameters (Love and Shida numbers) are based on the calculation of the relaxation amplitudes of gravity potential on the Earth surface and in its nucleus. Thereby a cross-correlation of QPV and the referred dynamic parameters of the Earth may be exist. This fact requires a separate studying.

Despite a low-intensity, anomalies of QPV gravity can be identified with confidence due to the peculiarities of the behavior of QPV curve time and the close inverse proportional correlation with the curves of vertical crustal movements. The latter one [Sobakar, 1972] is considered the result of commonness of processes in the upper mantle, affecting the QPV and the vertical movements. The total value of the QPV is treated as the sum of superpositions of variations of different origin, sign, period and amplitude. This total amplitude ultimately determines the evolution of Earth's gravity field caused by the evolution of the inhomogeneities of the crust and upper mantle.

3. The basis of monitoring. We call the *gravitational monitoring* a series of *periodically* repeated real-time *continuous* for a fixed period (Fig. 1) microgravity measurements and its processing subject to the influence of environment and area of application.

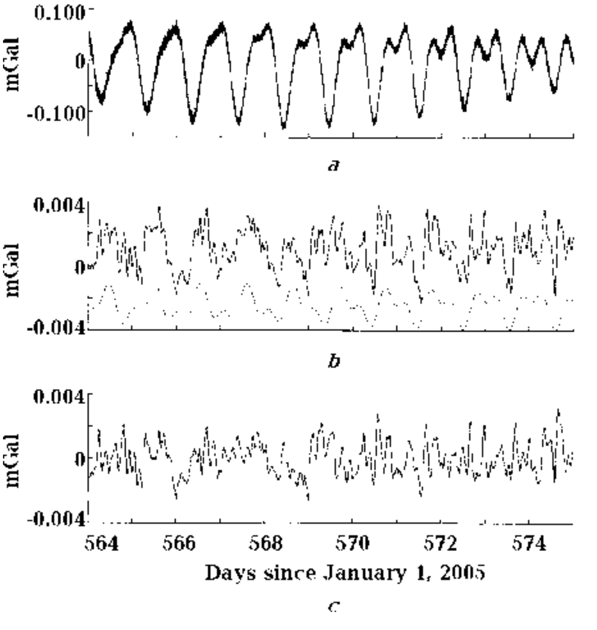


Fig. 1. 11-day series of measurements of gravity force: *a* — without filtering, *b* — with bandpass filtering, *c* — with correction for tidal effects.

The magnitude of the time interval depends on the quality of measurements, the measure of uncertainty of the observation data, the dynamics (amplitude and frequency) of the gravity.

Continuous connection of dynamics of the gravity and the environment parameters is the physical basis of gravity monitoring: thus to the undulations of the centimeter range are satisfied the gravity variations in a few mGal. If the deformation of surface relief of a certain area there is a direct consequence of the surface mass distribution, then gravity monitoring can be used to study a decompaction and fluid regime of the area studied.

The spatial distribution of variations of the vertical derivative values V_z of the gravity potential *directly correlates* with the area distribution of densities and temporal variations of V_z values clearly define the vertical variations of the fluid saturation.

Hardware base of the monitoring are a joint large-scale measurements of the terrain elevations by the GPS data and an absolute gravity values (hundreds of point on hundreds of km^2). The cheaper relative gravity measurement has serious limitations — the binding to the reference grid and the necessity for simultaneous accounting „zero creep". Nevertheless, in our case such measurements with proper methodical maintenance have the greatest prospect. A continuous measurements of gravity in boreholes may be used at some areas, as prevailing in the resolution that of the ground surveys due to the greater proximity to the disturbing sources and the elimination of surface effects. Some developments from the instrumental base of the marine gravimetry is advisable for use to compensate the influence of temperature and the other external factors.

4. On the extraction of a weak signal. In case studies of the 4D gravity monitoring (Geophysics, 2008. — **73**, № 6), the amplitudes of the signal are within the range of 20 mGal to 80 mGal. Within the boundaries of the active volcanoes of the signal amplitude increases to 300—600 mGal, and within watersheds ~200—250 mGal under a nonlinear accounting of "zero creep". Due to the repeatedness of measurements, fixing the residual gravity values at the observation point, we can estimate the accuracy of definition of the wanted signal in the time interval.

With the aim to extract a weak signal within the background noise in the gravimetry the methods of correlation analysis and calculation of some components of the gradients by the direct measurements of gravity are applied[2]. The signal wanted has distinguished by calculating the difference anomalies $\Delta g_d = \Delta g_m - \gamma h_z - \Delta g_{\mathrm{def}} - \Delta g_w$, where Δ — the difference between 2 adjacent time samples, γ — a free air correction, h_z — a vertical displacement; Δg_{def} — a Bouguer anomaly of deformation[3]; $\Delta g_w = 2\pi G \rho_w \varphi \delta_z = 42 \varphi \delta_z$ — the impact of groundwater. Also the additional connection to independent observations at a reference point located near the investigated area is used.

A certain improving of the weak signal in the background noise can be received through statistical filtering effect of the temperature fluctuations using the algorithms with fuzzy logic [Andó, Carbone, 2004]. If there is lack of length of series observations, may be useful a low-order polynomial approximation with the appropriate "calibration" of the polynomial order. Besides, there is advisable the comparing of the filtering results with the data obtained from a nearby checkpoint from the area of observations.

As in the case of the QPV gravity measurements, there are (Geophysics, 2008. — **73**, № 6) noted the correlation of a weak signal with vertical shifts. Assuming the different frequency of gravity strength and noise variations it is used a frequency filtering to enhance the signal wanted. The analogy can be seen again in the marine gravimetry. In the plain terrain areas the signal has a small gradient, and this approach, in our opinion, is ineffective. In such case the impact of noise must be considered in other ways — by the *changing the geometry* of observation networks, with the help of the temporal filtering, the *derivatives calculation*, and so on, as mentioned in [Sobakar, 1972].

5. On the method of monitoring. To organize the monitoring in it's methodical way, perhaps, is best as in [Sobakar, 1972], and to study the metrology nuances on the geodynamic polygon with a set of geophysical measurements. Lack of infrastructure and equipment will significantly influence on the costs of monitoring at the landfill — its increases by the uncertain value. The using of a digital recording will avoid some difficulties in the early stages of surveying by simplifying the scheme of surveying and also it accelerates the creation of a digital model of the object. To overcome the financial and technological deadlock we see in the cooperation of different institutions with common usage of equip-

[2] Just as in the marine gravimetric surveying are applied the calculation of the vertical and horizontal gradients of gravity and their complex interpretation. This method of interpretation is tested on offshore oil-gas structures [Yurgin, 2006].

[3] Contribution from changes in volume due to compression of environment around the disturbing source, which implies the displacement of density boundaries in a heterogeneous environment.

ment, personnel, methods and the common overview of the research on the common object[4].

The application of the classical scheme of measurements on a *regular* network of points and the subsequent recalculation of the gravity values by the well-known Poisson integral is suitable for regional studies (Geophysics. — 2008. — 73, № 6), but in the local conditions, often used for gravity monitoring [Bolotnova*,* 2007], it has a number of shortcomings [Dubovenko*,* 2002]. Besides, sometimes for many reasons the organization of regular network is impossible, and the conversion from an irregular network on a regular basis is more complex task than the inversion of the geological media structure from data measured.

A solution of the inverse problems of gravimetry with data given on a pseudo regular network with using the environmental models such as "endless profile" leads to ill-conditioned systems of linear equations, generating meaningless results. Because of this, and to proceed from mostly short length of the actual measurement profiles, it is expedient an alternative approach.

To interpret the measurements on the short profiles is proposed [Dubovenko, 2002] the system of the linear integral equations with rapidly decreasing kernels:

$$S_{n+1}^{+}(x)=$$

$$= v(x)-\frac{1}{2\zeta_n(x)}\int_{-\infty}^{\infty} S_n^{+}(\xi)\left(\cosh\frac{\pi(\xi-x)}{2\zeta_n(x)}\right)^{-1} d\xi + S_n^{+}(x),$$

$$S_{n+1}^{-}(x)=$$

$$= v(x)-\frac{1}{2\zeta_n(x)}\int_{-\infty}^{\infty} S_n^{-}(\xi)\left(\tanh\frac{\pi(\xi-x)}{2\zeta_n(x)}\right)^{-1} d\xi + S_n^{-}(x),$$

$$\zeta_0(x)=S_0^{+}(x)+S_0^{-}(x)=v(x),$$

$$\zeta_0(x)=S_0^{+}(x)+S_0^{-}(x), \quad n=\overline{0,\infty}.$$

With the account of the above the method of [Bolotnova, 2007] is effective only in certain conditions (a regional background is a polynomial of 1-st degree; there are known the *densities* and *positions* of the boundaries of gravitating bodies on the surface, and these bodies are similar or have a common contacts). It implies in particular the construction of a spatial density model of the medium divided into 3 stages: the separation of gravity sources anomalies and the identification of *effective* depths of their occurrence and the *quasidensity* (zero approximation), then the detection of *true* depths and densities of disturbing bodies by the solution of the 2D inverse problem (1-st approximation) and the final solution in the ADG-3D package.

We propose in the method [Bolotnova, 2007] to use the software [Starostenko et al., 2004] and the program kit obtained in the PhD study [Dubovenko, 2002].

6. On the interpretation of data. The purpose of monitoring is to assess the depth of the source of anomalies and the changes of the volume according to the deformation data of the relief. It requires a knowledge on the surface mass distribution (from the gravity data). Deformations of the earth surface are received by the GPS data, having a series of advantages over traditional surveying methods[5]. Near-surface heterogeneities of the medium structure (as karsts, baird, areas of flooding and loosening), the complex structure of the area (folding, salt tectonics, faults), the factors of the absorption of wanted signal (the temperature, the instrumental effects) are limiting the efficiency of monitoring, without reducing its practical value.

In (Geophysics, 2008. — **73**, № 6) does not take into account the peculiarity of the gravity variations: a fluctuations in the value of its derivatives depend on the fluctuations of the low-level geophysical events (as anomalous atmospheric masses (Fig. 2),

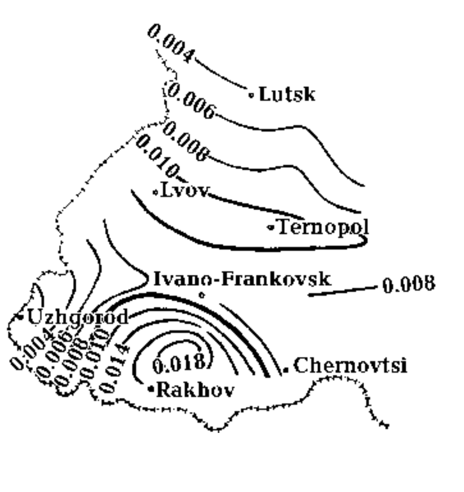


Fig. 2. Western Ukraine gravity change as a result of movement of air masses [Dvulit, 1999].

[4] This way of the integrated monitoring (a collaborative gravity network) comes well many western companies.

[5] The independence from the time of day and the weather conditions, the automation, the continuity, the completeness, the reliable binding to the network.

the snow masses, the groundwater level, forest cover and changes in topography (Fig. 3) due to anthropogenic activities. We can take into account these effects through the entering corresponding corrections [Dvulit, 1999] into the solution of direct problems of gravimetry in the areas of study (it is assumed that due to long-term monitoring period of station is known the structure beneath the area).

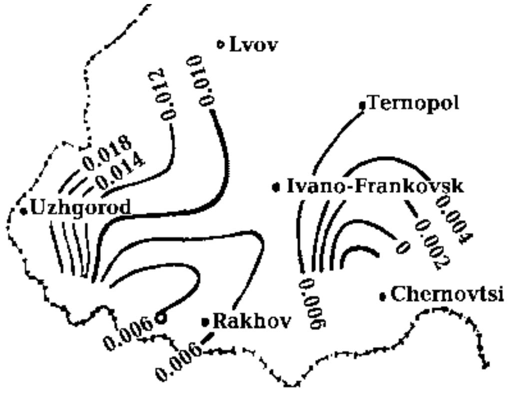


Fig. 3. Western Ukraine gravity changes as a result of mass transfer in the subsurface area [Dvulit, 1999].

The unjustified simplification of the analytical models of the geological media with the aim to reduce the ambiguity of interpretation in many cases may be the cause of incorrect results of calculations of the geometry sources and the vertical and lateral distribution of the density inhomogeneities. This especially takes place in cases where the external environment around the anomalous source is far from the assumptions of homogeneity. Reliable quantitative interpretation of the dynamics of the masses, for example, in the case of monitoring of hydrocarbons deposits can be produced providing the *well-known geometry* of the gravitating bodies (by the seismic data) and by the integrated interpretation of gravity field and deformation of relief data.

To avoid the ambiguity mentioned the the maximal accounting of the given *a priori* information about the media studied is needed. We propose to carry out it in 2 reciprocal supplementary ways:

1) by the constructing an appropriate model concepts (star-shape domains of known density inside the compact sets in the Banach space data);

2) by the adding into the discrepancy functionals in regularizing algorithms for some stabilizers of differential form, which eigenfunctions coincides with the eigenfunctions of the initial operators.

The section1 is justified in [Dubovenko, 2002], while section 2 — in [Chorna, 1999]. The solution of the specific inverse problems by the regularization is advisable by the algorithms of [Regularizing..., 1983] and similar one — on the basis of [Dubovenko, 2002; Starostenko et al., 2004].

7. Conclusions. The reasons considered above for gravity monitoring leads to next general issues.

The QPV of gravity should be taken into account in interpreting the results of 4D gravity in order to introduce appropriate corrections to the gravity surveys of different ages, to the long-term precision topographic mapping, to the clarifying the rheology of the investigated area, etc.

The weak signal must be extracted from noise by the *geometry control* of observation networks, by the temporal filtering or the *derivatives calculation*.

The measurements data interpretation on the short profiles give best results with the system of the linear integral equations with rapidly decreasing kernels being incorporated into existing 2D inversion.

The monitoring data must be corrected for the impact of fluctuations of the low-level geophysical events by the [Dvulit, 1999] technique.

An *a priori* information about the geological media may be accounted both by the selection of an appropriate media model and the special correction of regularization algorithms for ill-posed problems.

Repeated measurements of the gravity has a variety of applications but after the correction of the monitoring technique the results can be extended into the branch of QPV usage specified in [Sobakar, 1972]. The steps above seems to be necessary but maybe not sufficient to reduce the ambiguity of gravity monitoring interpretation. An experimental confirmation is expected.

From the gravity inversion of the monitoring data one can establish the *basic* image of density variations[6] not the absolute density values. There are great prospects for the interpretation of the temporal variations of gravity anomalies arising from changes of water-oil contact, or the level of reservoir water in the depths or any wells. It can be used as an inexpensive way of gravity monitoring of underground ecosystem of megapolises and the other geoecological solutions (the tracing the effects of floods, the landslides, the dynamics of pollution of underground basins, etc.).

---

[6] A decreasing of Δg stands for a decrease of hydrocarbons volume due to their production and thus, the lowering of gas-oil contact, but the increasing Δg stands for raising the level of the water layer of formation.

References

Aleksidze M. A. The solution of some fundamental problems of gravimetry. — Tbilisi: Metsniereba, 1985. — 412 p. (in Russian).

Andó B., Carbone D. A test on a neuro-fuzzy algorithm used to reduce continuous gravity records for the effect of meteorological parameters // Phys. Earth Planet. Int. — 2004. — **142**. — P. 37—47.

Bolotnova L. A. Eco-geological study of the state of geological environment in urban areas: geophysical aspects / V. V. Filatov, L. A. Bolotnova // IX Geophys. readings after V. V. Fedynskiy, 1—3 March 2007: Abstr. proceedings. — Moscow, 2007. — P. 43—44 (in Russian).

Bychkov S. G. On the calculation of gravity anomaly in the Bouguer reduction // IX Geophys. readings after V. V. Fedynskiy, 1—3 March 2007: Abstr. proceedings. — Moscow, 2007. — P. 73—77.

Chorna O. A. Investigation of inverse problems of the logarithmic potential theory for bodies resembling the given ones: Thesis for a cand. degree on phys.-mat. sci. / National Academy of Sciences of Ukraine. — Kiev, 1999. — 26 p. (in Russian).

Dubovenko Yu. I. Restoration of the contact boundary in layered medium // Geophys. J. — 2002. — **24**, № 6. — P. 36—41 (in Ukrainian).

Dvulit P. D. Methods of accounting of geophysical-tors on the variation of the gravity field of the Earth. — F. Dr. theses in Engineer. Sci: 05.24.01. Lviv Polytechnical. — Lvov, 1999. — 225 p. (in Ukrainian).

Regularization algorithms and a priori information / Eds. A. N. Tikhonov, A. V. Goncharsky, V. V. Stepanov, A. G. Yagola. — Moscow: Science, 1983. — 200 p.

Sobakar G. T. Quasiperiodic variations of the gravity field of the Earth, their nature and applied scientific value // Geophys. Proceedings AS USSR. — 1972. — **46**. — P. 31—42 (in Russian).

Starostenko V. I., Legostaeva O. V., Makarenko I. B., Pavlyuk E. V., Sharypanov V. M. On the automated input into a computer the images of the geological and geophysical maps with gaps of 1st kind and the interactive visualization of 3-D geohysical models and their fields // Geophys. J. — 2004. — **26**, №1. — P. 3—13 (in Russian).

Yurgin O. V. High-precision gravity prospecting for measurement of gravitational effects of shallow origin: Thesis for a cand. degree on engineer. sci. — Perm, 2006. — 26 p. (in Russian).

Yurkina M. I. Definition of measurements of the gravity field and the vertical crustal movements by the repeated gravimetric and levelling observations // Geodesy and Cartography. — 1978. — № 4. — P. 30—35 (in Russian).

Shallow coseismic slip deficit due to large (M7) strike-slip earthquakes

© ***Y. Fialko, 2010***

Institute of Geophysics and Planetary Physics, Scripps Institution of Oceanography,
University of California San Diego, La Jolla, USA
yfialko@ucsd.edu

Inversions of space geodetic data (in particular, Interferometric Synthetic Aperture Radar and Global Positioning System) from several large (moment magnitude ~7) strike-slip earthquakes indicate that coseismic slip in the middle of the seismogenic layer (at depth of 4—5 km) is systematically larger than slip at the Earth's surface. Fig. 1 shows an example of slip inversion from the April 4, 2010, M7.2 El Mayor (Mexico) earthquake, and Fig. 2 shows a compilation of slip inversions from severa well-documented events [Fialko et al., 2005], including our recent results for the El Mayor earthquake.

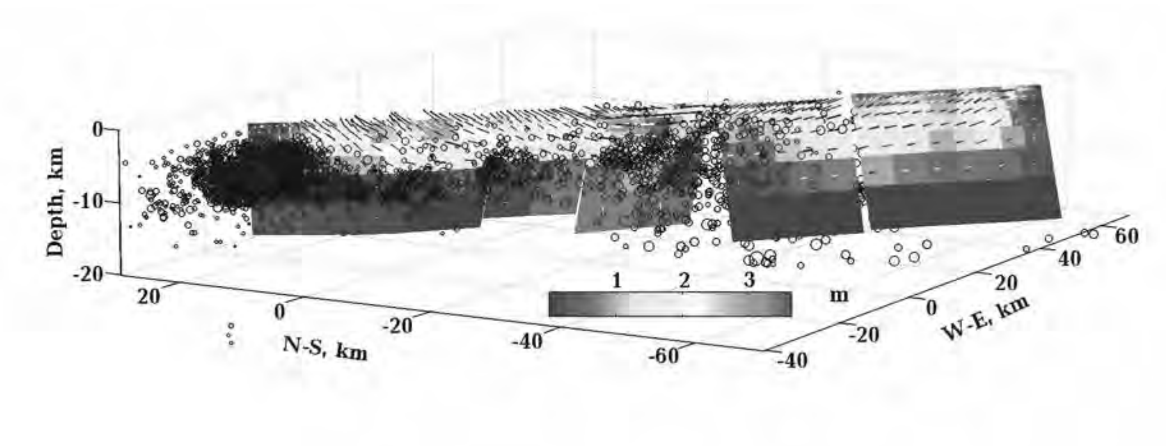


Fig. 1. Coseismic slip model of the El Mayor earthquake derived from inversion of InSAR and GPS Figure data. Colors denote the slip magnitude and arrows denote the sense of slip on the west side of the fault. Black circles denote precisely relocated hypocenters of aftershocks from the time period of 2 months following the mainshock (courtesy of Egill Hauksson).

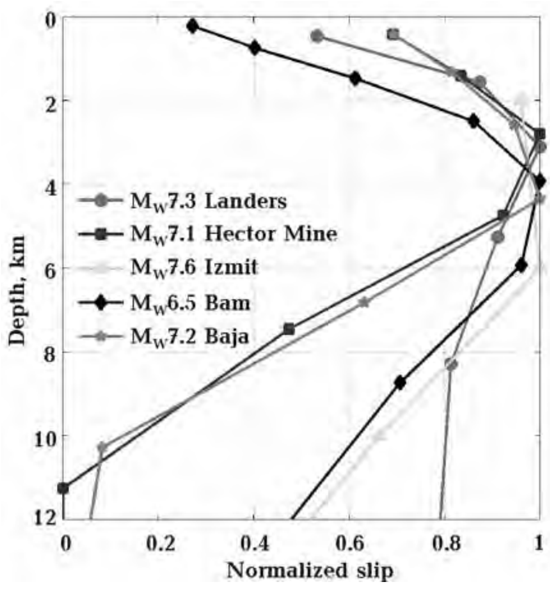


Fig. 2. Along-fault averaged distribution of slip for several large strike-slip earthquakes well constrained by the space geodetic data [Fialko et al., 2005]. The slip distribution from the El Mayor earthquake (magenta curve) follows the general pattern, with slip maximum in the middle of the seismogenic layer and shallow coseismic slip deficit.

This decrease in slip toward the surface, termed "shallow slip deficit", appears to be consistent with the idea that the uppermost brittle layer is velocity-strengthening, as suggested by experimental data [Marone, 1998; Scholz, 1998], there remain a question of how the coseismic slip deficit is accommodated throughout the earthquake cycle [Fialko et al., 2005]. To the best of our knowledge, events included in Fig. 2 were not associated with either shallow interseismic creep or robust shallow afterslip (in the amount sufficient to remove the coseismic slip deficit in the shallow crust) [Jacobs et al., 2002; Fialko, 2004; Fialko et al., 2005; Fielding et al., 2009]. We explore a possibility that the shallow slip deficit is associated with immature and/or infrequently slipping faults and is caused by the bulk inelastic yielding of the host rocks in the shallow part of the brittle crust.

References

Fialko Y. Evidence of fluid-filled upper crust from observations of post-seismic deformation due to the 1992 Mw 7.3 Landers earthquake // J. Geophys. Res. — 2004. — **109**. — P. B08,401.

Fialko Y., Sandwell D., Simons M., Rosen P. Three-dimensional deformation caused by the Bam, Iran, earthquake and the origin of shallow slip deficit // Nature. — 2005. — **435**. — P. 295—299.

Fielding E. J., Lundgren P. R., Burgmann R., Funning G. J. Shallow fault-zone dilatancy recovery after the 2003 bam earthquake in iran // Nature. — 2009. — **458**. — P. 64—68.

Jacobs A., Sandwell D., Fialko Y., Sichoix L. The 1999 (Mw 7.1) Hector Mine, California, earthquake: Near-field postseismic deformation from ERS interferometry // Bull. Seism. Soc. Amer. — 2002. — **92**. — P. 1433—1442.

Marone C. Laboratory-derived friction laws and their application to seismic faulting // Ann. Rev. Earth Planet. Sci. — 1998. — **26**. — P. 643—696.

Scholz C. H. Earthquakes and friction laws // Nature. — 1998. — **391**. — P. 37—42.

The onset of plate tectonics on super-Earth's using a damage rheology

© ***B. Foley[1], D. Bercovici[1], W. Landuyt[2], 2010***

[1]Yale University Department of Geology and Geophysics, New Haven CT, USA
bradford.foley@yale.edu
david.bercovici@yale.edu
[2]University of California San Diego, Scripps Institute of Oceanography, San Diego CA, USA
wlanduyt@ucsd.edu

Numerical simulations of mantle convection with a damage — grainsize feedback are used to develop scaling laws to predict conditions at which super-Earths would have plate tectonics. In particular, we introduce a new criterion for the onset of plate tectonics on terrestrial planets: that the viscosity of the lithosphere must be reduced to some critical value, which we assume to be the mantle viscosity. We formulate this criterion using the viscosity ratio between the pristine lithosphere and underlying mantle (μ_0/μ_1). These conditions are mapped out in regime diagrams of μ_0/μ_1 versus the damage fraction (f_a). The regime diagrams show that the transition from stagnant lid to mobile surface occurs for higher μ_0/μ_1 as f_a increases, with a power law relationship between those two variables; moreover, decreasing the healing constant (k_a) at the surface shifts the transition boundary to higher μ_0/μ_1. A scaling law is developed assuming that the transition between regimes occurs when damage, driven by convective stresses, reduces the viscosity in the lithosphere to a viscosity comparable to the mantle viscosity. This scaling law explains the numerical results well and can be applied to terrestrial planets. For the Earth, damage is efficient in the lithosphere, and viscosity can be reduced by 10 orders of magnitude with grains being reduced to a size on the order of a micron. When applied to super-Earth's, we find that larger planets are capable of larger viscosity reductions, but the viscosity ratio increases with planetary size at roughly the same rate. Therefore, contrary to previous results [e. g. O'Neill, Lenardic, 2007; Valencia et al., 2007], we find that the size of the planet has little effect on the convective regime that planet lies in. Factors such as surface temperature and thermal evolution may be more important in explaining the convective style of terrestrial planets.

References

O'Neill C., Lenardic A. Geological Consequences of Super-sized Earths // Geophys. Res. Lett. — 2007. — **34**. — P. 19204—19208.

Valencia D., O'Connell R. J., Sasselov D. D. Inevitability of Plate Tectonics on Super-Earths // Astrophys. J. — 2007. — **670**, № 1. — P. L45—L48.

Ancient CPU-GPU simulation of evolving fracture networks in a poro-elasto-plastic medium with pressure-dependent permeability

© *B. Galvan, S. Miller, 2010*

Bonn University, Bonn, Germany

Fluid flow in the earth is controlled by fracture networks that evolve in response to far field stress, local stress perturbations, and the pressure state of the fluid within them. The se-processes are very important for many geophysical systems, including earthquakes and volcanoes. Modelling the underlying physics is challenging because the time scales involved, from the elastic wave speed of crack growth to pressure diffusion and flow, make the se-problems numerically cumbersome. Our approach to

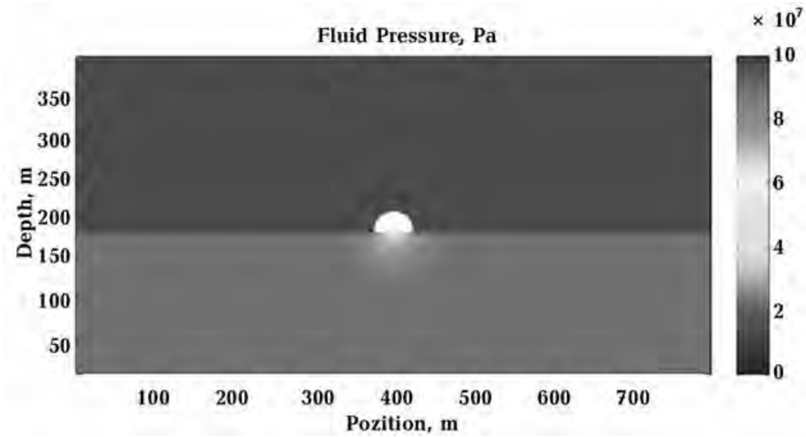


Fig. 1. CPU-GPU Poro-elasticity: 800×400points, grid size of 25 m. One day of simulation. Computation time: 42 min.

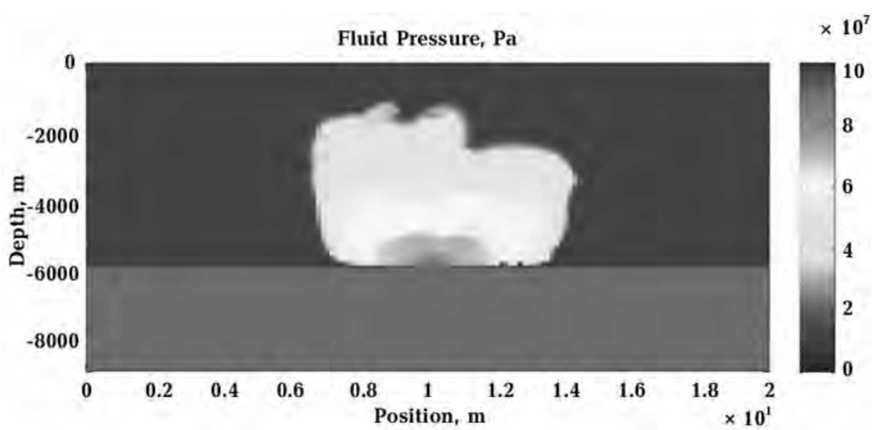


Fig. 2. Poro-elasto-plastic CPU (MATLAB): 150×100 points. Grid size is133 min *X* and 90 min *Y*. One day of simulation. Computation time: about 7 hours.

model the se-processes is to couple the elastic-plastic response of the solid porous matrix to a pressure dependent (nonlinear) diffusion model for the fluid flow. Changes in the fluid pressure introduce changes in stresses in the porous media, which may lead to either hydro-facture or shear fracture

within the solid. See page forces, forces related by gradients of pore pressure, can also promote delocalized crack formation. Many models of fracture propagation have been developed using finite elements or other numerical methods in order to overcome the high deformation of the grid, however costly re-meshing algorithms are necessary to accurate model the evolving crack. The complete model, nonlinear diffusion and poro-elasto-plasticity, is very computationally expensive. GPU technology allows high resolution modelling and easy implementation of explicit finite difference methods in an efficient way. We have taken advantage of many-cores GPU technology together with CPU and developed a high-resolution fully explicit finite difference model of nonlinear diffusion coupled with the mechanical response of poro-elasto-plastic medium (Fig. 1). In our algorithm, we can model both the propagation of previously de?ned fractures and fracture generation and growth in response to the evolving stress field. Our model includes shear and tensile cracking, which plays a dominant role in the hydraulic properties of the poro-elastic media as well as changes in the rheological properties. High resolution 2D simulations are presented showing the hydro-mechanical evolution of systems driven by high pressure sources at depth, such as some aftershock sequences and with application to volcano-mechanics. Using CPU-GPU approach numerical resolution can be increased to more than three times and computational time is decreased as much as at enth-compared with the CPU alone approach (Fig. 2).

Thermal conductivity of the deep Earth's minerals

© ***A. Goncharov, 2010***

Geophysical Laboratory, Carnegie Institution of Washington, Washington, USA
goncharov@gl.ciw.edu

Knowledge of thermal conductivity of the deep Earth's materials is critical for understanding of the Earth's thermal structure, evolution, and dynamics. Here we report on direct measurements of the lattice and radiative thermal conductivity of mantle and core materials under the pressure-temperature (*P-T*) conditions approaching those in the Earth's mantle and core by using optical spectroscopy and pulsed laser techniques in diamond anvil cells (DAC).

We developed and tested a new flash-heating high-pressure technique to measure thermal diffusivity, which involves time-resolved radiometry combined with a pulsed IR laser source [Beck et al., 2007]. The results for MgO, NaCl, and KCl obtained to 32 GPa and 2600 K agree with previous studies at low pressure and high temperature and enable tests of models for the combined pressure-temperature dependence of thermal conductivity. Preliminary results on the thermal conductivity of magnesium silicate perovskite to 125 GPa and 4000 K and [Goncharov et al., 2010] suggest a larger value than what was previously estimated, although the uncertainty is very large. Future accurate experimental measurements of the phonon contribution to the thermal conductivity of lower mantle materials will require a number of carefully crafted experiments under high pressure and temperature conditions to determine the thermal conductivity of all the materials used in the DAC. Measurements of the thermal conductivity of Ar are currently in progress and they will be presented at the meeting.

To determine the thermal conductivity of Fe and its temperature dependence at high pressures we use combined continuous and pulsed laser heating techniques. A thin plate of Fe is positioned in a medium (e.g., Ar), laser heating is applied from one side and the temperature is measured from both sides of the sample radiometrically. The thermal conductivity is determined by fitting the results of finite element calculations to the experimental results. This work is currently in progress.

Another technique of measurements of the thermal conductivity, time-domain thermoreflectance (TDTR), has been recently applied for the DAC studies [Hsieh et al., 2009]. A collaborative study of the thermal conductivity of MgO single crystal (as a benchmark sample) at high pressures with a group of Prof. D. Cahill (University of Illinois) is currently in progress, and the preliminary results will be reported at the meeting.

We will also present optical absorption data for lower mantle minerals to assess the effect of composition (including iron oxidation state), structure, temperture, and iron spin state on radiative heat transfer. The ultimate goal is to determine through these measurements the radiative thermal conduc-

tivity of the Earth's lower mantle. Optical absorption spectra have been measured at pressures up to 133 GPa for major mantle minerals, including ferropericlase (Mg, Fe)O, silicate perovskite $(Mg_{0.9}Fe_{0.1})SiO_3$, and postperovskite $Mg_{(1-x)}Fe_xSiO_3$ (x=0,1÷0,3). We find that optical absorption spectra of lower mantle minerals depend on composition (including iron oxidation state), structure, and iron spin state. We find that the presence of ferric iron in perovskite and ferropericlase strongly affects the optical properties, while the effect of the spin pairing transition may be more secondary [Goncharov et al., 2006; 2008; 2009; 2010]. We also show that post-perovskite exhibits larger than perovskite optical absorption in the near infrared and visible spectral ranges which may have a profound effect on the dynamics the lowermost mantle. Absorption spectra of ferropericlase up to 800 K and 60 GPa show minimal temperature dependence.

The estimated pressure-dependent radiative conductivity, k_{rad}, from these data is 2—5 times lower than previously inferred from model extrapolations [Goncharov et al., 2009], with implications for the evolution of the mantle such as generation and stability of thermo-chemical plumes in the lower mantle. Further work is required for an accurate assessment of the radiative component of the thermal conductivity of lower mantle minerals, including the study of compositional and structural properties, as well as the iron spin state. These include (but are not limited to) study of mantle minerals with compositions more realistic for the Earth's interior (e.g., containing Al).

I would like to acknowledge the following individuals for their contributions to this project: V. V. Struzhkin, D. A. Dalton, M. Wong, J. Ojwang, P. Beck, S. Jacobsen, S.-M. Thomas, J. Montoya, S. Kharlamova, B. Haugen, A. Savello, B. Militzer, R. Hemley, H. K. Mao, R. Kundargi, P. Lazor, Z. Konopkova, J. Siebert, J. Badro, D. Antonangeli, F. J. Ryerson, W. Mao, W.-P. Hsieh, D. G. Cahill. I acknowledge support from NSF EAR 0711358 and 0738873, Carnegie Institution of Washington, DOE/BES, DOE/ NNSA (CDAC), and the W. M. Keck Foundation. I wish to thank C. Aracne for her help in the thinning and cutting of the ferropericlase samples.

References

Beck P., Goncharov A. F., Struzhkin V. V., Militzer B., Mao H. K., Hemley R. J. Measurement of thermal diffusivity at high pressure using a transient heating technique // Appl. Phys. Lett. — 2007. — **91**. — P. 181914.

Goncharov A. F., Struzhkin V. V., Jacobsen S. D. Reduced radiative conductivity of low-spin (Mg,Fe)O in the lower mantle // Science. — 2006. — **312**. — P. 1205—1208.

Goncharov A. F., Haugen B. D., Struzhkin V. V., Beck P., Jacobsen S. D. Radiative conductivity and Oxidation State of Iron in the Earth's Lower Mantle // Nature. — 2008. — **456**. — P. 231—234.

Goncharov A. F., Beck P., Struzhkin V. V., Haugen B. D., Jacobsen S. D. Thermal conductivity of lower mantle minerals // Phys. Earth Planet. Int. — 2009. — **174**. — P. 24—32.

Goncharov A. F., Struzhkin V. V., Montoya J., Kharlamova S., Kundargi R., Siebert J., Badro J., Antonangeli D., Ryerson F. J., Mao W. Effect of Composition, Structure, and Spin State on the Thermal Conductivity of the Earth's Lower Mantle // Phys. Earth Planet. Int. — 2010. — **180**. — P. 148—153.

Hsieh W.-P., Chen B., Li J., Keblinski P., Cahill D. G. Pressure-tuning of the thermal conductivity of a layered crystal, muscovite // Phys. Rev. — 2009. — **80**. — P. 180302(R).

Earthquake as kinetic process

© ***O. Groza[1], V. Groza[2], 2010***

[1]Institute of Geophysics, National Academy of Sciences of Ukraine, Kiev, Ukraine
groza@igph.kiev.ua
[2]National Aviation University, Kiev, Ukraine
valentina.groza@gmail.com

1. At present time the forecast of earthquake is one of the most actual problems of geophysics and to a considerable degree one of the primary tasks of Earth physics. The basic unresolved question of

the earthquakes forecast is the prognosis of time of strong earthquakes occurrence. There are three models: dilatant-diffusion model, avalanche-unstable fracture model and stick-slip model. Unfortunately, while adequately describing the development of earthquakes, these models cannot predict earthquake. Actually they are only scenarios of earthquakes. At the same time it is essentially important that all these models consider ***earthquake as a process***. The models in question are based on solid mechanics and the physics of rock fracture. We propose the other approach based on thermodynamics, phase-transition theory and chemical kinetics. It allows to enter explicitly time into description of the process due to Arrhenius equation (as activation time). For elementary dislocation it is 10^{-13} s.

2. The kinetic approach allows to explain why aftershocks relaxation (Omori's law) has hyperbolic character and considerably differs from standard exponential relaxation of mechanical systems. The combination of the Boltzmann distribution law (statistical thermodynamics) and the Arrhenius equation (chemical physics) gives Omori's law ($N \sim t^{-1}$) directly.

From the same standpoint the role of fluctuations in the relaxation processes has been also analysed. Taking into account fluctuations it is necessary to replace the standard relaxation equation by

$$\frac{d}{dt}N = -\frac{N}{\tau_{\text{relax}}} + \phi(t)\sqrt{N} .$$

The solution is "stretched exponent", that is has long (hyperbolic) tail.

The kinetics of relaxation to equilibrium is limited by the speed of establishing the concentration fluctuations, which depends on the diffusion. In this case relaxation has character $N \sim t^{-3/2}$ instead exponential [Zel'dovich, Ovchinnikov, 1977]. Thus, in the real process $N \sim t^{-C}$ and $C \in [1;1.5]$.

3. The kinetic approach allows to look at diffusion in the crystals in the different way. The basic idea is that the diffusion process is not continuous — each act of displacement is accompanied by a relaxation. If Fick's law is explicitly added by the relaxation term, then instead of the diffusion equation the cable equation is obtained (it is similar for generalization of Fourier law realized by Cattaneo). Here it is essentially important that the problem of infinite rate of diffusion in this case disappears.

4. The solid rupture is traditionally considered as critical event, and strength is accepted to a constant of solid. Experience shows that it naturally depends on time and temperature. At present it is possible to state that such ***a limit of strength does not exist***. Tensile stress (load) p, fracture time τ and temperature T are uniquely related to each other [Zhurkov, 1968]:

$$kT \ln \frac{\tau}{\tau^*} = U - \text{const } p .$$

According to Russian Academician S. N. Zhurkov, the mechanism of rupture is connected with thermal fluctuation dissociation of bonds responsible for the strength. The sense of thermal fluctuation mechanism is that the potential barrier interfering rupture of bond is overcame due to of energy fluctuation. I. e. it is takes place over-barrier transition with characteristic exponential dependence of expectation time on temperature.

Our approach consists in the fact that transition occurs not due to the activation (energy excess), but due to the decrease of barrier height. The background is that the Zhurkov formula is equivalent in fact to ordinary thermodynamic relation

$$t = t_* \exp\left(\frac{\Delta G}{kT}\right).$$

The Gibbs "free energy" G has the physical dimension of energy but it is not energy per se. The Gibbs function is the pseudo-potential, which shows the natural direction of the dynamics of a thermodynamic system. The surface tension is defined is as $\gamma = \left(\frac{\partial G}{\partial s}\right)_{T,p,N_i}$. Reducing the height of the barrier means that the slope of the tangent to the barrier top decreases (in other words, the surface tension decreases). It is possible state the reverse — decreasing of surface tension reduces the height of the energy barrier. Since the surface tension is associated with the work expended to rupture of intermolecular bonds, then it is caused by these with bonds and inversely. Actually, γ is represented as ***work*** (per unit area) — cohesion work, i. e. it is a measure of intensity of work necessary for rupture. There are many reasons of decreasing the surface tension and thus reducing the strength, that is why it is difficult to define the strength limit uniquely.

References

Zhurkov S. N. Kinetic concept of solids strength // Bul. Academ. Sciences of the USSR. — 1968. — № 3. — P. 46—52 (in Russian).

Zel'dovich Y. B., Ovchinnikov A. A. Asymptotic of establishing equilibrium and concentration fluctuations // J. Experiment. Theor. Phys. Lett. Theoretical Physics. — 1977. — **26**, № 8. — P. 588—591 (in Russian).

Separation of thin layered geological medium fields

© ***D. Gryn', N. Mukoyed, 2010***

Institute of Geophysics, National Academy of Sciences of Ukraine, Kiev, Ukraine
dgrin@igph.kiev.ua

Within geological medium, as is known, various types of waves appear and multiply quickly and their propagation is accompanied by interferential phenomena. Complication of wave field is especially observable under condition of thin layered medium while conducting prospecting works by high frequency seismic methods. Application of more complex wave fields for studies of quantitative and qualitative features of geological medium is able to bring to incorrect conclusions. Therefore, for example, for solving the problems of seismic studies based on dynamic factors wave fields are to be of the same type and not damaged by accidental and regular waves-disturbances.

In our case difference method will be used which has physical basis under it [Gryn' M., Gryn' D., 2003]. The process of appearance, propagation and multiplying of various waves is accompanied by their interference. Therefore it seems natural to use procedures inverse to additive process: the search of algorithms for definition of form of separate waves or their groups and successive separation of the wave fields and their extraction. Difference method of target wave separation which is worked out is such one when according to direction of dominant wave on the temporal section or according to direction of assumed travel-time curve the differences between each pair of adjacent tracks are being determined successively. In this case, let us remind shared elements are extracted. However adjacent tracks of residual wave field superpose with inverse sign, in other words they are dubbed and on the edges of running processing windows the signals of target waves remain, therefore edge effects arrear, and for solving the problem we have conditions on the edges. Operators of bringing residual waves to initial form but with already extracted target waves have been worked out for elimination of dubbing and taking into account edge conditions.

Temporal section of target waves was determined as difference between input wave field and residual one. The procedure of target wave separation may be repeated in the direction of other dominant waves or according to other travel time curves.

Let us note that under land surface conditions of observation essential reason of instability of wave field effects of HFF may be considered with its variability of parameters, conditions of excitation and observing, and the major disturbances strong surface channel and main fields which superpose all the band of frequencies of reflected waves. Residues of these waves-noises have negative effect on the results of data processing by their dynamic properties.

Let us give an example of application of difference method on averaging of several tracks in the running window along the given direction according to the results of CMP obtained in the area near West Donbas mine, the Ternavska anticline (Fig. 1, *a*). The main disturbances for these data are residual modes of surface wave which frequency range coincides with frequency of useful reflected waves. The velocity of such waves is about 350 (±100) m/s. They have the same energy of amplitude as reflected waves and are present along all the profile.

The running window within which seismic tracks are averaging and separation of target waves and waves-noises takes place was realized on the base of 60 m, that is only 3 tracks are involved with a step of observation between them Δx=30 m. Sharpness of characteristics of the direction of a group of seismic receivers depends on the observation base. Under conditions of sub-horizontal occurrence of reflecting horizons the effect of the base upon tar-

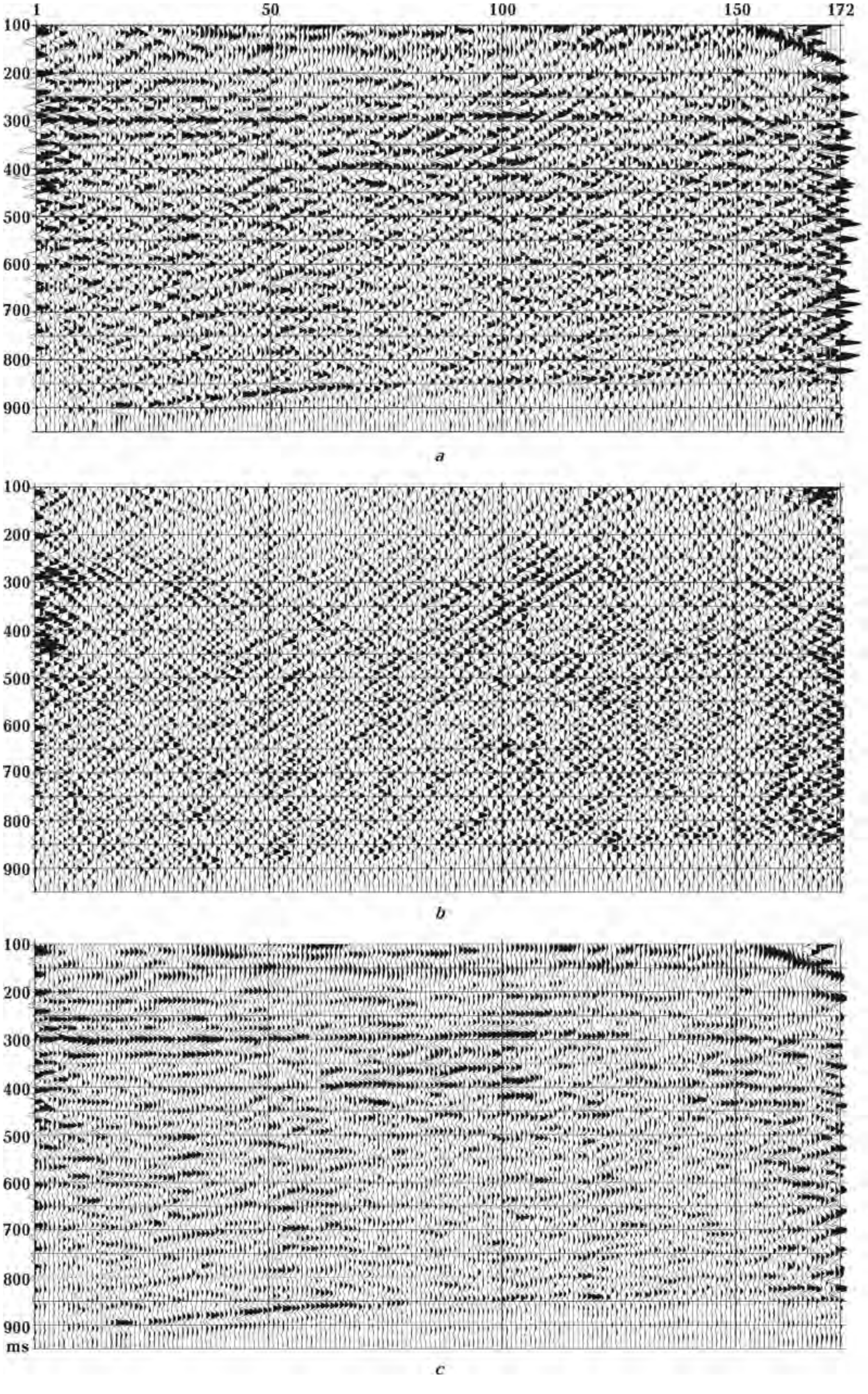


Fig. 1. Results of separation of reflected waves and waves-disturbances by difference method (Ternavska anticline, areas near West-Donbas mine): *a* — input data CMP; *b* — residual temporal section; *c* — temporal section of target reflected waves CMP.

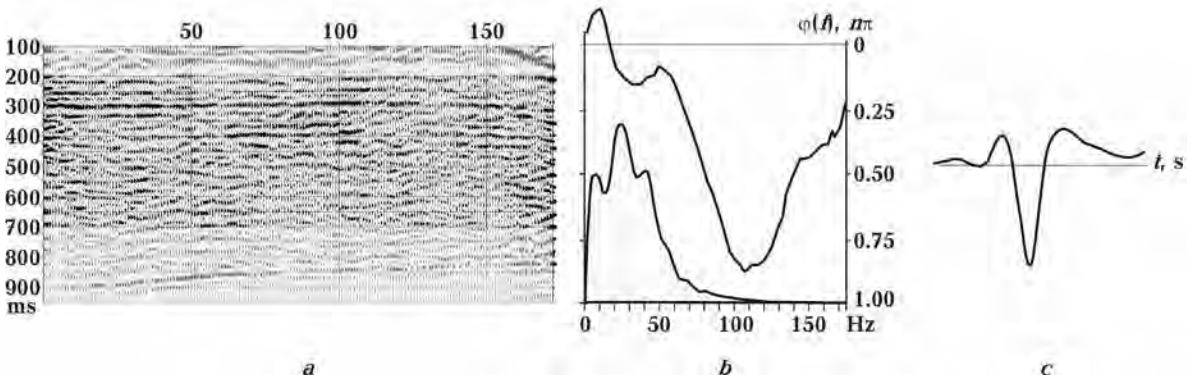


Fig. 2. Elementary signal obtained from the temporal section of target (sub-horizontal) reflected waves (CMP, Ternavska anticline, the area near West-Donbas mine): *a* — wave field used for statistical accumulation, *b* — AFH of elementary signal, *c* — elementary signal.

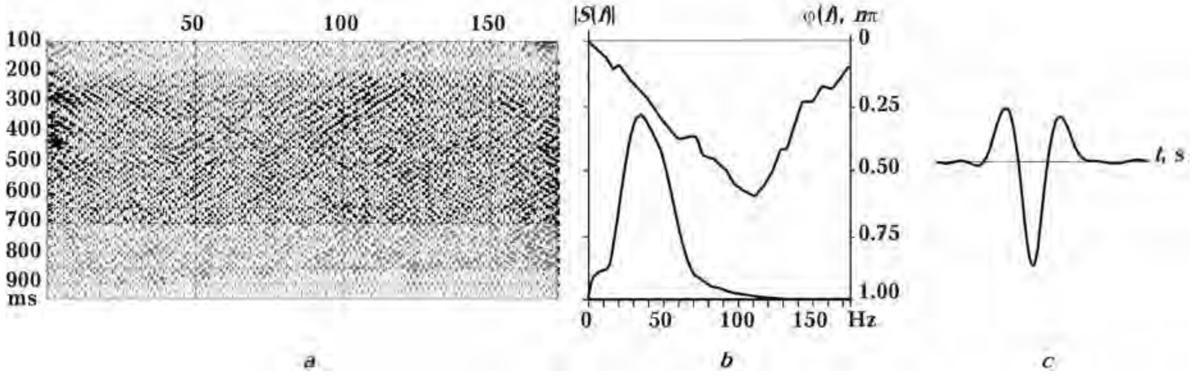


Fig. 3. Elementary signal obtained from the temporal section of the field of the residues of surface waves (CMP, Ternavska anticline, the area near West-Donbas mine): *a* — wave field used for statistical accumulation, *b* — AFH of elementary signal, *c* — elementary signal.

get waves is not strong but is observable on the residual temporal section. In this case the base is small and the angle of direction is wide. As a result of applying differential algorithm, on the residual temporal section (Fig. 1, *b*) diffracted waves and residual modes of surface waves have been revealed as well as disordered vibration slightly intense process.

Target waves on the temporal section (Fig. 1, *c*) are not complicated by disturbances, their dynamic and kinematic indications are not changed. They acquire stability and accuracy concerning input reflected waves, they are well correlated.

Non-complicated wave fields can be used, in particular, for determination of elementary signal that is an important stage for interpretation of seismic data. It is known that seismogram consists of impulse characteristics, elementary signal and different by their origin waves-disturbances. Temporal and spatial change of elementary signal gives additional information about physical properties of geological medium. It is as well important for increase of resolving capacity of seismic data because it is used in deconvolution.

For separation of elementary signal from seismograms statistical method of accumulating amplitude spectrum and continuous phase spectrum in complete angles [Gryn' M., Gryn' D., 2005], because there is a possibility of application of some elements of statistical analysis to them, in particular, determining of their mathematical expectation $M[\varphi(\omega)]$ through the whole range of frequencies of the signal spectrum.

As one can see from the given Figures elementary signal obtained from the target waves is change to some extent. It can be explained with the fact that reflecting boundaries coincide with the direc-

tion of statistical summation. As a result amplitude spectra are reinforced and complicated by deflections. The signal, depicted in Fig. 3 does not have this deficiency and looks as a “classical” elementary signal. It can be used for processing of fact materials by the method of phase de-convolution.

References

Gryn' D. N., Gryn' N. E. Algorithms for useful waves separation // Geophys. J. — 2003. — **25**, № 4. — P. 84—98 (in Urainian).

Gryn' M. Ye., Gryn' D. M. Statistical evaluation of phase spectra of seismic signals // Theoretical and applied aspects of geo-informatics. — Kyiv, 2005. — P. 126—137 (in Ukrainian).

The atmosphere heating due to wideband acoustic and shock waves propagating

© ***V. Gusev, 2010***

Lomonosov's Moscow State University, Moscow, Russia
vgusev@bk.ru

Acoustics waves propagating in the stratified atmosphere influence on its state. One of such mechanisms is the heating of atmosphere due to wave dissipation. It is well known [Golicyn, Romanova, 1968; Romanova, 1970] that the stratification of the atmosphere leads to some important effects associated with acoustics wave propagation. First of all is the exponential increase of velocity of particle of medium. It's mean that the nonlinear effects must be taken in account. The second effect is the significant increase of effective coefficient of dissipation. In addition, nonlinearity leads to formation of shock waves with narrow shock front. Finally the wave dissipation and corresponding energy flow is more significant in stratified atmosphere.

Acoustic waves are the important mechanism of interaction between different geospheres. Waves generated due to seismic activity and earthquakes influence on the atmosphere state. This phenomenon is important for prediction of long distance wave propagation, weather forecast and so on. Another application is the investigation of seismic activity themselves and prediction of strong seismic events [Gusev, Sobisevitch, 2010].

For wave profiles in stratified atmosphere the analytical solutions at large heights were obtained :

for periodical initial sinusoidal signal

$$V_S=\frac{1}{1+s}\left(-\theta+\pi\tanh\left[\frac{\pi}{4\Gamma(1+s)}\left(1+\sqrt{1+\frac{8\Gamma(1+s)^2}{\pi^2 s_0}}\right)\frac{\theta}{1+s/s_0}\right]\right),\ -\pi<\theta<\pi,$$

where the term with hyperbolic tan describes the shock front; and for positive phase of single *N*-shaped impulse

$$V_N=-\frac{\theta}{1+s}+\frac{1}{2\sqrt{1+s}}\left(1+\tanh\left[\frac{1}{4\Gamma\sqrt{1+s}}\left(1+\sqrt{1+\frac{8\Gamma(1+s)}{s_0}}\right)\frac{\theta+\sqrt{1+s}}{1+s/s_0}\right]\right),\ -\sqrt{1+s}<\theta<0.$$

Here $\theta=t-x/c_0$ is the retarded time, $s=\frac{2H}{z_{nl}}\int_0^x e^{x/2H}dx=2H\left(e^{x/2H}-1\right)$ is the effective distance, x —

height, Γ— coefficient of dissipation, $s_0 = \frac{2H}{z_{nl}}$, H is the standard atmosphere.

Using these expressions one can compute the heating atmosphere rate in accordance with equation

$$c_p \rho_0 \frac{\partial T}{\partial t} = -\frac{\partial}{\partial x} cE .$$

Here E is full energy of acoustical impulse

$$E = \rho_0 \int_{-T(z)}^{T(z)} u^2(\theta, z) d\theta .$$

This equation shows that temperature changing goes due to change of the energy flow. Taking into account that $\rho_0 = \rho_{00} e^{-x/H}$, $T(z) = T_0 \sqrt{1+s}$, one can obtain:

$$E = \frac{2\rho_{00} u_0^2 T_0^3}{3\sqrt{1+s_0\left(e^{x/2H}-1\right)}} \to \frac{2\rho_{00} u_0^2 T_0^3}{3\sqrt{s_0}} e^{-x/4H} .$$

Consequently the temperature increasing rate is

$$\frac{\partial T}{\partial t} = \frac{c u_0^2 T_0^3}{3 c_p} \frac{s_0}{2H} \frac{e^{3x/2H}}{\left(1+s_0\left(e^{x/2H}-1\right)\right)^{3/2}} \to \frac{\rho_{00} c u_0^2 T_0^3}{3 c_p \rho_0} \frac{1}{2H\sqrt{s_0}} e^{3x/4H} .$$

Thereby at large heights the significant temperature increasing takes place due to stratification and density decreasing. This phenomena radically differs from the influence of periodical signal, the amplitude of which reaches the saturation at large heights, so the temperature increasing rate due to periodical signal is almost independent on height.

References

Golicyn G. S., Romanova N. N. Vertical propagation of acoustical waves in atmosphere with variable on heights viscosity // Izv. AN USSR. Physics of Atmosphere and Ocean. — 1968. — **4**, № 2. — P. 210—214.

Romanova N. N. On vertical propagation of short acoustical waves in the atmosphere // Izv. AN USSR. Physics of Atmosphere and Ocean — 1970. — **6**, № 2. — P.134—145.

Gusev V. A., Sobisevitch A. L. Propagation of wideband and shock waves induced by seismic activity in the stratified atmosphere // Proc. 28th Intern. Conf. on Mathemat. Geophysics. — Pisa (Italy), 2010. — P. 76.

Accurate deteriminations of vibrational and radiative thermal transport in perovkite, rocksalt, and related structures

© ***A. Hofmeister, 2010***

Department of Earth and Planetary Sciences, Washington University, Missouri, USA
hofmeist@levee.wustl.edu

That thermal diffusivity is connected with cooling front speed has gone unrecognized until recently [Hofmeister, 2010]. Consequently, ballistic radiative transport affecting virtually all measurements inten-

ded to probe the vibrational mechanisms, even cryogenic, has been overlooked [Hofmeister, 2010]. In addition, failure to correct for refraction, not simply reflection, effects has provided large systematic errors in estimating radiative thermal conductivity from spectra obtained in the diamond anvil cell for lower mantle phases. [Hofmeister, 2010; (in review)]. Recent discovery that thermal diffusivity (D) is linked to thermal expansivity (α) [Hofmeister, (in review); Hofmeister, Whittington (in review)] coupled with overestimation of transport values for simple solids by acoustic models indicate that a much different theoretical approach wants consideration. To address these issues, to provide uncompromised values of thermal transport properties, and a means to extrapolate such data to lower mantle conditions, various spectroscopic-based measurements on analogues have been conducted and a new model is under construction.

We have recently measured the phonon component of thermal diffusivity (D) for lower mantle structures from ambient temperature (T) up to ~2000 K using contact-free, laser-flash analysis, from which effects of ballistic radiative transfer were removed. We focused on 13 compounds (e. g., synthetic $YAlO_3$:Tm, natural $Ca_{1.01}Mn_{0.001}Fe_{0.007}Ti_{0.99}O_3$) with perovskite and pervoskite-like structures, a dozen alkali halides, and a few magnesiowьstites, and also studied a wide variety of glasses and upper mantel materials. Perovskites [Hofmeister, (in review)] in the absence of phase transitions) are best described as D^{-1} following a low order polynomial in T. Ordered, cubic perovskites occupy a single trend, defining the contribution of the ideal lattice. Distortion, disorder, polymorphism, and temperature affect D^{-1} in a manner that is consistent with the damped harmonic oscillator-phonon gas model which relates phonon lifetimes to infrared peak widths. Combining our data with cryogenic measurements of $YAlO_3$ and $LaAlO_3$ [Agarwal et al., 2005] and similarly for fused silica [Agarwal et al., 2005] shows that the best description for $D^{-1}(T)$ is a proportionality to αT from ~0 K to the limit of measurements. At low T, $D^{-1} \sim T^3$, so acoustic modes dominate and $k_{lat} = k_0 + k_1 T$. Defects being present preclude scattering at sample walls, adding a small constant D_0^{-1} ~0,0001 mm^{-2} s as $T \to 0$, and an additional contribution of $k_{dfct} T^3$. Forms previously inferred for thermal insulators include systematic errors stemming from ballistic radiative transfer and/or interface resistance, and misunderstand mechanisms. Our results show that optical phonons largely govern heat transport of complex insulators, including glasses. Alkali halides behave differently wherein interactions of optic and acoustic modes govern heat transfer up to melting [Yu, Hofmeister, (in prep.)].

Visible-UV spectra of Fe^{2+} and Fe charge transfer in single-crystal perovskite-types have overall moderate absorption coefficients and flat baselines, consistent with reflectivity data, confirming that DAC spectra are plagued by insufficient baseline corrections. We find that diffusive radiative thermal conductivity values are similar to results obtained for olivines, permiting recasting of results to focus on iron concentrations for a given site speciation (e.g., [Hofmeister, 2007]).

Combining spectroscopic with direct heat transport measurements reveals microscopic mechanisms permitting extrapolation to the mantle. A detailed model with application to diverse materials will be presented in this talk.

References

Agarwal R. L., Riplin D. J., Ochoa J. R., Fan T. Y. Measurement of thermo-optic properties of $Y_3Al_5O_{12}$, $Lu_3Al_5O_{12}$, $YAlO_3$, $LiYF_4$, $LiLuF_4$, BaY_2F_8, $KGd(WO_4)_2$, and $KY(WO_4)_2$ laser crystals in the 80—300 K temperature range // J. Appl. Phys. — 2005. — **98**. — P. 103514.

Hofmeister A. M. Thermal conductivity of Earth’s deepest Mantle // Superplume: Beyond Plate Tectonics / Eds. D. A. Yuen, S. Maruyama, S. I. Karato, B. F. Windley. — Dordrecht: Springer, 2007. — P. 269—292.

Hofmeister A. M. Scale and directional errors in geophysical models and measurements involving heat transport: Implications for global power and temperatures // Izvestia (in review).

Hofmeister A. M. Scale aspects of heat transport in the diamond anvil cell, in spectroscopic modeling, and in Earth's mantle // Phys. Earth Planet. Inter. — 2010a. — **180**. — P. 138—147.

Hofmeister A. M. Thermal diffusivity of perovskite-type compounds at elevated temperature // J. Appl. Phys. — 2010b. — **107**. — P. 103532.

Hofmeister A. M., Whittington A. G. Effect of hydration and annealing on thermal diffusivity of fused quartz, fused silica, and their melts at high temperature from laser-flash analysis // J. Non-Crystalline Solids (in review).

Yu X., Hofmeister A. M. Thermal diffusivity of alkali and silver halides // J. Appl. Phys. (in prep).

Identification of magnetic carriers of original and secondary NRM components recorded in Devonian sediments from Podolia, SW Ukraine

© **M. Jeleńska[1], M. Kądziałko-Hofmokl[1], V. Bakhmutov[2], I. Poliachenko[2], P. Ziółkowski[3], 2010**

[1]Institute of Geophysics, Polish Academy of Sciences, Warsaw, Poland
bogna@igf.edu.pl
[2]Institute of Geophysics, National Academy of Sciences of Ukraine, Kiev, Ukraine
bakhm@igph.kiev.ua
[3]Faculty of Geology, University of Warsaw, Poland

Palaeozoic sediments are widespread in the west and southwest of the East-European platform. They are presented by carbonate-terrigenous rocks which thicknesses are increases westwards. The attention of geologists and paleontologists has been attracted for a long time to the Silurian — Lover Devonian sedimentary rocks because of quality of their exposure on the high and steep slopes of rivers and valleys, almost horizontal position, weak metamorphism and the abundance and breadth of fossils.

Most of paleomagnetic poles of Silurian and Devonian age published for the Russian Platform are coincident with the Late Palaeozoic part of the APWP. So, there is a suspicion that these poles are not well dated or are based on secondary magnetization. The Silurian-Devonian part of APWR is based mainly on extrapolation between best quality poles. Although apparently well defined, the Silurian-Devonian part lying close to the Carboniferous segment of the APWP needs verification by new reliable data, and the main problem is identification of magnetic carriers of NRN components recorded in Devonian red sediments.

New Paleomagnetic study of Devonian ferruginous sandstones and siltstones from Podolia revealed that the main direction was recorded during remagnetization in Permo — Carboniferous time. Thermal demagnetization of Natural Remanent Magnetization (NRM) showed that this component was carried by mineral with blocking temperature (T_b) about 600 °C. In several samples, at the end of demagnetization curves, besides this main component, we isolated Devonian direction with T_b close to the value of hematite (670—690 °C).

Thermomagnetic analysis giving decay curves of saturation remanence during heating SIRM(T) made for a whole rock gave T_b characteristic for hematite, but the presence of other minerals was not observed, especially mineral of $T_b \approx 600$ °C was not seen. Heating to 700 °C did not change composition of magnetic minerals. Thermomagnetic analysis made for the strongest component of NRM is similar to its thermal demagnetization — the main carrier of NRM is mineral with $T_b \approx 600$ °C. Intensity of NRM is about 1 % of SIRM intensity. It means that the main magnetic mineral observed on SIRM(T) curves — hematite — did not record any stable paleomagnetic direction. Comparison of hysteresis parameters of rock and AF demagnetization curves of NRM revealed that the magnetic grains which are the carriers of the main component of natural remanence are as hard as the grains of main mineral. Although their T_b is close to T_b of magnetite (≈600 °C) very high coercivity and remanence coercivity exclude magnetite or maghemite. The alternative is hematite with small content of titanium. Proper identification of this mineral has crucial significance for interpretation of NRM components. Regarding primary Devonian component found in some samples at the end of demagnetization curves we believe that it was recorded in small amount of hematite grains possibly of different origin then majority of hematite being the source of SIRM.

Petrologic studies based on scanning electron microscopy (SEM), wavelength dispersive spectroscopy (WDS) and X-ray diffraction (XRD) analysis revealed the presence of three main magnetic carriers:

1) detritic grains of hematite with small content of Ti — up to 3 % (size up to 100 µm),
2) authigenic, pure hematite crystals (1—2 µm size) occurring in the ferruginous cement of sandstones,

3) unidentified (Ti-hematite?) iron oxide, formed within the disintegrating detritic chlorite and biotite grains.

The detrital hematite (with small content of Ti) is a primary magnetic mineral contained inside the rock. This is a good candidate for being a carrier of the Devonian component of NRM. Unidentified iron oxides (Ti-hematite?) can be responsible for the Permo-Carboniferous remagnetization. Authigenic, pure hematite crystals (1—2 μm size) occurring in the ferruginous cement of sandstones are the main source of SIRM but majority of grains does not carry any stable component of NRM.

Lessons for Ukraine about recent strong earthquakes in the world

© ***A. Kendzera, Yu. Lisovoi, T. Amashukeli, L. Farfuliak, Y. Semenova, 2010***

Institute of Geophysics, National Academy of Sciences of Ukraine, Kiev, Ukraine
kendzera@igph.kiev.ua

Experience of catastrophic earthquakes that occurred one after another in Haiti (12/01/2010, with Mw=7.0) and in Chile (01/12/2010 with Mw=7.0), makes seismologists to re-evaluate their effects and to compare the situation with the seismic protection in these countries with the situation in Ukraine. Both earthquakes are confined to the powerful seismically active zone of the planet. Earthquake in Haiti occurred within a seismically active zone associated with the zone of collision of the Caribbean plate with the South America plate. An earthquake near Chile — with the feat of the Nazca plate under the South American continental plate [http://upload.wikimedia ..., 2010]. In both cases, the earthquake occurred in areas where strong seismic events is not uncommon, which made seismologists and leadership of both countries in advance to shape up for strong earthquakes.

Unfortunately, from a comparison of maps of general seismic zoning (GSZ) of the territory of Haiti [http://neic.usgs …, 2010] and maps of macroseismic manifestations of the 01/12/2010 earthquake [http://earthquake.usgs …, 2010], the intensity of seismic manifestations of the earthquake was, in fact, higher than predicted by seismologists to map of the Haiti GSZ. The level of projected acceleration of seismic vibrations on the map, which, with probability 90 % will not be exceeded over the next 50 years, corresponds to the average acceleration of seismic vibrations in the 7-balls earthquake. In fact, during the 12/01/2010 earthquake in the Port-au-Prince capital city of Haiti were observed 9 balls macroseismic effects (on 12 point scale). Clearly, projected onto the 7-ball impact homes and buildings could not remain 9-balls intact. As a result, the main shock and several hundreds of aftershocks have killed more than 280 thousand people, several million people lost their homes and jobs. According to the Inter-American Development Bank's the losses caused by the earthquake could reach 14 billion dollars [http://www.rbc.ua/rus …, 2010]. In addition, the experience of similar past disasters is well known that after their income level of the population is reduced on average by 30 %, despite the assistance provided by the international community.

The earthquake near the coast of Chile, was much more powerful, but according to official information, the number of his victims was much lower (780 person), primarily because the country for many years considerable attention devote for earthquake-protection design and construction, as well as for the protection from tsunamis. Especially intensive, this work is carried out after the 22/05/1960 quake with Mw=9.5, which is considered as the strongest since 1900, when the registration of seismic events in the world have been widely used the instrumental techniques.

Comparison of the earthquakes effects in Haiti and Venezuela shows the importance of properly assessing the level of Seismic risk of the sites of existing and planned buildings and structures. Adopted at this time in the world the concept of seismic protection includes the need for protection from earthquakes by each investor, owner and developer who are building houses and industrial buildings in seismic zones. At the same time, it should be noted that self-investors, owners and developers are unable to obtain the seismological information about the magnitude of the parameters of the maximum seismic effects, which with a given probability of exceeding can be realized at the site of the existing or projected development, and is needed for its seismic protection. This task must be decided by the State.

In particular, the Ministry of Regional Policy and the building of Ukrainian together with the National Academy of Sciences have developed and introduced into operation at 2007, State Building Codes B.1.1:12-2006 “Building in seismic regions of Ukraine” [State …, 2006], where in Appendix A, the table of communities with specification of seismic shaking projected intensity, and in Appendix B — the general seismic zoning maps, which shows the predicted intensity of seismic shaking on a MSK-64 macroseismic scale, which is likely 90, 95 and 99 percent will not be exceeded over the next 50 years. In the main text of this document the provides rules for the use of seismic data as well as rules for the protection of structures and buildings in the different seismic conditions [State …, 2006].

The territory of Ukraine to the south and southwest is comprehended by the influence of powerful seismically active zone of the planet, which resulted from the collision of large tectonic plates: Eurasian, African, Arabian and Indian. The belt stretches from the Azores through the Mediterranean and Black Sea, Caucasus, Central Asia and further to the Hindu Kush, Tibet — the island of Sumatra, and further south, where it connects with the Pacific planetary seismically active zone. Influence from this zone extends to the western regions of Ukraine, Bukovina, south-western part of the Odessa region, south of Mykolaiv, Kherson, Zaporozhye regions and the territory of Crimea. The belt includes the Carpathian arc with strong subcrustal earthquakes in the Vrancea area, which in the past 5 times shaken not only the territory of Ukraine, but even Moscow and St. Petersburg. Earthquakes in the territory of Ukraine were in the past, recorded by seismic stations and are felt by the people at present and, unfortunately, will be in the future.

Seismic risk in Ukraine is high also because of insufficient knowledge of local seismicity and the understatement of the real seismic hazard assessment regulatory by document SNIP-II-7-81 "Building in seismic areas" [Seismic …, 1980], which operated in Ukraine until 2007. Determination of the real parameters of seismic hazard requires instrumental seismological observations of the local seismic activity and of the powerful remote seismic events.

In the conditions of increasing anthropogenic loads and a significant depreciation of fixed assets in Ukraine the risks associated with the hazardous effects of earthquakes significantly increased, which, in turn, increases the level of technological risk in different sectors of the economy. Accompanied by faults, landslides, mudflows, tsunamis and other hazards, earthquakes can cause considerable material and social consequences.

In recent years, with a sufficiently short time intervals, there were a catastrophic earthquake (12.05.2008 in China with Mw=7.8; 05.10.2008 in Kyrgyzstan with Mw=6.6; 06.04.2009 in Italy with Mw=6.3; 13.01.2010 at the Haitian with Mw=7.0; 26.02.2010 in Japan with Mw=7.2, 27.02.2010 in Chile with Mw=8.8; 04.03.2010 in Taiwan with Mw=6.4 etc.), which led to deaths and huge financial losses. In most cases, the destruction of structures and buildings is due to underestimation of the real seismic hazard of areas. In turn, destroyed the house killing, maiming and causing man-made disasters. Losses from earthquakes can be substantially reduced with appropriate technical and organizational preparations for them. Properly determining the level of seismic hazard and its inclusion could to avoid casualties and material losses minimized.

In preparation for future earthquakes in the Ukraine it is current the studies of the seismic resistance of existing buildings and structures in areas where the real seismic hazard on the new seismic GSM-2004 maps [State …, 2006] proved to be higher than specified on the regulatory CP-78 map [Seismic …, 1980] current up to 2007. The input data should serve on observations of local and teleseismic earthquakes at seismic stations located in the studied areas, or as close as possible to them.

The world's modern science-based concept of effective seismic protection include: the identification of quantitative parameters of real seismic hazard and risk reducing, the vulnerability of populated areas by improving the seismic resistance of existing buildings and structures, development and implementation of earthquake-resistant construction norms that meet the real seismic hazards, monitoring of seismic design and regular maintenance of buildings and facilities, raising awareness by education and training, early warning of the emergence of a strong earthquake and rapid response, rehabilitation victim populations and areas; insurance against the effects of earthquakes.

Experience in the field of seismic protection of such developed countries as Japan, USA, Canada, France, Italy and others, shows that the basis of seismic protection in Ukraine should be the introduction of earthquake-resistant design and construction of housing and industrial facilities on the basis of objective knowledge about the quantitative parameters of real seismic hazard in their areas of deployment and on concrete construction sites. Knowledge of the real seismic hazard, along with reliable data on the seismic vulnerability of structures is necessary for earthquake resistant design and develop measures to reduce the seismic risk. The main link, which provides objective data for ac-

tivities of protection against earthquakes, are seismic observations.

S. I. Subbotina Institute of Geophysics of NAS provides activity of a seismic stations network, which actually performs the role of the national seismological network for providing information for all seismic protection works. The network provides standardized data on seismic manifestations on the territory of Ukraine. On these data the evidence-based forecasts of seismic hazard values are determined. It is necessary for central and local authorities to ensure the stable development of the seismic regions, as well as for the research institutes of other ministries and agencies working in related industries of earthquake-resistant design and construction.

Results of seismic observations are widely used in solving problems in key directions of fundamental research of IGPh of NAS: the study of the tectonics, structure, geodynamics, and evolution of continental and oceanic lithosphere; construction three-dimensional integrated geophysical and petrophysical models of geological structures in order to predict mineral development and introduction of new technological systems for processing and interpreting geophysical data; geophysical studies of the environment in order to predict seismic hazards and other threats to natural phenomena. Geodynamic processes that are constantly changing stress-strain state of geological environment, not only in seismically active zones, but as it is now scientifically proven, in the territories of ancient platforms of planet, requires permanent monitoring tools.

The integration of seismic and other geophysical studies can learn communication geophysical fields with the preparation of strong earthquakes sources.

Conclusion. Earthquake-resistant design and development of anti-seismic measures require knowledge of the quantitative parameters of the real seismic hazard and seismic data on the vulnerability of structures. The main link supplying objective data for activities to protect against earthquakes are seismological observation.

To obtain reliable baseline data is necessary to ensure the further expansion (increase in the number and uniformity of the distribution) network of seismic stations and its reequipment by modern equipment and software.

References

http://upload.wikimedia.org/wikipedia/ru/2/22/Tectonic_plates(rus).png

http://neic.usgs.gov/neis/eq_depot/2010/eq_100112_rja6/neic_rja6_w.html

http://earthquake.usgs.gov/eqcenter/shakemap/global/shake/2010rja6/

http://www.rbc.ua/rus/newsline/show/mezhamerikanskiy_bank_razvitiya_ushcherb_prichinennyy_ emletryaseniem_ gaiti_mozhet_ dostigat_14_mlrd_doll_ 16022010

Seismic zoning of the USSR. (Methodological framework and regional description of the 1978 map) // Eds. V. I. Bune, G. P. Gorshkov. — Moscow: Nauka, 1980. — 308 p. (in Russian).

State building codes SBC B.1.1-12: 2006 "Building in seismic regions of Ukraine”. — Kiev: Ministry of Construction, Architecture and Housing and Communal Services of Ukraine, 2006. — 84 p. (in Russian).

Melt segregation and matrix compaction: closed governing equation set, numerical models, applications

© ***Ya. Khazan[1], O. Aryasova[1], 2010***

Institute of Geophysics, National Academy of Sciences of Ukraine, Kiev, Ukraine
ykhazan@gmail.com; oaryasova@gmail.com

Partially molten systems are commonly modeled as an interpenetrating flow of two viscous liquids and are therefore described in terms of fluid mechanics [Drew, 1983; McKenzie, 1984; Nigmatulin, 1990]. In the gravitational field a liquid filling a viscous permeable porous matrix is in mechanical equilibrium only if its pressure gradient is equal to the hydrostatic one, and the pressures of the liquid and matrix are the same. If the liquid and matrix densities differ, with the liquid forming an interconnected network, the two conditions cannot be satisfied simultaneously, and the liquid segregates from the matrix while the latter compacts. The averaged momentum and mass conservation equations for a multi-phase medium are formulated separately for every phase. Considering the energy conservation

equation, this results in 4*N*+1 equations for a *N*-phase medium while the number of unknowns is 5*N* (3*N* velocity components, *N* pressures, temperature, and *N*–1 independent phase fractions). Therefore, for the problem to be fully determined it becomes necessary to add *N*–1 coupling equations. Khazan (2010; on review at GJI) and Khazan and Aryasova (Rus. Earth Phys., 2010, in press) derived a general equation (the mush continuity equation, MCE) closing the governing equation set. Its simplified 1D form valid for a two-phase system in the case of low-melt-fraction mush and linear matrix rheology, together with equation describing the rate of the inelastic porosity change [Scott, Stevenson, 1986], constitute a closed subset of governing equation set:

$$\frac{\partial}{\partial z}\frac{k(\varphi)}{\mu}\left(\frac{\partial(p_l-p_m)}{\partial z}-\Delta\rho g\right)=\varphi\frac{p_l-p_m}{\eta},$$

$$\frac{\partial\varphi}{\partial t}=\varphi\frac{p_l-p_m}{\eta}, \qquad (1)$$

where p_l, and p_m are the melt and matrix pressure, respectively, φ is the melt fraction or porosity, $k(\varphi)\propto\varphi^n$ is the matrix permeability, $\Delta\rho=\rho_m-\rho_l$ is the difference between the matrix, ρ_m, and melt, ρ_l, densities, η and μ are matrix and melt viscosities, correspondingly, n=2 to 3, g is acceleration due to gravity; Z axis points upward. Let L be the thickness of the partially molten zone, and φ_0 be the maximum of the initial porosity distribution. In terms of dimensionless coordinate $\zeta=z/L$, time $\tau=t\Delta\rho gL/\eta$, melt overpressure $\Pi=(p_l-p_m)/\Delta\rho gL$, and porosity $\psi=\varphi/\varphi_0$ the equations may be written as

$$\frac{\partial}{\partial\zeta}\psi^n\left(\frac{\partial\Pi}{\partial\zeta}-1\right)-\gamma_c\psi\Pi=0,\quad \frac{\partial\psi}{\partial\tau}=\psi\Pi,$$

where

$$\gamma_c=\frac{L^2}{\delta_c^2},\quad \delta_c=\sqrt{\frac{k(\varphi_0)\eta}{\varphi_0\mu}}, \qquad (2)$$

γ_c and δ_c are referred to as the compaction/segregation parameter and length, respectively. If coordinate is normalized by the compaction length, the first of Eqs. (2) does not contain γ_c [Grègoire et al., 2006] but it appears instead in the boundary conditions.

In what follows two characteristic situations referred to as segregation and compaction are considered. The former is a model of the evolution of a bounded partially molten zone. Its outer boundary coincides with solidus where the porosity and pressure difference vanish. The boundary and initial conditions are $\Pi(\tau,0)=\Pi(\tau,1)=0$, $\varphi(0,\zeta)=4\zeta(1-\zeta)$. For compaction (of bottom sediments, e. g.), it is assumed that the bottom is impermeable, and porosity at τ=0 is the same throughout the layer, so that: $\partial\Pi(\tau,0)/\partial\zeta=1$, $\Pi(\tau,1)=0$, $\psi(0,\zeta)=1$.

The solutions to Eqs. (2) are shown in Fig. 1 for segregation, and Fig. 2 for compaction. One may

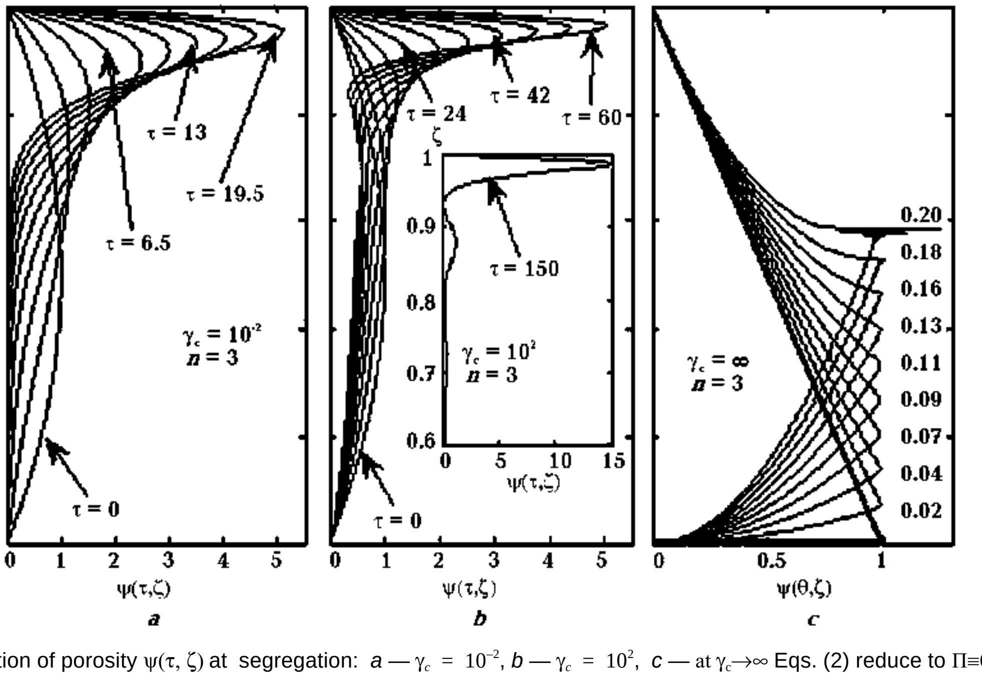


Fig. 1. Evolution of porosity $\psi(\tau,\zeta)$ at segregation: *a* — $\gamma_c=10^{-2}$, *b* — $\gamma_c=10^2$, *c* — at $\gamma_c\to\infty$ Eqs. (2) reduce to $\Pi\equiv0$, $\partial\psi/\partial\zeta\theta=-\partial\psi^n/\partial\zeta$ with и being a formally introduced time variable $\theta=\gamma_c\tau$. Note that the first and the second waves at $\tau=150$ (*b*, inset) contain 57 and 13 % of the melt, respectively, with the rest of the melt residing in the tail.

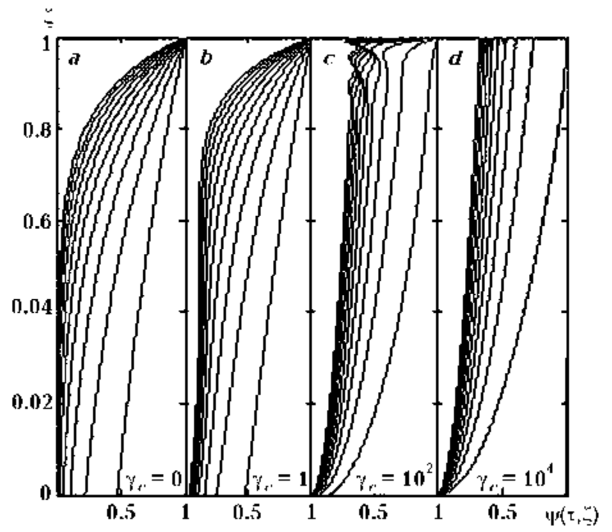


Fig. 2. Compaction of the bottom sediments at: *a* — $\gamma_c = 0$, *b* — $\gamma_c = 1$, *c* — $\gamma_c = 10^2$, *d* — $\gamma_c = 10^4$ ($n = 3$).

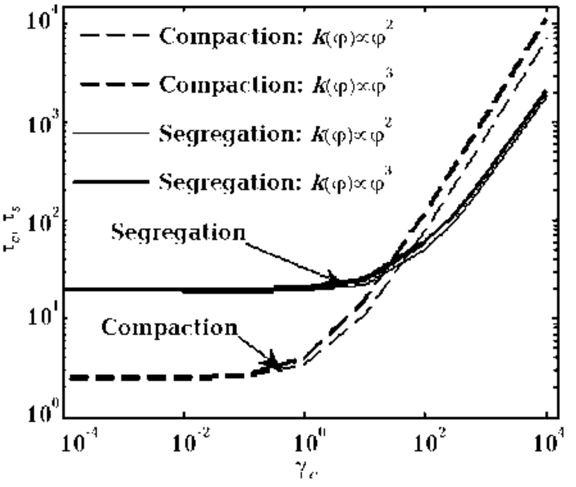


Fig. 3. Characteristic time of compaction τ_c and segregation τ_s vs. γ_c.

see from Fig. 1 that at low ãc practically all the melt segregates to the roof with amplitude of the porosity growing with time (Fig. 1, *a*). The pressure gradient remains hydrostatical in the enriched layer and evolves to zero in the low-melt fraction tail. At high γ_c (Fig. 1, *b*) a wave structure develops with the dimensionless pressure being generally low and sigh reversible, and a significant part of the melt remaining trapped in the tail. The case $\gamma_c = \infty$ (Fig. 1, *c*) corresponds to $\Pi \equiv 0$ (or $p_l = p_m$). The porosity amplitude remains the same (i. e. no segregation occurs), and it takes $\partial\psi/\partial\zeta$ a finite time to reach the -8 implying a numerical instability, which is absent from the finite γ_c models. The variation of porosity while a liquid is expulsed from a compacting porous layer (Fig. 2) is similar to that at segregation indicating that a property to generate a wave-like structure becomes more pronounced with increasing γ_c, i. e. at high melt viscosity. A large pluton layering [Wager, Brown, 1968] may be due to this wave structure, which is supported by the observation [Brown, 1973] that layered intrusions are commonly intrusions of a tholeiitic basalt while those of the alkali basalt parentage are rare, which may be due simply to about an order higher viscosity of the tholeitic magmas.

The dependence of characteristic compaction, τ_c and segregation, τ_s, times on γ_c , is shown in Fig. 3. In dimensional variables an approximate fit to these results may be written as follows:

$$t_c \approx 2.49\frac{\eta}{\Delta\rho g L} + \frac{L}{V_D}, \quad t_s \approx 19{,}5\frac{\eta}{\Delta\rho g L} + 0.25\frac{L}{V_D},$$

$$V_D = \frac{\Delta\rho g k(\varphi_0)}{\mu\varphi_0}, \tag{3}$$

where V_D is the Darcy's velocity. The L^{-1} scaling of the compaction/segregation times at low γ_c effectively constrains the thickness of compacting porous sediments as well as the maximum possible thickness of the partially molten zone. Really, if the mushy layer thickness increases gradually, due to, for instance, sedimentation with a rate of r_d then the steady sediment thickness, L_d, may be estimated as $L_d/r_d = t_c$ wherefrom $L_d \approx 1.7\sqrt{\eta r_d/\Delta\rho g}$. Similarly, let a protokimberlite melt result from a decompression melting of a diapir floating at a velocity V_d with its temperature varying along an adiabate. The melting starts when the diapir top reaches the intersection level of the adiabate and solidus, and maximum possible thickness of the molten zone, L_s, may be estimated as $L_s \approx\ \approx 4.5\sqrt{\eta V_d/\Delta\rho g}$. The estimates of L_d and L_s are valid if $\gamma_c >> 2$ for the compaction problem or $\gamma_c>>80$ for a segregation one. Also, Darcy's velocity is to be large, namely $V_D >> r_d$ at compaction and $V_D>>0.25V_d$ at segregation. These estimates relate to an evolution of a porous layer filled with a low viscosity liquid, and may be used to estimate, for instance, a steady thickness of porous marine sediments, or a maximum possible thickness of a partially molten zone filled with a low viscosity magma (kimberlite, carbonatite) at the moment of segregation. To illustrate the latter case, adopt the following parameter values: $\eta = 10^{19}$ Pas, $\Delta\rho = 100$ kg·m^{-3}, $V_d = 3$ cm·y^{-1}, $k(\varphi)=a^2\varphi^3/270$ [Wark et al., 2003], grain size $a = 1$ mm, $\varphi_0 = 0.01$, $\mu = 0.1$ Pas. Then compaction/

segregation length $\delta_c = 6$ km, $V_d = 30$ cm·y^{-1}, $t_s = 0.2$ My, $L_s = 8$ km, $\gamma_c = 1.7$. As soon as melt segregates, new partially molten zone grows, and the sequence of the events repeats until the whole diapir passes by the melting level. A diapir size, D, can be estimated based upon diameters $D = 20$ to 80 km of low-amplitude uplifts known to correlate with kimberlite fields [Kaminsky et al., 1995]. Therefore, the decreasing dependence of the segregation time on a mushy layer thickness implies formation of clusters of $D/L_s = 3$ to 10 low volume eruptions of almost the same age and composition. An attractive feature of the model is that it relates the kimberlite origin to a localized incipient melting.

References

Brown P. E. A layered plutonic complex of alkali basalt parentage; the Lilloise Intrusion, East Greenland // J. Geol. Soc. London. — 1973. — **129**. — P. 405—418.

Drew D. A. Averaged field equations for two-phase flow // Ann. Rev. Fluid Mech. — 1983. — **15**. — P. 261—291.

Grégoire M., Rabinowicz M., Janse A. J. A. Mantle mush compaction: A key to understand the mechanisms of concentration of kimberlite melts and initiation of swarms of kimberlite dykes // J. Petrol. — 2006. — **47**. — P. 631—646.

Kaminsky F. V., Feldman A., Varlamov V., Boyko A., Olofinsky L., Shofman I., Vaganov V. Prognostication of primary diamond deposits // J. Geochem. Explor. — 1995. — **53**. — P. 167—182.

McKenzie D. The generation and compaction of partially molten rock // J. Petrol. — 1984. — **2**. — P. 713—765.

Nigmatulin R. I. Dynamics of multi-phase media. — New York: Hemisphere, 1990.— **1**. — 507 p.

Scott D. R., Stevenson D. J. Magma ascent by porous flow // J. Geophys. Res. — 1986. — **91**. — P. 9283—9296.

Wager L. R., Brown G. M. Layered Igneous Rocks. — Edinburgh, London: Oliver, Boyd, 1968. — 588 p.

Wark D., Williams C., Watson E., Price J. Reassessment of pore shapes in microstructurally equilibrated rocks, with implications for permeability of upper mantle // J. Geophys. Res. — 2003. — **108(B1)**. — DOI:10.1029/2001JB001575.

Interactive visualization of large-scale numerical simulations with GPU-CPU systems

© ***M. Knox, P. Woodward, 2010***

Laboratory of Computational Science and Engineering,
University of Minnesota, Minneapolis,
MN, USA

We present a method for pipelining results from large-scale fluid dynamical simulations in such as way as to exploit the exponentially increasing computational capacity of the latest generation of multicore CPUs, many-cores and GP-GPUs. Exploiting this technique, together with an integration with several data post-processing and visualization utilities has enabled numerical experiments in computational fluid dynamics to be performed interactively on a new, dedicated system in our lab at the University of Minnesota. This method provides an immediate, user controlled visualization of the resulting flows on the LCSE PowerWall display as well as through a globally accessible html and java web interface. The code restructuring required to achieve the necessary computational performance boost, as well as the interactive visualization are described. Requirements for these techniques to be applied to other codes are discussed, and our plans for tools that will assist programmers elsewhere to exploit these techniques are briefly described. Examples showing the capability of the new system and software are given for various applications in turbulent hydrodynamics, stellar flows, and mantle convection.

High resolution study of temporal variations of induction vectors

© T. Klymkovych[1], I. Rokityansky[2], Yu. Horodysky[1], A. Isac[3], 2010

[1]Carpathian Branch of Institute of Geophysics, National Academy of Sciences of Ukraine, Lvov, Ukraine
tamara@cb-igph.lviv.ua
[2]Institute of Geophysics, National Academy of Sciences of Ukraine, Kiev, Ukraine
e-mail: rokityansky@gmail.com
[3]Institute of Geophysics of Romanian AS, Bucharest, Romania
margoisac@yahoo.com

The study of temporal variations of induction vectors (**C**) has a long story [Chen, Fung, 1993; Kharin, 1982 and many others]. The companion paper [Rokityansky et al., 2010] (see it for a notations and introductory material) emphasizes on the importance of periodic variations study and presents cases of annual variations. In [Klymkovych et al., 2007; 2009], new high resolution processing program has been developed and applied to magnetic observatory (MO) N. Selyshce data and periodic variations of induction vector parameters have been obtained both for annual and diurnal periods. In this work, high resolution program is applied to the data of MOs Surlari (some 30 km to SE from Vrancha zone and Carpathian electrical conductivity anomaly, Romania) and Dymer (40 km to North from Kiev, NE slope of Ukrainian shield to Dnieper-Donetsk Depression filled by sediments). We used 1 s digital data of three geomagnetic field components and make their averaging over 10, 20, 30, 40 or 60 s to receive input data for consequent processing.

2.5 years: 2008, 2009 and half of 2010 were processed. At all three stations both diurnal and annual variations are clearly seen on some of components. In Dymer the dependence is most clear and magnitude of annual variation attains 0.2 at the longest period 40—60 s at the northern component A, at shorter periods annual variation presents at both components. In Surlary annual variation is seen at all periods except longest one. In Surlari several monthly means behave as outliers that may be related with geodynamic processes in active Vrancha zone. Comparison with the earthquakes appearance is in state of study.

The main body of our talk will be devoted to presentation of numerous graphs received at the tree mentioned observatories and their analysis and discussion.

Diurnal variations are present at all three observatories and they mainly repeat the behavior of annual ones. The day-time external sources differ from night-time ones and both depend on geomagnetic activity. Then diurnal variation of **C** can be (at least partly) prescribed to change of the source parameters. Controlled sources are free of that influence. Dipole soundings in Central Asia and Baltic shield with distance between transmitter and receiver from 10 to 1000 km measured diurnal apparent resistivity variation from 5 to 20 % closely correlated with tides [Zhamaletdinov et al., 2004]. This controlled source experiments prove that noticeable periodic variations of transfer functions can have the tidal nature Stress in the lithosphere active zones can be several orders larger than tidal one. So geodynamic processes shurely can give rise **C** variations.

We review cases of strong lithosphere emission (ULF 0.01—10 Hz) of magnetic field before strong earthquakes Spitak, Loma Prieta, Grevena-Kozani, Biak, Chi-Chi with noticeable enhancement of vertical component, and hence with variation of **C**.

In China dozens 3-component geomagnetic observatories monitor monthly mean induction vector components $|A|$ and $|B|$. Before and after strong EQs, the components noticeable change. For example, northern component |A| of induction vector for period 20min before M6.2EQ 10.01.1998 show half year evolution with maxima 2 month before and during EQ [Zeng et al., 2002]. And what is the most remarkable: the maximum $\Delta|A|$ occur 400 km to ESE from epicenter, over epicenter region no anomaly is observed ("selectivity" effect). So, we can make the conclusion that response function variations can be caused by lithospheric emission or by the change of conductivity or by both.

We are greatly thankful to staff and supervisors of geomagnetic observatories Dymer N. Selishce and Surlari for data used in this work.

References

Chen P. F., Fung P. C. W. Time Changes in Geomagnetic Transfer Functions at Lunping before and after the 1986 Hualian Earthquake [Ms=7.6] // J. Geomag. Geoelectr. — 1993. — № 45. — P. 251—259.

Kharin E. P. Changes in transfer functions with time // Geophys. Surveys. — 1982. — № 4. — P. 455—466.

Klymkovych T. A., Horodyskyy Yu. M., Kuznetsova V. G., Maksymchuk V. Yu. Results of continuous investigations of induction vectors time changes in the seismoactive Transcarpathian trough // Geodynamics. — 2007. — № 1. — P. 41—48 (in Ukrainian).

Klymkovych T. A., Horodyskyy Yu. M., Kuznetsova V. G., Maksymchuk V. Yu. Studies of temporal changes of induction vectors parameters in the Transcarpathian seismically active trough // Geophys. J. — 2009. — **31**, № 6. — P. 147—152 (in Ukrainian).

Rokityansky I., Klymkovich T., Babak V., Savchenko T. Periodic variations of induction vectors // Geophys. J. — 2010. — **32**,№ 4. — P. 139—143.

Zeng X., Liu J-Y., Lin Y., Xu C. The evolution of dynamic images of geomagnetic field and strong earthquake // J. Atmospher. Electr. — 2002. — **22**. — P. 191—205.

Zhamaletdinov A. A., Mitrofanov F. P., Tokarev A. N., Shevtsov A. N. The influence from lunni-solar tidal deformations on results of control source EM monitoring for the seismic activity // Presentation at 32 Intern. Geological Congress (Florence, August 2004). — 2004.

New system of views on the Earth structural evolution: beyond plate tectonics

© ***V. Kobolev, Yu. Orovetsky, 2010***

Institute of Geophysics, National Academy of Sciences of Ukraine, Kiev, Ukraine
kobol@igph.riev.ua

For the past years a necessity has arisen to revise principles of the Earth's tectonic evolution due to increasing dissatisfaction with the modern geodynamic paradigm — concept of plate tectonics. Plate tectonics is viewed to be absolute truth although this approach violates the major dialectic principle of competiting scientific ideas. In our opinion:

1) palaeomagnetic data, which are a main basis of mobilism, were subjectively interpreted;

2) plate tectonics did not become a universal global theory of the Earth.

In developing plate tectonics the major gnosiological mistake was isolating the Earth from surrounding cosmic environment where the Earth is an integral and active part. Such an approach artificially eliminated a dynamic rotational effect. However, this effect seems to be the only factor capable of providing endogenic energy of the planet according to a scheme: rotation-gravity-pressure, pressure-frictional temperature. Only at the end of this generalized sequence of events the second active factor of developing the Earth was triggered under super high thermodynamic regimes of the future core. It was the liquid phase of initial planetesimal material in the form of magmatic melt, which is authentic to selective composition of accretional substratum. It automatically follows that:

1) the inner core of the Earth is matrix of solid refractory phase under high pressure;

2) a model for accretion is heterogeneous whose components are characterized by individual composition, including radioactive thermal generators.

Melting in closed environment is accompanied with autoclave effect resulted in increase of pressure in the liquid outer core. This mechanism is responsible for transformation of dynamic gravitational energy into kinetic thermally active one in the central part of the planet. Despite the different physical nature both types of energy proved to be functional. The metastable system can be set free from this situation only when its lid is distorted by tectonic rapture, which represents a low viscosity channel. The equatorial bulge of the planet controls the place of distortion. Here rotation of the Earth has formed a radial zone of the most intensive tensional stress of rotating rifting. This zone serves as a path-

way for vertical migration of melt from the outer core, the melt upwelling being caused by maximum centrifugal acceleration, high inner pressure and decompressional increase in a melt volume. The combination of these factors creates a long living wedge-shaped rupture and precludes the closure of a low viscosity tube. This situation creates persistent magmatism in the form of mantle plumes of complex composition including present-day potentially riftogenic equatorial zone. Similar ancient equatorial tensional features also are rotational rifting middle ocean ridges. Hence, the Earth dynamic rotational effect ignored by plate tectonic concept is capable of giving internally consistent interpretation of the nature of global tectonic elements of the Earth — MOR — without the mechanism of the mantle convection.

Using mantle convection in plate tectonics is predetermined by driving mechanism in this concept. Due to the absence of another plausible mechanism of plate moving mantle convection is used as driving force that propels plates, the convection is being caused by mostly radioactive heating the mantle material. However, in a classical sense this widely known physical phenomenon can occur only in gas and gas-liquid environment. In the case of the Earth an extremely large viscosity of the mantle material the estimation of which is based on indisputable seismological observations precludes from convention. To avoid this critical situation the convection is considered to occur at geological scale of time. The flows of the mantle materials are taken as principal cause for migrating lithospheres' plates. Although there exist many schemes of mantle convection, all of them resulted from numeral theoretical modeling. Therefore scales, rates and even reality of mantle convection are still a matter of contentious debates. To describe this phenomenon in mathematical terms, boundary conditions are imposed. As particular details of physical process are not known, these conditions are sometimes simplified and distort a true sense of phenomenon. Therefore erroneous results effect ultimate geophysical conclusions. The criticism of mantle convection is mainly based on the observation that a solidus temperature of the mantle material practically coincides with its gradient that precludes from thermal convection in the lower mantle. Taking into considerations this pluralism of opinions of mantle convection one must interpret the problem as not solved or even not adequately put forward.

Based on the study of rocks composition, isotopic-geochronological heterogeneity of the oceanic upper mantle has been definitely determined. The mantle was generated 3—1 billion years ago synchronously the main stage of forming the continental Earth's crust. It follows that it cannot survive in the convecting mantle. So, insisting on mantle convection would not be a correct approach.

However, one cannot reject convective heat-mass transport in the form of local magmatic bodies, which are characterized only upward flows of material. These bodies are collectively termed as "plume tectonics". They have occurred since the Prephanerozoic serving as thermal valve for getting away of extra heat outside the Earth.

Having abandoned large-scale mantle convection, we don't consider a subduction — obduction mechanism of plate moving derived from it because this mechanism is rather artifact than a subject of constructive scientific discussion.

Vertical transporting magmatic melt to the upper layers of the Earth in the form of mantle diapirs or plumes leads to the equivalent deficit of mass in the subcore according to the universal law of mass conservation. This deficit is compensated by subsidence the Earth's surface resulting in negative morphological features. This process seems to manifest itself in a worldwide increase in a depth of the World Ocean with time as inferred from sea drilling as well as in fivefold excess of subsidence over uplift in the geoid and M surface.

Horizontal movements are related to the change in the principal moment of inertia of the Earth: $J=mR^2$ (m — mass, R — radius) and derivative from it fluctuations of angular velocity in its rotating. In describing a physical sense of the equation we must emphasis that the only variable parameter proving a necessary effect is the radius of the Earth. Its change seems to be related to phase transformation of the first kind (fusion and crystallization) — in other word to genesis of magma. This inference is rather reliable because magma genesis as derived from the present-day seismic tomography sometimes occurs at the mantle depths up to the core resulting in mantle diapirs or plumes. In fusing material the local Earth's radius increases while crystallization leads to its decrease. These transformations appear to change an angular velocity of the Earth (ω) due to the principle of inertia moment.

According to seismological data there are two asthenospheres in our planet. The upper asthenosphere underlays the lithosphere and is spatially discrete. Despite this fact supporters of plate tectonics consider that over it lithosphere plates move. The lower asthenosphere is a liquid spherical layer E (outer core or subcore of the Earth) without any sufficient horizontal and vertical disruptions. There-

fore the highly dense inner core of the Earth inertially continues its rotation in the spherical layer of low viscosity when the Earth changes a rotating velocity. In a case of acceleration ω, the rotation of the core will retard relative to displacement of the Earth's shell (westward drift). On the contrary a decrease in ω will lead to an increase in a rotation velocity of the core relative to a rotation velocity of the shell (eastward drift). In other words the outer core is characterized by spherical symmetry in a rotational field that provides optimal conditions for lateral gliding of the solid shell over the liquid upper layer E. The Earth must inevitably react to these deep inertial disturbances by appropriate horizontal movements of masses relative to the axis of the magnetic dipole that will be clearly documented by the palaeomagnetic method. To the contrary of plate tectonics such a dynamics is free from constraints concerning spatial discreteness of the upper asthenosphere.

Palaeomagnetic poles of the planet migrate together with the moving mantle. To tell more accurate poles themselves don't migrate: displace their former locations on the Earth's revealed by palaeomagnetic measurements. Small eccentricity of palaeomagnetic and geographic poles is averaged out for 10^4 years. Therefore it can be neglected at geological time. Palaeomagnetic equators change their positions following migration of palaeomagnetic poles as they are coupled.

Our system of views of a structural evolution of the Earth relies on a dynamic rotational-gravitational mechanism and subcore magmatism accompanied it. A lateral migration of the Earth's surface occurs not along the basement of lithospheric plates but over the basement of a solid shell of the Earth, over the liquid surface of the outer core, which is not spatially discrete. This mechanism produced the equatorial bulges of rotational riftoges on the planet. These features of planetary tectonic divergence forming with time the dense network of divisibility in the tectonosphere favour its long conductive heat by rising overheated subcore material. As a result a temperature regime is created for selective fusing primary heterogeneous accretional substratum. In the mantle large regions of inertially reactive seismic wave-guides are formed and separation of fusible ingredients is complete. In a case of their abundance the thick continental crust is originated their deficit produces the oceanic crust. It is not excluded a similar autometamorphic mechanism of building discrete regions in the asthenosphere with entire spectrum of magmatic melts in them. Deep processes of the global rifting seem to be common from the formation of the liquid outer core. However, subsequent tectonic events sometimes transformed old rifts to such an extent that they are now not recognizable. Nevertheless even their remaining features are of paramount interest for a tectonic analysis. Therefore we consider that the study of this problem only starts. In future it will be needed to actively develop the quantitative aspect of palaeomagnetism (including oldest rocks) to first shed light into deep rotational, essentially riftogenic divisibility of the Earth.

Depending on morphologic hierarchy deep magmatogens rise to the outer shell of the planet in the form of diapirs or plumes producing above themselves positive relief including old platform areas and compatible with them compensating lows up to building oceanic depressions (Yuen et al., 2007).

As a consequence we arrive at a fundamental conclusion: a rotational- gravitational mechanism of the Earth accompanied with deep magmatism maintains its complex unstable mechanical system of permanent structure-forming on the surface of the integral continuous liquid subcore. In this context a derivative rotational rifting is the principal mechanism for structural transformations of the Earth's tectonosphere.

As for the plate tectonic paradigm our forgoing discussion shows inefficiency of its basic dynamic premise — mantle convection. The statement is based on non-uniqueness of solving the convection problem that rule out it of the plate tectonic mechanisms. In the absence of mantle convection there are no migration of lithospheric plates, subduction and obduction — the principle elements of neomobilism. The progressive role of the plate tectonic paradigm is indisputable only in one aspect: it is based on a huge piece of the present-day geological and geophysical information mostly on the oceanic tectonosphere. Nevertheless its criticism without suggesting something else is captiousness. An alternative system of views is briefly presented in this paper. Its major elements are of physical nature: they rely on basic oscillating processes which in turn rest on the universal law of conservative of energy. Due to its merit it is presented as a missing link between two antipodal geological ideologies of fixism whose historically formed canons remain inviolable and mobilism of its new version.

Low velocity zones in the Earth's crust

© ***V. Korchin, 2010***

Institute of Geophysics, National Academy of Sciences of Ukraine, Kiev, Ukraine
korchin@igph.kiev.ua

In the resent years fragmentary crustal low velocity zones were revealed by DSS profiles at depths of 5—22 km around the Earth. However, their nature remains not quite clear.

Interdisciplinary interpretation of DSS data including petrophysical thermobaric modelling the ithospheric composition brings more insight into the nature of these anomalous zones. In most cases they are considered as thermodynamical phenomena rather than a result of changing composition when mineral material is transformed by pressure and temperature at the depth of their occurrence.

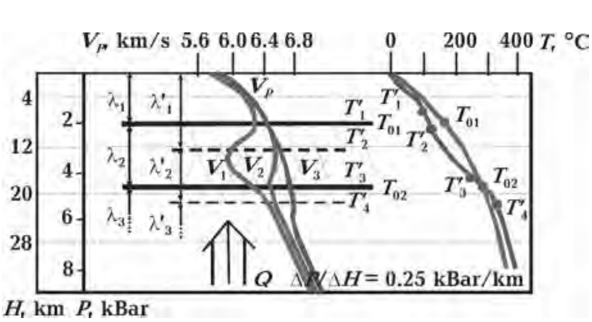
Multimethod laboratory studies of sample show that under *PT*-conditions at 5—15 km depths rocks are subjected to cataclastic and dilatational changes. Amajor mechanism responsible for this behaviour is a resultant effect of irregular and differently oriented tensions in the sample. In contacts between grains they reach values which exceed the strength limit of individual minerals that destructs integrity medium at a microlevel.

Here the rocks are characterized by low Young and shear modules, high brittleness (low Poissons's ratio), high discompaction (high dilatancy), low thermal conductivity (λ). The discompacted state of rocks at 5—20 km depths is a fundamental characteristic of the Earth's crust. It results from the counteraction of pressure and temperature at these depths. The inversion zones established by laboratory experiments in most cases well coincide with low velocity zones in the Earth's crust from DSS profiles.

As low velocity zones result from temperature destruction of rocks uncompensated by pressure at 5—18 km depths, changes in T at these depths can lead to change in intensity of the thickness of these zones and rate of decrease in V_P within them. Crustal thermobaric zones are shown to increase, decrease and disappear depending on $\partial T/\partial H$, $\partial P/\partial H$, λ, T. Instability of the crustal thermobaric zones of low velocity result in their episodic occurrence in the crust and their vertical and horizontal migration depending on temperature fluctuations in the crust.

The low velocity zone in the earth's crust is characterized by the lowered values of λ ($\lambda_1<\lambda_2<\lambda_3$) (Figure). It is the reflecting horizon for a heat flow with the thermal activity processes at large depths as a source. Presence of layer with the lowered heat conductivity on the way of the thermal energy distribution results in the temperature increasing at the lower part of layer and its decreasing at the upper one. That is why the equilibrium *PT*-conditions of the low velocity zone existence are disturbed.

The state of the upper layer of zone is equalized with the rock's state of the upper horizons with a temperature drop in the upper part of this zone. The upper edge of zone goes downward. The border with T_{01} values goes down to T_{02} values position. Simultaneously, there is the zone's foot overheat that is proportionally to the difference of heat conductivity of zone's mineral environment in the lower part of the bedding rocks. The lower foot of zone with T_{02} values goes down to the level of T_{04} values position. The higher pressure stops the growth of a zone due to compensation of thermal structural violations of rocks. Thus the zone area changes the configuration — its power can be increased (with the increase of intensity of deep heat flow) or this zone will disappear (with the sufficient heat lowering from a depth).



Low velocity zone parameters change as a function of deep heat flow values (Q) changing.

Comparison results of geodetic and seismic assessment of the Earth's crust deformation process (by example of the Tien Shan)

© A. Kostuk[1], S. Yunga[2], 2010

[1]Research Station, RAS, Bishkek, Kyrgyzstan
kostuk@gdirc.ru
[2]Institute of Physics of the Earth, RAS, Moscow, Russia
syunga@ifz.ru

Presence of significant heterogeneities in deformation field of the Tien Shan emphasizes nonuniformity of crust movements. Applying of different methods allows more accurate estimation of the deformation state in the region. At the same time, using few data sources can be very helpful in the results verification. Features of geophysical methods not always allow assessment of crust condition in some zones of the studied areas, but use of complex approach can help to expand an information set.

In the present paper, we have attempted to estimate the deformation state of the Tien Shan with the help of two different methods and the obtained results comparison. Both seismological data [Kostuk, 2008] and GPS observations results [Zubovich et al., 2007; Kostuk et al., 2010] were involved as data sources. In the process of the seismotectonic deformation (seismic strain release) research, three deformation regimes — trust, transpression, and trust-vertical regime — were determined for the Northern Tien Shan territory. The Lode-Nadai coefficient analysis indicates compression and shear strain in the most part of the studied territory and tension state only in minor parts of the crust, while the seismotectonic deformation rate intensity is $2{\cdot}10^{-9}$ year^{-1}.

Calculation of the contraction\extension axes direction based on GPS data showed that crust contraction in the region in general occurs in north-north-western direction, with small changes from zone to zone. It was defined that deformation field is quite heterogeneous; areas of high contraction rate and maximum shear strain rate were marked out. Some small areas of dilatation were localized. Deformation rate intensity was estimated according to GPS data and was $2{\cdot}10^{-8}$ year^{-1}.

Comparison of results of seismotectonic analysis and GPS data indicated that there is coincidence in the axes directions and deformation regimes. At the same time, despite the similarity of tendencies of deformation regimes, the deformation rate intensity by GPS is by a factor of ten larger than the siesmotectonic deformation rate intensity that conforms to the results of other researches dedicated to the other regions [Zobin, 1987; Radziminovitch et al., 2006].

In so doing, comparison of the contraction axes azimuths by GPS and seismological data showed significant concordance. In particular cases, there was determined almost complete concordance of directions, while in other cases marked difference took place. Azimuth according to GPS made 356° (rms=14.5°), and by the earthquake moment tensor solution data was 353° (rms=14.5°). Considering the root mean square deviation we could state that different methods provided the same estimation of the contraction direction azimuth. At the same time, average deviation between contraction axes by two different methods in each point was 14.5°. Thus, a considerable predomination of the north-north-western direction was noticed. Obtained results were confirmed by neotectonic structural grain, near-latitudinal trends of ranges and basins, reverse and thrust faults of the same orientation.

Additional estimation of the contraction axes directions the territory of California (USA) and island Honshu (Japan) showed similar results. Thus, the azimuth for California by GPS made up 40° (rms=29°), and by seismological data — 46° (rms=31°) and the average deviation between contraction axes directions in each point was 16°. In island Honshu these values equaled: 110° (rms=38°), 104° (rms=39°) and 20°, respectively that also proved the results obtained.

This work was partially supported by the Russian Foundation for Basic Research RFBR 09-05-00687-a.

References

Kostuk A. D. Source parameters of moderate-sized earthquakes in the northern Tien Shan // Vestnic KRSU. — 2008. — **8**, № 1. — P. 100—105 (in Russian).

Kostuk A. D., Sycheva N. A., Yunga S. L., Bogomolov L. M., Yagi Y . Deformation of the Earth's crust in the Northern Tien Shan according to the earthquake focal data and satellite geodesy // Izv. Physics of the Solid Earth. — 2010. — № 3. — P. 52—65.

Radziminovitch N. A., Melnikova V. I., San'kov V. A., Levi K. G. Seismicity and seismotectonic deformations of the crust in the Southern Baikal basin // Izv. Physics of the Solid Earth. — 2006. — № 11. — P. 44—62.

Zobin V. M. Source mechanism of earthquakes and Kamchatko-Komandor region seismotectonic deformation // J. Volcanology and Seismology. — 1987. — № 6. — P. 78—92 (in Russian).

Zubovich A. V., Makarov V. I., Kuzikov S. I., Mosienko O. I., Shchelochkov G. G. Intracontinental mountain building in Central Asia as inferred from satellite geodetic data // Geotectonics. — 2007. — № 1. — P. 16—29.

Electric conductivity of the Earth crust in the North-Eastern Part of the Alpine-Himalayan Orogenic Belt

© ***S. Kulik, T. Burakhovich, 2010***

Institute of Geophysics, National Academy of Sciences of Ukraine, Kiev, Ukraine
kulik@ndc.org.ua

Regional anomalies of high electric conductivity in the depth of the Earth crust characterize alpine tectonic structures. This is also true of the Alpine-Himalayan orogenic belt (AHOB), the mountain formation that encompasses western part of South-Eastern Asia, north-east of Africa and south of Europe. It separates Eastern-European (EEP), Siberian, Chino-Korean and Southern-Chinese platforms from the Afro-Arabian and Indian platforms, it stretches from Gibraltar in the west and covers part of the western and southern Europe, Mediterranean See, northern Africa and Indonesian archipelago.

This belt splits into several branches. The main one stretches from Pyrenees through Alps and Carpathians to Balcanides and northern Anatolia, Caucasus, Kopet Dag and Himalayas. It was suggested that there is one more northern Dobrudzha-Crimean-Caucasian branch [Kulik, 2009].

Carpathian and adjacent regions from the geological standpoint include south-western part of EEP and alpine folding region of Carpathians together with frontline and inner Miocene depressions as well as pre-alpine epyrogenic zones (Scythian, Misian and Dobrudzha).

Tarkhankut conductivity anomaly (CA) was identified in the western Crimea [Kulik, Burakhovich, 1999] and has comlex configuration at the depth of 10 km. Its cumulative longitudinal conductivity (*S*) is 5000 Sm. Its most conducting parts are located in the Black See basin, Karkinit-North-Crimean depression and Almian-Cimmerian trench.

In the sub-latitudinal direction from Tarkhankut peninsula to Novoselov uplift stretches CA 20—30 km wide and with *S* = 500 Sm. It is located at the depth of 5 km. Further on it changes the direction to north-western and can be partially traced along narrow fin like slope of the crust foundation. In the mountainous Crimea there is an anomalous zone with *S* = 1000 Sm located in the region of converging isolines on the map of density of quake epicenters. Conductivity zone at the depth of 2 and 5 km with corresponding *S* equal to 2500 and 5000 Sm can be identified in the eastern part of Crimea. This zone geographically coincides with location of mud volcanoes of Kerch — Tamansk region that can be possibly controlled by tectonic fractures with roots lying at the depth of 5—7 km.

Northern Dobrudzha fold-shift structure 50 km wide stretches in the north-west direction for 200 km. It can be traced inside Black See basin at the distance of 50 km but it's not connected with mountainous Crimea. It is quite likely that struc-

tures of the Teisseyre — Tornquist zone already start taking part in formation of this branch of AHOB. In the north-east the folding formation wedges out near latitudinal Trotush fracture which separates Eastern and Southern Carpathians. In Peri-dobrudzha and Northern Dobrudzha at the depths of 10—20 km and 40—80 km there stretches CA with electric resistivity in a range of 40 to 100 Ω·m [Burakhovich et al., 1995].

An anomaly of electric conductivity in the earth crust of Western Carpathians is related to the juncture zone of Flysch Carpathians and inner units including Pennian and Marmarosh zones [Burakhovich, 2004]. In Southern Carpathians there is a CA located in the juncture zone of Inner nappies that separates Pannonia and Transylvania, and Southern Carpathians but not Peri-Carpathian depression. An anomaly of the western part of Ukrainian Shield (USh) and its slope is galvanically related with Flysch zone of Eastern Carpathians and Marmarosh belt. Western branches of the CA are located in a zone of deep Podolian fracture and the juncture of south-western edge of EEP and Scythian platform. Dobrudzha is represented by a separate conducting object. It is absolutely obvious that in the studied region there is no universal and homogeneous asthenosphere.

Geoelectric models or crust CA do not always correspond to geology on a surface. For example, Pennian and Marmarosh belt as well as Flysch Carpathians are not a continuous CA in the Earth Crust. An anomaly of Precambrian USh and EEP wedges into alpine Carpathians. North-western branch of AHOB has some distinctive features characteristic to mobile belts; above all it's a week manifestation of the crust destruction in the beginning alpine stage of development.

A nature of a CA in the Earth Crust and Mantle can be different. First of all, it can be related to specifics of fluid (hydrothermal) regime deep in the Earth, to existence of melted rock phase in the crust. Second of all, it can be related to existence of inclusions with electronic conductivity. The most widespread representatives are graphite, sulphides bearing gneisses and shales which have graphite as one of their constituencies, graphite substance, pyrite, pyrrhotite and sometimes shungite. And finally, it can be due to a combination of inclusions with electronic conductivity and fluid which form an interconnected net of conducting channels.

References

Burakhovich T. K. Quasi 3D geoelectric model of Carpathian region // Geophys. J. — 2004. — **26**, № 4. — P. 63—74 (in Russian).

Burakhovich T. K., Kulik S. N., Logvinov I. M. Geoelectric model of the Earth crust and upper Mantle of Predobrudzha depression and Northen Dobdrudzha // Geophys. J. — 1995. — **17**, № 4. — P. 81—87 (in Russian).

Kulik S. N. Northern branch of Eurasian anomalies of electric conductivity // Geophys. J. — 2009. — **31**, № 4. — P. 168—180 (in Russian).

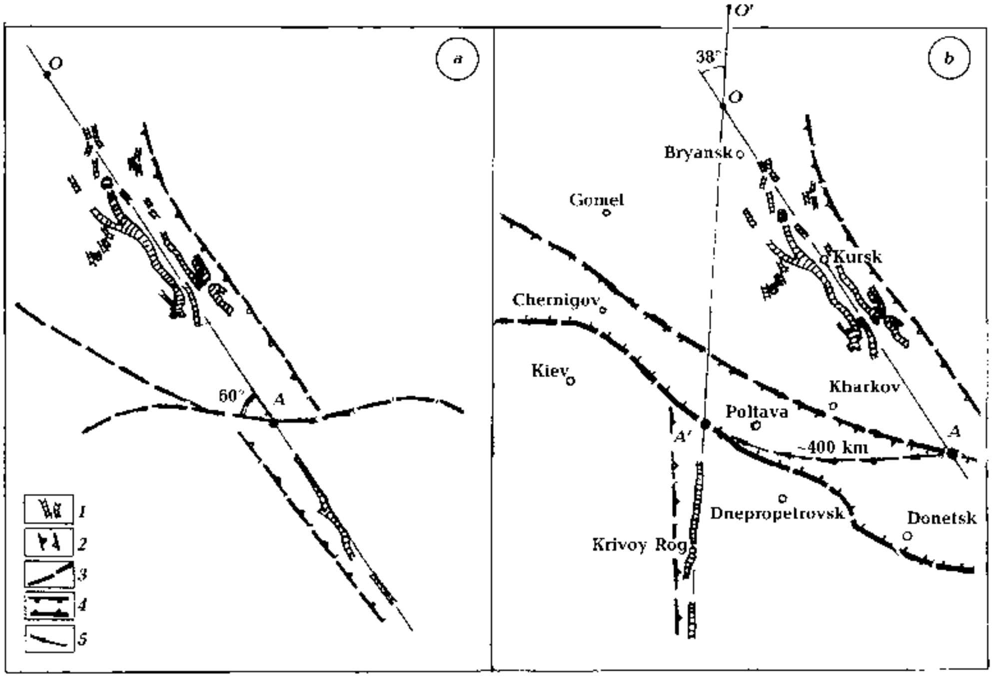
Kulik S. N., Burakhovich T. K. Quasi 3D geoelectric model of tectonosphere of Crimea // Geophys. J. — 1999. — **21**, № 3. — P. 123—126 (in Russian).

Towards the problem of genesis of Pripyat-Dnieper-Donetsk avlacogen

© ***V. Kurilenko, E. Petrova, T. Gusynina, 2010***

Institute of Geological Sciences, National Academy of Sciences of Ukraine, Kiev, Ukraine
gusynina@gmail.com

1. One of many problems in dynamics of lithosphere is the origin and development of rift systems inside and on the skirts of ancient platforms, in particular, the Pripyat-Dnieper-Donetsk avlacogen in body of East-European platform. The version about an origin of this avlacogen as a result of "superregional" right-hand shift lengthways Sarmat-Turan lineament, or more global (transcontinental) prolongation of this lineament to the west and to the east corresponding to the Schetland-Tsinlin fault-displacement [Roslyi, 2006; Isberg, Starchik, 2007], is well known. Horizontal



Model for formation of Pripyat-Dnieper-Donetsk system of formation of paleorifts: *a* — location of board`s zones of paleorifts and structures of iron-ore formations in earlyproterozoics time (1000 m. years ago); *b* — present location *(1* — magnetic anomalies in earlyproterozoics time (Krivorog`s and Kursk series [Zankevich, 2006]; *2* — boundaries of proterozois geosynclines zone; *3* — proterozois fault in massif of the Sarmat`s shield; *4* — boundaries fault of paleorifts; *5* — the trajectory of movement of conventional point A–A^1; O–O^1 — dislocation of rotation axis of the Ukrainian shield).

displacement of shift within the limits of described region makes 250—400 km.

Our reconstruction confirms displacement on 400 km and assumes turn of the Ukrainian shield clockwise on 38° with respect to southern suburb of the East-European platform in area of the Voronezh massif. The radius of turn is 650 km, and the center of rotation is gradually displaced to the "north" on 150 km. As a result initial points O and A (see Figure) have occupied positions O^1 and A^1.

The above reconstruction is based on the assumption of genetic connection of the magnetic anomalies of the Krivoy Rog — Krementchug and Kursk iron-ore formations as uniform linear structure in early proterozoic time. Slanting break (under an angle 60° to an axis) of this structure has begun right-hand shift, formation and expansion of rift cleft.

2. The process of transregional shift started at the beginning of late proterozoic era (1 bln years ago), proceeded non-uniformly, being entered during general planets tectogenes epochs, it was marked by formation of “rifey graben” in a south-east part of the future Dnieper-Donetsk paleorift, it brightly showed itself by formation of described rift system in late devonian epoch and has practically come to naught in cretaceous-paleogen times. However and nowdays in a landscape and a geological structure of region it is possible to observe neotectonic attributes of the latent movement: ring and linear aircosmic anomalies are displays of tangential and normal deformations in a sedimentary cover, listric faults [Geology ...,1991]. Shift right-hand deformations are clear visible along borders of rift forming deep breaks, lengthways the Smelov-Kholm diagonal break, in places of breaks of the Sarmat-Turan lineament, they are well traced along chains of salt rods in the central and south-east parts of Dnieper-Donetsk paleorift [Geology ...,1991; Kurilenko, Janshina,1988; Roslyi, 2006].

3. Rift formation combined with stretching, extension and crushing of basement blocks, it was accompanied by faulting of every possible types, listric chipping off, overturning and dropping of separate blocks, extensive landslides. Deformations of a stretching were non-uniform along described system of paleorifts: for the Dnieper-Donetsk graben it was 2—5 km in its extreme north-west, 5—7 km in a middle part and 10—18 km in a southeast. The Pripyat graben was generated mainly under influence of shift deformations, and broadening here did not exceed 2,4 km.

The paleorifts width also is changeable along all the system spreading. The Pripyat graben extends in the western direction from 110 up to 160 km at

thickness of a sedimentary cover from 2,5—4 km above ledges of the base up to 5,5—6,0 km above the immersed blocks. The Dnieper-Donetsk graben extends in a southeast direction from 75—90 km up to 110—130 km, being correlated with increase of a sedimentary cover in board zones from 3—4 km in the west up to 6—7 km in the east, and along an axial zone — from 6 up to 18 km in the same direction.

4. The bottoms of paleorifts ("rift valleys") are formed by "the breccia of rubbing" arisen under influence of transcontinental shift and consisting mainly from different sizes products of grinding blocks of crystalline rocks from basement and vulcanites. The range of the sizes of these "products" is very wide: from blocks in volume in hundreds cubic kilometers up to boulders and pebbles. A filler of these breccia are products of erosion and drift from onboard sites (mainly clastits), endogenous materials (effusive and halogens), chemic- and biogenic materials (carbonates). The same initially not consolidated deposits provided noncompensated filling of paleorifts.

Proceeding from the above stated representations, and taking into account an idea about of structure (fractality) and "geoblock divisibility" of the earth's crust [Krasnyi, 2005; Zankevich, 2006], the structure of paleorifts (their board`s and bottom) can be represented as system of relatively stable weakly deformed ("rigid") blocks divided by labile (unstable) zones of "hummocking". Stable blocks under influence of transregional shift deformations exercise some progress-rotary movement, and labile zones compensate superfluous pressure, playing a buffer role between blocks. Indicators of labile zones are anticlinal folds and chains of positive structures in a sedimentary cover. The majority of structures have attributes of imposed folding (dragging, squeezing, etc), complicated by halokinesis. Within the limits of labile zones the salt domes, often built in rhythmical chains or ring formations are located all. The overwhelming majority of oil and gas fields containing the lion's share of oil-gas provinces is related to labile zones.

Thus, the new approach is outlined in the tectonic zoning of the Pripyat-Dnieper-Donetsk oil-gas province and allocation on this basis of perspective zones of oil-gas accumulation that should raise a level of a scientific substantiation of accommodation of volumes of exploration.

References

Geology and oil-gas content of Dnieper-Donetsk depression. Deep breaks and combined oil-gas traps / Eds. V. K. Gavrish, A. I. Nedoshovenko, L. I. Ryabchin. — Kiev: Nauk. dumka, 1991. — 172 p. (in Russian).

Isberg R. E., Starchik T. A. Multifactor model of late paleozoic`s geodynamics for the Pripyat paleorift // Lithosphere. — 2007. — **27**, № 2. — P. 25—35 (in Russian).

Krasnyi L. I. Tectonics at the turn of XIX—XX and XX—XI centuries. — St. Petersburg: VSEGEI, 2005. — 164 p. (in Russian).

Kurilenko V. S., Yanshina N. A. Influence of geodynamic pressure on formation of salt structures of Dnieper-Pripyat gas and oil province // Geology of oil and gas. — 1988. — № 12. — P. 25—29 (in Russian).

Roslyi I. S. Regional riftgenesis, geodynamics and oil-gas content of Dnieper-Donetsk avlacogen. — Kiev: UkrDGRI, 2006. — 330 p. (in Ukrainian).

Zankevich B. O. Geodynamics and breaks tectonics during formation of Dnieper-Donetsk protorift // Energetics of Earth, its geologic-ecologic manifestation, scientific and practical utilization: — Kiev: Pub. Co. "Kiev University", 2006. — P. 155—160 (in Ukrainian).

Constraining the composition, density and thermal state of the lithospheric mantle of the Siberian craton from inversion of seismic data

© ***O. Kuskov, V. Kronrod, A. Prokofyev, 2010***

Institute of Geochemistry and Analytical Chemistry, RAS, Moscow, Russia
ol_kuskov@mail.ru

Quantitative estimation of the temperature distribution in the Earth's mantle is a key problem in

petrology and geophysics. In this study, we discuss the method of estimating temperature, composition, density and thickness of the subcontinental lithospheric mantle beneath the Siberian craton from absolute seismic velocities. The phase composition and physical properties of the lithospheric mantle were modelled within the Na_2O-TiO_2-CaO-FeO-MgO-Al_2O_3-SiO_2 system including the non-ideal solid solution phases. For the computation of the phase diagram for a given chemical composition, we have used a method of minimization of the total Gibbs free energy combined with a Mie-Grüneisen equation of state. Our forward calculation of phase diagram, seismic velocities and density and inverse calculation of temperature includes anharmonic and anelastic parameters as well as mineral reaction effects, including modes and chemical compositions of coexisting phases. Sensitivity of density and velocities to temperature, pressure and composition was studied. Inverse code computes the temperature distribution in the upper mantle from seismic and compositional constraints. The output results contain the self-consistent information on phase assemblages, densities and velocities. The approach used here requires a small number of thermodynamically defined parameters and has important advantages over earlier procedures, which contain no information about entropy, enthalpy and Grüneisen parameter. We inverted for temperature the recent velocity models of the Siberian craton as well as the IASP91 reference Earth model. Several long-range seismic profiles were carried out in Russia with Peaceful Nuclear Explosions (PNE). The velocity models from PNEs recorded along these profiles were used to infer upper mantle temperature profiles beneath the Siberian craton. The seismic profiles were inverted on the basis of low and high temperature xenoliths of garnet peridotites from kimberlite pipes of the cratons in order to gain insights into the temperature sensitivity to variations in the composition and mineralogy of xenoliths. Such a test can provide constraints on the compositional (vertical and lateral) heterogeneity of the upper mantle. 1D and 2D thermal and density profiles of the lithospheric mantle for the Siberian craton are discussed. We derive a lithosphere thickness of roughly 300 km for the Siberian craton by the intersection of the calculated temperature profile in the conductive region with the potential mantle adiabat.

Surface heat flow and thermal structure modelling of the Lithospere in the Black Sea region

© **_R. Kutas, 2010_**

Institute of Geophysics, National Academy of Sciences of Ukraine, Kiev, Ukraine
kutro@ndc.org.ua

The Black Sea Basin is a deep marginal depression within the Alpine belt. It is surrounded by tectonic features of different ages from pre-Cambrian to Neoalpine whose major elements mainly extend to the Black Sea shelf.

Low heat flow density (20—40 mW/m^2) dominates in the Black Sea. The lowest (< 30 mW/m^2) values have been recorded in central parts of the Western and Eastern Black Sea Basines with maximal sediment thickness. The area of low values occupies the most Western Black Sea Basin, where the “granitic” layer of the crust is absent. The thermal field is slightly differentiated. In the Eastern Black Sea Basin the thermal field is more differentiated. Here several high and low heat flow anomalies are distinguished. Low heat flow covers the most part of the Eastern Black Sea depression, slopes of the Andrusov and Shatsky elevation. A series of limited low (20—30 mW/m^2) heat flow anomalies are identifiable along the Crimea and Caucasian coast. Several high heat flow anomalies are distinguished in the central, northern and southern parts of the depression.

On the periphery of the Black Sea depression the heat flow changes mainly in the range of 20—150 mW/m^2. Abnormal heat flow density tends to occur mainly along the zones of active faults, mud volcano, mud diapirism, fluid and gas fluxes.

On the continental slope and shelf zone of the Black Sea a distribution of heat flow is influenced by land features. Its variation is controlled by geodynamic peculiarities and geological history of adjacent tectonic feature on land. Significant variations in heat flow indicate different ages of tectonic elements and/or repeated tectonic rejuvenations at different time. Heat flows increase from older struc-

ture units to younger ones. On the slope of ancient pre-Cambrian Platform the heat flow values are relatively low (35—45 mW/m^2). In the Paleozoic Scythian Plate heat flow increases to 50—65 mW/m^2. A number of geothermal anomaleous zones are distinguished here. High heat flows of some 70—80 mW/m^2 are found in the Karkinit riftogenic trough, Cenozoic Indol-Kuban depression.

The thermal state of the lithosphere depends on two main factors: thermal energy balance and heat transfer conditions. The energy balance is formed by intralitospheric energy sources, mainly radiogenic, and by the amount of heat which is supplied from below (through its basement). Heat transport within the lithosphere is predominantly by conduction. However, in active regions, effective thermal conductivity varies in time. As a result, transient heat flow anomalies are produced, which are complicated by thermal disturbances due to magmatic activity, sedimentation, erosion and horizontal displacement of the lithosphere plates. In constructing a well-grounded thermal model for the lithosphere, the dynamics of the all these processes should be considered. This requires the use of modelling based on complicated physical, mathematical, geophysical and geological phenomena and methods.

In the general case, temperature and heat flow distribution in the inhomogeneous lithosphere dominated by conductive heat transfer satisfies the transient heat conduction equation. The problem may be simplified by its subdivision into two ones: stationary and transient. The stationary problem describes the thermal field of the inhomogeneous lithosphere with thermal conductivity produced by radiogenic heat sources and the mantle heat flow. The transient problem describes temperature and heat flow variations due to short-time changes of temperature, heat generation or heat exchange conditions. The stationary field is taken to be a background (normal field) for the separation of transient anomalies. This problem was solved by finite differences methods.

Transient geothermal anomalies in the studied areas are associated with sedimentation, climate changes, lithosphere extension and astenosphere uplift. The accuracy of the thermal history calculations was checked using the following criteria: thickness and depths of specific lithofocies and basement surface on the present cross-section, thickness of the earth's crust the present values of heat flow and temperatures in the sedimentary rocks.

The modelling results are presented in the form of cross-sections of the lithosphere of temperature and heat flow distribution for two profiles crossing the Western and Eastern Basin of the Black Sea depression. Based on the results of the modeling of the mantle and the earth's crust heat flow components have been determined. Contribution of the sedimentary layer in the central part of the Black Sea Basin is 10—12 mW/m^2, contribution of the whole crust is 13—16 mW/m^2. The contribution of the mantle is 45±4 mW/m^2. It decreases to 30±5 mW/m$_2$ on the Scythian Plate and to 20±3 mW/m$_2$ on the pre-Cambrian Platform. The surface heat flow decrease in Black Sea Basin is mainly due to intensive accumulation of Pliocene-Quaternary sediments. The high mantle component is due to young tectonic activity. Our thermal modelling covers the depth range of the relatively cold thermal layer with temperature below 1300 °C. The 1300 °C temperature level is found at depth between 75—90 km in the central part of the Black Sea Basin, 100—130 km in the Scythian Plate and 160—180 km in the southern slope of the pre-Cambrian Platform area.

Reflection of tectonic structures of platform cover of the North of Russian plate in atmospheric field, character of geomagnetic variations and deep's decontamination

© *Y. Kutinov, Z. Chistova, 2010*

Institute of Ecological Problems of the North, Ural branch, RAS, Arkhangelsk, Russia
kutinov@iepn.ru

In 2001—2009 we measurements of atmospheric pressure above fault-crossing were carried out, and the fact of constant "deficiency" of atmospheric pressure was established. These minima have received the working name — "static" and have difficult structure with increase of values in the centre

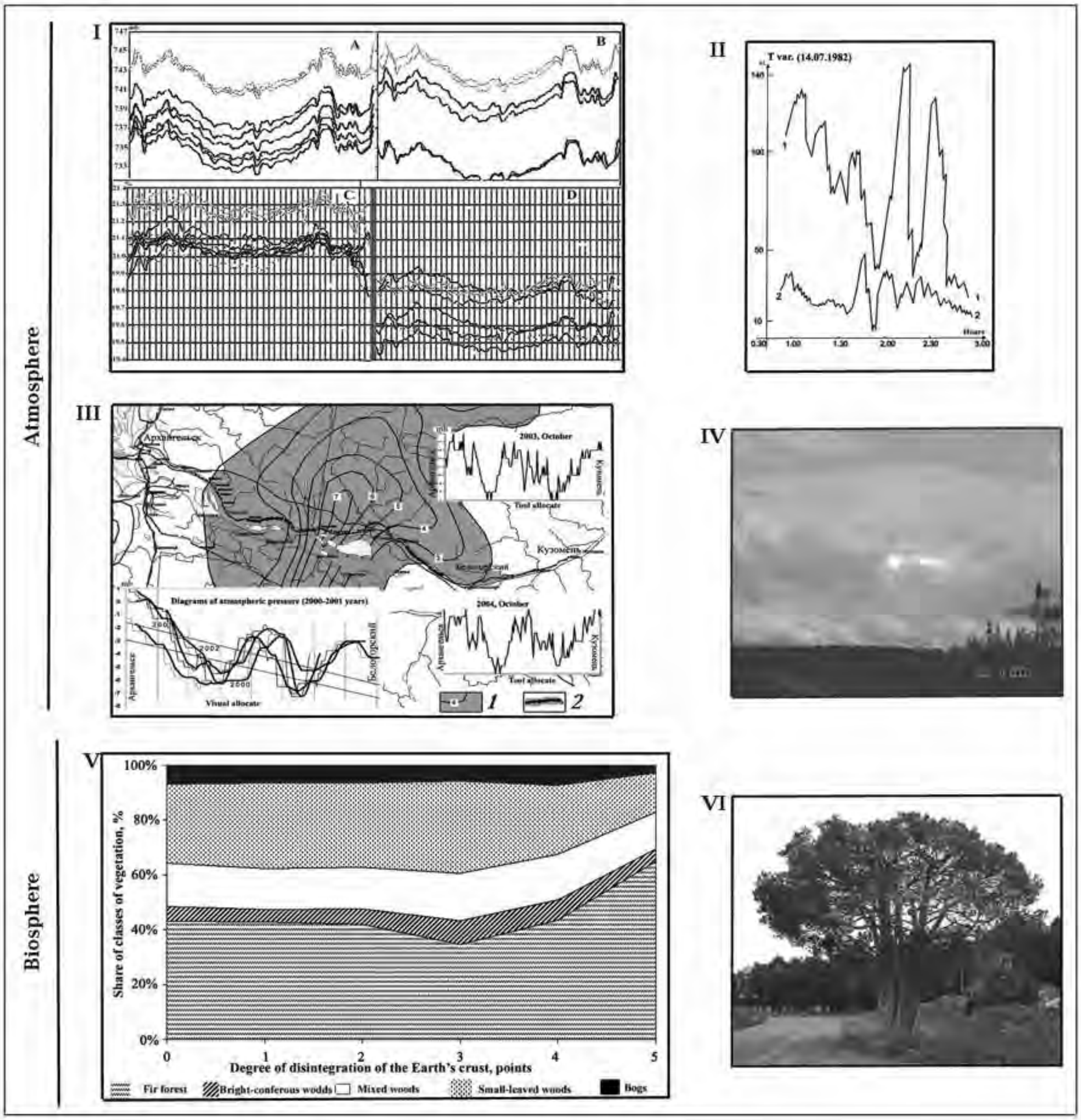


Fig. 1. Model of Geospheres interactions on the area of fault-crossing (atmosphere, biosphere): I — diagrams of atmospheric pressure (A, B) and contents of oxygen (C, D); II — diagrams of magnetic variations in fault-crossing and behind its limits; III — structure of atmospheric minimum (*1* — isolines of density of faults; *2* — anomalies of "deficiency" of atmospheric pressure); IV — structure of overcast; V — structure of vegetative cover; VI — dichotomy of trees.

and downturn on periphery (Fig. 1, III) the numerous measurements which have been carried out in different years and the seasonal periods, have shown that the allocated minima are static and do not undergo seasonal changes.

The revealed fact of change of dynamics shot wave geomagnetic variations at the moment of magnetic storms in fault-crossing [Kutinov, Chistova, 2004] (Fig. 1, II) and presence of zones of the increased conductivity (Fig. 2, II, III) allows to assume occurrence in tectonic structures induced magnetic-telluric currents and, as consequence, ionization of air above tectonic structure and units of faults. The original structure of overcast above fault-crossing speaks about change of electric conductivity of atmospheric air (Fig. 1, IV). And constantly observably pinkish shade can be interpreted as display of effect Cherincov' luminescence arising due to compression of rocks.

In space pictures of cyclones in northern hemisphere results of nuclear interaction of neutrons and

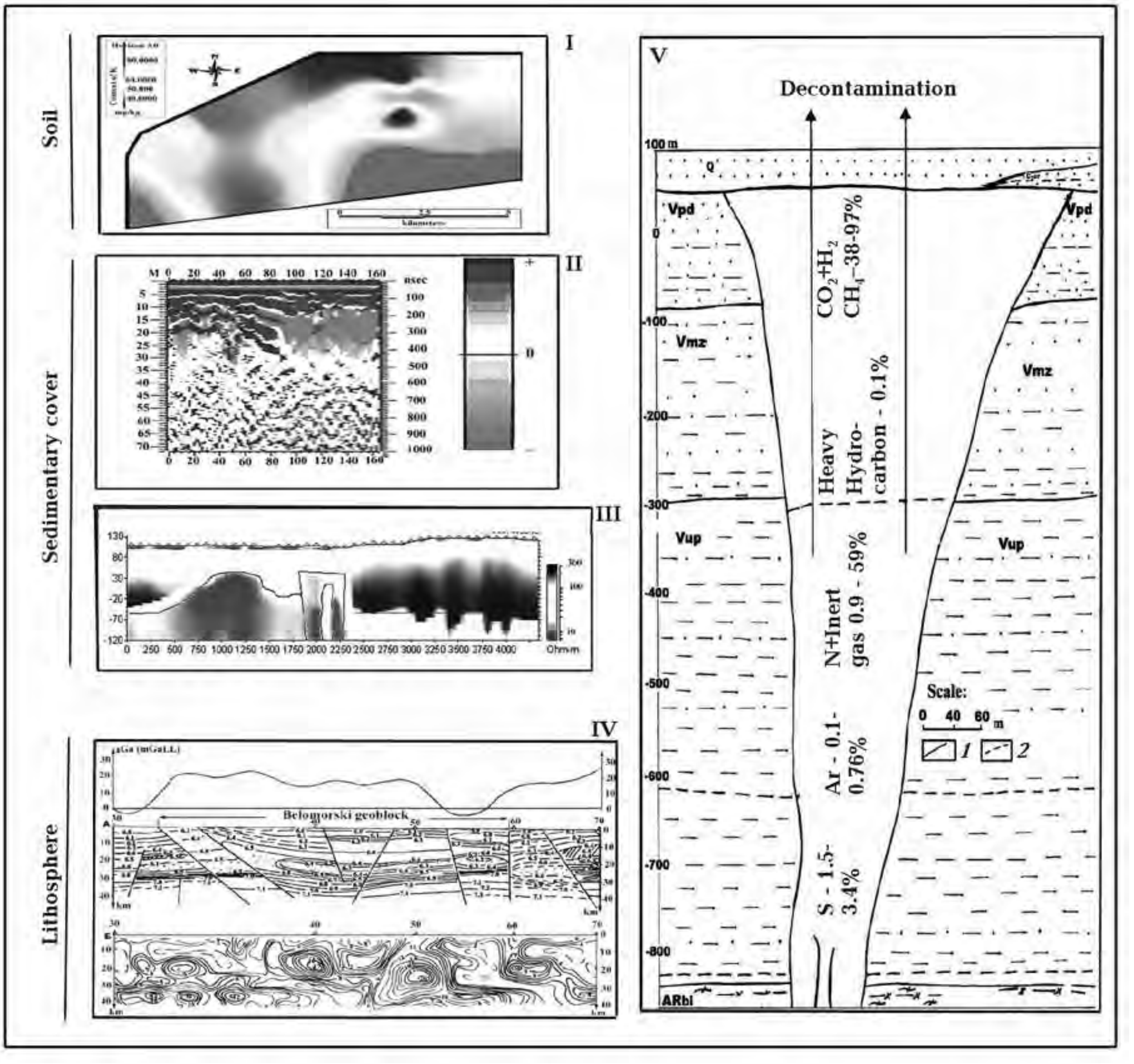


Fig. 2. Model of Geospheres interactions on the area of fault-crossing (geological medium): I — contents K in horizon A0; II — results of georadar-tracking researches; III — geoelectric section; IV — section on data DSZ; V — section of fault-crossing (geological boundary: *1* — established, *2* — assumed).

high-energy protons with an ozone cloud of a planet as the separate petals twirled counter-clockwise [Akhundov et al., 2007] are clearly visible. Getting in a nucleus of ozone, neutrons and high-energy protons translate it in the excited condition which is shown all over again as a silvery cloud, then in due course the cloud grows fat and, at last, becomes dark, having formed water. Water, in turn, drops out on a surface of the Earth as deposits — a rain, snow or hailstones. I. e., formation of a luminescence, difficult structure of overcast, other character of loss of deposits is possible. By us it is established, that in conditions of the European North frequency of loss of deposits and their quantity in the centre and on periphery of fault-crossing of tectonic dispositions which territorially coincide with stationary minima of atmospheric pressure for July—August essentially differ. Deposits in the centre of tectonic units dropped out much less often, and their quantity on 26-is less than 38 %.

In 2008 and 2009 by us were carried out on profile Arkhangelsk — Pinega for specification of dynamics of change of the contents of oxygen in near-ground layer of atmosphere on the area of fault-crossing. Received in 2008 and 2009 results speak, that, despite of practically full convergence of diagrams of atmospheric pressure, the picture of the contents of oxygen in 2009 differs from similar in 2008 (Fig. 1,

I). The contents of oxygen depends from *PT*-conditions and inflow of deep" gases. Values of atmospheric pressure during gauging were practically identical a temperature mode is characterized about zero values and has no significant distinctions. Thus, there is only an increase inflow deep' gases, first of all CO_2.

Our data testify to presence of influence of tectonic infringements on Environment due to occurrence induced currents, deep decontamination and change of structure atmospheric fields. The counter system "influence — response" is observed, i. e. not only change of a geomagnetic field and atmospheric pressure influence on is intense — deformed a condition of the geological Environment, but also the Environment influences sun-meteorological parameters. I. e., in area of tectonic units vertical through channels difficult geospheres interactions, fascinating lithosphere, hydrosphere, biosphere and an atmosphere are formed. The model of lithosphere, hydrosphere, atmosphere and biosphere interactions in areas of fault-crossing is developed (Fig. 1, 2).

Researches is executed at financial support RFBR, the grant 08-05-99816 "Active processes in the environment, their monitoring and forecasting in the territory of Arkhangelsk region" and Programs DSE of the Russian Academy of Science N 9 " Geospheres interactions", Project " "Studies process of interaction geospheres in active geological structure in the North of Russian Plate".

References

Akhundov I. D., Guseinov M. A., Solodilov L. M. Magnetic storms, variations geomagnetic and magnitotelluric fields at electromagnetic radiation from focus of earthquake // Razvedka i okhrana nedr. — 2007. — № 2. — P. 34—38 (in Russian).

Kutinov Y. G., Chistova Z. B. A hierarchial number of displays alcaline-ultrabasic magmatism of Arkhangelsk adamantine province. Their reflection in geological and geophysical data. — Arkhangelsk: OAO "IPP "Pravda Severa", 2004. — 283 p. (in Russian).

Geodetic estimations of the modern motions on Tien Shan

© ***S. Kuzikov, 2010***

Scientific Station, RAS, Bishkek, Kyrgyzstan
ksi@gdirc.ru

We can obtain information about formation and a posterior transformation of crust, in particular, from geological and structurally-tectonic researches or maps. More often we have only final result of change of geological objects and we do not know how this result has been reached in the course of time. Absence of such data has led to occurrence of extreme opinions about mode of intra-continental deformation of lithosphere. According to one of them, the prevailing part of movements realize through sliding of blocks on faults [e. g., Peltzer, Saucier, 1996; Replumaz, Tapponnier, 2003]. The alternative notion is based on the prevalence of plastic deformations and properties of a nonlinear-viscous liquid in crust [e. g., Flesch et al., 2001]. Long time the Research station of RAS (RS RAS) realizes geodetic researches of different scale, which allow to estimate quantitatively modern near-surface movements of Tien Shan crust and partially to understand the geodynamic problem designated above.

In Central Asia the regional GPS researches are in progress from 1992, by present time ~550 sites of periodic measurement are dispersed on ~1.7 million km^2 in territory of Kyrgyzstan, Kazakhstan, Uzbekistan, Tajikistan and China. The kinematic-statistical analysis of horizontal velocities measured for last 10—15 years, testifies about presence here quasi-rigid areas of crust (domains) in the size from ~30×50 to ~600×800 km^2 in which modern velocity of deformation is negligibly small [Kuzikov, Mukhamediev, 2010]. The inter-domain space (IDS) separate the quasi-rigid domains (QRD). IDS has width from first km to several hundreds km, in which velocity of displacement (to ~10 mm/year) can considerably exceed deviations from rigid whole in QRD (on the average — 0.35 mm/year). Total area of QRD

concedes a little of IDS territory as ~46 and ~54 % accordingly. In structure of IDS the spatially-kinematical regularity in 4 steady directions is allocated: NE (on the average ~54°) has left-hand component of shift; Latitudinal (~88°) has mainly cross-section shortening; SE (~116°) has elements of the right-hand shift; Meridional (~165°) has cross-section extension. The spatial analysis has shown absence of correlation between modern IDS and the active faults of Tien Shan, though on separate segments spatial and kinematic coincidence can be found. Thus, within IDS there can be both displacement on planes of faults, and elastic and-or plastic deformations.

In ~20—25 km to the southeast from Bishkek, in foothills of the Kirghiz range, RS RAS perform regular (1 time in 2 weeks) linear-angular (tacheometric) measurements from 2006 for detailed studying of deformation variations on 2 local sites. Tacheometric researches are combined with geodetic levelling, GPS measurements and other geophysical works. Each of these local sites occupies less then 0.75 km^2 and between them of ~5 km in direction W-E. Measured baselines between fundamental geodetic benchmarks have length from ~150 to ~1400 m. Since December 2007 to April 2008 on both local sites some northern benchmarks were anomalously displaced and then have returned almost on former places. Maximums of change of lengths on both local sites are fixed to the middle of March 2008 and have on a longitude ~ –18 mm on ~403 m (~ -4.5×10^{-5}) and on latitude ~14 mm on ~150 m (~9.3×10^{-5}). Thus, there was synchronous and approximately identical size of an elastic deformation for northern parts of the two local sites removed from each other on ~5 km. Probably, it is result of influence of neotectonic thrust located in ~500—1000 m to the north.

Approximately in the same area foothills of the Kirghiz range two profiles of northern directions have lengths ~14 and ~17 km for tacheometric observations on fundamental geodetic benchmarks are located. Since 1992 to 2009 on some segments of these profiles are lengthening and shortening the baselines with linear deformations to |~6.8×10^{-5}| on ~115 m and more. On some segments of profiles the change of directions of linear deformation is observed. The movements on some base lines it is possible to explain by displacement on planes of neotectonic faults, however on more base lines have elastic and plastic deformations, most likely.

At building of the dam by powerful explosion (~3 thousand tone of an explosive) has been made for the hydropower station Kambarata-2 on the river Naryn (near of Toktogulsky water-storage basin) on December, 22nd 2009. There was a probability of motions on the fault located in ~ of 300—500 m from epicenter of explosion. RS RAS exercised the geophysical observations within 2 days before explosion, during day of explosion and 2 days after. During this time 8 GPS stations on 4 sites exercised the continuous measurements around the explosion epicenter on distance from ~1.4 to ~5.3 km. As have shown the GPS data at daily averaging, almost on all investigated base lines immediately after explosion the increase in distances on 0.6—1.6 mm (on the average — 1.1 mm) was observed. Next day after explosion the same base lines have decreased on 0.2—0.9 mm (on the average — 0.5 mm). By the end of measurements the minimum of measured lengths of base lines for all time of supervision has been reached. Thus, around of epicenter there was elastic stretching immediately after explosion which after was replaced with shortening of all base lines as a result on 0.4—2.3 mm (on the average ~1.4 mm). Thus, the powerful industrial explosion has not essential influences on displacement of crust around hydropower station Kambarata-2.

References

Flesch L. M., Haines A. J., Holt W. E. Dynamics of the India-Eurasia collision zone // J. Geophys. Res. — 2001. — **106 (B)**. — P. 16,435—16,460.

Kuzikov S. I., Mukhamediev Sh. A. Structure of the Present-Day Velocity Field of the Crust in the Area of the Central-Asian GPS Network // Izv. Physics of the Solid Earth. — 2010. — **46**, № 7. — P. 584—601.

Peltzer G., Saucier F. Present-day kinematics of Asia derived from geologic fault rates // J. Geophys. Res. — 1996. — **101 (B)**. — P. 27,943—27,956.

Replumaz A., Tapponnier P. Reconstruction of the deformed collision zone between India and Asia by backward motion of lithospheric blocks // J. Geophys. Res. — 2003. — **108 (B6)**. — P. 2285. — DOI: 10.1029/2001JB000661.

Some common features in the picture of distributions of elastic heterogeneities of the crust and upper mantle of the Northern Caucasus accordingly to the earthquake converted-wave method, the deep seismic sounding and seismology

© ***A. Kuzin*[1], *L. Shumlyanska*[2], *2010***

[1]Institute of Oil and Gas, RAS, Moscow, Russia
amkouzin@ya.ru
[2]Institute of Geophysics, National Academy of Sciences of Ukraine, Kiev, Ukraine
lashum@ukr.net

Analysis is based on generalizations of regional ECWM and DSS works [Belyaevsky et al., 2006; 2007]. We used a model of the velocity of longitudinal waves for the mantle, calculated by the method of Teylor's approximation by Geyko V. S. [Geyko et al., 2005; Bugaienko et al., 2008]. Due to the fact that seismic methods differ by the type and frequency spectrum of the used waves in this work we consider the relative values of the velocity only.

Epicenters of the earthquakes weakly correlates with distributions of velocities of longitudinal (V_P) and transverse (V_S) waves and V_P/V_S in the crust and below the M boundary that are constructed accordingly to the ECWM and DSS data. These distributions are evidently dominated by the direction orthogonal to the strike of the folded structure of the North Caucasus and its main regional faults. Some correlation with discontinuous tectonics can be seen along the 45—46° longitude (fragment of the Transcaucasian regional fault), where at the latitude 44° a stepwise shift to the south for a cut of V_P/V_S is observed. In general, contours of the parameter V_P/V_S reflect more clearly the distribution of velocity heterogeneities in the crust compared with V_P and V_S slices. Clearly visible is the flexural bend of the contours along the longitude 46° coinciding with a high absorption zone [Shempelev et al., 2010]; more contrast arrear the maximum of decreased V_P/V_S values beneath the Stavropol uplift (45—44° latitude, 41—43° longitude) and prevailed in central parts of plots south-western strike of V_P/V_S isolines. The highest values of V_P, V_S and V_P/V_S are in better agreement with the regions of recent volcanic activity compared to the discontinuous tectonics of the Northern Caucasus folded structures. Comparison with the contemporaneous geokinematic tectonic map of the region [Kopp, 2005] allows us to interpret the distribution pattern of V_P, V_S and V_P/V_S in the crust of the North Caucasus as a reflection of its horizontal compression by the Arabian plate.

If we turn now to the results of processing and interpreting of seismological data, on the section corresponding to the 50 km depth a correlation between the earthquakes focies with the gradient zone of low values of the longitudinal wave velocities becomes evident. In the next section (H=100 km) a picture of V_P/V_S distribution similar to the lower part of the crust attracts one's attention. Lower values of V_P/V_S for the Stavropol uplift correlate with a projection of low V_P values. This area coincides with area of the recent volcanic activity (Elbrus, Kazbek, etc.). Taking into account presence of gas fields within the Stavropol uplift and its frame the region of low V_P/V_S values in the lower crust may be explained by high gas content. In the middle crust the area of the relatively low V_P/V_S values expands that agrees with such interpretation. On sections at 150 and 200 km the V_P distribution pattern changes dramatically. From the depths of 150 to 200 km the low-velocity area beneath the Stavropol uplift is replaced by the high-velocity one, while the prevailed direction of the velocity contours changes to the south-west and south-east.

At depths of 250 and 300 km of the mantle beneath the North Caucasus is represented by the high-velocity area. In the depth interval of 350—400 km a pattern of the velocity distribution changes again — the sublatitudinal strikes of the low velocity isolines become apparent in the northern and southern parts of the region. In the 450—500 km depth interval the V_P in the northern part becomes

more slow, we assume that underthrusting of the Scythian plate beneath the East European platform may occur at this depth interval.

From the above analysis we assume that from depths interval of approximately 70—120 km inversion of the velocity distribution and correspondingly of the distribution of mantle heterogeneities starts. [Krasnopevtseva, Kuzin, 2009] on the seismic profile Volgograd — Nakhichevan have shown that the relatively high-velocity folded structure of the Greater Caucasus has a tendency to dive under the Scythian plate, this interval corresponds to the immersion of M (*H*=50 km). At about the same interval a consistent series of mantle earthquakes with depths of focies 74, 97, 100, 115, 123, 150 km was recorded along the profile. Obviously, such a coincidence of focal depths of earthquakes and the beginning of the interval of inversion of elastic inhomogeneities distribution in the upper mantle is not accidental.

Vertical sections provide an opportunity to analyze the distribution of longitudinal velocities along 45, 43 and 41° N to a depth of 2500 km. Beneath the Stavropol uplift a picture of the velocity distribution differs significantly. To the east of 41—42° E the upper mantle represented by alternating layers: a low-velocity layer at a depth interval 50—150 km replaced by high-velocity layer at 150—250 km interval and again turn into low-velocity layer that cross the 670 km border of the upper mantle and extend down to 1300 km. In the lower mantle velocity changes do not exceed ±0.025 km/s from the reference zero velocity. In the western part of the area both the depth of the layers and velocity values change with the tendency to increase. The depth of the upper low-velocity layer increases to 300 km, of the underlying high-velocity layer — down to 500 km, while the low velocity layer appear at depths of 500—700 km. Anomalies of the velocity in the lower mantle are noteworthy. In contrast to the eastern part, here the alternation of high and low-velocity anomalies with deviations of ±0.10 km/s from a depth of 1300 km to 2500 km are observed. Stavropol uplift and Volcano Elbrus with their specific set of anomalies of geophysical fields such as positive anomalies of the thermal field and electrical conductivity are confined to the area of gradient change in the distribution of longitudinal velocities which can be traced throughout the section to a depth of 2500 km.

In general, there is a good correlation between different surface structures of the crust of the North Caucasus and the distributions of velocity of longitudinal waves at all sections.

References

Belyaevsky V. V., Egorkin A. V., Solodilov L. N., Rakitov V. A., Yakovlev A. G. Some results of applying methods of natural electromagnetic and seismic fields in the North Caucasus // Phys. Earth. — 2007. — № 4. — P. 4—14 (in Russian).

Belyaevsky V. V., Egorkin A. V., Zolotov E. E., Rakitov V. A., Avenisyan V. I., Konovalov Y. F., Nedyadko V. V. In-depth geological and geophysical studies by seismic prospecting (ECWM) and resistivity (MTS, GMTS, AMTS) methods in the regional profiles Eisk — Stavropol — Neftekumsk — Caspian Sea (850 km) and Corfe-Top Penzhina (500 km). Analysis and compilation of deep geophysical studies conducted in the North Caucasus, Kamchatka, and southern Siberia (report). — Moscow, 2006 (in Russian).

Bugaienko I. V., Shumlyanskaya L. A., Zaiets L. N., Tsvetkova T. A. Three-dimensional *P*-velocity model of the mantle of the Black Sea and the adjacent territory // Geophys. J. — 2008. — **30**, № 5. — P. 145—160 (in Russian).

Geyko V. S., Tsvetkova T. A., Shumlyanskaya L. A, Bugaienko I. V., Zaiets L. N. Regional 3-D *P*-velocity model of the mantle of Sarmatia (south-west of the East European Platform) // Geophys. J. — 2005. — **27**, № 6. — P. 927—939 (in Russian).

Kopp M. L. Mobilistic neotectonics of platforms in South-Eastern Europe. — Moscow: Nauka, 2005. — 340 p. (in Russian).

Krasnopevtseva G. V, Kuzin A. M. The mapping of tectonic activity of the junction zone of the Caucasus and the Scythian plate according to the interpretation of seismic profile of the DSS “Volgograd — Nakhichevan”. Geologic hazards // Mater. XV All-Russian Conf. with int. participation. — Arkhangelsk: Institute of Ecological Problems of the North ASC UB RAS, 2009. — P. 250—253 (in Russian).

Shempelev A. G., Feldman I. S., Belyavsky V. V., Kuhmazov S. U. Results of deep geophysical investigations of the eastern part of the Terek-Kuma Depression // Mater. XLIII tectonic meeting. 2. — Moscow: GEOS, 2010. — P. 450—455 (in Russian).

Neural network for seismic shaking intensity modeling

© **M. Lazarenko, V. Korolev, 2010**

Institute of Geophysics, National Academy of Sciences of Ukraine, Kiev, Ukraine
misha@nds.org.ua

The seismic zonation realizes one of major economic but most complicated tasks of seismology — numerical estimation (assessment) of seismic hazard (on the patch of earth surface), actually performing the prediction of shaking intensity distribution, using ill-found observations and conceptual regulations. The discussed approach to the problem is an attempt of filling the methodological gaps of this prediction by means of networks of artificial neurons — a powerful instrument of statistical analysis, allowing to build the behavior model of shaking intensity, using the limited set of observed examples of this behavior.

A neural-net model was formed on multi-layer, feedforward, fullconnected, controlled neuron network, using for training the error back propagation method and the set of parameter vectors — accessible to us geological, physical and morphological properties of seismic waves propagation medium. For the target the macroseismic estimation of shaking intensity was used.

A highest seismic hazard is threatening Ukraine from the Romanian earthquakes of Vrancea zone. "Domestic" sources do not represent a serious danger, except, possibly, the Crimea, where 1927 event and specificity of region make it a target of zonation.

Vrancea source. The seismic waves propagation media may be regarded as a filter, distorting the wave field, and the projection of elements of this media on an Earth's surface as a digital image or raster, which is shown on Fig. 1.

Every element, or pixel, is described by the vector of parameters, which components are the number of accessible to us descriptions of physical properties of geological media, functionally related to the response of this media on excitation by seismic waves. Factors that govern the seismic field distortion and control a diversity of shaking intensity distributions over the Earth's surface can conditionally be divided into three groups: regional or deep, local, and shallow (Tab. 1).

Table 1. Components of training set for the model of intensity of Ukraine

Parameters	Units	Range
Gravity	10^{-5} m/s^2	–95.4—111.0
Magnetic intensity	10^2 nT	–3.91—11.0
Heath flow	W/m^2	20.0—90.0
Apparent resistance	om	1.5—3712.0
Neotectonic movment amplitude	m	–3904.0—2084.0
Modern movements velocity	mm/year	–5.10—4.64
Basement depth	km	0—16.0
Fault density	n/pixel	0—4
Horizontal relief section	km/km^2	0.16—2.46
Vertical relief section	m	4.3—413.0
Hypocentral distance	km	230.8—1492.9
Back azimuth	Degree	171.3—330.6
Magnitude	Richter	6.7—7.2
Source depth	km	90—120
Shaking intensity	MSK-64	2.5—7.0

A near zone, that envelopes the southwest of the country, is exposed to body waves, macroseismic effect of which is controlled to a considerable degree by the local inhomogeneties and source mechanism. Shaking intensity in a distant zone is governed by the surface waves, for which defining are regional features of geological structure functionally related to integral characteristics of the stationary physical fields. Macroseismic measurements in metric of MSK-type scale are based on the reactions of standard sensors, which are largely determined by character of coupling with the Earth's surface. The mediated characteristic of such a contact can serve for the level assessment of its degeneration under influence of endogenous and exogenous factors, determined by the horizontal and vertical relief sections.

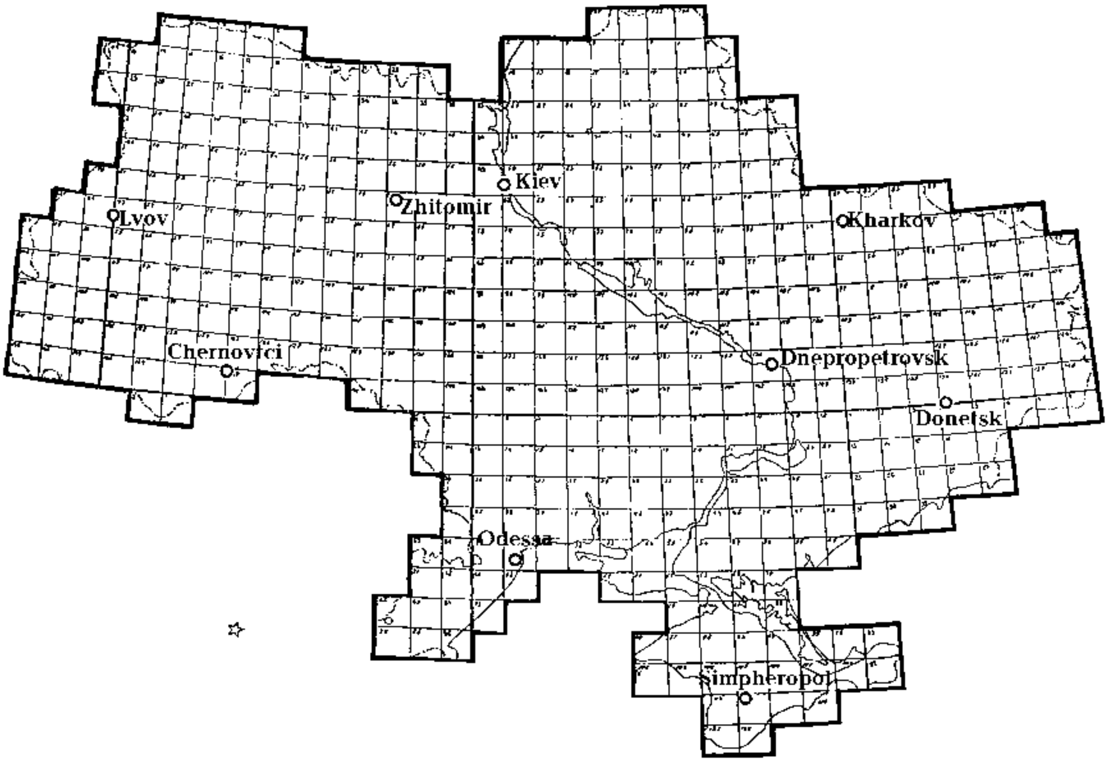


Fig. 1. Raster image of Ukraine.

As targets the mean values of the macroseismic estimations for a given pixel were considered. For Vrancea earthquakes five training sets were formed: in three of them as targets macroseismic evaluations of ’77,’86, and ’90 earthquakes were used. In fourth, for the pessimistic scenario, the worst of the first three were selected. In fifth the first three and 26 pixels of known macroseismic evaluations of ’40 Vrancea earthquake were integrated. As an example on Fig. 2 the izoseismal map for Ukraine of Vrancea ’86 earthquake and pessimistic scenario for XX century quakes are presented.

When compiling the training set for the neural networks for simulation of shaking intensity caused by the single event, such parameters as hypocentral depth and magnitude are not valid as parameters, because they are identical for all vectors-objects of training set and therefore not informative. Using the macroseismic estimations of four earthquakes a neural model allows to integrate these parameters and, due to a capacity for generalization, to model the shaking intensity, caused by a source with characteristics, different from such, used for training, what is shown on Fig. 3 for the extreme parameters of Vrancea source known from historical retrospections.

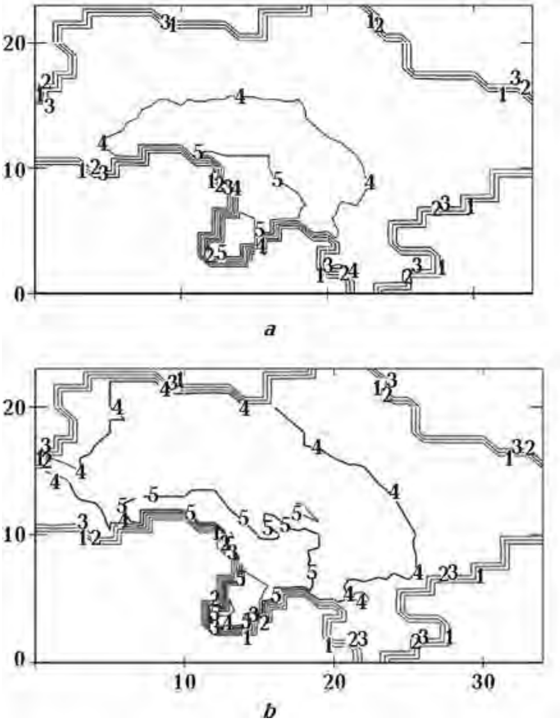


Fig. 2. Shaking intensity distribution in Ukraine in grades of MSK-64 scale for Vrancea1986 earthquake (*a*) and pessimistic scenario for strong Vrancea XX century earthquakes (*b*).

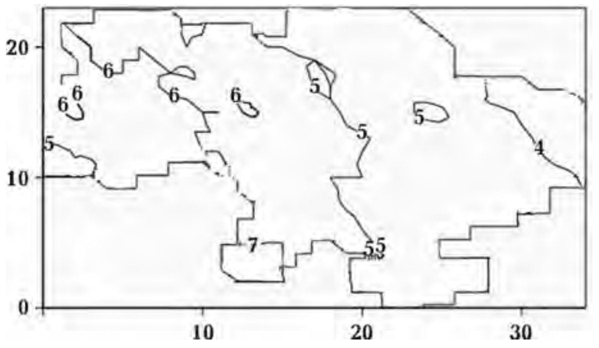


Fig. 3. Prediction of shaking intensity distribution in Ukraine in grades of MSK-64 scale for Vrancea, M=8.1, *h*=150 km.

Microzonation of Yalta. Big scale seismic zonation, obligatory for construction of civil and industrial objects in seismoactive regions, must be realized with due regard for number of factors concerning not only physical and mechanical properties of soil, their geological and morphological characteristics but also using some standard assessments relating these characteristics with responses to possible seismic force. The neural network can solve this problem.

Table 2. Components of vector parameters for Yalta neural model

Parameters	Units	Range
Magnitude	Richter	3.7—6.8
Source depth	km	17—22
Range	km	120—170
Back azimuth	Degree	18.2—26.8
Soil type	Boolean	0.1
Sediment thickness	m	2—20
Water table	m	0—20
N-W extent	Fault #	
N-E extent	Fault #	
Elevation	m	25—300
Tilt	Degree	15—30
Exposition	Degree	90—315
Shaking intensity	MSK-64 scale	3.6—8.3

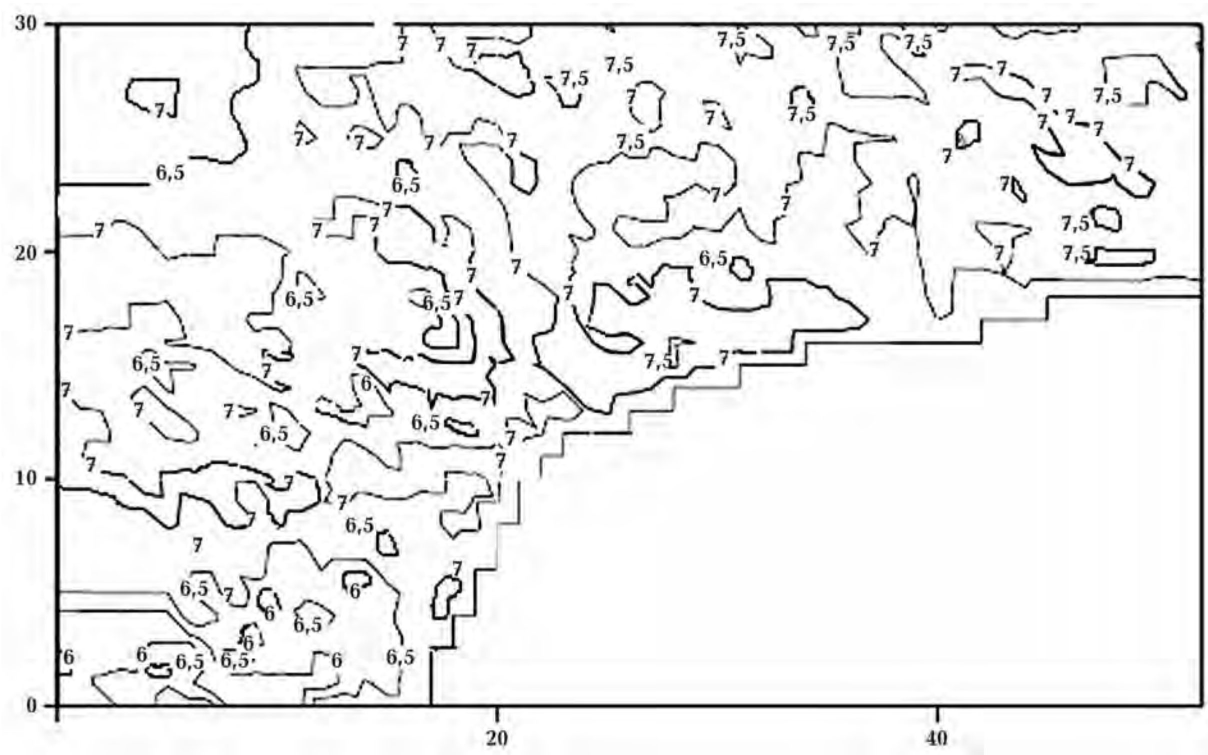


Fig. 4. Prediction of shaking intensity distribution in Great Yalta in grades of MSK-64 scale for ’27 Yalta earthquake type.

Based on macroseismic evaluations of Yalta ’27 and ’80 earthquakes, according to the algorithm used for Vrancea case, for parameters describing the geological medium and listed in Tab. 2, the neural network was trained and used for imitation of the shaking intensity behavior on Great Yalta terrain (Fig. 4).

Technical and algorithmic complex of monitoring of the dangerous geodynamics phenomena

© **O. Liashchuk, 2010**

Main center of the special control, Makarov-1, Ukraine
alex_liashchuk@mail.ru

It is set that mechanical changes in the earth's crust cause the change of parameters of all of the geophysical fields — electromagnetic, acoustic, seismic, influence on speed of output of gases from the earth's crust et al. The overhaul of the last looks to co-operation of the geophysical fields is resulted in work [Liperovsky et al., 2008]. These changes are most noticeable at such high-power phenomena, as earthquakes. At what changes in the geophysical fields take a place and registered not only after a basic shove but also during preparation of earthquake and can serve in quality forecasters.

On the basis of world information and own researches we are offer the qualitative model of co-operation of the geophysical fields during development of earthquakes and education of forecasters [Liashchuk et al., 2007]. So as a result of formation of defects as a result of change of the resiliently deformed state (mechanical tension) of the earth's crust before an earthquake, there are hertzian waves and underground acoustic noises. It is related to that every act of formation micro- and macrodefect excitation of acoustic and optical vibrations of crystalline grate, and consequently and by the radiation of acoustic and electromagnetic waves. In same queue the radiation of acoustic waves can result in an accelerating mechanism, essence of which in because intensive formation of defects, which is generated a stress deformation of breeds in the district of the future forms ultrasonic waves which in same queue substantially increase speed of transfer of gases (to the radon in a that number) in the matrix of mountain breeds the epicentre of earthquake. As a result of exit from breeds on the surface of radio-active gas of radon, there is ionic composition of the atmosphere and there is an anomalous electromagnetic radiation in an atmosphere. The increase of tension brings to the compression breeds over in the place of future cell of earthquake, as a result also there is an intensive exit of gases from the earthly bowels of the earth (so-called effect of degassing). At forming of main break, when the system already is in the unstable state, there are noise long-period vibrations of earthly surface, which result in appearance of vertical low-frequency acoustic vibrations — infrasound. Arriving at the overhead layers of atmosphere (ionosphere), infrasound begins to influence on chaotic motion of the charged particles (ions). Motion of ions acquires a certain orientation, what ionosphere currents are as a result of. Ionosphere currents, caused the vibrations of the earth's crust, and also atmosphere ionized before an earthquake can influence on distribution of VLF radio waves, which spread in a waveguide Earth-ionosphere.

Taking into account aforesaid, in the Main center of the special control created system for the exposure of possible predict effects of, which includes for itself the complex of the seismic, electromagnetic, infrasonic, radon measurings and can broaden other geophysical methods. An apparatus for conducting of measurings is oriented to measuring of low-frequency background processes in the earth's crust and atmosphere.

Practice of prognosis researches shows that as a reliable forecaster for every earthquake, none of common geophysical methods can not come forward, as before earthquakes which took a place, in times of systematic supervisions there were cases of and erroneous anomalies, and "admission of purpose".

The analysis of long-term data of row of geophysical (mainly seismological) forecasters showed that probability of successful prognosis on each of them did not exceed 0.5. One of possible exits from a situation there is the general use a few signs. It is thus necessary to go out from that every separate forecaster represents that, whether other side manysided and not to the end of clear process of preparation of earthquake and is not informing enough from the point of view statistics.

As a result of analysis of the accumulated information we are choose the row of prognosis criteria for each of geophysical methods which are on ob-

servation of MCSM posts. The estimation of probability of that an earthquake will take a place is conducted, taking into account probabilities of possible forecasters for the region of mountains of Vrancha. For each of criteria, offered for a compatible analysis probabilistic indexes settled accounts during throughout the year, a selection is taken in which. An integral criterion which took into account influencing of found out every forecaster settled accounts in future.

It is set that most payment is given by radon and electromagnetic forecasters. However, none of them independently exceeded the value of probability of origin of earthquake for the region of Vrancha (R=0,358). But before an earthquake 12.05.2005 (M=5,1), when all worked criteria are select, probability of origin of earthquake a complex was R=0.77, that in 2,1 times exceeds probability of the simple guessing.

Subsequent development of methods of complex researches and receipt of the unique integral description is on observation posts, will enable yet more to promote reliability and efficiency of prognosis estimations.

References

Liashchuk O. I., Savel'ev V. Yu., Pavlovich V. M. Complex method for search of probable forecasters of earthquakes in district of vrancha mountains // Geodynamics. — 2007. — № 1(6). — P. 55—59 (in Russian).

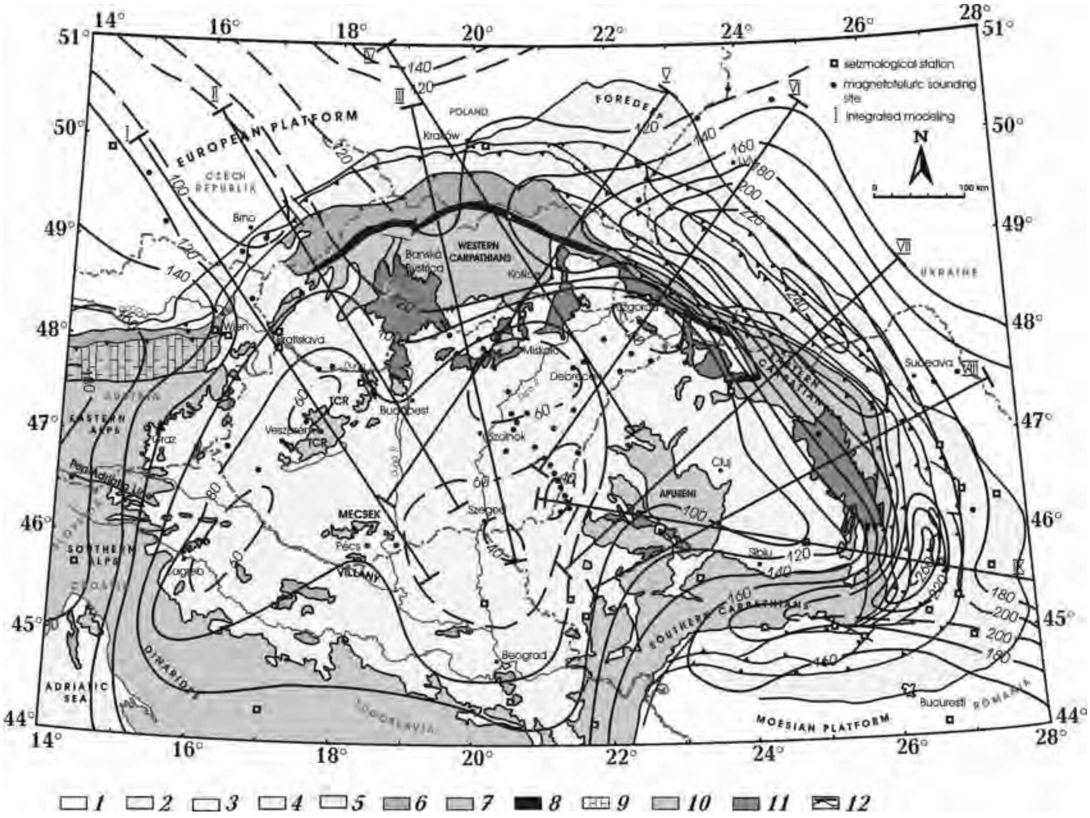
Liperovsky V. A., Pokhotelov O. A., Liperovskaya E. V., Meister C.-V. Physical models of coupling in the lithosphere-atmosphere-ionosphere system before earthquakes // Geomagnetism and Aeronomy. — 2008. — **48**, № 6. — P. 795—806 (in Russian).

Thermal state of the West Carpathian lithosphere — measured data and modelling results

© *D. Majcin[1], M. Bielik[2], M. Král[3], 2010*

[1]Geophysical Institute of SAS, Bratislava, Slovakia
geofmadu@savba.sk
[2]Department of Applied and Environmental Geophysics,
Faculty of Natural Sciences,
Comenius University of Bratislava, Bratislava, Slovakia
bielik@fns.uniba.sk
[3]Geothermex, Pezinok, Slovakia
geothermex@centrum.sk

We present the results received by the study of the thermal state of West Carpathian lithosphere both by direct methods and by modelling approaches. The direct methods are repre-sented by tables, graphs and maps of measured data — temperature distributions and heat flow density data collected and published mainly in [Atlas …, 1995]. The maps of thermal characteristics constructed in various depths levels of the upper part of the crust are there supplemented by related geological structures. The measured geothermal data were processed by classical interpolation and extrapolation methods. The modelling approaches are represented by results of stationary methods applied on cross sections along six profiles crossing the Carpathian arc [Majcin, 1993], by transient models [Majcin, Tsvyashchenko, 1994; Majcin et al., 1998] and by special 2D integrated modelling [Zeyen, Bielik, 2000; Zeyen et al., 2002; Dérerová et al., 2005; 2006] that combines interpretation of surface heat flow, gravity, topography and geoid data, which was used for calculation of the lithospheric thickness along nine geotransects passing through the Pannonian-Carpathian basin region. The temperature fields were calculated by the means of the finite difference method and of the finite element method. The density of calculated data allows to construct maps with the temperature distribution and distribution of



Map of lithospheric thickness in the Carpathian/Pannonian basin region: *1* — North European planform and Moesian platform, *2* — Foredeep, *3* — Subcarpathian unit, *4* — Krosno-menilite group and external Moldavides, *5* — Internal Moldavides, *6* — Magura group, *7* — Outer dacides, *8* — Pieninske bradlove pasmo, *9* — Northern calcareous Alps, *10* — Alpine-Carpathian-Pannonian internides, *11* — Neogene volcanides areas, *12* — Main tectonic lines.

the vertical component of the heat flow density on various depth levels, on Moho-discontinuity and also to construct the map of the supposed lithosphere thickness (Figure).

References

Atlas of Geothermal Energy of Slovakia / Eds. O. Franko, A. Remšík, M. Fendek. — Bratislava: Dionýz Štúr Institute of Geology, 1995. — 96 p.

Dérerová J., Bielik M., Dudášová V. Preliminary map of the lithospheric thickness in the Pannonian-Carpathian basin region obtained by means of 2D integrated modelling // Contrib. Geophys. Geod. — 2005. — **35**, № 2. — P. 163—172.

Dérerová J., Zeyen H., Bielik M., Salman K. Application of integrated geophysical modeling for determination of the continental lithospheric thermal structure in the eastern Carpathians // Tectonics. — 2006. — **25**, № 3. — Art. N TC3009.

Majcin D. Thermal state of the west carpathian lithosphere // Studia geophys. et geod. — 1993. — **37**, № 4. — P. 345—364.

Majcin D., Dudášová V., Tsvyashchenko V. A. Tectonics and temperature field along the carpathian profile 2T // Contrib. Geophys. Geod. — 1998. — **28**. — P. 107—114.

Majcin D., Tsvyashchenko V. A. Effect of magmatism on temperature field in the northern part of the Transcarpathian depression // Contrib. Geophys. Geod. — 1994. — **24**. — P. 72—86.

Zeyen H., Bielik M. Study of the lithosphere structure in the Western Carpathian-Pannonian basin region based on integrated modelling // Geophys. J. — 2000. — **22**, № 5. — P. 70—82.

Zeyen H., Dérerová J., Bielik M. Determination of the continental lithospheric thermal structure in the Western Carpathians: integrated modelling of surface heat flow, gravity anomalies and topography // Phys. Earth Planet. Int. — 2002. — **134**, № 1—2. — P. 89—104.

Heat flow refraction on structures with conductivity contrast

© D. Majcin, M. Hvoždara, D. Bilčík, 2010

[1]Geophysical Institute of SAS, Bratislava, Slovakia
geofmadu@savba.sk
geofhvoz@savba.sk
geofdubi@savba.sk

This contribution is devoted to the analysis of the refraction of the heat flow caused by the subsurface structures with contrasting thermal conductivity values. We enhanced the fundamental calculation and interpretation results [Carslaw, Jaeger, 1959; Ljubimova et al., 1976; 1983; Czeremensky, 1977, …] related to these effects by some new model configurations and by qualitative and quantitative analysis of their influence on the temperature and on the heat flow density distribution. The basic refraction effects were studied on models with the disturbing bodies bounded by the coordinate surfaces and buried in homogeneous half-space or in horizontally layered media [Hvo•dara, Majcin, 1985; Hvo•dara, 2008; 2009]. These model types were supplemented by more realistic 2D and 3D disturbing model structures with the contrasting thermal conductivity coefficients (various polygonal and polyhedral bodies). They were analysed in papers of [Hvoždara, Schlosser, 1985; Majcin, 1992; Hvoždara, Valkovič, 1999, Hvoždara, 2008; Hvoždara, Majcin, 2009] and other. The great attention was paid to the model problems related to the refraction of the heat flow near the border of the sedimentary basins also combined with the refractions on the Earth's surface topography [Majcin, Polák, 1995].

The solutions of mathematical problems were presented in the exact analytical form or they were received by the numerical approaches. The boundary element method and the finite difference method were the most frequently employed in our calculations.

The calculated model temperature distributions, the surface heat flow density data and also the distributions of the heat flow density vector components are analysed also with regard to the interpretation of measured surface data, to influence on calculation of representative heat flow density and to construction of the terrestrial heat flow maps over the geological structures with different thermal conductivity coefficients. The new models show the great importance of the refraction effects on contrasting structures in all mentioned branches of the geothermics. The anomalous temperature distributions, the step changes of the heat flow density components calculated in the directions not normal to the structure boundaries characterised by the step change of the conductivity parameters and the declination of heat flow density vectors from vertical direction near these boundaries force to apply refraction effects to measurements and interpretations mainly near the sedimentary basins borders and near the vertically or aslant layered structures or such narrow contrast rock zones. Such structures are typical and frequently occurred also inside the tectonic region of the West Carpathians.

References

Carslaw H. S., Jaeger J. C. Conduction of heat in solids. — Oxford: Claredon Press., 1959. — 510 p.

Czeremensky G. A. Applied geothermics. — Leningrad: Nedra, 1977. — 224 p. (in Russian).

Hvo•dara M. Geothermal refraction anomaly due to a spherical body buried in the halfspace // Contrib. Geophys. Geod. — 2000. — **30**, № 3. — P. 261—277.

Hvo•dara M. Groundwater and geothermal anomalies due to a prolate spheroid // Contrib. Geophys. Geod. — 2009. — **39**, № 2. — P. 95—119.

Hvo•dara M. Refraction effect in the heat flow due to

3-D prismoid, situated in two-layered Earth // Contrib. Geophys. Geod. — 2008. — **38**, № 4. — P. 371—390.

Hvoždara M., Majcin D. Calculation of a heat-flow anomaly generated by a cylindrical inhomogeneity // Contrib. Geophys. Geod. — 1885. — **15**. — P. 51—58.

Hvoždara M., Majcin D. Geothermal refraction problem for a 2-D body of polygonal cross-section buried in the two-layered Earth // Contrib. Geophys. Geod. — 2009. — **39**, № 4. — P. 301—323.

Hvoždara M., Schlosser G. Anomaly of the telluric and thermal field by the presence of a two-dimensional body in the homogeneous halfspace // Contrib. Geophys. Geod. — 1985. — **15**. — P. 35—49.

Hvoždara M., Valkovič L. The refraction effect in the geothermal heat flow due to a 3-D prism in two layered Earth // Studia geophys. et geod. — 1999. — **43**. — P. 407—426.

Ljubimova E. A., Ljuboshits V. M., Nikitina V. N. Effect of contrasts in the physical properties on the heat flow and electromagnetic profiles // Geoelectric and geothermal studies / Ed. A. Ádam. — Budapest: Akadem. Kiado, 1976. — P. 72—102.

Ljubimova E. A., Ljuboshits V. M., Parfenjuk O. I. Numerical models of temperature fields in the Earth. — Moscow: Nauka, 1983. — 124 p. (in Russian).

Majcin D. Refraction of heat flow on the near-surface structures with thermal conductivity contrast // Contrib. Geophys. Geod. — 1992. — **22**. — P. 67—80.

Majcin D., Polák S. Refraction of heat flow near the border of the sedimentary basins with topography // Contrib. Geophys. Geod. — 1995. — **25**. — P. 99—112.

Secular variation of the geomagnetic field in Europe for the 1985—2005 years

© ***V. Maksymchuk, Yu. Horodysky, D. Marchenko, 2010***

Carpathian Branch of Institute of Geophysics, National Academy of Sciences of Ukraine, Lvov, Ukraine
vmaksymchuk@cb-igph.lviv.ua

Secular variation (SV) is a typical feature of the Earth magnetic field. Doing the magnetic surveys for the different purposes, creating the maps of the anomalous magnetic field, it is very important take into account the knowledge about the time spatial structure of the Earth magnetic field. Geomagnetic observatories and data measured at the repeat stations (SV points) are offers the main source of information about the time spatial structure of SV. Using this data, constructed maps of the secular variations of geomagnetic field gave us imaginations about the morphology of SV in studied regions and theirs comparison at different time let us to detect the focuses of the secular variations and investigate theirs kinematics. Auspicious conditions take place in the European region for the detail study of the SV according to the huge network of the magnetic observatories.

Spatial structure of the SV in European area is demonstrated in such papers as [Orlov et al., 1968; Pushkov, 1976; Maksymchuk et al., 2001] in which shown that the very dynamic structure of SV attend in the second part of XX century in Europe: disintegration of the Caspian (Iran) SV focus in 60th and formation of the new SV focus in central Europe in 70th [Maksymchuk et al., 2001; Maksymchuk, 2002].

The main goal of this work — compilation of the new maps of the secular variation of geomagnetic field for the European region in the beginning of XXI century and investigations of the characteristics of time spatial structure on the basis of these new maps.

As we can see from the Fig. 1—2 occurrence of the global positive focus with the epicenter in the Apennine — Balkan region is the main feature of the secular variation of the geomagnetic field during the 1985 — 1995 years in Europe. According to the data from IGRF-10 global magnetic model the intensity of this focus by *Z*-component come to the 24 nT/y during the 1985—1990 years and 22 nT/y during the 1990—1995 years. This focus was concentrated basically in all part of Central and Western Europe.

Analyzing the data from the magnetic observatories we come to conclusions that this SV focus in comparison to IGRF data not such strong but also take place in European continent. However, its struc-

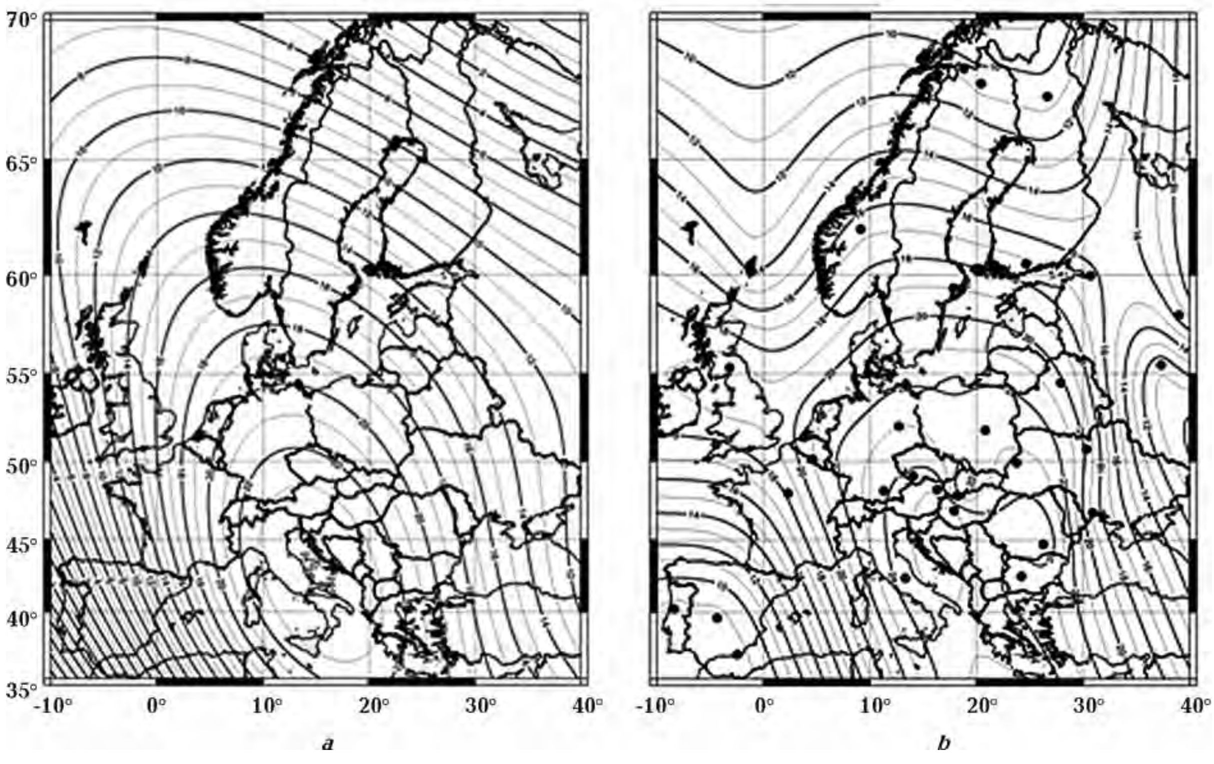


Fig. 1. Secular variation form 1985 to1990 of *Z*-component: *a* — IGRF-10 model, *b* — magnetic observatories data.

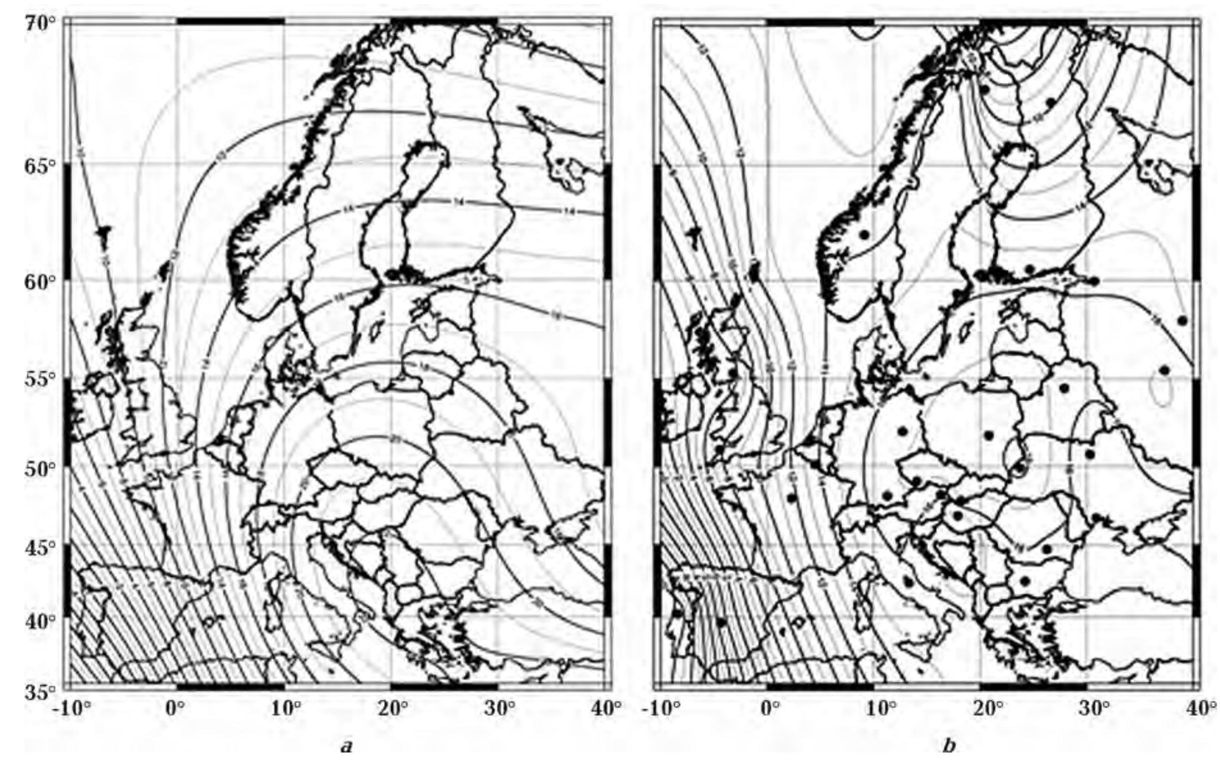


Fig. 2. Secular variation from 1990 to 1995 of *Z*-component: *a* — IGRF-10 model, *b* — magnetic observatories data.

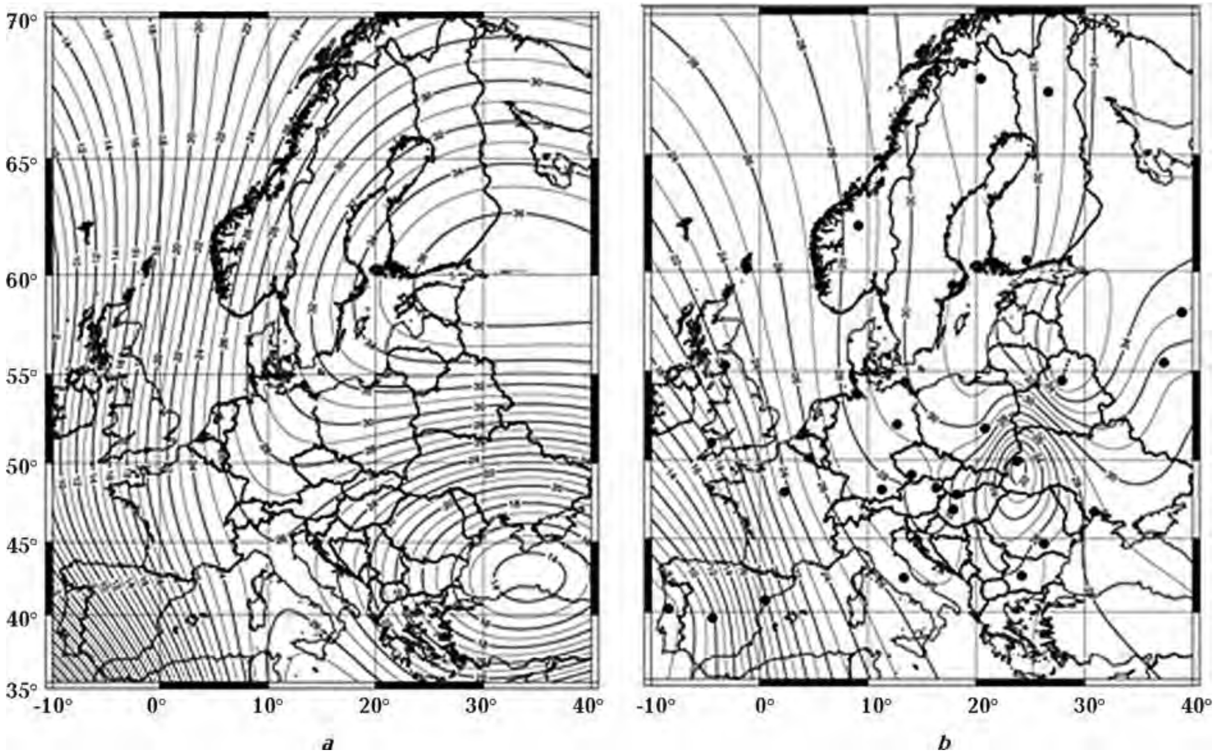


Fig. 3. Secular variation from 1995 to 2000 of *Z*-component: *a* — IGRF-10 model, *b* — magnetic observatories data.

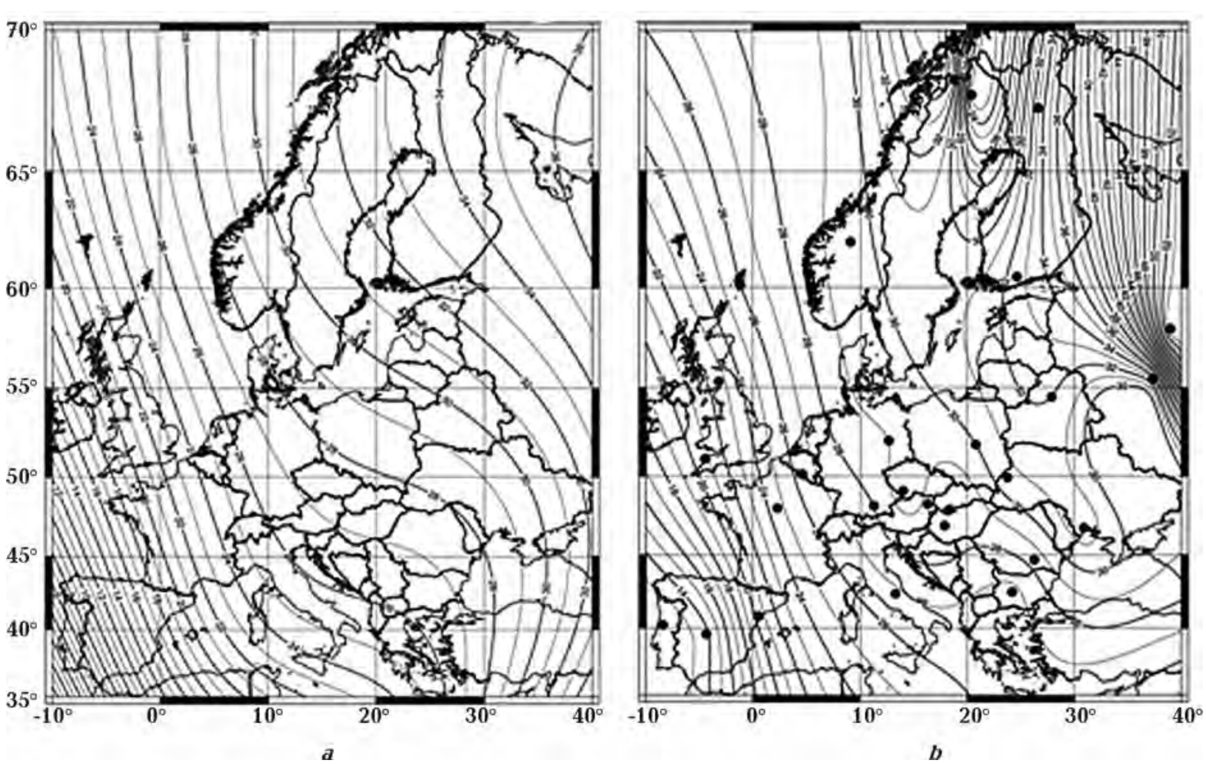


Fig. 4. Secular variation from 2000 to 2005 of *Z*-component: *a* — IGRF-10 model, *b* —magnetic observatories data.

ture more complicated particularly for the 1990—1995 years (Fig. 2, *b*), where its intensity noticeably lower (18 nT/y) in comparison to IGRF-10 model (22 nT/y) and epicenter is located in Poland region.

Different changes in SV structure happen in 1995—2005 years. In fact during the 1995—2000 years the Balkan SV focus is cease to be effective. In the area of Black Sea the global minimum of secular variation (16 nT/y) from IGRF data become apparent (Fig. 3, *a*). The central and western part of Europe is under the influence of the global focus in the north-west part of Europe. Instead of IGRF model the global minimum according to the magnetic observatories is absent in the Black Sea region, while the SV structure in the area of Rumania and East Ukraine sophisticated by the regional minimum (22 nT/y, Fig. 3, *b*).

During the 2000—2005 years IGRF — 10 model do not contain particular anomalies in the SV structure (Fig. 4, *a*). Secular variations field slightly unvarying decrease in the north — west and western direction. However, magnetic observatories data more expressive indicate that the morphology of the SV field allocate the global focus in the north-west part of Europe (Fig. 4, *b*).

For the X, I and D components secular variation structure do not disagree with the structure of *Z*-omponent. In general, comparison of the SV structures based on IGRF model and observatories data indicate about its adequacy. In western part of Europe the differences much higher than in the eastern part [Maksymchuk et al., 2010].

For our opinion we have grounds to maintain that the SV focus which toke place in the Europe during the 70th in the end of XX century was collapsed. Time of its existence do not exceed more than 25—30 years. By the spatial and time characteristics it could be referred to the short periodic SV focus and its nature can be related to the magnetic field generation in the Earth kernel.

We would like to express our sincerely thanks to the National fund of the fundamental researches which make the foundation in the frame of scientific project “Secular variation of the geomagnetic field in Europe” № F28.6/043.

References

Maksymchuk V. Time spatial structure of the secular variation of geomagnetic field in Europe. — Lvov: Scientific association of Shevchenko (Geophysics), 2002. — P. 57—67.

Maksymchuk V., Gorodysky Yu., Kyznecova V. Dynamic of the anomalous Earth magnetic field. — Lvov: Eurosvit, 2001. — 308 p.

Maksymchuk V., Gorodysky Yu., Marchenko D. Time spatial structure of the secular geomagnetic variations in European region in the beginning of the XXI sc. // IXth International Conference on Geoinformatics. — Theoretical and Applied Aspects (11—14 May), 2010. — Kiev, Ukraine, 2010.

Orlov V., Ivchenko M., Bazarganov A., Kolomuiceva G. Secular variation of the geomagnetic field during the 1960—1965 years. — Moscow: IZMIRAN, 1968. — 68 p.

Pushkov A. Secular variation of the geomagnetic field based on paleomagnetic and archeomagnetic data // Geomag. Res. — 1976. — № 17. — P. 9—14.

Results of the geomagnetic survey on the Ukrainian repeat stations network for the 2005 year epoch

© ***V. Maksymchuk*[1], *M. Orliuk*[2], *V. Tregubenko*[3], *Y. Horodysky*[1], *Y. Nakalov*[1], *V. Myasoyedov*[2], 2010**

[1]Carpathian Branch of Institute of Geophysics, National Academy of Sciences of Ukraine, Lvov, Ukraine
vmaksymchuk@cb-igph.lviv.ua
Institute of Geophysics, National Academy of Sciences of Ukraine, Kiev, Ukraine
orlyuk@igph.kiev.ua
[3]Ukrainian State Geological Prospecting Institute, Kiev, Ukraine
vitr@ukrdgri.gov.ua

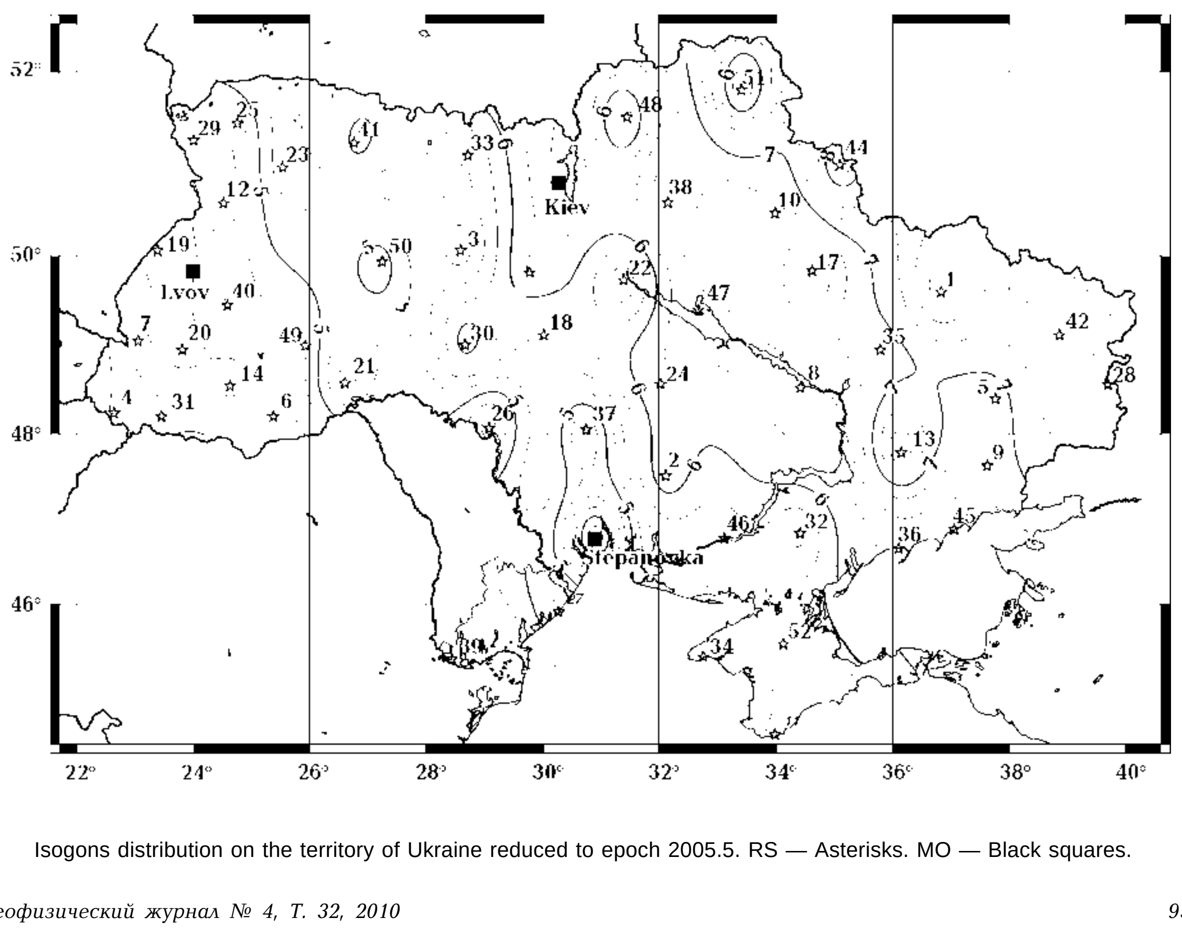
During 2003—2007 years there was renewed and enlarged the Ukrainian geomagnetic repeat stations (RS) network by the co-workers of Carpathian Branch of Subbotin Institute of Geophysics, Sub-

botin Institute of Geophysics and Ukrainian State Geological Prospecting Institute. At present time RS network contains 51 points. The distances between RS are about 100 km, i. e. the density of RS is about 1 point for 10 000 km^2. Similar networks are created in most European countries. The works of this scientific branch are coordinated by MagNetE (Magnetic Network in Europe) organization, which was founded in Potsdam in 2003. For accurate reduction of geomagnetic field components it is necessary to refer the RS measurements data to the continuous magnetic variation observations that are carried out on close by magnetic observatories (MO) or set of MO. There are 3 MO in Ukraine “Kyiv”, “Lviv” and “Odesa”, besides for the reduction accuracy increasing we can use the data of neighbouring countries MO such as “Belsk”, “Tihany” etc. as well as the data of permanent magnetic variation on geophysical stations such as “Nyzhnje Selysche” etc.

The main task of magnetic RS measurement consists in creating the maps of normal geomagnetic field components and theirs secular variation (SV) rates. Alongside of geomagnetic fundamental problems decision the results of RS measurement allows to perform reduction of different time magnetic data to common epoch and unified normal field level. This is very important for creation of aggregated anomalous field maps of large areas. The results of RS magnetic measurements may be very useful in navigation and topographic mapping where magnetic declination D and its yearly changes are given.

Actuality of RS network magnetic measurements and creating the newest maps of normal magnetic field as well as its SV rate on the territory of Ukraine is emphasized also because of appearing of SV rate focus at the end of XX century in the Eastern Europe. The appearing of this focus makes it more difficult to use the worked out local anomalous magnetic field models and investigate this field temporal changes for tectonic magnetic investigations as well as for geophycical exploration. Comparison of SV rates calculated due to model IGRF-2005 with rates obtained on MO of Europe reveal as noticeable distinctions of theirs special structures and morphology of time series between them as well [Maksymchuk et al., 2010].

We did follow the international recommendations [Newitt et al., 1996] when selecting the place of RS founding and performing measurements of magnetic field components. The scalar of geomagnetic field



Isogons distribution on the territory of Ukraine reduced to epoch 2005.5. RS — Asterisks. MO — Black squares.

vectors were measured by proton magnetometers with sensitivity 0.1 nT. Magnetic declination and inclination (I) were determined with ferrosonde magnetometer mounted on demagnetized theodolite of 1 arcsec scale accuracy. The reductions of magnetic field *X*-, *Y*-, *Z*-components were done to middle of observation years epochs and to common epoch 2005.5 as well. These reductions were performed referencing the data of permanent observation of MO “Belsk”, “Kyiv”, “Lviv”. Standard deviations of obtained results are in the range from 2 nT to 3.5 nT for *X*-, *Y*-, *Z*-components and lesser then 30″ for *I* and 50″ for *D*. These results were summarized in catalogue of Ukrainian RS for the 2005.5 epoch. We also created a set of maps for geomagnetic field components.

Comparison of components values that were obtained on Ukrainian RS network with the same components calculated due to IGRF-2005 model shows, that differences for linear (*X*, *Y*, *Z*) components lie in the range from several to several hundreds of nT. Apparently these differences are caused mainly by effect of magnetic anomalies localized in the Earth’s crust. The map of magnetic declination *D* (isogons) has a particular applied interest. Such map due to 1st cycle of Ukrainian RS network measurements is shown on Figure. The values of *D*, reduced to epoch 2005.5 on the territory of Ukraine lie in the range from 4° in the western region to 8° in the eastern region. The isogons shown on Figure noticeably differ from the same calculated by model IGRF-2005. Unlikely to model isogons the observed ones are of very complicated configuration. One can easily distinguish several anomalies of regional scale on the background of global trend. The general features of isogons distribution configuration are in concordance with tectonic structure and anomalous magnetic field of regional scale.

Conclusion. The RS network creation on the territory of Ukraine allows make use of the obtained data in process of new generation IGRF model construction. Even results of 1st cycle measurements may be useful as for IGRF model more precise definition and for tectonomagnetic investigations as well. Undoubtedly it is necessary to fulfill the next cycle of measurements on the created RS network and if it would be possible to enlarge the number of RS.

References

Newitt L. R., Barton C. E., Bitterly J. U. Guide for magnetic repeat station surveys. — Boulder: IAGA, 1996. — 112 p.

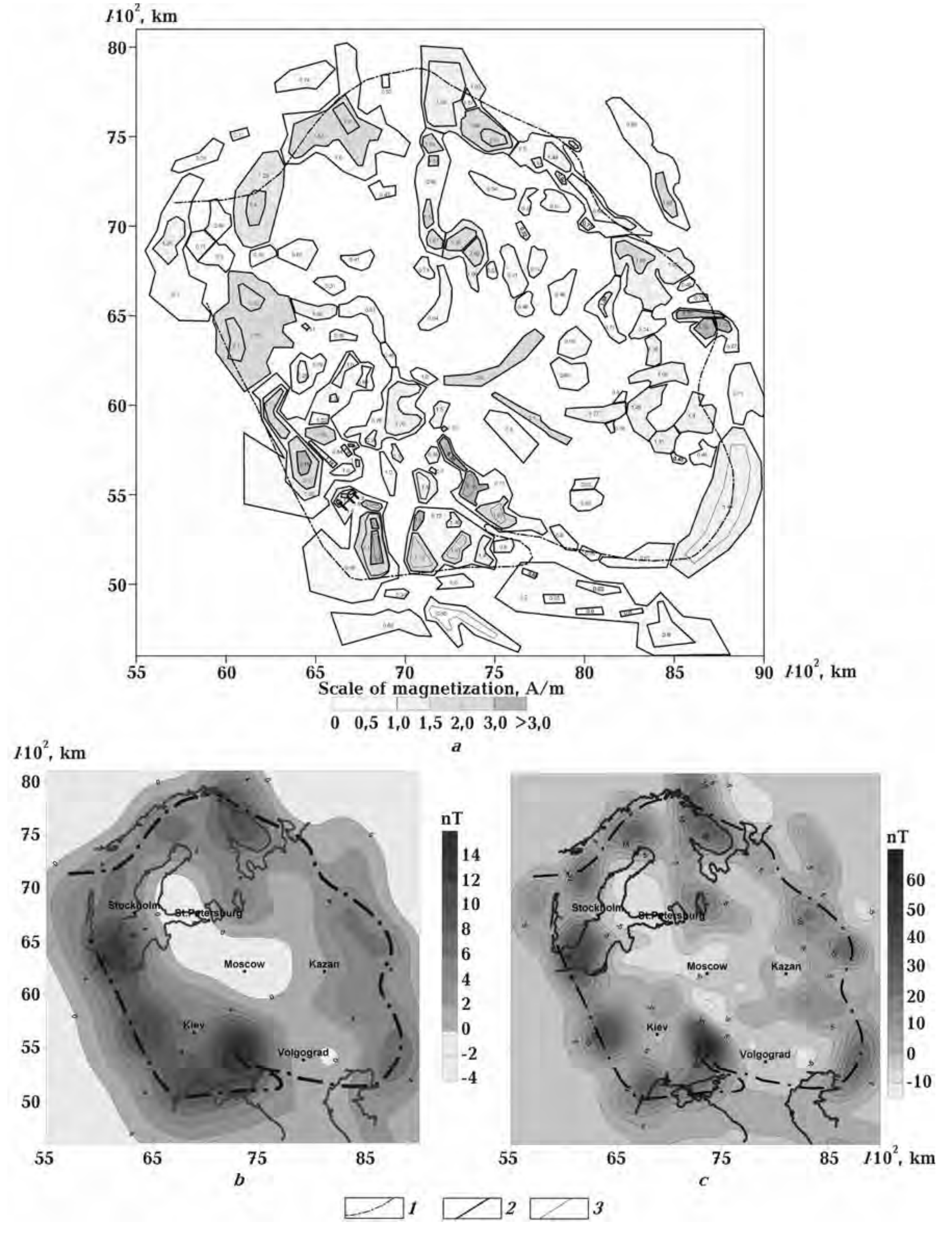
Maksymchuk V., Orlyuk M., Tregubenko V., Horodysky Yu., Nakalov Ye., Myasoyedov V. Land absolute magnetic survey on the basic network of repeat stations in Ukraine for the epoch 2005.5 // Geophys. J. — 2010. — **32**, № 5. — P. 82—85 (in Ukrainian).

3D magnetic model of the East European Craton and its effect at near-surface and satellite heights

© ***A. Marchenko, M. Orliuk, 2010***

Institute of Geophysics, National Academy of Sciences of Ukraine, Kiev, Ukraine
andrey_marchenko@ukr.net
orlyuk@igph.kiev.ua

Creation of 3D regional magnetic model of the East European Craton (EEC) for spherical Earth’s needs corresponding cartographic support notably availability of a geomagnetic maps of a geomagnetic anomaly of the total intensity scalar $(\Delta B)_a$ and its normal component B_{IGRF}. At present time there are published and digital maps of a geomagnetic field, that give a possibility to perform a small-scale zoning, to separate a regional component $(\Delta B)_{a.reg.}$, as well as to evaluate inhomogeneity degree of the Earth’s magnetic field. The first map of anomaly magnetic field for studied territory has been developed under the editorship of Z. A. Makarova [The Map …, 1977]. Next important achievement in magnetic mapping was creation a map of anomaly magnetic field of the Europe under the editorship of T. N. Simonenko and I. K. Pashkevich [The Map …, 1990]. Digital map of the world anomaly magnetic



3D magnetic model of the East European Craton (*a*) and magnetic anomalies from a model on height 400 km (*b*) and 200 km (*c*): *1* — boundary of the EEC, *2* — contours of lower, *3* — upper magnetic sources (in case of the inclined lateral sides).

field [Purucker, 2007] published under the aegis of UNESCO became the results of common 50-years researches concerning analyses of different-time and non-uniformly scaled terrestrial, marine, aero- and

satellite surveys. These maps enabled to separate a regional component of the EEC magnetic field and to propose as a first approximation a 3D magnetic model of the Earth's crust [Orliuk, 1984; 1996; 2000; Orliuk, Pashkevich, 1995; Pashkevich et al., 1990]. Digital map of the regional component of EEC anomaly magnetic field was developed [Orliuk et al., 2007] with using the results of the works [Orliuk, 2000; Purucker, 2007]. Developing 3D Earth's crust magnetic model of a big territories it is important to take into account the values of Earth's normal magnetic field B_{IGRF}. For the EEC on the epoch of 2005 [http://ccmc.gsfc.nasa…] minimal values of the field B_{IGRF} are observed in south-western part of the territory (48000 nT) and maximum values — in the north and north-eastern of the territory (56000 nT).

First approximation of regional magnetic model for EEC was formed with using digital anomaly magnetic maps, Precambrian basement depths, temperature within the crust and petromagnetic rock. 3D regional magnetic model of the territory (Figure) was developed in the sequel using program-algorithmic complex [Kovalenko-Zavoisky, Ivashchenko, 2006] to solve direct task of magnetometry in spherical coordinates. The models of magnetic sources were set a few spherical blocks, each of which was characterized homogeneous magnetic susceptibility, and different, in the case of necessity, values component of the normal geomagnetic field.

Depth of magnetic sources was set in limits from 10 km (depth of a top edge of magnetic sources) to 40 km (depth of a base surface). The field calculated by model was compared in terms of quantity with the interpreted field. After several iterations the minimal differences between these fields were achieved.

Under obtained model of the EEC there are a large Earth's sections with magnetization values from 0,5 to 1,75 A/m and which sizes are 200—300 km. The sources having magnetization values 1,0—2,0 A/m and sizes of 40—100 km are located in the limits of these blocks. The magnetization values more that 2 A/m are inherent to the solids that are the sources of such regional magnetic anomalies as one: Kursk (>6,35 A/m), Odessa (3,5 A/m), Lvov (3,18 A/m), Gaisyn (3,23 A/m), West-Ingulets (3,6 A/m), Kiev (2,71 A/m), Kungursk (3.72 A/m) et al.

Intensity of magnetic field from 3D magnetic model at height of 10 km changes in limits ΔB_a=–(300—1200) nT, on height of 200 km ΔB_a=–(15—70) nT and at height of 400 km ΔB_a=–(4—14) nT.

As you can see from figure sources of magnetic anomalies are situated to boarder part of the EEC.

References

Colles R. L., Haines G. V., Jansen van Beek G. Magnetic anomaly maps from 40°N to 83°N derived from Magsat satellite data // Geophys Res. Lett. — 1982. — **9**, № 4. — P. 281—284.

http://ccmc.gsfc.nasa.gov/modelweb/models/igrf.html

Kovalenko-Zavoisky V. N., Ivashchenko I. N. Mathematical support of ΔB_a field interpretation // Geophys. J. — 2006. — **28**, № 5. — P. 18—30 (in Ukrainian).

Orliuk M. I. Compiling technique and first results of 4D magnetic model of the Earth's crust of the Ukraine // Reports of NAS of the Ukraine. — 1996. — № 5. — P. 95—99 (in Russian).

Orliuk M. I. Magnetic model of Earth's crust of Volhyn and Podolie edge of the East-European Platform as well as its petrologic and tectonic interpretation // Studies of Platform's areas regional magnetic anomalies. — Kiev: Nauk. dumka, 1984. — P. 152—162 (in Russian).

Orliuk M. I. Spatial and space-time magnetic models of different rank structures of continental type lithosphere // Geophys. J. — 2000. — **22**, № 6. — P. 148—165 (in Russian).

Orliuk M. I., Kovalenko-Zavoisky V. N., Ivachenko I. N., Marchenko A. V. Regional magnetic anomalies interpretation subject to Earth sphericity // Thesis for VIIIth International conference Monitoring of a dangerous geological processes and environmental ecological state. — Kiev, 2007. — P. 76—77 (in Ukrainian).

Orliuk M. I., Pashkevich I. K. Magnetic model of south-western edge of the East-European Platform // Geophys. J. — 1995. — **17**, № 6. — P. 31—36 (in Russian).

Pashkevich I. K., Markovsky V. C., Orliuk M. I., Eliseeva S. V., Mozgovaia A. P., Tarashchan S. A. Lithospheric magnetic model of the Europe.— Kiev: Nauk. dumka, 1990. — 168 p (in Russian).

Purucker M. E. Magnetic Anomaly Map of the World // EOS. — 2007. — **88**, № 25. — P. 263.

The Map of the Anomaly Magnetic Field $(\Delta T)_a$ of the Europe. —1:5 000 000 / Eds. T. N. Simonenko, I. K. Pashkevich. — Kiev: GUGK, 1990. — 2 sheets.

The Map of the Anomaly Magnetic Field $(\Delta T)_a$ of the USSR (continental part and some adjacent water areas). — 1:2 500 000 / Ed. Z. A. Makarova. — Moscow: GUGK, 1977. — 16 sheets.

Dispersion and scatter of elastic waves in a pre-stressed and fractured geological medium

© **B. Maslov, 2010**

Institute of Mechanics, National Academy of Sciences of Ukraine, Kiev, Ukraine
maslov@inmech.kiev.ua

It is known [Crampin, Peacock, 2008] shear-waves propagating in anisotropic rocks split into two approximately orthogonal polarisations that travel at different velocities. Such seismic birefringence aligned azimuthally is widely observed in almost all igneous, metamorphic, and sedimentary rocks in the Earth's crust in almost all geological and tectonic regimes. The causes and interpretation of shear wave splitting in the Earth's crust are still not clearly understood [Maslov et al., 2006]. Although, in principle, shear-wave splitting is simple in concept and easy to interpret in terms of systems of anisotropic symmetry, in practice there are subtle differences from isotropic propagation that make it easy to make errors in interpretation.

So the solution of such problems is of interest not only revealing of prominent features of wave movement in the non-heterogeneous media, as that: dispersions, attenuations, but also and revealing of the reasons causing these effects. For long-wave processes the geo structure may be considered as some homogeneous media with the overall elastic properties [Maslov et al., 2001]. However in such approach it is impossible to reveal dependence of speed elastic waves from frequency that is observed in experiments on frequency of an order of several thousand hertz. To investigate the phenomena of a dispersion and attenuation in micro non-uniform media one uses the so-called dynamic effective characteristics defined from the equations of movement for representative volume [Maslov, 1982].

Here the problem of the overall dynamic characteristics determination for random geo structure with initial stress strain state in components is considered. The basic equations of incremental theory of elasticity are resulted in [Maslov, 2008]. Basic of them are the equations of balance of an initial state

$$\sigma^R_{ma,a} = 0 . \qquad (1)$$

The equations of elastic motion for actual state

$$\sigma^A_{ma,a} = \rho \frac{\partial^2 u_m}{\partial t^2}, \quad \sigma^A_{ma} = F_{mb} s^{ba},$$
$$s^{ba} = \partial W / \partial e_{ab} . \qquad (2)$$

Boundary and initial conditions

$$\begin{aligned} &\sigma^A_{ma} n^A_a = P_m, \quad \mathbf{x} \in S, \\ &u_m(\mathbf{x},0) = f_m(\mathbf{x},0), \quad \mathbf{x} \in S, \\ &u_m(\mathbf{x},t) = \psi_m(\mathbf{x}), \quad t = 0, \\ &\frac{\partial u_m}{\partial t} = \psi^1_m(\mathbf{x}), \quad t = 0 . \end{aligned} \qquad (3)$$

Constitutive law for increments [Crampin, Peacock, 2008]

$$\begin{aligned} &\sigma^A_{im} = L^{ijab} H_{ab}, \\ &L^{iamb} = F_{ik} F_{mn} \frac{\partial^2 W}{\partial e_{ak} \partial e_{nb}} + \delta_{im} \frac{\partial W}{\partial e_{ab}}, \\ &e_{ab} = \frac{1}{2} \left(F_{ma} F_{mb} - \delta_{ab} \right), \\ &F_{ma} = \delta_{ma} + H_{ma}, \quad H_{ma} = u_{m,a} . \end{aligned} \qquad (4)$$

The frequently used in nonlinear geodynamics plastic potential is

$$\begin{aligned} &W = \frac{1}{2}\lambda p_1 + \mu p_2 + 3\gamma \frac{n}{1+n} p^{1+1/n}, \\ &p_1 = e_{mm}, \\ &p_2 = e_{mn} e_{nm}, \\ &p = \frac{2}{3}\left(I_1^2 - 3 I_2\right)^{1/2} = \left(\frac{2}{3} e' \cdot e'\right)^{1/2} . \end{aligned} \qquad (5)$$

In this case

$$\lambda_{abcd} = 2\mu K_{abcd} + 3\text{æ} J_{abcd} + \frac{3}{2} E_{abcd} \,,$$

$$E_{abcd} = \frac{2}{3} \hat{e}_{ab} \hat{e}_{cd} \,, \;\; \hat{e}_{ab} = e'_{ab} \,/\, p \,,$$

$$l_{abmn} = F_{mk} \lambda^{abkn} \,, \;\; s_{ab} = l_{abmn} H_{mn} \,,$$

$$I_{abcd} = \frac{1}{2} \left(\delta_{ac} \delta_{bd} + \delta_{ad} \delta_{bc} \right) ,$$

$$J_{abcd} = \frac{1}{3} \delta_{ab} \delta_{cd} \,, \;\; K_{abcd} = I_{abcd} - J_{abcd} \,, \qquad (6)$$

I_1, I_2 — main invariants of finite deformation tensor [Maslov, 1982; Crampin, Peacock, 2008].

The state of homogeneous preliminary compression is considered in detail. Then, having restricted to a case of small gradients of initial displacements, the incremental elasticity tensor L_{abcd} is obtained. Substituting in (4) we gain the equations of motion which under the form presented here are like the Lame linear theory of elasticity equations. Fourier transformation led to equation for fluctuations of displacement, with circular frequency dependency. Random geo structures in which casual fields are statistically homogeneous and ergodic concerning not deformed reference representative volume are considered. On the boundary of elementary macro volume the fluctuations of displacements are equal to zero. So this case provides a perfect analogy of approach to problems of the linear theory of elasticity and incremental theories. As to the solution in incremental theories we are interested in averaged gradients of displacements in components while in the linear theory of micro non-uniform geological media the problem consists in determination of averaged on components deformations (the symmetrized gradients). Green's function of the equations in long-wave approach looks like, similar to a case of the linear theory. Constants are expressed in speeds of longitudinal and shear waves.

Substituting the solution of a statistical dynamic problem in the macroscopic equations of motion, we consider in a detail a case of a plane harmonic wave. From the dispersive equation it is found phase and group speeds of waves. Attenuation factors are obtained as functions of constituent properties, frequency and initial stress state. The account of preliminary plastic deformation leads essential variations of speed values. Concrete examples of calculation of dependence of phase speed of a shear wave from frequency in a case when components are in a state of long term initial plastic deformation are considered. Natural state of media as reference example is been modeled too. As result, influence of an initial plastic state has the same order, as influence of frequency of a wave spreading.

Azimuthally-aligned shear-wave splitting is widely observed so the splitting may be used as diagnostic of some form of seismic anisotropy and stressaligned fluid-saturated micro cracks as the cause of azimuthally-aligned shear-wave splitting [Maslov, 1982; Maslov et al., 2001]. Shear-wave splitting is modeled here by dependence of incremental elasticity (4) from stressed state. And contra versus the splitting is some kind of diagnostic for some form of seismic anisotropy. The next idea is possibility to investigate stress-aligned fluid-saturated micro cracks [Maslov et al., 2001] as the cause of azimuthally-aligned shear-wave splitting.

As we outlined earlier [Maslov et al., 2006] for the analysis of a long term motion of geo structure it is useful the continuum damage concept. The micro cracks distributed in regular intervals or casually in a material, may be offered as the variable of a degree degradation of elastic properties. The measure continuum damage may be considered as formal reduction of the area of cross-section section of the sample. Then it is possible to enter effective stress and the destruction moment to identify with achievement damage values. Damage accumulation is stochastic process by the nature therefore even at performance of qualitative, well controllable field experiments, the big statistical variability of data is observed. We use further a hypothesis of equivalence of elastic energy of a material in initial state and the damaged material. If the free from stress configuration of elementary volume in a point has passed in the new form described by a field of plastic deformations $e^T_{ab}(\mathbf{x}, t)$ then constitutive law (4) may be rewritten in form

$$\sigma_{ij} = L^{ijab} \left(e_{ab} - e^T_{ab} \right) . \qquad (7)$$

Such a model of incremental elastic behavior of the geological media does not assume change of elasticity owing to occurrence of a field of deformations of transformation. Thus, formally some element of a source is supposed free from initial stress if deformations are equal in it to the deformations of transformation mentioned earlier (7). The general models of cracks or the destructions of ruptures represented as a surface of rupture of a field of dislocations also in a limit can be described as field distribution $e^T_{ab}(\mathbf{x}, t)$ in a narrow zone. If to put a crack of a zone of transformation aspiring to zero corresponding components will aspire to infinity so that there is the rupture of dislocations equivalent to the phenomenon of destruc-

tion. Thus deformations we present here through Dirac δ-function. Therefore the solution of a problem with some kind of damage degradation also can be presented through Green dynamic function [Maslov, 1982].

The crack density [Maslov et al., 2006] used for calculation is approximately equal to one hundredth of the percentage of shear-wave velocity anisotropy in aligned cracks in a reference initial medium. Fluid-saturated micro cracks model suggested to evaluate viscous effects dispersion, scatter and splitting of elastic waves in pre stressed and fractured geological medium.

References

Crampin S., Peacock S. A review of the current understanding of seismic shear-wave splitting in the Earth's crust and common fallacies in interpretation // Wave Motion. — 2008. — **45**, № 6. — P. 675—722.

Maslov B. P. Overall dynamic characteristics of composite materials with initial stress // Prikl. Mech. — 1982. — **18**. — № 6. — P. 75—80 (in Russian).

Maslov B. P. Thermal-stress concentration near inclusions in visco-elastic random composites // J. Engineering Mathematics. — 2008. — **61**. — P. 339—355.

Maslov B. P., Prodaivoda G. T., Vyzhva S. A. A new mathematical modeling method of rupture processes in Lithosphere // Geoinformatics. — 2006. — № 3. — P. 53—61 (in Russian).

Maslov B. P., Prodayvoda G. T., Vyzhva S. A. Mathematical modeling of elastic wave velocity anisotropy in a cracked geological medium // Geophys. J. — 2001. — **20**, № 2. — P. 191—212 (in Russian).

Estimating the stresses within the lithosphere: parameter check with applications to the African Plate

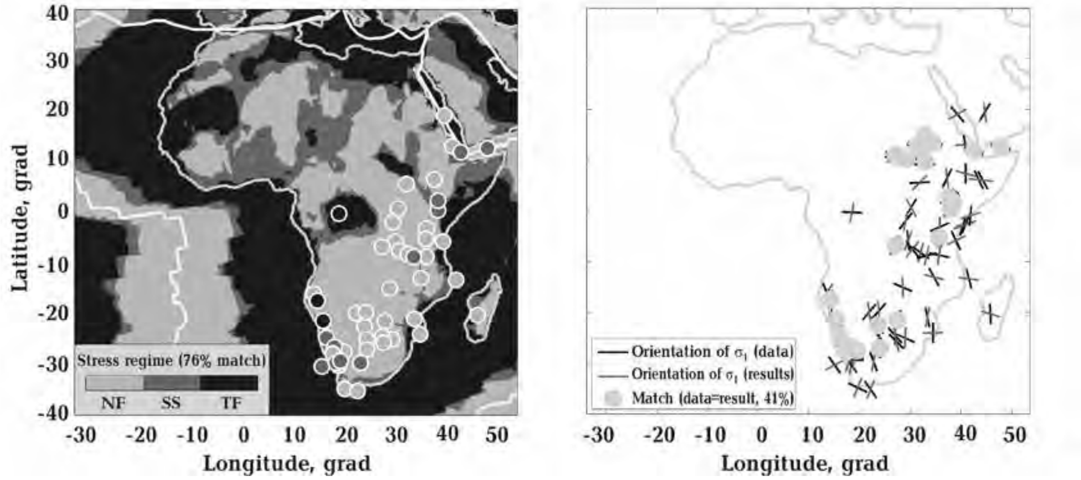
© ***S. Medvedev*[1] *and "The African Plate" Working group*[1,2]*, 2010***

[1]Physics of Geological Processes, Oslo University, Oslo, Norway
sergeim@fys.uio.no
[2]Center for Geodynamics, NGU, Trondheim, Norway

Several mechanisms control the state of stress within plates on Earth. The list is rather long, but well known and includes ridge push, mantle drag, stresses invoked by lateral variations of lithospheric density structure and subduction processes. We attempt to quantify the influence of these mechanisms and to construct a reliable model to understand modern and palaeo-stresses using the African plate (TAP) as an example.

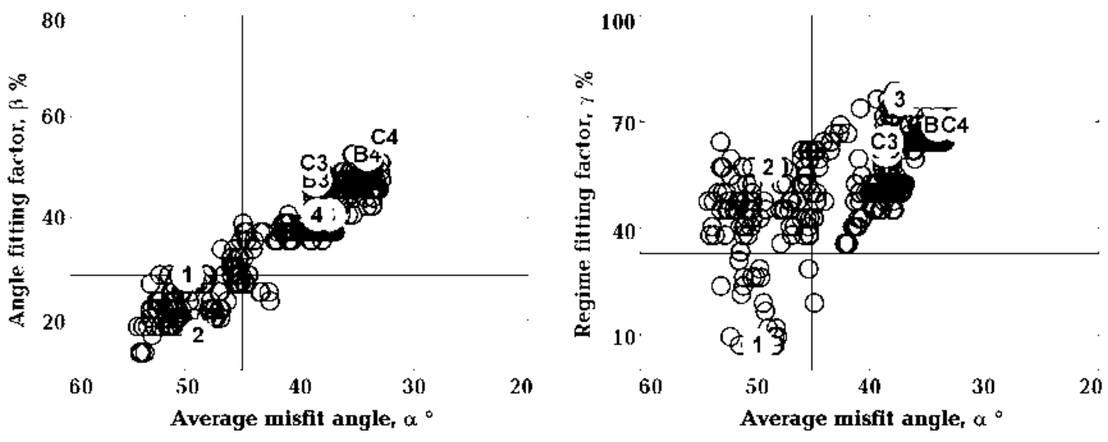
Constructing the base model lithosphere of TAP we follow [Steinberger et al., 2001]. Combining data on topography, age of ocean floor and global model for crust structure, CRUST2 [Bassin et al., 2000], we compute the gravitational potential energy (GPE) for the entire TAP. GPE, proportional to the double integration of the density profile through thickness of the model lithosphere, describes the forces rising from lateral density heterogeneities within lithosphere. In particular, GPE of the base model accounts for push from the mid-oceanic ridges surrounding TAP and stresses rising from the crustal thickness changes.

The finite-element based suite ProShell was utilized to calculate stresses using the real, non-planar geometry of TAP. The modeled results are tested and iterated to match the observed stress pattern recorded or derived from observations. We combined several studies to complete set of observational data. That includes non-seismic data from WSM [Heidbach et al., 2008], compilation of the field observation [Bird et al., 2006], and integrated inversion of focal mechanism data [Delvaux, Barth, 2010]. Fig. 1 presents the distribution of data on stress regimes and orientation of most compressive mean stress. We adopted several numerical characteristics describing proximity of model results and observations: 1) the average misfit angle is the mean difference in orientations; 2) the angle fitting factor is the percentage of the number of observa-



a *b*

Fig. 1. Results for model 3 represents typical distribution of the stress regimes with TAP (*a*) and orientation of maximal compressive stresses (marked as σ_1 on the (*b*) panel). The results of the model are compared to observations (see text for description of data). The data represented by markers on the (*a*). Green discs cover the results with orientation within 90 % confidence interval of observations on the (*b*) panel.



a *b*

Fig. 2. Illustration of variation of fitting parameters for different sets of numerical experiments. All circles represent results for different sets of parameters variations, circles filled with green represent successful representatives of each set (marker 4 covers marker for model 3 on (*a*), marker C3 covers B3 and marker C4 covers C3 on (*b*) panel). See text for description of the numerical experiments series and definitions of fitting parameters. Blue lines present random average values, the results that follow below or (*a*) from these lines represent light autocorrelation with observations.

tions which fits to model results within 90 % confidence interval of the data; 3) regime fitting factor is the percentage of the successful match of observed and modeled regimes.

Fig. 2 presents the fitting characteristics for approximately 700 model runs. The figure also shows that the results may fall below limit provided by random average. The results of base model (Fig. 2, model 1) compares poorly with observations. This model presents the simplest combination of simple models and widely available data and it assumes that the top of the mantle lithosphere (Moho) has constant temperature, which is clear oversimplification for model of TAP, which includes mid-oceanic ridges and thick continents. The model 2 (Fig. 2) assumes that the Moho temperature is proportional to the thickness of the crust above. This model, however, does not show significant improvement while compared to model 1 for variety of the coefficients of proportionality between crustal thickness and Moho temperature, ΔT.

Two previous models are based on the prescribed thickness of the crust (given by CRUST2) and model topography does not match exactly the observed topography of TAP. In model 3 we assume that the CRUST2 model is inaccurate. We stretched the thickness of the model crust so that after isostatical adjustment observed and model topography match exactly. Varying ΔT within model 3 we found that the optimal value for constant ΔT within TAP and improve significantly the match between model results and observation.

The density of mantle within models 1—3 depends only on thermal state of mantle, which in turn depends on the age and crustal thickness. The observations, however, point out existence of significant compositional (and thus, density) variations of the mantle beneath TAP. In model 4 we assume that part of mismatch between CRUST2 — based topography and observed topography is associated mantle density variations. That was emulated by variations of effective thermal situation, simply by assuming ΔT varies laterally.

In addition to the stresses directly resulted from GPE, we considered several additional complications of the model. In series B we considered basal drag caused by sub-mantle flow derived from mantle convection model. We couple this flow filed to models 3 and and vary parameters of coupling. Whereas the model B3 shows little improvement compared to model 3, the basal drag with reasonable parameters of coupling improves significantly model with variable density of the lithospheric mantle (model 4 vs, model B4).

All the models considered above are based on uniform rheological properties of TAP. This is very strong simplifying assumption. In model series C we considered simplest variations of rheological properties, assigning weakening along mid-oceanic ridges. The results improve (model C4) when weakening related to young age of the ocean floor is by up to two orders of magnitude.

References

Bassin C., Laske G., Masters G. The Current Limits of Resolution for Surface Wave Tomography in North America // EOS Trans AGU. — 2000. — **81**. — P. F897.

Bird P., Ben-Avraham Z., Schubert G., Andreoli M., Viola G. Patterns of stress and strain rate in southern Africa // J. Geophys. Res. Sol. Earth. — 2006. — **111**. — P. Bo8402. — DOI:10.1029/2005JB003882.

Delvaux D., Barth A. African stress pattern from formal inversion of focal mechanism data // Tectonophysics. — 2010. — **482**. — P. 105—128.

Steinberger B., Schmeling H., Marquart G. Large-scale lithospheric stress field and topography induced by global mantle circulation // Earth Planet. Sci. Lett. — 2001. — **186**. — P. 75—91.

Kola Super-deep — evidence of fluids in the Crust

© ***S. Milanovsky, 2010***

Institute of Physics of the Earth, RAS, Moscow, Russia
svetmil@mail.ru

The program of deep continental drilling became qualitatively a new stage in progressing of knowledge of the Earth crust. The major point of this new knowledge became the evidence of deep-seated fracturing of the crust. Geothermal investigations in Kola hole (SD-3) have been combined with a wide range of the adjoining studies which are carried on in this hole — hydrogeology, petrology, geochemistry of RAE, rock mechanics, numerous geophysical observations. It has given the chance to study thermal conditions of the Earth crust more deeply. The report includes some important results of geothermal in SD-3 [Ljubimova et al., 1985; Kremenetsky et al., 1986; Arshavskaya et al., 1987; Borevsky et al., 1985; 1997; 1998; Milanovsky, 1998]. Along with measuring, they included interpreting of a modification of a heat flux and its components with depth. It is necessary to name as the most essential result detection of link of a thermal field with hydro physical zonality of the crust and its frac-

turing. By geothermal study in SD-3 it was established, that heat flow density is enlarged with depth from 30 mWm^{-2} to 49.5 mWm^{-2}, locally to 68 mWm^{-2} [Borevsky et al., 1997; 1998; Milanovsky, 1998]. These values practically have a little varied after conducting of the subsequent mass measuring of a thermal conductivity of cores from SD-3 [Popov et al., 1999]. It was found, that by the most essential reason of growth of heat flow with depth, along with paleoclimatic effect which is limited with depth the downward filtering of meteoric waters is [Ljubimova et al., 1985; Borevsky et al., 1985]. On geothermal data Darcy velocity of a downward filtering in Proterozoic metamorphic rocks — 0.4 cm per year has been estimated. The evaluation of rate of this filtering has appeared is close to rate of modern uplift of blocks of a surface on Baltic Shield. The refraction of a vertical component of a temperature gradient on sloping interfaces of stratums of contrasting thermal conductivity is found. It is demonstrated, that geothermal parameters respond the physical-mechanical boundary lines [Milanovsky, 1998, Abdrakhimov et al., 1999] determined by complex analyses of SD-3 section [Borevsky et al., 1987; 1998; Milanovskiy, Borevsky, 2000]: Detailed level-by-level allocation of RAE (U, Th and K) of SD-3 cross-section [Kremenetsky et al., 1986] was studied. Average heat generation of the rocks in Protrusion complex is $0.41 \cdot 10^{-6}$ Wm^{-3}, in Achaean complex — $1.47 \cdot 10^{-6}$ Wm^{-3}. The contribution of Low Proterozoic complex in an integral heat flux is 2.8 mWm^{-2}, and of Achaean complex is 6.86 mWm^{-2}. Link of metamorphic processes with non-uniformly scaled redistribution of U and Th in the rocks on depths up to 10 km was found. Comparison of heat flux value in Kola super-deep with heat generation model allows to conclude:

1) in Pechenga (Proterozoic) complex the heat flux depends from radiogenic heat sources a little; the controlling factors instituting fluctuations of heat flow value are hydro-geological, structural and thermal;

2) in Archean part heat generation growth result in decreasing of heat flux with depth on the average ~5 mWm^{-2}. Along with deep studies, in Kola region field work on temperature gradient analysis 36 prospecting holes on the Ni-ore field "Verchnee" have been made. Salinity of fluid in a number of holes was measured, and also a thermal conductivity of 1375 samples of rock cores from 21 holes was mesured [Christoph et al., 1996; Schellerschmidt et al., 2003a; 2003b]. The heat flow in 19 boreholes on “Verhnee” varied between 31—45 mWm^{-2} with a mean 38 $mW м^{-2}$ [Mottaghy et al., 2005]. In the majority of boreholes the heat flux tests the considerable modifications with depth that correspond to the analogous variations of a heat flow observed in the upper part of SD-3. The carried out analysis [Mottaghy et al., 2005] allows drawing a conclusion, that this regularity is not a consequence of production operations, and reflecting a natural appearance. The reason of this effect — combination of advective filtration in fractured rocks, structure factor and paleoclimat. The preliminary analysis of a heat flux has demonstrated that filtration (fracturing) plays a defining role at the subordinate effect of varying surface temperature and the insignificant contribution of structural heterogeneity of rocks. Near surface geothermal studies have allowed to detect the space in homogeneity of a thermal field in the upper crust. Analysis of hydro-geothermal field has shown its link with stress field, fault tectonics and accordingly with inhomogeneous lateral permeability of the upper crust. The obtained data have been used for 2D thermal modeling of Pechenga Synclinorium and for calculation of deep temperatures in the crust. From a stand dilatancy model [Nikolaevskiy, 1996] analysis geothermal, seismic, geoelectric, density and petrologic models of old crust [Milanovsky, 1984; Milanovsky, Nikolaevskiy, 1989; 2000] was carried out. Comparison of *PT*-conditions on Conrad and Moho boundaries their correspondence to boundary lines of stick-slip and dislocation plasticity accordingly was established. The range of a bright dilatation for geomaterials coincides with the position of low velocity zone in SD-3 section.

The author expresses gratitude to many colleagues for their participation and the help in carrying out various parts of the present study. This work has been supported by Soros Foundation and INTAS-93 — 273 grant.

References

Abdrakhimov M. Z., Milanovsky S., Milanovsky V. Yu. Traskin Influence of Water and Drilling Fluid on the Structure and Permeability of Metamorfic Rocks at Depth 7—12 km in Kola Well // Ann. Geophys. — 1999. — **17**. — P. 77.

Arshavskaya N., Galdin N., Karus E., Kuznetsov O., Lubimova E., Milanovskiy S. Yu., Nartikoev V. D., Semashko S. A., Smirnova E. V. Geothermic investigations // The Superdeep Well of the Kola Peninsula / Ed. Kozlovsky. — Springer, 1987. — P. 387—394.

Borevsky L. V., Kuznetsov Yu. I., Milanovskiy S.Yu. New data about peculiarities of physical proper-

ties in the Kola superdeep hole // Ann. Geophys. — 1998. — **16**. — P. C85.

Borevsky L., Milanovsky S., Yakovlev L. Fluid-Thermal Regime in the Crust-Superdeep Drilling Data // Proc. World Geothermal Congr. — Florence, 1995. — P. 975—981.

Borevsky L. V., Vartanyan G. S., Kulikov T. V. Hydrological essay // The Superdeep Well of the Kola Peninsula / Ed. Kozlovsky. — Springer, 1987. — P. 271—287.

Borevsky V., Milanovsky S. Yu., Morgachev I., Orlov V. N. Hydrogeology of the Upper Crust in the Area of Kola Hole — Geothermal Aspects // Ann. Geophys. — 1997. — **15**.— P. C142.

Christoph C., Schellerschmidt R., Kukkonen I., Milanovsky S., Morgachov V., Borevsky L. New temperature data recorded in boreholes around the Kola superdeep borehole — prelimenary results // Heat Flow and the Structure of the Lithosphere: 4th International Workshop, Trest Castle. — Czech Republic, 1996. — P. 21.

Kremenetsky A. A., Milanovskiy S. Yu., Ovchinnikov L. N. A heat generation model for continental crust on deep drilling in the Baltic Shield // Tectonophysics. — 1989. — **159**. — P. 231—246.

Kremenetsky A., Ovchinnikov L. N., Milanovskiy S. Yu. Geotermal studies and heat generation model of Precambrian crust of a North-East part of the Baltic Shield // Geochemistry of abyssal rocks. — Moscow: Science, 1986. — P. 131—149 (in Russian).

Ljubimova E. A., Milanovskiy S. Yu., Smirnova E. V. New results of analysis of a heat flux on Baltic Shield // History of evolution of a thermal field in allowed bands of a various endogenous regime of the countries of East Europe. — Moscow: MGC, 1985. — P. 93—110 (in Russian).

Milanovsky S. Yu. Deep geothermal structure and mantle heat flow along Barents Sea — East Alps geotraverse // Tectonophysics. — 1984. — **103**. — P. 175—192.

Milanovsky S. Yu. Fluid-thermal regime in the crust — kola hole data. — Corinth Workshop, 1998. — P. 42.

Milanovskiy S. Yu. Geothermal structure of Precambrian crust // Structures in the Continental Crust and Geothermal Resources. Abstract Volume, 24—27 September. — Italy: Siena University, 2003. — P. 75.

Milanovskiy S. Yu., Borevsky L. V. Hydrogeology of the Upper Crust near Kola Hole–Geothermal Aspects // Geothermics at the Turn of the Century, University of Evora. — Portugal, 2000. — P. 75.

Milanovsky S. Yu., Nikolaevsky V. N. Continental crust — general view on seismic data, rheology, thermal state and petrology // Geothermics at the Turn of the Century. — Portugal: University of Evora, 2000. — P. 43.

Milanovsky S. Yu., Nikolaevskiy V. N. Thermomechanical analysis of a constitution of a continental crust (along geotravers Barents sea — Eastern Alpes) // Phys. Earth. — 1989. — № 1. — P. 83—91 (in Russian).

Milanovskiy S. Yu., Borevsky L. V., Kremenetsky A. A. Geothermal field of Precambrian crust // Proceedings of International Conference "The Earth Thermal Field and Related Research Methods". — Moscow, 2002.

Mottaghy D., Schellschmidt R., Popov Y. A., Clauser C., Kukkonen I. T., Nover G., Milanovsky S., Romushkevich R. A. New heat flow data from the immediate vicinity of the Kola superdeep borehole: Vertical variation in heat flow confirmed and attributed to advection // Tectonophysics. — 2005. — **401**. — P. 119—142.

Nikolaevskiy V. N. Geomechanics and fluid-dynamics. — Moscow: Nedra, 1996. — 448 p.

Popov Y. A., Pevzner S. L., Pimenov V. P., Romushkevich R. A. New geothermal data from the Kola superdeep well SG-3 // Tectonophysics. — 1999. — **306**. — P. 345—357.

Schellerschmidt R., Popov Y., Kukkonen I., Nover G., Milanovsky S., Borevsky L., Monttaghy D., Clauser C. Heat transfer processes in the upper crust — a case study for the region around the Kola superdeep borehole, Russia // IUGG Abstracts, Sapporo, Japan. — 2003a. — **A**, № 0920. — P. A.174.

Schellerschmidt R., Popov Y., Kukkonen I., Nover G., Milanovsky S., Borevsky L., Monttaghy D., Clauser C. New heat flow data based on geothermal measurements in the immediate vicinity of the Kola superdeep well SG-3 // Geophys. Res. Abstracts. — 2003b. — **5**. — P. 07720.

Fracturing of the Crust — Geological and Geophysical View

© **S. Milanovsky, V. Nikolaevskiy, 2010**

Institute of Physics of the Earth, RAS, Moscow, Russia
svetmil@mail.ru

In suggested analysis of a status and development of the Earth crust rupture experiments under high *P*-*T* conditions of rock samples are used in their comparison to geophysical studies, namely to available information about deep-seated fractures and faults in the crust and the upper mantle. Using scaling approach (transmission of data about a finite status of rock cores on scales of the earth crust) in comparison to results of deep seismic sounding, magnetotelluric, petrophysic and geochemistry data.

Initial representations are that. If rock massifs on strength properties are close to the properties to granite, brittle failure (including cataclastic) is possible up to Moho boundary and, therefore, a crust as a whole hydraulically permeable for water and gases. The quantitative deviations in strength (amphibolites, peridotites, serpentinites, basalts, etc. from granite) result in to wide gamma of alternatives of a constitution of the crust responding an observable geologic variety. (Including to differences continental and oceanic)

Including water as geologic factor ensures difference of crustal and mantle rocks, changes dynamics of destruction, and installing units of self-organisation during lithosphere evolution. Presence of water at destruction in the lower crust result in faults in amphibolites, to melting of granite, canceling Kennedy — Ito limitation on phase boundaries "basalt — eclogite" and provides appropriate kinetics of transformation events demanded in common theories modifications of material on Moho and its transmission and accumulation in lithosphere column. Known peculiarities in metamorphism and metasomatism also are connected with presence and absence of water.

In the earth crust there are in essence relevant differences in brittle destruction. They depend on a geotherm with depth and a concurrence of vertical and horizontal stresses that explains existence of waveguides by a flattening of deep-seated faults in middle crust. Modifications of seismic rates now it is stipulated not only petrology of the rocks, but also by level of their fracturing. Voidage of system of cracks is responsive to field distortions of the stresses manifested both at earthquakes, and at quasi-stationary development of tectonic events.

Boundary element method applied to plume dynamics

© **G. Morra[1], D. Yuen[2], F. Cammarano[3], 2010**

[1]Department of Geological Sciences, University of Sydney, Sydney, Australia
[2]University of Minnesota, Minneapolis, Minnesota, USA
[3]Institute of Earth Sciences, ETH., Zürich, Switzerland
gabrielemorra@gmail.com

We apply the fast multipole formulation of the boundary element method (FMM-BEM) to the temporal evolution of a rising mantle plume interacting with a mid mantle density/viscosity discontinuity. Detailed monitoring of the possible evolutions in time how the plumes may have a steady, a pulsating or a stalled behaviour. We map out the density and viscosity conditions controlling the three patterns and show that realistic radial mantle Earth profiles allow them to happen. We evaluate therefore possible scenarios for the dynamical evolution of the lower mantle convection and propose which ones are compatible with the surface geological observation of island plumes.

Mathematical model of ageing of natural and manmade objects in monitoring systems

© **V. Mostovyy, S. Mostovyi, 2010**

Institute of Geophysics, National Academy of Sciences of Ukraine, Kiev, Ukraine
mostovoy1@voliacable.com

The phenomenological mathematical model of an estimation of fatigue and aging processes of natural and manmade objects is proposed in this work. The model is based on the mainstream representations existing in material science. Information, obtained by authors while monitoring the Fourth Block of Chernobyl Nuclear Power Plant and the industrial constructions, allows to state, that the process of aging can be represented in space of attributes, each component of which describing an elastic property of materials, which form an investigated object. Since speeds of propagation and the form of pressure and share waves depend on the elastic properties of the materials, it follows that the changes of these properties results in the changes of spectral characteristics of the emission signals. One can see such changes in aging materials. Thus, while monitoring the Forth Block of Chernobyl Nuclear Power Plant, we observed that the Fourier spectrum of a background of natural emission have shifted from the one, that had been stationary before.

More specifically the center (meidan) of the spectrum became lighter and the tails (low- and high-frequency areas) became heavier. This effect can be explained by two major reasons. The first reason is the defragmentation of the elements of the construction, that results in an increase of eigenfrequencies of separate fragments due to a decrease of their geometric sizes. The second reason is an increase of geometric sizes of the defects (fractures) of separate fragments of the object, that results in a decrease of the frequency of emission signals of these defects.

Later the authors applied a similar approach to investigation of the objects that age less intensively. The eigenfrequencies of such objects were in the seismic spectrum band. In a stationary state in the regime of passive monitoring we observed that the vector, describing the state of the object, was migrating within a rather small ellipsoid of rotation in the space of attributes. Such behavior was observed until an occurrence of fatigue. From the point of view of materiology, fatigue is the developing local structural damages arising under the cyclic loadings of a material. Typically, the maximal values of the stress in a cycle are smaller than the highest stress limit for a given material.

Structural failure of a material consists in loss of bearing ability of an element or the whole structure. It begins when tensions in the material become close to limiting ones, causing excessive deformations, and when the material during a full cycle does not come back to an initial state, displaying the phenomenon of hysteresis.

Any redistribution of energy in a material is accompanied by the origination of the emitted signals. Emission of signals is the stress waves generated by a sudden internal redistribution of stress in a material. In turn such a redistribution is typically caused by sudden changes in the internal structure of a material. The possible reasons of the internal structure changes are occurrence and growth of fractures, movement and transformation of a phase in monolithic materials, and disintegration of its components.

Cyclic tensions result in fatigue of a material. Fatigue results in the irreversible deformations. In the model that we consider the process of aging is defined by changes of parameters of a material. It is represented in a space of attributes.

In particular, such structural changes in time stem from the geological faults, which are the basic sources of earthquakes.

If one models behavior of geological faults as behavior of the materials, then one can consider the signals of emission generated by a fault to be a source of information about their fatigue and aging.

Dynamics of the parameters of the emission signals reflects changes of elastic properties of a substance in faults. It means that the changes of the dynamic parameters of the emission signals are connected with the dynamic characteristics of these faults. Moreover, due to presence of a stochastic background noise at monitoring procedure, one needs to have a model that takes such randomness into account.

The key question is the choice of informative parameters for the space of attributes, in which it is necessary to carry out the dynamic analysis of behavior of the parameters, and to build a solving rule for a forecast of a fault condition based on this analysis.

Thus the choice of the space of attributes that represents aging and fatigue becomes a crucial problem. Since information about the condition of an object is in the form of characteristics of emitted signals, and consequently information is indirect; we can only carry out the indirect measurements of propagation of emission waves. The dynamic changes of these waves are represented in the dynamics of their spectral characteristics. The components of the space of spectral characteristics represent the parameters, which are statistically connected to the characteristics of an object.

Our mathematical model takes into account two stochastic components of emission process. The first one is the point process of the moments of occurrence of emitting signals; the second one is the process of formation of a shape of the fluctuating signals. Stochastic characteristics of such a compound random process reflect the change of the elastic characteristics of the material.

The problem of estimation of the parameters of the considered stochastic process is reduced to an estimation of their a posteriori distribution. The dynamics of these parameters represents the processes of accumulation of fatigue and aging of the object. Our decision-making model for evaluation of the level of fatigue is based on risk criteria.

The space of attributes is a subspace of the image space of wavelet transform. In this space the emissions signals are represented by the amplitudes, scale factors and parameters of shift.

In the model it is possible to use both physically feasible signals, i.e. signals that satisfy the conditions of causality and stability, and physically unfeasible signals, i.e. the signals that do not satisfy these conditions. To represent physically feasible functions one can use the orthonormal system of the Haar functions in a Hilbert space, where inner product is given by an integral of the product of the functions, and the norm of a function is the standard L^2 norm. To represent emission signals occasionally it is convenient to choose physically unfeasible functions, which satisfy the condition of stability, but do not satisfy the condition of causality.

For example, consider the derivatives of the density function of the normal distribution with free parameters ó and ì. The obtained functions are not orthogonal (in the Hilbert space defined above), but, if the the parameters ó and ì take values in a certain set, these functions can be close to orthogonal, i.e. the scalar product of two functions with various ó and ì can be close to zero.

Now, consider passive monitoring. Information about an object is enclosed in emission signals, which are registered together with a natural background noise. It is natural to assume, that these signals form a stochastic process. One can model such a process in many different ways, e.g. as a Poisson process, which is described by only one parameter, or as a process, which is described by a vector of parameters of a large dimension. On the one hand the latter model is more complicated and it requires more a priori information about an object, which is being monitored. On the other hand it can give more insight about it and thus is useful. An example of such a process is a non-stationary binomial (or Bernoulli) process.

In order to take into account a natural background noise, one can model it as a stochastic process, which *additively* accompanies the process of registration of the emission signals. It can be assumed to be a stationary or a quasi-stationary stochastic process. Quasi-stationarity might stem from a seasonal or a daily change of the parameters of the underlying process.

The usage of a wavelet transform for an approximation of emission signals allows one to *minimize* the number of parameters of an approximation of a signal, since the wavelet basis can be formed from a fragment of the (random) process of emission of signals.

Under an investigation of a real object the system that we built collects data, processes it in real time and makes a decision about the state of the object. It important to emphasize that our system is a self-learning system, thus it uses data to learn the stationary state and the dynamics of the changes of the object.

Big bang modelling in core of the Earth and origin of oil and gas

© ***Ju. Muraveynyk, 2010***

Department of Marine Geology and Sedimentary Ore Formation,
National Academy of Sciences of Ukraine, Kiev, Ukraine
jmurav@mail.ru

In 1879 Professor George H. Darwin propounded the view that the Moon formed a part of the Earth [Pickering, 1907]. In 1957 Professor W. B. Porfir'ev has reported new conception on the youthful Neogene time of migration and formation of oil fields. He has promulgated, that petroleum erupted from great depths [Porfir'ev, 1968]. Since 1973 author has been working in the department of aca-

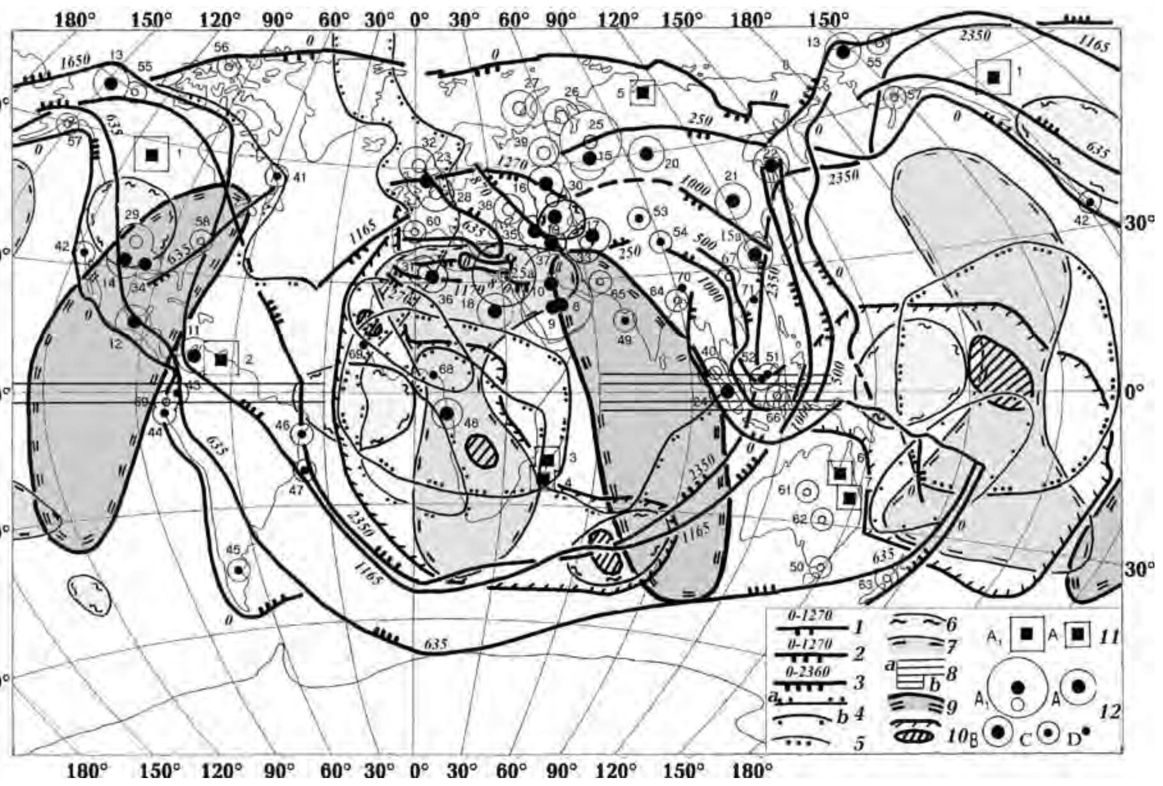


Fig. 1. Map the deep structure of the Earth and distribution of main oil and gas fields [Muraveynyk, 2000; 2003]. Zawaritski-Benioff zones — margin zones of continent — eugeosynclinale, depth (km): *1* — Tethis, Proterozoic, 1990 m. y.; *2* — Arctic Ocean, Proterozoic, 1115 m. y.; *3* — Pacific Ocean, Mesozoic, 240 m. y. *4* — upper mantle (*a* — slow anomalies — 0,2 % of *P*-wave velocities (V_P) at 1165 km depth [Zhou, 1996]. Slow anomalies — 0,2 % V_P (splitting-functions of free oscillations of the Earth)); *5* — lower mantle; *6* — outer core; *7* — inner core [Giardini et al., 1988]; *8* — isotropic layer (*a* — as large as 400 km in thickness at the top of the inner core (60°—140° E), *b* — 200 km in thickness at the top of the inner core (30—130° W) [Garcia, Sourian, 2000]); *9* — slow anomalies — 0,2 % V_P at 370 km of the inner core radius [Morelli et al., 1986]; *10* — low velocity anomalies V_S of S_{diff} phases (SH) in D" layer [To, Romanowich, 2009]; *11* — bitumen (very heavy oil) fields (geological reserves) (A_1 — 100 billion tons, A — 1 billion tons)); *12 — fields (recoverable reserves):* A_1 — unique (10 000) (*a* — oil (million tons), *b* — gas (billion m^3)), A — supergiant (1000), B — giant (1000—500), C — largest (500—100), D — large (100—50). See the list of main oil and gas fields [Muraveynyk, 2000; 2003].

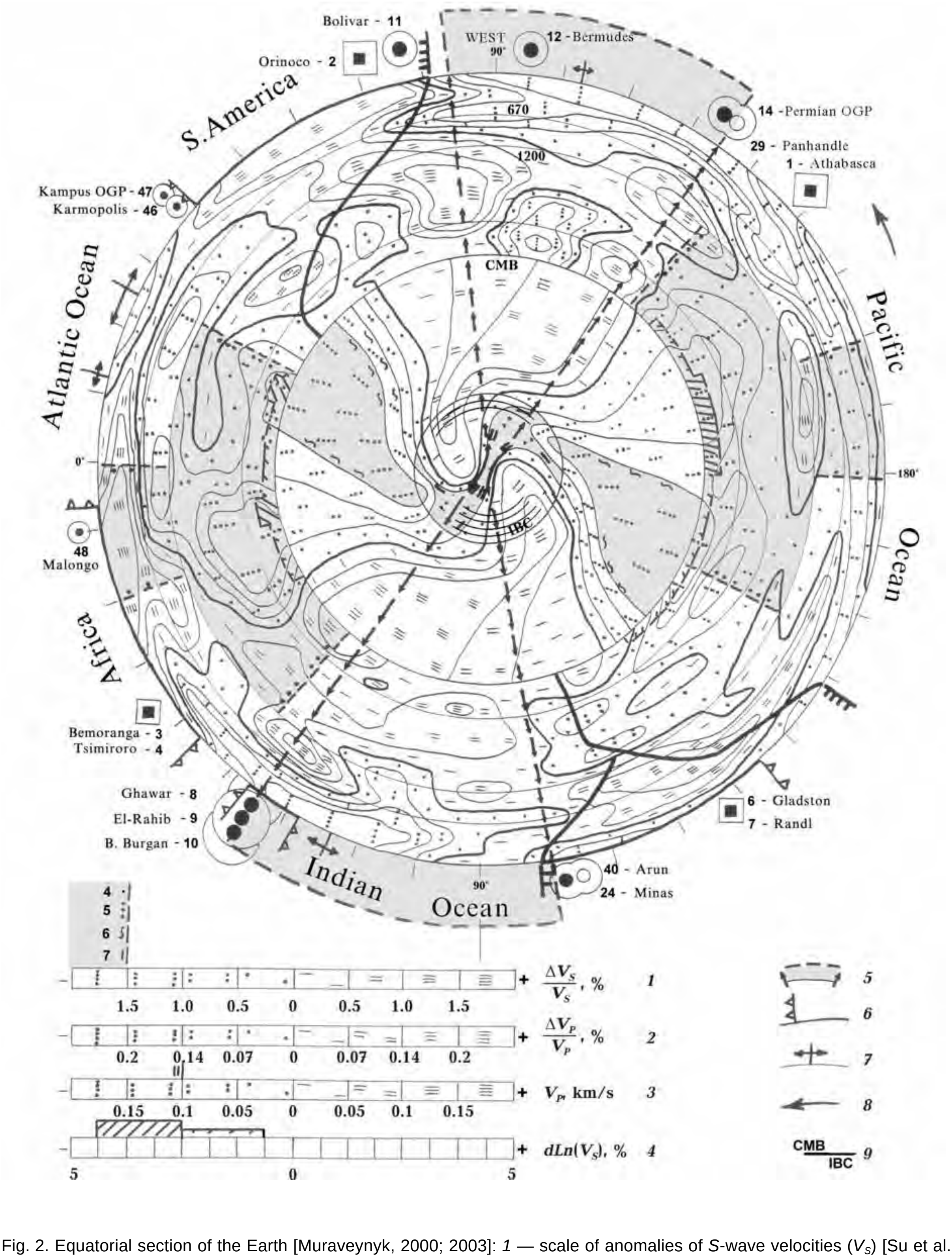


Fig. 2. Equatorial section of the Earth [Muraveynyk, 2000; 2003]: *1* — scale of anomalies of *S*-wave velocities (V_S) [Su et al., 1994]; *2* — scale of anomalies of V_P (splitting-functions of free oscillations of the Earth) [Giardini et al., 1988]; *3* — scale of anomalies of V_P at 370 km of the inner core radius [Morelli et al., 1986]; *4* — scale of anomalies of V_S S_{diff} phase (SH) in the D" layer; *5* — vertical projection on the surface of the Earth of slow anomalies — 0,2 % V_P at 370 km of the inner core radius [Morelli et al., 1986]; *6* — continental slopes; *7* — mid-oceanic ridges; *8* — spin of the Earth; *9* — CMB — core mantle boundary in depth 2891 km, IBC — inner boundary core at radius 1221 km. See the rest of legend in Fig. 1.

demician W. B. Porfir'ev "Geology and origin of oil and gas fields" at the Institute of Geological Sciences of the National Academy of Sciences of Ukraine. This ideas have been developed and used for systematizing data about existing oil and gas fields and coordinating research of new ones [Muraveynyk, 2000; 2003].

The further development of this ideas, supported by the modern data about the Earth inner structure forms ground for a new hypothesis about the Earth history. Anomalies of low velocity seismic waves in the inner and outer core, lower and upper mantle allow to map relicts of big bang (explosion) in the inner core under the Indian Ocean and antipodal under the Pacific. The D" region is the most widely and globally sampled by diffracted waves, S_{diff} and P_{diff}, which typically travel along the CMB over more than 30 degrees of epicentral distance. Using these phases is essential for mapping the 3D structure in the D" layer. In particular, horizontal velocity jumps of 3—4.5 per cent have been reported in the D" layer at the border of the two large-scale low velocity provinces (LLV *P*), often also called 'superplumes', in the south Pacific and under Africa, based primarily on the analysis of Sdiff phases [To, Romanowich, 2009]. Superplumes in the mantle under these oceans reflect termic influence of the closed big bang (without part separation of the planet) 65 m. y. ago. 240 m. y. ago at the beginning of the Mezozoic the big bang happened in the core with separation of the part of the planet under the Pacific Ocean with the forming of the Moon. Zawaritski-Benioff zones (subduction zones) mark edges of the bang cone in the lithosphere. These zones are recognized by the anomalies of low velocity seismic waves down to the core of the Earth. 1115 m. y. ago separation of satellite Mercury from theArctic Ocean happened. 1990 m. y. ago satellite Venus separated from Tethys. 3500 m. y. ago satellite Mars was formed from the suggested integral green stone eugeosynclinales of Aldan, Africanian, Australian, Indian, North and South America, Ukrainian cratons. The history of the Earth, Jupiter and Saturn was a history of brown dwarfs, separated after big bang of the Sun 5500 m. y. ago. Volcanic active satellite Io separated from Red Spot of the Jupiter 65 m. y. ago. The history of the Earth divided into 175 m. y. cycles (anomalistic galactic year) with big bangs in the beginning of the Cenozoic, Mezozoic, etc. The termic energy of this explosions affect lithosphere and atmosphere, determined interruptions in life evolution on the Earth, as well as distributions of ore deposits in margins of the bang cones in lithosphere. Oil and gas have been generated by closed big bang in the inner core of the Earth 65 m. y. ago. The heterogeneity of the Earth core controls oil-gas fields distribution in the Earth's crust. The 60 % of theWorld oil proved reserves are located in the Persian Bay Province — on the top of vertical heterogeneity in the inner and outer core (Fig. 1, 2).

References

Garcia R., Sourian A. Inner core anisotropy and heterogeneity level // Geophys. Res. Lett. — 2000. — **27**, № 19. — P. 3121—3124.

Giardini D., Li X.-D., Woodhouse J. H. Splitting functions of long-period normal modes of the Earth // J. Geophys. Res. — 1988. — **93**, № B 11. — P. 13716 —13742.

Morelli A., Dziewonski A. M., Woodhouse J. H. Anisotropy of the inner core inferred from PKIKP travel times // Geophys. Res. Lett. — 1986. — **13**, № 13. — P. 1545—1548.

Muraveynyk Ju. A. Big Bands in the Earth's core as a basic of theoretical geology // Ukranian geologist. — 2003. — № 2. — P. 35—46 (in Russian).

Muraveynyk Ju. A. Influence heterogeneity of core on placing of oil and gas fields in the earth's crust // Dop. Nation. Acad. Sci. Ukraine. — 2000. — № 6. — P. 137—142 (in Russian).

Pickering W. H. The Place of origin of the Moon — the volcanic problem // J. Geolog. — 1907. — **XV**, № 1. — P. 23—38.

Porfir'ev W. B. Genetic environment of commercial oil pools // Geolog. J. Akad. Nauk Ukrainian SSR. — 1968. — № 4. — P. 3—33 (in Russian).

Su W.-J., Woodward R. L., Dziewonski A. M. Degree 12 model of shear velocity heterogeneity in the mantle // J. Geophys. Res. — 1994. — **99**, № 4. — P. 6945—6980.

To A., Romanowicz B. Finite frequency effects on global S diffracted traveltimes // Geophys. J. Int. — 2009. — **179**. — P. 1645—1657.

Zhou H.-W. A high resolution P wave model for the top 1200 km of the mantle // J. Geophys. Res. — 1996. — **101**, № 12. — P. 27791—27810.

Strain state and crustal deformation in the central part of the ingul megablock of the Ukrainian Shield according to structural data on the Novoukrainka massif and the Subbottsy-Moshoryno fault zone

© ***S. Mychak, L. Farfuliak, 2010***

Institute of Geophysics, National Academy of Sciences of Ukraine, Kiev, Ukraine

Mychak_S@ukr.net
myronivska@list.ru

The central part of the Ingul megablock of the Ukrainian Shield (US) is located between the Zvenigorod-Bratsk and Kirovograd fault zones, which is tectonically and metalogenically unique. That part of the US is the major section of a transregional fault belt that extends from the south to the north for 1000 km between the towns Kherson and Smolensk. This Kherson-Smolensk belt is represented by a set of submeridional faults and large intrusions, the Korsun'-Novomirgorod pluton of gabbro — anorthosites and rapakivi granites (KNP) and the Novoukrainka massif of trachytoid granites and monzonites (NU-massif) (Figure). They are divided by the latitudinal Subbottsy-Moshoryno fault zone (SMFZ). The NU-massif was intruded at ca. 2050—2035 Ma, while the KNP at ca. 1750 Ma.

The Novoukrainka massif and the Korsun'-Novomirgorod pluton. The structural research of the Novoukrainka massif is important to understand geodynamic processes in the lithosphere of the central part of the Ukrainian Shield and the formation of the Kirovohrad ore region with deposits and occurrences of uranium, lithium, gold, lead and zinc, copper, tin and silver [Granitoids ..., 1993; Starostenko et al., 2010].

Structural studies of the Ingul megablock were conducted in 2007—2009. Many features of crystalline rocks like dynamic metamorphic mineral parageneses in cracks, zones of schistosity, cataclasis and mylonitization, spatial orientations of trachytoid textures, striation and furrows on sliding mirrors were investigated. As a result, stress conditions and the sequence of deformation events as defined by the interrelation of strain structures were obtained for the period between 2.05 and 1.75 Ga, which is isotopic age of the NU and KNP intrusions.

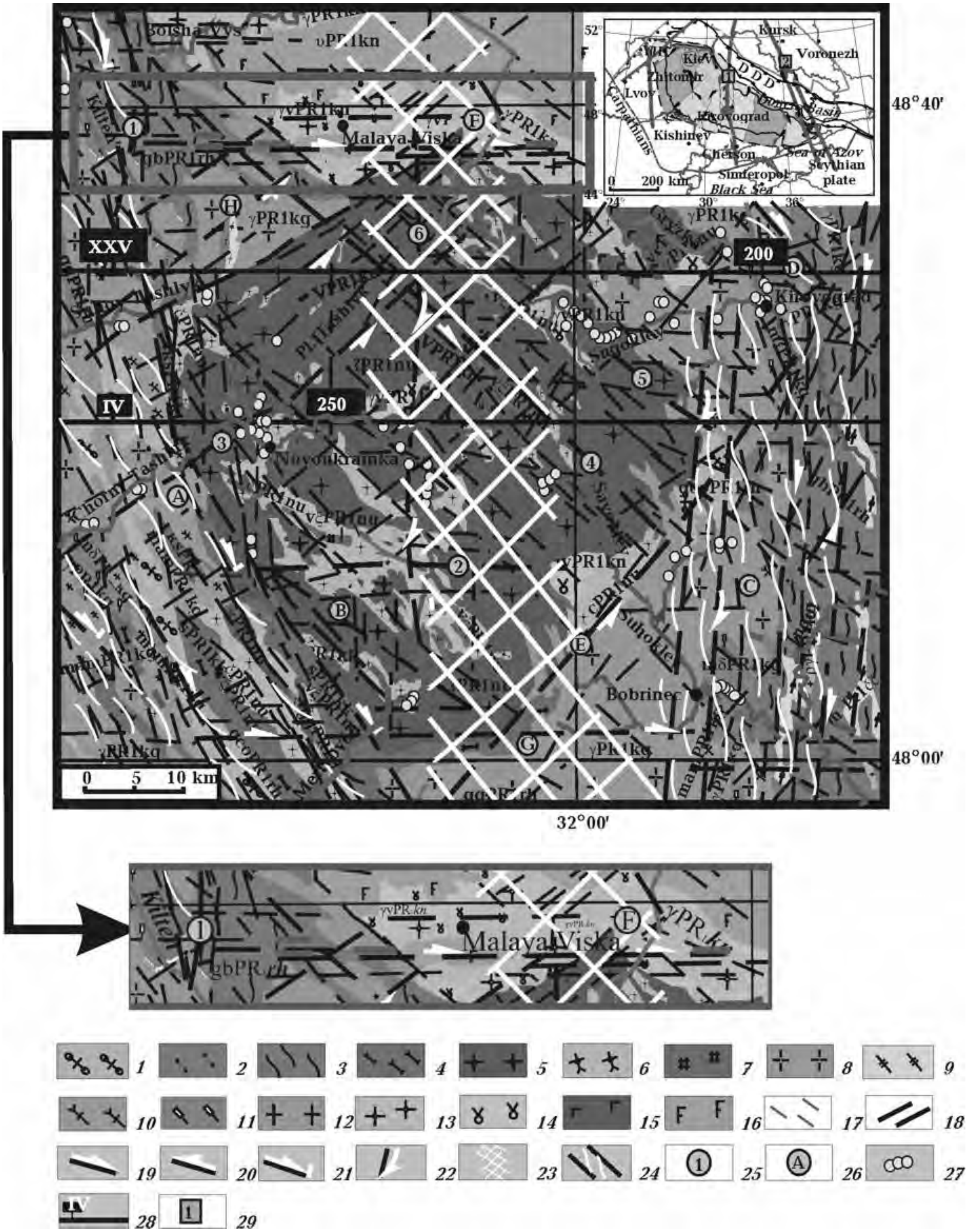
The formation and deformation in the NU-massif were connected with stress conditions, which caused the $\sigma_1\sigma_3$ planes both subhorizontal and inclined. Generally, 67 % of studied fractures in the NU-massif are sub-vertical and 33 % are inclined (<70°).

The stress parameters for the NU-massif are close to those published by [Belichenko, Gintov, 1996] for the KNP i. e.: the Korsun' phase — compression (σ_1) 6/00[1] , tension (σ_3) 276/00; the Gorodysche phase — compression (σ_1) 171/00, tension (σ_3) — 81/00 (Table). The preservation of strain during the time interval of ca. 250 Ma between the NU and KNP intrusions, when several deformation and fault stages occurred, is difficult to explain. We connect the early strain stage of the NU-massif to a strong EW extension of the lithosphere in the central part of the Ukrainian Shield along the future Kherson—Smolensk submeridional fault belt. This is a reason to separate the early stress phase in the NU-massif as the independent "Kherson–Smolensk" deformation stage, which repeated during the KNP intrusion after 250 Ma.

Since all faults before and after this event were shears [Gintov, 2005], there are no doubts that the Kherson-Smolensk fault belt was formed with a shear component, i.e. due to transtension. The orientation of compression axis of 8° deviates to the right from the direction of this belt by 15°. This suggests a right-lateral shear component of general deformation.

During some stages transtension could pass to transpression, because the emplacement and crys-

[1] 6 — dip-azimuth / 00 — dip angle.



Structural map of the central part of the Ingul block [as based on Kirovgeologiya' and the authors' data]. *Ingulo-Ingulets series: 1* — gneisses and biotite-cordierite schists ($gcoPR_1rh$); *2* — gneisses and garnet-biotite schists ($ggPR_1rh$); *3* — biotite gneisses ($gbPR_1rh$); *4* — pyroxene and biotite-pyroxene orthogneisses (sPR_1kk). *Novoukrainka complex: 5* — host granites and migmatites with biotite and garnet porphyroblasts (ãPR_1nu); *6* — host granites and migmatites with pyroxene-biotite porphyroblasts (čPR_1nu); *7* — monzonites and quartz monzonites ($v\xi PR_1nu$). *Kirovograd complex: 8* — granite and migmatite (γPR_1kg); *9* — composite gneisses (m^1PR_1čč); *10* — plagioclase migmatites and granites ($mamPR_1kg$); *11* — porphyroblastic plagioclase migmatite ($m\delta PR_1kg$); *12* — aplite granite and pegmatite (ñãPR_1kg). *Korsun'-Novomirgorod complex: 13* — ovoid rapakivi granite (γrPR_1kn); *14* — hybrid rocks (gabbro-monzonites, quartz monzonites) (γvPR_1kn); *15* — gabbro, gabbro-norites, norites, gabbro-diorities, gabbro-anorthosites (vPR_1kn); *16* — anorthosites (labradorite) (uPR_1kn); *17* — dykes of

tallization of the granite bodies took place under side compression.

The Subbottsy-Moshoryno fault zone (SMFZ). The latitudinal Subbottsy-Moshoryno fault zone extends for 200 km within the Ingul megablock, between 48°34.5′ and 48°45.5′ north (see Figure). 750 structural measurements were carried out in 53 sites. Our results show that the SMZF faults are steep, dipping between 70 and 90°. There is evidence of the shear nature of the SMZF such as the mainly sublatitudinal flat-dipping (30—55°) cracks, and thrusting in 3 % cases. Furrows and striatiuon on rare sliding mirrors indicate both right- and left-lateral slip components along sublatitudinal and submeridional structures. The presence of right-lateral and left-lateral R- and R′-shears almost everywhere agrees with this kinematics [Gintov et al., 2008].

Table sums up the structural characteristics of the Novoukrainka massif and of the SMFZ and deformation stages for the period of 2.05—1.75 Ga.

Conclusion. The obtained results confirm the earlier idea [Gintov, 2005] about a strong extension of the lithosphere in the central part of the Ukrainian Shield which took place ca. 1.8 Ga ago. At this

Major stages and phases of deformation in the central part of the Ingul megablock of the Ukrainian Shield

Stage	Phase	Axes of stress		Type of stress	Deformation	Age, Ga
		σ_1 compression	σ_3 tension			
Krivoi Roh	Krivoi Roh	70/30	320/30	compression	Slip reverse fault	≥2.05
Kherson-Smolensk	Kherson-Smolensk	8/00	278/10	tension	transtension	2.05
Kirovoghrad	Kirovoghrad	48/00	318/00	compression	Transtension (right lateral shear)	1.9
Kirovoghrad	Lelekovka	3/00	273/05	compression	Transtension (right lateral shear)	1.9
Kirovoghrad	Bobrinets-Zhivanovka	62/05	330/35	compression	Transtension (right lateral shear)	1.8—1.9
Korsun’-Novomirgorod	Korsun’	6/00	96/00	tension	Transtension	1.75
Korsun’-Novomirgorod	Gorodysche	171/00	81/00	tension	Transtension	1.75
Korsun’-Novomirgorod	Kompanievka	90/00	360/00	compression	Transtension (right lateral shear)	1.75
Subbottsy-Moshoryno	Subbottsy-Moshoryno	134/00	45/00	tension	Transtension (right lateral shear)	~1.75
Subbottsy-Moshoryno	Adzhamka	47/00	317/00	compression	Transtension (right lateral shear)	~1.75

diabases, lamprophyres (β PR_1—PR_2); *18* — en echelon and elementary shears (kinematic indicators for the initial stage); *19* — right-lateral shear; *20* — left-lateral shear; *21* — slip-normal fault; *22* — slip-reverse fault *and thrust*; *23* — Kherson-Smolensk transregional belt; *24* — folding along faults; *25* — faults (Kirovgeologiya’s data) (1 — Novopavlovka—Yaroshevka, 2 — Devladovo—Butovo, 3 — Adabashev, 4 — Nerubaevo—Lozovatsk, 5 — Shestakovka—Voroshilovka, 6 — Novokonstantinovka); *26* — fault zones, letters in circles are (A — Zvenigorodka-Bratsk, B — Novoukrainka, C — Kirovograd, D — Lelekovka, E — Mar’evska, F — Subbottsy-Moshorino, G — Bobrinetsy, H — Gladossk); *27* — sites of structural studies; *28* — profiles of DSZ (deep seismic zoning) IV and XXV (200 and 250 — picket numbers); *29* — deformation zones are shown on the right up map of the US (1 — Kherson-Smolensk belt, 2 — Donetsk-Bryansk belt).

time the Shield was divided by the submeridional Kherson-Smolensk intracratonic fault belt, 60—70 km wide. The phases of transtension were interrupted by transpression phases, however extension predominated. This defined the emplacement both the Novoukrainka and Korsun'-Novomirgorod pluton.

References

Belichenko P. V., Gintov O. B Stress straine and deformation of the crustal Ukrainian Shield in the period formation of the Korsun'-Novomirgorod Pluton gabbro-anortothyte and rapakivi (tectonophysic data) // Geophys. J. — 1996. — **18**, № 2. — P. 59—69 (in Russian).

Gintov O. B. Field tectonophysics and its application for the studies of deformations of the Earth's crust of Ukraine. — Kiev: Feniks, 2005. — 572 p. (in Russian).

Gintov O. B., Orlyuk M. I., Mychak S. V., Bakarzhieva M. I., Farfuliak L. V. Subbotsko-Moshorinsky stage of the Earth's crust deformation of the Ukrainian Shield // Geophys. J. — 2008. — **30**, № 6. — P. 23—39 (in Russian).

Granitoids of the Ukrainian Shield. Petrochemistry, geochemistry, ore content. Guide / Ed. N. Scherbak. — Kiev: Nauk. dumka, 1993. — 231 p. (in Russian).

Starostenko V. I., Kazanskiy V. I., Popov N. I., Drogitskaya G. M., Zayats V. B., Makivchuk O. F., Tripolskiy A. A., Chichetov M. V. From surface structures to integral deep model of the Kirovograd ore are (Ukrainian Shield). 1 // Geophys. J. — 2010. — **32**, № 1. — P. 3—34 (in Russian).

Computer modeling of nonlinear dynamic processes in structured geophysical media

© ***S. Mykulyak, 2010***

Institute of Geophysics, National Academy of Sciences of Ukraine, Kiev, Ukraine
mykulyak@ukr.net.

In different kinds of deformation processes practically all rocks reveal specific properties such as nonlinearity, hysteresis, dilatancy and dependence on the rate of deformation. These nonlinear properties are usually attributed to the structural constitution of the materials and to the processes taking place on contacts of structural elements: crystals, grains, granules, etc. The experiments with neutron diffraction [Darling et al., 2004] confirm the dependence of the non-classical properties of sedimentary rocks (sandstones, marble and limestone) on the deformation processes of small material volumes near bonds and contacts, inhomogeneous stresses in the grains and the pore space available for grain motion. For the explicit study of this dependence the computer simulation of dynamic deformation processes in the structured medium has been performed.

The structured medium is modeled by the discrete system of 2D deformed elements (grains). Three types of grain interaction: a) elastic, b) viscoelastic and c) elastoplastic are considered. The

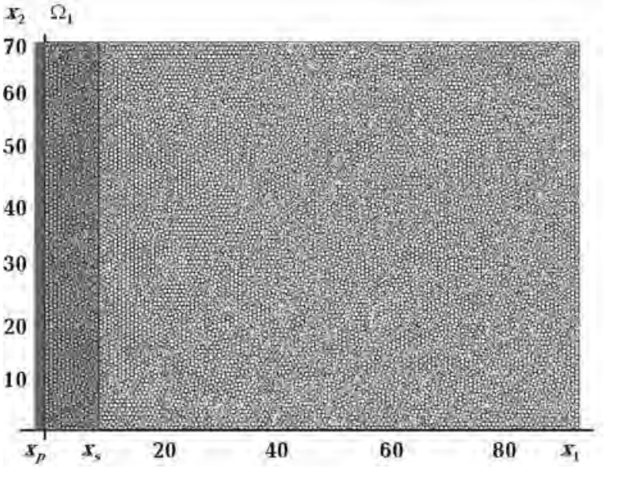
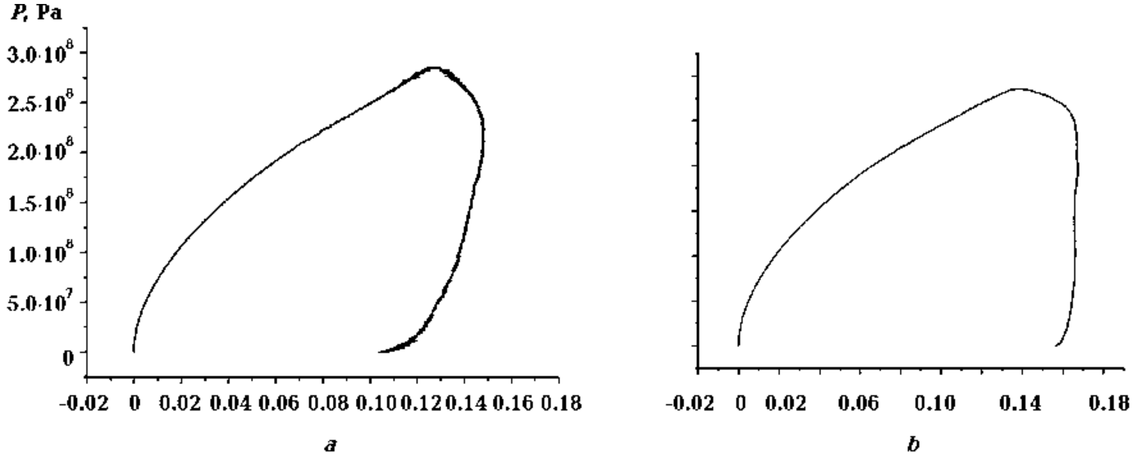


Fig. 1. The grains massif.



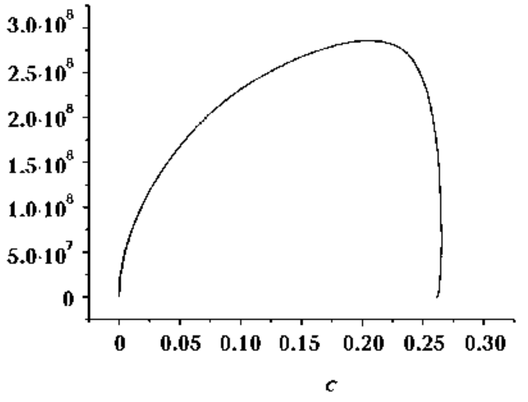


Fig. 2. The stress-strain diagrams for three types of grains interaction: *a* — elastic, *b* — viscoelastic, *c* — elastoplastic.

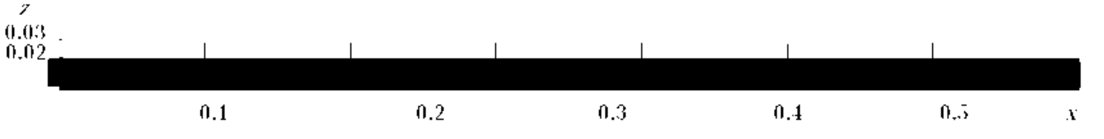


Fig. 3. The structured massif in which propagates the nonlinear wave.

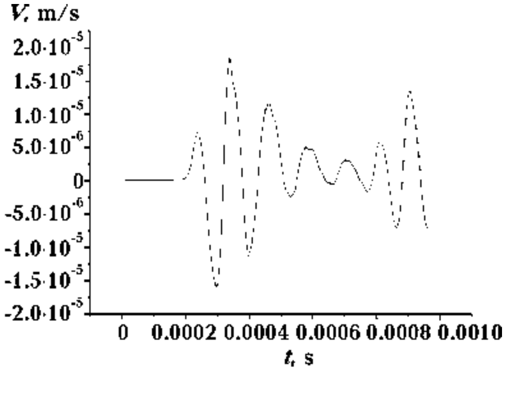


Fig. 4. Averaged velocities V_x vs. time t at the distance x=0.16.

molecular dynamic technique is used for simulation the dynamic of the discrete medium [Cundall, Strack, 1979]. The grains massif is placed in a rectangular aria (Fig. 1). The massif is deformed by the piston, which is driven by the force acting in the *x*-direction

$$f = f_0 \sin^2(\pi t / t_{\max}). \tag{1}$$

The thin wall with the coordinate x_s is located inside the massif. Knowing coordinates of piston x_p and x_s one can to determine the actual strain $\varepsilon(t)$ of the thin layer Ω_1

$$\varepsilon(t) = 1 - \frac{x_s(t) - x_p(t)}{x_s(t_0) - x_p(t_0)} \tag{2}$$

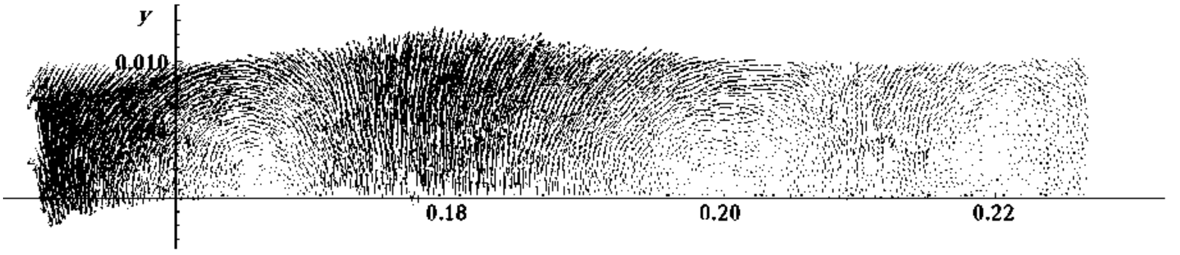


Fig. 5. The vector field at the time t=0.96 ms.

and to build the stress-strain diagram. The stress-strain diagrams for three types of grains interaction are presented in Fig. 2. All diagrams are nonlinear and hysteretic. The hysteresis squares in the viscoelastic and elastoplastic cases are greater then in the elastic one.

The second part of the report is devoted to the propagation of nonlinear wave in structured media in gravitation field. The massif consists of 56000 elements with the elastic Hertzian contacts (Fig. 3). The wave is generated by the same procedure as in the first case. Averaged mass velocities are calculated at six distances away from the piston by averaging the velocities of particles in thin layers. The dependences of the averaged velocities on time are presented in Fig. 4. The propagating wave rapidly decays being transformed then into a periodically one. Fig. 5 shows that in the massif periodical wave structures are formed. If the massif is in a prestressed state the wave attenuates slowly and the wave structures do not arise. The prestressed state is created by the z-direction weighting.

References

Cundall P. A., Strack O. D. L. A discrete numerical model for granular assemblies // Geotechnique. — 1979. — **29**, № 1. — P. 47—65.

Darling T. W., TenCate J. A., Brown D. W., Clausen B., Fogel S. C. Neutron diffraction study of grain contacts to nonlinear stress-strain behavior // Geophys. Res. Lett. — 2004. — **31**. — P. L166041—L166044.

Efficient method for solving the resistivity sounding inverse problem

© ***N. Myrontsov, 2010***

Institute of Geophysics, National Academy of Sciences of Ukraine, Kiev, Ukraine
myrontsov@ukr.net

The aim of electromagnetic sounding including the logging is to determine medium parameters on the base of measurement data. In other words, it is necessary to associate each vector $\mathbf{g}$ from the measurement space $\mathbf{G}$ to vector $\mathbf{p}$ from the space of model parameters $\mathbf{P}$. The finding of such correspondence determines the essence of solving the inverse problem.

Traditionally in solving the logging inverse problem, it is accepted to use a minimization of the functional:

$$F\left(\rho_1^T,\ldots,\rho_n^T\right)=\sqrt{\sum_{i=1}^{n}\left(\frac{\rho_i^T-\rho_i^P}{\delta_i\rho_i^T}\right)^2}\ , \qquad (1)$$

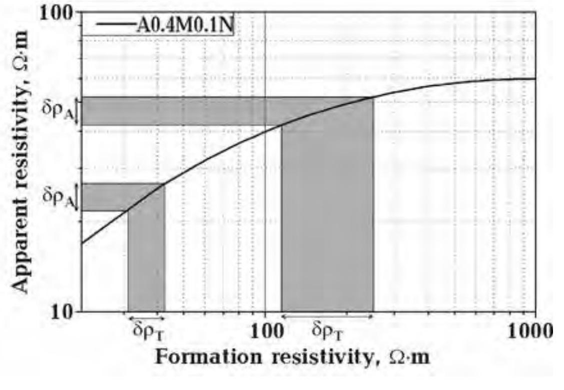
where: n is the number of sounds in the equipment, ρ_i^T are computed theoretical values of apparent resistance (AR) of the model under consideration, ρ_i^P are values obtained really in AR measuring and δ_i is the value of error for i-th sound. The values of model parameters, to which computed ρ_i^T correspond at each step of the iterative process of minimization of

the functional (1) shall be the solution of the inverse problem. This approach was devised and described in details in many articles (L. E. Kneller, A. P. Potapov, M. I. Epov, G. K. Gorbik, S. M. Zundulevich, A. E. Kulinkovich, M. D. Krasnogon etc.). At the present time this method is commonly used in practice (for example in programs: Mikar, Electra, VIKIZ etc.), we shall refer it to as “now used method”.

In the present work, it is shown that practical use of such approach is not quite correct since instead of vector $\mathbf{g}$ the spatial domain $\mathbf{g}+\delta\mathbf{g}$ should be our initial condition (taking into account an error, a result of any variation is non-numerical, a confidence interval (CI)). Accordingly, the inverse problem solution shall be not $\mathbf{p}$ vector, but a $\mathbf{p}+\delta\mathbf{p}$ spatial domain. The results of minimization (1) reflect only the relationship between vectors $\mathbf{g}$ and $\mathbf{p}$, but do not reflect any relationship between $\mathbf{g}+\delta\mathbf{g}$ and $\mathbf{p}+\delta\mathbf{p}$. For example, Figure demonstrates the dependence of apparent resistivity ρ_A on formation resistivity ρ_T for resistivity logging sound A0.4M0.1N. As it is shown in the figure, the values of $\delta\rho_T$ corresponding to the same value of $\delta\rho_T$ can change substantially depending on a part of range. And in accordance with the above-stated, in this case the interval of $\delta\rho_T$, but not the value of ρ_T itself, is the solution of inverse problem. Thus, the method of inverse problem solving should primarily minimize the domain of $\mathbf{g}+\delta\mathbf{g}$. As was found, it can be easily realized. The idea of the proposed method consists in the replacement of functional (1) by functional:

$$F\left(\rho_1^T,\ldots,\rho_n^T\right)=\sqrt{\sum_{i=1}^{n}\left(\frac{\rho_i^T-\rho_i^P}{\lambda_i\rho_i^T}\right)^2}\,, \qquad (2)$$

where: λ_i are weighting coefficients determined from the condition $\inf\limits_{\lambda_1,\ldots,\lambda_n}\left(\left\|\delta\mathbf{p}(\delta\mathbf{g})\right\|\right)$ and in solving the inverse problem determining the measure of influence on the confidence interval of every of model parameters, respectively.



Apparent resistivity (ρ_A) as a function of formation resistivity (ρ_T).

Table 1. Parameters of different bed models

Type of bed	Fluid content	ρ_T, Ω·m	ρ_{x0}, Ω·m	D/d
1	water-saturated	4.5	20	5
2	gas-saturated	50	30	5
3	oil-saturated	8.5	30	4

Table 2. Compared error in solving the inverse problem with using two methods (I — now used, II — proposed) for 7IK equipment

Type of bed	I			II		
	ρ_T, %	ρ_{x0}, %	D/d, %	ρ_T, %	ρ_{x0}, %	D/d, %
1	37.1	12.0	23.7	5.4	2.5	5.3
2	15.6	16.3	23.1	6.4	4.1	6.4
3	41.5	42.8	34.0	3.7	6.1	3.1

Table 3. Compared errors in solving the inverse problem with using two methods (I — excisting, II — proposed) for MEK equipment

Type of bed	I			II		
	ρ_T, %	ρ_{x0}, %	D/d, %	ρ_T, %	ρ_{x0}, %	D/d, %
1	19.4	32.4	72.1	13.3	15.2	13.1
2	14.1	26.1	51.6	4.9	13.0	12.7
3	17.8	29.2	47.4	5.3	14.1	18.2

To estimate the efficiency let us give some examples of comparing the proposed method of solving the inverse problem with the now used method. For that end, let us consider models of typical invaded beds corresponding the conditions of the Dnieper-Donetsk depression (model parameters of considered beds are given in Tabl. 1; where: ρ_T is the formation resistivity, ρ_{X0} is the invasion zone resistivity, D is the diameter of invasion zone, d is the rated well diameter). The 7IK seven-sound equipment for induction logging (a modified analogue of AIT Schlumberger) and the MEK multisound equipment for electric logging (a modified analogue of HRLA Schlumberger) were chosen as the sounding equipment.

The results of comparison between these methods for 7IK are given in Tabl. 2, and the ones for MEK are given in Tabl. 3. It is evident that the proposed method is significantly more precise than the one used traditionally. Similar calculations were performed for all spectrum of models of payout beds relating to the Dnieper-Donetsk depression and Western Siberia. It shall be noted that effective practical use of the proposed method has become possible owing to the development of computers since it require considerable computer resources: actually to determine the confidence interval for each of determined parameters of every concrete bed it is necessary to solve the inverse problem for several different values of initial data.

The following conclusion was made on the base of conducted study: the solution of inverse problem based on the minimization of functional (2) is more correct and accurate than in case of use of the minimization of functional (1).

Method for improving the spatial resolution of resistivity logging

© ***N. Myrontsov, 2010***

Institute of Geophysics, National Academy of Sciences of Ukraine, Kiev, Ukraine
myrontsov@ukr.net

The main aim of resistivity logging is to determine geometric and electrical parameters of a model of borehole environment. Subsequent problems of geophysical investigations of well, such as determinations of fluid saturation, daily flow of fluid production and others will be solved the more precisely, the more precisely these parameter are determined. Sounds in the complex differ each from other as to the depth of investigation and the vertical resolution (along the axe of well). Naturally, the vertical resolving power is worse for sounds with larger depth of investigation. In this connection, the necessity to build sounding system for logging with the maximum high vertical resolution of all sounds including the most subsurface ones.

A creation of such equipment based on traditional principles is complicated by the necessity to use frequency, spatial or time separation, what complicates considerably the design (a creation of effective equipment with more than two sounds was found practically impossible). A creation of such equipment for induction logging are also complicated because of fundamental design limitations.

A factorization is believed an affective approach to create sounding system for logging with the maximum high vertical resolution of all sounds including the most subsurface ones. The factorization permits to solve separately the inverse problem along the axe of well and along a normal to it. It means that in each point of sound's position we can believe that the bed has infinite thickness (is free of shoulder effect). In this case, the conductivity values will change only along the normal to the axe of well.

The following methodical approach was used for induction logging: to determine the resistivity according to the apparent resistivity measured within the frame of the linear Doll theory using a solution of the first kind Fredholm equation of convolution type. The present method was tested on model material from various complexes (4IK, 7IK, AIT Schlumberger). The example of application of such method to data of 4IK equipment is shown in Fig. 1 (sounds: I0.5; I0.85; I1.25; I2.05. The numbers corresponds to the length of each sounds). It is evident that using the proposed approach permits to factorize the problem with high degree of accuracy. In the work, it is also shown that after such factorization the vertical resolution of each sound is limited only by the error of measurement and the value of recording step along the axe of well.

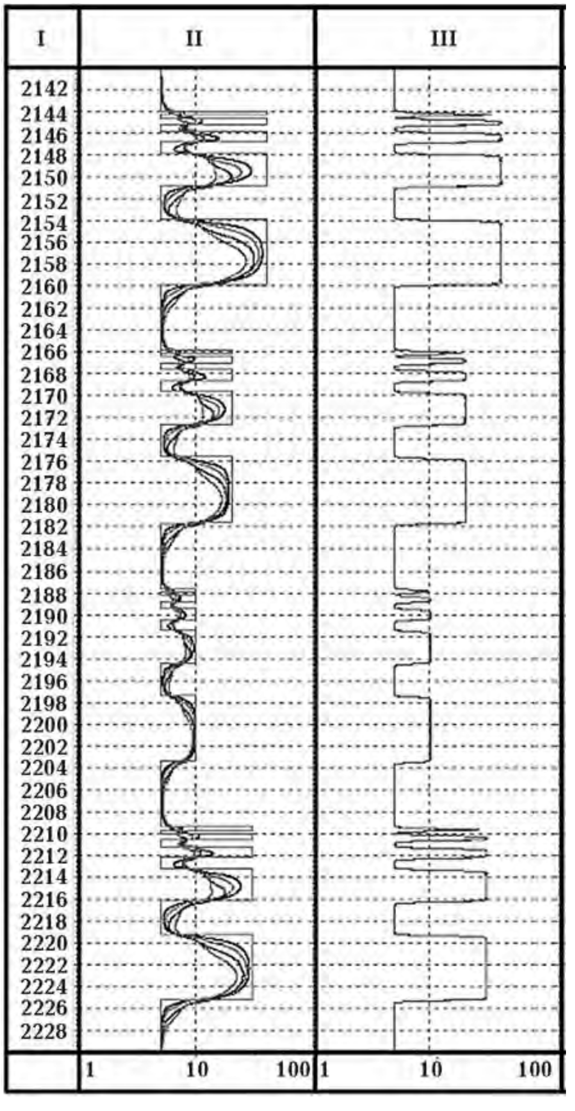


Fig. 1. The example of factorization of 2D inverse problem of inductive logging: I — depth, II — measured apparent conductivity and specified conductivity of beds, III — reconstructed conductivity.

The assumption on absence of current interaction in medium also is a restriction of this method. This restriction is not critical since the linear Doll approach describes many cases being topical for practice with high degree of accuracy. Besides, a lot of authors linearize the problem using a correction for skin effect. In the course of investigation, it was shown that use of correction for skin effect is only some approximation, which introduces its own error being, in essence, unavoidable, but it permits to find some, undoubtedly approximate, solution. The modelling has shown that solution based on using a correction for skin effect can lead to qualitatively incorrect results. One of obvious advantages of described method consists in its applicability to already existing equipment of inductivity logging.

In contrast to inductivity logging problems, the problems of electric logging are nonlinear in essence. So, the variant of algorithmic solution is inapplicable for electric logging. In this work, the new type of multisound electric logging equipment (MEK) is proposed. The principle of lateral logging, but without a necessity of frequency, spatial and time separation, is used as principle of its action.

The idea of the method consists in the possibility to realize a simultaneous measurement of currents, every of which penetrates down to strictly defined depth. In this case, high vertical resolution is reached by means of use of the principle of lateral logging.

The example of MEK borehole logs for invaded profile is shown in Fig. 2. It is evident that proposed method also factorizes the problem with high degree of accuracy. It is demonstrated that the vertical resolution of each sound is limited mainly by the error of measurement and the value of step recording along the axe of well as well as the sound's size.

The MEK design and the principle of measurement proposed in the work have a number of advantages: the possibility to be used in horizontal wells; the insusceptibility to the Groningen effect; the constructive ease of realization and small overall dimensions.

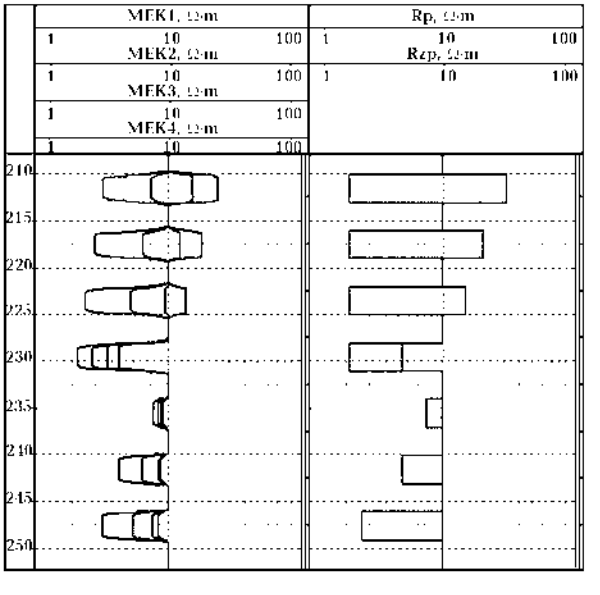


Fig. 2. The example of factorization of 2D inverse problem of electric logging: MEK1, MEK2, MEK3, MEK4 are resistivities obtained by different depth sounds; Rp is the resistance of virgin part of bed; Rzp is the resistance of invaded zone.

The efficiency of proposed methods of electric and inductivity logging was analyzed under the conditions of Western Siberia and the Dnieper-Donetsk depression. On the grounds of performed analysis, the conclusion that MEK and 7IK have much better characteristics in comparison with commonly used BKZ-BK-IK complex and some of other multisound complexes used on the territories of Ukraine, Russia, Kazakhstan and other countries was made. They also are not inferior to similar complexes developed by leading geophysical corporations as to their characteristics.

Extensometric researches in Ukraine: methods, instruments, results

© *A. Nazarevych[1], L. Nazarevych[2], V. Nasonkin[3], O. Boborykina[3], 2010*

[1]Carpathian Branch of Institute of Geophysics, National Academy of Sciences of Ukraine, Lvov, Ukraine
nazarevych-a@cb-igph.lviv.ua
[2]Department of seismicity of Carpathian region of Institute of Geophysics,
National Academy of Sciences of Ukraine, Lvov, Ukraine
nazarevych.l@gmail.com
[3]Tavrichesky National University, Simferopol, AR Crimea, Ukraine
b0b04ka14@mail.ru

Extensometric seismoprognostic researches are conducted in Ukraine for over 20 years. They are concentrated in the Transcarpathians and the Crimea as the most seismoactive regions of the country (Figure). In Transcarpathians the quartz extensometers was working [Latynina et al., 1992; 1993; Verbytsky et al., 2003; Verbytsky, Nazarevych, 2005; Nazarevych, 2006]. Now works 3 de-



Points of extensometric researches in Ukraine (marked by red triangle): 1 — RGS "Beregove"; *2* — RGS "Koroleve"; Geophysical Observatory of TNU (AR Crimea, Sevastopol, Cape Chersonese).

vices. At different times they were equipped with various measuring and recording systems [Latynina et al., 1993; Verbytsky et al., 2003; Verbytsky, Nazarevych, 2005; Nazarevych I., Nazarevych A., 1999; 2006]. In parallel in one of the stations for some time the 2 — axis tiltmeter was worked. Recently, we have developed and put into operation in one of quartz extensometers in regime geophysical station (RGS) "Beregove" (see Figure) the computerized measurement and recording system with a noncontact capacitive sensor of micromoving measuring. The system has a primary tool sensitivity 10 nm (about 10^{-9} in relative units) at 2 count per second and can obtain the sensitivity 1 nm in the signal accumulation mode (1 count per 10 s). For temperature control and accounting of parasitic thermoelastic deformation of constructions constituent the system is equipped with a temperature control channel with a sensitivity 0.01 °C.

In Crimea on Geophysical observatory (Sevastopol) of Vernadsky name Taurichesky National University the extensometric laser interferometer complex was created and works [Shliakhovyj et al., 2007; http://www.tnu.crimea.ua/tnu/str_praz/observatory/index.htm]. The complex consists of 2 equal "shoulder" ("shoulder" length is 5 m) two-ray laser interferometers of Michelson type with separated beams using the frequency-stabilized laser as a wavelength standard. Their basic metrological characteristics are following: the sensitivity on strains (ADC LSD unit) — 0.16 nm, the instrumental long-term drift — not more than 2.5×10^{-8} units per year. There is computer registration, measurements are made at intervals 4 s. In the same place 2 — axis tiltmeter which was created in Poltava gravimetric observatory of Subbotin name Institute of Geophysics of NASU also works.

During the extensometric observations the number of more or less intensive predictive deformation anomalies which accompany the preparation of local earthquakes was recorded. In Transcarpathians one of the most intensive was precursor of sensible 1989 Vynogradove earthquakes with M=2.9 (I=5.5) [Nazarevych A., Nazarevych L., 2008; Nazarevych, 2010], which was registered in extensometric station "Muzhiyevo" ("Beregove-1") at the epicentral distance 23 km. Anomaly started 5 months before earthquake and had absolute amplitude 30,8 mkm relative to trend component (11×10^{-7} in relative units). In the period of preparation and after earthquake the nature of deformation processes in rock massifs in observation area was changed: by extensometer **d1** the average annual compression with value $\approx10.5\times10^{-7}$ was changed by expansion with value $\approx4.1\times10^{-7}$, by extensometer **d2** the average annual compression with value $\approx23\times10^{-7}$ decreased to $\approx9.6\times10^{-7}$. Also we can note that there was a similar nature (expansion) and correlated in time changes of deformation (**d1**) and registered on a nearby point of geoacoustic observations acoustic anomalies [Nazarevych, 2010].

An example of deformation precursor of the Crimea — Black Sea region earthquake is recorded in a distance of about 250 km anomaly, which accompanied the preparation of the 07.05.2008 earthquake with a magnitude M=4.9, epicentre coordinates 45.36°N, 30.92°E and focal depth about 10 km. Duration of anomaly was about one and half months, the absolute amplitude relative to trend component was 1,92 mkm ($\sim4\times10^{-7}$ in relative units).

Comparison of values of recorded deformation anomalies with data of theoretical studies on propagation of deformations from the future earthquake emerging focal zone [Dobrovolsky, 1991] shows that registered anomalies are in value by 10—100 times higher than results of theoretical estimations with taking into account the size of the source [Nazarevych A., Nazarevych L., 2009] for earthquakes of corresponding energetic class/magnitude. The reason for this can be features of tectonic structure of these regions lithosphere and the presence here of horizontal tectonic stresses [Nazarevych L., Nazarevych A., 2006]. These results indicate that potential and prospects of extensometric method in seismoprognostic monitoring are substantially greater than it was consider before.

References

Dobrovolsky I. P. The theory of tectonic earthquake preparation. — Moscow: IPhE RAS, 1991. — 219 p. (in Russian).

http://www.tnu.crimea.ua/tnu/str_praz/observatory/index.htm (in Russian).

Latynina L. A., Baysarovych I. M., Brymyh L., Varga P., Yurkevych O. H. Deformation measurements in the Carpathian-Balkan region // Phys. Earth. — 1993. — № 1. — P. 3—6 (in Russian).

Latynina L. A., Yurkevych O. I., Baysarovych I. M. The results of deformation measurements in Beregovo area // Geophys. J. — 1992. — **14**, № 2. — P. 63—67 (in Russian).

Nazarevych L., Nazarevych A. Seismicity and geomechanics of Ukrainian Carpathians region lithosphere // Proc. of XYIII-th congress of the Carpathian-Balkan geological association. September 3—6, 2006, Belgrade, Serbia. — Belgrade, 2006. — P. 402—403.

Nazarevych A. Extenzometric research in Beregovo area in Transcarpathians // Proc. of SSSh. — Lvov, 2006. — Volume XVII. Geophysics. — P. 129—139 (in Ukrainian).

Nazarevych A. V., Nazarevych L. Ye. Deformation precursors of Carpathian earthquakes: separation methods and analysis results // Theoretical and applied aspects of Geoinformatics. — Kiev, 2008. — P. 311—320 (in Ukrainian).

Nazarevych A. V., Nazarevych L. Ye. Scale-energy correlation ratio for Transcarpathian earthquakes sources: some consequences and energetic verification // Theoretical and applied aspects of Geoinformatics. — Kiev, 2009. — P. 279—298 (in Ukrainian).

Nazarevych A. V. Geophysical precursors of some sensible Transcarpathian earthquakes as a reflection of the formation of focal zones // Theoretical and applied aspects of Geoinformatics. — Kiev, 2010. — P. 274—285 (in Ukrainian).

Nazarevych A., Nazarevych L. Optoelectronic measuring channel to quartz extensometer // Geodynamics. — 1999. — № 1(2). — P. 116—120 (in Ukrainian).

Shliakhovyj V. P., Tregubenko V. I., Shliakhovyj V. V., Boborykina O. A., Nasonkin V. A. Some results of digital seismic and tidal observations at Cape Chersonese (Sevastopol) // Geodynamics. — 2007. — № 1(6). — P. 29—36 (in Ukrainian).

Verbytsky T. Z., Gnyp A. R., Malytsky D. V., Nazarevych A. V., Verbytsky Yu. T., Ignatyshyn V. V., Novotna O. M., Narivna M. I., Yarema I. I. Microseismic and extensometric studies in the Carpathians: results and prospects // Geophys. J. — 2003. — **23**, № 3. — P. 99—112 (in Ukrainian).

Verbytsky T. Z., Nazarevych A. V. Extensometric and geoacoustic studies in Transcarpathians // Studies of modern geodynamics of Ukrainian Carpathians / Ed. V. I. Starostenko. — Kiev: Nauk. dumka, 2005. — P. 113—131 (in Ukrainian).

Small-scale convection produces sedimentary sequences

© S. Nielsen[1], K. Petersen[1], O. Clausen[1], R. Stephenson[2], T. Gerya[3], 2010

[1]Aarhus University, Department of Earth Sciences, Denmark
sbn@geo.au.dk
kenni@geo.au.dk
orc@geo.au.dk
[2]Geology and Petroleum Geology, School of Geosciences, College of Physical Sciences, Meston Building, King's College, Aberdeen, Scotland
r.stephenson@abdn.ac.uk
[3]Department of Geosciences, ETH-Zürich, Zürich, Switzerland
taras.gerya@erdw.ethz.ch

It is generally acknowledged that heat transfer in the sub-lithospheric mantle is dominated by convection that maintains an adiabatic temperature gradient close to 0.6 K/km. Transfer of the advected heat to the conductive lithosphere takes place at the base of the lithosphere, which is maintained at a relatively constant temperature in the vicinity of 1300 °C. However, the thermo-mechanical details of this highly dynamic boundary condition at the base of the lithosphere are frequently approximated by a fixed temperature at the assumed long-term equilibrium depth of the base of the lithosphere (the plate model). The present contribution investigates this approximation. We apply a two-dimensional, numerical, thermo-mechanical model of the lithosphere and upper mantle [Petersen, 2010] to asses the effects resulting from a more correct representation of the sub-lithospheric small-scale convection, which is responsible for heat transfer in the sub-lithospheric mantle. Given a particular mantle rheology, our model shows small-scale convection, and converges over time towards a self-consistent, quasi-steady-state with a stable lithosphere, the thickness of which depends on the chosen creep

parameters (within experimental constraints) and hence on the vigour of small scale convection and the heat transfer. At the base of the long term stable lithosphere, a thermal boundary layer is formed in which the heat exchange between the convecting sub-lithospheric mantle and the lithosphere takes place. Small ascending diapers of warmer material slow down and spread out laterally at the base of the lithosphere, pealing off colder material that descends back into the upper mantle. The buoyancy effects of this partly chaotic mass movements cause low-amplitude and relatively rapid vertical movements of the surface of the lithosphere, which show only limited horizontal correlation. The faster vertical movements occur with periods from 2—20 Myr and have amplitudes up to 20—40 m. Long term surface movements have higher amplitudes and are caused by quasi-static organisation of the convective pattern in the sub-lithospheric mantle, which last long enough to influence the thermal state of the lithosphere. Because of the visco-elastic nature of the lithosphere, the more rapid buoyancy changes are filtered by a stiffer lithosphere than long term buoyancy changes. The shorter periods therefore correlate for slightly larger distances.

Extension of the convecting equilibrium model causes fault-controlled continental rifting and subsidence, followed by protracted thermal subsidence, much like the well-known plate model. However, in contrast to the plate model, the elevated asthenosphere is not instantaneously decoupled from the convecting upper mantle below, and cooling is thus not entirely conductive above the former base of the lithosphere. This causes significantly protracted cooling and slower and more linear post-rift subsidence. This model exhibits improved consistency with subsidence data from several rifted margins and intra-continental basins. Because of the small scale convection the long-term subsidence pattern in the presence of small-scale convection is superimposed by the aforementioned low-amplitude vertical movements due to convection dynamics at the base of the lithosphere. These movements are a recurrent and a potential cause for the development of stratigraphic sequences at similar time scale. Such sequences are commonly assumed to be caused by eustatic variations. The results therefore have important implications for inferences on global eustatic variations inferred form sedimentary sequences by e.g. back stripping analyses and assumptions about the thermal subsidence history based on the plate model of lithospheric cooling. Our results are furthermore important for the assessment of hydrocarbon potential of sedimentary basins in terms of stratigraphic correlation and thermal maturation.

References

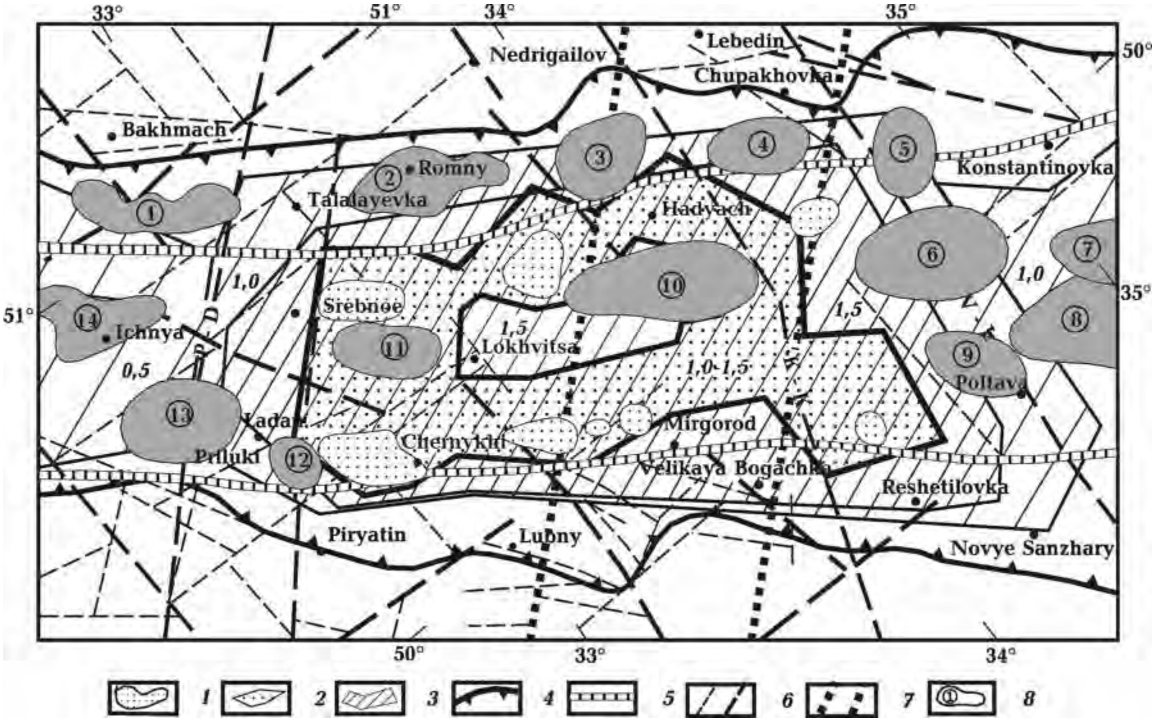
Petersen K. Continental rifting in the presence of small-scale convection — subsidence, stratigraphy and upper mantle strength: PhD-thesis, Aarhus University, 2010.

Nature of sources of the magnetic anomalies in the Central Depression of the Dnieper-Donets Aulacogen

© *M. Orliuk, 2010*

Institute of Geophysics, National Academy of Sciences of Ukraine, Kiev, Ukraine
orlyuk@igph.kiev.ua

The nature of sources of the local and regional magnetic anomalies is an important element of the fundamental and applied studies aimed at elucidating the deep structure, composition and evolution of the Earth's crust. The present paper investigates the nature of the magnetization of different crustal layers of the Central Depression (CD) of the Dnieper-Donets Aulacogen (DDA) with special emphasis on elaboration of regional and local geomagnetic criteria for prognosing the oil and gas potential of the Earth's crust of the study area [Orliuk, 1994; Orliuk, Pashkevich, 1996; Orliuk et al.,1998; 2000]. The CD is situated between the cities Ichnya and Poltava [Chirvinskaya, Sollogub, 1980]. The crystalline basement surface is situated at depths from 2 km in the Aulacogen boundary areas and at 5—12 km in the central part. A regular basement depth increases from N to SE is observed [Ilchenko, 1997;



Sources of the magnetic anomalies in the consolidated crust of the Central Depression: *1* — local magnetic bodies with magnetization of 1.5—2.5 A/m; *2* — contours of the magnetic inhomogeneities of the upper crust, magnetization in A/m; *3* — contours of the magnetic inhomogeneities of the lower crust; *4* — marginal fault of the aulacogen; *5* — boundary of the Central Graben of the DDA (compacted part of the aulacogen) and faults of the rank; *6* — fault of the second and third rank by gravimagnetic data; *7* — projection of the exposure of the litospheric lineament G at the day surface the former separating the lithosphere with different thickness; *8* — contours of local depression.

Kozlenko, 1982]. Against the background of the regional change of the crystalline basement surface depth some local basins are distinguished. The Dimitrovskaya (1), Romenskaya (2), Sinevskaya (3), Kachanovskaya (4) and Sidoriachskaya (5) basins are located in the northern edge of the Aulacogen. The Solokhovskaya (6), Chutovskaya (7), Landoriskaya (8) and the Reshetilovskaya (9) basins are placed in the Aulacogen centre (at the Poltava and Akhtyrka longitude) (Figure). The Lutenskaya (10), Srebnenskaya (11) and Ichnianskaya (14) basins are situated in the central part of the Aulacogen, while the Ladanskaya (12) and Prylukskaya (13) basins are close to the southern boundary. The basins situated near the northern aulocogen (with the 6.0—7.5 km basement depths) are separated from the Aulacogen centre basins (7.0—12.0 km depth) by a peculiar swell with depths of 4.5—6.0 km to the crystalline basement surface. According to seismic data, the basement surface is disturbed by numerous faults of different strike.

The M uplift to 35 km is observed in the central part of the DDA [Sollogub, 1986]. The maximal gradient is recognized in the northern and southern aulocogen. The marginal aulocogen is featured by M depths >40 km, the gradient of the M for the northern boundary being steeper than that for the southern one. The magnetic model of the CD of DDA reflects the three-stage distribution of the magnetic sources in the Earth's crust. The upper stage consists of effusive-pyroclastic rocks of the Frasnian and the Famennian stages and lies in the lowermost sedimentary cover. Its mean weighted magnetization is 1.0—3.0 A/m. An analysis of the MS of a sedimentary cover enabled us to establish some regularities. 1) The increase in the magnetic susceptibility (MS) values of rocks from north to south is expected. Such a MS distribution corresponds to the consolidated crust magnetization, which kind of "contamination" with magnetic minerals of the whole crust in the area of the Lokhvytsya regional magnetic anomaly. 2) The increase of MS of the same type rocks with depth. This regularity is often masked by a certain periodicity in the distribution of the χ values associated with the structure of the sedimentary cover and perhaps with the character of the oxidation-reduction regime. 3) A clear differentiation of the MS values for the rocks of the bore-

holes with oil and gas fields. The magnetic sources in the upper consolidated crust (the upper edges at 3.0—15.0 km and the lower ones at 10.0—18.0 km depths respectively) have the magnetization of 1.0—2.5 A/m. The magnetic bodies of the lower crust are characterized by the magnetization of 1.0—1.5 A/m. The magnetic sources of the consolidated Earth's crust of the Central Depression have been formed at the stage of the Earth's crust extension during the aulacogen formation. This regime was favourable for the deposition of thick sedimentary masses and the accumulation of the organic substance from which the oil and gas accumulations were generated later. The MS values of different lithologic types of rocks obtained by studying the core samples show that the hydrocarbon formation and migration were accompanied by the change in the magnetization of the sediments.

References

Chirvinskaya M. V., Sollogub V. B. Deep structure of the Dnieper-Donetz aulacogen by geophysical data. — Kiev: Nauk. dumka, 1980. — 180 p. (in Russian).

Ilchenko T. V. Some aspects of the evolution of the Dnieper-Donets rift by DSS data // Geophys. J. — 1997. — **19**, № 3. — P. 69—80 (in Russian).

Kozlenko V. G. A system interpretation of geophysical fields. — Kiev: Nauk. dumka, 1982. — 220 p. (in Russian).

Orliuk M. I. Oil and gas potential of the Earth's crust of the Ukraine in connection with its magnetization // Oil and gas industry. — 1994. — **3**. — P. 16—19 (in Russian).

*Orliuk M. I., Pashkevich I. K.*Some aspects of the relation of the oil and gas potential with the magnetization of the Earth's crust of the Ukraine // Geophys. J. — 1996. — **18**, № 1. — P. 45—51 (in Russian).

Orliuk M. I., Kravchenko S. N., Entin V. A. Magnetic characteristic of the rocks of the sedimentary cover of the Central Depression of the Dnieper-Donets aulacogen. Oil and gas of the Ukraine. Materials of the 6th international scientific-practical conference. — Ivano-Frankovsk, 2000. — **1**. — 303 p. (in Russian).

Orliuk M. I., Maximchuk V. E., Vakarchuk G. I., Chepil P. M. Magnetometric studies with the regional and local prognosis of the oil and gas potential of the Earth's crust of the Dnieper-Donets Bazin // Geophys. J. — 1998. — **20**, № 3. — P. 92—102 (in Russian).

Sollogub V. B. Lithoshere of the Ukraine. — Kiev: Nauk. dumka, 1986. — 184 p. (in Russian).

Spacial-temporal structure of the magnetic field in territory of Ukraine

© M. Orliuk, A. Romenets, Yu. Sumaruk, T. Sumaruk, 2010

Institute of Geophysics, National Academy of Sciences of Ukraine, Kiev, Ukraine
orlyuk@igph.kiev.ua
sumar@mail.lviv.ua

The Earth's magnetic field (EMF) is one of the principal geophysical factors concerning the processes in a different planet covers and the planet in whole. Numerous phenomena in magnetosphere, ionosphere, atmosphere and biosphere are due to the magnetic field state as well as to the geomagnetic activity. Space-temporal structure of the Earth's magnetic field *B* is defined by field total from different sources:

$$B = B_n + B_a + B_e + \delta B_v$$

where B_V is the Earth's normal main field that is generated by the processes in the liquid core and at the border with the mantle and that is defining global space and temporal structure of the planet field; B_a is the anomalous magnetic field (one of the lithosphere) that is due generally to the rocks mag-

netization; B_e is the external field that is due to the influence of solar and cosmic radiation as well as to the Sun magnetic fields and circumterrestrial space; δB_v is the variations field.

Geomagnetic anomaly of the total scalar ΔB of the territory of the Ukraine has a very complex character after the data of surface and airborne survey. Anomalies sizes and intensities are depending on the geological structure of the Earth crust and on the magnetic sources.

Continuous registration of the EMF induction as well as of the induction of northern B_x, eastern B_y and vertical B_z components is carrying out by geomagnetic observatories (GO). On the territory of the Ukraine during long period of time there three GO: “Kyiv”, “Lviv” and “Odesa”. After the survey data it is shown that the principal changes have place in the main EMF, especially for the territory of the Ukraine the value is upon the average B_n=1200 nT for the last 50 years. This field were used by us to evaluate the magnetizing effect in the magnetic field secular variations (B_{SV}).

Magnetic field secular variations B_{SV} is defined as a difference between successive average annual values of three orthogonal components and total intensity of the geomagnetic field that is observed uninterruptedly by GO. Calculating those differences it is assumed that the variations with the periods less that one year and that are generated by external sources are excluded automatically. However the variations of the geomagnetic field generated by the ring magnetic current that are reflected in the horizontal (δB_H) and vertical (δB_z) field components are of the same sign. Therefore during magnetically active years δB_H-component is always smaller and δB_z-component is bigger than in the quiet years. The same effect is produced by the solar-day variation δB_s. Under the influence of the external sources the secular variations δB_{SV} obtained by average annual values will have the components connected with solar activity and, correspondingly, with magnetic one.

Changing magnetic field is inducing from the external sources in the main Earth’s layers the currents whose magnetic field is overlapping the dipole field. So the average annual intensity values of the geomagnetic field and its components have besides a dipole field) a contributions from external sources as well as from the magnetizing effect and induction currents in the main layers of the Earth. A very actual goal is to disjoint field by components from every source.

Geomagnetic observatories of the Ukraine “Kyiv”, “Lviv”, “Odesa” are placed in the regions with different geological structure that is reflected by the magnetic field intensity. GO “Kyiv” is located in the region of weakly intensive Kiev regional magnetic anomaly ΔB=85 nT, GO “Lviv” on the periphery of the intensive Lvov anomaly ΔB=250 nT, and GO “Odesa” — in the gradient zone of Odesa anomaly ΔB=−20 nT. Thereby it should wait a different values of observatories cushion courses.

To separate a components connected with external and internal sources it needs to subtract from average annual field value for this observatory its dipole part generated by currents at the core-mantle border. Dipole field value B_{IGRF} as well as the values of all EMF components were calculated from IGRF 1945—2010 Model Coefficients 2010.

It is necessary to divide the obtained difference into two parts: one from external magnetospheric and ionospheric currents, another from magnetization of the magnetic sources and currents in the cushion courses. External sources influence on the average annual values of the geomagnetic field is reflected best of all in the horizontal B_H-component, internal sources influence — in the vertical B_Z and total field component B.

Contribution of the external sources for all the observatories are evaluated by the difference of average annual values for all the days and by the quiet days (B_H–B_{Sq}).

At present for GO “Kyiv”, “Lviv” and “Odesa” using a new criterion to estimate EMF disturbance the anomalies that occurred due to the magnetizing effect in the anomalies B_{SV} are calculated. They originated from the change of the rocks magnetizing field value. It follows from the supposition that in case the inductive component $I_i=\chi H$ is conditioning the total rocks magnetization the proportion $\Delta D=\Delta B/2Bn$ must be constant for any time interval. The calculations shown that this field component during last 50 years make: −0.75 nT for GO “Odesa”, 2.25 nT for GO “Kyiv” and 6.3 nT for GO “Lviv”.

Thus the report evaluated the space-temporal structure of the EMF on the territory of the Ukraine during last 50 years, it proposed the technique to evaluate the contribution of external and internal sources in the secular variation anomaly as well as it obtained first numerous evaluations after the data of the Ukrainian observatories.

Granitoids localization in collisional overthrust structures subject to thermal conditions-numerical modeling

© O. Parphenuk, 2010

Institute of Physics of the Earth, RAS, Moscow, Russia
oparfenuk@mail.ru

High temperature metamorphism and widespread granite magmatism are common peculiarities of many ancient continental collision structures. Deeply eroded areas of the Archean and Proterozoic continental shields formed in the process of tectonic evolution including horizontal shortening and collision expose at the surface middle to the lower crust rocks uplifted by overthrusting from the depths of 20—40 km. This phenomenon seems to be valid also for modern collision zones. The massive layer of granite melt approximately of 10 km thickness is observed at 10—15 km depth by seismic methods in the resent orogens such as the Himalayas and Caucasus [Rosen, Fedorovsky, 2001]. The Palaeozoic Variscan orogen in Europe is characterized by large volumes of felsic granites intruded during HT-LP metamorphism and exposed in deeply eroded parts of the Variscan belt (South Bohemian Batholit) [Gerdes et al., 2000].

Fundamental features of collision zones reflect the effect of the main tectonic event — horizontal shortening in compression setting, collision of two continental plates accompanied by the thickening of the crust and the surface uplift. Extensive development of horizontal and oblique motions of crustal plates and blocks leads to the disturbances in the thermal regime, heat flow, the surface and Moho topography. The main petrologic mark of such collision is granite melt generated at different depth's levels and exposed at the surface as a result of the denudation and uplift.

Thermal-kinematic model of continental collision calculates pressure, velocity and temperature fields and includes horizontal shortening, brittle overthrusting in the upper crust compensated by the lower crust viscous flow and erosion of the thickened crust. Finite-element 2D modeling is used to examine the thermal and kinematic conditions for high-temperature metamorphism and the depth and timing of crustal melting in the case of rheologically layered lithosphere [Parphenuk et al., 1994; Parphenuk, 2005]. The thermal effects during collision process and postorogenic stage are studied.

Calculation of lithospheric temperature field is based on crustal thickening by overthrusting with dip angle of faulting of 15—30° and shortening rate in the range of 0.5—2 cm/y. Total amount of horizontal shortening is 100 km. We assumed that erosion and concurrent sedimentation begins after an additional crustal portion of a substantial thickness is exposed. The equation of energy conservation is solved for the case of Lagrange coordinates with material time derivative [Turcotte, Shubert, 1985]:

$$c_i \rho_i \frac{DT}{Dt} = \lambda_i \nabla^2 T + H_i \, ,$$

where c is specific heat, ρ is density, λ is the thermal conductivity, and H is the heat generation rate. The model consists of three layers: 20 km brittle upper crust (i=1), 20 km ductile lower crust (i=2) and 80 km lithospheric mantle (i=3) with different thermal, kinematic and rheological parameters.

The calculations show the possibility of the partial melting and granite melt generation subjected to the main thermal parameters of the model — the initial temperature distribution (heat flow higher than 60 mW/m^2) and radiogenic heat production. The temperature increase can be fairly significant (up to 250 °C) at depths level of 10—30 km confirming the idea of crustal origin of the continental collisional granites. The partial melting (wet granite solidus) starts in the thickened crust in the vicinity of thrust fault and widens in the direction of thrusting and to the lesser depths. Maximum temperature increase along the fault zone is 300 °C.

2D collision model confirms the observation of a wide range of *PT*-conditions over short distances in metamorphic belts [Chamberlain, Karabinos, 1987]. As a result of upward motion along the fault, the additional loading redistribution in the course of erosion, and the viscous compensation at the level of the lower crust, *PT*-histories will be completely different for the points along the thrust fault. For example, for the convergence and erosion rates of 0.5 and

0.025 cm/y, respectively, maximum erosion level of ~9 km of uplifted crust is reached at 45 Ma after the onset of collision (at postcollisional stage). The material will be transported from a depth of 20 km to a depth of about 5 km while the rocks that were initially located at a depth of 3.5 km will experience a rather complicated *PT*-evolution. At the postcollisional stage (after 20 Ma of shortening) the compressional regime is changed by extension with very low velocities.

Local effect may result from the frictional heating along the slip zone during the overthrusting. The frictional heat production is proportional to the product of the shear stress across the slip plane, the velocity of obduction and coefficient of friction. The additional heating can rise the temperature by 50—150 °C at 10—20 Ma in the vicinity of slip zone in the case of horizontal shortening rate of up to 4 cm/y and thrust sheet thickness up to 20 km [Brewer, 1981]. This local and moderate additional heating (in comparison with crust thickening effect) is much less in the case of slower thickening.

The following set of parameters is critical to initiate crustal melting and granite formation: initial temperature distribution with heat flow density value higher than 60 mW/m^2, relatively high radiogenic heat production, slow crustal thickening (0.5—1 cm/y for 10—20 Ma) and slow exhumation. The results of the modeling confirm other model estimates [England, Thompson, 1984; Gerdes et al., 2000].

The research is supported by the Russian Foundation for the Basic Research (09—05—01032).

References

Brewer J. Thermal effects of thrust faulting // Earth Planet. Sci. Lett. — 1981. — **56**. — P. 233—244.

Chamberlain C. P., Karabinos P. Influence of deformation on pressure — temperature paths of metamorphism // Geology. — 1987. — **15**. — P. 42—44.

England P., Thompson A. B. Pressure-temperature-time paths of regional metamorphism. Part I: Heat transfer during the evolution of regions of thickened continental crust // J. Petrology. — 1984. — **25**. — P. 894—928.

Gerdes A., Worner G., Henk A. Post-collisional granite generation and HT-LP metamorphism by radiogenic heating: the Variskan South Bohemian Batholith // J. Geolog. Soc. — 2000. — **157**. — P. 577—587.

Parphenuk O. I. Thermal regime of collisional overthrust structures // Izvestiya. Phys. Solid Earth. — 2005. — **41**, № 3. — P. 238—240.

Parphenuk O. I., Dechoux V., Mareschal J.-C. Finite-element models of evolution for the Kapuskasing structural zone // Can. J. Earth Sci. — 1994. — **31**. — P. 1227—1234.

Rosen O. M., Fedorovsky V. S. Collisional granitoids and the Earth crust layering. — Moscow: Nauchnyi Mir, 2001. — 188 p. (in Russian).

Turcotte D., Shubert J. Geodynamics. — Moscow: Mir, 1985. — **I**. — 376 p. (in Russian).

Seismic structure of the upper mantle and problems of geodynamics

© N. Pavlenkova, G. Pavlenkova, 2010

Institute of Physics of the Earth, RAS, Moscow, Russia
ninapav@ifz.ru

During the last decades of the XX century severall long-range seismic profiles were carried out by Russian institutions in oceans and in the continents. The longest profiles are the Angola-Brazil geotraverse in the Southern Atlantic with the investigation depth of 100 km [Pavlenkova et al., 1993] and a system of profiles with large chemical and Peaceful Nuclear Explosions (PNE) in the Northern Eurasia with the wave penetrating depth of 700 km [Fuchs, 1997; Pavlenkova G., Pavlenkova N., 2006]. The studies show that the revealed structural peculiarities of the oceanic and continental upper mantle are difficult to describe in a simple lithosphere-asthenosphere system.

The Angola-Brazil geotraverse shows that the oceanic basin lithosphere is of 60—70 km thickness and it is underlined by the low velocity layer (the asthenosphere). However beneath the mid-oceanic ridge instead of the asthenosphere uplift, two local low velocity zones (asthenolites) are revealed at depth of 20 and 50 km. The seismic velocities between these zones are too high (up to 8.5 km/s) for such high heat flow area, they may be explained only by the anisotropy effects.

In the cratonic regions of the Northern Eurasia the thermal lithosphere was proposed from the heat flow data at depth of 200—250 km. The seismic data have not revealed any decrease of the velocities at these depths. On the contrary the low velocity layers are often observed inside the lithosphere at depth of 80—100 km. Two basic boundaries were traced over the study area: N boundary at the low velocity layer bottom, and L boundary at a depth of 180—240 km. All the boundaries are not simple discontinuities, they are thin layering zones with the alternation of high and low velocities in inner layers.

The *N* and *L* boundaries divide the upper mantle in three layers of different plasticity. It follows from regular change of the upper mantle horizontal heterogeneity. The most heterogeneity is observed in the uppermost mantle: the velocities change from the average 8.0—8.1 km/s beneath the high heat flow areas (the West Siberian Plate) to 8.3—8.4 km/s in some blocks of the Siberian Craton and of the Urals. At the depth of 100—120 km the local high velocity blocks disappear and low velocity layers are often observed. These structural features propose that the depth of 100—120 km is a bottom of a brittle part of the lithosphere. Another visible change of the matter plasticity is observed at depths of 200—250 km where the mantle structural pattern is changed too: the velocities decrease beneath the *L* boundary uplifts, which makes the isostatic equilibrium of the upper mantle. At these depths the *Q*-factor is also decreased [Egorkin, Kun, 1978].

The other large explosion experiments and the world seismological studies show that these boundaries may have a global significance. The geophysical and geological data reveals some additional characteristics of these complicate mantle boundaries. They are the higher electrical conductivity zone favoring the existence of fluids at a depth interval of 100—150 km. The most part of the xenoliths comes from the depths around 100, 150 and 200 km and the xenoliths from the Siberian Craton kimberlites taken from the depths of these seismic boundaries have indications of film melting [Solov'eva et al., 1989]. In different tectonic regions, inside the continents and in the continental margins, the most earthquakes are located at depths of around 100 and 200 km.

The correlation the xcenolits origin depth and the earthquake clusters with the regional mantle boundaries could no be an accidental correlation and it shows that the depths of the regional boundaries are critical depths where some regular transformations of the matter are happened.

One possible explanation of these upper mantle properties involves the deep fluids. The concentration of fluids at certain *PT*-levels changes mechanical properties of the matter, they initiate partial melting and metasomatism of the mantle material which results in the velocity changes. The practically infinite energy sources for earth-quakes are the explosive chain reaction of the decomposition, triggered by decompression within the fault zone [Gilat, Vol, 2005]. The matter flow along these weak zones results in origin of the seismic boundaries with the velocity anisotropy.

The determined upper mantle weak zones can have a great effect on all dynamic processes. Together with deep faults they form a channel system for the mantle fluids and matter transportation. The weak zones play an important role in the horizontal displacement of the lithosphere blocks and in formation of tectonic structures. During tectonic activation the weak layers can be transformed in the asthenolites by partial melting and provoke the plume tectonics.

References

Egorkin A. V., Kun V. V. P-wave attenuation in the upper mantle of the Earth // Izvestiya. Phys. Solid Earth. — 1978. — **4**. — P. 25—36.

Fuchs K. Upper mantle heterogeneities from active and passive seismology, NATO ASI Series (1.Disarmament Technologies — Vol. 17) // Contribution ¹336, International Lithosphere Program. — Dordrecht: Kluwer Acad. Publ., 1997. — 366 p.

Gilat A., Vol A. Primordial hydrogen-helium degassing, an overlooked major energy source for internal terrestrial processes // HAIT J. Science and Eng. — 2005. — **2**, № 1—2. — P. 125—167.

Pavlenkova G. A., Pavlenkova N. I. Upper Mantle Structure of the Northern Eurasia from Peaceful Nuclear Explosion Data // Tectonophysics. — 2006. — **416**. — P. 33—52.

Pavlenkova N. I., Pogrebitsky Yu. E., Romanjuk T. V. Seismic-density model of the crust and upper mantle of the South Athlantic along Angola-Brasil geotraverse // Phys. Sol. Earth. — 1993. — № 10. — P. 27—38.

Solov'eva L. V., Vladimirov B. M., Kiselev A. I., Zavijalov L. L. Two stages of mantle metasamatites of deep xenoliths from Yakutia kimberlites and their relation to lithosphere processes // Precambrian metasamotites and their ore deposits. — Moscow: Nauka, 1989. — P. 3—17 (in Russian).

Scaling and Performance Analysis of Underworld: Towards the One Billion Particle Target

© *R. Petersen, D. Stegman, 2010*

Institute of Geophysics and Planetary Physics, Scripps Institution of Oceanography,
University of California San Diego, La Jolla, USA
rpetersen@ucsd.edu
dstegman@ucsd.edu

We investigate the scaling performance of Underworld, a geodynamic modeling framework, on high performance computing resources. These results inform the configuration and allocation of resources committed to study the complex geodynamic processes in and around subduction zones. We use a 3D thermal convection model that includes a temperature and stress dependent rheology as a proxy for the computational difficulty of the eventual subduction problems. This proxy model is designed with significant variation in viscosity, in conjunction with the non-linear temperature and stress dependent rheology this results in a computational problem that is significantly more challenging than the similar isoviscous convection problem.

”Using an allocation of 30000 service units on Texas Advanced Computing Center (TACC) cluster, Ranger, we ran a suite of models that exercised Underwold by solving problems with element subdomain sizes of 16×16×8 and 16×16×16 per core. For each of subdomain size we ran the models at several global resolutions, from what we call "tiny" models (32×32×32) to what we refer to as "huge" (192×192×192). The global resolutions selected require CPU core allocations from 100’s to 1000’s.

Underworld supports both a basic FEM solution method and Particle In a Cell (PIC). We solve the thermal convection problem using both methods to verify the equivalence of solutions. At the highest resolutions using the PIC method the number of particles approaches 1.5 million. We continue to explore this model with an eye towards systems populated by up to 1 billion particles.

Timing results are measured as the walltime per model timestep. A common steady-state model is first calculated over several thousand timesteps. This steady-state model is then restarted at the appropriate resolution whence the performance data is gathered.

Stress modeling in the Central Asia crust, importance of gravity stresses

© *V. Pogorelov, A. Baranov, R. Alekseev, 2010*

Laboratory of Theoretical Geodynamics, Institute of Physics of the Earth, RAS, Moscow, Russia
vpogorelov@list.ru,
baranov@ifz.ru

The Southern and Central Asia is a tectonically complex region which characterized by the great collision between the Asian and Indian plates. Its tectonic evolution is strongly related to the active

subduction process along the Pacific border. Stress investigation in the continental crust is a very important problem not only for science but also for the practical purposes. There are four main factors which produce tectonic stresses: gravity anomalies of the crust, density inhomogeneities, deformation from area with intraplate collision, residual elastic deformations and underthrust stresses conditions from convective mantle. We present the stress model of the crust and lithosphere for the Central and Southern Asia on the basis of the finite element modeling. For the crust we take the elasto-plastic rheology with Drucker-Prager criterion. In the lithosphere the elasto-plastic model with von Mises criterion is assumed. We investigated stresses which are produced by the crustal density inhomogeneities and surface relief. The calculations are done using the U-WAY finite element code [Vlasov et al., 2004] developed at the Institute of Applied Mechanics Russian Academy of Sciences (similar to the Nastran program). Density inhomogeneities are based on the AsCRUST-08 crustal model [Baranov, 2010], which has resolution of 1×1 degree. AsCRUST-08 was built using the data of deep seismic reflection, refraction and receiver functions studies from published papers. The complex 3D crustal model consists of three layers: upper, middle, and lower crust. Besides depth of the boundaries, we provided average *P*-wave velocities in the upper, middle and lower parts of the crystalline crust and sediments. The seismic *P*-velocity data was also recalculated to the densities and the elastic moduli of the crustal layers using the rheological properties and geological constraints. Strength parameters of rocks strongly depend on temperature, tectonic and fluid pressure. Fluid pressure can reduce resistance forces in faulting rock, tectonic pressure increases these forces.

Results. Isotropic pressure in crustal layer is approximately equal to 0.6—0.8 from lithostatic values, for example 900 MPA on the 40 km depth (Poisson ration changes in the crustal layer from 0.25 to 0.32 in accordance to its mineral properties). In the mantle isotropic pressure practically equals to lithostatic values which corresponds to Poisson ratio 0.5. Lateral pressure variations in the crustal layer are limited by 10—15 % (negative pressure anomaly under Tibet orogen reaches 15 %).

Shear stresses gradually increase with depth and reach approximately 650 MPA in the lower crust under Tibet orogen and 300 MPA on the 30km depth. The models in this work are simplified in several aspects. However our purpose was to compare gravity stresses in the normal continental crust and under Tibet orogen with anomaly thick crustal layer.

References

Baranov A. A. A New Model of the Earth's Crust in Central and South Asia // Izvestiya. Physics of the Solid Earth. 2010. — **46**, № 1. — P. 34—46.

Vlasov A. N., Yanovsky Yu. G., Mnushkin M. G., Popov A. A. Solving geomechanical problems with UWay FEM package // Computational Methods in Engineering and Science / Ed. V. P. Iu. — Potsdam: Taylor & Francis, 2004. — P. 453—461.

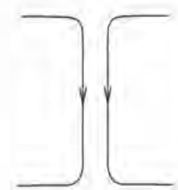
Main tectonic regularity in the structure of continental margins

© *O. Prykhodchenko, I. Karpenko, 2010*

Oil and Gas Exploration Department, Ukrainian State Geological Prospecting Institute,
Kiev, Ukraine
alenaprihodchenko@ukr.net
karpenko@ukrdgri.gov.ua

The lithosphere plate tectonics theory describes the process of oceanic crust opening and closure in geological history of the Earth using the Wilson cycle [Keary, Vine,1991]. Upon the end of the cycle the oceanic crust being formed at its early stages is almost completely destructed in the process of subduction. As for the continental margin it is modified during the cycle with formation of volcanic and non-volcanic islands arcs, back- and fore-arc sedimentary basins, and orogens. During the next

Comparison of models evolution of the ocean and continental margins during the complete Wilson cycle

Model of the ocean evolution (Khain, 2004)		Model of the continental margin evolution			
Geosyncline	Plate tectonic «Wilson cycle»	Stages of Wilson cycle	Substage, time (million years)	The course of crust-mantelle substances under the continental margin	Contents of stages
Inland rise (A continental rift)	Continent into pieces; new ocean basin opening	Divergecy	0 Start of forming a new ocean basin		Rifting when continent breaks up
Geosyncline stage	Evolution of new ocean depression, forming deep (15-20km) basin, which is filled in sediments (continental slope and new ocean floor)		200 Ocean widens		Ocean widens. Ocean crust is forming. New quasi-oceanic subocean crust is forming on the place of future continental margin
		Convergency	400 Convergence begins, an ocean plate subducts, creating a volcanic chain at active margin, I orogenic stage		Closing of the ocean basin. Creating a volcanic chain at active margin and subcontinental crust
	First stage of closure the ocean basin, creating of volcanic chain at active margin		600 Thermal subsidence stage		Cooling and subsidence of the mantle diapir when the ocean is closed. Formation of thermal sedimentary basins.
Partial inversion	The ocean basin closes in some part of the ocean depression, two continents collide and began the stage of overthrusting begins	Collision	800 Partial inversion , II orogenic stage		Uplift of the thermal sedimentary basins as a result of dissolution in mantle of cooler lower crust, which is plunging into the mantle
Closing of the ocean basin			1000 Closing of the ocean basin and overlthrusting, III orogenic stage		Overlthrusting of the inversed part of the crust on the passive continental margins and formation of new continental crust
The continent erodes and became a platform		The continent erodes and became a platform	1200		The continent erodes and became a platform

stage of cycle the previously formed continental margin is subjected to deep transformation again leaving in the structure of newborn margin only some relics of the previous ocean crust known as ophiolites. However, as the study proves, complete destruction of the previous continental margin is not reached. Always or quite often it is preserved a significant part of newborn continental crust accreting laterally an existing continental plate and modified during further transformations passing though consecutive stages of states that could be called a vertical line of the tectonostages for particular continental margin. Evidence for that conclusion is an age rejuvenation of the continental crystalline crust while moving from the central parts (shield) towards their outskirts (continental margin). It is proposed the geological timescale of tectonostages derived from the Wilson cycle and established their time boundaries for the last 2500 million years. Along with the developed model for continental margins evolution it allows application of the concept of horizontal sequence of tectonostages transition into vertical and vice versa to study structure of continental margins [Karpenko, Prykhodchenko, 2009]. It is supposed that for the Wilson cycle of 1200 million years every continental margin is subjected to the tectonic process as follows. During the first stage of a divergent epoch (0—200 Ma) a new oceanic basin is forming due to a continental rift. Present-day example of such a rift one can consider the Red Sea Rift and latitude-oriented rift system between North and South America stretched into the Pacific and Atlantic Oceans. Predecessor of the future Red Sea ocean was Tethys and Prototethys paleo-oceans originated during the stages of 590,75—385,75 Ma and 992,5—793,0 Ma ago. The Tethys is corresponding to present-day Alpine-Himalayan orogenic zone and related sedimentary basins, and the Prototethys ones to the Donbass Foldbelt and its eastern prolongation into Karpinskiy Ridge. Rejuvenation of continental margins age towards the periphery of the continents set the problem of studying evolution of those margins applying concept of vertical and horizontal sequences of tectonostages. For this purpose the model of evolution (tectonic stratification) of continental margins is developed. It includes six stages of tectonic evolution: origination of a new ocean and its opening (divergent epoch of the Wilson cycle), stage of the oceanic basin shortening and thermal subsidence (convergent stage), the stage of partial inversion, and the next stage of the complete inversion along with the compression thrusting (collision stage) (Table). Corresponding to the stages is the types of crust being formed (ocean, quasi-ocean, quasi-continental, continental). The stages are divided into geosynclinal and orogenic sub-stages (the Bertran cycle). It is demonstrated that tectonostages and orogenies are matching (Alpine, Hercynian, Caledonian, Baikal and others) for the last 1500 million years. Actually, the features and direction of changes in vertical and horizontal sequences of continental margin tectonostages is a basic tectonic regularity to be studied because it determines existing types of sedimentary petroleum-prone basins, sedimentary complexes and separate prospects considered as hydrocarbon traps.

References

Keary P., Vine F. J. Global Tectonics. — Blackwell Scientific Publ., 1991. — 302 p.

Karpenko I. V.. Prykhodchenko O. E. Tectonostages of the Wilson cycle // Scientific Proc. Ukr. State Geological Prospecting Institute. — 2009. — № 3—4. — P. 96—107 (in Ukrainian).

Model study of influence of internal stresses on deformation and seismic processes in convergent plate boundary zones by the example of Lake Baikal ice cover

© *S. Psakhie[1], E. Shilko[1], S. Astafurov[1], A. Dimaki[1], V. Ruzhich[2], 2010*

[1]Institute of Strength Physics and Materials Sciences, SB RAS, Tomsk, Russia
shilko@ispms.tsc.ru
[2]Institute of the Earth's Crust, SB RAS, Irkutsk, Russia
ruzhich@crust.irk.ru

An important class of problems in mechanics of heterogeneous media (including geological ones) is studying regularities of deformation and destruction of specific quasi-two-dimensional (plate) systems,

whose structural elements are mainly located in one plane. A classical example of a natural plate medium is the lithosphere. Macroscopic geometry of the lithosphere and mechanic characteristics of substrate stimulate its fragmentation (breaking into ensemble of interacting plates) and appearance of specific deformation mechanisms, connected with removal of mature material from the plane of deformation (subduction) and formation of a new one (spreading). Studying zones of subduction and their influencing the stressed medium condition is one of the most urgent geotectonic and geodynamic problems, connected with understanding regularities of deformation processes in the lithosphere. Due to huge spatial and temporal scale of deformation processes in such zones, one of the perspective ways to analyze their peculiarities is physical modeling with the help of simplified model systems. As the results of previous researches have shown [Hamaguchi, Goto,1978; Psakhie et al., 2009], a perspective model medium for studying tectonic processes (in particular, the conditions of subduction zone formation and development) is a plate ice cover of large water reservoirs. The present paper is devoted to evaluation of typical level of stress in plate medium and the role of underride/subduction as relaxation mechanism by the example of Lake Baikal ice cover.

The conducted full-scale research have shown that regularities of localization of interplate deformations in the Lake Baikal ice cover are determined by distribution, value and sign of internal plate stresses. In particular, convergent interplate movements, leading to forming and developing underride zones (analogous to subduction zones in the lithosphere), are the results of increase in positive (stretching) stresses. Decrease in value and change of stress sign to negative result in partial consolidation of blocks consisting in "healing" some of previously active interfaces and localization of small, mainly divergent interblock movements on the rest of the interfaces. These regularities are consistent with modern conception on the connection between sign and value of regional tectonic stresses near interplate boundaries in the lithosphere and type of relative displacement of tectonic plates (convergent or divergent). It is important to mention that stress distribution inside the consolidated (i.e. not separated by through-thickness cracks) fragments of the ice cover is rather homogeneous and correlates mainly with the direction of movement of the fragments themselves. At the same time, stress state of neighbouring fragments can differ greatly. In accordance with traditional definition [Zoback,1992], stresses determining deformation processes on the ice cover interplate boundaries can be regarded as "tectonic". Thus, measurement results prove the existence of "plate tectonics" in the ice cover of Lake Baikal and support its usage for the physical modeling of tectonic processes in the lithosphere being grounded.

On the basis of measurements of internal plate deformations the threshold stresses of activation of convergent processes in the underride zones as high-rank deformation-induced structures are estimated. The value of these stresses is connected with inner cohesion on the most solid parts of interplate boundaries and, as a rule, varies within the range 2—10 % of the compression strength of plate material. In case of "healed" boundaries (after rather long "calm" periods of deformation activity) the activation threshold value can rise anomalously high (20—30 % of plate material strength). The recent research results show that high internal stresses can provoke changes of the character of deformation processes in a block-structured medium, including the appearance of "precursors" of dynamic convergent events and effects of fragmentation of consolidated blocks. It gives the ground to the supposition that anomalies of deformation regime of the Earth's crust, registered at various times before large earthquakes, seem to be connected with reaching a certain threshold level of stress in the area of registration. Basing on the data obtained on the ice cover we can suppose that a characteristic value of such strains can reach 20—30 % of rock strength.

It is important to mention that activation of interplate boundaries in the ice cover as a multiscale block-structured medium is preceded by the involvement of low-rank deformation mechanisms. As the seismic monitoring data show, the intensity of their involvement rises abruptly when the activation moment approaches. Alongside with it, immediately before the activation the number of relatively high-energetic seismic events increases, which reflects growing characteristic scale of the involved deformation mechanisms with the increase in internal stresses.

All said above indicates that both ice cover and the lithosphere are multiscale media with a hierarchical system of relaxation mechanisms. Each mechanism corresponds to a typical activation threshold (stress). Relaxation (and deformation) mechanisms with maximum involvement threshold are connected with the formation and functioning of interblock boundaries. Thereby, the ice cover of Lake Baikal gives a unique possibility to study the influence of a strained state on the regularities of deformation accommodation processes in block-structured (plate) media of different nature, particularly, in the lithosphere.

References

Hamaguchi H., Goto K. A study on ice faulting and icequake activity in the Lake Suwa, (2) Temporal variation of m-value // The Sci. Rep. of the Tohoku Univer. — 1978. — Ser. 5. 25. — № 1. — P. 25—38.

Psakhie S. G., Dobretsov N. L., Shilko E. V. Model study of the formation of deformation-induced structures of subduction type in block-structured media. Ice cover of Lake Baikal as a model medium // Tectonophysics. — 2009. — **465**. — P. 204—211.

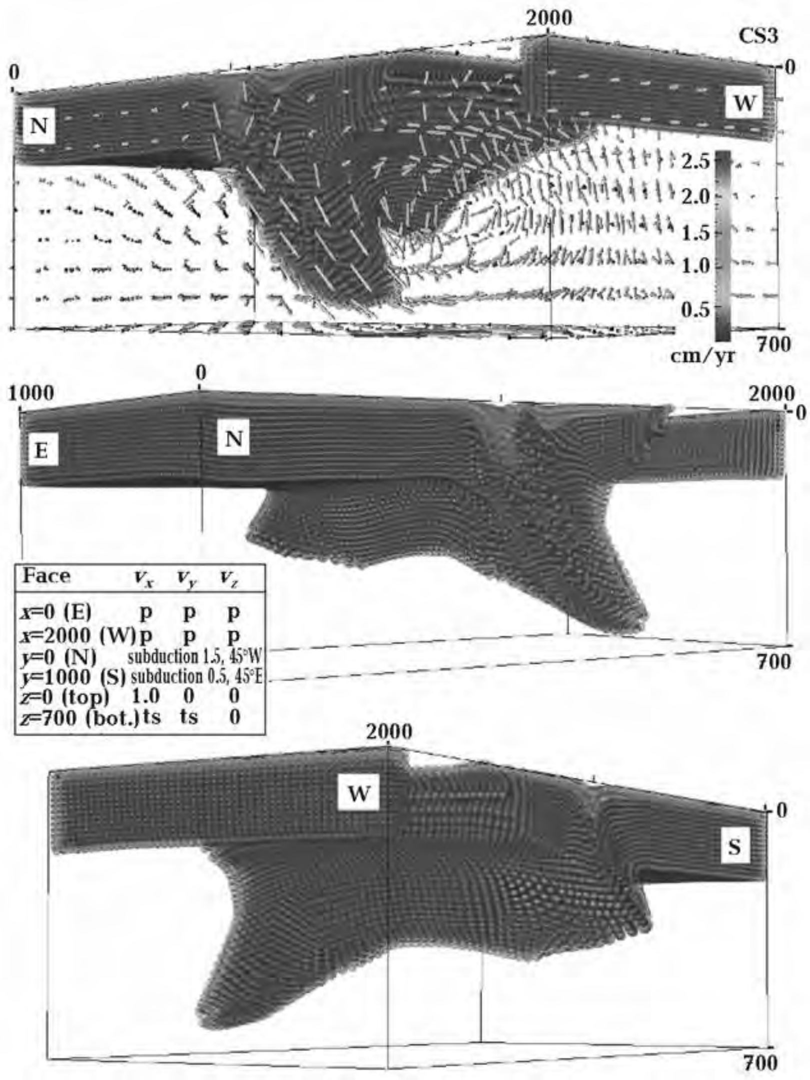
Zoback M. L. First- and second-order patterns of stress in the lithosphere: The world stress map project // Geophys. J. Res. — 1992. — **97**(B8). — P. 11703—11728.

Three-dimensional mantle lithosphere deformation at collisional plate boundaries: A subduction scissor across the South Island of New Zealand

© R. Pysklywec[1], S. Ellis[2], A. Gorman[3], 2010

[1]Department of Geology, University of Toronto, Toronto, Ontario Canada
russ@geology.utoronto.ca
[2]Institute of Geological and Nuclear Sciences, Lower Hutt, New Zealand
S.Ellis@gns.cri.nz
[3]Department of Geology, University of Otago, Dunedin, New Zealand
andrew.gorman@otago.ac.nz

The continental plate collision across the South Island of New Zealand is highly oblique (dextral) and is bounded by oppositely verging ocean plate subduction zones — with north-west dipping Hikurangi subduction to the north and east-dipping Fiordland-Puysegur subduction to the south [e. g.; Okaya et al., 2007; and references therein]. As such, the region can be considered as a type of "subduction scissor". Within this tectonic context, we use three dimensional computational geodynamic models to consider how convergent mantle lithosphere can be modified by scissor and strike-slip effects. Bounding subduction at both ends of the continental collision causes flow of the descending mantle lithosphere in the direction along-strike of the model plate boundary, with thinning in the centre and thickening towards the subduction zones that bifurcates the continental mantle lithosphere root. With dipping bounding subduction, the mantle lithosphere root takes on a more complex morphology that folds over from one subduction polarity to the other, but remains as a continuous feature as it folds under the collision zone (Figure). In the absence of bounding subduction, the plate convergence causes a linear (along-strike) mantle lithosphere root to develop. A rapid strike-slip motion between the converging plates transfers material in the plate boundary-parallel direction and tends to blur out features that develop in this direction — such as descending viscous instabilities. The along-strike variations in the morphology of the mantle lithosphere root that develop in the models — viz., thickening of the root towards the subduction edges, thinning in the center — are consistent with recent, albeit poorly constrained, geophysical interpretations of the largescale lithospheric structure of the South Island [Kohler, Eberhart-Phillips, 2002; Scherwath et al., 2006]. We speculate that this reflects the nature of the evolution of the South Island collision as a limited continental segment of the plate boundary that it is dominated and guided by adjacent well-developed/developing ocean plate subduction. The modelling provides insights into how varying "three-dimensional effects" could influence the evolution of the continental mantle lithosphere at the South Island and may have implications for understanding other collisional zones where a continental plate ends or transitions into ocean plate subduction.



Model CS3 at 29 Myr. Three views of the inverted anvil-type morphology of the mantle lithosphere (marked distances in km). Inset table indicates velocity boundary conditions on the six surfaces of the box. The locations of the faces are indicated by intercepts of the planes as well as their corresponding compass direction in the convention adopted here. The velocity magnitudes are in cm/yr and indicate the total magnitude for the spatially variable boundary conditions on the individual faces; 'p' refers to a periodic boundary condition, 'fs' refers to free slip.

References

Kohler M., Eberhart-Phillips D. Three-dimensional lithospheric structure below the New Zealand Southern Alps // Geophys. J. Res. — 2002. — **107**.

Okaya D., Stern T., Davey F., Henrys S., Cox S. Continent-continent collision at the Pacic/Indo-Australian plate boundary: back- ground, motivation, and principal results / Eds. D. A. Okaya, T. A. Stern, F. J. Davey. A continental plate boundary: tectonics at South Island, New Zealand // Amer. Geophys. Union. — 2007. — **175**. — P. 1—18.

Scherwath M., Stern T., Davey F., Davies R. Three-dimensional lithospheric deformation and gravity anomalies associated with oblique continental collision in South Island, New Zealand // Geophys. J. Int. — 2006. — **167**.

Rocks with elasticity in mantle convection

© Yu. Rebetsky, 2010

Institute of Physics of the Earth, RAS, Moscow, Russia
reb@ifz.ru

All modern mantle convection equations are based on pure viscous media model, which has compressibility only in frames of thermoelastic problem solution (impact of temperature on volume change and absence of such impact from pressure — positive and negative elastic dilatation and from deviator stresses — inelastic dilatation) [Trubitsyn, 2008]. Analyzing the results obtained in these studies one may ask: how much we can trust these results? This question follows from our knowledge that mantle is a rigid crystalline rock and not a fluid; and also from understanding the difference in mechanisms of viscous fluid flow and ductile behavior of solid body.

It is well-known that Poisson coefficient of crystalline rocks varies in wide range from 0.15 to 0.40, most often observed values are 0.25, which essentially differs from values for fluids — 0.5. Seismic data in the crust and mantle are compatible with coefficient close to 0.25, except some local anomalous areas, which are mostly concentrated in the crust. This let us assume that mantle rocks have elastic properties and their ability to flow is conditioned by rather low yield strength magnitude; (elasticity) in the lithosphere and high rates of diffusion and re-crystallization processes in the low mantle. Taking into account the knowledge of real rock state it is interesting to understand what we are missing, when in mantle convection problem we replace ductile flow of solid rocks having elasticity by viscous fluid flow without elasticity.

In the recent publications [Rebetsky, 2008] it has been shown that in the problem of gravitational forces acting on rock massive, triaxial pressure with depth goes closer to lithostatic (weight of the rock column) due to inelastic deformation taking place in confined conditions (neighbor rocks, which are in the same conditions, limits horizontal spreading. Such deformation under gravitational forces leads to the increment of confining stresses in horizontal direction and to the vertical compaction in the same time [Jager, 1962]. This mechanism could be called as *gravitational elasto-plastic compaction*. If the rocks react on gravitational loading only in elastic manner, then for Poisson coefficient 0.25 horizontal pressure would be only 1/3 of vertical one [Dinnik, 1926]. Inelastic strains developing under lateral confining stresses brings *additional horizontal confining stresses* and elastic compaction of rocks [Rebetsky, 2008]. If the rocks as fluids would have Poisson coefficient 0.5 (ideal rubber) then gravitational stresses will not cause deviatory stresses and normal stresses in any direction will be equal to rock column weight.

Inelastic deformation at different tectonoshpere levels is conditioned by different mechanisms: in the crust — due to fracture flow (upper and middle crust) or quasi plastic midgrain flow (lower crust) when Coulomb stresses reach threshold value; in under crust lithosphere — due to the ductility flow [Nikolaevsky, 1996] when deviatory stresses reach yield strength; in lower mantle — due to the diffusion and re-crystallization mechanisms of viscous flow. If the rock specimen which underwent such elasto-plastic compaction under gravitational forces will be drilled out from rock massive (maintaining horizontal confining condition) then only additional horizontal confining stresses occurred at gravitational compaction stage will be left. In the rock specimen not healed at post-deformation stage by later mineralization these stresses will disappear practically immediately after canceling lateral confinement. For the rock specimen having such new formation, sudden destruction may occur after extracting the specimen from drilling holder. In this case, above mentioned additional confining pressure should be treated as residual stress forming in the specimen specific type of mutually compensating stress state.

What happened when we drill out the rock specimen from certain depth? In such case, first of all the weight of upper layers are canceled, relaxation occurs, but stress relaxation is not complete. In such relaxation conditions, when lateral confinement still acts, vertical stresses completely dropped; and horizontal ones — according to Poisson coefficient ν — *elastic relaxation law*. For rocks having ν=0.25 only 1/3 of overlaying column weight (lithostatic pressure) is

relaxed. Elastic relaxation law together with lateral confinement and erosion processes at surface conditions occurrence in rocks residual stresses when vertical uplift, what was marked at first time in [Goodman, 1989]. It has to be noted, if rocks would have Poisson elastic coefficient 0.5 (rubber), then elastic relaxation of gravitational stress state leads to equal decrement of both vertical and horizontal stresses, what actually happened in all modern computation of mantle convection.

Evaluations of the gravitational stress state energy are known $2.5 \cdot 10^{32}$ J. It is by three orders larger than kinetic energy of the planet and by four orders larger than energy of thermal convection. Our evaluations show that residual horizontal stresses of gravitational stress state (2/3 of lithostatic pressure and $\nu=0.25$) compose circa half of total energy of elastic strains. This energy will relax through vertical convection movements causing additional (relative to ideal viscous fluid) plastic deformations, which *finally will be transitioned into heating*. Comparing the residual stress energy of unit volume released when uplifting from the core up to upper mantle boundary with the work spent on vertical transferring of this volume in thermal convection we will get $8 \cdot 10^9$ J и $3 \cdot 10^9$ J respectively. *Thus, energy confined in residual stress state is more than the energy spent on vertical uplift of unit volume*.

Therefore, our analysis has demonstrated that in all modern computations of thermal convection in the mantle in solutions is missing one of the most important components in energy balance — residual stress state conditioned by gravitational elastic-plastic compaction. In the presentation in the frames of traditional viscous model the problem will be posed and the solving equations followed from it, which take into account existence of the residual stresses in mantle and its impact on mantle convection will be given.

The research is supported by RFBR grant 09—05—01213a.

References

Dinnik A. N. About rock pressure and calculation column of circle mine // Ingeniring worker. — 1926. — № 3. — P. 1—12 (in Russian).

Goodman R. E. Introduction to rock mechanics. (2nd Edition). — New York: John Wileyand Sons, 1989. — 583 p.

Jager J. C. Elasticity Fracture and Flow. — London: Methuen and Co. LTD, 1962. — 208 p.

Nikolaevsky V. N. Geomechanics and fluid dynamics. — Moscow: Nedra, 1996. — 446 p. (in Russian).

Rebetsky Yu. L. Mechanism of tectonic stress generation in the zones of high vertical movements // Fiz. Mezomekh. — 2008. — **11**, № 1. — P. 66.

Rebetskii Yu. L. Possible mechanism of horizontal compression stress generation in the Earth's crust // Doklady Earth Sciences. — 2008. — **423A**, № 9. — P. 1448—1451.

Trubitsyn V. P. Equations of termal convection for uncompressibility viscous mantle with phase transition // Phys. Earth. — 2008. — № 12. — P. 83—91 (in Russian).

Seasonal variation of induction vectors

© I. Rokityansky[1], T. Klymkovych[2], V. Babak[1], T. Savchenko[1], 2010

[1]Institute of Geophysics, National Academy of Sciences of Ukraine, Kiev, Ukraine
rokityansky@gmail.com
[2]Carpathian Branch of Institute of Geophysics, National Academy of Sciences of Ukraine, Lvov, Ukraine
tamara@cb-igph.lviv.ua

In the geoelectromagnetic studies of electrical conductivity of the Earth's interior, the response function (RF) is supposed to be any function (impedance, apparent resistivity, induction arrow, horizontal MV tensor…) derived from the Earth's electromagnetic (EM) data which provides us with possibility to determine the conductivity structure in the Earth. Ideally RF depends only on the Earth's conductivity and does not depend on the properties of external EM field used.

Widely used RF for EM monitoring is induction vector **C**:

$$\mathbf{C} = Ae_x + Be_y \,, \qquad (1)$$

where e_x and e_y are unit vectors, x — is pointed to

North, y — to East, z — downward, A and B form a 1×2 matrix which transforms the horizontal magnetic field (B_x, B_y) observed at a station into the vertical component B_z

$$B_z = AB_x + BB_y \, . \qquad (2)$$

In (1), (2) all quantities are complex and depend on period T of variations, thus supposing that we deal with observed magnetic field $\mathbf{B}(T)$ after harmonic (Fourier) analysis of total field.

The real $\mathbf{C}_u = A_u e_x + B_u e_y$

and imaginary $\mathbf{C}_v = A_v e_x + B_v e_y$

parts of the vector **C** are referred to as the real and imaginary Wiese (or Parkinson) induction vectors or arrows.

Real induction arrows possess an important property: in the notation of Wiese, they are directed away from good conductor, in Parkinson's notation — to good conductor.

Really observed $\mathbf{B}(T)$ is composed of

$$\mathbf{B}(T) = (\mathbf{B}_{en} + \mathbf{B}_{in} + \mathbf{B}_{ia}) + \mathbf{B}_{noise} + \mathbf{B}_{LE} \, , \qquad (3)$$

where: $\mathbf{B}_{en}$ — normal external primary magnetic field (of period T) of the currents in ionosphere and magnetosphere; $\mathbf{B}_{in}$ — normal internal secondary magnetic field of the currents induced in hypothetical horizontally layered (1*D* conductivity) Earth; $\mathbf{B}_{ia}$ — anomalous secondary field arising on local/regional conductivity anomaly as result of re-distribution of the currents responsible for $\mathbf{B}_{in}$.

For commonly used in magnetotellurics idealized model of Tikhonov — Cagniard (plane wave vertically incident on horizontally layered Earth) the normal field in (3) has only horizontal components *x* and *y*, B_z in (2) is purely anomalous. If two last terms in (3) can be neglected, the [A, B] matrix and induction vector carry pure information on conductivity anomaly. And if induction vector varies with time one can suppose that conductivity structure changes.

In reality, at least 3 more factors can vary RF, so RF variation with time can be caused by 1) variation of the properties of external source field i.e. by its deflection from T—C model, 2) noise, 3) superposition of transient internal EM fields — lithospheric emission (LE). The latter cause together with the change of lithosphere electrical conductivity manifest geodynamic processes including earthquake (EQ) and volcano activity preparation and are of great interest. Variability of TF was reported many times during last 50 years including two reviews of early studies by Niblett and Honkura, 1980 and Kharin, 1982. After transition to geomagnetic field digital registration, reliability of TF study was essentially improved.

From common considerations we can suppose that EQ and volcano eruption precursors should have an aperiodic temporal regime appearing once or several times before EQ. Then, regular periodic TF variations can be treated as a background for the precursors study.

Annual (or seasonal) variation of **C** components were presented in works [Fujita, 1990; Moroz Yu., Moroz T., 2006; Moroz et al., 2006; Korepanov, Tregubenko, 2009]. Consider their results.

In Fig. 1 the results of induction vectors study in Japan is presented. Annual variation appears most clearly at the northern component in Kakioka (KAK) observatory where real vector attains maximum at the period 50 m and imaginary one change its sign [Shiraki, Yanagihara, 1975]. In Fig. 1, *d* (averaged for 13 years monthly mean data), annual variation is clearly seen especially at long periods where it exceeds error given by vertical bars. A_v changes its level according frequency response of C_v. Fig. 1, *c* shows long term trend which can be related with EQ occurrence, in particular, with Kanto EQM7.8 in 1923.

Fig. 2 presents the results of three years monitoring in Kamchatka. C_u exhibits highly interesting behavior: at the shortest period 250 s, annual variation is maximal 0.1/half year with minimum in summer season, at longest period 6000 s the variation equals 0.05/half year with maximum in summer season. At the periods 1000 and 3000 s the variation is small. Quite different behavior exhibits C_v (Fig. 2, *c*). Analysis of frequency characteristic (Fig. 2, *b*) together with geoelectric structure of the region give ground for attempt to explain RF behavior.

Fig. 3 displays annual variation only for Patrony observatory where it attains almost 0.1/half year at long and short periods and reduces in 3 times at periods around 1000 s where C_u attains maximum (Fig. 3, *b*). Sign of variation does not change. In Enhaluk observatory annual RF variation does not exceed 0.02 and does not seen in the noise.

V. I. Tregubenko during more than 10 years drives MV monitoring in Ukraine. He applayed best processing program and developed reliable monitoring processing procedure for EQ prediction and also received annual RF variations. According his opinion these variations can be seen most clearly in phase (Fig. 4).

Conclusion.

1. Annual (or seasonal) variation of induction vector components really exists and in some cases has rather pronounced magnitude.

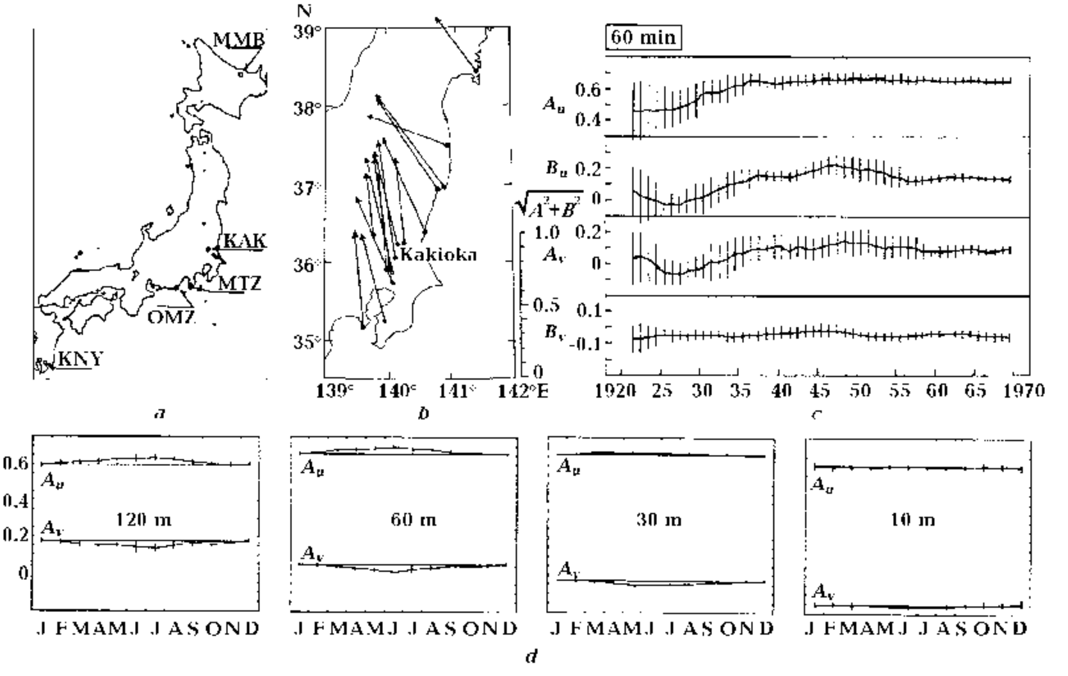


Fig. 1. Results from Japan: *a* — Observatories position; *b* — $\mathbf{C}_u$ in central Japan for T=15÷60 m [Kuboki, 1972]; *c* — ten years running averages of $\mathbf{C}$ components in Kakioka for the period 60 m, vertical lines show 95 % confidence intervals [Shiraki, Yanagihara, 1977]; *d* — seasonal variation given by monthly means of 1976—1988 Kakioka data for four periods.

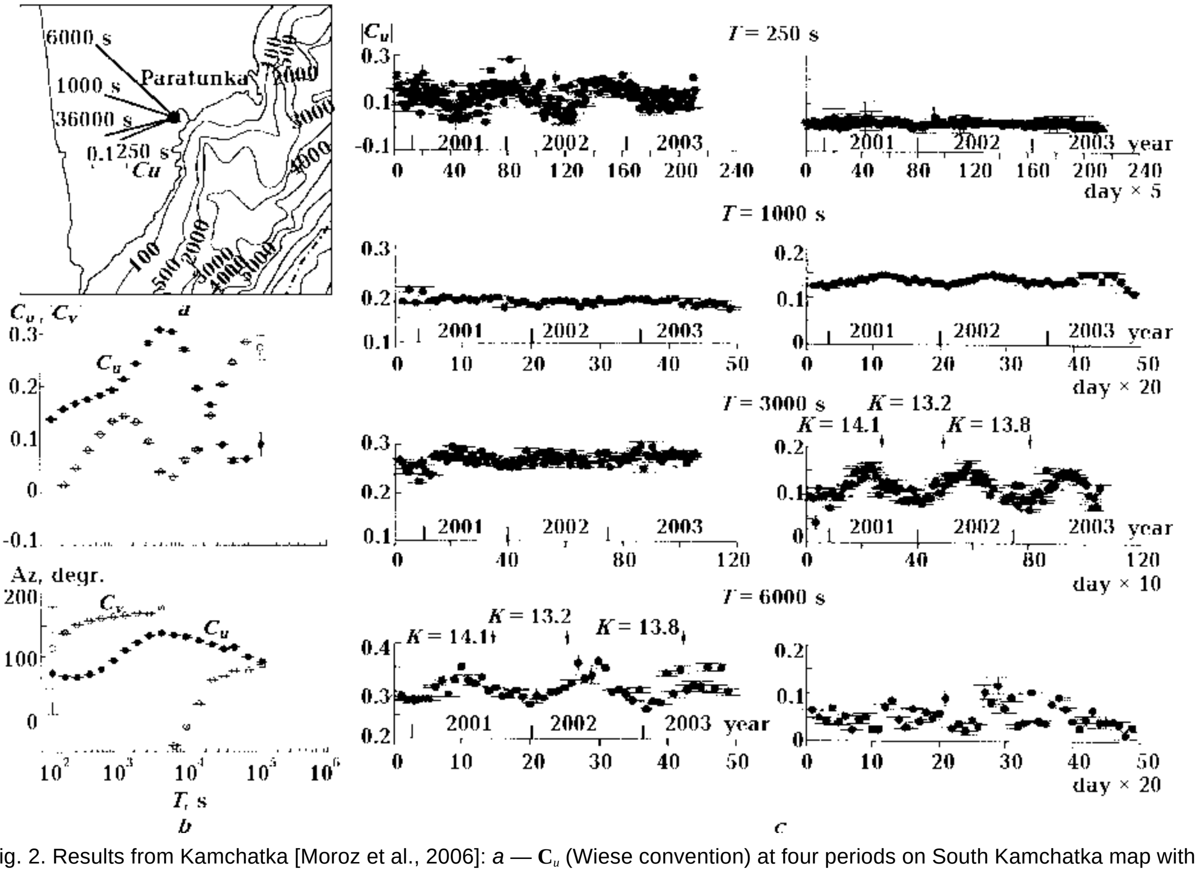


Fig. 2. Results from Kamchatka [Moroz et al., 2006]: *a* — $\mathbf{C}_u$ (Wiese convention) at four periods on South Kamchatka map with Pacific bathymetry lines marked in meters; *b* — modulus and azimuth of $\mathbf{C}_u$ and $\mathbf{C}_v$ versus period for Paratunka observatory; *c* — three years monitoring of $\mathbf{C}_u$ and $\mathbf{C}_v$ with averaging 5, 10 or 20 days (which indicated at horizontal axis legend) at four periods. Arrows show the time of strong (K>13) EQs at the distance 150 km or less from Paratunka observatory.

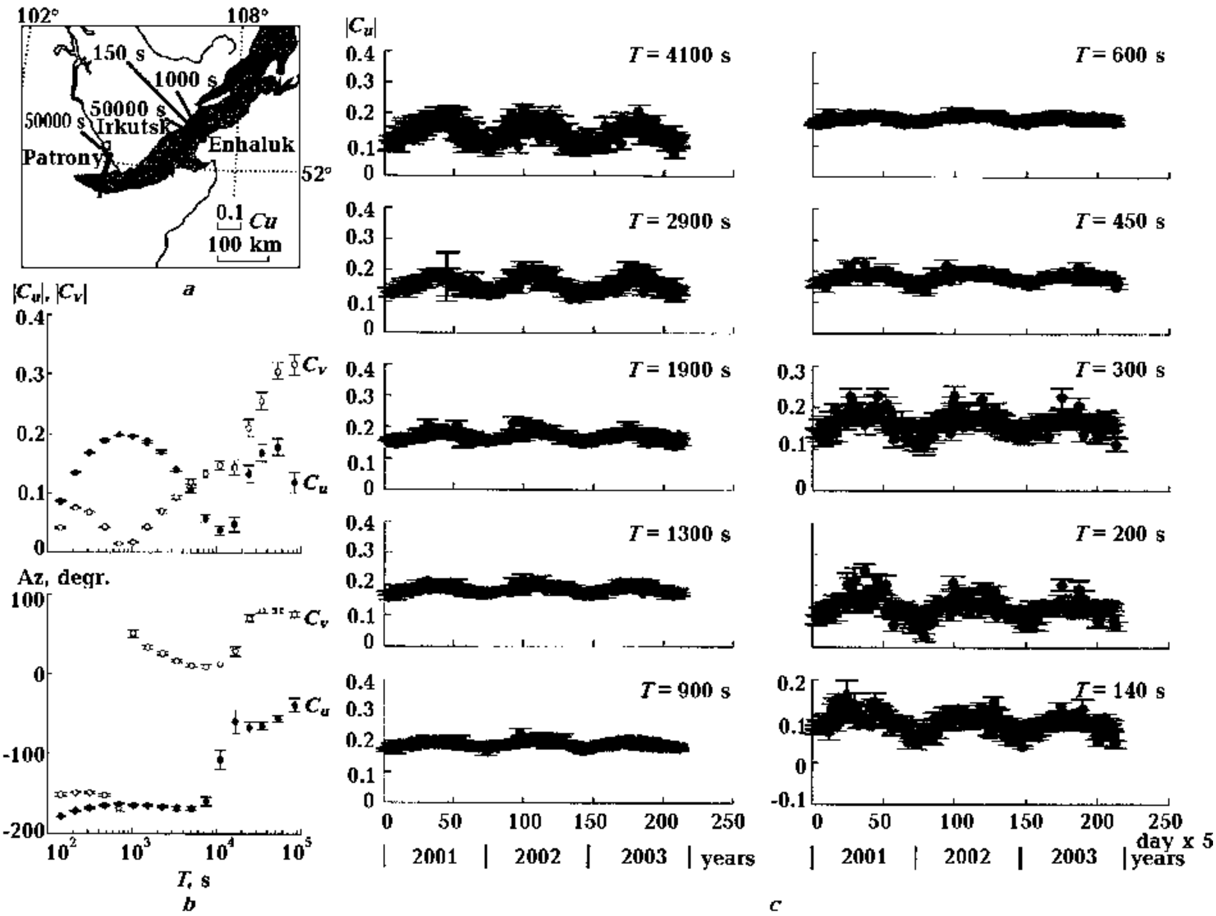


Fig. 3. Baykal rift [Moroz Yu., Moroz T., 2006]: *a* — real induction vectors (Parkinson convention) for two observatories for three periods; *b* — modulus and azimuth of $\mathbf{C}_u$ versus period for Patrony observatory; *c* — three years monitoring of $\mathbf{C}_u$ with averaging 5 days at ten periods.

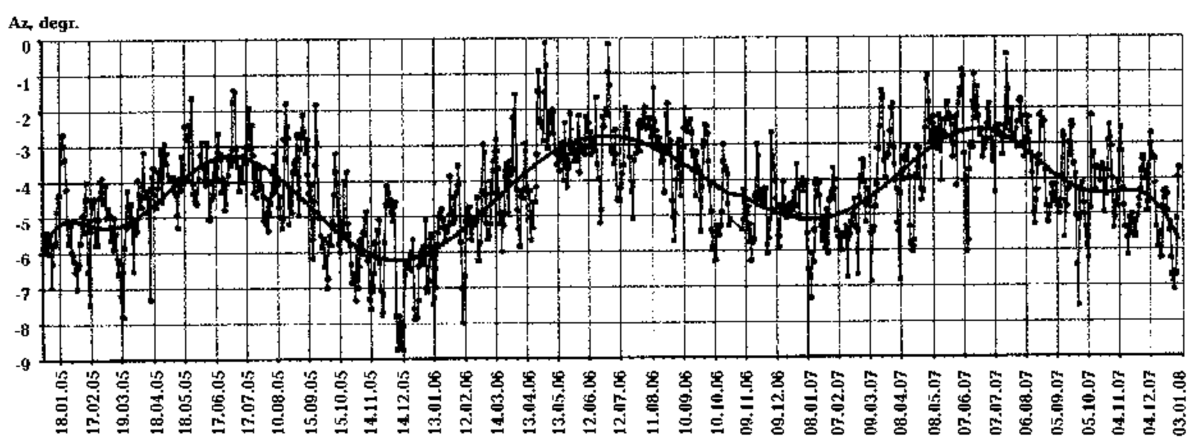


Fig. 4. Phase of the tipper meridional component (arg A) variation at T=1000 s in Blue Bay (South Crimea) Each point is duirnal arg A value after averaging in 5 days window [Korepanov, Tregubenko 2009]

2. In looking for EQ precursors (supposing be aperiodic) annual variation should be well studied and reduced.

3. Causes of annual variation may be a) the change of electrical conductivity in the Earth's interior, forming induction vectors; b) seasonal variation of the external source parameters leading to deflection from T—C model. c) superposition of seasonally variable parts of the last terms in equation (3).

References

Fujita S. Monitoring of Time Changes of Conductivity Anomaly Transfer Functions at Japanese Magnetic Observatory Network // Memoirs of the Kakioka magnetic observatory. — 1990. — **23**, № 2. — P. 53—87.

Korepanov V. E., Tregubenko V. I. Features of construction and trends of modern instruments development for magnetotelluric and magnetovariational soundings // Geophys. J. — 2009. — **31**, № 4. — P. 181—190 (in Russian).

Kuboki T. The Anomaly of Geomagnetic Variation in Japan (Part V) // Memoirs of the Kakioka magnetic observatory. — 1972. — **15**, № 1. — P. 63—80 (in Japanese).

Moroz Yu. F., Moroz T. A. Magnetovariational studies in the Baykal lake region // Fizika Zemly. — 2006. — № 11. — P. 93—98 (in Russian).

Moroz Yu. F., Smirnov S. E., Moroz T. A. The results of monitoring of geomagnetic field variations in Kamchatka // Fizika Zemly. — 2006. — № 3. — P. 49—56 (in Russian).

Shiraki M., Yanagihara K. Transfer Functions at Kakioka (Part I) // Memoirs of the Kakioka magnetic observatory — 1975. — **16**, № 2. — P. 143—155 (in Japanese).

Shiraki M., Yanagihara K. Transfer function at Kakioka (Part II). Reevaluation of Their Secular Changes // Memoirs of the Kakioka magnetic observatory. — 1977. — **17**, № 1. — P. 19—25 (in Japanese).

High Rayleigh Number Mantle Convectionon GPU

© D. Sanchez[1], D. Yuen[1], G. Wright[2], G. Barnett Jr.[3], 2010

[1]Minnesota Supercomputing Institute, University of Minnesota, USA
[2]Department of Mathematics, Boise State University, USA
[3]Department of Applied Mathematics, University of Colorado, Boulder, USA

The performance, potential growth, availability, and affordability of GPUs has made them attractive to scientists for many years. Although historically cumbersome and difficult to use for scientific software, the introduction and refinement of high-level development tools, such as CUDA, have made GPU computing accessible. With the advent of architectures, such as NVIDIA's Fermi, which explicitly cater to scientists by enabling more memory, faster access to that memory, and better double-precision support than ever before, members of the computational world are finding GPU difficult to ignore.

Using finite-difference methods with second-order accuracy in space and third-order accuracy in time, we investigate 2D and 3D thermal convection at the infinite Prandtl number limit, at resolutions on the order of 1000×2000 2D and 400×400×200 3D grid points. Our CUDA code makes extensive use of

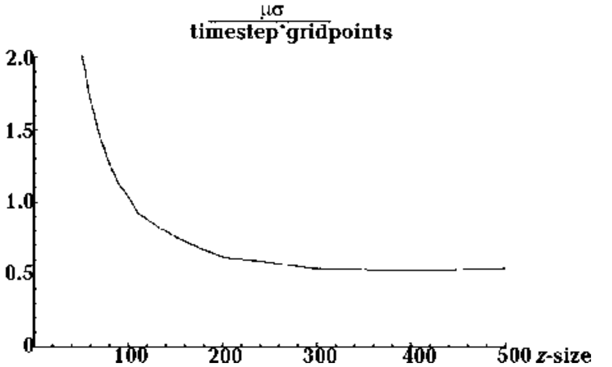


Fig. 1. Performance scaling with grid size on Tesla C1060.

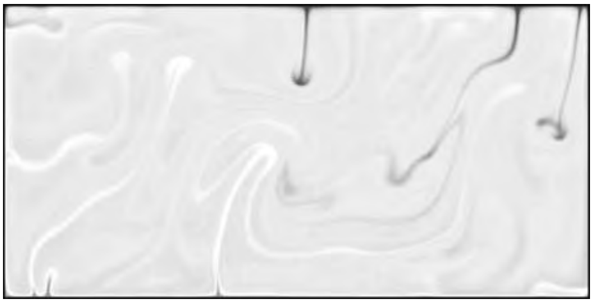


Fig. 2. 2D mantle convection at a Rayleigh number of 10^9.

highly-optimized CUBLAS routines, allowing us to unlock a significant fraction of GPU's performance. This performance has enabled us to study the behavior of high Rayleigh number simulations, on the order of 10^9, in 2D and 10^7 in 3D over sufficient time scales to see evidence of flow-reversal (Fig. 1).

We compare our CUDA code's performance with Jacket-accelerated Matlab code and CPU-only Matlab code across the Tesla C1060, Tesla C2050, and GTX 480 (Fig. 2).

Observation and analysis of ULF data associated with M_b=4.5 Koyna-Warna (India) earthquake

© A. Sharma, A. Patil, 2010

Space and Earth Sciences, Department of Physics, Shivaji University Kolhapur, India
sharma_ashokkumar@yahoo.com

In recent years ULF (Ultra Low Frequency) emission is detected during the seismic activity and this emission is recognized as one of the most promising candidate for earthquake prediction. In this paper, we present measurements of magnetic field anomalies detected for moderate earthquake that occurred on 29 July, 2008 having magnitude (M_b) 4.5. The ULF observation system uses three-component induction coil magnetometer and it has been installed at Shivaji University Kolhapur (16.40°N, 74.15°E), India.

Data of moderate earthquake have been analyzed using spectral density and polarization methods [Hattori et al., 2002a, b]. Long term data analysis shows that, two anomalous enhancements in intensity of magnetic field were observed about two and one months before the earthquake. Short term data analysis shows that, maximum enhancement in intensity of magnetic field was prominent within ±1 hours around the main shock time and it started to be observe four to five days before the earthquake. The enhancement in intensity of magnetic field is examined in terms of space magnetic pulsation and ULF emission associated with earthquake by using polarization parameter [Hayakawa et al., 2007; Sharma et al., 2008] and planetary index (K_p). It is concluded that there is no relation between enhancements in intensity of magnetic field and geomagnetic activity.

References

Hattori K., Akinaga Y., Hayakawa M., Yumoto K., Nagao T., Uyeda S. ULF Magnetic Anomaly Preceding the 1997 Kagoshima Earthquakes // Seismo-Electromagnetics: Lithosphere-Atmosphere-Ionosphere Coupling / Eds. M. Hayakawa, O. A. Molchanov. — 2002. — P. 19—28.

Hayakawa M., Hattori K., Ohta K. Monitoring of ULF (ultra-low-Frequency) Geomagnetic Variations Associated with Earthquakes // Sensors. — 2007. — **7**. — P. 1108—1122.

Hayakawa M., Ohta K. M., Nickolaenko A. P., Ando Y. Anomalous Effect in Schumann Resonance Phenomena Observed in Japan Possibly Associated with the Chi-Chi Earthquake in Taiwan // Annales Geophys. —- 2005. — **23**. — P. 1335—1346.

Sharma A. K., Patil A. V., Haridas R. N., Bhosale R. V. ULF emissions associated with seismic activity recorded at Kolhapur Station // Current Sci. — 2008. — **94**, № 8. — P. 25.

Deep structure and geodynamics of the euro-arctic region

© N. Sharov, 2010

Institute of Geology, Karelian Res. Centre, RAS, Petrozavodsk, Russia
sharov@krc.karelia.ru

The Euro-Arctic region includes the Barents Plate, the northern Baltic Shield, the northern Timan-Pechera Plate and the northeastern Russian Plate. In the west, the study region is bounded by the Svalbard Archipelago, in the east by the Novaya Zemlya Archipelago and in the north extends as far as the latitude of the Franz Josef Land Archipelago. In the region, the Kola Superdeep Borehole was drilled to a depth of 12 km and over 450 000 linear kilometres of seismic profiles were worked out, about 1/3 of which as a part of regional studies. Deep horizons were mapped, two- and three-dimensional models of geological structures were developed and deep faults were traced using the seismic method [Lithospheric ..., 2005]. Seismic data provided a basis for interpretation by other geophysical methods.

The basic characteristics of the lithospheric structure in the domain of transition from the passive continental margin to the oceanic depression were revealed by integrated interpretation of the data that show the main pattern of the deep structure of the Euro-Arctic region at its different levels. The continental parts of the platforms have an average crustal thickness of 40—50 km, the upper and lower crustal storeys having a commensurate thickness. The plasticity level is at a depth of 20—25 km, and usually corresponds to the lower crust surface. Upper crust heterogeneities are compensated by the mantle, in which either one layer with a velocity of about 8.0—8.2 km/s or two complementary layers with velocities of 8.0—8.1 and 8.4 km/s are distinguished above the compensation level. Locally, in palaeosuture zones the layering of the substrate increases, and lenses with velocities of 7.6 km/s or over 8.5 km/s appear in it. The consolidated crust of the shelf is as thin as 15—25 km, in contrast to oceans, where the maximum thickness of the consolidated crust is not more than10 km. Another characteristic of the shelf plate is a greater contribution of the lower ("basaltic") layer to the consolidated crust column up to the almost complete disappearance of the upper crustal ("granitic") layer.

Available technical facilities and marine and ground monitoring methods were used to form a system of hodographs of refracted and deep reflected waves to examine the wave field structure over a wide distance range and to study in detail the geological structure of the earth crust and the upper mantle in the transition zone between the Baltic Sea and the Barents Sea depression. At the Baltic Shield-Barents Plate jointing the basement plunges in stepwise manner. The sedimentary cover increases in thickness to 15—20 km, and crustal thickness decreases to 28—30 km. A layer with a velocity of 7.0 km/s was revealed in the thickest sedimentary cover zone in the crystalline basement of the plate. A lower-crustal layer with a velocity of 7.0—7.4 km/s was detected locally on the Baltic Shield in rifting zones. Therefore, its crust-mantle mixture, formed in tectono-magmatic activation zones, can be interpreted.

New seismological data on the deep structure of the eastern Baltic Shield have confirmed the correctness of the reconstruction of the deep structure in which the earth crust of the modern continent and shelf was chiefly formed in Archaean time, and Proterozoic structural facies complexes played a minor role. The structure of large Precambrian crustal blocks has largely preserved to the present time, and has only been modified in tectono-magmatic activation zones of limited size.

Geological-geophysical interpretation of seismic data on the Euro-Arctic region has revealed quite a number of discrepancies in geohistorical models and palaeoreconstructions, showing again that tectonics and geodynamics are now at a crucial stage: scientists search for a new paradigm to fit "plate-tectonic" and "oscillation" concepts into a general-purpose scheme.

In one group of models emphasis is placed on the stability of continental lithospheric blocks over billions of years, which does not prevent the permanent manifestation of high-amplitude intracontinental movements in aulacogens and "isolated depressions" without transformation of the continental crust into oceanic. This group of models is based on con-

ventional methods for interpretation of geological and geophysical data and is consistent with the concepts of an essential contribution of raid tectonics to the platform history developed in the past few years. In an alternative model of the destructive-accretionary history of the Barents-Pechera basin crust a distinctive methodology, used to reveal an old oceanic-type spreading belt buried at great depth under a young plate cover, is especially valuable. If these bold geophysical palaeoreconstructions are supported by geochemical and petrological data, then an integrated geological-geophysical methodology of analysis of the evolution of continents will be at a new, advanced level.

References

Lithospheric structure of the Russian part of the Barents region / Eds. N. V. Sharov, F. P. Mitrofanov, M. L. Verba, C. Gillen — Petrozavodsk: Karelian Res. Centre, RAS, 2005. — 318 p.

Earth's tidal tilt jumps and their relationship to earthquake source's physics

© *V. Shliakhovyi*[1], *V. Chernyi*[2], *V. Shliakhovyi*[1], *2010*

[1]Poltava Gravimetric Observatory of the Institute of Geophysics,
National Academy of Sciences of Ukraine, Poltava, Ukraine
gravics@gmail.com
[2]eMeter Corporation, San Mateo, USA
scherniy@yahoo.com

Institute of Geology and Seismology and Poltava Gravimetric Observatory of Institute of Geophysics of National Academy of Sciences of Moldova and Ukraine researched earth's crust tilt deforma-

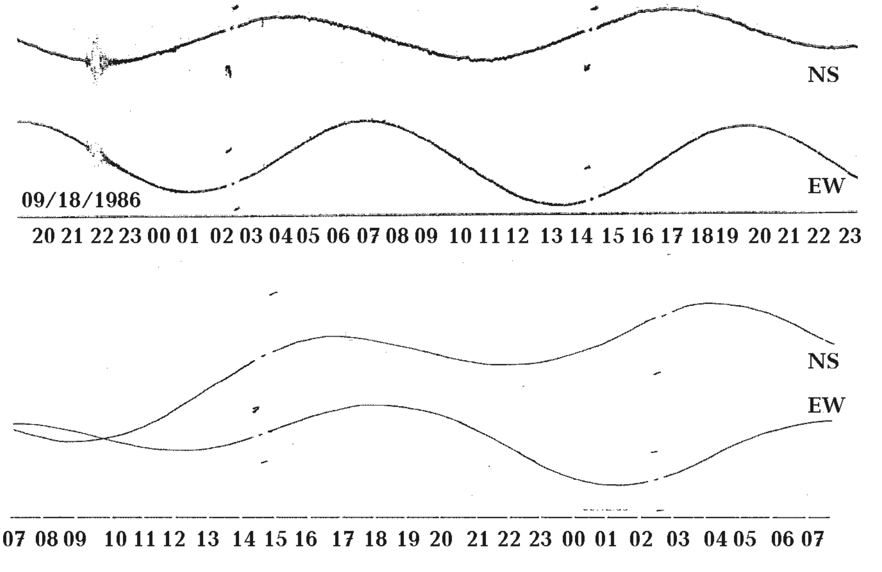


Fig. 1. Usual record of earth- tidal tilts at station "Chisinau". Top — with presence of seasonal microseisms and bottom — without.

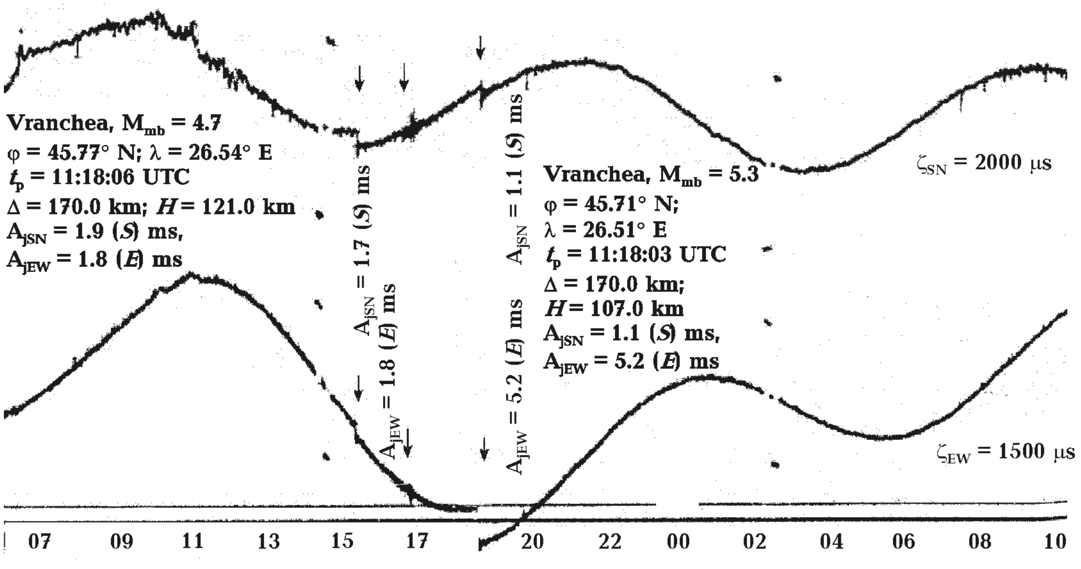


Fig. 2. The sample of earth-tidal tilts record with doubled Vranchea earthquakes and corresponding tilts jumps ("Chisinau").

Earthquakes parameters with corresponding tilt jumps

№ п/п	Data, time	M	Lat	Long	H, km	L, km	Jump, msec arc		P (press)		B		T (tension)	
							EW	NS	az	pl	az	pl	Az	pl
1	1.08.85 11:17	5.2	45.8	26.75	120	200	1.8	−1.7	135	8	42	19	248	69
2	1.08.85 14:35	5.5	45.35	26.52	105	195	5.2	−1.1	252	10	358	57	156	31
3	27.04.86 00:04	5.1	45.48	26.95	41	235	0.5	0.7	128	2	38	8	229	82
4	16.08.86 06:41	5.2	45.53	26.42	154	245	1.5	5.6	293	27	29	12	142	61
5	30.08.86 21:28	7.0	45.52	26.49	137	255	160	−49	330	20	238	7	131	69
6	16.12.86 22:33	4.8	45.59	26.56	142	235	2.4	2.4	272	9	8	32	169	57
7	23.09.87 20:40	4.5	45.6	26.59	140	220	1.4	0.8	276	26	19	25	146	52
8	8.01.88 16:50	4.8	45.54	26.26	135	258	12.3	1.5	311	0	220	77	41	13
9	30.05.90 10:40	6.5	45.87	26.87	89	215	460	−710	318	17	51	9	168	70
10	31.05.90 00:17	6.4	45.83	26.89	79	205	-100	180	27	22	123	15	244	63
11	26.06.90 07:54	4.3	45.75	26.8	82	200	-0.4	0.7	97	0	187	5	1	85
12	13.01.91 23:48	4.9	45.73	26.75	120	210	1.6	15	20	1	290	8	115	82
13	31.01.91 13:29	5.1	45.72	26.69	127	195	1.2	1.5	23	16	115	5	221	74
14	21.11.92 12:55	4.8	45.8	26.58	124	215	12.8	7	261	18	352	5	99	71

tion in the vicinity of earthquake source zone Vranchea during 14 years. Auto-compensating tiltmeters allow to broaden the spectrum of the research, including earth-tidal study, recent movement of the earth's crust, and geodynamic processes in area adjacent foci zone of Vranchea earthquakes — one the most active seismogenic regions in Europe.

Observation station was located in the mine, about 75 m underground and maximally distant from the technogenic and climotogenic sources of noise. High quality of data allows use of observations in study of strong earthquakes precursors; three of these stronger earthquakes (M~6.4÷7.0) occurred during observation period, which also allowed getting precious scientific results for whole spectrum of study areas. Some results of these studies were published [Schlikhovoi et al., 1989; 1997; 1998; Drumea et al., 1990], some — are still in progress. The study of jump events corresponding to strong earthquakes of Vranchea is important to study of their relation with regional geotectonic and to earthquake precursor study. This aspect of study is imperative due to the expected strong earthquake according to known seismic activity cycle of Vranchea

region. Usually, the jumps are recorded for earthquakes with M≥4,5. During the period of observation, 35 earthquakes of similar magnitude took place in Vranchea; five of which (M≤4,8) are missing jumps, four — concealed with mine noise, data for twelve is missing due to equipment malfunction and blackouts. We ended up with 14 sets of high quality jumps data displayed in Tab. 1 along with foci mechanism parameters. Examples of record of tidal tilts at station "Kishinev" at usual registration and with jumps at earthquakes are shown Fig. 1, 2. Analysis of data in table shows that jumps accompany all M≤5 earthquakes. Analysis shows that meaningful statistical relationship could be established between magnitudes of earthquakes (M) and amplitudes of jumps (Am). The dependency can be expressed by regression: M=(4.58±0.41)+(0.74±±0.11) lg |Am| with 10 % accuracy. The values and sign of the jump components depend on position of the fault's surface and azimuth line between obser-

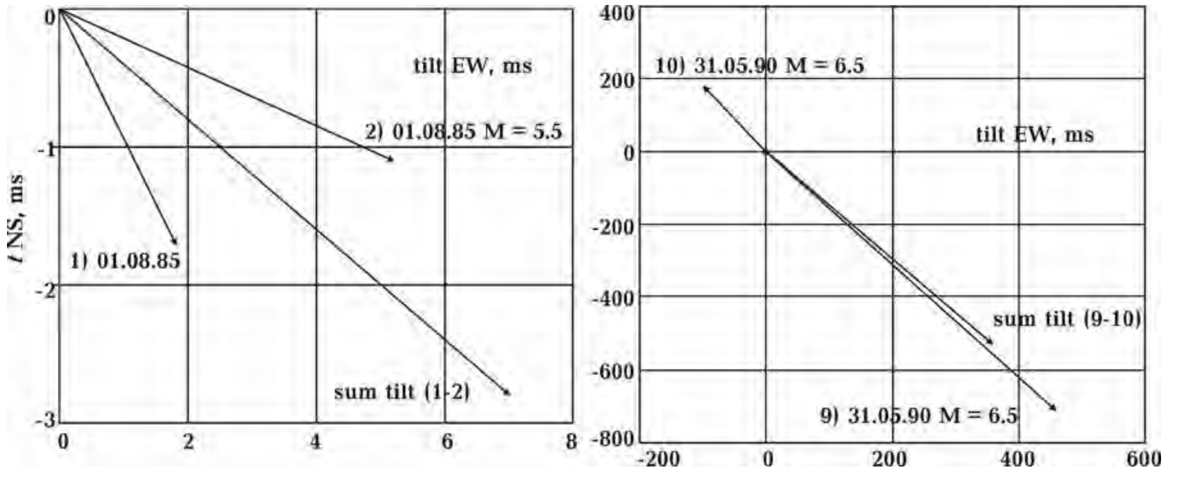


Fig. 3. Vector-diagram of tilt jumps.

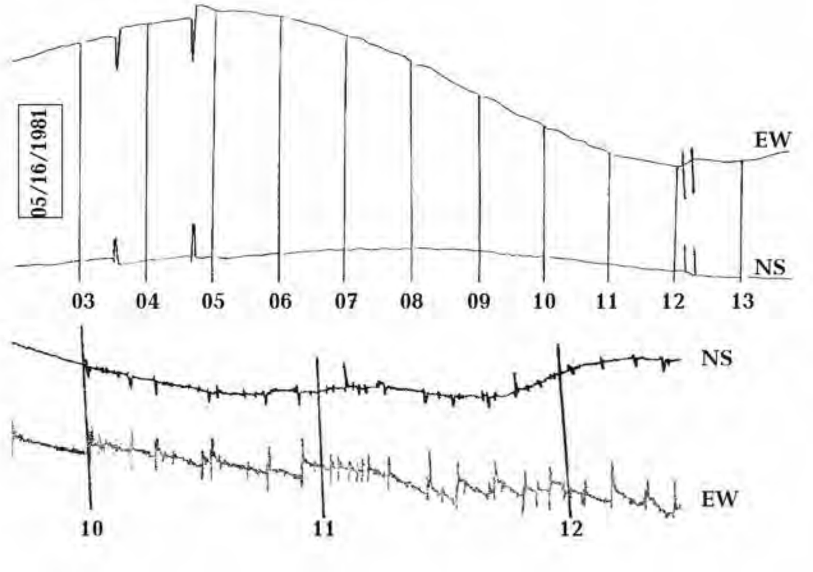


Fig. 4. Samples of tiltmetric records with the presence of technogenic tilt jumps originated by heavy traffic during the experiments: top — st. Sudievka and bottom — Dniester river bridge.

vation's location and earthquake focus. Tilt jumps vector-diagrams display this (Fig. 3). In case of doubled earthquakes (with close time of occurrences) we have clearly identified jumps for each earthquake respectively. In case of weak earthquakes the jumps are mono-directed, for strong — multi-directed. Tilt jumps quantitative interpretation follows fault- dislocation model, which precisely depicts foci processes. This approach allows determine earthquake geometrical and energetical parameters on the basis of several observation stations. The method represented in monograph "Earthquake mechanics" [Kasahara, 1981] was used to interpret observed data. Unfortunately, we only have one station data, thus can use only simple model (dip-slip). This model fits most of strong Vranchea earthquakes due to faults surface angle falling into 70°—85° and slips being vertical [Drumea et al., 1990]. Even for the simple model three stations observation are required. Assuming relation between magnitude and fault parameters (height, length), slip parameters were computed; the results of computation (except: May 1990 earthquakes) were in sync with the results derived by other methods [Drumea et al., 1990]. Jumps appeared on tidal tilt records aside from seismic events, and were considered as noise and ignored. Turns out, the jumps appeared as result of sudden overload of geophysical continuum. This was proven by real time sync tiltmetric observations in pit-hole at station Sudievka (Poltava suburb) and deformation study at Dniester river bridge (Bender). Records of these observations often contained peak impulses with residual tilts from 0,001 (in pit-hole) to 1 (bridge) arc.sec (Fig. 4). Some time these jumps were considered as instrumental noise, but then have established that they are caused by loadings from moving transport. Observations on the bridge delivered records of elastic and non-elastic tilt jumps; with lesser quantity and amplitude of jumps in areas where pillars were set in denser rocks. Most likely, tilt jumps are caused by non-elastic rock deformation. Moreover, tilt frequency and jump amplitude indicate critical condition of rock deformation. Based on the above-mentioned observations and results of the data analysis, we were able to arrive at following conclusions:

a) tilt jumps occur at geo-objects of different scale and composition, yet display same physical nature;

b) presence of jumps (deformations, slides) demonstrates unstable condition of geo-objects;

c) increase of amplitude and number of jumps indicates transformation of geo-object into more dynamic deformation phase that predeceases catastrophes such earthquake, landslide, mine collapse, and other; and, possibly, may be considered as direct precursor of natural and technogenic cataclysm;

d) tiltmetric observation are direct indicators of continuum deformational state, thus must be considered as necessary component in complex geophysical monitoring of deformational processes.

References

Drumea A. V., Shebalin N. V., Skladnev N. N. The Carpathian Earthquake of 1986. — Chisinau: Stiinza, 1990. — 334 p.

Kasahara K. Earthquake mechanics. — Cambridge University, 1981. — 260 p.

Schlikhovoi V. P., Cherny V. I., Ostrovsky A. E. Investigation of deformation processes in the area of the Vrancea focal zone using precise tiltmeters // 6th In. Symp. "Geodesy and Physics of the Earth", Potsdam (GDR), 1988. III. Recent Crustal Movements. — Potsdam, 1989. — P. 217—228.

Schlikhovoi V. P., Schlikhovoi V. P., Slusar E. G. Jumps of the Tilts at Earthquakes of Vranchea // 29th Ge-neral Assemble Int. Association of Seismology and Physics of the Earth's Interior, Abstract. (Thessa-loniki (Greece) August 18—28). — 1997. — P. 197.

Schlikhovoi V. P., Slusar E. G., Schlikhovoi V. P., Cherny V. I. Results of a study of tidal tilts near to Vranchea zone // Proc. Thirteenth Int. Symp. on Earth Tides. (Brussels, July 22—25, 1997). — Brussels, 1998. — P. 243.

3D velocity model of the crust and upper mantle of the Ukrainian Shield

© L. Shumlyanska, T. Tsvetkova, A. Tripolsky, V. Tripolska, 2010

Institute of Geophysics, National Academy of Sciences of Ukraine, Kiev, Ukraine
tsvet@igph.kiev.ua

We construct a unified *P*-velocity model of crust and upper mantle of the Ukrainian shield. The work was done in two stages. In the first phase were collected materials on the velocity models of the crust, obtained by long-term work by the study of the velocity parameters of the crust and upper mantle of the Ukrainian Shield by a method of deep seismic sounding [Sollogub et al., 1978; Ilchenko, Kryuchenko,1981; Ilchenko, 1984, 2002; Sollogub, 1986; Sollogub, Ilchenko, 1986; Lithosphere …, 1987; 1988; Tripolsky et al., 2000; Grad et al., 2003; Thybo et al., 2003]. Velocity characteristics of the crust, relief of the Moho were considered and analyzed. We construct a two-layer model for the average velocity, the division conducted crustal horizontal (laminar) and vertical (the structural division of a rectangular grid). Divide the crust into two layers is a traditional division of the boards of the northern hemisphere [Tripolsky, Sharov, 2004]. The two layer model includes: the first layer of 15 km and the second from 15 to the Moho. In addition to the velocity at the division of the crust was used comprehensive information about the tectonic, geological and geophysical structure of the crust of the Ukrainian Shield [Kuprienko et al., 2007; Omelchenko et al., 2008; Starostenko et al., 2002]. The second phase included the conversion of previously received travel time curves for *P*-velocity model of the mantle of Eurasia, obtained by the method of V. S. Geyko [Geyko, 2004]. Calculation was carried out using the software package developed by the T. A. Tsvetkova. For

Average velocity in the crust and V_P in the upper mantle under Ukraine shield

Struktures	V_{aver}, km/s, on 15 km	V_{aver}, km/s, on Moho	Depth of Moho, km	V_{aver}, km/s	V_P, km/s, on 50 km	V_P, km/s, on 75 km	V_P, km/s, on 100 km	V_P, km/s, on 125 km	V_P, km/s, on 150 km	V_P, km/s, on 175 km	V_P, km/s, on 200 km
Volyn block	6.21	6.91	50.9	6.69	7.285	8.062	8.122	8.145	8.226	8.277	8.333
	6.41	6.86	40.4	6.68	8.075	8.087	8.109	8.135	8.166	8.206	8.254
	6.32	6.81	40.27	6.63	8.015	8.042	8.052	8.117	8.165	8.22	8.286
	6.17	6.79	42	6.56	8.066	8.078	8.099	8.127	8.167	8.22	8.287
	6.16	6.73	39.8	6.51	8.069	8.082	8.101	8.129	8.166	8.214	8.275
Podol block	6.21	6.91	50.9	6.69	7.285	8.062	8.122	8.145	8.226	8.277	8.333
	6.26	6.78	47.06	6.61	8.059	8.087	8.120	8.155	8.197	8.245	8.305
Ros block	6.38	6.87	41.29	6.69	8.024	8.065	8.114	8.166	8.219	8.274	8.317
Bug block	6.17	7.03	54.33	6.73	7.317	8.143	8.193	8.235	8.273	8.314	8.356
Golovanevska suture zone	6.28	7.09	53.22	6.86	7.515	—	—	—	—	—	—
Ingul block	6.28	6.81	42.33	6.62	—	—	—	—	—	—	—
	6.18	6.8	42.3	6.57	—	—	—	—	—	—	—
	6.21	6.74	40.75	6.58	8.088	8.1356	8.1753	8.2106	8.246	8.284	8.325
	6.16	6.69	38	6.48	8.014	8.080	8.138	8.190	8.241	8.293	8.346
Krivoy-Rog-Kremenchug suture zone	6.25	6.99	52.67	6.77	7.418	8.137	8.175	8.213	8.301	8.301	8.35
Middle-Dnepr block	6.27	6.68	38.4	6.51	8.013	8.080	8.138	8.190	8.240	8.293	8.346
Orehovo-Pavlograd suture zone	6.28	6.75	42.6	6.57	7.995	8.062	8.114	8.162	8.210	8.262	8.313
Azov block	6.2	6.7	38	6.54	8.047	8.102	8.154	8.203	8.252	8.307	8.047

that purpose, as an amendment to the bark were used the values obtained for average velocity and depth of the Moho. Were analyzed for changes in the behavior of the velocity model [Geyko et al., 2006], which was used by the standard model of Jeffreys — Bullen and after the introduction of "real" model mean velocities of the crust. It is shown that up to 0.015 km/s changes are observed to depths of 150 to 300 km (Table). Maps of the distribution of average velocities for the crust, for the layers (15 km on the Moho, the average velocity of the crust as a whole) were built in the isolines and block diagrams. For the upper mantle velocity distribution built in the true velocity throw 25 km by a depth.

References

Geyko V. S. The general theory of seismic travel time tomography // Geophys. J. — 2004. — **26**, № 2. — P. 3—32.

Geyko V. S., Shumlyanskaya L. A., Tsvetkova T. A., Bugaienko I. V., Zaiets L. N. Three-dimensional model of the upper mantle of Ukraine on the arrival time of *P*-waves // Geophys. J. — 2006. — **28,** № 1. — P. 3—16 (in Russian).

Grad M., Gryn' D.. Guterch A., Janik T., Keller R., Lang R., Lyngsie S. B., Omelchenko V. D, Starostenko V. I., Stephenson R. A., Stovba S. M., Thybo H., Tolkunov A. DOBREfraction'99 — velocity model of the crust and upper mantle beneath the Donbas Foldbelt (East Ukraine) // Tectonophysics. — 2003. — **371**. — P. 81—110.

Ilchenko T. V. Kryuchenko V. A The results of integrated interpretation of seismic and gravity data along the profile of DSS XXV Babanka — Pjatihatki // Geophys. J. — 1981. — **3**, № 1. — P. 94—104 (in Russian).

Ilchenko T. V. Studies by the DSS along geotransekta EUROBRIDGE'97 // Geophys. J. — 2002. — **24**, № 3. — P. 36–50 (in Russian).

Ilchenko T. V. Velocity model of the Earth's crust along the profile Manevichi — Vinnytsia (Ukrainian Shield) // Geophys. J. — 1984. — **6**, № 4. — P. 7–-83 (in Russian).

Kuprienko P. Y., Makarenko I. B., Starostenko V. I., Legostaeva O. V. Three-dimensional density models of the crust and upper mantle of the Ukrainian shield // Geophys. J. — 2007. — **29**, № 5. — P. 3—27 (in Russian).

Lithosphere of Central and Eastern Europe: Geotraverses I, II, V / Ed. A. V. Chekunov. — Kiev: Nauk. dumka, 1987. —168 p. (in Russian).

Lithosphere of Central and Eastern Europe: Geotraverses IV, VI, VIII / Ed. A. V. Chekunov. — Kiev: Nauk. dumka, 1988. — 172 p. (in Russian).

Omelchenko V. D., Tripolsky A. A., Nosenko A. B. Velocity heterogeneity and Moho relief section of the Ukrainian shield // Geophys. J. — 2008. — **30**, № 6. — P. 113—126 (in Russian).

Sollogub V. B. Lithosphere Ukraine. — Kiev: Nauk. dumka, 1986. — 184 p. (in Russian).

Sollogub V. B., Ilchenko T. V. Seismic model geotraverse VIII // RAS USSR. — 1986. — **B**, № 12. — P. 15—18 (in Russian).

Sollogub V. B.. Chekunov A. V. Tripolsky A. A Results of the study the deep structure of the Ukrainian shield // Structure of the crust and upper mantle of Central and Eastern Europe. — Kiev: Nauk. dumka, 1978. — P. 136—147 (in Russian).

Starostenko V. I., Pashkevich I. K., Kutas R. I. Deep structure of the Ukrainian shield // Geophys. J. — 2002. — **24**, № 6. — P. 36—48 (in Russian).

Thybo H., Janik T., Omelchenko V. D., Grad M., Garetsky R. G., Belinsky A. A., Karataev G. I., Zlotsky G., Knudsen M. E., Sand R., Yliniemi J., Tiira T., Luosto U., Komminaho K., Giese R., Guterch A., Lund C.-E., Kharitiniv O. M., Ilchenko T., Lysynchuk D. V., Skobelev V. M., Doody J. J. Upper lithosphere seismic velocity structure across the Pripyat Trough and the Ukrainian Shield along the EUROBRIDGE'97 profile // Tectonophysics. — 2003. — **371**. — P. 41—79.

Tripolsky A. A., Kalyuzhnaya L. T., Omelchenko V. D. Features of the deep structure of plutons rapakivi granites and gabbro-anorthosite Ukrainian and Baltic shields (from seismic data) // Geophys. J. — 2000. — **22**, № 6. — P. 121—136 (in Russian).

Tripolsky A. A., Sharov N. V. The lithosphere of the Precambrian shields of the northern hemisphere of the Earth from seismic data. — Petrozavodsk: Karelian Res. Centre RAS, 2004. — 159 p. (in Russian).

Ultra low-frequency electromagnetic variation observed prior to development of an earthquake followed by tsunami

© L. Sobisevich[1], K. Kanonidi[2], A. Sobisevich[1], 2010

[1]Institute of Physics of the Earth, RAS, Moscow, Russia
[2]Institute of Terrestrial Magnetism,
Ionosphere and Radiowave Propagation, Troitsk, Russia
alex@ifz.ru

Analysis of experimental observations of variations in the magnetic field of the Earth recorded by instrumental complexes of the Northern-Caucasus Geophysical Observatory is performed. It is confirmed that it is possible to distinguish characteristic ultra-low-frequency (ULF) wave forms in the structure of the recorded electromagnetic signals preceding strong teleseismic events (earthquakes), especially ones being followed by tsunami.

The Alaska earthquake of March 27, 1964, with a magnitude of 9.2 was one of the strongest events in the history of instrumental seismic observations. At the end of 1964, G. W. Moore was the first to report about characteristic magnetic signals (forerunners), which appeared two hours before the earthquake [Fraser-Smith, 2008]. Investigation of forerunners of this class was continued [Gul'el'mi, 2007; Sobisevich et al., 2008a]. Anomalous electromagnetic signals before strong earthquakes were observed in a wide frequency range [Bakhmutov et al., 2003; Gul'el'mi, 2007; Sobisevich et al., 2008b]. The main efforts of scientists were focused on the study of anomalous broad-band electromagnetic disturbances [Barsukov, 1991]. Quasi-harmonic components almost fell out of consideration. This explains the fact that, during the last 50 years, ultra-low-frequency electromagnetic forerunners are periodically discussed, but so far there is no full agreement among geophysicists about the possibility of their reliable separation and practical application.

There is no satisfactory theoretical explanation of this effect so far [Alekseev et al., 2008; Gul'el'mi, 2008]. Therefore, field experiment becomes the first tool in the investigation of the revealed effect.

In recent years, systematic observations of magnetic field fluctuations with ultra-low frequency have been carried out at the Northern-Caucasus Geophysical Observatory of the Institute of Physics of the Earth (IPE RAS) equipped with modern geophysical instruments, including tiltmeters and triaxial magnetic variometers [Sobisevich et al., 2008a]. Analysis of the accumulated geophysical information about stimulated wave processes caused by remote earthquakes allowed us to confirm the existence of electromagnetic forerunners and distinguish anomalous wave forms with ultra-low-frequency of disturbances before strong teleseismic events 2—4 h before their beginning [Sobisevich et al., 2009].

Almost every earthquake with magnitude greater than 6 and followed by tsunami in 2007—2009 has been carefully analysed in terms of experimental observations over magnetic variations in the Northern-Caucasus geophysical Observatory (Table).

In every case there have been determined ULS geomagnetic variations, yet the first event registered and analysed was the Great Sumatera-Andaman earthquake back in 2004 (Fig. 1).

We refer to universal time here and further in this text. Analysis of magnetic variations has revealed the two time intervals with geomagnetic anomalies (possible precursors) may be clearly observed. Detailed representations of mentioned wave-forms are shown in the two incuts (1 and 2) while filtered anomalous ULF geomagnetic variations observed close to midnight December 24—25 are shown in Fig. 2.

It has been shown that quasi-harmonic wave forms of the geomagnetic variation determined in the time interval from 2006.12.24 23:58 to 2006.12.25 00:23 is containing information on electrodynamic processes in the domain of forthcoming seismic event.

It should be emphasized, that magnetic variometers are also registering well-known quasi-harmonic pulsations (Pc4 pulsations) of ionosphere origin. By comparing experimental records of the Pc4 geomagnetic

Date	Hypocenter/origin time	Location	Magnitude	Depth, km	Latitude	Longitude	Period of variations, s	Amplitude of variations, nT
01.04.2007	20:39:54.2	Solomon Islands	8.1	10.0	–8.3	156.9	120	1
16.07.2007	1:13:22.0	Japan	6.6	33.0	37.6	138.5	80	2.5
02.08.2007	2:37:42.3	Sakhalin	6.2	10.0	47.1	141.7	60	0.8
02.08.2007	3:21:42.8	Aleutian Islands	6.7		51.31	–180	60	0.8
15.08.2007	23:40:56.5	Near coast of Peru	8	40	–13.5	–76.6	120	1
02.09.2007	01:05:17.5	Santa-Cruz Islands	7.2	33.0	–11.3	165.8	60	2
12.09.2007	11:10:23.5	Indonesia	8.4	30.0	–4.4	101.5	75	1.8
30.09.2007	05:23:35.3	New Zealand	7.4	20	–49.31	163.8	50	3
14.11.2007	15:40:51.7	Northern Chile	7.7	60.0	–22.21	–69.93	80	2
03.12.2007		Canada					140	1.5
09.12.2007	07:28:24.0	Fiji	7.8	190.0	–25.8	–17.5	190	1.5
25.02.2008	0,35872	Indonesia	6.5	33.0	–2.5	99.9	80	3.5
09.04.2008	12:46:12.5	Loyalty Islands	7.3	40.0	–20.1	168.9	66	4
28.04.2008	18:33:34.2	Vanuatu Islands	6.4				52	4
12.05.2009	06:28:00.0	China	7.9	10.0	31.2	103.3	70	3.6
19.07.2008	2:29:28.7	Japan	6.9		37.6	142.2	75	1
11.09.2008	0:20:50.9	Japan	6.8	33.0	41.9	143.8	150	3
28.10.2008		USA			43.9	–69.6		
16.11.2009	17:02:31.8	South Peninsula Sulawesi	7.3	33	1.3	122.1	40	1
03.01.2009	19:43:53.0	Indonesia	7.6	33.0	–0.45	132.75	63	2.1
03.01.2009	22:33:40.2	Indonesia	7.3	33.0	–0.7	133.3	63	2.1
15.01.2009	17:49:36.8	East of Kuril Islands	7.4	33.0	46.9	155.2	126	3.4
11.02.2009	17:34:50.7	Indonesia	7.2	33.0	3.7	126.5	158	2
19.03.2009	18:17:38.8	Tonga Islands	7.6	33.0	–23.2	–174.6	95	1.2
28.05.2009	08:24:43.0	Caribbean Sea	7.3	10.0	16.7	–86.4	158	3
15.07.2009	09:22:31.8	New Zealand	7.8	33.0	–45.7	166.7	110	1.1
10.08.2009	19:55:38.5	Andaman Islands	7.5	33.0	14.1	92.92	126	2.9
10.08.2009	20:7:9.1	Japan	6.4	33	34.74	138.3	126	2.9
16.08.2009	7:38:21.7	Sumatra	6.7	50	–1.479	99.49	150	2
29.09.2009	17:48:11.0	Samoa Islands	8	20.0	–15.4	–172.2	150	4
30.09.2009	10:16:08.6	Indonesia	7.5	90.0	–0.8	99.9	150	4
07.10.2009	23:03:14.4	Vanuatu Islands	7.6	33	–13.01	166.5	250	2.5

pulsations with registered geomagnetic variations in question, one should note that for now there is no clear indication of what is the primary phenomena and what is the secondary one, in other words there is no clear indication that every magnetic variation in this frequency range is related to Solar activity only and is not related to electrodynamic processes accompanying the development of the domain of forthcoming seismic event.

For more than seven years we have been analyzing experimental records of ULF geomagnetic variations at the Northern-Caucasus Geophysical Observatory and based on this experience may we suppose that the initial phenomena is the geomagnetic signal generated in the domain of development of forthcoming seismic event.

In Fig. 3, 4 the time interval of several hours prior to the main shock of the Sumatra-Andaman earthquake featuring the fine structure of geomagnetic variation is shown.

Analysis of geodynamic settings in the course of preparation and development of the Sumatra-Andaman earthquake in combinations with records of magnetic variations has allowed to outline the specific type of quasi-harmonic ULF geomagnetic variations preceding an earthquake followed by tsunami. It has been suggested that the origin of mentioned geomagnetic variations is located within the

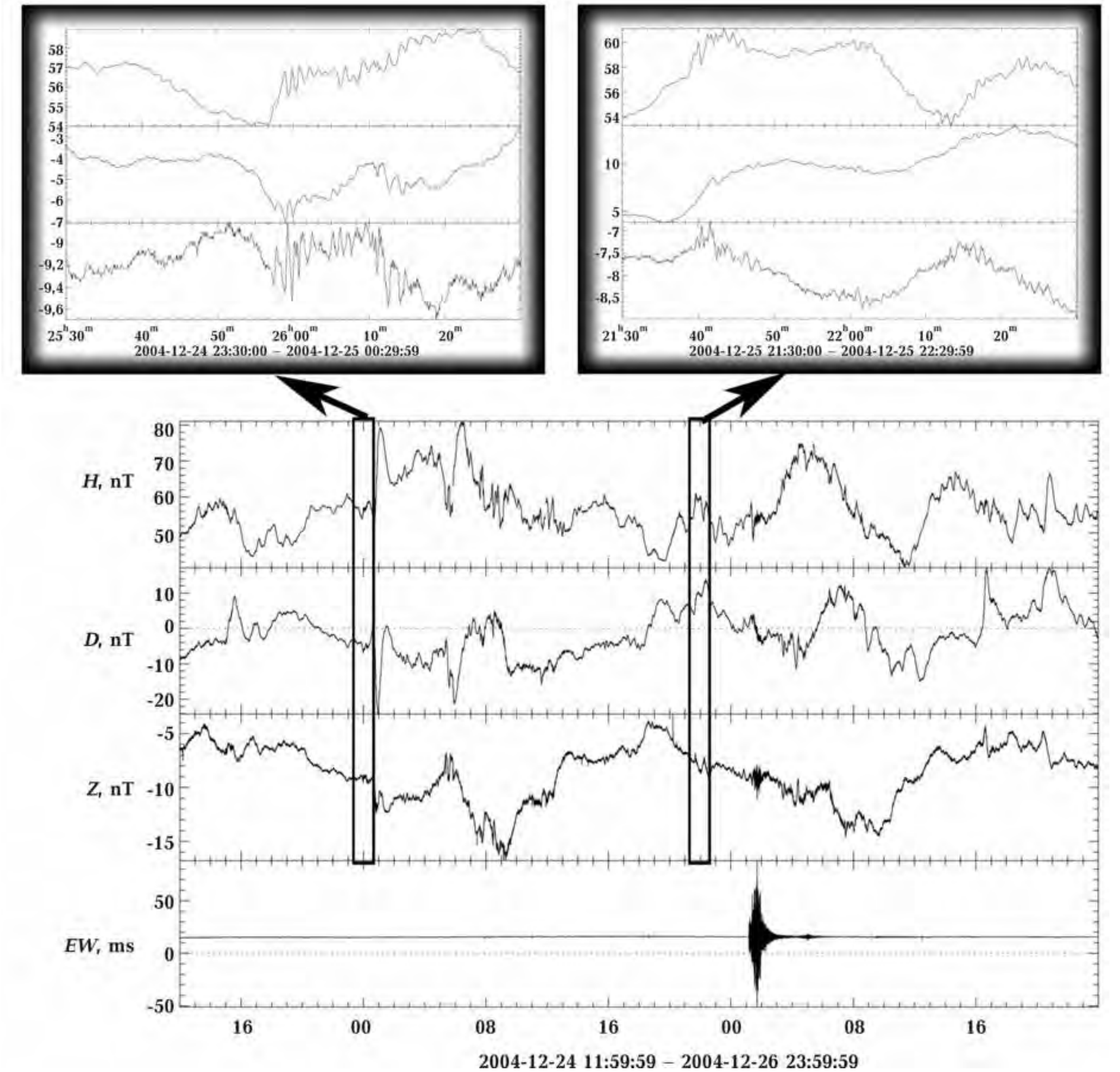


Fig. 1. Magnetic variations and tilt measurements recorded prior to the earthquake in Sumatra region as of 26.12.2004.

domain of a forthcoming epicenter and their amplitude observed at the distant locations (Laboratories 2 and 4, the Northern-Caucasus Geophysical Observatory, Elbrus volcanic area) varied from 0.5—1.2 nT.

Analysis of recorded data for the M=7.8 Northern Sumatera earthquake 06.04.2010 responsible for tsunami generation has confirmed the existence of ULF geomagnetic variations (Fig. 5, 6).

Analysis of ULF geomagnetic variations has revealed its quasi-harmonic nature and structure.

It should be emphasized, that experimental data collected by means of instrumental observations in the Northern-Caucasus Geophysical Observatory is of highest quality standards and thus is quite reliable in terms of short-time geomagnetic disturbances prior to development of an earthquake followed by tsunami (Table) are obtained for the first time and to the best of our knowledge there are no similar results obtained worldwide for now.

Results of experimental observations carried out in the Northern-Caucasus Geophysical Observatory are stored in the on-line flat file database (Public Domain) with the two following URLs: http://forecast.izmiran.ru/ and http://alex.uipe.ru/data/.

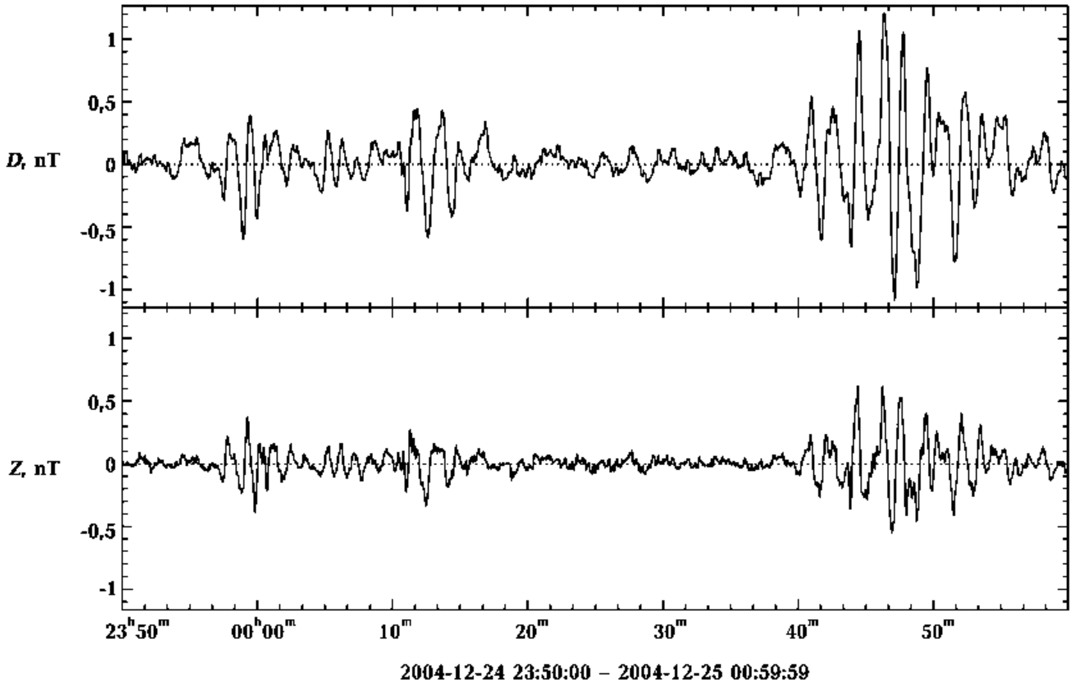


Fig. 2. Filtered quasi-periodic variations, featuring specific characteristics of geomagnetic disturbance originated approx. 24 hours prior to the Sumatra earthquake as of 26.12.2004.

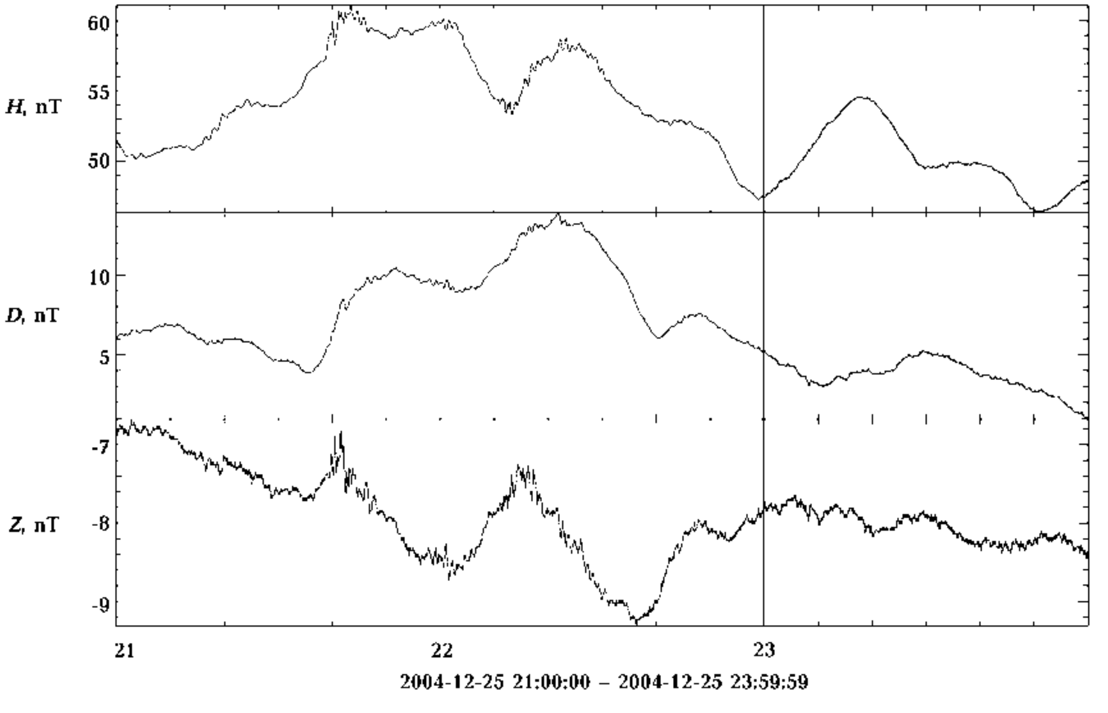


Fig. 3. Selected fragment of the record of magnetic variations in the region of Sumatra as of 26.12.2004.

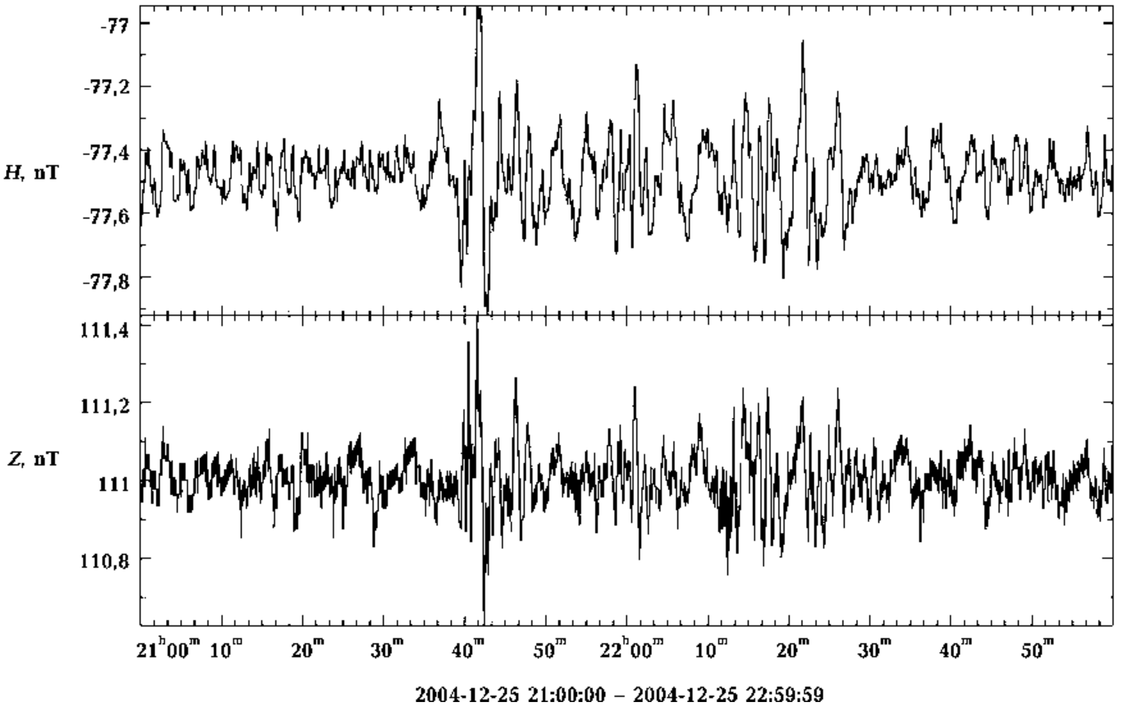


Fig. 4. The structure of geomagnetic variations preceding the Sumatra earthquake as of 26.12.2004.

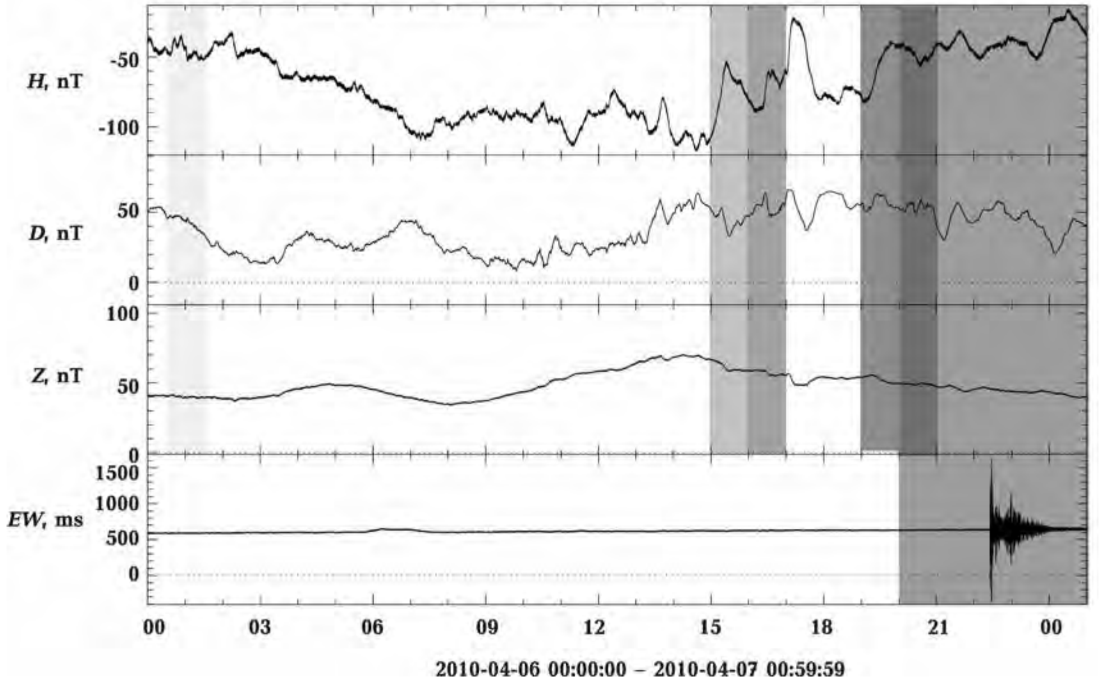


Fig. 5. The Northern Sumatra earthquake 06.04.2010 responsible for tsunami generation. Records of East-West tilt and triaxial magnetic variations. Colour selections represent specific fragments of the experimental records with anomalous ULF geomagnetic disturbances.

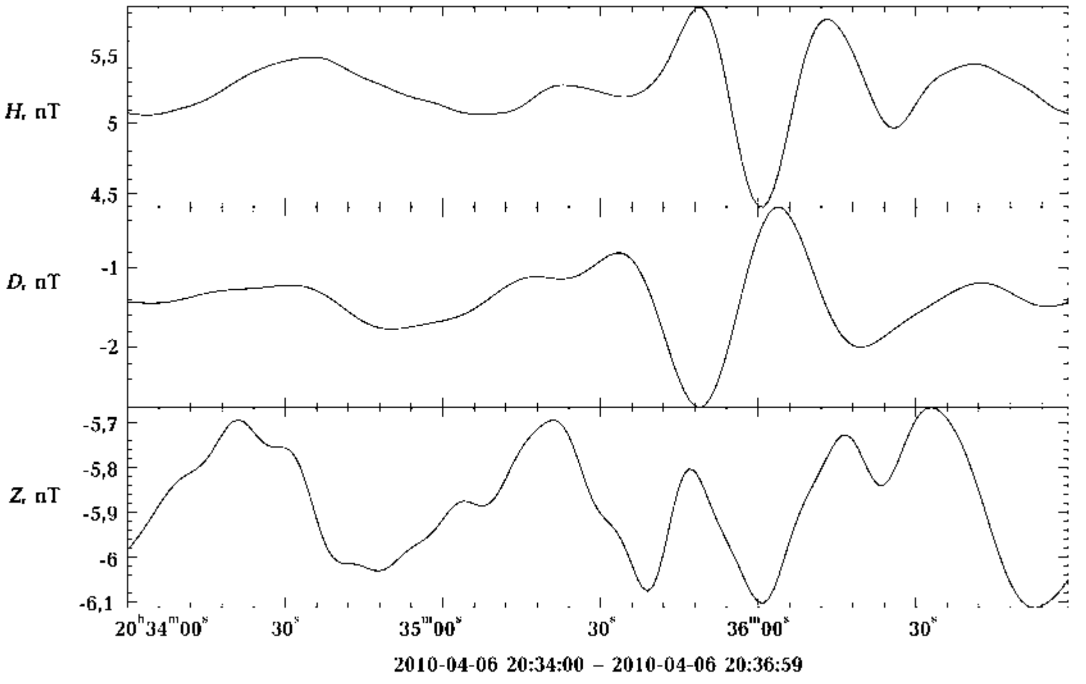


Fig. 6. Filtered and rescaled wave forms of the ULF geomagnetic disturbances observed one hour prior to the Northern Sumatra earthquake 06.04.2010.

This study was supported by the Russian Foundation for Basic Research (project nos. 09—05—00066 and 09—05—00431), and Program 4 of the Presidium of the Russian Academy of Sciences, and the Russian Science Support Foundation (www.science-support.ru).

References

Alekseev A. S., Glinskii B. M., Imomnazarov Kh. Changes of Natural Environment and the Climate. Natural Catastrophes. Seismic Processes and Catastrohes. — Moscow: IFZ RAN, 2008. — **1**. — P. 179—222 (in Russian).

Barsukov O. M. Solar Flares, rapid onsets and earthquakes // Phys. Solid Earth. — 1991. — № 12. — P. 93—96.

Bakhmutov V. G., Sedova F. I., Mozgovaya T. A. Morphological Features in the Structure of Geomagnetic Variations in Relation to March 25, 1998 Earthquake in Antarctica // Ukr. Antarkt. J. — 2003. — № 1. — P. 54—60.

Gul'el'mi A. V. Ultra-low-frequency electromagnetic waves in the Earth's crust and magnetosphere // Usp. Fiz. Nauk. — 2007. — **177**. — P. 1250—1276.

Sobisevich A. L., Gridnev D. G., Sobisevich L. E., Kanonidi K. Kh. Ultra low-frequency electromagnetic disturbances appearing before strong seismic events // Seism. Pribory. — 2008a. — № 44. — P. 12—25.

Sobisevich L. E., Kanonidi K. Kh., Sobisevich A. L. Changes of Natural Environment and the Climate. Natural Catastrophes. Seismic Processes and Catastrohes. — Moscow: IFZ RAN. — 2008b. — **1**. — P. 157—163 (in Russian).

Sobisevich L. E., Kanonidi K. Kh., Sobisevich A. L. Ultra Low-Frequency Electromagnetic Disturbances Appearing before Strong Seismic Events // Dokl. Earth Sciences. — 2009. — **429A**, № 9. — P. 1549—1552.

Fraser-Smith A. C. Ultralow-Frequency Magnetic Fields Preceding Large Earthquakes // EOS, Trans. AGU, 2008. — **89**. — P. 211.

http://www.agu.org/pubs/eos-news/

Study of deep underground structure of mud volcanoes in North-Western Caucasus by means of geological and geophysical methods

© L. Sobisevitch, A. Sobisevitch, 2010

Institute of Physics of the Earth, RAS, Moscow, Russia

sobis@ifz.ru

Results of complementary geological and geophysical studies of mud volcanic phenomena in North-Western Caucasus (Taman mud volcanic province) are presented. Geophysical field works have been carried out in 2005—2009 on the two different mud volcanoes: the Gora Karabetova and the Shugo mud volcano.

Usage of methods of vibroseismic sounding, traditional magneto-telluric sounding and relatively new method of low-frequency microseismic sounding allows obtaining several independent vertical cross-sections for the two different mud volcanoes down to the depth of 25 km. For the two different mud volcanoes their deep subsurface structure has been revealed and discussed with respect to regional tectonic settings, geology and geomorphology.

The Gora Karabetova mud volcano is one of the most active mud volcanoes in the Taman peninsula with primarily explosive behaviour while the Shugo mud volcano's activity pattern is different, explosive events are rare and both types of phenomena may be explained by the configuration of their feeding systems, tectonic position and deep pathways of migration of fluids.

References

Gorbatikov A. V., Sobisevich A. L., Ovsyuchenko A. N. Development of the Model of the Deep Structure of Akhtyr Flexure-Fracture Zone and Shugo Mud Volcano // Dokl. Earth Sci. — 2008. — **421A**, № 6. — P. 969—973. — DOI: 10.1134/S1028334X0806024X.

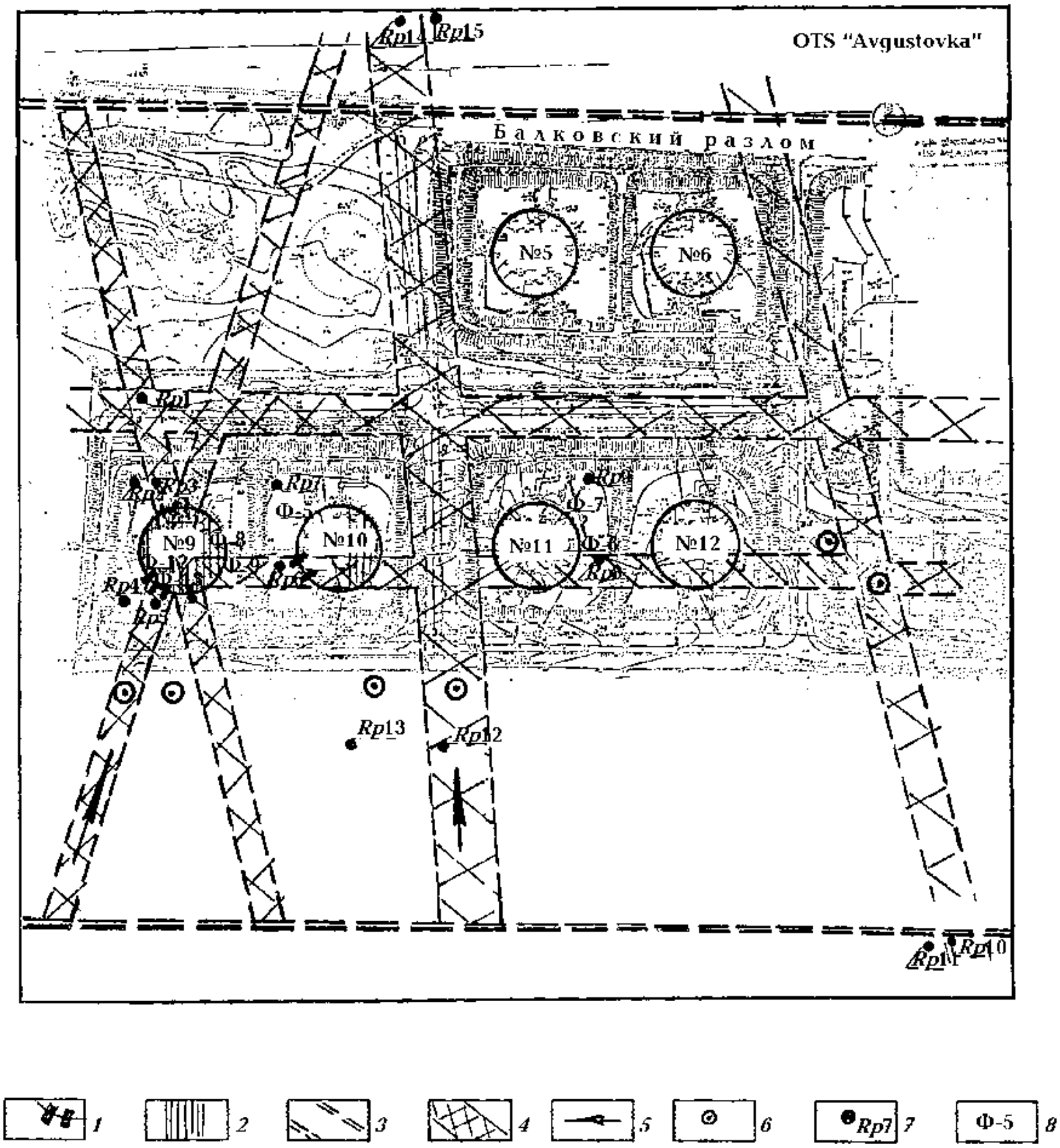
Sobisevich A. L., Gorbatikov A. V., Ovsuchenko A.N. Deep Structure of the Mt. Karabetov Mud Volcano // Dokl. Earth Sci. — 2008. — **422**, № 7. — P. 1181—1185. — DOI: 10.1134/S1028334X08070428.

Current assessment and accounting of geodynamic phenomena in engineering geology with geological and geophysical methods of investigation

© E. Sobolev, V. Vysotyuk, 2010

SSIE "Mars", Komsomolsk-Donetsk region, Ukraine
mnvp_mars@ukr.net

Despite the apparent inconsistency of the existing theoretical views on many aspects of the tectonic processes in the lithosphere, no one no longer doubt the assertion that the entire Earth's crust is divided into very difficult, though not devoid of certain laws, and a network of numerous raznorangovyh poligeneticheskih faults. In addition, because of the continuous mobility of the earth's crust,



The results of the impact GDZ at the tank farm NPS "Avgustovka": *1* — strain of tanks; *2* — underflooded facilities; *3* — boundary effects Balkivs'ka faults; *4* — GDZ 1 category, *5* — channel revenue "perched" on GDZ; *6* — well "zaverochnogo" drilling; *7* — geodetic benchmarks; *8* — geodetic marks on the foundation.

occurring primarily by the forces of cosmo-planetary origin, it constantly with a certain cyclic deformation occurs not only fragile, but also plastic [Nikolaev, 1988]. Thus, by discharging accumulated stresses due to rotational modes of the Earth, which is one of the main factors governing its equilibrium state [Tyapkin, 1998]. At the Earth's surface, these strains are usually manifested in the form of relatively narrow elongated linearly geomorphological forms, called the Geological lineament. This is especially true of large deep-seated tectonic faults, which are usually well manifested in deciphering aerospace images.

However, in engineering geology are often confronted with manifestations not only of major tectonic disturbances of global or regional scale, but also with the influence of a very common and extensively ramified network of medium and small-scale violations of local, local values. Moreover, these violations are similar to large can be charac-

terized as disjunctive and plicative kinds of deformations. As shown by careful analysis of large-scale topographic maps, they also are reflected in the present relief of the Earth in the form of elongated negative forms — the lineaments of a lower order. In the countryside, as a rule, such "micro" morphologically expressed bends channels of small rivers, streams, gullies, ravines, or just minor depressions, often barely noticeable visually.

It should be noted that in terms of the impact of existing tectonic faults in stability and functioning of various engineering structures, in our opinion, is not that important to order, as their modern geodynamic activity. Moreover, fixed in geophysical fields geodynamical active zones on the Earth's surface can appear also outside the zones of influence of existing tectonic disturbances. Apparently, the main criterion here is not so much the presence of the already established structure of the impaired as a direct manifestation of the time of observation of abnormal mechanical stresses, concentrated in the surface layers crust. In other words — is a modern geodynamic effect on the investigated rock mass is confined to the space in the form of a linearly elongated narrow zones and temporary determinant of the cyclical nature of recent tectonic movements. One can not help noticing more and technogenic factors of critical stresses in the reclaimed man of the rock massif, an increasingly relevant in the study of geodynamic phenomena.

One of the first on the existence of geodynamical active zones in the surface layers of the crust and the possibility of their successful study and mapping of attention Donetsk geologist collier YS Ryaboshtan in studies of structural features rock mass within the mine fields [Ryaboshtan, 1969]. He developed and successfully implemented in practice of geological research reclaimed rock mass method of structural-geodynamic Mapping — SGKE [Gorbushina, Ryaboshtan, 1974, Ryaboshtan, 1975]. This method is based on the use of emanation (radon-toron) shooting, later found the widest application in solving many practical problems in mining, various branches of geology and seismology, even in the prediction of earthquakes.

In subsequent years, the work of various departments of the Institute of Geophysical DonNIGRI and UkrNTEC (Donetsk) method has been significantly upgraded through the introduction of new hardware development, methodological innovation and integrated approach to the study of the problem. As geodynamic processes are reflected also in the electromagnetic field, when studying them more actively in addition to radiometric methods has begun to attract magnetometry and electrical [Sobolev, 2004]. That emerged a set of methods has been successfully applied in studies of engineering and geodynamic conditions of various objects (underground mining, quarries, dumps, natural slopes, waterworks, dams, residential buildings and promsooruzheniya, slopes of canals and pipelines, etc.).

Continually refined over more than one decade set of ground geophysical methods has passed a reliable tested in the study of geodynamic situation in the different sites and in particular on industrial sites pumping stations "Snihurivka" and "Avgustovka" Odessa DIC (Figure). As a result, a specially made zaverochnogo drilling with core sampling and determination of physical and mechanical properties of rocks, was found that within the identified geodynamic zones (GDZ) rock mass is characterized by reduction of the strength, deformation and physical characteristics at 11—50 %. Level ground water is turned on 0,6—0,9 m above. Are also characteristic of them was the presence of "perched", which is outside the zone was absent [Minutes …, 2000]. Thus justifying the concept of the geodynamic zone-block structure of an array of rock, which is already built, or only provides for the construction of engineering facilities for different purposes.

This concept as the basis of scientific and technical activities SSIE "Mars" (Komsomolsk Donetsk region), which is currently follower of these ideas in the annex to decision many of today's practical problems of Engineering Geology and Geo-ecology [Sobolev, Vysotyuk etc., 2007—2009].

Unfortunately, long recognized and accepted by many representatives of the scientific community views on the crucial role of the geodynamic factor in the occurrence of geological disasters (earthquakes, volcanic eruptions, landslides, mudslides, flooding, subsidence earth's surface et al), hitherto rejected by senior officials. That will depend on their adoption of building regulations, requiring designers necessarily and properly due consideration to the zone-block structure of reclaimed arrays. We believe this position is extremely irresponsible and totally inconsistent with today's challenges. As a result, those endless and often very tragic accident that occur in recent times more and more. In their series of Chernobyl [Strakhov et al., 1997], as well as the tragedy with passenger trains in the Urals [Divakov, 1998]. Their main reason for our firm belief is ignoring the importance of knowledge of the geodynamic setting near exploited very responsible engineering structures.

Recent advances in the study of geodynamic phenomena are pressing for an urgent review current building regulations. Necessary enter the appropriate additions and changes, requiring all participants in the construction and operation of criti-

cal facilities to identify the location of geodynamic zones on reclaimed tracts of rocks with the obligatory Map construction engineering and geodynamic zoning and take into account the geodynamic effect on the stability and security operations engineering objects [Sobolev, Vysotyuk, 2007].

References

Divakov V. I. Mikrogeodinamika. — Moscow: Russian University Peoples' Friendship, 1998. — 24 p.

Gorbushina L. V., Ryaboshtan Y. S. Mapping of zones of contemporary movements with the help of radiometry // Izv. universities. Ser. Geology and exploration. — 1974. — № 6. — P. 36—39.

Minutes of the Technical Meeting to review the work of OAO UkrNTEC and IGR of JSC "ITN" vol. In 2000, the NPS "Snihurivka" and NPS "Avgustovka" Odessa DIC. — Kiev, 2000. — 3 p.

Nikolaev N. I. Contemporary tectonics and geodynamics of the lithosphere. — Moscow: Nedra, 1988. — 491 p.

Ryaboshtan Y. S. From experience of application of emanation survey in the Donetsk pool. — Donetsk, PO Ukruglegeologiya, 1969. — 22 p.

Ryaboshtan Y. S. Methodological manual on structural-geodynamic mapping emanation method (CFS—E). — Donetsk: PO Ukruglegeologiya, 1975. — 86 p.

Sobolev E. G. Theory and practice magnetodynamic introscopy in solving engineering-geological and environmental problems (monograph). — Donetsk: Chestnut, 2004 — 264 p.

Sobolev E. G., Vysotyuk V. A. Site Engineering geodynamic zoning be built array: geodynamic causes of accidents, destruction and flooding of civil and industrial facilities // Ecology Environmental and safety. — Kiev: Knowledge, 2007. — № 2. — P. 36—40.

Sobolev E. G., Vysotyuk V. A. Technological features geodinamichemskogo mapping of the surface layers of the Earth by the method SSIE "Mars" // Proc. 6th NPC "Engineering protection of territories and objects in connection with the development of hazardous geological processes", 05—09.10.09, Crimea, Yalta. — SPC Ekologiya. Nauka. Technika. — 2009. — P. 35—37.

Sobolev E. G., Vysotyuk V. A. The influence of geodynamic zoning—based successful monitoring of the coastal array of rocks // Proc 4th RPC "Monitoring of the environment: scientific and methodological, regulatory, technical, software", 21—25.09.09, Crimea, Koktebel. — SPC Ekologiya. Nauka. Technika. — 2009. — P. 12—13.

Sobolev E. G., Vysotyuk V. A., Dolzhikov P. N. One geodynamic mechanism of the processes of flooding and landslides, soil (rock) arrays // Proc. 5th NPK Underflooding. 11—15.06.09, Berdyansk Zaporozhye region. — SPC Ekologiya. Nauka. Technika. — 2007. — P. 22—24.

Sobolev E. G., Vysotyuk V. A., Voyevoda B. I., Zhivora V. F., Schugorev V. A., Varvarovsky V. B., Klyuyko V. Ya. The need for radical additions and changes in building construction regulations and "DBN" Ukraine // Ecology Environmental and safety. — Kiev: Knowledge, 2007. — № 3. — P. 56—59.

Strakhov V. N., Starostenko V. I., Kharitonov O. M., Aptikaev F. F., Barkovsky E. W., Kedrov O. K., Kendzera A.W., Kopnichev Yu. F., Omelchenko W. D., Palienko W. P. Seismic phenomena in the vicinity of Chernobyl // Geophys. J. — 1997. — **19**, № 3. — P. 3—15.

Tyapkin K. F. Physics of the Earth. — Kiev: Vishcha Shk., 1998. — 312 p.

Vysotyuk V. A., Sobolev E. G. Geodynamic factor and its role in the formation of landslides in the hillside areas of terrain // Proc. 5th NPK impact of devastating floods, floods, dangerous geological processes on the functioning of utilities and life safety, 23—27.02.09, Yaremche Ivano-Frankivsk region. — SPC Ekologiya. Nauka.Technika. — 2009. — P. 92—93.

Vysotyuk V. A., Sobolev E. G. On improving methods to predict emergencies caused by geodynamic processes // Proc. Intern. NPK "Problems of Forecasting and prevention of natural disasters, natural and man-made and man-made origin, 05—09.10.09, Crimea, Yalta. — SPC Ekologiya. Nauka. Technika. — 2009. — P. 62—64.

Geodynamics of lithosphere as one of the crucial factors of mineral deposits formation of Ukraine

© V. Starostenko, O. Gintov, R. Kutas, I. Pashkevich, 2010

Institute of Geophysics, National Academy of Sciences of Ukraine, Kiev, Ukraine
earth@igph.kiev.ua
kutro@ndc.org.ua
oleg.gintov@gmail.com; innap@34mail.ru

Comprehensive studies of the lithosphere structure of Ukraine have been performed lately at the Institute of Geophysics NASU in connection with solving the problems of metallogeny, diamond-, gas- and oil-bearing [Starostenko et al., 2007]. These studies included: thourough analysis of geological-geophysical data on tectonics and deep structure of the Earth's crust and upper mantle; plotting the comprehensive three-dimensional geophysical and geodynamic model of lithosphere; generalization of global experience in application of geophysical, including tectonophysical, methods for the search and prospecting of different kinds of mineral deposits. The results of studies allow drawing some conclusions on the character of geodynamic processes, having an influence on formation and distribution of deposits on the territory of Ukraine.

It has been shown by the examples of the Ukrainian Shield, the Dnieper-Donets, the Carpathian and Azov-Black Sea oil-gas-bearing provinces that the regularities of formation, redistribution and concentration of mineral deposits are determined in many cases by special features of tectonosphere evolution arising from the mechanisms of global and regional movements of lithosphere plates.

The Ukrainian Shield (USh). Practically all large fault zones of the USh are *zones of shift with* acute predominance of horizontal component of banks displacements [Gintov, 2005]. They were arised in Neo-Archean and Early Proterozoic as right and left shifts, strike-slip and upthrow faults with amplitude of displacement as kilometers and tens of kilometers and transcending far beyond the limits of the Shield. Their roots according to different geophysical characteristics are relaited to in the mantle up to the depth of 100—200 km and more [Gintov, Pashkevich, 2010]. Existence of such ancient extensive zones of shift may be only explained by convective movements in the mantle, which took place as early as in Neo-Archean and Early Proterozoic. In Proterozoic numerous fault zones were also formed as listric ones or gently sloping overthrust.

According to the results of tectonophysical and paleomagnetic studies of dynamics of lithosphere of the USh a conclusion has been drawn that the Shield as a consolidated structure has existed since the boundary of 1.8—1.6 Ga. According to paleomagnetic data [Elming et al., 1998], it existed before and moved autonomously and even earlier, according to tectonophysical data [Gintov, Pashkevich, 2010], it was divided into several megablocks, which had their own trajectories of movements.

Joint analysis of kinematic and three-dimensional geophysical model of the Shield as well as of V_P tomographic model of the mantle up to the depth of 850 km [Geyko et al., 2006], allows to correlate the results of metallogenic studies of fault zones of the USh with materials of geodynamic reconstructions. Within the limits of the USh more than 75 percent of known metallogenic zones, ore areas and ore fields belong to well studied large fault zones. These are mainly the areas of development of mineralization and deposits of non-ferrous, rare, noble metals, uranium, rare earths et al. [Starostenko et al., 2007].

Dnieper-Donets oil-gas province (DDOGP). Numerous oil-gas deposits within non-anticline, the so-called "non-traditional" traps — on monoclines, half-anticlines, sub-thrust zones, within crystalline basement etc. have been discovered here lately. The majority of such deposits are related to the fractures of fault-, shift and upthrow (shear) fault types. These considerations brought a lot of scientists to the idea of great perspectives of anorganic hypothesis of oil origin and of important role of tangential forces and horizontal movements of lithosphere in formation of traps for hydrocarbons.

Numerical modeling of the process of the Dnieper-Donets aulacogene (DDA) formation by the back-stripping method within the limits of continental lithosphere stretching concept of D. McKenzie testifies the possibility of its formation in the Late

Devonian by the type of rift basins with formation of sub-oceanic crust [Stifenson et al., 1997]. Important role has been proved of shifting processes in formation of contemporary structure of DDOGP and of many types of oil-gas deposits. The system of faults of the DDA manifested during Alpine time as the largest right shift, which is the result of super-regional sub-longitudinal contraction, which covered during Meso-Cenozoic time the territories of the south and south-west of the East-European Platform (EEP). The explanation can be found in the known plate tectonic reconstructions: the pressure on the EEP from the south as a result of movements of the African and Arabian plates is passed through West-Black Sea and East Black Sea micro-plates [Nikishin et al., 2001; Patalaha et al., 2003; Kazmin et al., 2004].

The suture zone of the Donets Folded Structure (DFS) with the south slope of the Voronezh crystalline massif (Starobelsk-Millerov monocline) can be considered as an example of the influence of the processes of compression and shifting upon formation of hydrocarbon deposits. The suture zone is revealed by the series of over-thrusts of Carboniferous-Cretaceous deposits of the DFS upon the monocline — Krasnopopovskiy, Severodonetskiy, Marievskiy, Almaznyi, Iliychevskiy and other ones. Here, within the stripe not less than 50 km wide, a whole set of non-anticline type deposits within the limits of the monocline itself, in Krasnorechensk and Lisichansk gas-bearing areas have been discovered [Gintov, 2005; Starostenko et al., 2009].

The Carpathian Meso-Cenozoic Oil-Gas Province (COGP) is characterized by over-thrust structure of the Meso-Cenozoic strata, doubled and tripled cross-section of the Cretaceous, Paleogene and Neogene, is considered by the majority of geologists and geophysicists from the positions of plate tectonics.

According to the data of seismic tomography high-velocity lithosphere of EEP sinks under relatively low-velocity mantle of the Volyno-Podolian plate and the Carpathians from the depth of 50 to 250—300 km [Geyko et al., 2006].

It has been found by geothermic studies [Kutas, 2005] that for deposits and the areas of oil-gas accumulation, concentrated within the limits of Pre-Carpathian depression (in this case within the External zone of depression gas and gas-condensate deposits predominate, and within Internal one — oil deposits), increased temperature and heat flows are specific. Deposits form two stripes, narrow enough in zones of Carpatian direction Pre-Carpathian and Scole faults which are at a distance of 20—30 km from each other.

In the periphery of EEP accumulation of hydrocarbons in the deposits of accretion wedge could occur as early as Cretaceous and Paleogene. During collision stage redistribution of hydrocarbon potential occurred. Migration processes influenced essentially on hydrodynamic conditions, thermal regime, physical parameters of sedimentary strata. These parameters can be used for determination of the ways of migration and zoning of oil-gas areas.

With the help of numerical tectonophysical modeling the connection of formation and distribution of oil-gas deposits COGP with plate-tectonic mechanism of region formation has been analyzed [Gonchar, 2007]. Palinspastic sections of the frontal part of the Flish Carpathians and Pre-Carpathian depression have been complited. They reconstruct the process of formation of deposits under conditions of lateral accretion and formation of covers in case of obduction-subduction mechanism and explain zoning in distribution of oil and gas deposits within Pre-Carpathian depression.

Application of modern geodynamic concepts of the Carpathian region formation allows considerable widening of its perspectives of oil- and gas-bearing. North-western part of the External zone of Pre-Carpathian depression (Krukenitskaya sub-zone), autokhtonous deposits of Folded Carpathians, platform Meso-Cenozoic deposits of south-eastern part of External zone under the over-thrust of the Folded Carpathians, Trans-Carpathian depression are worth to be paid special attention.

Azov-Black Sea Oil-Gas Province (ABSOGP). A considerable part of the Province is located within the water areas. Therefore analysis of geodynamic processes in it is possible only on the background of geodynamic development of the whole Black Sea-Caucasian segment of the Alpine belt.

ABSOGP and COGP have got some common geophysical peculiarities. It allows treating them from similar geodynamic positions. ABSOGP adjoins to the southern tectonic border of EEP and here, as well as in the COGP, according to the data of seismic tomography [Geyko et al., 2006] submergence can be observed of relatively high-velocity lithosphere of the Craton under relatively low-velocity mantle of Dobrogea, Scythian plate, the Black Sea. The studies of geothermal regime of the region shows that oil-gas deposits are localized within the areas of increased heat flows, forming in this case two sub-parallel stripes: gas deposits are located within the zones of high heat flows and the oil ones — in their periphery. The important role is played by tectono-thermal activization in case of shift displacements of micro-plates [Kutas et al., 2002; 2007].

For the studies of ABSOGP conditions of formation the main interest belongs to Oligocene-Quaternary stage, which began 35—40 million years ago. The results of geothermal studies in the region show that for this period there is strong enough correlation between location of oil-gas deposits and anomalies of heat flow [Kutas et al., 2002; 2007]. At this stage the Black Sea — Caucasian region develops in the indentor regime under the action of Arabian, Pannonian and Adriatic plates [Patalaha et al., 2003]. In addition, the movement of the Black Sea plate within northern points of compass was of reverse character that is indicated by tectonophysical data on the Crimean peninsula: the phases of sub-longitudinal contraction was interrupted by shorter phases of even stretching [Gintov, 2005].

For promising areas of ABSOGP — north-western shelf of the Black Sea and the Kerch-Tamanian depression the detailed schemes of fault tectonics of consolidated crust have been compile [An integrated …, 2006]. They emphasize the leading role of shift deformations during formation of fault and fold structures of the Meso-Cenozoic cover, to which (especially to the knots of fault crossing) hydrocarbon deposits are related. It has also been found by marine geophysical studies that zones of deep faults and neo-tectonic disturbances connected with them are the channels of migration of gas-fluid flows [Kobolev, Kutas, 1999].

References

An integrated three-dimensional geophysical model of the lithosphere of the Ukrainian Shield in connection with magmatism, tectonics and the formation of minerals // Report of the Institute of Geophysics by S.I. Subbotin of NASU / Ed. V. I. Starostenko. — Kiev, 2006. — 510 p. — Fund of UkrNIINTI, № state registration 102U002478 (in Russian)

Elming S. A., Mikhailova N. P., Kravchenko S. N. The Ñonsolidation of the East European Craton; a Paleomagnetic Analysis of Proterozoic Rocks from the Ukrainian Shield and Tectonic reconstructions Versus Fennoscandia // Geophys. J. — 1998. — **20**, № 4. — P. 71—74 (in Russian).

Geyko V. S., Shumlanskaya L. A., Bugaenko I. V., Zayets L. N., Tsvetkova T. A. Three-dimensional model of the upper mantle of Ukraine on the arrival time of *P*-waves // Geophys. J. — 2006. — **28**, № 1. — P. 3—16 (in Russian).

Gintov O. B. Field tectonophysics and its application in studying the crustal deformation of Ukraine. — Kiev: Phoenix, 2005. — 572 p. (in Russian).

Gintov O. B. Tectonophysics in solving important economic problems (review of research in the CIS countries) .1 // Geophys. J. — 2009. — **31**, № 5. — P. 3—31 (in Russian).

Gintov O. B., Pashkevich I. K. Tectonophysical analysis and geodynamic interpretation of the three-dimensional geophysical model of the Ukrainian Shield // Geophys. J. — 2010. — **32**, № 2. — P. 3—27 (in Russian).

Gonchar V. V. Rheological control of the accretion and cover styles of deformation and stress state of suprasubduction orogen // Geophys. J. — 2007. — **29**, № 6. — P. 116—137 (in Russian).

Kazmin V. G., Lobkovsky L. I., Pustovitenko B. G. Contemporary kinematics of the microplates in the Black-sea-South-Caspian region // Okeanology. — 2004. — **44**, № 4. — P. 600—610 (in Russian).

Kobolev V. P., Kutas R. I. Geophysical researches of gas release structures on the northwestern part of the Black Sea // Tectonics and oil- and gas-content of the Azov-Black-sea region. — Simferopol, 1999. — P. 53—55 (in Russian).

Kutas R. I. Geodynamic processes and thermal state of lithosphere of the Carpathian region // Research of modern geodynamics of the Ukrainian Carpathians. — Kiev: Nauk. dumka, 2005. — P. 132—139 (in Russian).

Kutas R. I., Kobolyev V. P., Paliy S. I. Geothermal conditions and oil- and gas bearing of the North-Black-sea — Ciscaucasian region // Oil and Gas Industry. — 2002. — № 5. — P. 9—11 (in Russian).

Kutas R. I., Kravchuk O. P., Bevzyuk M. I., Stakhova L. I. Results of geothermal studies in the northern part of the Black Sea // Geophys. J. — 2007. — **29**, № 4. — P. 45—65 (in Russian).

Nikishin A. M., Korotayev M. V., Bolotov S. N., Yershov A. V. Tectonic history of the Black-sea basin // BMOIP. — 2001. — **76**, issue 3. — P. 3—17 (in Russian).

Patalakha E. I., Gonchar V. V., Senchenkov I. K., Chervinko O. P. Indenter mechanism in geodynamics of the Crimean-Black-sea region. Forecast of HC and seismic hazard. — Kiev: Publishing house PP "EMKO", 2003. — 226 p. (in Russian).

Starostenko V. I., Gintov O. B., Pashkevich I. K., Burakhovich T. K., Kulik S. N., Kuprienko P. Ya., Makarenko I. B., Orlyuk M. I., Tsvetkova T. A. Regularities in the distribution of ore mineral deposits in con-

nection with the deep structure and dynamics of the lithosphere of the Ukrainian Shield // Geophys. J. — 2007. — **29**, № 5. — P. 3—34 (in Russian).

Starostenko V. I., Lukin A. E., Kobolyev V. P., Rusakov O. M., Orlyuk M. I., Shuman V. N., Omelchenko V. D., Pashkevich I. K., Tolkunov A. P., Bogdanov Yu. A., Burkinsky I. B., Loiko N. P., Fedotova I. N., Zakharov I. G., Chernyakov A. M., Kuprienko P. Ya, Makarenko I. B., Legostayeva O. V., Lebed T. V., Savchenko A. S. Model of deep structure of the Donets folded construction and surrounding structures according to the regional geophysical observations // Geophys. J. — 2009. — **31**, № 4. — P. 44—68 (in Russian).

Stephenson R. A., Van Weiss Ja. D., Stovba S. N., Shymanovsky V. A. One-dimensional numerical modeling of tectonic immersion of DD within the concept of extension of the continental lithosphere by Mac Kenzie // Geophys. J. — 1997. — **19**, № 3. — P. 25—41 (in Russian).

Deep structure and geodynamics of the Kirovograd ore district (Ukranian Shield): correlation of geological and seismic data

© *V. Starostenko[1], V. Kazansky[2], G. Drogitskaya[1], N. Popov[1], A. Tripolsky[1], 2010*

[1] Institute of Geophysics, National Academy of Sciences of Ukraine, Kiev, Ukraine
earth@igph.kiev.ru
[2]Institute of Geology of Ore Deposits, Petrography, Mineralogy and Geochemistry, RAS, Moscow, Russia
director@igem.ru

The central part of the Ukrainian shield, where the Kirovograd ore district is located, has been the subject of prolonged investigation of the Institute of Geophysics in cooperation with another research Institutions. Around 20 years ago, A. V. Chekunov et al. (1989) proposed a geodynamic model of this territory, derived from geophysical and geological data. The model is illustrated by the geotraverse VIII Odessa — Krivoy Rog, which intersects the Kirovograd (now Ingulets) lithospheric block and adjacent protogeosynclines (Fig. 1). The Kirovograd block is distinguished from them in seismic velocities in crust and at the Moho discontinuity and in thickness of the crust (35—38 km against 54—58 km). The block is cut by steep faults and gentle tectonic zones which extend into upper mantle. The suggested model explained these phenomena by the continuous development of a mantle plume or a protoasthenolite, which originated at the beginning of Early Proterozoic, influenced the deposition of the ingulo-ingulets series and caused the emplacement of granites, anorthosites and rapakivi granites in crust at the mature stage.

The current study of deep structure of the Kirovograd ore district [Starostenko et al., 2010], is based on the correlation of geological and seismic data, using modern technologies, and accounts for new isotopic dating [Shcherbak et al., 2008]. The study proceeds from a broad interpretation of space boundaries of the Kirovograd polymetal ore district and the incorporation of uranium, lithium, gold and titanium deposits in these boundaries (Fig. 2).

The study indicates that in the Kirovograd ore district, the Paleoproterozoic magmatism started after deposition of the ingulo-ingulets series and developed in two short-lived (30—40 Ma) stages. During the first stage (2.06—2.02 Ga), the crustal Novoukrainsk-Kirovograd granitoid massif formed. During the second stage (1.75—1.72 Ga), the mantle-derived Korsun'-Novomirgorod rapakivi-anorthosite massif originated. In conjunction, they constitute the Novoukrainsk-Korsun'-Novomirgorod pluton which defines the surface structural pattern of the ore district.

Lithium, uranium and gold deposits are located in the Novoukrainsk-Kirovograd granitoid massif and the connected Kirovograd and Zvenigorod fault zones [Bakarzhiev et al., 2005]. Lithium deposits are close in age (2.0 Ga) to the Novoukrainsk-Kirovograd massif and associated with local granite-migmatite domes. Uranium deposits are dated at 1.8 Ga, overprinted on the massif and controlled by its rejuvenated structural elements. Gold deposit's age is unclear. In combination, the deposits outline a wide

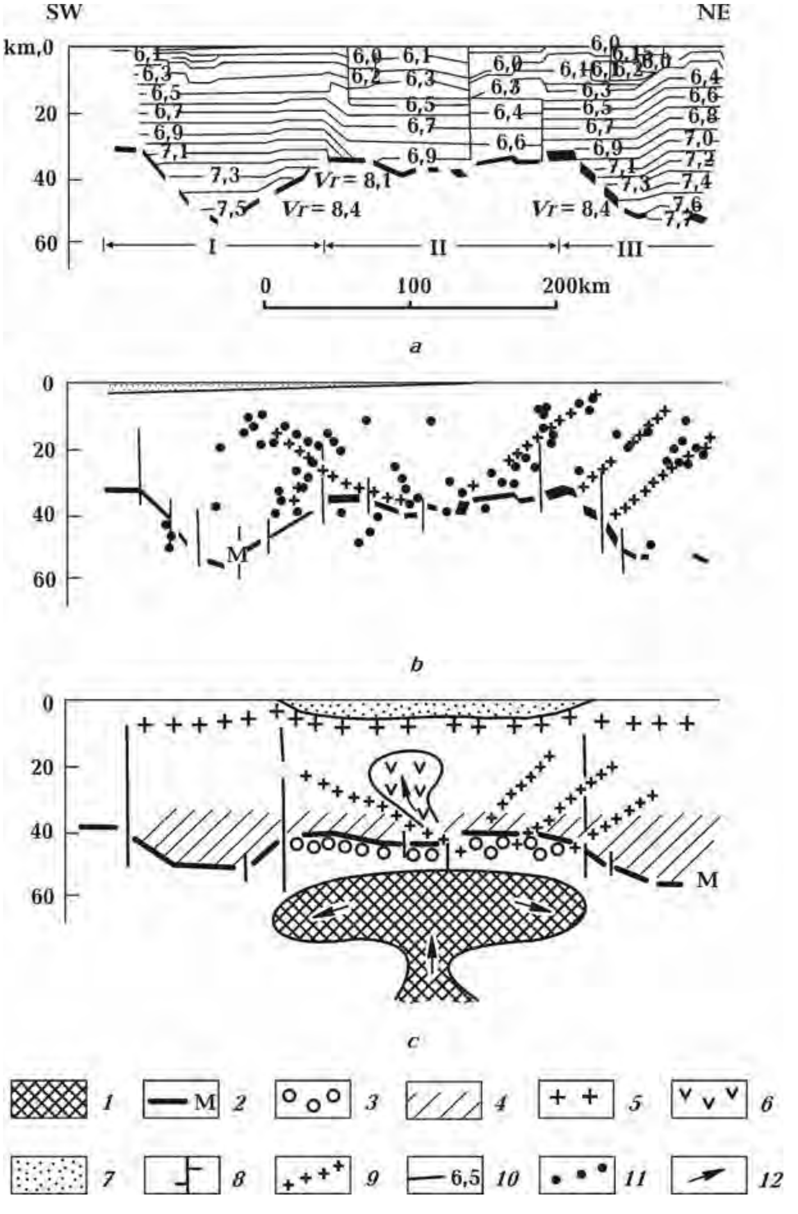


Fig. 1. Deep structure of the Kirovograd lithospheric block along the geotraverse VIII (modified after Chekunov et al., 1989): *a* — velocity section, *b* — seismic section, *c* — geodynamic section *(1* — protoasthenolite; *2* — Moho discontinuity; *3* — zone of the matter transformation at the crust-mantle boundary; *4* — basaltic layer; *5* — crystalline basement; *6* — mantle-derived magmatic rocks in crust; *7* — sediments; *8* — faults; *9* — gentle thrusts; *10* — seismic velocities (km/s); *11* — diffraction points; *12* — direction of the matter transfer); I — Odessa-Yadlov protogeosyncline; II — Kirovograd lithospheric block; III — Krivoy Rog protogeosyncline.

(30—35 km) longitudinal band going in parallel to the Subbotin-Moshorin fault zone and across the Novoukrainsk-Korsun'-Novomirgorod pluton. It was previously assumed that within the latitudinal band, the uranium deposits and host rocks had been subsided by east-west faults that preserved them from erosion [Genetic …, 1995]. Nowadays the band is related to a deep sublatitudinal trough in the Moho discontinuity relief (Fig. 3). The discovery is the first to establish the spatial association of Paleoproterozoic hydrothermal ore deposits with a middle-scale anomaly of the crust-mantle boundary [Starostenko et al., 2007].

The Korsun'-Novomirgorod rapakivi-anorthosite massif is devoid of Li, U, Au deposits and contains titanium mineralization of magmatic origin. Where-

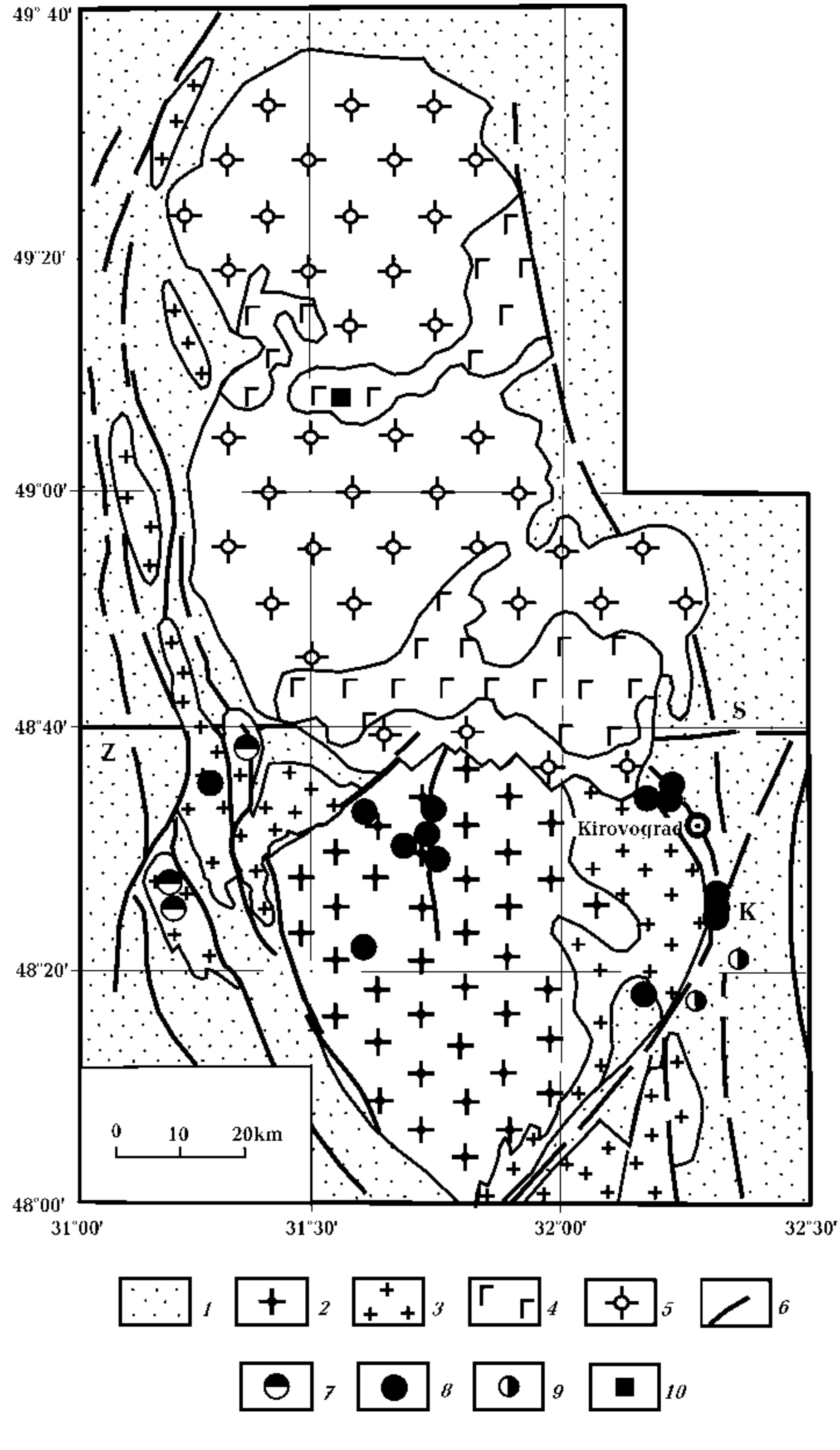


Fig. 2. Geological map of the Kirovograd polymetal ore district (modified after Starostenko et al., 2010): *1* — stratified ingulo-ingulets series; *2*, *3* — Novoukrainsk-Kirovograd massif (*2* — diorite-monzonite complex, *3* — granite-migmatite complex); *4*, *5* — Korsun'-Novomirgorod massif (*4* — gabbro-anorthosites, *5* — rapakivi granites); *6* — faults; *7—10* — ore deposits (*7* — lithium, *8* — uranium, *9* — gold, *10* — titanium). Fault zones: K — Kirovograd, S — Subbotin-Moshorin, Z — Zvenigorod.

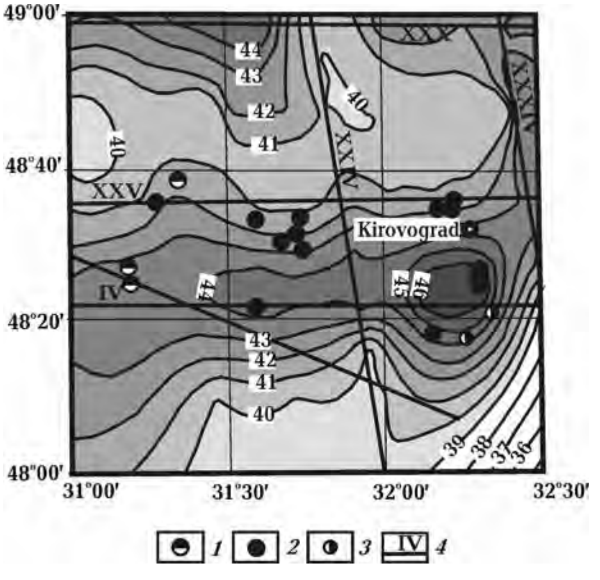


Fig. 3. Projection of ore deposits on the Moho discontinuity relief (depth isolines in km): *1*—*3* — ore deposits (*1* — lithium, *2* — uranium, *3* — gold); *4* — DSS profiles.

as the Novoukrainsk-Kirovograd massif and the ingulo-ingulets series build up an intrusive-ultrametamorphic basement of the district, the autonomous Korsun'-Novomirgorod massif is inserted in the basement. By seismic methods, the first is traced to a depth of 15—20 km, the second to a depth of 40—50 km, that is below the Moho boundary (Fig. 4). Against this background seismic anomalies are interrupted over and below the mantle trough. It should be emphasized that this seismic "gap" extends from the surface into the upper mantle.

The above-listed geological, age and seismic data suggests that the Kirovograd ore district developed under three different geodynamic environments (Fig. 5). The first was marked by the formation of the Novoukrainsk-Kirovograd granitoid massif as a constituent of the intrusive-ultrametamorphic basement, the second resulted in the tectonic activization of the basement, the third was dominated by the emplacement of the Korsun'-Nowomirgorod rapakivi-anorthosite massif. Taking into consideration a unique combination of tectonic structures, intrusive rocks, deposits and geodynamic environments, we regard the Kirovograd ore district as a Paleoproterozoic center of intense conjugated mantle-crust magmatism and endogenous ore formation.

The work is performed according to a research agreement between IGPH and IGEM and supported by the program P-22 Rassian Academy of Sciences.

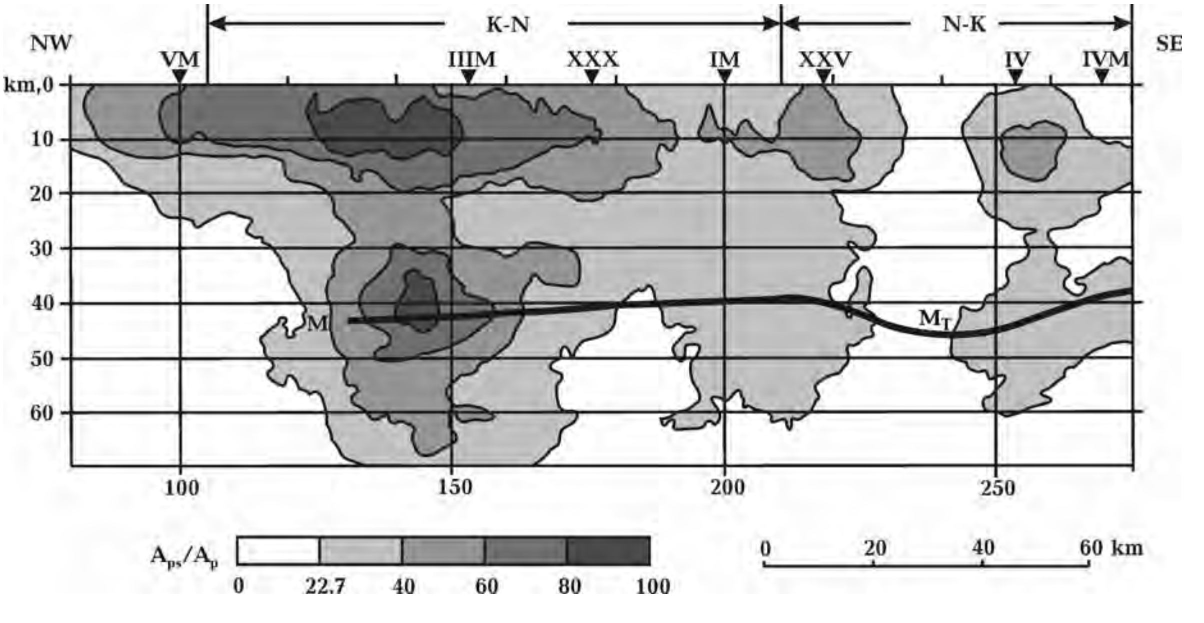


Fig. 4. Convertability of environment by MCWE data along vertical section of the Novoukrainsk-Korsun'-Novomirgorod pluton. A_{PS}/A_P — ratio of the converted wave amplitude to same of *P*-wave generates by former one. K-N — Korsun'-Novomirgorod rapakivi-anorthosite massif; N-K — Novoukrainsk-Kirovograd massif; M — M discontinuity; M_T — mantle trench. VM, IIIM, IVM — intersection points by deep sections along MCWE profiles; XXX, XXV, IV — intersection points by deep sections along DSS profiles.

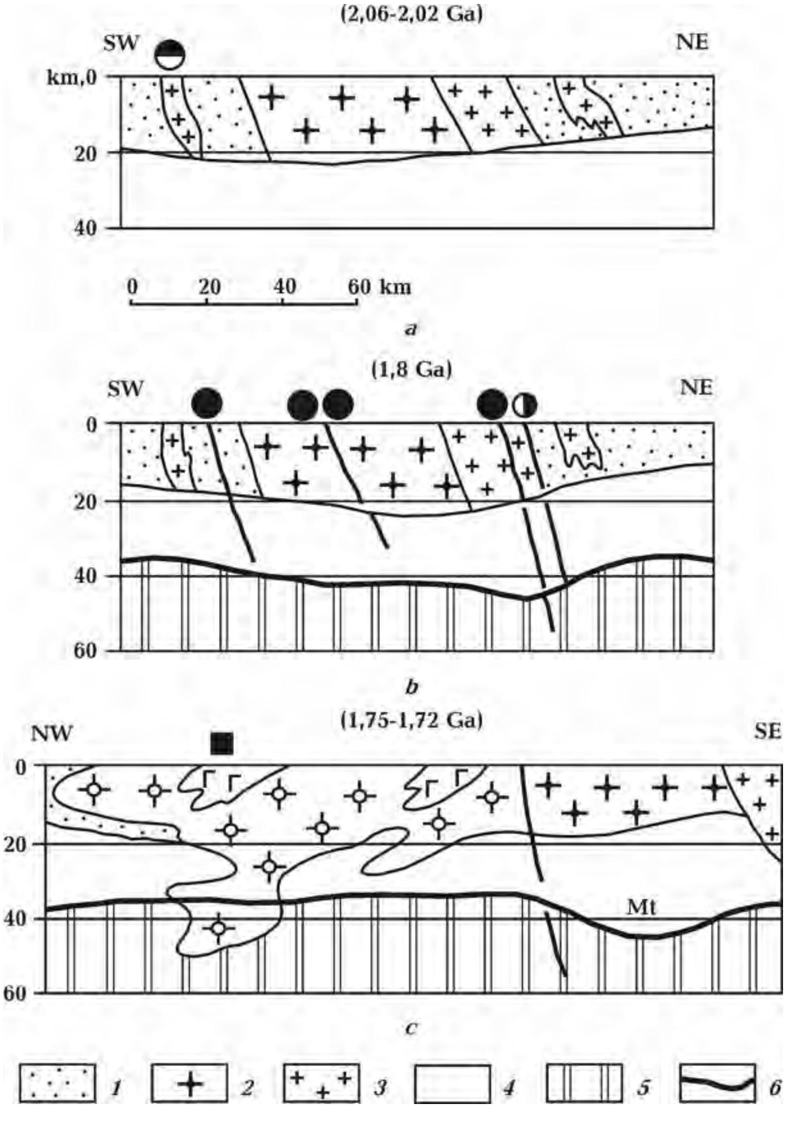


Fig. 5. Geodynamic and metallogenic evolution of the Kirovograd ore district: *a* — formation of the intrusive-ultrametamorphic basement and lithium deposits; *b* — tectonic activization of the basements and metasomatic uranium ore formation; *c* — emplacement of mantle-derived anorthosites and rapakivi granites accompanied by titanium mineralization. Figure captions: *1—3* — intrusive-ultrametamorphic basement (*1* — stratified ingulo-ingulets series; *2* — diorite-monzonite complex; *3* — granite-migmatite complex); *4* — middle-low crust; *5* — upper mantle; *6* — Moho boundary; Mt — mantle trough. For other captions see Fig. 2.

References

Bakarzhiev A. Kh., Makivchuk O. F., Popov N. I. Development of mineral-resource base of Ukraine // Razv. okhr. nedr. — 2005. — № 10. — P. 50—58 (in Russian).

Chekunov A. V., Sollogub V. B., Galetskii L. S., Kurlov N. S. Geodynamic model of the central part of the Ukrainian shield and the Krivoy Rog superdeep borehole // Geophys. J. — 1989. — **11**, № 4. — P. 3—13 (in Russian).

Genetic types and occurance mode of uranium deposits of Ukraine / Eds. Ya. N. Belevtcsev, V. B. Koval. — Kiev: Nauk. dumka, 1995. — 396 p. (in Russian).

Shcherbak N. P., Artemenko G. V., Lesnaya I. M., Ponomarenko A. N. Geochronology of Early Precambrian of the Ukrainian shield. Proterozoic. — Kiev: Nauk. dumka, 2008. — 299 p. (in Russian).

Starostenko V. I., Kazansky V. I., Drogitskaya G. M., Makivchuk O. F., Popov N. I., Tarasov N. N., Tripolsky A. A., Sharov N. V. Relationships of surface structures of the Kirovograd ore district (Ukrainian shield) with local heterogeneities of the crust and the Moho discontinuity relief // Geophys. J. — 2007. — **29**, № 1. — P. 3—21 (in Russian).

Starostenko V. I., Kazansky V. I., Popov N. I., Drogitskaya G. M., Zayats V. B., Makivchuk O. F., Tripolsky A. A., Chicherov M. V. From surface structures to the integrated deep model of the Kirovograd ore district (Ukrainian shield), I // Geophys. J. — 2010. — **32**, № 1. — P. 3—33 (in Russian).

Variations in the crustal types of the Dnieper-Donets Basin and surrounding areas from 3D gravity modelling

© V. Starostenko, P. Kuprienko, I. Makarenko, O. Legostaeva, A. Savchenko, 2010

Institute of Geophysics, National Academy of Sciences of Ukraine, Kiev, Ukraine
irinam@igph.kiev.ua

There are two reasons for constructing a new three-dimensional density model of the Dnieper-Donets Basin (DDB) and surrounding areas. 1) A lack of reliable data on the structure of the deep horizons in the sedimentary cover and crystalline crust. 2) Recently fresh geological and geophysical data have been obtained for the upper sedimentary layers (up to depths of 5—6 km) from seismic data (DSS and MCSP) along the DOBRE1 and DOBRE2 profiles [Grad et al., 2003, Maystrenko et al., 2003].

In this study modern software has been applied [Starostenko et al., 1997; 2004]. It has a principal advantage over standard approaches because density maps of individual layers are automatically input into a PC, enabling geological environments to be approximated very accurately. A technique of constructing a 3D model and converting it into a schematic map of layers types are described in detail elsewhere [Kuprienko et al., 2007].

3D modelling has resulted in a new pattern of the density for the whole crust of the DDB and surrounding areas. It has been used to compile schematic maps for a thickness of the "granitic, "dioritic" and "basaltic" layers (the upper, middle and lower crust). Earlier based on the generalization of relationships of velocity vs. depth and density vs. velocity for different types of the crust, it has been put forward a conditional subdivision of the whole crust into three stages without sharp boundaries between them. They have been defined as the upper, middle and lower crust. Due to traditions they have been named as "granitic, "dioritic" and "basaltic" layers. Their parameters are as follows: 1) ρ<2.75 gcm^{-3}, V_P<6.30 kms^{-1}; 2) ρ=2.75÷2.90 gcm^{-3}, V_P=6,30÷÷6,80 kms^{-1}; 3) ρ>2.90 gcm^{-3}, V_P>6.80 kms^{-1} respectively. Petrologically the first range of the parameters is a mixture of acid and intermediate rocks. The second series is composed of a mixture of intermediate and basic rocks (granodiorites, diorites, charnokites, many gneisses, shists, metabasic rocks, and gabbroids). The third row consists of intrusive rocks of basic and ultrabasic composition and metamorphic rocks (granulites, amphibolites) [Lithospheric …, 1993].

A relationship of a thickness of each layer to a total thickness of the crust demonstrates the contribution of each layer into a total thickness of the crust. The name of the crustal type corresponds to prevailing portion of any layer.

The portion of "granitic" layer (Fig. 1, *a*) within the DDB iz characterized by a ratio of 0—0.4. The highest values correspond to the southern flank of Poltavskii megabloc (0.4), the northern side and the southern preflank zone of the Lokhvitskii and Poltavskii megablocs, as well as most of the northern flank, where the percent ratio is 0,3. The smallest proportion of the layer belongs to the central zone of megablocs (0.0—0.1). On the rest of the areas layer portion is 0.0—0.2.

The portion of "dioritic" layer (Fig. 1, *b*) is the largest in the south of the DDB, in south-east of the northern flank, in the central zone and southern preflank zone of the Chernigovskii, and Poltavskii and Lokhvitskii megablocs (0.4—0.5). A small portion of this layer occurres in the southeastern part of the central zone of the Iziumskii megabloc and in the north-western Donbass (0.0—0.1). The rest of the area is characterized by the values of 0.2—0.3.

The maximum portion of the "basalt" layer (Fig. 1, *c*) is associated with the north-western Chernigovskii megablock and the north-western part of the central zone in the Lokhvitskii megabloc, the south-eastern Iziumskii megablock and the whole Donbass (0.5—

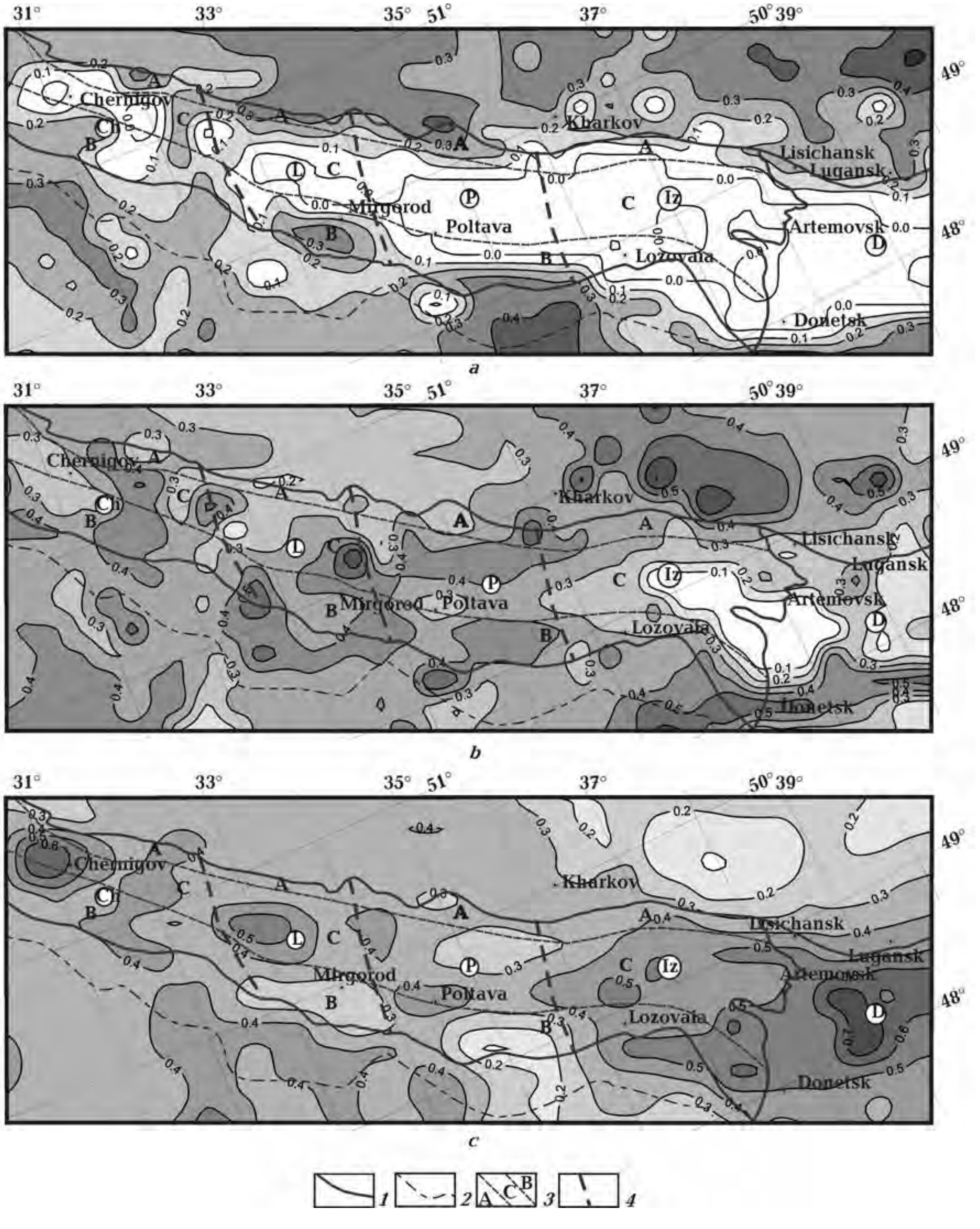


Fig. 1. Contribution of the "granitic" (*a*), "dioritic" (*b*) and "basaltic" (*c*) layers to a whole thicness of the crust in the Dnieper-Donets Basin and Donbass: *1* — the boundary of the DDB; *2* — the boundary of the northern flank of the DDB; *3* — the longitudinal division of the DDB (after Arsiriy et al., 1984) *zones*: A — northern flank, B — sothern flank, C — Central; *4* — the transversal division of the DDB (after Dolenko and Varich, 1989) *megablocks:* Ch — Chernigovskii, L — Lokhitskii, P — Poltavskii, Iz — Iziumskii, D — Donbass.

0.7). The smallest ratio of the layer (0.2) is related to the southern preflank zone of the Poltavskii megabloc and the northern edge of the Iziumskii megablock. In the rest of area the ratio is 0.3—0.4.

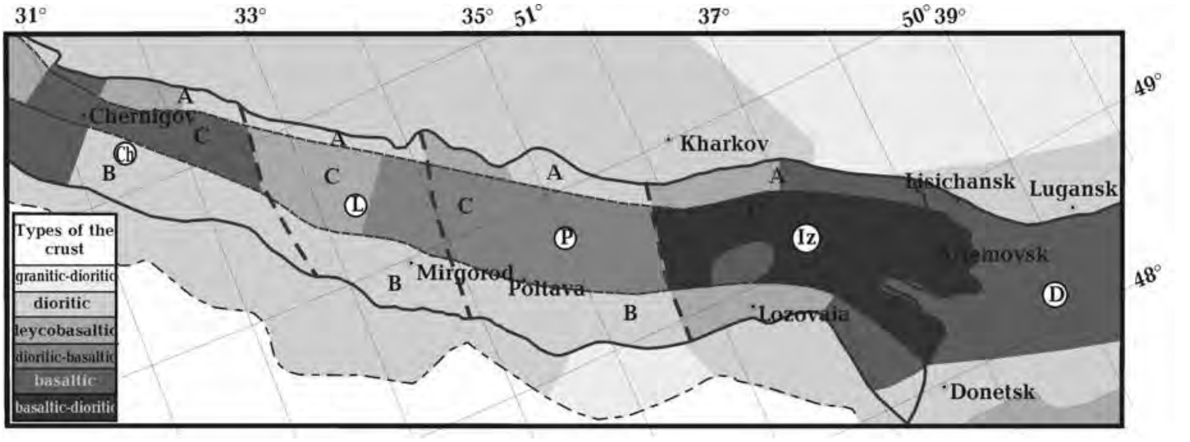


Fig. 2. Schemetic map of prognostic composition of the Earth's crust in the DDB and Donbass from 3D gravity modelling. See Fig. 1 for conventions.

Based on this information, six types of the crust are determined for the DDB and Donbass (Fig. 2).

The granitic-dioritic crustal type has the smallest distribution which mainly occurs on the southern flank of VCM (the Svatovo-Troitskii, Rossoshanskyii blocks). Its small massif occurs on the northern flank of the Ush (the southern flank of the Poltavskii megablock).

The dioritic type of the crust is distributed in the northwest and central parts of the southern slope of VCM, in the southeast of the northern flank zone of the Chernigovskii and Poltavaskii megablocs, in the northern flank zone of the Lokhvitskii block, in almost whole southern flank zone, on the southern edge, as well as in northern and southern Donbass.

Leykobazaltic type of the crust is characteristic of the north-western Chernigovskii and Lokhvitskii megablocs, north-western parts of the northern flank zone in the Chernigovskii, Poltavskii, Iziumskii megablocs, as well as the north-western portion of the southern flank zone of the Iziumskii megabloc.

Dioritic-basaltic type dominates in the central region of Poltavskii and the south-east of the central zone of the Lokhvitskii megablocs.

Basaltic type of the crust is spread in the southeast of the northern and southern flank zones of the Iziumskii megabloc, the most part of Donbass, in the central zone and in the north-western part of the southern preflank in the Chernigovskii megabloc. An isometric area is present in the southern part of the central zone in the Iziumskii megabloc.

Basaltic-dioritic type of the crust occurs only in the central zone of the Iziumskiy megabloc. Its parameters are intermediate between basaltic type, which is distributed in the central part of the Donbass, and diorititic — basaltic, typical for the central zone of DDB. *A question arises whether the belt of the basalt-diorite type of the crust is the transitional zone between the DDB and Donbass?* We should like to give a positive answer to this question.

In conclusion, the granitic-dioritic type of the crust dominates in the flank zones while the basaltic and basaltic-dioritic types are spread in the central belt of the DDB and Donbass. It demonstrates the increase in basicity of the rocks from the flanks to the centre of the depression that proves an axial compaction.

References

Grad Y., Gryn' D., Guterch A., Janik T., Veller R., Lang R., Lyngsie S. B., Omelchenko V. D., Starostenko V. I., Stephenson R. A., Stovba S. N., Thybo H., Tolkunov A. DPBRE-fraction'99—velocity model of the crust and upper mantle beneath the Donbas Foldbelt (East Ukraine) // Tectonophysics. — 2003. — **371**, № 1—4. — P. 81—110.

Maystrenko Y., Stovba S., Stephenson R., Bayer U., Menyoli E., Gajewski D., Huebscher C., Rabbel W., Saintot A., Starostenko V., Thybo H., Tolkunov A. Crustal-scale pop-up structure in cratonic lithosphere: DOBRE deep seismic reflection study of the Donbas fold belt, Ukraine // Geology. — 2003. — **31**, № 8. — P. 733—736.

Starostenko V. I., Legostaeva O. V., Makarenko I. B., Pavlyuk E. V., Sharypanov V. M. On automated computering geologic-geophysical maps images with the first type ruptures and interactive regime visualization of three-dimensional geophysical models and their fields // Geophys. J. — 2004. — **26**, № 1. — P. 3—13 (in Russian).

Starostenko V. I., Matsello V. V., Aksak I. N., Kulesh V. A., Legostaeva O. V., Yegorova T. P. Automation of the computer input of images of geophysical maps and their digital modeling // Geophys. J. — 1997. — **19**, № 1. — P. 3—13 (in Russian).

Kuprienko P. Ya., Makarenko I. B., Starostenko V. I., Legostaeva O. V. 3-D density model of the Earth's crust and upper mantle of the Ukrainian Shield // Geophys. J. — 2007. — **29**, № 5. — P. 3—27 (in Russian).

Lithospheric of the Central and East Europe . Generalization of the researches results / Ed. A. V. Chekunov. — Kiev: Nauk. dumka, 1993. — 258 p. (in Russian).

Lithospheric inhomogeneity in the Black Sea from geophysical data

© V. Starostenko, I. Makarenko, O. Rusakov, I. Pashkevich, R. Kutas, O. Legostaeva, 2010

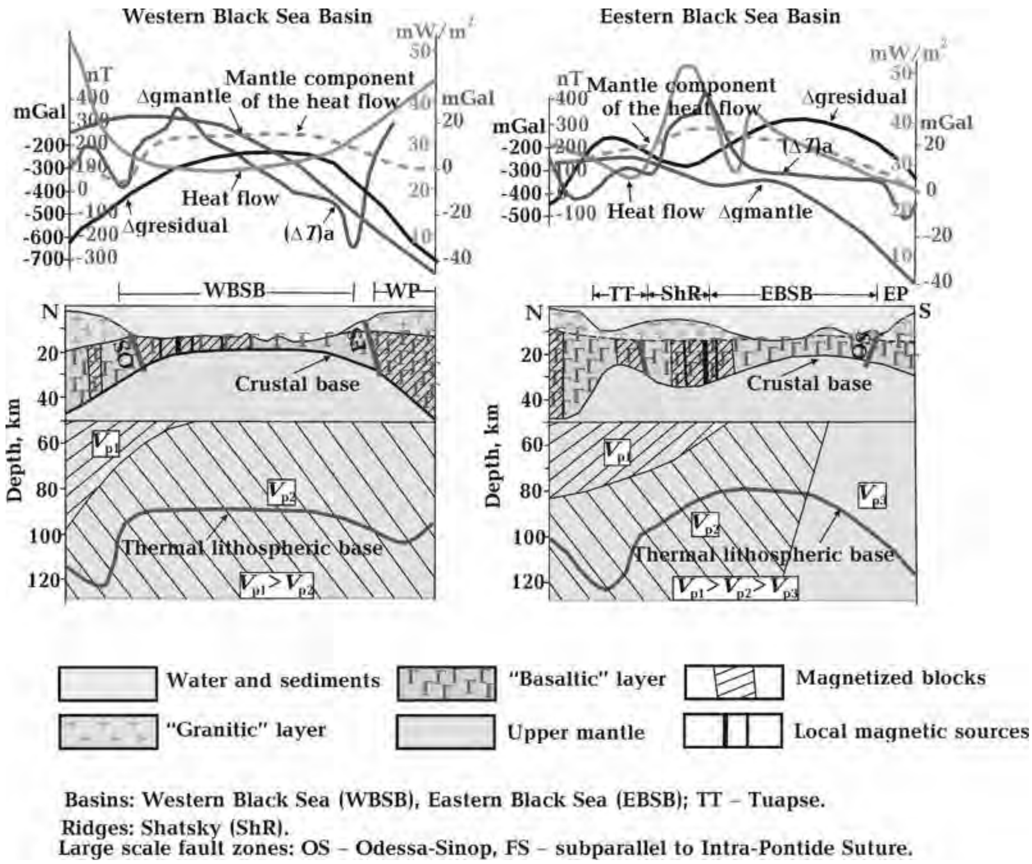
Institute of Geophysics, National Academy of Science of Ukraine, Kiev, Ukraine
irinam@igph.kiev.ua
eart@igph.kiev.ua
rusakov@igph.kiev.ua

The international interest in the Black Sea geology is based on its key role in understanding the tectonic evolution of the middle Tethyan Realm and its hydrocarbon potential. The present-day tectonic setting of the Black Sea has been mainly derived from multi-channel surveys and sparse DSS data. The available information is however insufficient to produce a coherent geodynamic model for the region.

The purpose of this study is aimed at examining the lithospheric structure and relationship between near-surface and deep features using jointly the magnetic, gravity, heat flow, seismic and tomographic data (Figure).

A first integrated analysis has resulted in a new and mutually consistent image of lithospheric density, magnetic, thermal and velocity inhomogeneities. A most detailed map of faults systems has been compiled for the consolidated crust. A substantial and important difference in the crustal and mantle structure and geophysical parameters of the Western and Eastern Black Sea basins has been revealed. The "non-granitic" crust occurs only in the central portion of the Eastern Black Sea basin whereas it spreads practically within the whole Western Black Sea basin. Heat flow is more intensive and differentiated in the Eastern Black Sea basin than in the Western Black Sea basin. The topography of the thermal lithospheric lower boundary is dome-like beneath the Eastern Black Sea basin and it is flat in the Western Black Sea basin. Different mantle seismic velocities as well as the fabric of the crustal magnetic and gravity anomalies are characteristic of the two sub-basins. Over the rift zone a distinct local heat flow anomaly is observed in the Eastern Black Sea basin. On the contrary, in the Western Black Sea Basin the rift zone is not individually manifested itself in thermal field. The low density mantle exists beneath the rift zone in the Eastern Black Sea basin whereas any distortions of a density distribution are related to similar zone in the Western Black Sea basin.

The large mantle fault zones have been delineated in the Black Sea with the prominent Odessa-Sinop fault zone, which has mostly predetermined the dissimilarities mentioned because it has divided the old continental crust into two large blocks. Orthogonality of the rifts in the Western and Eastern Black Sea basins clearly demonstrates that they have been sequentially formed as two separate tectonic units. The Western Black lithosphere has rifted earlier than that of the Eastern Black and their post-rift histories have been autonomous and individual.



Lithospheric schematic cross-sections through the Black Sea Basins from geophysical data.

Plate Tectonics from the Top-down

© D. Stegman[1], W. Schellart[2], F. Capitanio[2,3], R. Farrington[3], 2010

[1]Scripps Institution of Oceanography, University of California, San Diego, La Jolla, USA
dstegman@ucsd.edu
[2]School of Geosciences, Monash University, Melbourne, Australia
wouter.schellart@monash.edu
[3]School of Mathematical Sciences, Monash University, Melbourne, Australia
Fabio.capitanio@monash.edu
Rebecca.farrington@monash.edu

Subducting slabs represent the continously recycled cold thermal boundary layer of the Earth's convecting mantle, and are thought to be the primary driving force for plate tectonics. Subducted tectonic plates (slabs) sink through the mantle and pull the plate they are attached to, but this subduction can be accommodated by two modes: the forward motion of the subducting plate or backwards motion of the plate boundary. The latter is the process of slab rollback and is associated with retreating trenches.

Over the past decade, both analogue and numerical models of subduction have been developed which consider the dynamics of a single, isolated plate sinking into a passive upper mantle. These models offer a novel way to investigate aspects of plate tectonics and mantle convection through single-sided, asymmetric subduction with a coupled

lithosphere-mantle system, but are restricted to the upper 1000 km of the mantle and 50 million years of progressive time-evolution. While such models assume plates with simplified rheologies, uniform thickness and uniform density contrasts appropriate for mature oceanic lithosphere, their resultant 3D subduction dynamics are quite rich. The subducting plate and the sinking slab are coupled through a stress guide in the middle of the subducting plate (the strong core) as well as by virtue of poloidal and toroidal flows induced in the surrounding mantle. We will present the latest generation of these numerical models and provide an overview of how these models can be used to investigate the development of trench curvature, how the subduction rate is partitioned between forward plate advance and slab rollback, and how slab morphologies in the upper mantle are a product of these plate and trench motions.

As a result of numerous experiments, five distinct styles of subduction emerge as the entirety of possible ways a plate can subduct and these have been quantitatively described in a regime diagram with predictive capability. We propose that the variety of subduction regimes are generated primarily as a direct consequence of the presence of the modest barrier to flow into the lower mantle. The regime diagram can be understood from the competition between the weight of the slab and the strength of the plate, which are related to each other through an applied bending moment, and this competition produces a particular radius of curvature (for which we provide a simple scaling theory). Based on this regime diagram, and observations of the bending moment at several trenches, we propose that modern plate tectonics operates entirely within only 2 of these styles, but we speculate that other modes may have been the predominant style of subduction in the Precambrian.

Additionally, for the regime operating on present-day Earth (the Folding mode), we show that slab width (W) controls these modes and the partitioning of subduction between them. Using models from the Folding regime and a global subduction zone data set, we show that subducting plate velocity scales with $(W)^{2/3}$, whereas trench velocity scales with 1/W. These findings explain the Cenozoic slowdown of the Farallon plate and the decrease in subduction partitioning by its decreasing slab width. The change from Sevier-Laramide orogenesis the orogenesis to Basin and Range extension in North America is also explained by slab width; shortening occurred during wide-slab subduction and overriding-plate — driven trench retreat, whereas extension occurred during intermediate to narrow-slab subduction and slab-driven trench retreat.

Dynamic of gas hydrate deposits evolution under subaqueous conditions

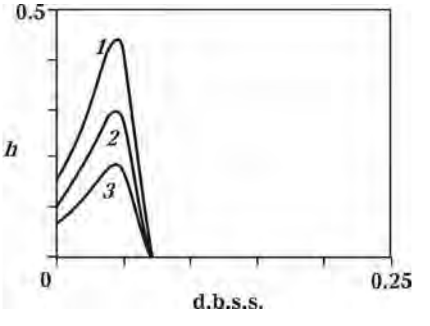
© *E. Suetnova, 2010*

Institute of Physics of the Earth, RAS, Moscow, Russia
elena_suetnova@mail.ru

At present, more than 100 areas of gas hydrate manifestations in sediments have been revealed by various geophysical (mainly seismic) methods. Subsurface filtration is the most powerful process of gas and fluid transport into hydrate stability zone to form gas hydrate deposits in sediments [Davie, Buffet, 2002]. Pressures and temperatures favorable for the formation and stability of gas hydrates are widespread in seafloor structures, particularly, at continental margins, where accumulated sediments contain appreciable amounts of biological material, ensuring gas (mainly methane) influx into crustal fluids. Depths of hydrate stability interval and hydrate saturation are different in natural conditions. These differences were interpreted usually in the frame of thermal regime peculiarity. Peculiarity of sediment accumulation processes was not considered usually, but the sedimentation regime determined the evolution of porosity, permeability, fluid pressure and filtration rate in accumulating sediments [Suetnova, Vasseur, 2000]. Thus, to understand the mechanisms of accumulation and evolution of hydrate deposits in sediments during geological history it is necessary to study the complex geophysical process of porosity, filtration and hydrate accumulation evolution. The author's recent results of numerical modeling of gas hydrate accumulation in dependence on geophysical condition of sedimentation are presented below.

Methods and results. Gas and fluid filtration is

determined by compaction during sediments pill growing, so, hydrate accumulation depends on sedimentation and compaction history of sediments. Interrelated processes of filtration and visco-elastic sediment compaction during sediment column growing are accounted for system of nonlinear differential equations supplemented by appropriate boundary conditions [Suetnova, Vasseur, 2000]. The system was reduced to a dimensionless form in order to reveal its characteristic scales [Barenblatt, 1982]. The dimensionality analysis of parameters and variables of the system reveals the compaction-related length L and time T scales characteristic of the problem considered [Suetnova, Vasseur, 2000]. Thus, the system in the dimensionless form with these scales contains the dimensionless characteristic similarity numbers $V=V_0/\ L/T$, and D=вз/T and, consequently, the depth and time distributions of the dimensionless porosity, the velocities of the sediment matrix and pore fluid, and the hydrate concentration, which are obtained as solutions of the system of equations, depend on these similarity numbers. Changes in the values of permeability, viscosity, and sedimentation rate alter the values of the characteristic similarity numbers of the compaction process, controlling the fluid flow in sediments [Suetnova, Vasseur, 2000]. Therefore, regular patterns of accumulation of gas hydrates in a growing layer of sediments depending on their physical and hydrodynamic properties and sedimentation rates can be determined as a function of the similarity numbers of the problem of visco-elastic compaction. To reveal the dynamic of hydrate accumulation the set of model calculation were performed using geophysical data on known hydrate regions. The influences of hydrate saturations on free pore volume and Damkohler number were taken into account in the calculations [Suetnova, 2007]. Results of the calculations show that hydrate accumulation essentially influences on pore fluid filtration process. Calculations of time-dependent evolution of gas hydrate deposits show that the rate of hydrate accumulation is higher in the case of developing overpressures compaction than in equilibrium compaction process; provided that real sedimentation rate and final sediment thickness and overburden pressure are equal in both case, but rheological and hydrodynamic property are different (Figure, Table).



Comparison of hydrate saturation versus distance from sediment surface, normalized to sediment final thickness, resulting after 2 m.years of sedimentation. Number of curve corresponds to the values of parameters, listed at table 1 at the same lines number.

№	t	V_0, m/s	m_0	η, Pa·s	μ, Pa·s	ρ_f, kg/m^3	ρ_s, kg/m^3	B, 1/Pa	k_0, m^2	V	D
1	7.7	10^{-10}	0.3	$5\cdot10^{20}$	$2.6\cdot10^{-3}$	$1.0\cdot10^{3}$	$2.65\cdot10^{3}$	10^{-9}	10^{-14}	0.06	0.06
2	0.77	10^{-10}	0.3	$5\cdot10^{21}$	$2.6\cdot10^{-3}$	$1.0\cdot10^{3}$	$2.65\cdot10^{3}$	10^{-8}	10^{-15}	0.6	0.6
3	0.77	10^{-10}	0.3	$5\cdot10^{21}$	$2.6\cdot10^{-3}$	$1.0\cdot10^{3}$	$2.65\cdot10^{3}$	10^{-9}	10^{-15}	0.6	0.06

Conclusions. The results of modeling interrelated processes of sediment compaction, filtration and hydrate accumulation during geological history of sediment pile forming gives the theoretical and numerical base to understand the dependence of hydrate accumulation dynamic on mechanical and hydrodynamic processes in sediments which determined it's dynamic during geological time.

References

Barenblatt G. I. Similarity, Self-Similarity, and Intermediate Asymptotics. — Leningrad: Gidrometeoizdat, 1982. — 255 p. (in Russian).

Davie M. K., Buffet B. A. A comparison of methane sources using numerical model for the hydrate formation. Proceeding of the 4 international conference of gas hydrate. — Japan: Yokogama, 2002. — P. 25—30.

Suetnova E. I. Accumulation of Gas Hydrates and Compaction of Accumulating Sediments: The Interaction Problem // Dokl. Akad. Nauk. — 2007. — **415**(6). — P. 818—822 (in Russian).

Suetnova E. I., Vasseur G. 1-D modeling rock compaction in sedimentary basin using visco-elastic rheology // Earth Planet. Sci. Lett. — 2000. — **178**. — P. 373—383.

Secular variations at Ukrainian magnetic observatories

© Yu. Sumaruk, 2010

Institute of Geophysics, National Academy of Sciences of Ukraine, Kiev, Ukraine
sumar@mail.lviv.ua

Secular variations (SV) are the main origin of the information on the processes inside of the Earth, that geomagnetic field generate. SV are calculated by means of the mean year values of the geomagnetic field components measured at the magnetic observatories. It is generally accepted, that SV consist of two components, the first component is generated by internal origins, and second — by the external ones [Kalinin, 1984]. The external origins are magnetospheric-ionospheric currents. Variations from ionospheric currents have different sign and therefore their mean per year values are equeal about zero. Magnetospheric ring current is created during magnetic storms. The current flows to the West and therefore it creates negative variation of horizontal component (*H*) and positive ones in vertical component (*Z*). In *Z*-component the effect intensifies to the high latitudes and in *H*-component — to the equator. In the years of low solar and magnetic activities, quantity of the magnetic storms is little. It means that the mean year values of *H*-component are lesser and *Z*-component — greater in such years, and vice versa in the years of high solar activity. There are shortperiod and longperiod SV generated by external sources. About one-two year period SV are high correlated with geomagnetic activity. It mean that their sources are magnetosphere-ionosphere currents [Sumaruk, 2001]. However in [Ladynin, Popova, 2008] assumption is made that these quasibiennial SV-variations are connected with the changes of the dipole field parameters, i. e. they have internal sources. The most probable quasibiennial SV have as external so internal sources. Existence of quasibiennial variations on the SV graphs on quiet and also disturbed days is argument for such assumption. Longperiod SV include elevenyear [Shevnin et. al, 2009] and eightyyear (80-year) [Sumaruk, 2001] variations. The goal this work is:

1) to investigate SV on Ukrainian magnetic observatories;

2) to separate components connected to solar and geomagnetic activities. We used mean year values of geomagnetic field three components on all (*a*), quiet (*q*) and disturbed (d) days at magnetic observatories "Lviv" (LVV), "Kyiv" (KIV) and "Odesa" (ODE).

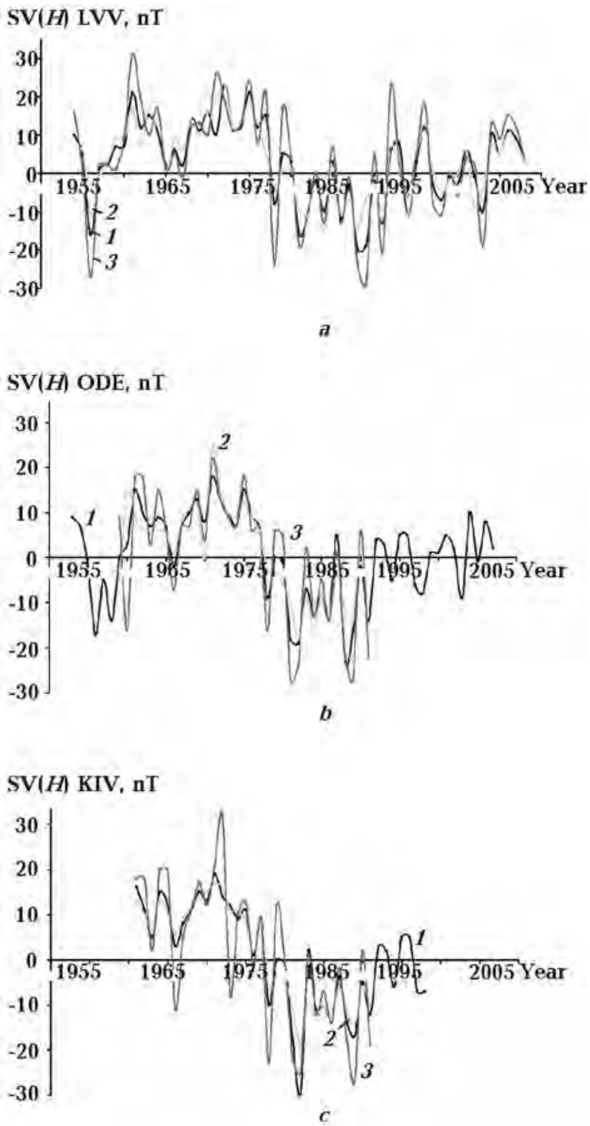


Fig. 1. SV in *H*-component at magnetic observatory LVV (*a*), ODE (*b*), KIV (*c*), all (*1*), quiet (*2*) and disturbed (*3*) days.

Fig. 1 shows SV in *H*-component at magnetic observatory LVV (*a*), ODE (*b*), KIV (*c*) on all (black), quiet (green) and disturbed (red) days. Short period variations at three observatories in *H*-component change in phase, but their amplitudes are different. The greatest amplitudes on all, quiet and disturbed days are observed at LVV. At all observatories short-period SV have greater amplitudes on disturbed days.

Fig. 2 shows SV in *Z*-component at magnetic observatory LVV (*a*), ODE (*b*), KIV (*c*) on all (black), quiet (green) and disturbed (red) days, and Fig. 3 the same for *D*-component. In Z- and *D*-components for shortperiod SV one may see the same as for *H*-component, but amplitudes are lesser as for disturbed days so for all and queit days. Shortperiod

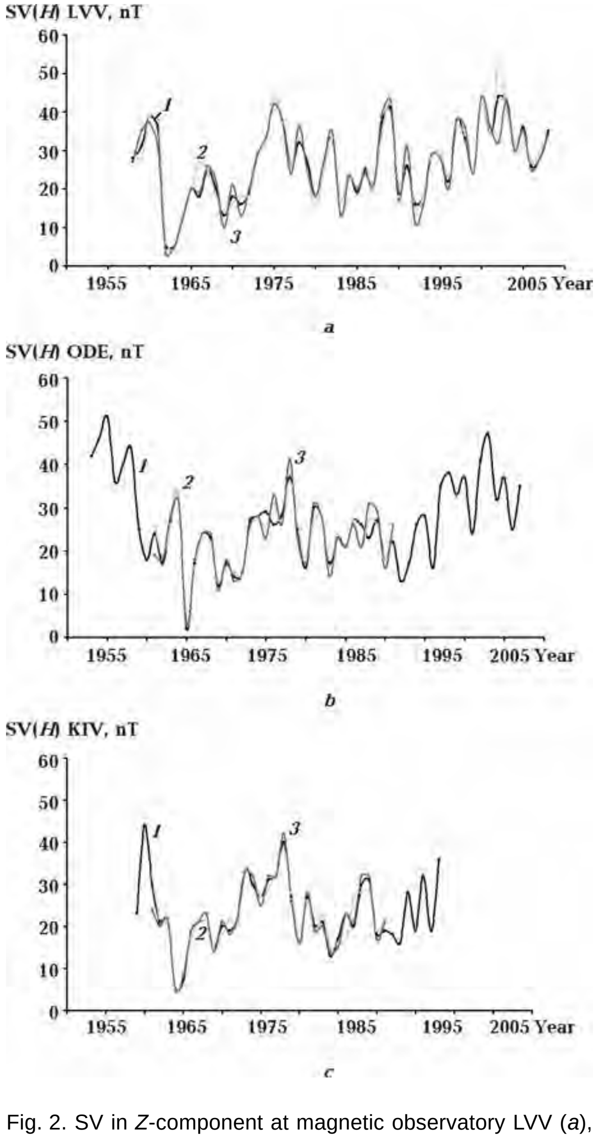


Fig. 2. SV in *Z*-component at magnetic observatory LVV (*a*), ODE (*b*), KIV (*c*) all (*1*), quiet (*2*) and disturbed (*3*) days.

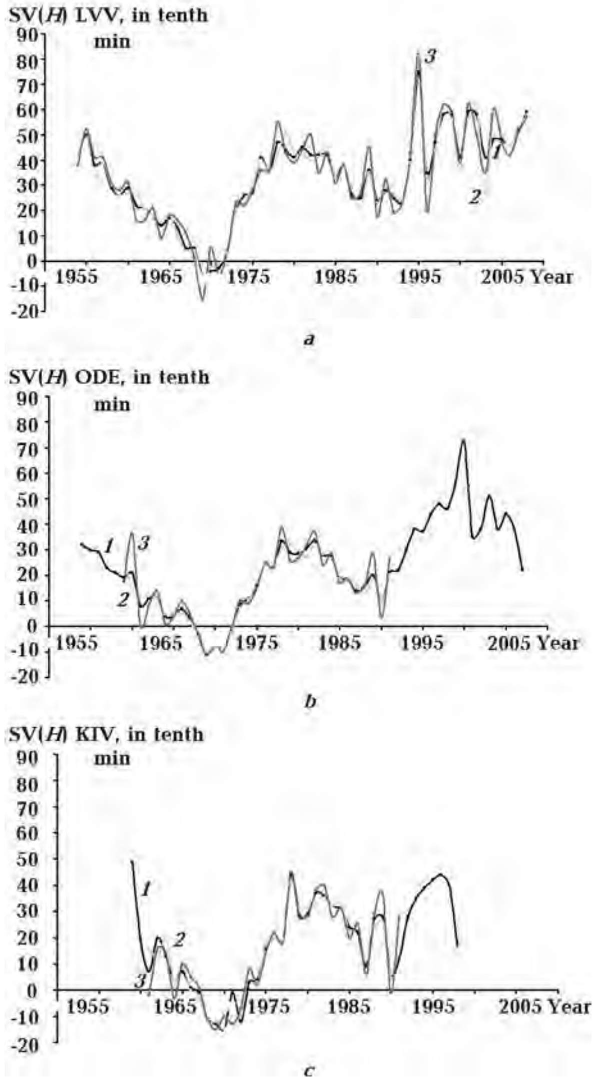


Fig. 3. SV in *D*-component at magnetic observatory LVV (*a*), ODE (*b*), KIV (*c*) all (*1*), quiet (*2*) and disturbed (*3*) days.

SV in *Z*- and *D*-component change in opposite phase to *H*-component phase. It is factor to evidence the external sources of these variations. Shortperiod variations we exclude by trapets method. After excluding shortperiod SV, about 11-year SV are seen dictinctly. These variations are connected to changes of cyclic solar activity. On the growth (fall) stage of solar activity, the SV decreases (increases).

Smoothing at 11-year running window exclude cyclic changes of SV. By excluding shortperiod and cyclic SV variations, we received quasisinusoidal curve. Unfortunaly Ukrainian magnetic observatories observed only part of the quasisinusoid. It was shown in [Sumaruk, 2001] that such observatories as Hartland (HAD, observational row from 1846), Coimbra (COI, from 1866), Voejkovo (LNN, from 1869) ob-

served SV with period about 80 years. It may suppose, that 80-years SV also have external source so far as they correlate to mean per solar cycle Wolf numbers.

References

Kalinin Yu. D. Secular geomagnetic variations. — Novosibirsk: Nauka, 1984. — 160 p. (in Russian).

Ladynin A. V., Popova A. A. Quasiperiodical fluctuations of the secular variations velocity of the geomagnetic field on the data of world net observatories for 1985—2005 // Geologia i geofisica. —2008. — **49**, № 2. — P. 1262—1273 (in Russian).

Shevnin A. D., Levitin A. E., Gromova L. I., Dremukhina L. A., Kainara L. N. Solar cyclic variation in magnetic components of the observatory "Moscow" // Geomagnetizm i aeronomija. — 2009. — **49**, № 3. — P. 315—320 (in Russian).

Sumaruk Yu. P. On external sources of secular variations of the Earth magnetic field // Contributions to Geophys. and Geod. — 2001. — **31**, № 1. — P. 353—354.

Quasi-biennial variations of the solar and geomagnetic activities

© T. Sumaruk, P. Sumaruk, 2010

Institute of Geophysics, National Academy of Sciences of Ukraine, Kiev, Ukraine
sumar@mail.lviv.ua

In the spectrum of the solar activity expressed with Wolf numbers or other indices, the period about 2—3 years is distinguished [Gnevyshev, 1977; Apostolov, 1985]. Quasi-biennial oscillations (QBO) manifest itself on all geliolongitudes and it was shown in [Ivanov-Kholodny et al., 2003], the common structure of the QBO exists on the Sun.

Statistical analysis of the connection between QBO and solar magnetic fields shows high correlation between phenomena [Ivanov-Kholodny et al., 2004]. The same QBO were found out in the interplanetary environment [Okhopkov, 1998], in the critical frequencies of the ionosphere layers E and F_2 [Ivanov-Kholodny et al., 2000; 2003], in some geophysical and meteorological processes [Rakipova, Ephimova, 1975; Gabis, Troshichev, 2001; Fadel et al., 2002]. The best QBO manifests itself at the beginnings of the solar cycles as a fade out oscillations. The amplitude of the first oscillation is the greatest and then it decreases to the end of the cycle. At the growth phase of the solar cycle activity the periods of the oscillations are about three years, but at the minima they are about two years [Kononovich, Shefov, 2003].

The physical interpretation of the QBO in the solar activity is based on the changes of the solar convective zone parameters G. S. Ivanov-Kholodny et al. draw conclusion, that QBO have the same origins in all phenomena [Ivanov-Kholodny et al., 2004]. Yu. D. Kalinin [Kalinin, 1952] was first, who discovers QBO in the magnetic field variations. Availability of the QBO in the geomagnetic field variations in middle latitudes was shown in [Sumaruk T., Sumaruk P., 2009]. Our purpose is to see of QBO in the geomagnetic field secular variations (SV) and their correlation to solar and geomagnetic activities.

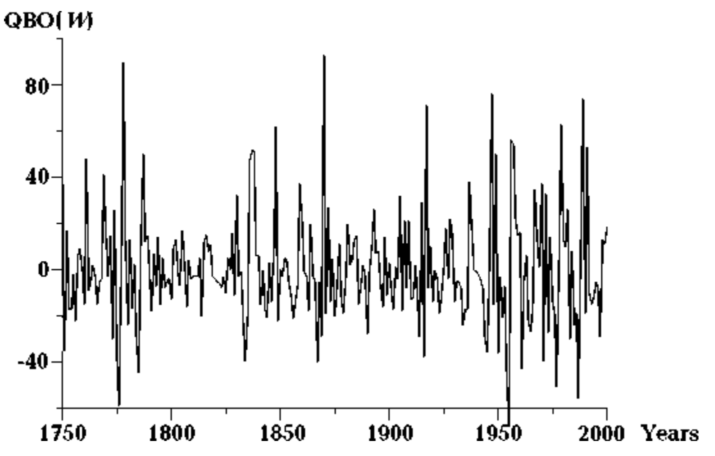


Fig. 1. QBO(W) for 1750—2000.

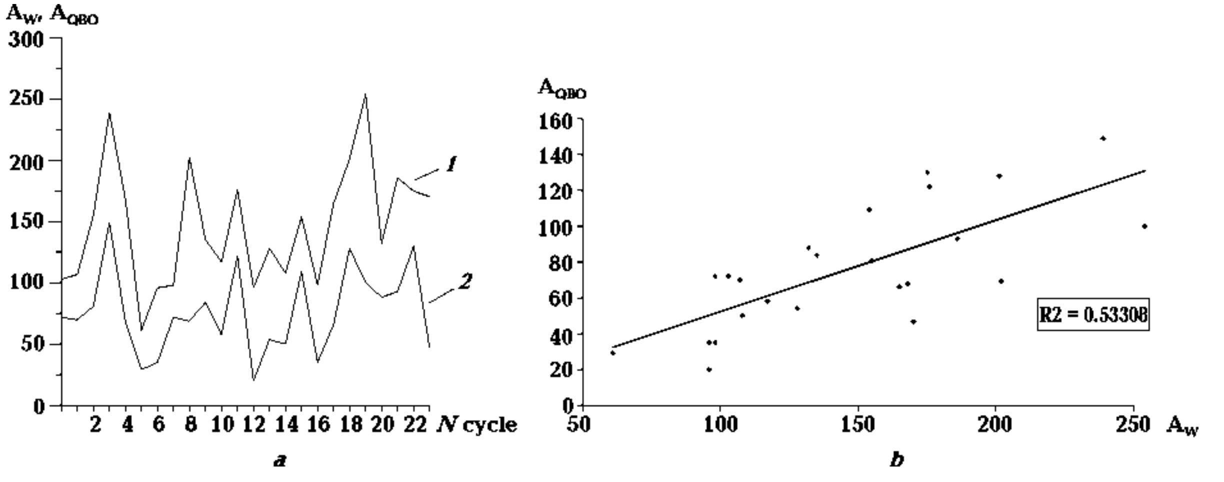


Fig. 2. Amplitudes of the Wolf number A_W (*1*) and amplitudes of QBO (W) A_{QBO} (*2*) for every solar cycle (*a***)** and correlation between A_W and A_{QBO} (*b*).

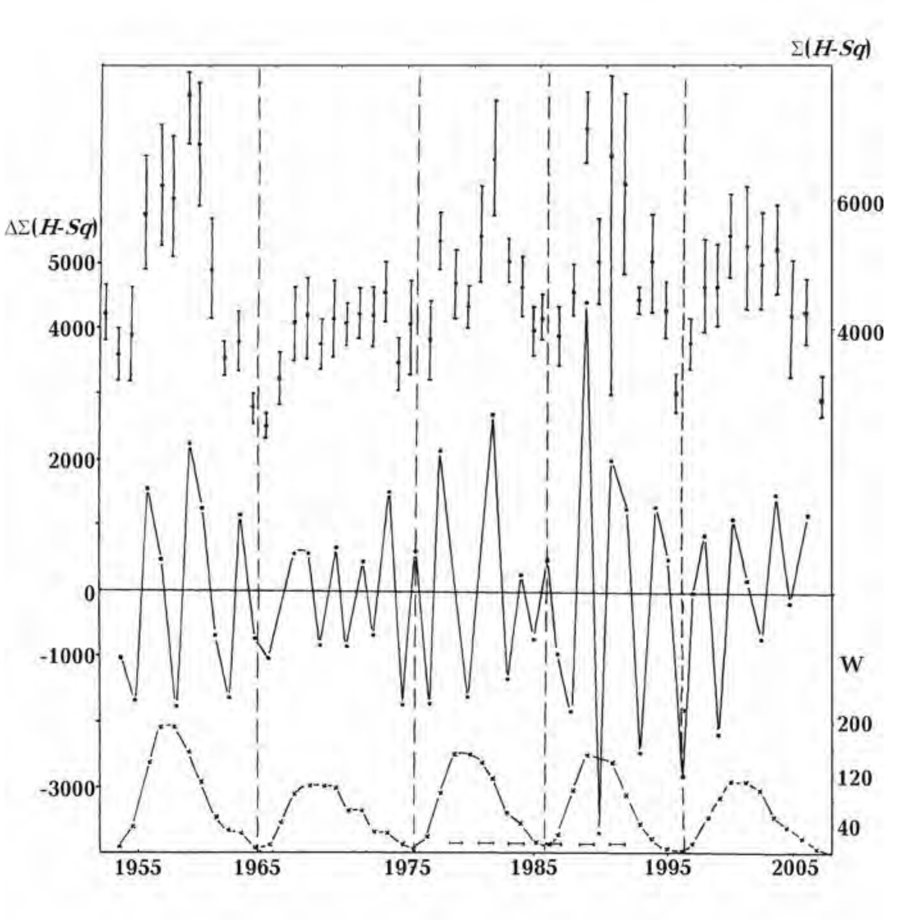


Fig. 3. Mean per year $\Sigma(H\text{–}S_q)$ values and their dispersion, $\Delta\Sigma(H\text{–}S_q)$, Wolf number for 1954 till 2005.

The starting data were the mean year Wolf numbers (*W*) and values of horizontal component (*H*) at magnetic observatory "Lviv". The measure of magnetic activity was the mean monthly per year sum of differences between hourly absolute values of *H* and correspondent *H* on five international quiet days

(S_q)–(Σ(H–S_q)). SV were calculated as difference between successive mean year values of H. To select QBO was used method of [Ivanov-Kholodny, Chertoprud, 1992], which consist in finding differences of double values of correspondent parameter and the same for previous and next years.

Fig. 1 shows QBO(W) for 1750—2004. From three to five oscillations are observed during every solar cycle. Amplitudes of oscillations are maximal at the beginnings and decreases to the ends of the cycles. In the odd solar cycles the amplitudes are to a great extent larger. Two cycles odd and even present as if one group and it reflect the change of sign of the Sun polar magnetic field.

Fig. 2, *a*. presents the amplitudes of the Wolf number (*1*) and amplitudes of QBO (W) (*2*) for every solar cycle.

The high correlation between values exists. Fig. 2, *b*. shows it dependence.

As E. Gibson shows [Gibson, 1973] about eighty year solar cycle exist. Amplitudes of QBO(W) also show the same cyclisity. Minimal amplitudes of QBO(W) was observed in cycle № 5, the next minimum was in cycle № 12 and the next — cycle № 20. Solar activity increased from cycle № 14, the same increasing shown amplitudes of QBO(W).

As it was shown T. Sumaruk [Sumaruk T., Sumaruk P., 2009] QBO exist also in middle latitude geomagnetic variations. Geomagnetic activity was measured by the monthly Σ(H–S_q) for geomagnetic observatory "Lviv". So far as the amplitudes of S_q change with the seasons [Sumaruk T., Sumaruk Yu., 2004; 2005] it means that seasonal variations of Σ(H–S_q) were excluded.

Fig. 3 shows mean per year Σ(H––S_q) values and their dispersion from 1954 till 2005. Central curve shows QBO of Σ(H–S_q)–ΔΣ(H–S_q). Bottom curve shows mean year Wolf number. Scale values of Σ(H–S_q) — on right, of ΔΣ(H–S_q) — on the left. Vertical lines show solar activity minima. Amplitudes of the QBO of Σ(H–S_q) change from one cycle to other and in the cycle. Periods of Σ(H–S_q) QBO change from two to four years.

At the bottom of Fig. 3 thick horizontal lines show the interval of time when east wind exist in the equatorial atmosphere [Gabis, Troshichev, 2001]. The wind is the characteristic of many meteorological processes. One may see that time of the east direction of the wind coincides to positive peaks of QBO in the geomagnetic activity indices. It means that one may use these QBO as prognosis factor.

So far as QBO in solar activity reflects in the geomagnetic activity, and the last manifests itself in secular variations (SV) the geomagnetic field, it may be waits of QBO in the SV. Au:Fig. 4 shows QBO in the SV (red) of H-component at magnetic observatory "Lviv" four 1953—2008. The bottom curve shows QBO in the Σ(H–S_q) (blue). It is easy to sea good negative correlation between values. Deflection from correlations is observed in 1957 and 1979, the years of maximal solar activity. Amplitudes of QBO in SV(H) increase from 20 to 23 solar cycles.

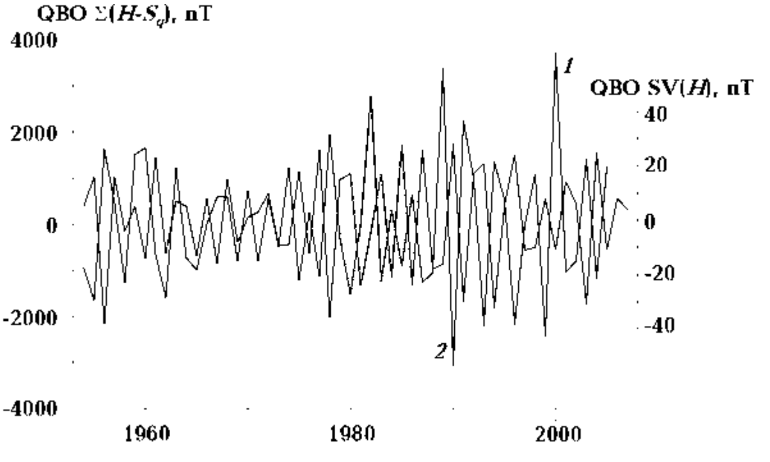


Fig. 4. QBO in the SV of H-component at magnetic observatory "Lviv" four 1953—2008.

References

Apostolov E. M. Quasi-biennial oscilation in sunspot activity // Bull. Astronom. Inst. Czechsl. — 1985. — **36**, № 2. — P. 97—102.

Fadel G. M., Semenov A. I., Shefov N. N., Suhodoev V. A., Martsvaladze N. M. Quasi-biennial variations of the temperature of the mesopause, lower troposphere and solar activity // Geomag. Aeronom. — 2002. — **42**, № 2. — P. 203—207 (in Russian).

Gabis I. P., Troshichev O. A. Influence of the short period variations of the UV-radiation of the Sun on the stratospheric circulation // Geomag. Aeronom. — 2001. — **41**, № 3. — P. 408—419 (in Russian).

Gibson E. G. The quiet Sun. — Washington, NASA, 1973. — 408 p.

Gnevyshev M. N. Essential features of the 11-year so-

lar cycle // Solar Phys. — 1977. — **51**, № 1. — P. 175—183.

Ivanov-Kholodny G. S., Chertoprud V. Yu. Analysis of the extrema quasi-biennial variations of the solar activity // Astronom. Trans. — 1992. — **3**, № 1. — P. 81—84.

Ivanov-Kholodny G. S., Mogilevsky E. I., Chertoprud V. Yu. Geliologitude effect in the solar and ionospheric quasi-bienual variations // Geomag. Aeronom. — 2003. — **43**, № 2. — P. 161—165 (in Russian).

Ivanov-Kholodny G. S., Mogilevsky E. Y., Chertoprud V. Yu. Quasi-bienual variations of solar magnetic field and geliogeomagnetic activity // Geomag. Aeronom. — 2004. — **44**, № 3. — P. 291—295 (in Russian).

Ivanov-Kholodny G. S., Nepomniashchaya E. B., Chertoprud V. Yu. Changes of the quasi-bienual variations parameters of the Eart's ionosphere // Geomag. Aeronom. — 2000. — **40**, № 4. — P. 126—128 (in Russian).

Kalinin Yu. D. On some quastions of studing of the geomagnetic field secular variations // Trudy IZMIRAN. — 1952. — № 8(18). — P. 5—11 (in Russian).

Kononovich E. V., Shefov H. H. Fine structure of the eleven year ciclysity of the solar activity // Geomag. Aeronom. — 2003. — **43**, № 2. — P. 166—173 (in Russian).

Okhopkov V. P. On connection of the quasi-bienual variations of comical rays and displays of solar activity // Geomag. Aeronom. — 1998. — **38**, № 2. — P. 159—161 (in Russian).

Rakipova L. R., Ephimova L. K. Dynamics of the upper layers of the atmosphere. — Leningrad: Gidrometizdat, 1975. — 256 p. (in Russian).

Sumaruk T. P., Sumaruk P. V. Quasi-biennial variations of the geomagnetic field of the Earth // Dopovidi NANU. — 2009. — № 1. — P. 114—116 (in Ukrainian).

Sumaruk T. P., Sumaruk Yu. P. On the count of level of irregular variations at the middle latitudes // Geophys. J. — 2004. — **26**, № 6. — P. 139—142 (in Ukrainian).

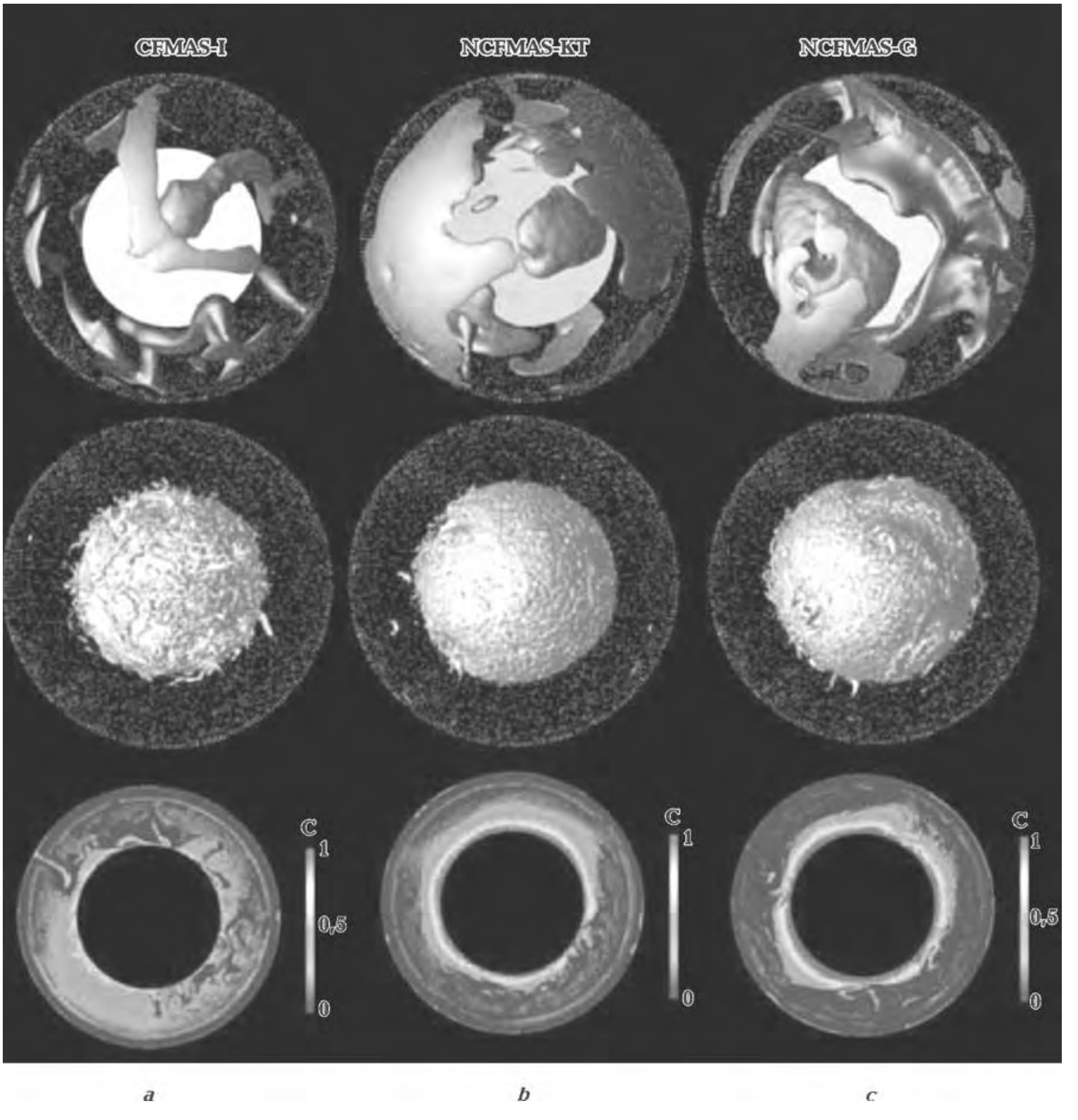
Sumaruk T. P., Sumaruk Yu. P. On the origins of S_q-variations of geomagnetic field at the middle latitudes // Geophys. J. — 2005. — **27**, № 2. — P. 299—303 (in Ukrainian).

3D Spherical models of coupled mantle thermo-chemical evolution, plate tectonics, magmatism and core evolution incorporating self-consistently calculated mineralogy

© ***P. Tackley[1], T. Nakagawa[1], F. Deschamps[1], J. Connolly[2], 2010***

[1]Institute für Geophysik, ETH Zürich, Zürich, Switzerland
ptackley@ethz.ch
[2]Insitute für Geochemie und Petrologie, ETH Zürich, Zürich, Switzerland

High pressure and temperature experiments and calculations of the properties of mantle minerals show that many different mineral phases exist as a function of pressure, temperature and composition (e. g., [Irifune, Ringwood, 1987]), and that these have a first-order influence on properties such as density, which has a large effect on the dynamics, and elastic moduli, which influence seismic velocity. Numerical models of thermo-chemical mantle convection have typically used a simple approximation to treat these complex variations in material properties, such as the extended Boussinesq approximation. Some numerical models have attempted to implement multiple, composition-dependent phases into thermo-chemical mantle convection (e. g., [Tackley, Xie, 2004]) and to calculate seismic anomalies from mantle convection simulations based on polynominal fitting for temperature, composition and mineral phase [Nakagawa, Tackley, 2006]. However, their linearised treatments are still approximations and may not adequately represent properties including effect of composition on phase transitions. In order to get closer to a realistic mineralogy, we calculate composition-dependent mineral assemblages and their physical properties using the code PERPLEX, which minimizes free energy for a given combination of oxides as a function of temperature and pressure [Connolly, 2005], and use this in a numerical model of thermo-chemical mantle convection in a three-dimensional spherical



Simulation results using three different compositions for basalt and harzburgite, showing (red isosurfaces) hot upwellings (blue isosurfaces) cold downwellings, (green isosurfaces) subducted crust, (bottom row) slices of compositoin. For full details see [Nakagawa et al., 2010].

shell, to calculate three-dimensionally-varying physical proporties. In this presentation we compare the results obtained with this new, self-consistently-calculated treatment, with results using the old, approximate treatment, focusing particularly on thermo-chemical-phase structures and seismic anomalies in the CMB region and the transition zone [Nakagawa et al., 2009; 2010]. The numerical models treat the evolution of a planet over billions of years, including self-consistent plate tectonics arising from plastic yielding, melting-induced differentiation, and a parameterised model of core evolution based on heat extracted by mantle convection. Results indicate while the behaviour is broadly similar between the self-consistent treatment and the parameterised treatment, details of the behaviour depend quite sensitively on exact compositions, particularly in the contents of Al and Na [Nakagawa et al., 2010]. This approach is also being used to study Mars, Venus, Mercury and super-Earths (Figure).

References

Connolly J. A. D. Computation of phase equilibria by linear programming: a tool for geodynamic modeling and an application to subduction zone decarbonation // Earth Planet. Sci. Lett. — 2005. — **236**. — P. 524—541.

Irifune T., Ringwood A. E. Phase transformations in a harzburgite composition to 26 GPa: implications for dynamical behaviour of the subducting slab // Earth Planet. Sci. Lett. — 1987. — **86**(2—4). — P. 365—376.

Nakagawa T., Tackley P. J. Three-dimensional structures and dynamics in the deep mantle: Effects of post-perovskite phase change and deep mantle layering // Geophys. Res. Lett. — 2006. — **33**(L12S11). — DOI:10.1029/2006GL025719.

Nakagawa T., Tackley P. J., Deschamps F., Connolly J. A. D. Incorporating self-consistently calculated mineral physics into thermo-chemical mantle convection simulations in a 3D spherical shell and its influence on seismic anomalies in Earth's mantle // Geochem. Geophys. Geosyst. — 2009. — **10**(Q03004). — DOI:10.1029/2008GC002280.

Nakagawa T., Tackley P. J., Deschamps F., Connolly J. A. D. The influence of MORB and harzburgite composition on thermo-chemical mantle convection in a 3-D spherical shell with self-consistently calculated mineral physics // Earth Planet. Sci. Lett. — 2010. — **296**(3—4). — P. 403—412.

Xie S., Tackley P. J. Evolution of helium and argon isotopes in a convecting mantle // Phys. Earth Planet. Int. — 2004. — **146**(3—4). — P. 417—439.

Induced small-scale convection in the asthenosphere in continent-continent collision zones

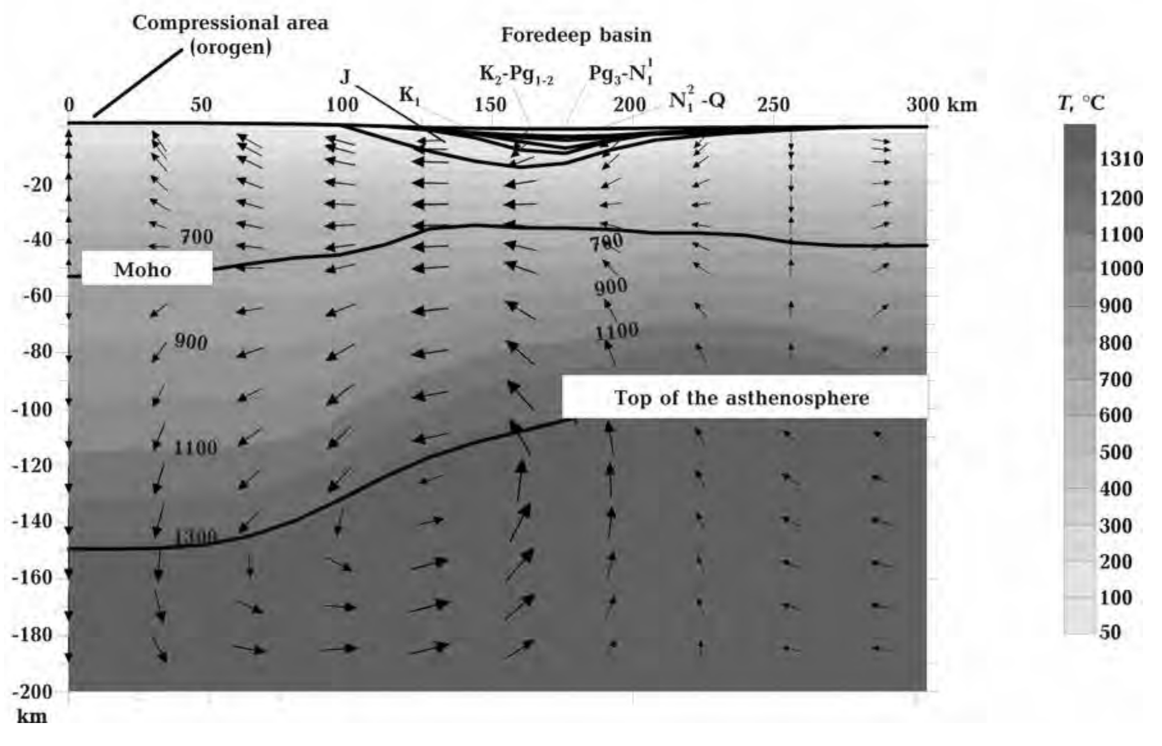
© E. Timoshkina, V. Mikhailov, 2010

Institute of Physics of the Earth, RAS, Moscow, Russia
tim@ifz.ru
mikh@ifz.ru

We investigated interaction of the lithosphere and the asthenosphere in continent-continent collision zone using a rheologically stratified model of the Earth outer shell including sedimentary layer, the lithosphere, the asthenosphere and uppermost part of the mantle. [Mikhailov et al., 1996]. The lithosphere — asthenosphere boundary is a rheological one and determined by position of specified isotherm. Equation for the top of the model includes detailed description of sedimentation and erosion. The model is asymptotically matched to the model of mantle convection what solves the problem of boundary conditions at its lower boundary. The model permits modelling of active extension and compression by mantle-induced or intraplate forces as well as relaxation of mechanical and thermal disequilibrium arose at active tectonic stages.

Active tectonic deformations of the Earth's outer shell by external mantle-induced or intraplate forces disturb thermal and mechanical equilibrium within this shell. Our model demonstrates that these disturbances lead to formation of small-scale convection within low-viscosity asthenosphere. This convection plays important role in restoration of thermal and mechanical equilibrium in the Earth outer shell and it style depends also on the surface (sedimentation and erosion) processes. Small-scale convection lasts over a long period of time after cessation of external tectonic forces, causing deformations in overlying lithosphere. In a continent-continent collision environment the small scale convection amplifies uplift of orogenic belts and causes subsidence at their periphery. We consider the small scale convection to be the main driving mechanisms of foredeep basins formation [Mikhailov et al., 1999; Timoshkina et al., 2010].

To illustrate this model we perform results of detailed modelling of the Great Caucasus orogen formation. To assign correctly initial conditions to the beginning of compressional stage, we considered preceding stages including: 1) extension of continental lithosphere in the early Jurassic; 2) subsequent post-extensional subsidence; 3) compressional (collisional) stage, when the system orogen — foredeeps forms. Parameters of the lithosphere and the asthenosphere and parameters of exten-



Distribution of temperature (gray scale), position of main boundaries in the lithosphere and sedimentary cover and small-scale convection in the model of the Great Caucasus — North Caucasus foredeep formed in result of four compressional events before beginning of the present-day compressional one. The right side of the symmetric figure is shown. The centre of the orogen is at the left (x=0). The maximum length of arrows corresponds to 1.3 mm/year.

sional — compressional processes were selected to provide a result close to the Great Caucasus — North Caucasus foredeeps, including topography, deep structure, thermal regime, subsidence history, gravity anomalies and so on.

The suggested model shows a good agreement with the data on the foredeeps structure and evolution. In particular, it is able to explain thickness of sediments in foredeep basins and their shape, formation of foredeeps not only at the front but also at the back of compressional thrust belts, uplift of a foredeep during compression in the belt and rapid subsidence after cessation of external compression.

Comparison of the numerical results with the observed data on the North Caucasus foredeep permits new interpretation of existing geological data [Timoshkina et al., 2010]. In particular, it is possible to conclude, that the system orogen — foredeep resulted from at least five active compressional events separated by periods of relatively weak tectonic activity. The first compressional event took place before the formation of the Maykopian series, i. e. 39.5 Ma, and could be related to the closure of the Arabian Ocean and subsequent beginning of the continent-continent collision in the Lesser Caucasus. There is still no consensus on when compression and orogeny in the Caucasus region commenced, many researchers estimate beginning of the compression by considerably later date. The four further compressional events can also be recognised — one of them being between 16.6 and 15.8 Ma, the others — between 14.3 and 13.7 Ma and between 7.0 and 5.2 Ma. These stages coincide well with geological data. The present day stage is also an active compression one.

References

Mikhailov V. O., Myasnikov V. P., Timoshkina E. P. Dynamics of the Earth' outer shell evolution under extension and compression // Izvestiya. Physics of the Solid Earth. — 1996. — **32**, № 6. — P. 496—502.

Mikhailov V. O., Timoshkina E. P., Polino R. Foredeep basins: the main features and model of formation // Tectonophysics. — 1999. — **308**. — P. 345—360.

Timoshkina E. P., Leonov Yu. G., Mikhailov V. O. Formation of orogen — foredeep system: geodynamic model and its comparison to the North Caucasus data // Geotectonics. — 2010. — № 5. — P. 1—20.

Mantle seismic tomography beneath East-European Platform

© *T. Tsvetkova, 2010*

Institute of Geophysics, National Academy of Sciences of Ukraine, Kiev, Ukraine
tsvet@igph.kiev.ua

3D *P*-velocity model of the mantle under East-European platform was received as the solution of the seismic tomography problem by Taylor approximation method, which was supposed by V. S. Geyko [Geyko, 2004]. The solution don't depend from the referent model selection and can be imagine in Cartesian and spherical coordinate system. The used tomography method permits recovering the mantle model being optimal in the given metric in respect with the whole totality of *P*-wave first arrival traveltime data within the frame of selected basic model of interpretation. It includes the apriory assumptions? Theory and algorithms of numerical inversion, parameterization of velocity function, the smoothing method and other regularizing factors. The results are imagine in horizontal, longitude and latitude sections of the model. The generalized velocity-depth caracteristics $V_{\text{aver}}(z)$ were used in definitions high and low velocities and residual of velocities

$$V_{\max} = \sup_{\varphi,\lambda\in S} V(\varphi,\lambda,z), \qquad (1)$$

$$V_{\min} = \inf_{\varphi,\lambda\in S} V(\varphi,\lambda,z), \qquad (2)$$

$$V_{aver}(z) = z\left(\int_0^z \frac{d\zeta}{\sum(\zeta)} \iint_{S(\zeta)} \frac{d\varphi d\lambda}{V(\varphi,\lambda,\zeta)}\right)^{-1}, \qquad (3)$$

where $S(\zeta)$ is the domain into horizontal section at the depth ζ, and $\sum(\zeta)$ is its space in the coordinates φ, λ.

The first time arrival from the ISC from 1964 to 2005 year were used as the input data.

The 3D *P*-velocity model analysis shows the next properties:

1) common velocities characteristic for received mantle model under EEP is layer velocities structure, which defined by inverse changing of phone velocity for each layer: high velocity tomographic lithosphere layer(upper mantle velocity characteristic), low velocity Golitsin — Geyko layer (transition zone velocity characteristic), high velocity zone of division-1? low velocity middle mantle, high velocities zone of division-2, low velocities low mantle, Mantle under EEP surrounding, except eastern part, characterized by common inverse relate to mantle velocities characteristics under EEP;

2) by velocities characteristics tomographic lithosphere under EEP can be devided on three layers: 50—100±25 km, 100±25—200±25 km, 200±25 km — tomographic lithosphere bottom;

3) mantle velocity boundary under EEP don't coincides with EEP tectonic boundary. Maximum agreement is on the depth 50 km, and maximum changing at the Golitsyn — Geyko depth;

4) as a whole by velocity characteristics mantle under EEP can be divided into three parts:

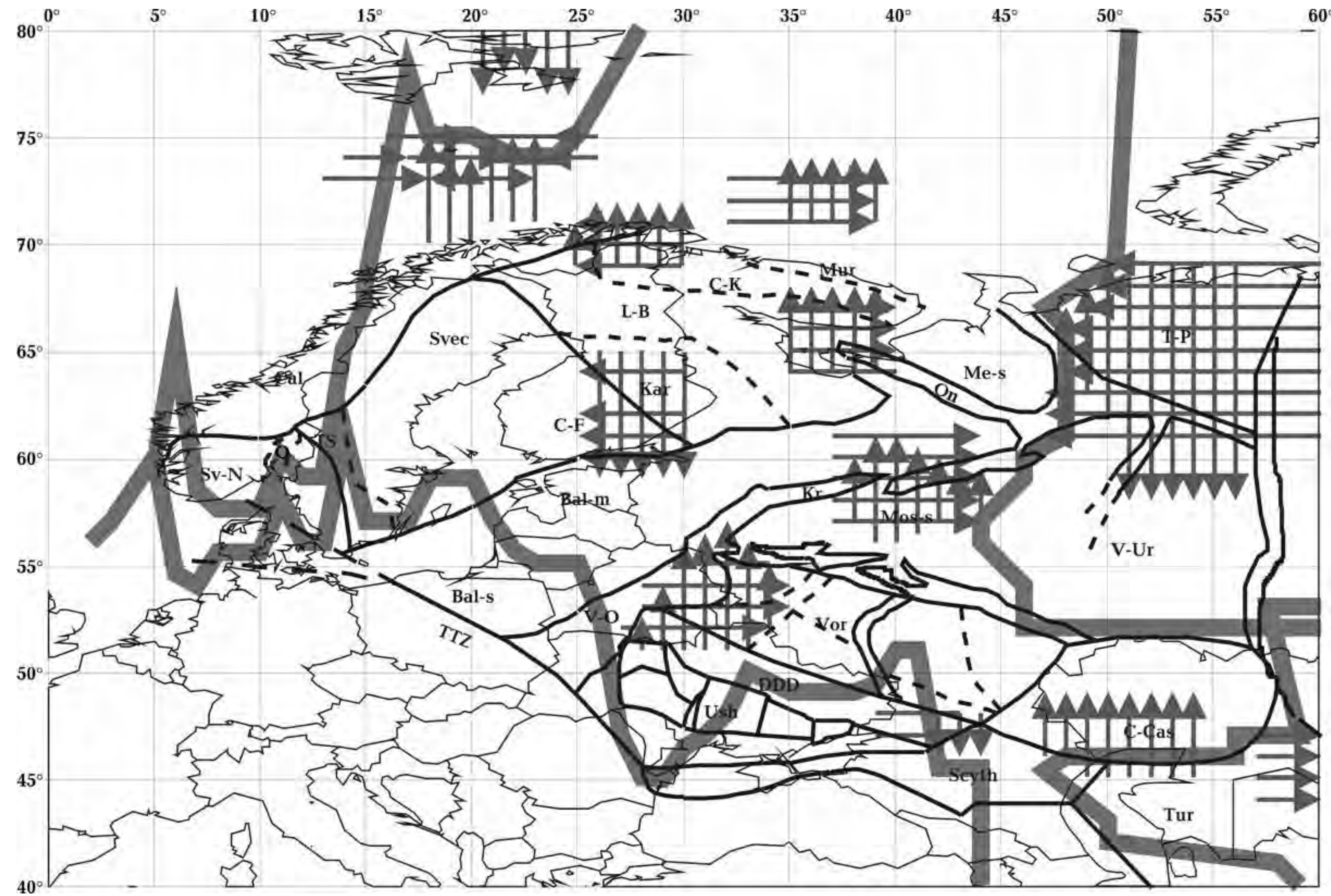
• boundary mantle velocity region of interaction with 1 type activation;

• main part with two type mantle velocity activations;

• east part of mantle under EEP, which has different velocity characteristics from another mantle part. The first type of velocity activations correspond to propagation of high velocity layers from the Golytsin — Geyko layer under surrounding regions to the low velocity Golytsin-Geyko layer under EEP and increase the part of high velocities in upper mantle layers under surrounding zone to EEP. Second type of velocity activation correspond to subvertical low velocities layers propagation from the middle mantle to the upper mantle. It is pick out inclined layers, which mainly corresponded boundary mantle velocity region of interaction (Figure);

5) mantle under Barents-Pechora Platforme units with mantle under EEP by velocity characteristics

So that by velocity characteristics we have both horizontal process and the vertical process in the mantle under East European Platform.



Velocity boundaries of 1 and 2 types of activations: Bal-m — Baltic monocline, Bal-s — Baltic syneclise, C-Cas — Cis-Caspian depression, C-F — Central-Finland massif, C-K — Central-Kola block, DDD — Dniper-Donetsk depression, Kal — Scandinavian Caledonides, Kar — Karelian block, Kr — Krestovsky avlacogen, L-B — Lapponial-White sea belt, Me-s — Mezen syneclise, Mos-s — Moscow syneclise, Mur — Murmansk block, O — Oslo graben, On — Onega graben, Scyth — Scytian plate, Sv-N — Sveconorwegian block, Svec — Svecofenian block, T-P — Timan-Pechora plate, T-S — Transscandinavian belt, TTZ — Teyseyr-Tornquist zone, Tur — Turanian plate, V-O — Volyn-Orsha avlacogen, V-Ur — Volgo-Uralia, Vor — Voronezh massif, USh — Ukrainean Shield.

References

Geyko V. S. A general theory of the seismic traveltime tomography // Geophys. J. — 2004. — **26**, № 2. — P. 3—32 (in Russian).

The disturbances of the equilibrium state of the rotating Earth and the physical nature of its tectonic activations and modern earthquakes: generality and differences

© ***K. Tyapkin, M. Dovbnich, 2010***

National Mining University, Dnepropetrovsk, Ukraine
dovbnichm@mail.ru

Most scientist in the whole world supposed Earth tectonogenesis and particularly its tectonic activations are controlled by endogenous forces caused by intra earthy spontaneously physical geological and geochemical processes flowed in its interior. The role of external factors leaded to the disturbances of the Earth equilibrium state determined the nature of the geodynamic processes appearance was showed in monograph being published recently [Tyapkin, Dovbnich, 2009]. In this work the new notions are justified and stated. In accordance with it observed geodynamic processes caused by the interaction between our planet and its surrounding space fields. So face of the Earth and its interior structures form under the influence of two opposed groups of forces according to it: the phenomena leaded to the keeping the dynamic equilibrium of the rotating Earth (geoisostasy) happen under the influence of one group; the other forces group aspired to disturb this equilibrium state. The physical nature of the first group forces is studied well enough. This group control peneplanization processes of the Earth surface trying to rich its equilibrium figure-ellipsoid. The source of the second group forces are the stresses occurred in tectonosphere as a result of the Earth rotation regime variations: changes of the angukar velocity and the displacements of the rotating axes relatively to geoid.

For the first time the geoisostasy conditions was stated and insonified on the XXVII session of IGC [Tyapkin, 1984]. Based on this conception M. M. Dovbnich gained the calculation algorithm of the stress fields in tectonosphere, caused by variations of the Earth of rotation regime. They were described in the II part of monograph in detail [Tyapkin, Dovbnich, 2009]. I can be find in free access in internet [www.nmu.org.ua/ru/scientific/publications/].

The analysis of the global stress fields occurred in the Earth tectonosphere as a result of the rotating regime variation made it possible to make following conclusions.

1. A main contribution in the global filed of the rotating stresses in tectonosphere make a component caused by the displacement of the Earth rotation axes relatively to the geoid. The value of these stresses of this component exceeds breaking point of tectonosphere rocks (10^7 Pa), so it can be seen as a reason of the Earth tectonic activations.

2. The contribution of stress field component caused by the variation of the angular velocity of the Earth rotation is much less. Maximum value of this stress component can rich the value 10^5 Pa. So, the Earth tectogenesis in essence determined by the component of the global field in tectonosphere, caused by displacement of the Earth rotation axes relatively to the geoid.

The Earth tectonic activations appeared in the tectonosphere zones, in which the rotation stresses rich the values exceeded breaking point of its constituent rocks. The specified tectonosphere fault system is developed as a result of every tectonic activations. This system is presented as hierarchically subordinated faults of two mutually orthogonal directions. The interaction of the both direction faults created an appropriate blocks system. Relational block displacements on the faults initiate a denudation sedimentary process generating a mainframe terrigenous matter necessary for surface structure formation.

Experience of our scientists argued that in Eurasia six Precambrian fault systems of tectono-

sphere are easily fixed. Its parameters are characterized by the strick azimuth: 0° and 270°; 17° and 287°; 35° and 305°; 45° and 315°; 62° and 332°; 77° and 347°, less fixed fault systems with strick azimuth intermediate relatively with azimuth mentioned above. So, only in Precambrian there took place six large-scale tectonic activations of the Earth, regardless of much smaller — activations phases.

Earthquakes present as a oscillations of the Earth surface, caused by abrupt energy release in rather localized tectonosphere zones called sources. Talking about the forces nature caused the earthquakes famous american geologist Bruce Bolt said: the same forces geological or tectonic creating mountains, rift valley, ridges and deep-water trays, the same forces are the primary reason of the earthquakes. The nature of these global forces is not so clear [Bolt, 1981]. Fully share this opinion we can state, that the source of the forces caused the earthquake origin is the mentioned above global stress field occurred in the Earth tectonosphere as a result of its rotation regime variations.

The distinctive features of modern earthquakes from ancient tectonic activations are: its much less energy intensity; corresponding between origination sources and ancient fault structures; and also — much higher frequency of the earthquakes appearance argued about that the preparation before the earthquakes need much less time. All features mentioned above can be explained by that the modern tectonosphere is less homogeneous relatively with Pracembrian tectonosphere. Earlier tectonic activations of the Earth caused the appearance of the weak areas with lower strength ($<10^7$ Pa). These areas are the zones of Precambrian different scale faults. This feature allows scientists to use it as an additional criterion for the earthquake prognosis.

Based on the possibility to calculate the global stress fields and all study features of earthquakes demonstration our university together with the UkrNIMI NAN Ukraine (Donetsk, Ukraine) are going to make research dedicated to creation of rational forecasting earthquake technique, included relational to it dynamic phenomena in mines, catastrophic consequences of which cause grand losses for mining industry of Donbass. Authors will be glad for collaboration.

References

Bolt B. Earthquakes. — Moscow: Mir, 1981. — 256 p. (in Russian).

Tyapkin K. F. A new model isostasy of the Earth // Abstracts XXVII Geologorum Conventus. — Moscow, 1984. — **3**. — P. 438—439.

Tyapkin K. F., Dovbnich M. M. New rotation hypothesis of structure development and its geological mathematically ground. — Donetsk: Knowledge, 2009. — 342 p. (in Russian).

www.nmu.org.ua/ru/scientific/publications/

High-quality seismic imaging and interpretation of prospective features in a thrust zone of onshore Ukraine

© O. Tiapkina, O. Polunin, 2010

Nadra Group, Kiev, Ukraine
yutyapkin@rambler.ru
aipolunin@yahoo.com

Introduction. For many years, the Dnieper-Donets Basin (DDB) in Ukraine has attracted extensive exploration activities. In this mature petroleum-bearing sedimentary basin, significant efforts are made to searching for and exploration of hydrocarbon traps in a variety of complex-structure land environments. Geophysicists face, to name a few, overburdens of intense lateral structure variations and large velocity contrasts [Tiapkina et al., 2006], settings of complex salt tectonics [Tiapkina et al., 2008], and highly folded and faulted thrust zones. Interpretation of seismic data in these complex environments is quite a challenge. The objective of this study is to demonstrate, with examples from a thrust zone, which comprises several productive fields and prospective areas, how integration of high-quality

depth processing with seismic structure and attribute interpretation can improve reservoir characterization and well planning.

Geological setting of the study area. The area of interest for this study is located in the south-eastern part of the DDB adjacent to the Donets Basin. It belongs to a thrust zone that includes several producing fields and prospective areas (Fig. 1). All these brachyanticlines adjoin the main compound thrust fault, which trends NW—SE in the western part and W—E in the eastern part. The geological section of the territory is composed of Paleozoic, Mesozoic and Cenozoic sedimentary rocks. In the Spivakivske field, commercial quantities of hydrocarbons are produced from prolific Bashkirian and Early-Permian reservoirs, whereas in the Drobyshivske field, several wells encountered significant amounts of hydrocarbons in Bashkirian, Moscovian and Gzelian predominantly sandstone reservoirs and proved economic. In some wells, these reservoirs are fractured, which is confirmed by core analysis and mud loss during drilling.

The complex tectonic setting of the region suggests that the Paleozoic rock mass was underwent a compressive stress regime in the course of the Main Cimmerian phase of the Hercynian tectoge-

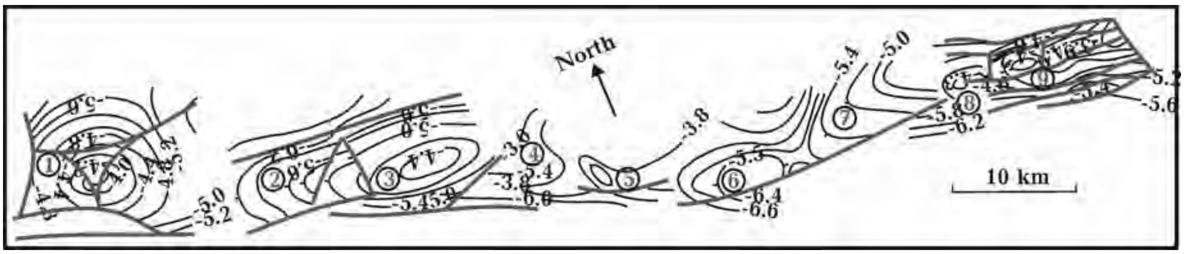


Fig. 1. Schematic map showing the structure and location of the (1) Pivnichno-Volvenkivska, (2) Zakhidno-Spivakivska, (3) Spivakivske, (4) Snizhkivska, (5) Kamyanska, (6) Svyatogirska, (7) Torska, (8) Zakhidno-Drobyshivska and (9) Drobyshivske productive fields and prospective areas within an extensive thrust zone of the south-eastern part of DDB (Ukraine).

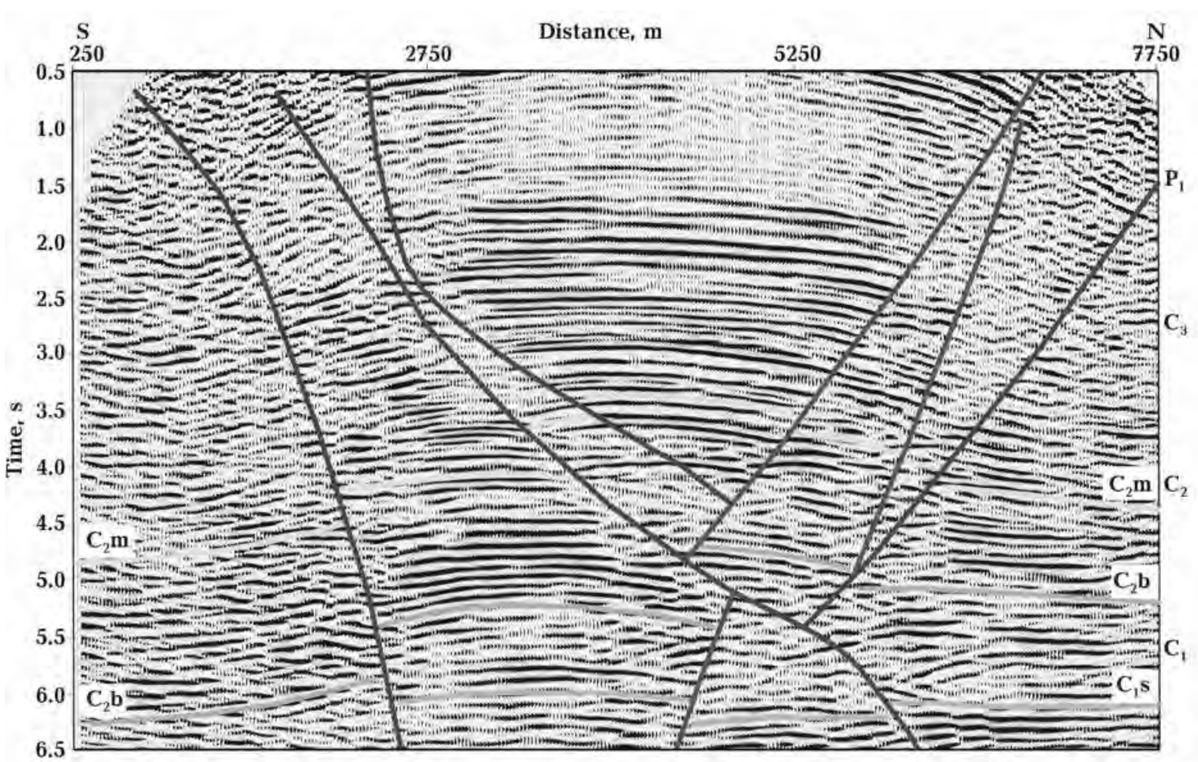


Fig. 2. Typical seismic section passing across the complex horst-anticlinal structure with jump-up thrust faults on the left flank and compensative jump-up faults on the right flank.

nesis in Middle Jurassic. This horizontal stress induced extensive strike-slip faulting and large-amplitude anticlinal uplifting. Then, during on-going compressive deformations, stress was redistributed within the Paleozoic rocks. As a result, in the lower part of the deformed unit, of the Early and Middle Carboniferous (C_1—C_2) age, horizontal stress increased and produced intense compound thrust and jump-up faults. Their planes incline to the northern side of the DDB, where stress was maximal. At the same time, in the upper part of the deformed strata, of the Late Carboniferous (C_3) and Early Permian (P_1) age, stress was released and transformed into tension, specifically on the opposite limbs of the folds. As a result of this local tension regime, the northern flanks of the structures were affected by multiple compensative jump-up faults, dipping southwards to the axial planes of the anticlines. The same forces pushed up the structural crests and formed fault-bounded horst-anticlines. Both types of the controlling faults, with the former being more pronounced, propagate and can readily be identified on seismic images up to the wide-spread pre-Triassic unconformity surface (Fig. 2). They cross and go out in the Lower Carboniferous deposits.

High-quality imaging of prospective features. Before, the study area was investigated by 2D seismic and proved to be productive from several wells. Nevertheless, it can still contain significant amounts of unexplored hydrocarbons. However, the isolated, limited areal extent, intricate geometry, and fault nature of these traps are major exploration and development challenges for 2D seismic. For this reason, a 3D seismic survey was acquired over this geologically complex area with the objective to generate new drilling prospects. In order to make further interpretation more successful, a high-quality objective-oriented depth processing sequence was applied. Before embarking on depth migration, we process any data in time to attenuate noise and enhance signal (see [Tiapkina et al., 2008; Tiapkina et al., 2010] for more details). Then, because of a complex structure of rocks and rapid lateral velocity variations in the thrust environment, we switch the processing sequence to depth processing. This is the only way to minimize the pitfalls of interpreting structures from time sections and obtain geologic sections better correlated to well depths. Depth migration in thrust settings requires an interpretive approach to building a plausible depth-velocity model, the key determinant in successful depth imaging. To this end, we integrate seismic and well data along with structural-geology constraints into the velocity model. We start with selecting several main geologic interfaces with regard to the main velocity contrasts in the area. For each layer, time-migrated picked horizons associated with RMS velocities and velocity gradient estimation deduced from well data allow the conversion of a time macro model into an initial depth model through map-migration techniques. This initial model is then refined iteratively in order to make it geologically and geophysically consistent using GeoDepth software. Interpreters and structural geologists are closely involved in each step of this process to ensure that the velocity models are confident with well data and the known structural regime. Applying the advanced tool enables a more confident delineation of hydrocarbon traps within the zone of interest due to better positioning structural elements and better imaging faults. Since some traps in the area are controlled by faults, it is therefore essential to improve

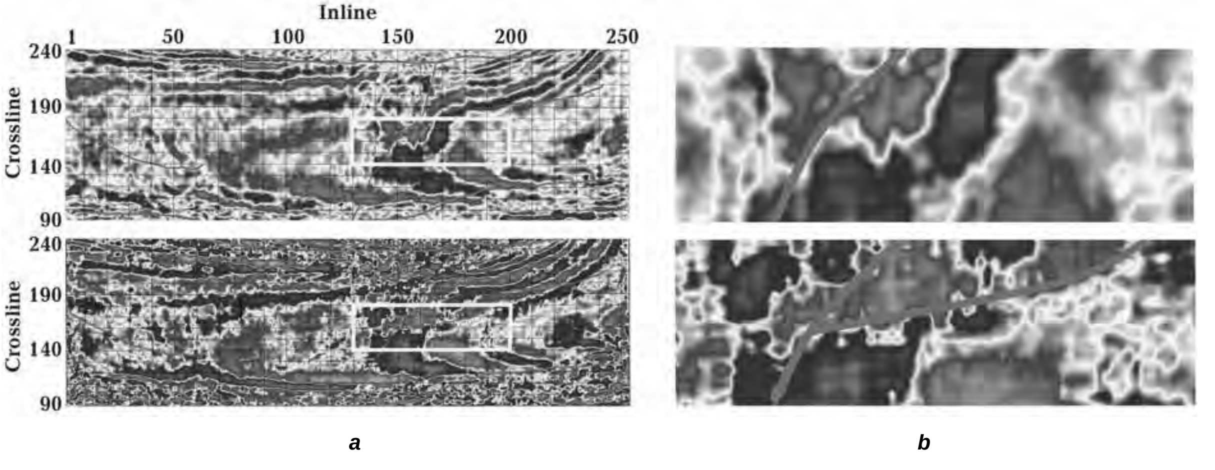


Fig. 3. Time slices extracted from the instantaneous phase attribute show a better interpretability of the structure after PSDM (bottom) than after postSTM (top) — *a*, zoom-in on the time slices from the left demonstrates an improved fault resolution and clarity after PSDM (bottom) as compared with those after postSTM (top) — *b*.

fault resolution and clarity and the ability to map events across these faults. Fig. 3, *a* shows that the structural elements after Kirchhoff prestack depth migration (PSDM) are more pronounced than those after Kirchhoff poststack time migration (postSTM). In Fig. 3, *b*, a zoomed portion of the left-hand side, demonstrates that an axial-parallel small-scale fault on the crest of the main domal uplift of the structure can be identified and tracked much more confidently after PSDM than after postSTM

The seismic data interpretation workflow utilized and some results of reservoir characterization in this thrust zone are described in [Tiapkina et al., 2010]. The results of reservoir delineation and reservoir description allowed the drilling plans for new exploratory and development wells to be refined.

References

Tiapkina O., Voitsytski Z., Khoma R. Seismic depth imaging in onshore and offshore Ukraine — Case studies // 68th EAGE Conf., Extended Abst. — 2006. — P. 175.

Tiapkina O., Voitsytski Z., Sydorenko G., Parkhomenko T. Imaging and mapping of hydrocarbon traps in areas of complex salt tectonics in Ukraine — Case studies // 70th EAGE Conf., Extended Abst. — 2008. — P. 076.

Tiapkina O., Solovyov I., Polunin O. Imaging and mapping of hydrocarbon traps in a thrust zone from onshore Ukraine — A case study // 72nd EAGE Conf., Extended Abst. — 2010. — P. 312.

Heat flow pattern and fault structures in Donbas

© ***O. Usenko, 2010***

Institute of Geophysics, National Academy of Sciences of Ukraine, Kiev, Ukraine
tectonos@igph.kiev.ua

A map showing the heat flow pattern at depth in Donbas is based on the data of heat flow measurements in over 5000 boreholes(Fig. 1). An unprecedented degree of detail has been achieved making

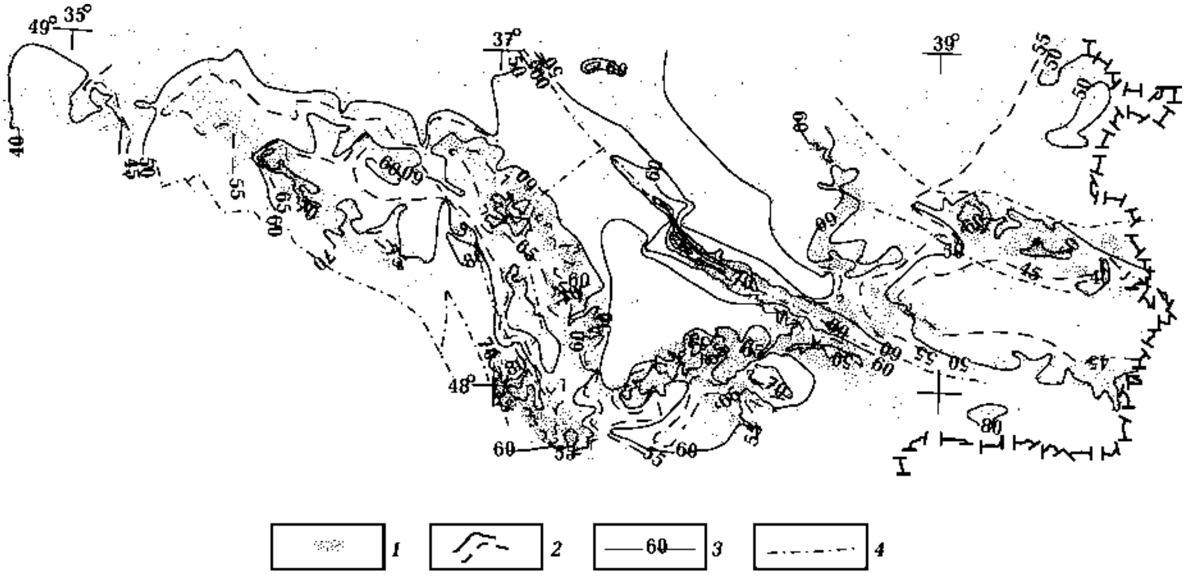


Fig. 1. A map of a heat flow (HF) of Donbas: *1* — points of definition HF; *2* — isolines HF; *3* — values HF (in Mw/m), *4* — fault zone.

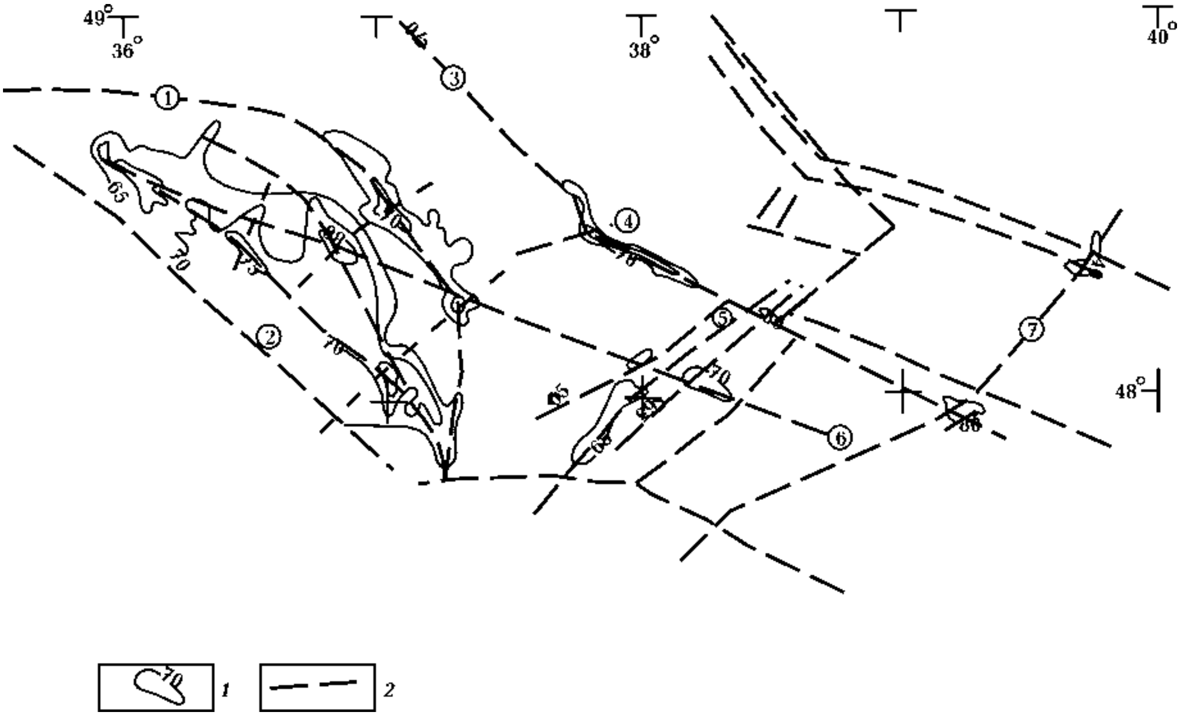


Fig. 2. The scheme of faults of the crystal base and anomalies HF: *1* — anomalies HF: positive, negative; *2* — faults of the crystal base. Figures in circles: *1* — Krivorozhsko-Pavlovskiy; *2* — Southern Donbasskiy; *3* — Axial; *4* — Mikhaylovsko-Yuryevskiy; *5* — Volnovakhsko-Chernukhkhinskiy; axial: *6* — Mushketovsko-Persianovkiy; *7* — Yelanchik-Rovenkovskiy.

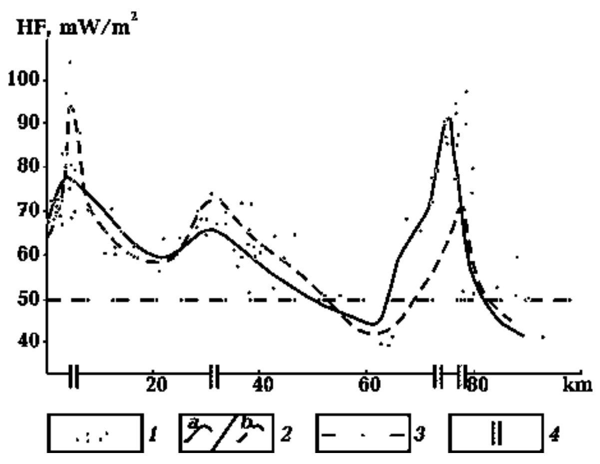


Fig. 3. HF along line AB: *1* — values HF by results of individual definitions; *2* — values HF on isolines: (*a* — in 2 km to the northwest, *b* — in 2 km to the southeast from a line AB); *3* — background values HF; *4* — faults of the crystal base.

it possible to draw maps to the scale of 1:200 000 for the entire region and 1:50 000—1:25 000 for individual areas.

Heat flow values have been calculated as a function of the average geothcrmal gradient between the surface and the borehole face (the temperature at the surface is assumed to be 10 °C) and the thermal conductivity of rocks there 1.65—2.6 W/mK.

The values of temperatures at the borehole faces were adjusted to allow for palcoclimatic variations. The effect of long-term climatic changes in the case of 1000—1400 m deep boreholes takes the form of a 2.9—3.2 °C decrease in the temperature observed at the borehole face. For the Main and Druzhkovsko-Konstantinovskaya anticlines we had to introduce a structural adjustment of –7 mW/m^2 at the curve of the fold, –4 mW/m^2 at the limb, with a gentle increase to +1 mW/m^2 at the transition to the Bakhmutskaya and Kalmius-Toretskaya troughs. In view of the fact that heat flow values were determined based on the temperatures measured at the faces of the boreholes going down to depths over 1000 meters, no hydrogeological adjustment was introduced because earlier studies had not revealed in the region at those depths any appreciable effect of the downpouring waters.

The territory is largely characterized by heat flow values ranging from 42 to 52 mW/nr (the Kalmius-Toretskaya and Bakhmutskaya troughs and the ter-

ritory north of the Nagolnyy Range to the Northern zone of fine folding). In the Northern fine folding zone the heat flow rises to 48—55 mW/m^2, further increases to 62 mW/m^2 at the junction with the Bakhmutskaya Trough, and amounts to 52—56 mW/ra^2 at the slope of the Voronezh block. Maximum heat flow values have been found at the slope of the Ukrainian Shield as well as in the areas of the Main and Druzhkovsko-Konstantinovskaya anticlines in the Donctsk-Makeyevka area. Average heat flow vc.iucs there amount to 63, maximum values reach 75 in the Donetsk-Makeyevka area, 103 at the slope of the Ukrainian Shield, and 104 mW/m^2 in the Nikitovskiy ore field confined to the Main anticline.

The most common heat flow values — 48 mW/m^2 — encountered in the area have been adopted as background values. The derived result is not much higher than the calculated or observed background heat flow in the Ukrainian Shield or Voronezh block (about 45 mW/m^2).

Virtually everywhere the anomalies stretch along the major folded structures of the basin and are quite extensive in length (up to 140 km) but not in width (4—10 to 20 km). They separate areas with relatively low heat flow values. Narrow anomalies correspond to deep-seated longitudinal faults, while background values are typical of blocks undisturbed by faulting. That the anomalies are associated with none other than location of fault zones (rather than folded structures) is clearly displayed in the southwestern part of Donbas (Fig. 2). Higher heat flow values there are confined to the intersection of the Mikhaylovsko-Yuryevskiy and Volnovakhsko-Chernukhkhinskiy faults rather than to the Volchanskaya syncline, whose axis intersects the anomaly at the 45 degrees angle. Heat flow highs mark the intersection of transverse and longitudival faults.

Quite intensive anomalies have been revealed at the southwestern edge of the basis. They run from northwest southeastwards above the Southern part of Donbass, Krivorozhsko-Pavlovskiy, and Mikhaylovsko-Yuryevskiy faults within the crystalline basement. Areas between closely spaced fault zones are characterized by heat flow values higher than background ones (56—58 mW/m^2), but immediately above the fault zones the heat flow values increase sharply (to 104 mW/m^2).

The diagram (Fig. 3) shows a profile of heat flow values measured within a 4 km — wide "corridor". Solid and dashed lines mark heat flow isolines (at the northern and southern borders of the "corridor," respectively). Dots show results of individual measurements. The diagram proves that the scatter of heat flow values is not due to an error in the heat flow determination but to variations in the thermal field intensity. There is no doubt whatsoever that the heat flow highs are confined to zones within the sedimentary layer above faults in the basement. A displacement of the Axial fault zone between the Main and Druzhkovsko-Konstantinovskaya anticlines is responsible for the displacement of the heat flow high. Sharp increases in the intensity have been noted over the entire length of the Mushketovsko-Persianovkiy (up to 85 mW/m^2) and Axial (up to 104 mW/m^2) faults. The northern fault zone is marked by insignificant (up to 55 mW/m) heat flow hikes.

The detailed determinations of heat flow values makes it abundantly clear that some of the faults are represented by up to 20 km wide zones (Southern Donbasskaya, Volnovakhsko-Chernukhinskaya. and others).

The Ukrainian Shield slope is cut by a network of closely spaced transverse and longitudinal faults, and this enables one to concur with geologists who view it as one integral zone. The heat flow map also reveals a displacement of the Volnovakhsko-Chernukhinskiy fault at the intersection of the longitudinal Mushketovsko-Persianovskiy and Axial faults that these authors have also noted. A displacement of the Axial fault at the transition from the Main to the Druzhkovsko-Konstantinovskaya anticline is obvious.

Thus, vertical movements of blocks, as indicated by the present level of erosion shear, were not the only type of displacement during previous episodes of intensification of the deep-seated processes. Horizontal movements with an amplitude of displacement of up to 10—15 km also took place. The currently observed elevated heat flow values associated with the efflux of heat and fluids (including hydrocarbons) are not the only indication of the existence of fault zones and their intersections. The presence of such structures is also indicated by magmatism, hydrothermal ore mineralization (gold, mercury and so on) left by past intensification episodes. One can observe at the intersection of the fault zones an abrupt change in the lithification of sedimentary rocks (including coal) as a result of changes in the level of the erosion shear in different blocks of the crystalline basement. It is therefore an important task to look for fault zones when prospecting for minerals. This task can be tackled with the help of detailed heat-flow maps. On territories involved in recent deep-seated processes, such faults can be pinpointed by hikes in the heat flow values. In the absence of recent intensification processes or of heat emanating from the depth, fault zones are marked by insignificant (up to 5 mW/m) negative heat flow anomalies (the northern part of the Yelanchik-Rovenkovskiy fault).

A fundamental possibility of identifying faults on

the basis of variations in the heat flow values has been demonstrated in the southwestern part of the region where anomalies trace the extension of the faults through the slope of the Ukrainian Shield.

Modeling of the nonlinear resonant response in sedimentary rocks

© V. Vakhnenko[1], O. Vakhnenko[2], J. TenCate[3], T. Shankland[3], 2010

[1]Institute of Geophysics, National Academy of Sciences of Ukraine, Kiev, Ukraine
vakhnenko@ukr.net
[2]Institute for Theoretical Physics, National Academy of Sciences of Ukraine, Kiev, Ukraine
vakhnenko@bitp.kiev.ua
[3]Los Alamos National Laboratory, New Mexico, USA
tencate@lanl.gov
shankland@lanl.gov

Sedimentary rocks, particularly sandstones, are distinguished by their grain structure in which each grain is much harder than the intergrain cementation material [Guyer, Johnson, 1999]. The peculiarities of grain and pore structures give rise to a variety of remarkable nonlinear mechanical properties demonstrated by rocks, both at quasistatic and alternating dynamic loading [Guyer, Johnson, 1999; TenCate, Shankland, 1996; TenCate et al., 2000; Darling et al., 2004]. We suggest a model for describing a wide class of nonlinear and hysteretic effects in sedimentary rocks at longitudinal bar resonance. In particular, we explain: hysteretic behaviour of a resonance curve on both its upward and downward slopes; linear softening of resonant frequency with increase of driving level; gradual (almost logarithmic) recovery of resonant frequency after large dynamical strains; and temporal relaxation of response amplitude at fixed frequency. Starting with a suggested model, we predict the dynamical realization of end-point memory in resonating bar experiments with a cyclic frequency protocol. These theoretical findings were confirmed experimentally at Los Alamos National Laboratory.

A reliable probing method widely applied in resonant bar experiments is to drive a horizontally suspended cylindrical sample with a piezoelectric force transducer cemented between one end of the sample and a massive backload, and to simultaneously measure the sample response with a low-mass accelerometer attached to the opposite end of the bar[2,4]. The evolution equation for the field of bar longitudinal displacements u as applied to above experimental configuration we write as follows

$$\rho\frac{\partial^2 u}{\partial t^2}=\frac{\partial\sigma}{\partial x}+\frac{\partial}{\partial x}\left[\frac{\partial\Im}{\partial(\partial^2 u/\partial x\partial t)}\right]. \qquad (1)$$

Here we use the Stokes internal friction associated with the dissipative function $\Im=(\gamma/2)\times$ $\times[\partial^2 u/\partial x\partial t]^2$. The quantities ρ and γ are, respectively, mean density of sandstone and coefficient of internal friction. The stress-strain relation (σ–$\partial u/\partial x$) we adopt in the form

$$\sigma=\frac{E\operatorname{sech}\eta}{(r-a)\,[\cosh\eta\,\partial u/\partial x+1]^{a+1}}-$$

$$-\frac{E\operatorname{sech}\eta}{(r-a)\,[\cosh\eta\,\partial u/\partial x+1]^{r+1}}, \qquad (2)$$

which for $r>a>0$ allows us to suppress the bar compressibility at strain $\partial u/\partial x$ tending toward $+0-\operatorname{sech}\eta$. Thus, the parameter $\operatorname{coch}\eta$ is assigned for a typical distance between the centers of neighboring grains divided by the typical thickness of intergrain cementation contact.

The indirect effect of strain on Young's modulus E, as mediated by the concentration c of ruptured intergrain cohesive bonds, is incorporated in our theory as the main source of all non-trivial phenomena. We introduce a phenomenological relationship between defect concentration and Young's modulus. Intuition suggests that E must be some monotonically decreasing function of c, which can be expanded in a power series with respect to a small deviation of c from its unstrained equilibrium

value c_0. To lowest informative approximation we have

$$E = (1 - c/c_{cr})E_+ . \qquad (3)$$

Here c_{cr} and E_+ are the critical concentration of defects and the maximum possible value of Young's modulus, respectively. The equilibrium concentration of defects $c\sigma$ associated with a stress σ is given by

$$c_\sigma = c_0 \exp(\upsilon\sigma / kT) , \qquad (4)$$

where the parameter $\upsilon>0$ characterizes the intensity of dilatation. Although formula (4) should supposedly be applicable to the ensemble of microscopic defects in crystals, it was derived in the framework of continuum thermodynamic theory that does not actually need any specification of either the typical size of an elementary defect or the particular structure of the crystalline matrix. For this reason we believe it should also work for an ensemble of mesoscopic defects in consolidated materials, provided that for a single defect we understand some elementary rupture of intergrain cohesion.

Fig. 1 shows typical resonance curves, i. e., dependences of response amplitudes R (calculated at $x=L$) on drive frequency $f=\omega/2\pi$, at successively higher drive amplitudes D. Solid lines correspond to conditioned resonance curves calculated after two frequency sweeps were performed at each driving level in order to achieve repeatable hysteretic curves. The dashed line illustrates an unconditioned curve obtained without any preliminary conditioning. Arrows on the three highest curves indicate sweep directions. This results of the computer simulations were adapted to experimental conditions appropriate to the data obtained by TenCate and Shankland for Berea sandstone [TenCate, Shankland, 1996].

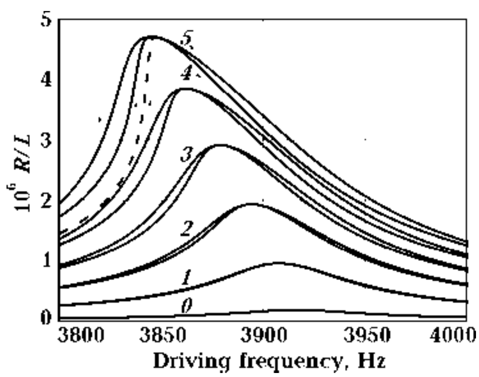


Fig. 1. Resonance curves $j=0, 1, 2, 3, 4, 5$ at successively higher driving amplitudes $D_j = 3.8(j + 0.2\delta_{j0})10^{-8} L$.

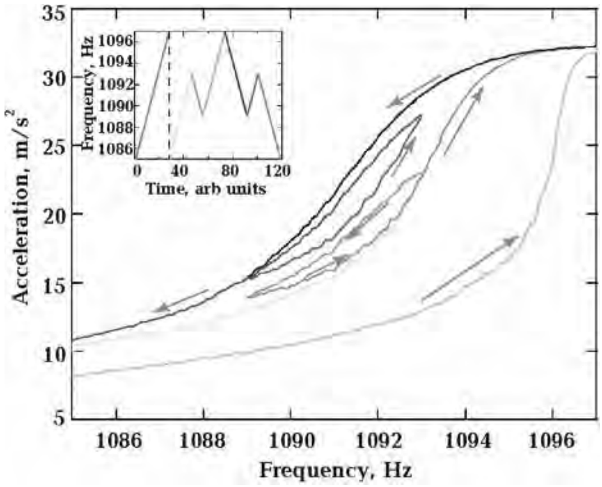


Fig. 2. Recovery of resonant frequency f_r to its maximum limiting value f_0.

Fig. 2 shows the gradual recovery of resonant frequency f_r to its maximum limiting value f_0 after the bar has been subjected to high amplitude conditioning and conditioning was stopped. We clearly see the very wide time interval $10 \le (t - t_c)/t_0 \le 1000$ of logarithmic recovery of the resonant frequency (Fig. 2), in complete agreement with experimental results. Here t_c is the moment when conditioning switches off and t_0=1s is the time scaling constant. Curves $j=1, 2, 3$ on lower Fig. 2 correspond to successively high water saturations $s_j=0.05(2_j-1)$.

The question of whether an effect similar to the end-point (discrete) memory that is observed in quasi-static experiments with a multiply-reversed loading-unloading protocol (see [Darling et al., 2004] and references there) could also be seen in resonating bar experiments with a multiply-reversed frequency protocol has been raised in [Vakhnenko et al., 2006] and was first examined theoretically. The graphical results of this investigation are presented in Fig. 16 in [Vakhnenko et al., 2005] One of the features of dynamical end-point memory, defined here as the memory of the previous maximum amplitude of alternating stress, is seen as small loops inside the major loop. The starting and final points of each small loop coincide, which is typical of end-point memory.

Following the theoretical results, we performed experimental measurements to verify our prediction [Vakhnenko et al., 2005]. The sample bar was a Fontainebleau sandstone and the drive level produced a calculated strain of about at the peak. Fig. 3 shows the low frequency sides of resonance curves

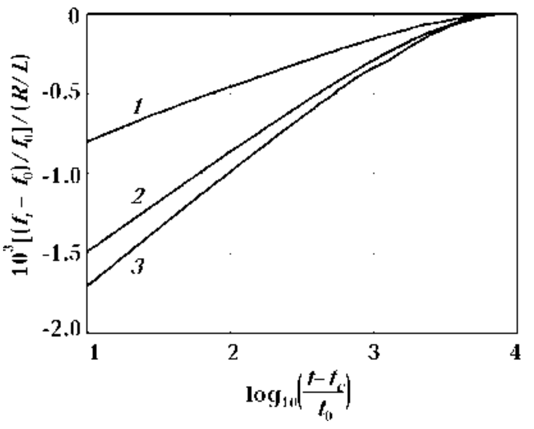


Fig. 3. The low frequency sides of experimental resonance curves for Fontainebleau sandstone.

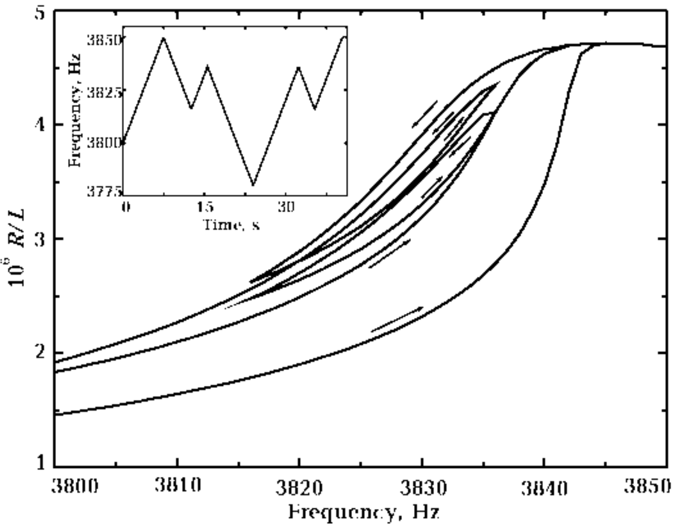


Fig. 4. The low frequency sides of the resonance curves calculated for Berea sandstone.

that correspond to the frequency protocol given on inset of Fig. 3. We clearly see that the beginning and end of each inner loop coincide, i. e., a major feature of end-point memory.

The experimental results for the Fontainebleau sandstone shown in Fig. 3 were reproduced by using our model equations though with constants (including a state equation) developed for Berea sandstone [Vakhnenko et al., 2005]. We note the good qualitative agreement between the experimental (Fig. 3) and the theoretical (Fig. 4) curves suggesting that our physical model is appropriate for both sand-stones.

Hence, the suggested model enables us to describe correctly a wide class of experimental facts concerning the unusual dynamical behaviour of such mesoscopically inhomogeneous media as sandstones. Moreover, as it is shown below, we have predicted the phenomenon of hysteresis with end-point memory in its essentially dynamical hypostasis. These theoretical findings were con-firmed experimentally at Los Alamos National Laboratory.

References

Darling T. W., TenCate J. A., Brown D. W., Clausen B., Vogel S. C. Neutron diffraction study of the contribution of grain contacts to nonlinear stress-strain behavior // Geophys. Res. Lett. — 2004. — **31**. — P. L16604(4).

Guyer R. A., Johnson P. A. Nonlinear mesoscopic elasticity: Evidence for a new class of materials // Physics Today. — 1999. — **52**. — P. 30—35.

TenCate J. A., Shankland T. J. Slow dynamics in the nonlinear elastic response of Berea sandstone // Geophys. Res. Lett. — 1996. — **23**. — P. 3019—3022.

TenCate J. A., Smith E., Guyer R. A. Universal slow dynamics in granular solids // Phys. Rev. Lett. — 2000. — **85**. — P. 1020—1024.

Vakhnenko O. O., Vakhnenko V. O., Shankland T. J. Soft-ratchet modelling of end-point memory in the nonlinear resonant response of sedimentary rocks // Phys. Rev. B. — 2005. — **71**. — P. 174103(14).

Vakhnenko V. O., Vakhnenko O. O., TenCate J. A., Shankland T. J. Dynamical realization of end-point memory in consolidated materials // Innovations in nonlinear acoustics: ISNA17—17th International Symposium on Nonlinear Acoustics. — AIP Conference Proceedings. — 2006. — **838**. — P. 124—127.

Computer simulation related to salt tectonics in the Dnieper-Donets basin

© D. Vengrovich, 2010

Institute of Geophysics, National Academy of Sciences of Ukraine, Kiev, Ukraine
vengr@rambler.ru

In this work we investigate thoroughly the mechanisms that generate salt diapirs in brittle rocks [Poliakov et al., 1996] using the fully dynamic model of natural materials with internal structure. The over-

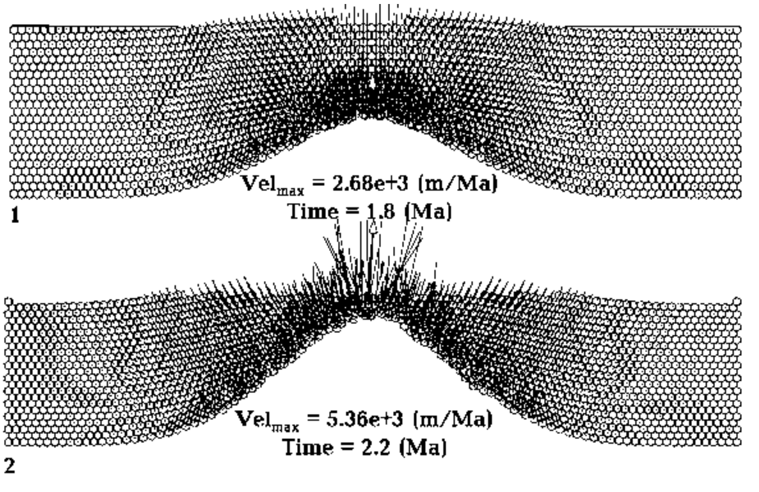


Fig. 1. Positions and velocities (arrows) of blocked sediments during salt diapir growing (model with taking into account erosion).

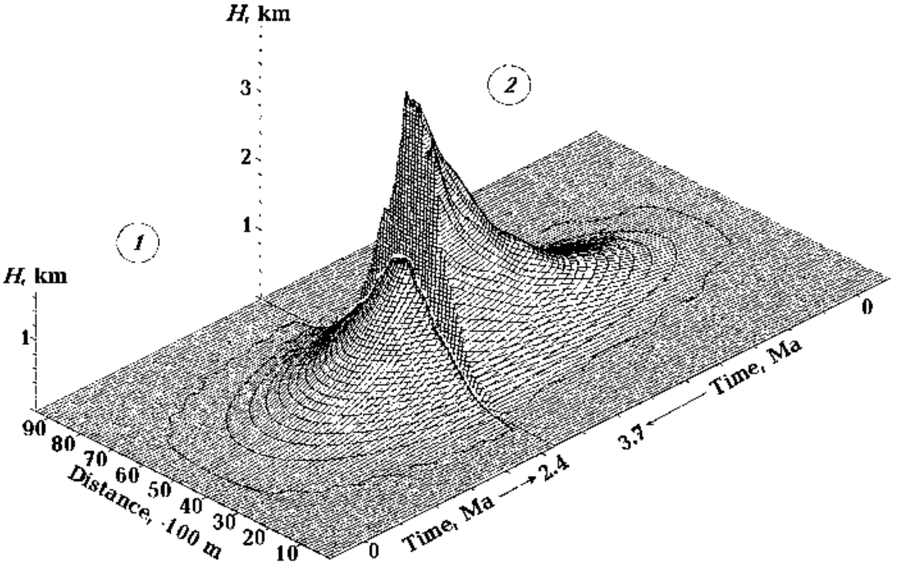


Fig. 2. Salt diapir growing in case of different thickness of sediment overburden: *1* — initial thickness is equal to 1.8 km, *2* — initial thickness is equal to 3.6 km.

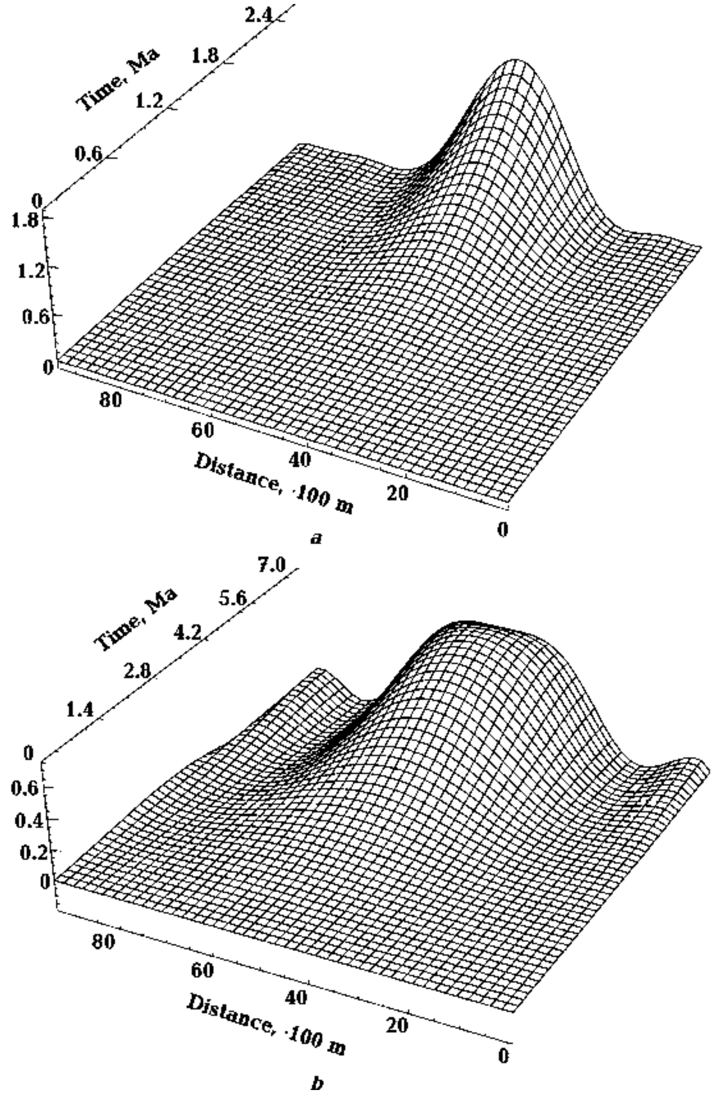


Fig. 3. Salt diapir growing in case of momentary erosion (*a*); diapir growing in case of simultaneously sedimentation 0.5 km/Myr (*b*).

burden and salt are represented by sandstone and salt blocks, capable to be separated or crushed under exterior load. In the 2D model we equate the dynamics of block media [Starostenko et al., 1999]:

$$m_k \frac{d^2\mathbf{x}_k}{dt^2} = \sum_j \mathbf{F}_{\mathrm{jk}} \ , \ I_k \frac{d\varpi_k}{dt} = \sum_j \mathbf{M}_{kj} \ ,$$

where m_k is mass of block k; I_k is moment of inertia of block k; $\mathbf{x},\omega$ are co-ordinate and angular velocity; forces are presented as summarized frictional force, forces owning to energy dissipation, elastic interaction force and gravity force [Poliakov et al., 1996]:

$$F_{ij} = F\mathbf{n}_{ij} = R(\varepsilon_{ij})\,\mathbf{n}_{ij}$$

$$\varepsilon_{ij}^{\substack{compresion \\ tension}} = \pm 2r - \left(\sum_{k=1,2} \left(x_i^k - x_j^k \right)^2 \right)^{1/2} .$$

Thus set are a brittle-elastic medium, which one frequently use at physical simulation in this field. In such model density contrast between salt and brittle overburden leads to the salt diapir generation. By additional causes can serve small regional sediments tensions, their erosion, local basement subsidence along fault. As a result of computer 2D-simulation and comparison with geologic datas on salt tectonic of the Dnieper-Donets Rift basin (Ukraine) is established, that buoyancy forces are capable to drive diapirs of salt into brittle overburdens.

Fig. 1 shows the result of computer 2D-simulation of salt diapir growing. Fig. 2. shows the comparison of salt diapir growing in case of different thickness of sediment overburden. Fig. 3. shows the comparison of salt diapir growing with and without erosion.

References

Poliakov A., Podladchikov Yu., Dawson E., Talbot C. Salt diapirism with simultaneous brittle faulting and viscous flow / Eds. G. I. Alsop, D. J. Blundell, I. Davison // Salt Tectonics, Geolog. Soc. Spec. Publ. — 1996. — № 100. — P. 291—302.

Starostenko V. I., Danilenko V. A., Vengrovitch D. B., Kutas R. I., Stovba S. M., Stephenson R. A., Kharitonov O. M. A new geodynamical-thermal model of rift evolution, with application to the Dniepr-Donets Basin, Ukraine // Tectonophysics. — 1999. — **313**. — P. 29—40.

Digital modeling of the rift processes in the Dnieper-Donets Basin, Ukraine

© *D. Vengrovich, V. Starostenko, V. Danylenko, 2010*

Institute of Geophysics, National Academy of Sciences of Ukraine, Kiev, Ukraine

A model of the lithosphere, incorporating both dynamic and thermal processes, has been developed by solving a coupled system of differential equations governing stress and temperature in a 2D block-structured geophysical medium [Starostenko et al., 1999; 2001]. Using the kinetic energy of block k in functional form:

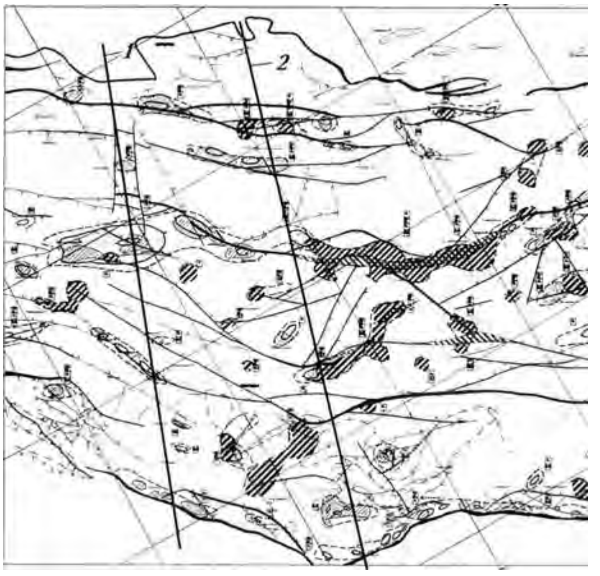


Fig. 1. Locations of seismic reflection profile Zachepilovka — Belsk (*1*) and Mikhailovka — Prokopenki (*2*) in the central part of the Dnieper-Donets Basin (DDB).

$$T_k = \frac{m_k}{2}\left\{\upsilon_{k-1}^2 + 2\beta\left(r_{ok-1} - r_{k-1}\right)\upsilon_{k-1}\frac{\partial\upsilon_{k-1}}{\partial\vec{r}_{ok-1}} + \right.$$

$$\left. + \beta^2\left(r_{ok} - r_{k-1}\right)^2\left(\frac{\partial\upsilon_{k-1}}{\partial r_{ok-1}}\right)^2\right\} +$$

$$+\frac{1}{2}\left(1 + b_k\right)^2\left(\omega_{k-1}\times\omega_{k-1}\right)I_{k-1}^{l,j} +$$

$$+I_{k-1}^{l,j}\left\{\frac{\beta^2}{2}\left(div\,\upsilon_{k-1}\right)^2 + \beta^2\frac{\partial\upsilon_{k-1}}{\partial r_{ok-1}}div\upsilon_{k-1}\right\} +$$

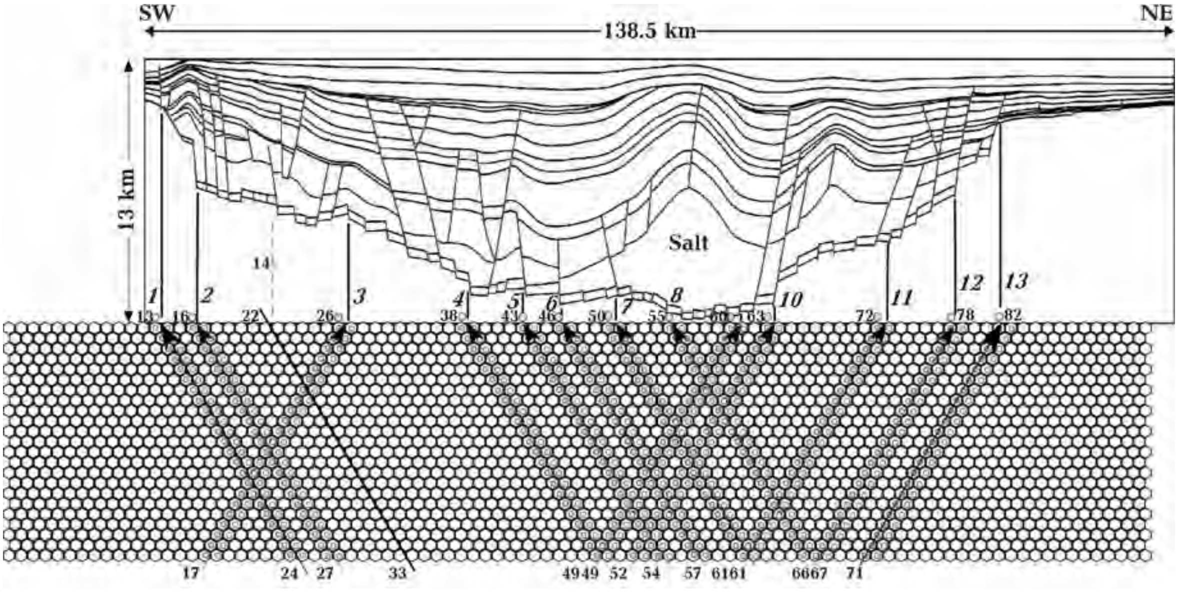


Fig. 2. Initial location of blocked layers of basin basement according to Zachepilovka — Belsk seismic profile: *1* ¯0 km (+); *2* ¯5.0 km (+); *3* ¯24.6 km (–); *4* ¯41 km (+); *5* ¯48 km (+); *6* ¯53 km (+); *7* ¯61 km (+); *8* ¯68 km (+); *9* ¯78 km (–); *10* ¯82 km (–); *11*¯98 km (–); *12* ¯106 km (–); *13* ¯113 km (–).

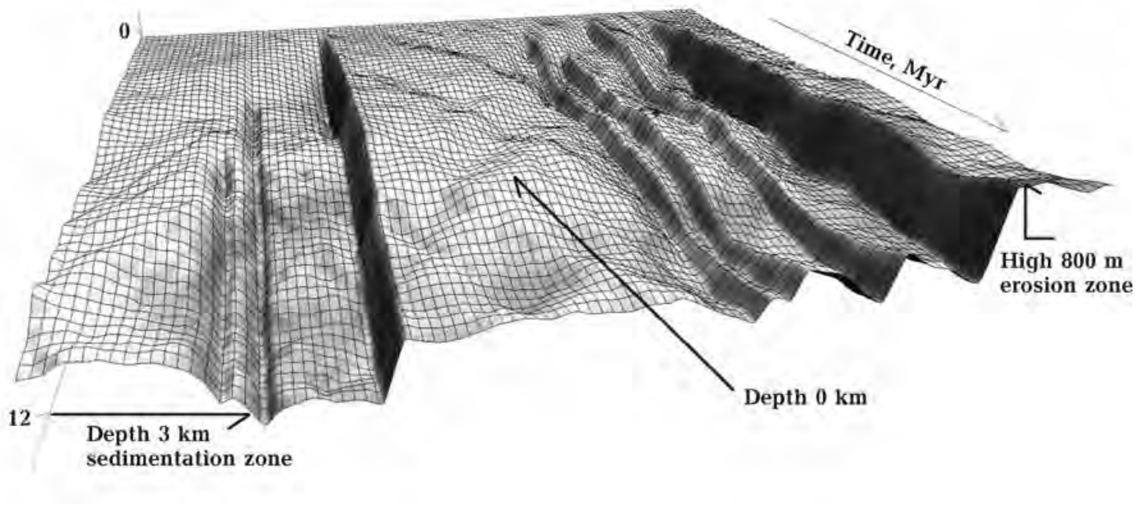


Fig. 3. Model predicted evolution of the sedimentary basin basement horizon along the Zachepilovka — Belsk profile from the beginning of the rift stage (370 Ma) until the late Fammenian.

$$+(1+b_k)[\omega_{k-1}\upsilon_{k-1}]\, m_k\, r_{ok-1}+$$

$$+\frac{1}{2}\beta\upsilon_{k-1} div\upsilon_{k-1} m_k\, r_{ok-1}.$$

We equate the dynamics of block media:

$$\frac{\partial}{\partial t}\left[\frac{\partial T_k}{\partial \mathbf{q}}\right]+\frac{\partial T_k}{\partial \mathbf{q}}+\frac{\partial U_k}{\partial \mathbf{q}}=\mathbf{F}'_k+\mathbf{F}''_k+\mathbf{F}_{kn}+\mathbf{F}_0,$$

$$k=1,2,..,n,$$

where m_k is mass of block k; $I_{k-1}^{l,j}$ is moment-of-inertia tensor of block k–1; $\mathbf{q}$, $\dot{\mathbf{q}}$, ω_I are generalized co-ordinate, linear and angular velocity; $\mathbf{F}'_k$ is summarized frictional force; $\mathbf{F}''_k$, $\mathbf{F}_{kn}$, $\mathbf{F}_0$ — forces owning to energy dissipation, elastic interaction and gravity.

The main rifting phase forming the Dnieper-Donets Basin (DDB) occurred in the Late Devonian (370—

363 Ma). In this approach the digital simulation of whole DDB region showed that after initial stretching and mantle thermal load the set of blocks became active over a period of 12 Myr.

Fig. 1 shows locations of test in presentation seismic reflection profiles Zachepilovka — Belsk (*1*) and Mikhailovka — Prokopenki (*2*) in the central part of the DDB according to geophysical observations. The mathematical 2D dynamic and thermal model is 140 km in length and 120 km deep and comprises three layers — 'granite', 'basalt', and mantle — with appropriate thermo-physical parameters. Fig. 2. shows the initial 'granite' and 'basalt' layers of blocks that have been built according to Zachepilovka — Belsk profile interpretations. Model results are shown in Fig. 3. as evolution of the sedimentary basin basement horizon along the Zachepilovkav — Belsk profile.

References

Starostenko V. I., Danilenko V. A., Vengrovitch D. B., Kutas R. I., Stovba S. M., Stephenson R. A., Kharitonov O. M. A new geodynamical-thermal model of rift evolution, with application to the Dniepr-Donets Basin, Ukraine // Tectonophysics. — 1999. — **313**. — P. 29—40.

Starostenko V. I., Danylenko V. A., Vengrovich D. B., Kutas R. I., Stephenson R. A., Stovba J. N. Modeling of the Evolution of Sedimentary Basins Including the Structure of the Natural Medium and self-organization processes // Phys. Sol. Earth. — 2001. — **37**, № 12. — P. 1004—1014.

Possibilities of seismic migration for interpretation of wide-angle reflection/refraction profiles

© A. Verpakhovska, V. Pylypenko, O. Pylypenko, 2010

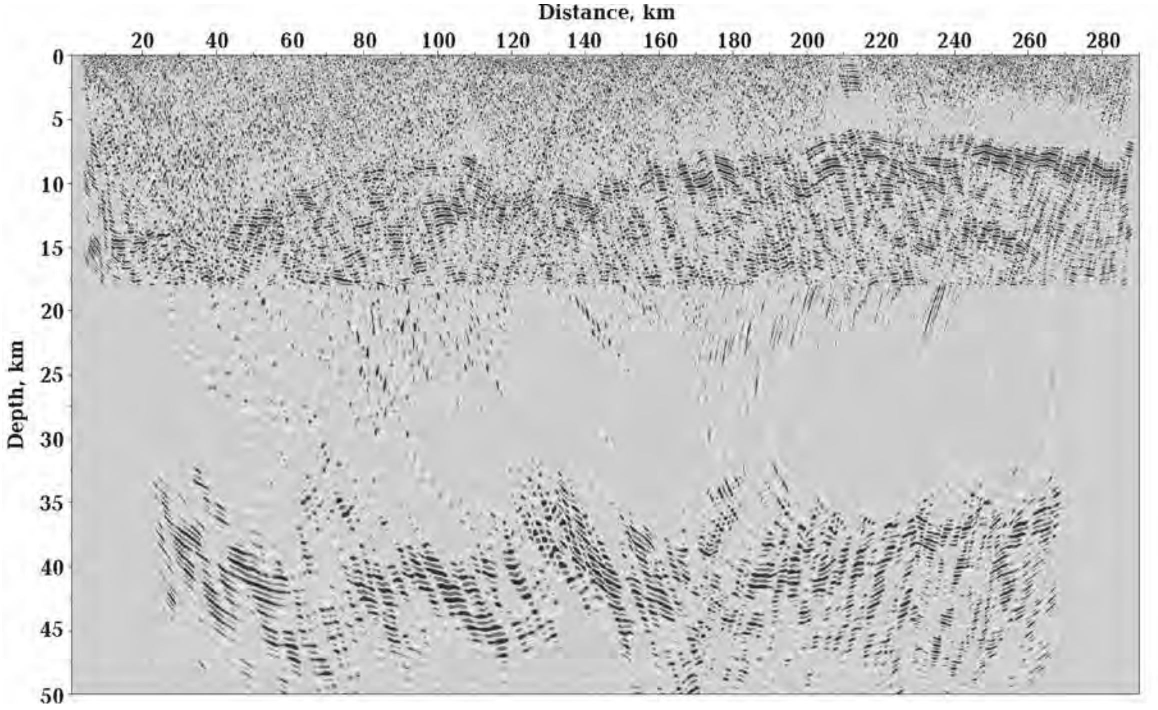
Institute of Geophysics, National Academy of Sciences of Ukraine, Kiev, Ukraine
alversim@gmail.com

The migration of observed wave field is key procedure of processing and interpretation of seismic materials as gives the chance to receive an image of a deep section of investigated area where boundaries of environment and feature of their structure are accurately traced. At present there are a considerable number of variants of wave field migration transformations, but one of the most important problems still is involving in process of migration of the wave field recorded at wide-angle observations.

The traditional method of reflected field migration is used successfully for that part of a wave field which is received in rather small distant from a source. At rare and irregular observation system the more stability image of environment can be received with application of finite-difference reverse time depth prestack migration [Pilipenko et al., 1999].

The refracted waves dominate in a distant part of a wave field, from a source. In seismic prospecting, at interpretation under the refracted waves frequently understand waves which conform to theories of head wave propagation sliding along refracting border and thus not penetrate into refracting thickness. Such understanding of the refracted waves mismatches their real propagation in the environment. However, accounting of their penetration into in refracting thickness leads to complexities, as in theoretical and practical realization of migration. Thus the main problem of wide application of the refracted diving wave field migration is ambiguity in definition position of wave refraction (that is connected with two points of refraction: a penetration in refracting thickness and an exit from it) as opposed to uniquely fixing of a reflection place for the reflected waves. Therefore, the refracted wave field finite-difference migration, offered by Pylypenko V. N. in the eighties of the twentieth century [Pylypenko, Sokolovskaya, 1990] remains while the unique method which is based on refracted diving waves. The given method of migration provides carrying over of a source from a day surface on a surface of refracting boundary in a point of a wave penetration into refracting thickness and to form the boundary image on a point of an exit of wave in covering layer [Pylypenko, Verpakhovskaya, 2003]. Such approach has allowed realizing a correct method of refracted wave field finite-difference migration. The developed method has been successfully tested on a practical seismic material, observed in different parts of the world [Pylypenko, Goncharov, 2000; Makris et al., 2008; Pavlenkova et al., 2009].

Finite-difference migration of refracted wave field



Depth migration section of seismic data (MONALISA2) from North Sea (the top part of a section is formed with the refracted wave field, and bottom — with the reflected wave field).

is based on continuations of time and wave fields for each shot gather. Thus, the difference approximation of eikonal equation on a special grid which as much as possible corresponds to wave propagation in environment is used for continuation of a time field, and reverse continuation of a wave field is performed via the finite-difference solving of the wave equation with application of a time-spatial grid. Finally, the individual images are stacked to produce a final image. The choice of finite-difference method solution explains its correctness and high stability.

Hereby, at researches the WARRP observation system frequently does not allow generating a full deep section by means of migration of a field of one type of waves. The combined approach of image environment formation where the top part of a section is formed with the refracted wave field (Figure), and bottom — with the reflected wave field can serve as an exit in similar situations. Such approach to migration execution has been successfully tested both on modeling and on practical materials and results make possible to talk about its high efficiency and capacity at studying of areas with different degree of deep structure complexity.

References

Makris J. N., Papoulia J. E., Pylypenko V. N., Kakrastahis V. K. Crustal Structure of the Saronic Basin and Western Central Corinthian Gulf from Active Seismic Observations // 31st General Assembly, Europian Seismological Commission. — Hersonissos, Crete Island (Greece), 7—12.09.2008. — P. 163.

Pavlenkova N. I., Pilipenko V. N., Verpakhovskaja A. O., Pavlenkova G. A., Filonenko V. P. Crustal structure in Chile and Okhotsk Sea regions // Tectonophysics. — 2009. — **472**. — P. 28—38.

Pilipenko V. N., Pavlenkova N. I., Luosto U. Wide-angle reflection migration for POLAR profile (Northern Scandinavia) // Tectonophysics. — 1999. — **308**. — P. 445—457.

Pylypenko V., Goncharov A. Seismic migration in near-vertical and wide-angle reflection and refraction studies: Towards a unified approach // Exploration Geophysics. — 2000. — **31**. — P. 461—468.

Pylypenko V. N., Sokolovskaya T. P. Imaging of seismic refracting boundary by a differential method // Geophys. J. — 1990. — **12,** № 5. — P. 48—54 (in Russian).

Pylypenko V. N., Verpakhovskaya A. O. Features of migrational transformation of the diving wave field // Geophys. J. — 2003. — **25**, № 1. — P. 42—54 (in Russian).

Hydrodynamic-type model of relaxing media

© V. Vladimirov, 2010

University of Science and Technology, Academy of Mining and Metallurgy, Krakow, Poland

We consider a mathematical model of geophysical medium, taking into account effects of temporal nonlocality. This model was derived by G. M. Lyakhov on pure machanical ground in late 70th of the XX century, and had been substantiated by V. A. Danylenko and co-workers a decade later within the framework of phenomenological thermodynamics of irreversible processes.

The set of travelling wave (self-similar) solutions of the modeling system is shown to possess a compacton-like solution, if an external force of specific form is present. In contrast to the classical compactons appearing in the Rosenau-Hyman equation, the compacton appearing in the model under consideration is manifested at specific values of the parematers. In spite of such restriction, the compactly-supported travelling wave solution seems to be of interest, since it is shown to attract the near-by, not necessarily self-similar solutions. Using the numerical experiments, we show that solutions to Cauchy problems are attracted to the compacton if some energy criterion is fulfilled, regardless of the shape of initial data.

Lithosphere structure of the Black Sea basin from seismic tomography and 3D gravity analysis

© T. Yegorova[1], T. Yanovskaya[2] , V. Gobarenko[1], E. Baranova[1], 2010

[1]Institute of Geophysics, National Academy of Sciences of Ukraine, Kiev, Ukraine
egorova@igph.kiev.ua
valja-gobar@mail.ru
[2]St. Petersburg State University, St. Petersburg, Russia
yanovs@yandex.ru

Black Sea Basin is a back-arc basin formed in the Latest Cretaceous (or at the Cretaceous-Palaeogene boundary) at the hinterland of the Pontide magmatic arc. At present the Black Sea Basin is a flat abyssal plain with the sea floor at a depth of 2 km, which overlaps two large sedimentary basins in the western and eastern parts of the sea (the West (WBS) and East Black Sea (EBS) Basins), filled with thick (up to 12—14 km) Cenozoic sediments. These two basins are separated by the Mid Black Sea Ridge — a NW-trended linear structure of the basement uplift. Thick sedimentary cover masks poorly investigated basement and heterogeneous crystalline crust that is most likely represented by a collage of different microplates and terranes of different affinities, welded together by accretion during the closure of Neotethys. Recent reinterpretation of some existed in the Black Sea profiles of deep seismic refraction study [Baranova et al., 2008; Yegorova et al., 2010] and new seismic experiment in the East Black Sea Basin [Shillington et al., 2009] have shown that the WBS and the EBS basins are underlain by high-velocity (6.6—7.0 km/s) thin oceanic and semi-oceanic crust of 5—7 km thickness confined by the Moho boundary placed at nearly 20 km depth.

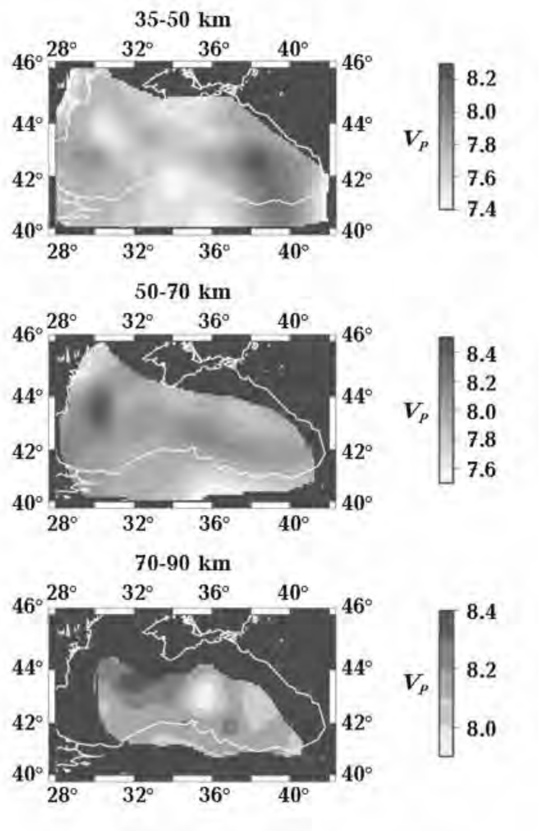
Despite active geological and geophysical exploration of the study region, little is known about the structure of lithospheric mantle below the Black Sea Basin. This information, together with distribution of recent seismicity, is of crucial importance for understanding the geodynamic situation and governed tectonic processes in the region [Gobarenko, Yegorova, 2010; Yegorova, Gobarenko, 2010]. The present contribution deals with investigation of the velocity structure of the Black Sea lithosphere by seismic tomography using the data from earthquakes occurred inside the study region and recorded by seismic sta-

tions located along the coastline of the Black Sea. This velocity model was converted into density model in order to calculate the gravity signal from the lithospheric mantle, which was compared with mantle gravity anomalies derived from 3D gravity analysis using the back-stripping method.

Velocity distribution in the upper mantle was calculated using the seismic tomography method, which encompasses partitioning the medium on cells and defining in them velocity corrections. Initial data were corrected for the crust impact, allowing us to derive precise information on velocity structure of the upper mantle. Resulting lateral variations of *P*-wave velocities in the mantle lithosphere of the Black Sea are shown in Figure by horizontal slices of average velocities for the depth of 35—50, 50—70 and 70—90 km.

Derived velocity distribution represents the Black Sea Basin not as a single velocity domain, but rather heterogeneous one, where one can see two distinct areas of increased velocities within the western and eastern parts of the Black Sea, which are separated by lower velocities in the central part of the sea. Gravity signal from the lithospheric mantle, calculated from density equivalent of this velocity model in Figure, outlines two areas of positive gravity (up to 80 mGal) in western and eastern parts of the Black Sea. They are separated by non-anomalous zone within the central part of the sea.

From the other side, mantle gravity anomalies were derived by back-stripping gravity analysis whereby gravity effect of constrained layers (seawater, sediments, crystalline crust) are removed from initial gravity field. The crust structure here is constrained by new results from active seismic experiments [Baranova et al., 2008; Shillington et al., 2009; Yegorova et al., 2010] Gravity calculations were performed on 10 km×10 km grid. Final residual anomalies of supposed mantle origin distinguish small positive values (to 40 mGal) in the western part of the Blacks Sea, whereas no significant anomalies were revealed in the eastern part — prevailing anomalies here range from zero to 20 mGal. These slight positive mantle anomalies might be indicative of isostatic equilibrium of the Black Sea



Distribution of the *P*-wave velocities in the Black Sea lithosphere.

deep structure, namely that negative gravity effect of sediments is substantially compensated by strong positive gravity impact of the Moho swallowing. In general these mantle anomalies agree with mantle gravity signal, derived from seismic tomography model (despite amplitude of the latter a bit higher of the former), and both are indicative of lack of the asthenosphere or mantle diapir at the depth less 100 km below the Black Sea. This corresponds also with very low surface heat flow density with prevailing values in the Black Sea of 30—40 mW/m^2 and low deep temperatures estimated to be 500—600° at the depth of 30 km [Kutas et al., 1997].

References

Baranova E. P., Egorova T. P., Omelchenko V. D. Reinterpretation of seismic materials of DSS and gravity modeling along the profiles 25,28 and 29 in the Black Sea and the Sea of Azov // Geophys. J. — 2008. — **30**, № 5. — P. 124—144 (in Russian).

*Gobarenko V. S., Yegorova T. P.*The lithosphere structure and geodynamics of the West and East Black Sea basins // Izvestiya, Phys. Sol. Earth. — 2010. — **46**, № 6. — P. 507—523.

Kutas R. I., Kobolev V. P., Tcvyashchenko V. A., Bev-

zuyk M. I., Kravchuk O. P. Geothermal model of the Black Sea Basin // Geophys. J. — 1997 — **19**, № 6. — P. 70—83 (in Russian).

Shillington D. J., Scott C. L., Minshull T. A., Edwards R. A., Brown P. J., White N. Abrupt transform from magma-starved to magma-rich rifting in the eastern Black Sea // Geology.— 2009. — **37**, № 1. — P. 7—10.

Yegorova T., Gobarenko V. Structure of the Earth's crust and upper mantle of West- and East-Black Sea Basins revealed from geophysical data and its tectonic implications / Eds. R. A. Stephenson, N. Kaymakci, M. Sosson, V. Starostenko, F. Bergerat // Sedimentary basin Tectonics from the Black Sea and Caucasus to the Arabien Platform, Geolog. Soc. — London: Spec. Publ., 2010. — **340**. — P. 23—41.

Yegorova T., Baranova E., Omelchenko V. The crustal structure of the Black Sea from the reinterpretation of deep seismic sounding data acquired in the 1960s / Eds. R. A. Stephenson, N. Kaymakci, M. Sosson, V. Starostenko, F. Bergerat // Sedimentary basin Tectonics from the Black Sea and Caucasus to the Arabien Platform, Geolog. Soc. — London: Spec. Publ., 2010. — **340**. — P. 43—56.

Important influences of depth-dependent lower-mantle properties on the formation of a plume-fed asthenosphere in the upper mantle

© D. Yuen[1], N. Tosi[2], O. Cadek[3], 2010

[1]Department of Geology and Geophysics, University of Minnesota, Minneapolis, USA
daveyuen@gmail.com
[2]German Space Agency, Berlin, Germany
[3]Charles University, Prague, Czech Republic

Asthenosphere is an old geological concept based on uncanny intuition of Reginald Daly in the 1920's. to explain surface geological observations with underlying mobility in mind.

The idea of a plume-fed asthenosphere has been around for a few years due to the ideas of Phipps-Morgan and his father Jason Morgan. Basiclly this calls for a dynamically induced mechanism instead of partial melting or a mineralogical phase change. Using a two-dimensional Cartesian code based on finite-volume method, we have investigated the influences of lower mantle physical properties on the formation of a low viscosity zone in the upper mantle in regions close to a large mantle upwelling. The rheological law is Newtonian and has both temperature- and pressure-dependences. An extended Boussinesq model is assumed for the energetics and both the spinel to perovskite and perovskite to post-perovskite phase transitions are considered. We have compared the differences in the behavior of hot upwellings passing through the transition zone in the mid-mantle for a variety of models, starting with constant physical properties in the lower-mantle and culminating with complex models which have the post-perovskite phase transitions and depth-dependent properties of both the thermal expansion coefficient and the thermal conductivity.

We found that the formation of the asthenosphere in the upper mantle in the vicinity of large upwellings is only possible in models where both depth-dependent thermal expansivity and thermal conductivity are included. The constant thermal expansivity and costant thermal conductivity models fail to deliver a hot low viscous zone, resembling the asthenosphere. Our findings argue for the potentially important role played by lower-mantle material properties on the development of plume-fed asthenosphere in the oceanic upper-mantle.

Current methods of assessment of the Kremechutskiy reservoir basin within Cherkassy region: Research of the ecological state of Kremenchug reservoir within Cherkassy region by ERS methods

© S. Zagorodnya[1], M. Novik[2], I. Radchuk[2], N. Shevyakina[1], 2010

[1]Institute of Telecommunications and Global Information Space,
National Academy of Sciences of Ukraine, Kiev, Ukraine
snej@ukr.net, 6802146@ukr.net
[2]Institute of Geophysics, National Academy of Sciences of Ukraine, Kiev, Ukraine
igo_r@meta.ua

Creation of the Dnipro cascade hydropower stations and reservoirs caused the gradual development of many complex environmental problems. In such a situation there is also Kremenchug Reservoir. Due to excessive exploitation of the reservoir area of shallow water for various reasons, but primarily due to human factors, decreased from 41.5 hectares to 30.6 hectares, of which over 10 thousand hectares of overgrown vegetation and surface were silted. Therefore, effective management decisions are necessary to control and improve the ecological condition of the Kremenchug reservoir.

We must have accurate, timely and complete information about the basic parameters of the current state of the environment components and anthropogenic factors that affect them. Most of these data can be obtained using the technologies of remote sensing (ERS) from space. These technologies offer more and more sophisticated hardware — software solutions and new approaches to the analysis of a wide range of subject — oriented problems. Analysis of these solutions and approaches, gives grounds to conclude that it is expedient to attract them to study structural relationships between socio-economic, technological, and natural resource factors that together determine the status, variability and correlation components of the natural environment in their interaction with technosphere. Using CRP allows methods and with great certainty to get objective information about the ecological state of an object and implement its Monitoring. In combination with technologies of geo-



Fig. 1. A space shot Ikonos (Cherkassy city).

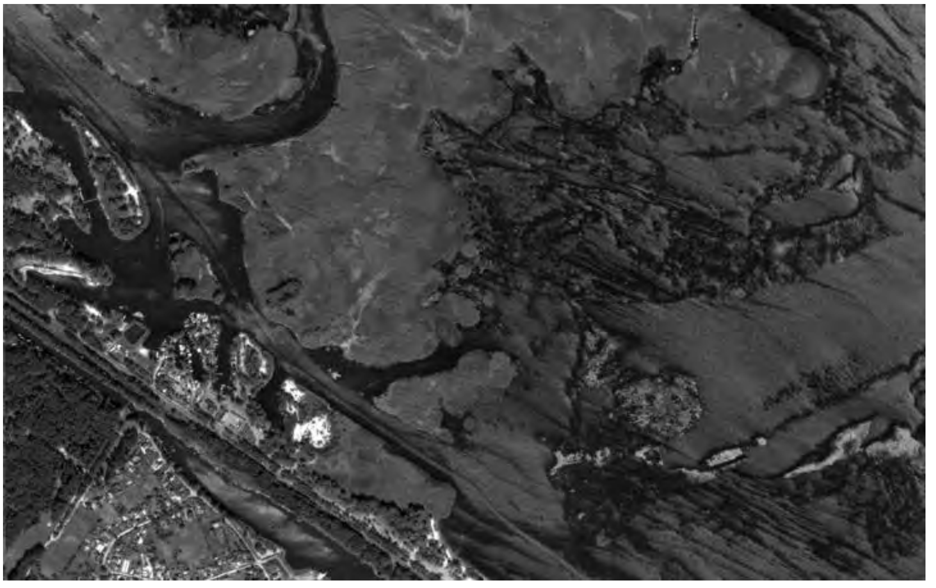


Fig. 2. Kosmos Ikonos (Kremenchug Reservoir).

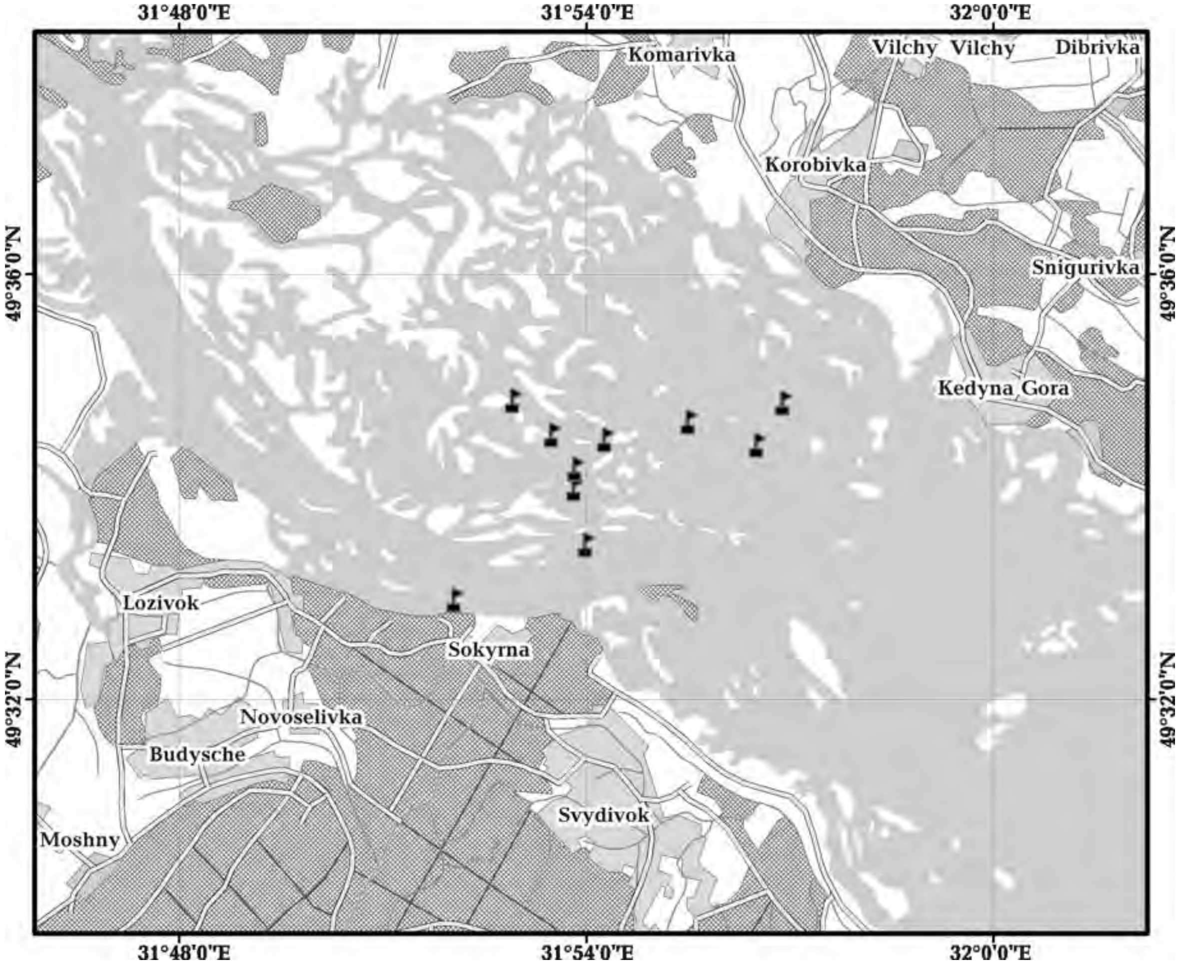


Fig. 3. Site selection stations surface water samples.

graphic information systems (GIS) remote sensing techniques allow us to quickly and comprehensively interpret environmental information content, quickly analyze and update it, combining with management decisions. That′s why these methods were used in the studies of ecological state of the Kremenchug reservoir. Kremenchug water reservoir located in Cherkassy, Poltava and Kirovograd regions. It is the main regulator of Dnieper cascade.

Useful capacity of reservoir is 9 km 3, which is 50% of working volume of all Dnieper cascade reservoirs. The total length of 149 km, maximum width — 28 km, average — 15.1 km, maximum depth — 20, medium — 6 pm His area of 225 hectares. And water resources 13.5 mlrd m^3 [Regional …, 2009].

Kremenchug reservoir placed dozens of intake. In the summer in most of the waters of the Kremenchug reservoir lake set mode.

At high temperature there is intensive "blooming" of water, there is accumulation of algae and their subsequent reproduction has negative consequences for the health and biological condition of water quality, resulting in oxygen deficiency occurs in the subsurface water at night. Forming various organic and inorganic substances, including toxic.

During research expeditions ecological condition Kremenchug reservoirs, which were organized by the Institute of telecommunications and global information space of NAS of Ukraine and the State Research — Production Center "Nature" NCA in June 2009 was carried out complex measurements of environmental parameters of water masses (Fig. 1, 2). Their interpretation of satellite images of medium involved (MODIS) and super-high distinction (Ikonos) [Krasovsky, 2008; Krasovsky, Petrosov 1999].

According to preliminary data results of visual contextual interpretation of images determined the optimal location of grid stations to collect samples for hydrochemical analysis. The criterion was defined zone sign of extreme brightness area waters, according to the value resolution image. This grid included 10 stations to collect samples. Check point located to create with. Sokyrne — pp. Korobivka so that each channel was tested and cities with a dead regime. Time of testing — the middle day, averaging parameters determined for the oxygen regime. Coordinates of sampling stations of surface water registered by technical means of GPS accuracy of 15 m (Fig. 3) selected samples at different depths. Instrumentation were carried out using water devices Hanna Instrunents HI and HI 98 130 98 121 according to the following list: conductivity, temperature, pH value and redox potential (Table). Also transparency was fixed (on disk Sekky).

It is known that pH-index of activity of hydrogen ions. Size influenced by a mass development of phytoplankton (eg, blue-green algae characteristic of the Dnieper cascade reservoirs) in the summer can be increased to 9.0—10.0; the period of mass death and decomposition of algae in acid pH shift side (sharp decrease in pH) [Nikanorov, 1989].

During research expeditions in the ecological condition of the materials space shooting, synchronous with the ground measurements of indicators of ecological state of water masses, methods of correlation and regression analysis was restored spatial — temporal distribution of these indicators across the top of the Kremenchug reservoir area.

The collected data show that the top of Kremenchug reservoir no significant man-made pollution phe-

Indicators of quality of surface water

№ station	Coordinates		Time selection 21.07.09	Depth, m	Clarity, m	Conductivity	Temperature, °C	Eh, мВ	Ph	Notes
	X, latitude	*Y*, logtitude								
1	49°54.684′	31°86.902′	11:35	4.9	2.2	330	24.8	+205	8.02	Cal solid-watched blossom water
2	49°55.779′	31°90.164′	11:50	3.2	1.8	330	24.8	+205	7.59	
3	49°56.660′	31°89.883′	12:10	1.5	1.5	330	24.5	+205	7.83	
4	49°56.964′	31°89.897′	12:20	2.4	2.2	330	24.5	+214	7.83	
5	49°57.497′	31°89.329′	12:35	3.6	2.0	330	24.6	+214	7.95	
6	49°58.038′	31°88.373′	12:45	2.4	2.0	330	24.7	+213	7.99	
7	49°57.424′	31°90.632′	13:00	3.4	2.0	330	24.6	+207	8.04	
8	49°57.704′	31°92.683′	13:05	3.0	2.4	330	24.7	+216	7.87	
9	49°57.338′	31°94.367′	13:15	2.3	2.0	330	24.7	+208	8.0	Completely clarity, available higher water vegetation
10	49°58.002′	31°95.008′	13:30	2.0	2.0	320	25.0	+220	8.06	

nomena and its ecosystem is in good order. Note that the research are systematic and not selective, which can not reflect the environmental situation in general, but at the time of sampling.

On this point may be noted that there is a need for regular and thorough environmental monitoring marine and coastal areas of the lake (of course, this applies not only in the region), which should include a wide range of issues, ranging from enterprise monitoring and control of waste emissions and process waste, thermal and chemical pollution of waters to determine the intensity of self-purification, secondary contamination of biota and other issues.

References

Regional report on the state of the environment in Cherkassy in 2008. — DUONPS in Cherkasy region. — 2009. — 199 p.

Krasovsky G. Y. Space security monitoring water ecosystems using GIS technology. — Kiev: Intertechnolohiya, 2008. — 480 p.

Krasovsky G. Y., Petrosov V. A. Introduction to methods of monitoring the environment of space. — Kharkov: Aerospace University them. N. E. Zhukovskoho "KhAI", 1999. — 205 p.

Nikanorov A. M. Hydrochemistry: learning. Allowance. — Leningrad: Gidrometeoizdat, 1989. — 205 p.

Influence of surroundings features on the velocity structure of mantle under South-East Asia from data of seismic tomography

© L. Zaiets, T. Tsvetkova, I. Bugaienko, L. Shumlanskaya, 2010

Institute of Geophysics, National Academy of Sciences of Ukraine, Kiev, Ukraine
tsvet@igph.kiev.ua

The region of Southeast Asia is characterized by numerous micro-plates, which are separated by a complex system of subduction zones, marginal and back-arc basins, strike-slip boundaries and accreted terrains. The western part of Southeast Asia is comprised of three tectonic plates: the Southeast Asia plate, the Burma plate, and the Indo-Australian plate. The Pacific plate has influence on

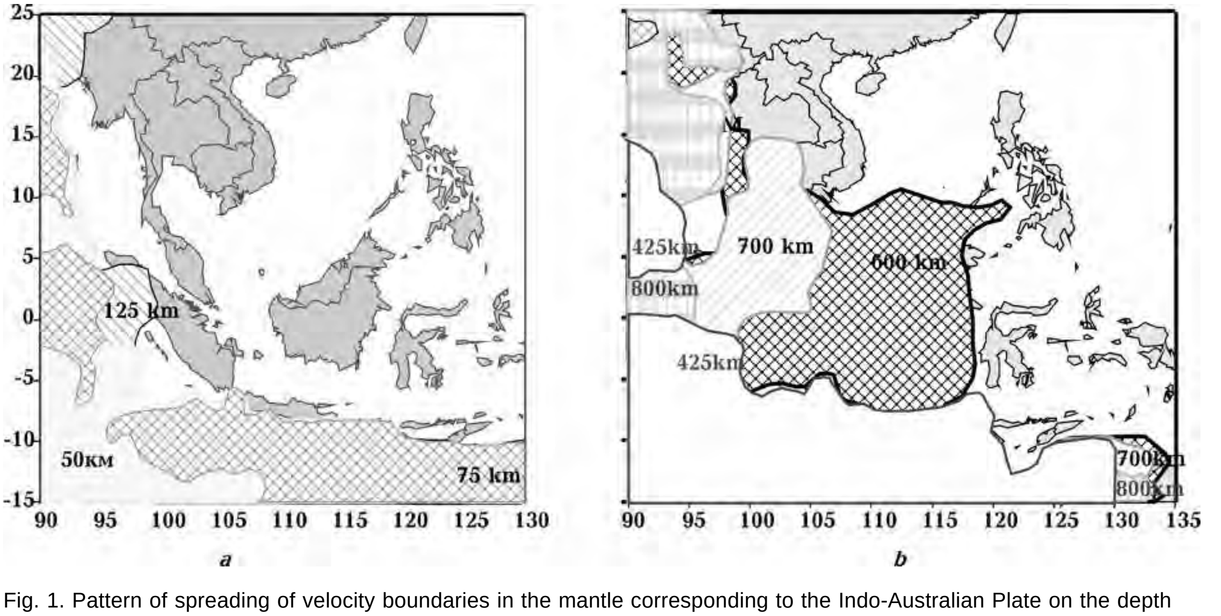


Fig. 1. Pattern of spreading of velocity boundaries in the mantle corresponding to the Indo-Australian Plate on the depth 50, 75, 125 (*a*), 425, 600, 700, 800 (*b*).

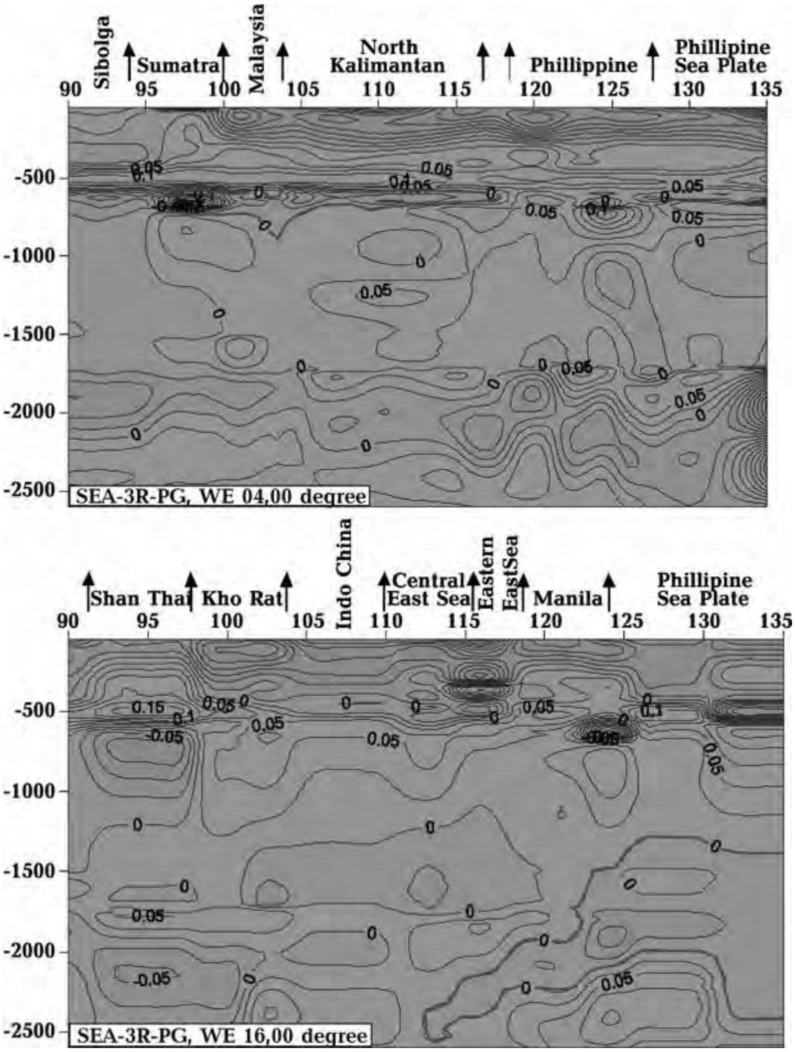


Fig. 2. The latitudinal cross-section of the 3D *P*-velocity model of mantle of the SE Asia.

east part. Tomographic methods can provide new information which can help to test tectonic models. The main objective of the research presented in this thesis is to improve our understanding about influence of surrounding structures on the velocity structure of mantle under South-East Asia of the on depths 50—2500 km. 3D *P*-velocity model of SE Asia has been obtained as a result of application of the method of Taylor approximation of solution of seismic tomography of *P*-waves arrival time introduced by V. S. Geyko [Geyko, Tsvetkova, 1989; Geyko, 1997; 2004). The solution is represented in a form of vertical sections (latitudinal and longitudinal) up to 2500 km depths with 1° spacing in residual in relation to one-dimensional referential model obtained as a result of seismic tomography analysis for Eurasia.

In obedience to our model there is prevailing influence on the structures of SE Asia of velocities structures, proper the Indo-Australian plate. The mantle of the Indo-Australian plate is characterized by a double-layer structure of upper mantle (heavy high-velocity seismic lithosphere and thin low-velocity layer), high-velocity transition zone of upper mantle, low-velocity layer of the zone-1 and quasi-homogeneous middle mantle. Each of layers has the features. Disparity of tectonic boundary of plate and boundary of distribution of low-velocity and high-velocity areas, corresponding to this structure, is thus marked (the boundary of velocity area is distinguished for residual 0.0 km/s to that at changing of sign of velocity heterogeneity) (Fig. 1). Maximal advancement of velocity layers of mantle structures of Indo-Australian plate — to 118° longitudes on a

depth 600 km. Other there is business with the east outskirts of SE Asia. Boundary of mantle of the Philippine plate, distinguished on the boundary of velocity areas observed in a middle mantle and zone-1. So, Philippine plate is selected a sloping low-velocity layer, going from the side of the Philippine plate (1300—2000 to the depth 2400 km). The boundary of plate on a low-velocity layer (on depths 1400—2400 km) comes to 112° longitudes. Partly the boundary of the Philippine plate can be selected on completion of high velocities layer which goes down on the depths of middle mantle and reaches in a westward to 110° longitudes, and under Java to 108° longitudes (600—1400 km). In an upper mantle the boundary of the Philippine plate is expressed by changing of depth of bedding of bottom and top of velocity layers. About the degree of influence of velocity structures corresponding to the Philippine plate on the structures of Asia judging is difficult. It is fact that the tectonic boundary of plate coincides with the exit of low-velocities from a bottom mantle. The South-China Sea is the knot of joining of structures of velocities, going from a south (Indo-Australian Plate) and from a north (velocities structure of South China). The picture of mutual introduction of layers of velocities is observed in upper mantle and transitional zone of upper mantle with 112° longitudes to 118° longitudes, within the limits of 10—20° latitude North (Fig. 2).

References

Geyko V. S. A general theory of the seismic travel-time tomography // Geophys. J. — 2004. — **26**, № 2. — P. 3—32.

Geyko V. S. Taylor approach of the wave equation and the eikonal equation in inverse seismic problems // Geophys. J. — 1997. — **19**, № 3. — P. 48—68 (in Russian).

Geyko V. S., Tsvetkova T. A. On unigueness in solution of unidimensional inverse kinematik problem of seismic // Geophys. J. — 1989. — **11**, № 6. — P. 61—67 (in Russian).

On the problem of correlation between the faults of the Ukrainian Shield and mantle fault zones

© B. Zankevich[1], N. Shafranska[2], 2010

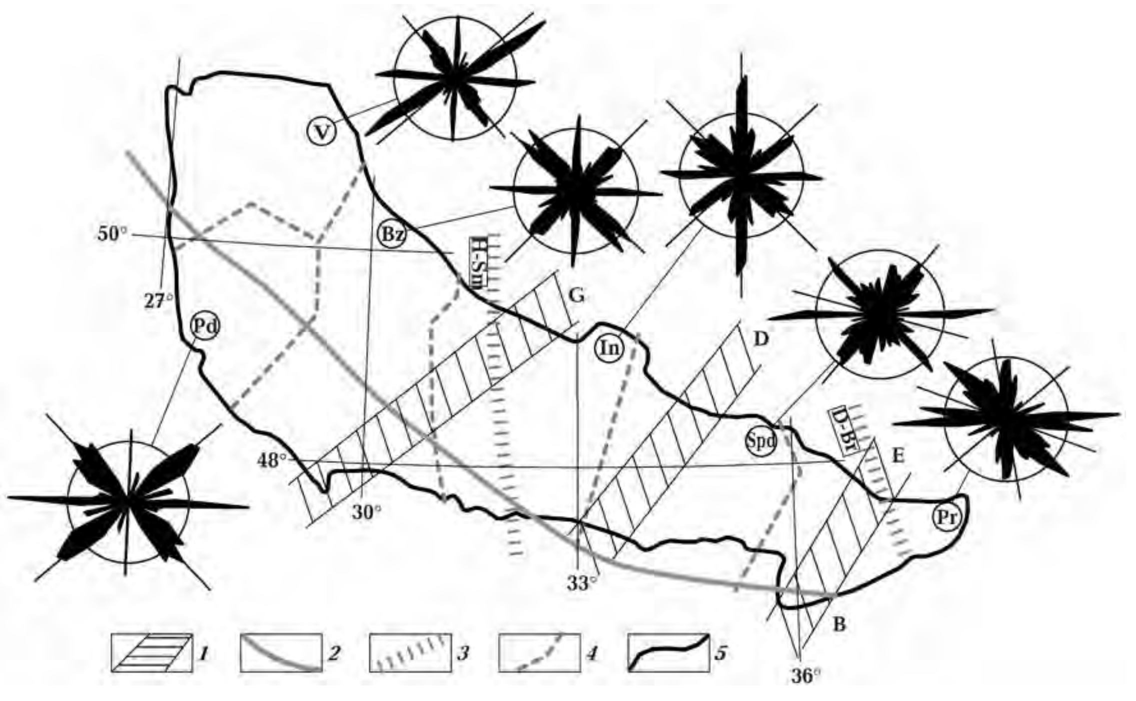
[1]Department of Marine Geology and Sedimentary Ore Formation,
National Academy of Sciences of Ukraine, Kiev, Ukraine
nikalmas@mail.ru
[2]Taras Shevchenko National University of Kiev, Kiev, Ukraine
shafranv@mail.ru

Fault ensembles of basement surface of the Ukrainian Shield (USh) have been analyzed by geological maps of Ukraine (9 maps, scale 1:500000—1:1000000, editors: O. Oleynic, 1978; Kalyayev, 1984; N. Krilov, 1988; D. Gurskiy, 2000; A. Kuzmin, 2002; D. Gurskiy, S. Kruglov, 2004; V. Kalinin, 2007; S. Kruglov, 2007) in the network of the problem [Starostenko et al., 2007].

Mantle faults of the USh and adjacent regions — zones of deep faults (lineaments) touching the surface of asthenosphere, according to [Sollogub, 1986] are “longitudinal” lineament B and NE zones, crossing upper mantle — G, D, E. Their geological-geophysical profiles are different, however these zones and trans-regional mantle sutures (H-Sm and D-Br) determine the structure pattern of Mohorovichich discontinuity surface (Figure).

Faults are systematized as circular extension diagrams of faults by each of maps. Diagrams of these maps equally well illustrate two known systems of faults — diagonal and orthogonal. Some other dependences of fault extensions are revealed on the diagrams for certain megablocks of the USh (see Figure).

Structural-paragenic approach [Rastsvetaev, 1987] adapted by us to the level of knowledge of Precambrian permits to interpret “structural-forming” directions. They have been obtained methodically independently though coincide with strikes of the mantle fault zones of USh. Such coincidence is observed relative to the nearest deep zones, dominating in corresponding parts of the USh. The mantle zones of NE strike G, D, E differ somewhat by strike azimuth, one can observe on the diagrams of



Diagrams of fault strikes of megablocks of the Ush: mantle tectonic zones: *1* — G, D, E by [Sollogub, 1986]; *2* — lineament B [Sollogub, 1986]; *3* — trans-regional sutures [Starostenko et al., 2007]; *4* — boundaries of megablocks; *5* — contour of USh.

megablocks the difference of strike azimuths of "structure-forming" NE directions (note: independently plotted). Change of strike azimuth is specific for "lengthgthwise" mantle lineament B; change of azimuth of "structural-forming" directions is also observed on diagrams of megablocks, from the South to the North: WNW—NW.

Diagrams, plotted by the map (V. Kalinin, 2007), are illustration of relations of USh′s faults strike with mantle faults. But diagrams of faults of all considered maps revealed the same dependences. Such significant coincidence of intersubjective data of the maps can be considered as an empirical regularity.

Empirical diagrams of USh and diagrams of secondary faults of shear zones models [Stoyanov, 1977] are analogous by angular ratios of maximums. This fact is the basis of working hypothesis on significant role of shear component of mantle sutures in formation (and activizations) of faults of the Earth's crust. Faults of the USh partly inherit directions of mantle zones but other fault directions are related to them regularly. The faults of the USh partly inherit the mantle zones directions but other directions of faults are related to them regularly.

References

Rastsvetayev L. M. Paragenetic method of structural analysis of disjunctive tectonic disturbances // Problems of structural geology and physics of tectonic processes. — Moscow: GIN Ac. Sci. USSR Publ., 1987. — P. 173—275 (in Russian).

Sollogub V. B. Lithosphere of Ukraine. — Kiev: Nauk. dumka, 1986. — 184 p. (in Russian).

Starostenko V. I., Gintov O. B., Pashkevich I. K., Burakhovich T. K., Kulik S. N., Kupriyenko P. Ya., Kutas R. I., Makarenko I. B., Orlyuk M. I., Tsvetkova T. A. Metallogeny of USh: regularities of disposition of ore deposits, their connection with deep structure and lithosphere dynamics // Geophys. J. — 2007. — **29**, № 6. — P. 3—31 (in Russian).

Starostenko V. I., Kazansky V. I., Drogitskaya G. M., Makivchuk O. F., Popov N. I., Tarasov N. N., Tripolsky A. A., Sharov N. V. Connection of surface structures of Kirovograd ore area (the Ukrainian Shield) with local heterogeneities of the crust and the relief of Moho discontinuity // Geophys. J. — 2007. — **29**, № 1. — P. 3—21 (in Russian).

Stoyanov S. S. Mechanism of disruptive zones formation. —– Moscow: Nedra, 1977. — 144 p. (in Russian).

What is a “Typical” Mantle Plume?

© A. Harris, Ch. Kincaid, 2010

University of Rhode Island, Graduate School of Oceanography, Narragansett, USA

Process models for mantle plumes, and indeed arguments for the existence of mantle plumes, are largely based on expected characteristics for these upwelling features. Typically plume models have large heads (>500 km), moderately slender tails (~100 km), uniform compositions (lower to upper mantle/Lherzolite), and high excess temperatures (200 °C or more). Here we present laboratory models of mantle convection with recycled, chemically laminated lithosphere which reveal a diversity in size, composition, temperature and both surface geological and geophysical expressions. Results suggest there is no typical mantle plume, but rather a range in plume classes. Examples from within the different classes can readily explain the diversity in plume surface expressions, from large igneous provinces with associated tails (time progressive island chains), to headless plumes and large (or small) headed plumes with no tails. The traditional large headed, uniform composition, high excess temperature plume was rarely seen in the 25 experiments conducted to date. Laboratory models utilized a glucose syrup ($Ra=10^5 \div 10^6$) for a working fluid. Mixtures of syrup and water were used to introduce density and viscosity contrasts between the ambient fluid and a dyed, chilled and layered slab representing recycled lithosphere. Generally, one layer of the slab was less dense than the ambient fluid (representing Harzburgite) and one layer was denser than the ambient fluid (representing Eclogite). A thermal boundary layer was developed at the base of a 20×20×15 cm tank by uniform basal heating. Interaction between the slab layers and fluid within the thermal boundary layer had a strong influence over the distribution of thermochemical heterogeneity within upwelling plumes. A range of repeatable plume styles emerged from this study. One prominent plume style is characterized by upwellings growing shortly after slabs enter the thermal boundary layer. These plumes are Harzburgite-rich and range from cooler (~100 °C) than ambient mantle to nearly equivalent with background temperature. Two common forms of chemical heterogeneity are seen, one in which these plumes have a thin (~10 km), Eclogite core. Plumes of this type that form from the edge of a slab pile have near perfect bilateral symmetry, containing half Harzburgite and half Lherzolite material from within the thermal boundary layer. Another common style of upwelling is recorded over a range of parameter combinations and occurs well after recycled material has reached and spread within the thermal boundary layer. These are hotter plumes (~200—400 °C excess temperature) with predictable distributions of both slab components (Harzburgite and Eclogite) and ambient thermal boundary layer material (Lherzolite). Length scales of thermochemical heterogeneity range from 1 km to >100 km depending on chemical density contrasts and local processes of instability formation within the basal boundary layer. A number of cases from distinct upwelling classes are digitized and used to drive synthetic melting and seismic models. Results show that more typical “plume-like” patterns can occur, but more commonly cases show extreme spatial and temporal discontinuities in melt production and seismic velocity patterns.

GPU support for sparse matrix calculations in PETSc, with applications to nonlinear Stokes

© D. Karpeev, 2010

Mathematics and Computer Science Division Argonne National Laboratory, Argonne, USA

Many geophysical phenomena (matle convection, glacier dynamics) are described by nonlinear Stokesian fluids coupled to various thermodynamic quantities. Linearization leads to variable coefficient linear

Stokes systems, which can exhibit poor convergence in absence of effective preconditioners. The emergence of GPU-based architectures offers dramatic hardware acceleration of many scientific computation tasks. Therefore it is natural to try to take advantage of GPU acceleration for many sparse matrix calculations, including Stokes systems. While achieving peak performance on sparse matrices is usually a challenge, we focus on enabling GPU support within one of the most popular sparse linear algebra and PDE library: PETSc (Portable Extensible Toolkit for Scientific computation). In this talk we will discuss our approach to enabling GPU acceleration for sparse matrix calculations, preconditioning, and the implications for Stokes solvers.

WebViz: A web-based collaborative interactive visualization system for largescale data sets

© E. McArthur[1], R. Weiss[1,2], D. Yuen[1,3], M. Knox[4], 2010

[1]Department of Geology and Geophysics, University of Minnesota, Minneapolis, USA
[2]Department of Computer Science, Macalester College, Saint Paul, USA
[3]Minnesota Supercomputing Institute, University of Minnesota, Minneapolis, USA
[4]Laboratory of Computational Science and Engineering, University of Minnesota, Minneapolis, USA

With larger, faster, and more affordable multi-core and massively parallel computers coming to the market and with the introduction of general purpose GPU computing, the number and size of data sets being produced by the scientific community is on a steep rise. Additionally, with the rise of digital communication technologies, it is more and more common for scientists to engage in international collaborations across large geographical distances. To make sense of the large amount of data now being produced and to make collaboration between scientists easier, a new paradigm for data visualization is necessary. We propose that collaborative visualization tools and a web-based approach to data visualization is an attractive solution [Woodward et al., 2007; Damon et al., 2008; Greensky et al., 2008; McLane et al., 2009].

We have created a web-based application for multi-user collaborative visualization called WebViz. Our web application allows users in geographically disparate locations to simultaneously and collectively visualize large data sets (on the order of gigabytes) over the Internet. Furthermore, by providing data visualization services "in the cloud," users all around the world can leverage our service regardless of their local compute capabilities.

WebViz leverages asynchronous java and XML (AJAX) web development paradigms via the Google Web Toolkit (http://code.google.com/webtoolkit/) to provide remote users with a web portal to LCSE's (http://www.lcse.umn.edu) large-scale interactive visualization system already in place at the University of Minnesota. LCSE's custom hierarchical volume rendering software provides high-resolution visualizations on the order of 15 million pixels and has been employed primarily for visualizing data from simulations in astrophysics, geophysics, and computational fluid dynamics [Porter, 2002; Porter et al., 2002; Greensky et al., 2008; McLane et al., 2009].

In the current version of our WebViz application, we have implemented a new, highly extensible backend framework built around HTTP "server push" technology. This design allows us to provide a rich collaborative environment and a smooth end-user experience. Furthermore, the web application is almost completely platform independent and is accessible via a variety of devices including netbooks, iPhones, and other web- and javascript-enabled cell phones.

Features in the current version of WebViz include: the ability for (1) users to launch multiple visualizations, (2) a user to invite one or more other users to view their visualization in real-time, (3) users to delegate control aspects of the visualization to others and (4) engage in collaborative chat and instant messaging with other users. These features are all in addition to a full range of visualization functions including 3D camera and object orientation/position manipulation, timestepping control, and custom color/alpha mapping.

References

Damon M. R., Kameyama M. C., Knox M. R., Porter D. H., Yuen D. A., Sevre E. Interactive visualization of 3D mantle convection // Visual Geosciences. — 2008. — P. 49—57. — DOI: 10.1007/s 10069-007-0008-1.

Greensky J., Czech W. W., Yuen D. A., Knox M., Damon M. R., Chen S. S., Kameyama M. C. Ubiquitous interactive visualization of 3D mantle convection using a web portal with java and AJAX framework // Visual Geosciences. — 2008. P. 105—115. — DOI: 10.1007/ s10069-008-0013-z.

McLane J., Czech W. W., Yuen D. A., Knox M., Wang S. M. Ubiquitous Interactive Visualization of Large-Scale Simulations in Geosciences Over a Java-based Web-Portal. — Concurrency and Computation: Practice and Experiences. — 2009. — (in press).

Porter D. H. Volume visualization of high-resolution data using PC Clusters. — 2002. — http:// www.lcse.umn.edu/hvr/pc_vol/rend_Lpdf/.

Porter D. H., Woodward P. R., Iyer A. Initial experiences with grid-based volume visualization of fluid low simulations on PC Clusters. — 2002. — http:// www.lcse.umn.edu/dhp1/ articles.html.

Woodward P. R., Porter D. H., Greensky J., Larson A. J., Knox M., Hanson J., Ravindran N., Fuchs T. Interactive volume visualization of fluid flow simulation data. Applied Parallel Computing, State of the Art in Scientific Computing, Proc. PARA 2006 Conf., LNCS 4699, — Heidelberg: Springer Verlag, 2007. — P. 659—664. — http://www.lcse.umn.edu/para06.

Molecular Paleoclimatology: Quantum Chemistry and the History of the Earth's Atmosphere

© J. Rustad, 2010

University of California, Davis, CA USA
james.rustad@gmail.com

The history of the composition of the Earth's atmosphere is one of the most important problems of our time. As the human race considers the possibility of planetary engineering to mitigate the potential effects of CO_2-induced global warming, clearer insight into the history of atmospheric PCO_2 and global temperature is required. For example, if PCO_2 values were 20 times higher at times in the geologic past, it may be premature to worry about anthropogenic increases in PCO_2 a factor of two above Pleistocene-Holocene values, which are anomalously low from the point of view of geologic history. Two major techniques for determining the history of atmospheric PCO_2 are the chemically based. The first depends on the isotopic composition of carbon incorporated into soil minerals during their growth. The second depends on the isotopic composition of boron incorporated into marine minerals during precipitation. Both methods depend crucially on knowing the equilibrium constant for isotope exchange between minerals, aqueous, and gas phases. There are major uncertainties in these equilibrium constants which strongly affect geochemical estimation of the history of PCO_2 in Earth's atmosphere. Here, I describe how quantum chemistry techniques can be used to reduce this uncertainty and make more reliable estimates of PCO_2 values.

Ab initio molecular dynamics and quantum chemistry techniques are used to calculate the structure, vibrational frequencies, and carbon-isotope fractionation factors of the carbon dioxide component [CO_2(m)] of soil (oxy)hydroxide minerals goethite, diaspore, and gibbsite. We have identified two possible pathways of incorporation of CO_2(m) into (oxy)hydroxide crystal structures: one in which the C^{4+} substitutes for four H^+ [$CO_2(m)_A$] and another in which C^{4+} substitutes for (Al^{3+},Fe^{3+})+H^+ [$CO_2(m)_B$]. Calculations of isotope fractionation factors give large differences between the two structures, with the $CO_2(m)_A$ being isotopically lighter than $CO_2(m)_B$ by≈10 per mil in the case of gibbsite and nearly 20 per mil in the case of goethite. The reduced partition function ratio of $CO_2(m)_B$ structure in goethite differs from CO_2(g) by<1 per mil. The predicted fractionation for gibbsite is>10 per mil higher, close to those measured for calcite and aragonite. The surprisingly large difference in the carbon-isotope fractionation factor between the $CO_2(m)_A$ and $CO_2(m)_B$

structures within a given mineral suggests that the isotopic signatures of soil (oxy) hydroxide could be heterogeneous.

Density functional and correlated molecular orbital calculations (MP2) are carried out on $B(OH)_3 \cdot nH_2O$ clusters (n = 0, 6, 32) and $B(OH)_4 nH_2O$ (n = 0, 8, 11, 32) to estimate the equilibrium distribution of ^{10}B and ^{11}B isotopes between boric acid and borate in aqueous solution. For the large 32-water clusters, multiple conformations are generated from ab initio molecular dynamics simulations to account for the effect of solvent fluctuations on the isotopic fractionation. We provide an extrapolated value of the equilibrium constant $á_{34}$ for the isotope exchange reaction $^{10}B(OH)_3(aq) + {}^{10}B(OH)_4(aq) = {}^{11}B(OH)_3(aq) + {}^{11}B(OH)_4\ (aq)$ of 1.026—1.028 near the MP2 complete basis set limit with 32 explicit waters of solvation. With some exchange-correlation functionals we find potentially important contributions from a tetrahedral neutral $B(OH)_3 \cdot H_2O$ Lewis acid–base complex. The extrapolations presented here suggest that DFT calculations give a value for $103\ln á_{34}$ about 15 % higher than the MP2 calculations.

Interaction of earthquakes and slow slip: Insights from fault models governed by lab-derived friction laws

© N. Lapusta, 2010

California Institute of Technology, Pasadena, CA, USA

Motion of plates in the Earth crust is accomodated through fault slip. That includes both fast events (earthquakes) and slow relative motion, as evidenced by seismic and geodetic observations. We study mechanics and physics of earthquakes using a unique simulation approach that reproduces both earthquakes and slow slip, with full inclusion of inertial effects during simulated earthquakes, in the context of a 3D fault model. The approach incorporates laboratory-derived rate and state friction laws, including the effects of shear heating during rapid, seismic slip, involves slow, tectonic-like loading, resolves all stages of seismic and aseismic slip, and results in realistic rupture speeds, slip velocities, and stress drops. Our simulations show that a number of observed earthquake phenomena can be explained by interaction of earthquakes and slow slip, including transition to intersonic rupture speeds during earthquakes, peculiar properties of small repeating earthquakes, and complex spatio-temporal patterns of earthquake sequences.

Numerical simulations of short-timescale geomagnetic field variations

© A. Sakuraba, 2010

Department of Earth and Planetary Science, University of Tokyo, Tokyo, Japan
sakuraba @eps.s.u-tokyo.ac.jp

Numerical modeling of the convection in the Earth's liquid outer core has succeeded in simulating generation of a dipole-dominated magnetic field and its intermittent polarity reversals. However, previous models have used unrealistically high viscosity for the core fluid because of computational difficulty to resolve small-scale turbulence that would otherwise happen. It is still an open question whether lower-viscosity Earth-type dynamo models can simulate the geomagnetic field and its time varia-

tions. Recent models have succeeded in reducing viscosity by about one order of magnitude, compared to previous models. However, such models seem to fail to produce an Earth-like strong magnetic field even though the viscosity is more realistic. I explained that this paradoxical result was caused by geophysically unrealistic boundary condition for the core surface temperature (Sakuraba, Roberts, *Nature Geosci.* **2009. — 2.** 802 p.). If the core surface temperature is laterally uniform like recent low-viscosity models, the magnetic field is dipolar but its strength is relatively weak. If the surface heat flux is laterally uniform, which allows a pole-equator temperature difference, westward (retrograde) thermal wind naturally blows beneath the core equator and generates a strong toroidal magnetic field by its omega effect. The resultant dipole moment is relatively strong too. I concluded that the former boundary condition was not only theoretically unrealistic at the Earth's core-mantle boundary, but failed to produce Earth-like magnetic fields.

Small viscosity generally enables the dynamo model to simulate field variations of short timescales. Here I report on attempts to find Earth-like signatures of short-timescale field variations in the low-viscosity geodynamo model. I focus on three characteristic geomagnetic secular variations: westward drift, torsional oscillations, and jerks. The simulated westward drift is confined in the equatorial belt like the geomagnetic field variations for the last 400 years. The drift is primarily caused by advection, but larger-scale (lower-wavenumber) fields tend to be stationary or rather move eastward, which suggests that some planetary-scale MHD waves modulate the field behaviors. The drift velocity is slower than the Earth's probably because the simulated magnetic Reynolds number is too small. The axial angular velocity of a cylinder in the liquid outer core can be defined as a function of the cylinder's radius and the time, and this shows wavelike propagation both toward the rotation axis and toward the core equator. The phase velocity is slightly slower than that predicted by the Braginsky's theory of torsional oscillations. All three magnetic field components in my model sometimes show zigzag variations in time like the geomagnetic jerk. The simulated jerk seems to be a local phenomenon, but the cause is still under investigation.

AUTOR INDEX